Information Technology: Transmission, Processing, and Storage

CDMA Radio with Repeaters

Joseph Shapira
Shmuel Miller

CDMA RADIO WITH REPEATERS

Information Technology: Transmission, Processing, and Storage

---

CDMA Radio with Repeaters
Joseph Shapira and Shmuel Miller

Digital Satellite Communications
Giovanni Corazza, ed.

Immersive Audio Signal Processing
Sunil Bharitkar and Chris Kyriakakis

Digital Signal Processing for Measurement Systems: Theory and Applications
Gabriele D'Antona and Alessandro Ferrero

Coding for Wireless Channels
Ezio Biglieri

Wireless Networks: Multiuser Detection in Cross-Layer Design
Christina Comaniciu, Narayan B. Mandayam and H. Vincent Poor

The Multimedia Internet
Stephen Weinstein

MIMO Signals and Systems
Horst J. Bessai

Multi-Carrier Digital Communications:
Theory and Applications of OFDM, 2nd Ed
Ahmad R.S. Bahai, Burton R. Saltzberg and Mustafa Ergen

Performance Analysis and Modeling of Digital Transmission Systems
William Turin

Wireless Communications Systems and Networks
Mohsen Guizani

Interference Avoidance Methods for Wireless Systems
Dimitrie C. Popescu and Christopher Rose

Stochastic Image Processing
Chee Sun Won and Robert M. Gray

Coded Modulation Systems
John B. Anderson and Arne Svensson

Communication System Design Using DSP Algorithms:
With Laboratory Experiments for the TMS320C6701 and TMS320C6711
Steven A. Tretter

A First Course in Information Theory
Raymond W. Yeung

Nonuniform Sampling: Theory and Practice
Edited by Farokh Marvasti

Simulation of Communication Systems, Second Edition
Michael C. Jeruchim, Phillip Balaban and K. Sam Shanmugan

(continued after index)

CDMA RADIO WITH REPEATERS

Joseph Shapira
Comm&Sens Ltd.

Shmuel Y. Miller
Celletra Ltd.

Springer

Dr. Joseph Shapira
President, Comm&Sens Ltd.
Haifa, Israel 34980

Dr. Shmuel Y. Miller
Executive Vice President, Celletra Ltd.
Yoqne'am, Israel 20692

CDMA Radio with Repeaters

Library of Congress Control Number: 2006935654

ISBN 0-387-26329-2 e-ISBN 0-387-49064-7
ISBN 978-0-387-26329-8 e-ISBN 978-0-387-49064-9

Printed on acid-free paper.

9 8 7 6 5 4 3 2 1

springer.com

Contents

PREFACE xv

ABBREVIATIONS xix

1 INTRODUCTION AND PREVIEW 1
1.1 Evolution of Distributed Radio Access in the Cellular Communications 1
1.1.1 The Cellular Communications Concept 1
1.1.2 The Coverage Challenge 3
1.1.3 The Cost of the Service 4
1.1.4 The Evolution of Repeaters in the Cellular Service 5
1.2 Classification of Repeaters 6
1.2.1 Distributed Wireless Communications 6
1.2.2 Repeaters in the Cellular Communications 7
1.2.3 Repeaters in Multiple Access Systems 9
1.2.4 Repeater Classification by their Backhaul Conduit 11
1.2.5 Repeater Classification by Application 14
1.3 Repeaters in the CDMA Cellular Network 14
1.3.1 Repeater Interaction with the Network, and Tuning 14
1.3.2 Impact of Repeaters on the CDMA Network 15
1.4 Cost Considerations 17
1.5 Theme of the Book 18
1.5.1 The Complexity of the Multiple Access Mobile Communications Channel 18
1.5.2 Propagation Modeling 18
1.5.3 System Modeling 20

1.5.4 Theme of the Book 20
1.6 Organization of the Book 20

2 CDMA AIR INTERFACE OVERVIEW 23
2.1 Cellular Wireless Communications 23
2.2 CDMA IS 95 Air Interface Overview 25
2.2.1 System Concept 25
2.2.2 Logical and Physical Channels 28
2.2.3 Power Control 30
2.2.4 Soft Handoff 32
2.3 Third Generation - 3G 34
2.3.1 The Motivation 34
2.3.2 The Standardization 34
2.3.3 The Features and Techniques 35
2.4 CDMA2000 36
2.4.1 Introduction 36
2.4.2 Forward Link 36
2.4.3 Reverse Link 37
2.5 WCDMA UMTS 38
2.6 CDMA Timeline 38
2.7 Forward Link Time Multiplexing 39
2.8 1xEV-DO 40
2.9 1xEV-DV 41
2.10 HSDPA 42

3 THE MOBILE RADIO PROPAGATION CHANNEL 45
3.1 Overview of the Mobile Wireless Channel 45
3.1.1 Introduction 45
3.1.2 Channel Characteristics 45
3.1.3 Path-Loss and Channel Fluctuations 46
3.2 Path-Gain Physics 47
3.2.1 The Transmission Equation 47
3.2.2 Wave Reflection from a Perfectly Conducting Plane 48
3.2.3 Reflection at the Interface between Dielectric Media 50
3.2.4 The Two-Ray, Flat Earth Propagation Model 53
3.2.5 Lateral Waves at the Interface – Forest Propagation 55
3.2.6 Diffraction 57
3. 3 Path-Gain Prediction Models 62
3.3.1 The Role of Measurement and of Modeling in Channel Characterization and Prediction 62
3.3.2 Physically Based Prediction Models 63
3.3.3 Building Penetration and Indoors Propagation 65

3.3.4 Heuristic Models 67
3.4 Multipath and Fading 67
3.4.1 Impulse Response 67
3.4.2 Coherent Time and Coherent Bandwidth 69
3.4.3 Fading Statistics 71
3.5 Polarization Effects 73
3.5.1 Polarization of Electromagnetic Waves 73
3.5.2 The Depolarization of Electromagnetic Waves 74
3.6 Antennas and Coverage 75
3.6.1 Introduction 75
3.6.2 Antenna Parameters 76
3.6.3 Gain of an Aperture Antenna and the Sidelobe "Skirt" ... 78
3.6.4 Wave Field Regions 79
3.6.5 Dipole Antenna 80
3.6.6 Colinear Arrays 80
3.6.7 Coverage Shaping 81
3.6.8 Antenna Diversity 86
3.6.9 Antenna Noise Temperature 92
3.6.10 Coupling between On-Site Antennas 94

4 RADIO ACCESS RELATED PERFORMANCE OF CDMA CELLULAR NETWORKS 101
4.1 CDMA Forward and Reverse Links 101
4.2 Reverse Link Coverage-Capacity Assessment 102
4.2.1 The Reverse Link Equation 103
4.2.2 Capacity Limit and Noise Rise 105
4.2.3 Impact of Tower-Top LNA (TTLNA) and of Diversity 106
4.2.4 Cells with Different Size and Load 106
4.3 Soft Handoff and the Definition of the Cell Boundary 107
4.3.1 The Reverse Link Cell Boundary 108
4.3.2 Cell Coverage and "Cell Breathing" 108
4.3.3 Cell Jamming 111
4.3.4 The Forward Link Cell Boundary 113
4.4 Forward Link Assessment 113
4.4.1 Derivation of the Forward Link Equation 113
4.4.2 The Orthogonality Function 115
4.4.3 Orthogonality and Diversity Gain 117
4.4.4 Orthogonality and Forward Link Power Control 120
4.4.5 Forward Link Capacity 120
4.4.6 User Distribution 123
4.4.7 Capacity Limit of the Forward Link 124

4.4.8 Coverage and Capacity - Call Blocking and Dropped Calls 124
4.4.9 Capacity Measurement 125
4.5 Link Balancing 125
4.5.1 Coverage Balance 126
4.5.2 Capacity Balance 126
4.5.3 Balancing the Links by Controlling the Pilot Power 126
4.5.4 Link Balancing by Beam Control 130
4.6 Load Balancing 130
4.7 Soft Handoff Search Window 131
4.8 Heterogeneous Cell Clustering 131
4.8.1 Cell Shaping 131
4.8.2 Microcells 134
4.8.3 Omni Cells 138
4.9 Network Optimization 142
4.9.1 Objectives 142
4.9.2 The Dimensions of Optimization 142
4.9.3 Scope and Dynamics of Optimization 144

5 DIVERSITY IN TRANSMISSION AND RECEPTION 149
5.1 Overview of Diversity in Communications 149
5.1.1 Introduction 149
5.1.2 Diversity Dimensions 153
5.1.3 Macro- and Micro-Diversity 157
5.2 Diversity Combining 158
5.2.1 Selection Diversity Processing 159
5.2.2 Equal-Gain Combining Diversity Processing 161
5.2.3 Maximal Ratio Combining Diversity Processing 162
5.3 RF Diversity Methods in CDMA Cellular Systems 166
5.3.1 Space Diversity 166
5.3.2 Polarization Diversity 167
5.3.3 Angle Diversity 169
5.4 Transmit Diversity 169
5.4.1 Time-Delay Transmit Diversity (TDTD) 170
5.4.2 Phase-Sweep Transmit Diversity (PSTD) 173
5.5 Relaying and Cascading Diversity in Remote RANs 174
5.5.1 Direct Diversity Relaying 174
5.5.2 Remote Transmit Diversity 176
5.5.3 PseudoDiversity Combining (*PDC*) – Relaying RL Diversity 177
5.5.4 Diversity Reception of Relayed Diversity Branches 178
5.6 The Impact of Diversity on the CDMA Cellular Network 178

5.6.1 Diversity in the Reverse Link 179
5.6.2 Transmit Diversity in the Forward Link 180
5.6.3 Time-Delay Transmit Diversity 180
5.6.4 Phase-Sweeping Transmit Diversity (PSTD) 185
5.6.5 Comparative Evaluation 187
5.6.6 Impact of Diversity on Network Probes and Status Measurement 187

6 REPEATERS EMBEDDED IN THE CDMA RADIO ACCESS NETWORK 193
6.1 Modeling of the Repeater in the CDMA Network 193
6.2 Classification of Repeaters by their Interaction with the Donor Cell 196
6.2.1 Embedded Repeaters 196
6.2.2 Range Extension Repeaters 196
6.2.3 Cell boundary Repeaters 197
6.2.4 Remote Repeaters 197
6.3 Interaction of the Repeater with the CDMA Network 198
6.3.1 Repeater Modeling – Reverse Link 198
6.3.2 Repeater Impact on Coverage and Capacity – Reverse Link 200
6.3.3 Forward Link Analysis 204
6.3.4 Repeater Links Balancing 207
6.4 Optimization of the Reverse Link 211
6.4.1 Derivation of the Optimization Equation 211
6.4.2 User-Density-Limited Cells 212
6.4.3 Capacity-Limited Cells 215
6.5 Repeater Coverage Overlap with the Donor Cell 217
6.5.1 Coverage Overlap Analysis 217
6.5.2 Coverage Overlap Control. 218
6.6 Multiple Repeaters 219
6.6.1 "Star" Architecture – Parallel Repeaters 219
6.6.2 Multi-hop Repeater Architecture 222
6.6.3 Comparison of Star and Cascade Repeater Linking 229
6.6.4 RF Distribution Network and the Distributed Antenna . 231
6.7 Search Windows 232

7 REPEATERS DESIGN AND TUNING IN CDMA NETWORKS 235
7.1 RF Repeaters 235
7.1.1 The Role of RF Repeaters 235
7.1.2 Network Diagram and Signal Flow 235
7.1.3 Repeater Generic Diagram 236

7.1.4 BTS Interface 237
7.1.5 Critical Signal Paths and Parasitic Coupling 239
7.1.6 Signal Distortions 240
7.2 Repeater Architecture 241
7.2.1 Governing Parameters and Design Principles 241
7.2.2 Distributed and Unified Repeater Architectures 249
7.2.3 Band-Filtered and Channel-Filtered Repeaters 251
7.2.4 Signal and Interference Budget 252
7.2.5 Gain and Filtering Chain 254
7.2.6 Level and Gain Control 257
7.2.7 Antennas in Repeater Systems 260
7.3 Repeater Design 261
7.3.1 Basic Design Rules 261
7.3.2 RF F1/F1 Repeater 274
7.3.3 Optical Fiber Repeater 278
7.3.4 Free-Space Optic Repeater 283
7.3.5 In-Band F1/F2 Repeater 285
7.3.6 Out-of-Band F1/F2 Repeater 291
7.3.7 MW F1/F2 Repeater 292
7.3.8 Repeater Tuning 294
7.4 Regulation and Type Approval 296
7.4.1 Regulatory Constraints 296
7.4.2 Type Approval 297
7.4.3 Type Classification 297
7.4.4 Test Parameters 297
7.4.5 Test Subtleties 298
7.4.6 Emission Requirements 299

8 BACKHAUL FOR RF DISTRIBUTED RADIO ACCESS NODES 303
8.1 Analog and Digital Backhauls 303
8.1.1 Analog Backhaul 303
8.1.2 Digital Backhaul 304
8.2 Classification of Backhauls 304
8.2.1 Coax 304
8.2.2 Optical Fiber (OF) 304
8.2.3 Free-Space Optics (FSO) 305
8.2.4 In-Band FSR 305
8.2.5 Out-of-Band FSR 305
8.2.6 MW FSR 305
8.3 Repeater Backhaul Parameters 306
8.3.1 Introduction 306

8.4 Repeater Backhaul Engineering 308
8.4.1 Design Rules 308
8.4.2 Coax Backhaul 310
8.4.3 Optical Fiber Backhaul 311
8.4.4 Free-Space Optic Backhaul (FSO) 316
8.4.5 Radio Point-to-Point Backhauls 319
8.4.6 Backhaul Enhancement by Diversity 321
8.5 Backhaul Cost Considerations 322
8.5.1 Cost Contributors 322
8.5.2 Cost 323

9 REPEATER ECONOMICS 325
9.1 Baseline Networks 325
9.1.1 Network Distribution in Typical Markets 326
9.1.2 Coverage – Capacity Model 327
9.2 Repeater Embedded Networks 329
9.2.1 Constituting Relations 329
9.2.2 Relevant Scenarios 330
9.3 Cost Constituents 330
9.3.1 Tower Cost 331
9.3.2 Tx Power Cost 332
9.3.3 Backhaul Cost 332
9.3.4 BTS and Repeater Cost 333
9.4 Cost Model for Area Coverage 333
9.4.1 Optimal Coverage of a Flat Area 333
9.4.2 Optimal Coverage of a Length of Road 336
9.5 Cost Model for Area Coverage by a Cluster of BTSs and Satellite Repeaters 337
9.5.1 Large Area Coverage 337
9.5.2 Supplementary Coverage 338
9.6 Summary 338

10 ADVANCES IN CDMA REPEATERS 341
10.1 Introduction 341
10.2 Performance Monitoring and Control 342
10.2.1 Application of a CDMA Modem in the Repeater 342
10.3 Stabilization by Gain Control 344
10.4 Interference Suppression 345
10.4.1 Digital Repeaters 345
10.4.2 Enhancing Isolation between the Backhaul and Service Antennas by Adaptive Interference Cancellation 346
10.4.3 Adaptive Interference Cancellation 347

10.4.4 Adaptive Cancellation of Radiated Interference 348
10.5 Receive Diversity in Repeaters 349
10.6 Transmit Diversity in Repeaters 350
10.7 Network Parameters Readout from the Wireless Modem 350
10.8 Antenna Control 351
10.9 Tagging of Repeater-Served STs 351
10.10 Location 351
10.11 Measurement of Traffic Load through the Repeater 352
10.12 Load Balancing between Cells and Sectors 352
10.13 High Data Rate Systems 353

EPILOG 357

APPENDIX A

REVERSE LINK INTERFERENCE IN HETEROGENEOUS CELL CLUSTERS 359
A.1 The Ring Model for Other Cells' Interference 359
A.1.1 Introduction 359
A.1.2 The Ring Model 360
A.2 The Embedded Microcell Model 363

APPENDIX B

EVALUATION OF THE POWER RISE EQUATION 369

APPENDIX C

ORTHOGONALITY FACTOR THROUGH THE CELL 373
C.1 Scattering and Reflections 373
C.1.1 The Reflection Coefficient *F* 374
C.1.2 The Population of Contributing Reflectors 376
C.1.3 The Reflection Contributions 377
C.2 Orthogonality Factor 379
C.3 Unified Factor – Transitions 381
C.3.1 Transition Near-Intermediate Zones 381
C.3.2 Transition Intermediate-Far Zones 382

APPENDIX D

SYSTEM NOISE AND DYNAMIC RANGE 383
D.1 Noise Figure 383
D.1.1 Definitions 383

D.1.2 System Noise 386
D.1.3 System Sensitivity 388
D.2 Dynamic Range 389
D.2.1 Basic NonLinear Model 389
D.2.2 Intermodulation Products 390
D.2.3 System Intercept Point 396
D.2.4 Dynamic Range 399
D.3 Beamforming and Combiners 401

APPENDIX E

ENVELOPE CORRELATION AND POWER CORRELATION IN FADING CHANNELS 405

APPENDIX F

EIGENVALUE ANALYSIS OF MRC 407

APPENDIX G

OPTIMAL SECTOR BEAMWIDTH 409
G.1 Model 409
G.2 Choice of Antenna Gain Function 410
G.3 Total Sector Traffic Power 411
G.4 Softer Handoff Boundary 411
G.5 Discussion 413
G.5.1 Limits on the Analysis 413
G.5.2 Optimal Beamwidth 413
G.5.3 Effect of the SrHO 413

APPENDIX H

CELLULAR BANDS AND FREQUENCY ALLOCATIONS 415

ABOUT THE AUTHORS 417

INDEX 419

PREFACE

Cellular Communications is about *Service, Technology and Economy. Public awareness and safety* is considered the fourth dimension in the equation, that rolls back to impact all of the other three.

Mobile communications has become an indispensable element of modern lifestyle. The 3G cellular systems focus on high data-rate multimedia services and a host of respective applications, mostly leisure-time oriented. At the other extreme, mobile communications is a most effective driving force in boosting the economy of developing communities. These two processes may share technology momentum and the economy of scale, but their substantial differences have to be recognized, at the time when the momentum of cellular deployment moves in that direction. The introduction of mobile wireless services to developing communities is challenged by the cost of infrastructure, operations and user terminals of the advanced networks, and the mixture of older generation systems to coexist with the new deployments. Affordability considerations and priority of services inspire innovative architectural and optimization solutions to the infrastructure, choice of applications and user terminals.

Mobile communications is the art of interaction of the ingenious transmission and reception of multiple messages, with the nature of propagation that paves their way. Both the propagation channel and the distribution of the multitude of users are not known exactly, posing a major challenge to the optimization of the multiple access network. The latter aims at minimizing capital and operational costs while matching the maximal load with satisfactory performance, recognizing that the load is not evenly distributed nor is it stationary in time. The optimization of 3G systems providing multimedia services is even more challenging. Statistical propagation modeling and network simulations fall short of representing the dynamics of the network and optimizing its performance. The combination of prediction models with online measurements is needed for network performance diagnosis. Proper distribution of access nodes, both BTSs and repeaters, and duly dynamic application of coverage and diversity means by antennas and power control, in response to the diagnosed parameters, will ensure an optimized utilization of the network resources.

Each of the CDMA cellular systems, IS 95, CDMA2000 or UMTS WCDMA, is a complex adaptively controlled digital modulation and processing system. Its radio interface is governed by surprisingly simple rules, however, relating to averaging of multiple transmissions to a noise like

interference. These basically simple rules allow for an understanding of the underlying processes and trends relating to coverage, capacity, grade and quality of service, which offer the radio engineer the insight needed to guide the planning, deploying, analyzing and optimizing of the network. Furthermore, the new data-optimized systems – 1xEV-DO and HSDPA, that share the network and the air interface with the CDMA systems, bring in different radio resource management rules. A different paradigm has to be attended to in optimizing the mixed services operating on the same network.

The schematic uniform, preferably hexagonal, grid of identical cells as conceived at the introduction of the service in early 80s, does not meet the continuous coverage requirements over a diversified environment and teletraffic densities. Way over half of the service area in each major market is coverage-limited and does not fully utilize its communications resources. The optimal cell size in these areas is governed by the cost structure of its constituents: tower, shelter, radio and processing equipment. Distributed radio access by repeaters, augmenting nodal base stations, substantially reduces the cost in such a rural coverage, as they do when stacked in multi-hop chains in coverage of long roads, when illuminating shadowed areas within the regular cell coverage ("radio holes"), and when providing access indoors.

Repeaters constitute an interactive part within the cellular CDMA network. Effective deployment of the repeaters, and optimization of repeater-embedded network - requires an intimate understanding of the CDMA air interface. The purpose of this book is to enrich the cellular scientist and engineer with the understanding of the interaction between the CDMA network dynamics and its embedded repeaters - and with the propagation channel, and offer them the insight into the processes and trends.

The interrelation of the parameters involved in the radio access is too complex and site-dependent to be accurately simulated, and any attempt to heuristically typify a model does not cast comprehension on others. This book takes the approach of simple modeling of the radio access behavior, with physically based canonical scenarios. The interrelation of these propagation models with the system performance models provides a convenient tool for understanding of the system performance, parametric dependence and dynamics. These models are supported by observed experience and occasional detailed calculations.

The book is written in simple language, enriched with graphical description of the scenarios and with trending plots. Ten chapters cover the cellular scene and rational for distributed access, the relevant aspects of the cellular standards, the characteristics of the mobile propagation, the inter-relations and dynamic of the CDMA network, the application of diversity transmission and reception, and the application of repeaters to the CDMA network and their impact and optimization of the repeater-embedded network.

Costing models for the application of repeaters are elaborated upon. Supporting chapters provide detailed structure and tuning parameters for repeaters and their backhaul relay. Chapter 10 - Advances in Repeaters, then reviews emerging technologies and applications.

ABBREVIATIONS

3G	3rd Generation cellular system
3GPP	3rd Generation Partnership Project *(produced the WCDMA standard)*
3GPP2	3rd Generation Partnership Project 2 *(produced the CDMA2000 standard)*
1x	Single carrier (1.25 MHz) version of CDMA2000
3X	Multicarrier (5 MHz) version of CDMA2000
ACP	Adjacent Channel Power
ACPR	Adjacent Channel Power Ratio
AFC	Automatic Frequency Control
AFL	Automatic Frequency Locking
AFLT	Advanced FL Triangulation
AGC	Automatic Gain Control
AIN	Advanced Intelligent Network
AISG	Antenna Interface Standardization Group
AMLC	Automatic Maximum Level Control
AMC	Adaptive Modulation and Coding
AMPS	Advanced Mobile Phone Service
AP	Access Point
APD	Avalanche Photo Diode
ARQ	Automatic Repeat Request
AWGN	Additive White Gaussian Noise
BDA	Bidirectional Amplifier
BER	Bit Error Rate
BFN	Beam Forming Network
BHCA	Busy Hour Call Attempt
BPF	Band Pass Filter
BPSK	Biphase Shift Keying *modulation*
BSC	Base Station Controller
BSS	Base Station Subsystem
BSSM	Base Station Subsystem Manager
BTS	Base Transceiver Subsystem
CAPEX	Capital Expenditure
CCP	Call Control Processor
CDE	Code Domain Error
CDF	Cumulative Distribution Function
CDG	CDMA Development Group
CDMA	Code-Division Multiple Access

CDMA2000	3rd generation CDMA standard *produced by 3GPP2*
CEPT	European Conference of Postal and Telecommunication Administrations
CFR	Code of Federal Regulations *(goes with a number)*
CIS	CDMA Interconnect Subsystem
COST WI	(Commission of European Communities) Walfish Ikegami – *an urban propagation model adopted by COST*
CSCG	Circularly Symmetric Complex Gaussian
CTIA	Cellular Telecommunications Industry Association
CW	Continuous Wave
D/A	Digital to Analog
dBO	dB of Optical gain
DFB	Distributed Feedback
DG	Digital Gain
DGU	Digital Gain Unit – *In the FL power and power control*
DRC	Data Rate Control
DTOA	Differential Time of Arrival
DU	Diversity Unit
DWDM	Dense Wavelength-Division Multiplex
EAM	Electro-Absorption Modulator
EGC	Equal-Gain Combining *of diversity branches*
EIA	Electronics Industry Alliance
EIRP	Effective Isotropic Radiated Power
ETSI	European Telecommunications Standards Institute
EV-DO	Evolution to Data Optimized. *Version of CDMA2000 standard*
EV-DV	Evolution to Data and Voice. *Version of CDMA2000 standard*
EVM	Error-Vector Magnitude
F1/F1	On-frequency relay
FA	Frequency Allocation. *The same as Channel*
FCAPiCh	Forward Common Auxiliary Pilot Channel
FCC	Federal Communications Commission
FCH	Fundamental Channel. *Used in call and low data rate*
FDAPiCh	Forward Dedicated Auxiliary Pilot Channel
FDD	Frequency-Division Duplex
FDM	Frequency-Division Multiplex
FDMA	Frequency-Division Multiple Access
FEC	Forward Error-correction Code
FER	Frame Error Rate
Finger	A time-delayed branch in the RAKE receiver
FL	Forward Link

FLPC	Forward Link Power Control
FM	Fade Margin
FP	Fabry-Perot *optical filter*
FPCh	Forward Paging Channel
FPiCh	Forward Pilot Channel
FSCCh	Forward Supplemental Code Channel
FSO	Free-Space Optics
FSR	Frequency Shifted Repeater (F1/F2)
G/T	Gain to Temperature ratio
GDV	Group Delay Variations
GM	Gain Margin – *-Gain+Isolation in dB*
GoS	Grade of Service
GPS	Global Positioning System
GSM	Global System for Mobile communications
HARQ	Hybrid ARQ
HLR	Home Location Registry
HPA	High-Power Amplifier
HSDPA	High Speed Downlink Packet Access
ICI	InterCarrier Interference
ID	Identification
iDEN	integrated Digital Enhanced Network
IF	Intermediate Frequency
i.i.d	independent identically distributed
IIP	Intermodulation Intercept Point *where the intermodulation product equals the signal power*
IM	Intermodulation
IMT2000	International Mobile Telephone standardization program by ITU
IP	Internet Protocol
IP3	Intermodulation Product of 3rd order
IR	Infrared
IS 95	cdmaOne 2nd generation standard
ITU	International Telecommunications Union
LHC	Left-Hand Circular *(polarization of electromagnetic wave)*
LNA	Low-Noise Amplifier
LO	Local Oscillator
LOS	Line of Sight
LPI	Low Probability of Intercept
LPIR	Low Probability of Intercept Radar
MIMO	Multiple In – Multiple Out *antenna arrays communications*
MMDS	Multipoint Microwave Distribution Service
MOU	Minutes of Use

MRC	Maximal Ratio Combining *of diversity branches*
MS	Mobile Station. *See ST.*
MW	Microwave *transmission conduit*
MZM	Mach-Zehnder optical Modulator
NBPF	Narrow-Band-Pass Filter
NE	Network Element
NF	Noise Figure
NLOS	Non Line of Sight
NMC	Network Management Center
NMS	Network Management System
NOC	Network Operations Center
Noise Rise	Measure of the total power received at the BTS relative to its thermal noise. *Also called RoT*
NSS	Network Switching System
OA&M	Operation, Administration and Maintenance
ODU	Out Doors Unit
OF	Optical Fiber
OFDM	Orthogonal Frequency-Division Multiplex
OFR	On-Frequency Repeater (F1/F1)
OPEX	Operational Expenditure
OQPSK	Offset Quadrature Phase Shift Keying *modulation*
OR	Optical Fiber Repeater
OTD	Orthogonal Transmit Diversity
PA	Power Amplifier
P.C.	Power Control
PC	Portable Computer
PCDE	Peak Code Domain Error
PCG	Power Control Group
PCS	Personal Communications Service. *A frequency allocation in the US (1850-1990 MHz).*
PCSCh	Power Control SubChannel
PDC	Pseudo Diversity Combining
PDF	Probability Distribution Function
PG	Path-gain. *The inverse of Path-loss*
PIN	P I N *diode*
PLL	Phase-Lock Loop
PMRM	Power Measurement Report Message
PN	Pseudo Noise. *PN code offset identifies the pilot.*
PolMatch	Polarization Matching
PSMM	Pilot Strength Measurement Message
PSTD	Phase-Sweep Transmit Diversity
PSTN	Public Switched Telephone Network

PTP	Point to Point
QAM	Quadrature Amplitude Modulation
QoS	Quality of Service
QPSK	Quadrature Phase Shift Keying *modulation*
RAKE	Receiver. *An optimum receiver (matched filter) structure consisting of several parallel receivers-correlators, one per time-delayed version of the signal. The output of all branches adds in a combiner to yield the statistic for decoding the transmitted symbol.*
RACh	Reverse Access Channel
RAN	Remote Access Node
RBC	Remote Beam Controlled *antenna*
RC	Radio Configuration
RET	Remote Electrical Tilt *for antenna*
RF	Radio Frequency
RHC	Right-Hand Circular *(polarization of electromagnetic wave)*
RL	Reverse Link
RMS	Root Mean Square
RNMS	Repeater Network Management System
RNS	Radio Network Simulation
RoT	Rise over Thermal *noise. See Noise Rise*
RRM	Radio Resource Management
RS	Rate Set
RSSI	Received Signal Strength Indication. *Total power measured at the receiver input, no detection.*
RTCh	Reverse Traffic Channel
RTT	Radio Transmission Technology *(goes with a number)*
SAW	Surface Acoustic Wave
SCDMA	Synchronous CDMA
SCh	Supplemental Channel, *used in time shared high data rate packets with channel scheduling*
SEL	Selection *of diversity branches*
SHO	Soft Handoff
SIMO	Single In Multiple Out *antenna arrays*
SNIR	Signal to Noise and Interference Ratio - *power ratio*
SNMP	Simple Network Management Protocol
SNR	Signal to Noise Ratio - *power ratio*
SOR	Service Option Request
SrHO	Softer Handoff
SSA	Supplementary Service Adjunct
ST	Subscriber Terminal. *Also called Mobile Station – MS*
STBC	Space-Time Block Code

STTD	Space-Time Transmit Diversity
SyncCh	Sync Channel
TDD	Time-Division Duplex
TDMA	Time-Division Multiple Access
TD-SCDMA	A TD standard within 3GPP
TDTD	Time-Delay Transmit Diversity
TDU	Transmit Diversity Unit
TE	Transverse Electric electromagnetic wave mode
TIA	Telecommunications Industry Association
TM	Transverse Magnetic electromagnetic wave mode
TMA	Tower Mounted Amplifier. *See TTLNA*
TOA	Time of Arrival *of the propagated wave*
Transmit Adjust	*The average sum of the P.C. corrections to the open loop P.C. bias K*
Tx Gain Adjust	Same as Transmit Adjust
TSTD	Time Switched Transmit Diversity
TTE	Tower-Top Electronics
TTLNA	Tower-Top LNA *(also TMA)*
UMTS	Universal Mobile Telecommunications System
USD	US Dollar
UTRA	UMTS Terrestrial Radio Access
VCO	Voltage Controlled Oscillator
VLR	Visitor Location Registry
WBPF	Wide-Band-Pass Filter
WCDMA	3rd generation CDMA standard *produced by 3GPP*
WDM	Wavelength-Division Multiplex
WWRF	Wireless World Research Forum
XPD	Cross Polarization Discrimination
XPR	Cross Polarization Ratio. *See XPD*

1

INTRODUCTION AND PREVIEW

1.1 Evolution of Distributed Radio Access in the Cellular Communications

1.1.1 The Cellular Communications Concept

The inception of the cellular mobile communications dates over 50 years ago, striving to provide multiple access communications to mobile users anywhere, any time. Technology closed the gap by the end of the 70s, and commercial services were launched, first in Tokyo, then the U.S. The rest is history [1].

Provision of the service *everywhere* means maintenance of sufficient level of signal for reception with the required quality of service over the whole area. This is termed *coverage.* Provision of *multiple access* – multiple independent duplex sessions, means division of the limited spectral resources between the sessions. The concept of *cell* means a *continuous limited coverage area* beyond which the spectral resources may be reused because the signal propagation decays away from the cell. The cellular system relies on hubs, called *base stations*, that communicate with each user in a STAR network (Fig. 1-1).

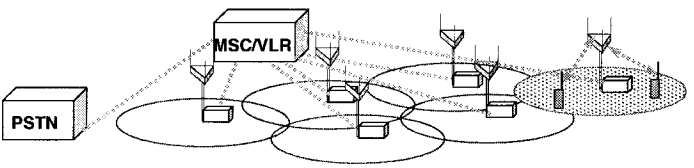

Figure 1-1. The cellular system. *Communications between subscribers in the same cell go through the BTS. Communications between cells and with the line telephone service are handled through fixed lines (dotted), and controlled by the Mobile Switching Center (MSC) that also hosts the Visitor Location Registry (VLR) and is linked to the Public Switched Telephone Network (PSTN)*

This way the base station antenna, located appropriately higher above the mobile users' level, can shed continuous and well-defined coverage and limit the variations of the link loss throughout the cell to some 80 dB. The part of the base station associated with the antenna, transmission and reception is called Base Transceiver Subsystem (BTS) (also called Node B in the UMTS system), while the part that controls the calls is Base Station Controller (BSC), not necessarily collocated. The full duplex communications flows in two separate frequency bands – *frequency-division duplex* (FDD), that is common to all major cellular standards. Systems that switch periodically between transmission and reception – *time-division duplex* (TDD), also serve for short ranges in the digital 2nd and 3rd cellular generation.

The coverage is determined by the signal level above noise and interference from other cells (Fig. 1-2). A guard zone is required to avoid inter-cell interference - the adjacent cells do not use the same frequency, and frequency reuse applies in every 7th cell (AMPS) and 3rd or 4th cell (GSM). The CDMA system, based on code-filtering rather than frequency and time filtering, reuses the same frequency in every cell while absorbing the adjacent cells' interference on behalf of reduced capacity. The omnidirectional signal distribution as in Fig. 1-2 creates round cell coverage. The most compact packing of circles is in a hexagonal grid, which is then the schematic deployment architecture for the cellular networks.

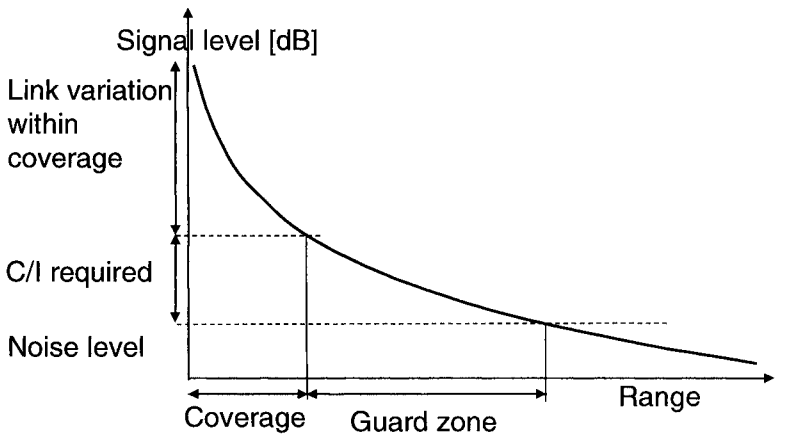

Figure 1-2. Signal strength, coverage and guard zone. *The coverage extends to the level of required C/I above the noise level. The guard zone extends to the noise level, where the same frequency can be used*

Extra overlap of the cells' coverage is required in order to assure a safe and uninterrupted communication session while in passage of a mobile from one cell to another – a process called handoff (or hand over) that involves a smooth transparent disconnect from one and reconnect to the other. The handoff in the CDMA network is soft (SHO), meaning that both cells are connected during the passage. This is possible because the same frequency is used throughout. The SHO allows for a smaller overlap margin. Cells are commonly split into *sectors* by directive antennas at the BTS, each covering an angular sector.

The purpose of sectorization is reducing the intercell interference, which allows for better frequency reuse and thus for an increase of the capacity of each cell. Sectorization into three, each covering 120^0, appears to be the most practical.

1.1.2 The Coverage Challenge

The ultimate limit on the capacity of the cellular network is the total number of links (modems) and the total power available for transmission from all BTSs in the network. The network is set to accommodate this in a uniform, hexagonal grid of cells and uniform distribution of users throughout the network. Networks exercise a small portion of their ultimate capacity, however. The users' density varies between extremely dense in urban areas to very sparse in rural areas. Over half of the cells in every major market are coverage-limited, seeking to cover large, sparsely populated areas, while capacity-limited cells in the urban core seek the confinement to a small coverage where the cell's capacity is utilized, and there is isolation from neighbor cells' interference. The topography and land cover – building, forests - limit the coverage of the BTS antenna and its uniformity, sometimes creating shadowed areas ("radio holes") within the cell coverage, while shedding excessively strong signals to adjacent cells in other cases. The hexagonal grid is then left as conceptual schematics and has to give way to a detailed architecture planning based on propagation rules, users' densities and air interface dynamics of the relevant system. The impact on the CDMA system may be divided into *in-cell/ sector related*, where shadowed areas or channel multipath conditions degrade the service; *network/ cell cluster related*, where excess of coverage overlap, or lack of it, disturbs the soft handoff process and increases interference or teletraffic loads are not well-distributed within the cell cluster; and *forward and reverse link balancing*, where these links in the CDMA systems are affected differently by the channel conditions and users' distributions due to their different structure which impairs the coverage balance between the links.

1.1.3 The Cost of the Service

The cellular communications service is an infrastructure-based industry, where the capital investment of the vast infrastructure precedes any accrued income. The cost of the BTSs amount to 70% of the investment in the network, and has a cardinal impact on the venture. The main cost constituents of the BTS are tower complex, comprising the tower, antennas and cables, the shelter and auxiliary infrastructure, the BTS equipment and the cost of the backhaul communications, either owned or leased. The cost of the tower complex ascends as its height cubed. The coverage area relates roughly to the antenna height above the land cover. These relations set a trade-off for the cell coverage area, and thus the number of cells to cover a given service area that delicately depend on the cost of the BTS equipment, shelter and backhaul. This is demonstrated in Fig. 1-3 (see Fig. 9-5 for details), with exemplary cost estimates.

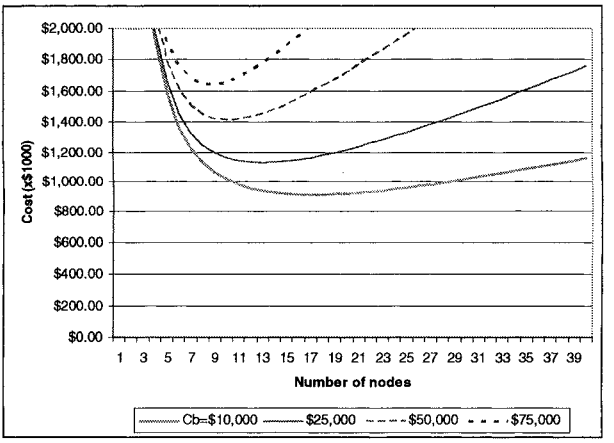

Figure 1-3. Cost of coverage of a rural area. *The cost of the tower is* $C[USD]=c=0.7[USD/m^{2.5}]\cdot height^{2.5}[m]$; *the height of the land cover is 20 m. Cost of BTS* C_b *ranges from $10,000 to $75,000*

The cost may be reduced by separating the BTS communications and processing part from the radio access, comprising the RF transmission part. By so doing, a single shelter and BTS can serve multiple radio access nodes and a larger coverage area. The aggregation of BTS resources (multiple sectors) in one shelter that is easily accessible for servicing and backhaul connection to the switch and distributing the antennas to relevant coverage areas via RF conduits, is sometimes called *BTS hotelling*. Each access node

has its dedicated resources and can exercise full capacity. Access nodes that branch off the main BTS antenna, and thus share the main cell's resources, are called *repeaters*. Their role is mainly coverage extension or hole-filling, but they may also be utilized to optimize the network performance, as elaborated on in this book.

1.1.4 The Evolution of Repeaters in the Cellular Service

The period 80s – mid 90s. The commercial cellular communications developed from a privileged mobile service to a popular personal service, with the first generation analog systems. The market was dominated by a few end-to-end manufacturers of the system, while most of the operators were government entities or otherwise regulated. The vendors, having full technical control and interest in the equipment business, did not provide nor promote distributed access equipment and repeaters. The cost of the BTS shelter and equipment was over half a million USD.

The period mid 90s – 2000. The introduction of the second generation and the proliferation of the service. The cost of the BTS was steadily decreasing, while the requirements for the service were ever increasing. The introduction of the digital communications standards allowed for new concepts for network enhancement, including "smart antennas", introduced by new niche industries, but hardly accepted by the market that is vendor-financed by the main infrastructure vendors. Repeaters spawned in Korea as a part of the new CDMA network, which – due to its frequency reuse throughout the network, accommodated repeaters without new network planning.

The period 2000 – 2003. A time of crisis in the communications industry. Vendor financing to the cellular operators diminished, and investments in the infrastructure froze, in spite of a steady growth of the subscriber base (Fig. 1-4).

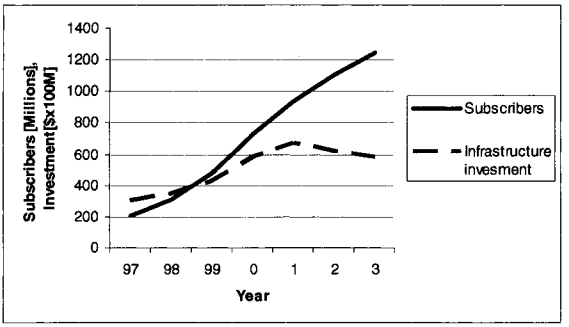

Figure 1-4. Subscribers growth vs. investment in infrastructure. *A steady growth of subscriber base vs. freeze in infrastructure*

The major infrastructure vendors began stripping off their RF business. The operators transformed their business model. The shortage evaporated many small RF businesses.

The period 2003 – present. The infrastructure industry forges into the digital and communications part, held by the traditional main vendors who focus on developing the 3G and service applications, and an RF access industry that provides the RF access, including amplifiers, cables, antennas, repeaters and integrated solutions. The operators take charge of their network, and seek cost saving network enhancement solutions. The RF access industry steadily merges to large, one-stop-shop companies. The cost of BTS drops steadily, leaving the cost of the tower as a dominant factor in the cost of the network. A move for standardization of the RF interface to the BTS supports this trend. Activity for standardization of remote RF access and repeaters in the 3G and broadband wireless standardization bodies is ongoing. The bulk of new networks deployment shifts to developing countries, where cost-awareness is at premium.

Next? The packet-switched multimedia network is to leverage on a wide area wireless broadband internet to provide the core networks between the BTSs, which may further fragment the traditional cellular infrastructure industry. The low-cost of the BTS may threaten the market of repeaters, which will have to develop more control features to compare offerings.

1.2 Classification of Repeaters

1.2.1 Distributed Wireless Communications

A signal transmitted from the source to the receiver undergoes deterioration effects: attenuation, distortion, added noise, etc. The effects on the signal on its passage are attributed to the *link*. The *link* relates the signal status at the end to that at the source. The physical means for relaying the *link* are typically termed by the specific type, e.g. microwave transmission, fiber optics, etc. In general, these are termed hereon the *conduits* for the signal. Long haul transmission through a conduit suffers deterioration. A *repeater* is a means to relay, amplify, and condition the signal along the conduit. Repeaters are used in a variety of communications systems, e.g. multi-hop microwave transmission, satellite communications, optical fiber links, and cellular communications. A *regenerative repeater* is essentially a receiver-transmitter chain that demodulates the transmission, detects the bit stream, and remodulates and transmits it, amplified and clean of noise. *Regenerative repeaters* apply to long haul *digital communications*. The rational for regenerative repeaters is signal consistency over the long haul, and not necessarily cost.

A BTS in the cellular communications system is basically a stack of *regenerative repeaters* that transform the signal from one conduit (the backhaul links) to another (the over-the-air transmission to multiple users in the coverage area) and also controls the sessions. Shortage of the coverage area, or link impairments within the coverage area, can be recovered by either introducing additional BTSs or by introducing *cellular repeaters*. The rational for the choice of cellular repeaters over BTSs is *cost*. Cellular repeaters are therefore simpler in structure and functionality than BTSs, and *are not regenerative*. They are essentially bidirectional amplifiers aimed at transparent amplification of the forward (down) and reverse (up) links of the over-the-air signal distribution to the users.

1.2.2 Repeaters in the Cellular Communications

The distribution of radio access nodes within the service area is constrained by topography and land cover – in coverage limited areas, and by users' density in capacity-limited areas. The relative cost of the infrastructure constituents drives a distribution of access nodes that do not yield the full features (and cost) of the BTS. *Remote sectors* are radio nodes consisting of antennas and respective amplifiers, located remote from the BTS shelter as needed for the coverage and linked directly to the communication resources (modems) of a sector by RF conduits (microwaves, fibers, RF cable, Free-Space Optics). They benefit of full communications resources and can accommodate full users' capacity in their coverage area. A cluster of remote sectors distributed around a stack of collocated BTS resources is called *BTS hotelling*.

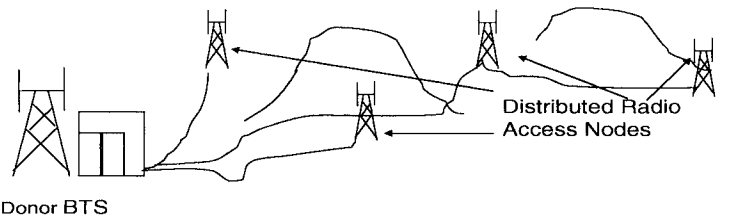

Figure 1-5. Distributed radio access nodes

Repeaters are relay stations for the signal. In the cellular service the repeater relays the transmission of the BTS to the subscribers in a coverage area, and vice versa. The repeater shares the modem stack (channel elements stack) of a donor sector in a BTS with the donor's antenna that serves its own

coverage area, by branching off the RF conduit to/from the antenna, or the IF at the front end of the BTS. It differs from *remote sector* in that the latter is connected directly to a dedicated modem stack and thus constitutes a BTS or a sector thereof whose antenna is remote from the equipment. The unique feature of the repeater in the network, then, is that it shares the RF resources with other RF distribution (antenna) and does not have dedicated controls to its coverage (e.g. pilot code, power control, etc.). Multiple repeaters may be connected in parallel ("star") or in a multi-hop chain. "On–frequency" (F1/F1) repeaters that are linked to the donor sector by communicating with the donor service antenna do not require a *donor unit* at the donor BTS, but only a *remote unit*. Remote sector, on the other hand, needs a *donor unit* at the BTS (Fig. 1-6).

BTS Hotelling is shown in Fig. 1-7. Several base stations are placed in one preferred location, forming a *BTS hotel* or *BTS farm*. The distributed radio coverage to be provided by the base stations is achieved via remote sectors. If two or three sectors share a single conduit to provide a remote BTS, the system is termed *remote cell*. The BTSs in the *BTS hotel* do not need to incorporate the high-power amplifiers, which capture most of the volume and the attendance in a typical BTS shelter.

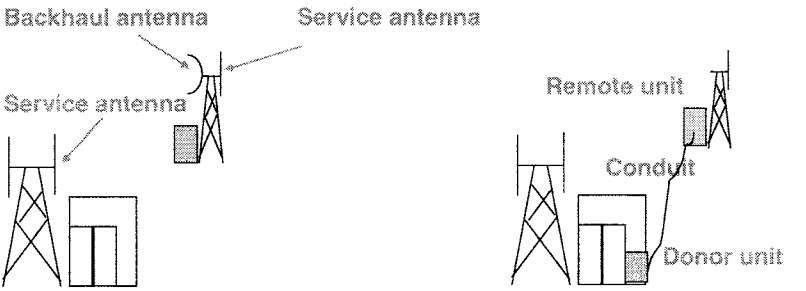

Figure 1-6. Repeater and remote sector. *Remote sector requires a donor unit at the BTS for connecting to the modem stack and transforming to the backhaul conduit*

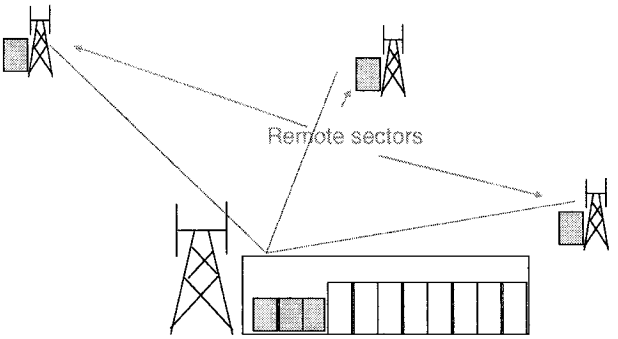

Figure 1-7. BTS hotelling

1.2.3 Repeaters in Multiple Access Systems

The cellular standards allocate links to each of the multiple access users in different ways, which influence the application of the repeaters in these networks.

FDD – frequency-division duplex. All the major cellular standards rely on a separate band allocation for the signals transmitted from the BTS to the users – *forward* (or *down*) links, and the signals transmitted from the users to the BTS – *reverse* (or *up*) links. All the forward links are stacked in a *forward link (FL) frequency allocation* (FA) band, while the reverse links are stacked in a *reverse link (RL) frequency allocation*, allocated by the authorities. Each individual user's link maintains the same duplex separation between its forward and reverse links, separated so as to make the duplexer and filters functions at the user terminal practical. The separation of the individual FL and RL in the 850 MHz systems and 900 MHz systems is 45 MHz, for example. The separation of the FL and RL bands depends on the band allocation to each operator. Repeaters in these services incorporate both links and have to maintain enough isolation between them, within the equipment and between the respective antennas, in order to avoid oscillations.

TDD – time-division duplex. This applies to certain short-range digital multiple access systems, such as PHS and DECT. The systems have to be digital and able to compress the transmission into a shorter time period, and allow for a period of reception. The forward and reverse links are switched periodically, using the same frequency allocation. Time-delay zones have to be incorporated in these transmission schemes to allow for the respective

delay through the repeaters and avoid coupling between the FL and RL. Active switching may apply in these repeaters to increase the isolation.

FDMA – frequency-division multiple access. These are the analog cellular standards, whereby each user's link has a *channel allocation.* This is 30 KHz in the AMPS system, for example. The system frequency reuse is typically 7 cells when each is sectorized to 3. *Band repeaters* incorporate band filters according to the band allocated for the repeater, which may be the full band allocated to the operator, or a fraction of it, according to the frequency planning. *Channelized repeaters* incorporate individual, narrow band, channel filters (e.g. 30 KHz). Multiple channel repeaters comprise a stack of channel filters. Remote control over the analog channel filters is cumbersome and not common. Installation of coverage extension repeaters requires a review of the frequency plan of the network.

TDMA – time-division multiple access. These are schemes for some of the 2G standards. They are in effect TDMA- FDMA, as they do allocate frequency channels, and time slots within them, and have similar frequency reuse plans. Thus, in the IS 136 the frequency allocation ("channel" or "carrier") is 30 KHz, reuse is 7/3 and time slot is 6.7 ms (3 slots per channel), while in the GSM the frequency allocation is 200 KHz, typical reuse is 4/3 and the time slot is 0.577 ms (8 slots per channel). Common application for cost reduction purposes is the *band repeater.* Remote control by switching in and out time slots of each channel in a *channelized TDMA repeater* is possible, and allows for network coverage control and load balancing. Installation of coverage extension repeaters requires a review of the frequency plan of the network.

CDMA – code-division multiple access. Both IS 95/CDMA2000 and UMTS WCDMA are *CDMA* standards. All users' links share the same FA (channel), which is 1.25 MHz for IS 95 and CDMA2000, and 5 MHz for UMTS. Incorporation of repeaters in the CDMA network does not require large scale replanning as with narrow band systems, but local parameter tuning. CDMA repeaters do not have the optional control on individual links, as in TDMA. Only channel or band filtering are available to this technology. The CDMA repeater is a transparent bidirectional amplifier serving users in a coverage area with the same pilot code (PN offset) as the donor sector. The users served in this area interact with the donor BTS in the same way as those connected directly to the donor, namely – they receive and respond to the same power control, access protocol and soft handoff.

1.2.4 Repeater Classification by their Backhaul Conduit

The type of conduits employed for cellular repeaters are:

- ✓ On-Frequency (F1/F1) Repeaters (OFR).
  - o F1/F1 free-space transmission. Do not require a dedicated backhaul conduit.
  - o RF cable transmission (typical for short-range, indoor distribution).
- ✓ Frequency Shifted Repeaters (FSR, or F1/F2). Require a dedicated conduit.
- ✓ In-band frequency shifted free-space transmission.
- ✓ Out-of-band frequency shifted free-space transmission.
- ✓ Microwave transmission.
- ✓ RF cable transmission (typical for short range, indoor distribution).
- ✓ Optical conduit.
- ✓ Fiber Optics transmission.
- ✓ Free-Space Optics (FSO) transmission.

On-frequency RF repeaters. The repeater draws the signal from the donor BTS antenna and transmits to the donor BTS antenna, like any other user in that coverage area. It typically employs a directive backhaul antenna in the direction of the donor, located at a convenient height, to get a gain advantage. The link between the donor BTS and the repeater operates at the service channels. The repeater amplifies the band allocated for the repeater coverage, which is the full band allocated to the donor sector, or a fraction thereof. Most repeaters, designed for coverage extension, relay between one to three CDMA channels. The repeater can have a band filter (*band repeater*) or multiple channel filters (*channelized repeater*). The latter is structured as a *heterodyne repeater*, where the signal is down converted to an IF level, where channel filtering takes place, and up converted for retransmission. *Channelized repeaters* can be tunable to remotely or preset select the desired channels for relaying to the repeater coverage. The repeater coverage may incorporate a single lobe or multi-lobe (typically 2 or 3 lobes), materialized by a single or separate amplifiers and antennas, that may operate with different amplifiers' and antennas' gain. All lobes share the same pilot. Further, a multi-hop chain, where each repeater feeds from the antenna of the previous one in the succession, is used to cover long stretches of roads (Fig. 1-8).

A major challenge with *on-frequency RF repeaters* is their proper installation and commissioning. Isolation higher than the gain through the repeater by over 15 dB, antenna to antenna, has to be maintained to avoid noise build up and repeater oscillation that result in a distorted output and corrupted communications. This is true separately for the FL and for the RL.

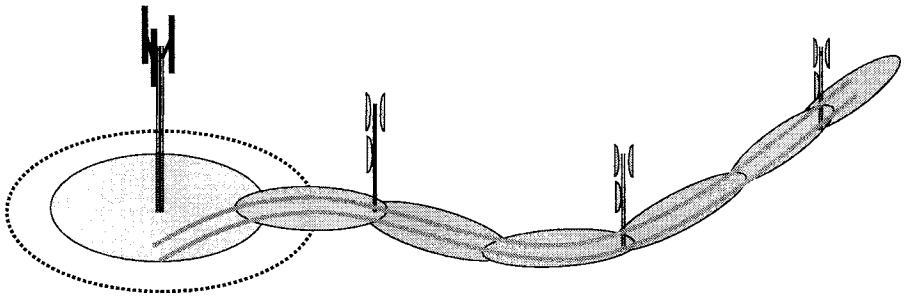

Figure 1-8. A multi-hop chain of on-frequency or FSR. *Each repeater consists of two lobes for coverage of a road*

This affects the installation on the tower – the backhaul antenna has to be isolated from the service antenna by an appreciable physical separation, which limits the applicable gain of the on-frequency repeater. The required physical separation for achieving the same isolation is larger for lower frequencies; it is larger at the 850 MHz band than in the 1900 MHz band. A common practice for maximal achievable gain of OFR is 90 dB. This sets a limit to the distance that OFR can be remote from donor BTS, to allow for a strong enough donor signal.

Frequency shifted repeater (FSR, or F1/F2). These are heterodyne repeaters for the frequency shift. The donor BTS RF signals are sampled with directional couplers and converted into a different frequency. This "F_2" frequency becomes the backhaul frequency.

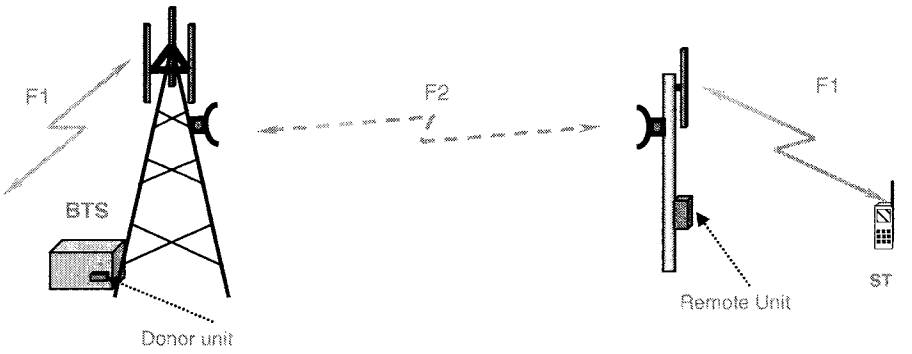

Figure 1-9. Frequency shifted repeater. *F2 may be in-band, out-of-band, or microwave*

In-band FSR. The backhaul frequency is allocated in an unused FA within the same band as that of the donor BTS, e.g. PCS – PCS, etc. Here the operator utilizes part of the spectrum for the link. In cases of rural or highway coverage, the operators use only a small part of their allocated spectrum. In such cases, it is beneficial to spend a part of the "unused spectrum" for the backhaul channels.

There must be some guard band between the service sub-band and the link sub-band, to allow for proper attenuation roll-off of the filters handling the backhaul and service signals. Typical achievable performance is operation at isolation levels of 20 dB below the set gain, or at least 70 dB. With special means and sufficient guard band, it is possible to achieve high gain (~110 dB) at only 55 db isolation.

Out-of-band FSR. In case the operator possesses a license to both 850 MHz and 1900 MHz bands, it would be advantageous to use the band that is different from the service band as the backhaul frequency. There is no sacrifice of guard band in this case, and the ultimate rejection of the filtering is achieved with better overall performance than with the in-band FSR. Typical isolation limits for this case are 55 dB.

Microwave repeater. The conduit is microwave (analog) point-to-point (PTP) transmission in the microwave PTP allocated bands (e.g. 2.6 GHz, 7 GHz, 15 GHz, 18 GHz). The higher microwave frequencies offer smaller size antennas or higher gain, and better ground clearance against fading, but higher rain attenuation. The microwave transmission conduit can transmit the FL and RL, and multiple links, by IF multiplexing in a single beam. The bandwidth obtainable at microwave transmission is higher than in the cellular operating bands. Thus it is possible to extend a multi-carrier full BTS (3-sectors) in 7 MHz or 14 MHz bandwidth in a cost-effective way.

Optical fiber Repeater (OR). The branched RF signals at the BTS are transformed to modulating the fiber optics, and are reconverted at the remote unit to RF. FL and RL can be multiplexed by wavelength-division multiplexing (WDM). Multiple links (e.g. diversity channels) can be similarly multiplexed or IF multiplexed in a single fiber.

Free-Space Optics (FSO) repeater. The RF is modulated on a laser transmission in free space between the BTS and the repeater location. FL and RF, and multiple links can be multiplexed by IF multiplexing in a single beam. FSO requires a clear line of sight, which limits its usability to fair weather and limited distances.

1.2.5 Repeater Classification by Application

Repeaters are low-cost coverage agents in the cellular network, and are candidates to replace BTSs in coverage-limited and shadowed areas for cost saving. The main applications of repeaters are:

Coverage extension. Enlargement of the cell coverage area. This applies where the cell coverage is limited by topography, or in cases where distributed repeaters is cost-saving vs. a high tower – high-power BTS. These solutions may have single or multi-lobe coverage, depending on the shape of the area that requires coverage, and may be designed to cover an area or a stretch of road, in which case a multi-hop chain is applicable.

Remote coverage. Allocation of capacity resources to a remote coverage area, not necessarily overlapping the donor cell area. A full 3 sector remote coverage repeater draws capacity from 3 sector donors in the donor cell. Typically one to three FAs are allocated for the remote service.

Hole-filler. These are repeaters installed so as to cover a shadowed area within the coverage area of the donor cell. They are designed for limited coverage, not to overly overlap with the main coverage area. The repeater relays the full band of the donor to maintain coverage continuity for all users in the donor cell.

Indoor repeaters. The indoors environment is compartmental, isolated from spaces and between floors, while the propagation within each is mostly line of sight. Low power repeaters, loosely coupled to the donor cell, serve the indoors. Multiple repeaters are cascaded in a multi-hop or parallel, typically by an RF cable or fiber.

Hot spot repeaters. These are used to cover a limited area where a dense activity takes place within a larger donor coverage area. The purpose of the hot spot repeater is to reduce the link loss, both in RL and in FL, and thus allow the donor cell to serve both a large area that is not densely populated by its main antenna, and the "hot spot" - by the repeater. These are typically low power repeaters.

1.3 Repeaters in the CDMA Cellular Network

1.3.1 Repeater Interaction with the Network, and Tuning

The repeater in the CDMA network is a bidirectional linear amplifier that transparently amplifies and relays both FL and RL. Within that, it relays the pilot signals, the traffic signals pertaining to all the users in the donor service (and not only those in the repeater coverage), and the power control commands in the FL, and traffic and signals/ report messages in the RL. Pilot search windows have to be adjusted to accommodate the additional delay to

the repeater coverage. This allows users to access the donor from the repeater coverage and move smoothly between the repeater and the donor coverage. Repeaters bordering other cells act as agents for their donor and exercise the soft handoff between the donor pilot code domain and the other cell domain.

The key parameters involved in the interaction of the repeater and the CDMA networks are its gain in both directions G_{RF}, G_{RR}, the transmission gain between the repeater backhaul antenna port and the BTS antenna port (or any other conduit connecting them) T_D, the repeater noise factors in the reverse and in the forward links, F_{RR}, F_{RF} and the repeater power limit in the FL. The net gain $y=G_R T_D$ of the repeater is a product of the transmission gain between the donor to the repeater - T_D, and the repeater gain G_R. The apparent noise factor of the repeater at the BTS input $\hat{F} \equiv G_{RR} T_D F_{RR}/F_{BTS} = y F_{RR}/F_{BTS}$ contributes to the *noise rise* in the BTS. This decreases the donor plus repeater capacity if the donor has an a priori set limit to the noise rise, but a strategy that allows for higher noise rise limit can maintain the capacity on behalf of the donor coverage loss. This is the main trade-off in optimizing the repeater service to its designed application.

Balance of the FL and RL gain in the repeater is required for maintaining the link balance in the coverage area. A change in the FL gain changes the pilot level in the repeater area, while the traffic level is controlled by end-to-end power control, so that the ratio between the pilot level and that of the traffic changes, impairing the link balance.

1.3.2 Impact of Repeaters on the CDMA Network

A CDMA network employing integrated remote radio access techniques can generally achieve improved coverage performance in terms of range extension, radio hole coverage, and link and load control.

Reduced link loss. This serves to *reduce the power transmitted from the BTS* to the users at the repeater coverage, thus freeing power to serve more users and increase FL capacity; to *require lower power from the repeater* than from the BTS (use lower-cost repeaters); to reduce the *Subscriber Terminal (ST) transmit power*, and to *reduce the overall power transmission* in a distributed coverage. The user in the coverage area of the repeater has higher transmission gain T_R to the repeater access than to the donor BTS - T_C. The overall transmission gain between the donor and the user is $T = T_D G_R T_R = y T_R$. The link gain advantage to the donor when relaying through the repeater is $T/T_C = y T_R/T_C$. It can be attributed in full to the repeater, when $y = T_D G_R = 1$, in which case the required repeater power is lower than that required from the donor to reach the same coverage area by the ratio $P_{repeater}/P_{BTS} = T_C/T_R$. Alternatively, the advantage can be shared with the donor BTS by setting $y<1$,

and used to also reduce the BTS power allocated to these users, which releases BTS power to serve more users and increase its capacity – if the donor is FL limited. The link advantage is exhibited in Fig. 1-10, where a repeater positioned at 3/4 of the cell range, to cover to the cell border, needs 24 dB lower transmission power than the donor BTS (if γ=1)[1].

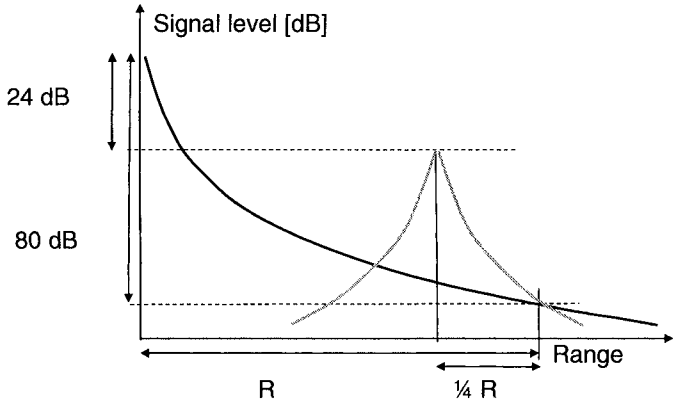

Figure 1-10. Power level vs. coverage range. *Transmit power for 1/4 the cell range is 24 dB lower*

The whole cell coverage area can be covered by 16 such repeaters, altogether transmitting -24+12=-12 dB lower power than that required from the single BTS antenna.

1.3.2.1 *Reduced link loss variations.* The variations of propagation loss within the coverage area, due to topography or obstructions, create shadowed areas. Serving these areas requires a substantial power boost that is costly and sometimes not practical, and that interferes with neighboring cells. These shadowed areas can be covered by repeaters.

1.3.2.2 *Link balancing.* The forward and reverse links in each cell are not automatically balanced in the CDMA system, and are set by tuning the pilot power according to the expected configuration and activity of the cell and its neighborhood. When this set status is changed ("cell breathing") the balance is impaired. A change of pilot power setting in a cell affects all its neighbors. When a more local tuning is needed it can be affected by changing the FL gain of a repeater covering that area. This affects the pilot level in the repeater coverage, while the level of the FL traffic is corrected by the FL power control (setting of the digital gain).

[1] The propagation loss exponent is assumed here to be γ=4.

1.3.2.3 *Load control.* The load throughout the network is rarely uniform, and changes in time. Repeaters placed remotely from their donor into other areas serve in shifting loads from one cell to another, remote, cell. This is controllable by changing the repeater gain.

In conclusion, the application of remote radio access nodes to a cellular CDMA network adds a powerful means for its enhancement. Both coverage and capacity can be much improved, with additional benefits to network quality (less access failures, less dropped calls, less blocking, indoor penetration, less interference) as well as to the mobile users (less transmitted power, longer battery life). To be successful, care must be exerted in correct planning, set-up and parameter tuning of the remote access units as well as the base stations involved.

1.4 Cost Considerations

The cost of remote radio access equipment must be a fraction of the BTS cost to justify its massive deployment. The cost saving of incorporating repeaters in the network depends on the application. These are briefly highlighted here. For a more detailed review of repeater economics see Chapter 9. A simple cost criterion is the number of boxes in the repeater system. Transmit power is another differentiator, and then special control and monitoring functions, to name a few, have major effects on cost. A classification of solutions by application in Table 1-1 helps in dimensioning their cost.

Table1-1. Classification of remote extension solutions

Application	Repeater Type	Backhaul	Coverage	Remote Unit Gain	Units
Urban, Sub-Urban	OFR	1-4 km	1-4 km	< 90 dB	1 –2
Sub-Urban, Rural, Highway	In-Band FSR	4-17 km	4-10 km	< 110 dB	2 – 3
Rural, Highway	Out-of-Band FSR	4-17 km	10-18 km	< 120 dB	2 – 3
Sub-Urban, Rural, Highway	Optical Fiber	5-20 km	5-20 km	< 60 dB	2 - 4
Highway	2-Lobe FSR	4-15 km	2x16 km	< 115 dB	3

1.5 Theme of the Book

"Things should be made as simple as possible, but not any simpler."

Albert Einstein

1.5.1 The Complexity of the Multiple Access Mobile Communications Channel

Every mobile wireless communications system comprises a *structured element*, consisting of the hardware and software encapsulated in the transmit and receive ends of the link, and the processing and control thereof, and an *unstructured element* – the propagation medium. The latter is too complex to be well-defined, and is dynamically time varying. A multiple access mobile communications system, as every cellular system is, has yet another layer of complexity and uncertainty relating to the subscribers' locations, motion and activity. While the first element is well-defined, is predictable and can be well simulated, the interaction of the communication system with the subscriber population through the propagation environment is by far too complex to accurately predict, design or simulate. The explosive growth of the cellular service during the last two decades repeatedly encounters a gap between the impressive evolution of technology through the generations and the large scale field performance, being short of the predicted service expectations time after time and needing a long series of field-derived optimizations to reach satisfaction.

This book strives to fill this void and provide the RF network engineers with the knowledge and insight into the radio interaction processes, and particularly in the CDMA cellular network. Inasmuch as the complexity is acknowledged, attention is set on the underlying physical and system rules of this complexity that portrays a structured characterization clattered by overlaying complexity. These underlying, relatively simple models, provide a comprehensive insight into the parametric behavior of the mobile communications system, while – at the same time, the characterization of the complexity clutter is left to statistical models riding over the structured models. Operational network probing and measurements serve to tighten the uncertainty of the statistical part and to calibrate the structured models.

1.5.2 Propagation Modeling

The cellular communications is served by terrestrial propagation between BTS antennas, preferably above the surrounding clutter, and STs that are mostly embedded within the clutter. The propagation process and modeling is

covered in Chapter 3. It can be classified into the energy transfer mechanism, also termed as path-loss, and the fast variations (fading) resulting from wave interference between reflected and scattered multipath. The former is important in terms of the local area and time average of the signal level, while the latter relates to the signal detectability by specific system. Propagation channel modeling for description of these phenomena may have two different objectives:

- ✓ Models aimed at characterization of the propagation along a path. These are conceived to match field measurements, and are used in network planning and optimization. These are of interest in this book.
- ✓ Models aimed at serving as a reference in testing the performance of the system equipment. These may bear similar statistics, time variations and dynamic range, but not necessarily the spatial relation to the environment. These are not considered here.

The path-loss is formulated in terms of basic wave propagation processes – in free space, at grazing ground reflection, over the forest canopy, grazing a layer of roofs, etc., and interaction between them that creates the complexity. While site-specific analysis may require detailed knowledge of the topography and structures overlay, the bulk radial propagation from the antenna has been characterized by various curve-fitting measurement-based models to radial regression exponents between 2 and above 4. These are well justified by the simple models of the free space (LOS) model of R^{-2} and the grazing propagation R^{-4} adopted throughout the book for describing cell-size propagation and explaining coverage areas and interaction between cells.

The scattering and reflecting environment that dominates the cellular service and is responsible for the multipath phenomena – is typified by inter-reflector distances that are much shorter than the coherent distance for the narrow band cellular systems of the first and part of the second generation. The multipath is thus coherently added at the receiver as flat fading adequately described by Rayleigh statistics, but with no insight into local processes. The CDMA waveform is broadband enough to time-wise resolve reflections, which serves to reduce the fade margin and the delay-diversity process. These processes are location dependent and have a structured description in terms of rays, while the fluctuation statistics serve to characterize the short distance multipath interaction of the transmitter or receiver with its close neighborhood. By using this approach the book develops system-related functions, e.g. orthogonality factor, delay-diversity, and their relations to the physical nature of the environment.

1.5.3 System Modeling

The CDMA system is extremely complex. However, it is conceived for simple interactions with the propagation channel within the multiple access, multiple BTSs environment, and its complexity serves to generate and exploit multiple diversity means and dynamic responses to mitigate, or at least tame, channel variations and teletraffic activity fluctuations [2]. Its spectrum spreading decorrelates delayed multipath, reduces the fading depth and allows for utilizing the diversity gain of the uncorrelated multipath in the "rake receiver". The random spreading code spreads and averages the interference sources, including other users, to become (almost) Gaussian white noise, against which the system is measured and self-adjusts. The combination of the power control and the soft handoff minimizes the interference within and between cells. The combination of these attributes forges each cell as a dynamic, "living" entity, operating as a group within the environment of other cells, and relieves the analysis from probing each user. The underlying rules stated above are simple and allow for simple monitoring, analysis, control and optimization.

The approach adopted in this book is to employ these system rules, together with the basic propagation rules, in analyzing their interaction.

1.5.4 Theme of the Book

Repeaters constitute an interactive part within the cellular CDMA network. Effective deployment of the repeaters, and optimization of a repeater-embedded network requires an intimate understanding of the CDMA air interface and its interaction with the propagation environment. The purpose of this book is to enrich the radio engineer with the understanding of the interaction between the CDMA network dynamics and its embedded repeaters, and the propagation channel, and offer engineers the insight into the processes and trends.

The book is aimed to be a *guide book*. It does not encompass all design details and procedures to be a handbook, nor is it meant to be. The gap it is designed to fill is the understanding of the interrelating processes within the CDMA system in the field, and with its embedded repeaters. Understanding these processes and trends offers guidance to the optimal solution – be it during network planning, routine troubleshooting, upgrading or optimizing.

1.6 Organization of the Book

The book is structured to be comprehensive and self-consistent in its approach:

Chapter One reviews the underlying network issues, needs for distributed radio access and repeaters and their role in the deployment, operation and optimization.

Chapter Two provides the features and functions of the CDMA standards that are relevant to the radio air interface.

Chapter Three is the mobile radio propagation chapter. It provides the physical basis for propagation modeling and interaction used throughout the book. Energy transfer canonical models ("path-loss") are derived for propagation over the terrain, over forests and groups of buildings, and through diffraction and reflection. The scattering mechanism is modeled to derive the multipath interference effects. Characteristics of antennas for the cellular service are then reviewed, including their applications in coverage control and for diversity transmission.

Chapter Four discusses the radio access related performance of the CDMA cellular network. The structure of the forward and reverse links is reviewed and their dependence on user distribution and activity, and the nature of the channel. The impact of orthogonality and multipath diversity on coverage and capacity is modeled and calculated. Link balancing, cell boundary and its "breathing", and their control are similarly modeled and parametrically evaluated, including microcells. Optimization techniques are then discussed.

Chapter Five treats radio-related diversity processes in the CDMA network. The multipath diversity is modeled and integrated to the link performance. Space, polarization and angle diversity techniques are reviewed. RF transmit diversity is analyzed, and time-delay (TDTD) and phase-sweep (PSTD) transmit diversity characteristics throughout the coverage are modeled and shown to be complementary. Add-on techniques for transmit diversity, applicable to base stations and to repeaters, are treated.

Chapter Six is a key chapter on the interaction of the repeaters with the CDMA radio access network. Both forward link (FL) and reverse link (RL) interaction are modeled in a way that reflects their impact on the donor and adjacent cells. Coverage and capacity trade-off is evaluated and optimized for different scenarios, from hole-filling, hot spot coverage to range extension and base station replacement, including multi-hop repeater chains. The impact of transmit and receive diversity application on repeaters is treated.

Chapter Seven analyzes the structure and performance of repeaters in detail. The amplification chain is reviewed, and balance between staged gain and noise and nonlinear effects is analyzed. Filtering parameters are discussed. Features relating to the different relay conduits (e.g. over-the-air, microwave, fiber, etc.) are treated. Set-up, tuning and control parameters are provided.

Chapter Eight discusses RF backhaul relay methods to distributed radio access and repeaters. Over-the-air in-band and frequency shift, microwave relay, fiber optics and free-space optics (FSO) are analyzed parametrically and compared. Design and tuning guidelines are provided.

Chapter Nine models the cost of repeater-embedded network. A model for large scale "Greenfield" deployment trades-off the cost constituents and the impact of the cost of the repeater vs. base station cost – on the size of each cell and the overall cost. Another model handles the "small scale" introduction of repeaters to an already existing network, for filling holes, extending coverage and covering "hot spots".

Chapter Ten reviews advances in repeaters, including antenna (tilt) control, receive and transmit diversity, link stability control, interference cancellation, monitoring performance and traffic, and projects the role of repeaters in high data rate and next generation of cellular.

REFERENCES

[1] G.I. Zysman, J.A. Tarallo, R.E. Howard, J. Friedenfelds, R.A. Valenzuela, and P.M. Mankiewich, *Technology Evolution for Mobile and Personal Communications*, Bell Labs Technical Journal, Jan-March 2000.

[2] A.J. Viterbi, *CDMA*, Addison-Wesley, 1995.

2

CDMA AIR INTERFACE OVERVIEW

2.1 Cellular Wireless Communications

Objectives - The cellular wireless communications emerged as an answer to a need for a fully mobile telephone service. The service objectives are *mobility*, *full duplex voice*, *ubiquity* – service everywhere and all the time, and *capacity* - multiple independent sessions within the same area. *Grade of service* (GoS) is measured by the availability of call access and uninterrupted session continuation, and *quality of service* (QoS) – by the quality of the voice, where comparison is made to the voice quality of the line telephone.

Architecture - The cellular wireless is composed of multiple *star networks*, each covering a limited area ("cell") where communication is conducted between users within that area and the hub ("base station"). The latter administers the sessions ("calls") and interconnects calls to users in other cells or in the wired telephone system via backhaul conduits and switching centers. The part of the base station incorporating the transmission is called *BTS – Base Transceiver Substation.* The *BSC, Base Station Controller*, handles the call administration. One BSC may control several BSCs.

Deployment - The coverage area of each cell is measured by the sufficiency of the link budget between the base station and the user, and its dominance over interference from other users in the same cell and in other cells. The process of detaching the link from one base station and establishing the link with another ("handoff") when a user moves from the coverage of one cell to another is automatic and transparent to the ongoing call.

Spectral band and efficiency - The wireless cellular architecture was conceived over 50 years ago but its first commercial deployment took place in the early 80s, with the availability of the enabling technologies. Relevant frequency range for this service, aiming at Non Line Of Sight (NLOS) coverage, but at the same time limited range to allow for reuse of the same frequency band in adjacent cells, ranges from decimeter wavelength (450 to 1000 MHz) for open areas, to centimeter wavelength (1000 to 2500 MHz) for

urban and indoors environments. Regulatory limitations on the frequency bandwidth allocated to the service, mainly based on priority allocation to other services (TV, military), has been a major challenge in the evolution of the wireless cellular technology. Spectral efficiency is a key parameter in the economy and scope of the service.

Duplex - FDD (Frequency-division duplex) is used in the cellular systems: transmissions from the base station to the user (*forward link* – FL, or *down link*) are separated from those from the user to the base station (*reverse link* – RL, or *uplink*) by a preassigned gap (45 MHz in the 850 MHz bands and the 900 MHz bands, 80 MHz in the 1800 and 1900 MHz bands, 90 MHz in Korean bands).

Multiple access - The first generation was based on analog modulation and filtering FDMA (Frequency-division multiple access) whereby calls in each cell were separated by frequency allocations of channels – 30 KHz in the US system AMPS. A guard zone is required beyond the coverage to avoid interference to other cells, which leads to reuse of the same channels only once in every 12 cells. The split of the circular (omnidirectional) cell to 3 directional sectors, by use of directional antennas, increases the isolation between cells thus achieving a reuse of 1/7.

The second generation, introduced in the early 90s, leverages on digital modulation and processing to increase the spectral efficiency and introduce new data services. The US TDMA (Time-division multiple Access) triples the capacity by time multiplexing 3 calls in each channel. It is an evolutionary standard into the same 30 KHz allocations. GSM, which has been allocated a virgin frequency band in Europe, opts for 8 time slots in a channel of 200 KHz, with respective reuse of 1/4. Frequency hopping techniques further increase the reuse.

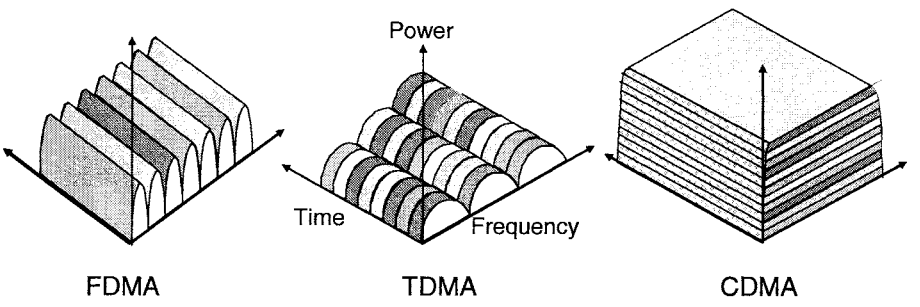

Figure 2-1. Multiple access schemes

CDMA (Code-division multiple access) was first proposed to the cellular service in 1989, and commercially introduced in the mid 90s. The system utilizes direct sequence spread spectrum technology to differentiate the user's channels by codes rather than by frequency filtering and time gating, thereby allowing for multiple access on the same channel throughout the network, with a reuse of 1. The channel bandwidth 1.25 MHz was chosen for multiple reasons: a) taking an evolutional strategy into the AMPS frequency allocation in the US, where 1.25 MHz captures 10% of the band allocated to each operator while doubling its capacity; b) technology maturity of digitizers and processors; and c) optimizing the time resolution (and then the number of delay-searching correlators – "fingers") to the main clusters of delayed multipath observed in the outdoors environment [1].

The ITU program IMT2000 standardized the third generation (3G). These are geared for a variety of mobile data services, including interactive multimedia and high data rate, in addition to voice. Two major standards emerged: UMTS (WCDMA) is a 4.5 MHz per channel CDMA, and CDMA2000 (1x and 1x-EV) – a 1.25 MHz per channel CDMA. In addition, two short-range TDD (Time-division duplex) standards have been approved: UTRA TDD and TD-SCDMA. The diversified requirements entail introduction of new techniques and resource management schemes: packet switching, scheduling, code and time multiplexing. The two standards' paths evolved around different perceptions of the transmission efficiency of the aggregate of services: CDMA2000 opted for dedicating a full channel for data optimized communications, which materialized as 1xEV-DO, separate from voice and low latency multimedia services in CDMA2000, while UMTS turned to combine all services in the 4.5 MHz channel.

2.2 CDMA IS 95 Air Interface Overview

2.2.1 System Concept

Spread Spectrum is a technology whereby the signal transmission is spread over a broad band. The spreading scheme is known only to authorized users, while for unauthorized ones the signal is embedded in noise and undetectable. This technology found wide usage in the defense applications as a Low Probability of Intercept (LPI) communications and anti-jamming method. This technology is applied to cellular communications in IS 95. The spectrum is spread by modulating the carrier by BPSK (QPSK in later versions) in the FL, and OQPSK in the RL, at a rate of 1.2288 MHz. The modulating sequence has a periodicity of 2^{41}-1 (the *long code*). The correlator integrates over 128 "chips", 0.8μs each, to form a signal bit at a rate of 9600

bps, thus achieving a processing gain of 21 dB to the desired signal over uncorrelated signals.

Reverse link – random code and power control. The long code is used on the reverse link to provide the link to the individual user. The transmission of other users is not coherently integrated by the per-user correlator in the BTS receiver, and appears as noise, well randomized by the long code. Same cell users and other cells' users are thus interfering to the desired signal. A power control scheme controls the transmission power of all in-cell users to be received at the BTS receiver with the same power level. Each user then contributes noise that is 21 dB lower than the desired signal. The contribution of all users piles up. Capacity limit is reached when the aggregate interference reaches the limit set by the modem detectability, *Eb/It* (energy per bit over the spectral density of noise plus interference). About 2/3 of the interference is generated by in-cell users; the rest comes from users in adjacent cells. The interference from the latter is bound by the Soft Handoff (SHO) process that applies the power control to users in the adjacent cells whose transmission exceeds the set threshold.

Forward link – the signal is spread by direct sequence spreading over the same bandwidth as the reverse link. The code structure is however different. The transmission from the BTS is one-to-many. Signal transmission to all users is synchronized, and each is identified by an orthogonal code. 64 length Walsh code is used, allowing for 55 to 61 user codes, and 1 to 7 paging codes, one synchronization code and one pilot code. A short spreading sequence of 2^{15} (the *short code*) multiplies the BTS transmission and identifies the BTS. The orthogonality of the Walsh codes eliminates any interference from other in-cell users, except for delayed multipath which adds noise. The *channel orthogonality factor*, indicating the fraction of the BTS transmission that is fully synchronized, is a channel quality measure for each user link. Interference from adjacent BTSs is significant only toward the cell edge.

Channel code and diversity – the modem threshold *Eb/It* (equivalent to *C/I* in analog systems), which sets the limit to the capacity, depends on the nature of the interference. *Error-correction codes* are applied to enhance detectability and reduce the required *Eb/It* . These codes add bits to the signal stream, that help in identifying the signal out of the interference by seeking an order in the signal corrupted by random noise. The powerful codes that are applied in the system are *convolutional codes*, which avoid excess delay in the decoding. This is an important factor in the service of full duplex voice, that allows for a delay not exceeding 40 ms. The spreading and transmission bandwidth (1.25 MHz) is larger than the coherent bandwidth of the propagation channel in open environments, thereby suppressing fading by its frequency diversity. The *rake receiver* incorporates a number of correlators ("fingers") that search for delayed replicas of the signal and optimally

combines them. Further suppression of fading in more densely packed environments - dense urban and indoors where the coherent bandwidth exceeds the system bandwidth, is provided by the fast *power control*, which compensates for the missing power through deep fades. This is effective for slow moving users, commensurate with the power control response time. Faster fading is mitigated by the *coder-interleaver*, that spreads the transmitted signal bits over a period of 20 ms such that errors are randomized over the code symbols to enable error correction. The bits are then reordered by the *deinterleaver-decoder* at the receiver. Antenna diversity is also applied at the BTS receiver, space or polarization diversity. Transmit diversity option is built into the CDMA2000 standard. However, add-on transmit diversity is an option for IS 95 also.

The IS 95 air interface is summarized in Fig. 2-2. 9600 bps data (block a) is coming out of the vocoder, encoded, interleaved and then spread and upconverted, and transmitted as a 1.23 MHz spread signal (block b). This is picked up at the receiver, along with its self-thermal noise (block e), other narrow band interference (block f), other users' transmissions in the cell (block g) and those of users in adjacent cells (block h). The rake receiver, comprised of down-converter, A/D, despreading correlators and deinterleaver-decoder, despreads the desired signal from the input (block c) while spreading the narrow band interference (block d).

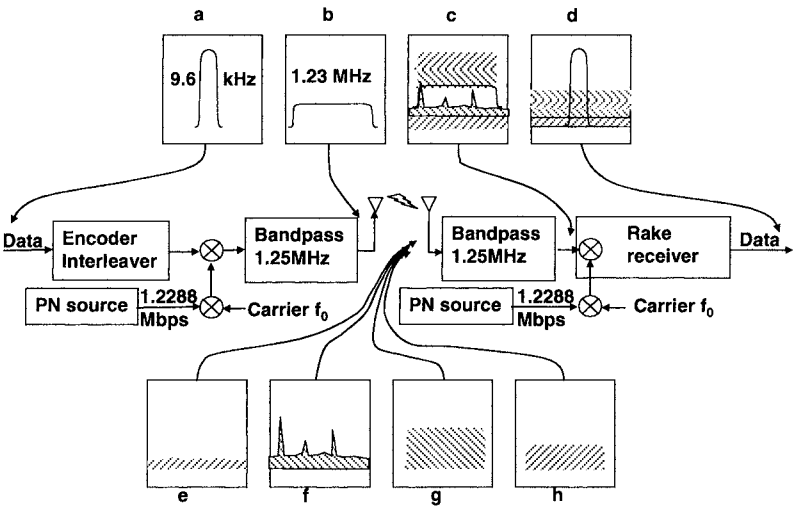

Figure 2-2. The IS 95 air interface concept

2.2.2 Logical and Physical Channels

2.2.2.1 Reverse Link

The reverse link of IS 95 has two logical transmit channels: *Reverse Traffic Channel* (RTCh) and *Reverse Access Channel* (RACh). RACh is used by the ST to establish a call or to respond to the system. RTCh is used only during a call, after the access has been established. Both are organized into 20 ms frames.

Reverse Traffic Channel has a variable data rate. RS1 (Rate Set 1) may use 1200, 2400, 4800 or 9600 bps data rate. RS2 may use 1800, 3600, 7200, or 14,400 bps data rate. These are built for use with a variable rate vocoder that automatically chooses the rate according to voice quality measures. The RS2 configuration employs a 1/2 rate convolutional encoder, while RS1 – a 1/3 rate encoder. The weaker protection for RS2 results in a higher *Eb/It* threshold and lower capacity than that of the RS1 configuration.

The ST transmission saves power in lower data rates by transmitting in bursts. The 20 ms frame is divided into 16 *power control groups* (PCG), 1.25 ms each. Full rate (9600 or 14400 respectively) transmission is continuous. 8 PCGs are masked out in half rate, 12 – in 1/4 rate and 14 in 1/8 rate. The masks are randomized within each frame.

Voice and data can be multiplexed on the same traffic channel. *Blank and burst* blanks out a full voice frame for data transmission. *Dim and burst* uses the blanked PCGs, this time in a continuous group in each frame, for data or signaling transmission.

Reverse access channels – are used by the ST when initiating a call, when performing an autonomous registration, and when responding to a paging message while being in an *idle state*. *Access probe* is a short transmission burst, timed randomly in order to avoid collision with *access probes* of other STs using the same RACh. An *access probe sequence* consists of a sequence of *access probes*, their transmission power increasing sequentially. A max of 16 access probes is transmitted in a sequence, and a max of 15 sequences can be transmitted.

The reverse link is Walsh code modulated, spread by the long code and then modulated OQPSK (Offset QPSK). The Q channel is offset by half a chip in order to smooth the transmission envelope and to allow higher efficiency ST amplifier operation.

2.2.2.2 Forward Link

The forward link of IS 95 has four types of channels: *Forward Pilot Channel* (FPiCh), *Forward Sync Channel* (FSyncCh), *Forward Paging Channel* (FPCh) (up to 7 channels) and *Forward Traffic Channel* (FTCh) (55 to 61 channels). Each channel is multiplexed and spread by Walsh codes. The

pilot channel is designated W_0 (Walsh code 0), the Sync – W_{32}, and the paging channels W_1 to W_7. The traffic channels are randomly designated. Each channel is then individually amplified. The channel gains are determined by transmission considerations, including the pilot power allocation and the power control to the traffic channels. Once amplified, each channel is split to quadrature (I and Q) channels, and each arm is PN modulated by a *short code, common to all channels in the same sector.* All channels are then added up voltage wise, to form the base-band mask, which is shaped by a digital filter for minimum spectral spill off, upconverted and QPSK modulated for transmission. The information in the I and Q channels is the same, and the efficiency is that of BPSK. The quadrature modulation is applied in order to smooth the transmission envelope.

Half rate convolutional encoders are used in the FSyncCh, FPCh and FTCh. The transmissions are organized in 20 ms frames.

Pilot channel is a PN modulated carrier. It is always spread by Walsh code W_0, and then by a unique PN offset code that identifies the cell/ sector. The pilot is a reference time signal that allows the ST to acquire the system, provides phase reference for coherent detection, and provides the ST with signal strength measurement for *Soft Handoff* (SHO) window gates. The pilot strength is a network tuning parameter. All BTSs are time-synchronized, aided by GPS. The codes of the pilots throughout the system are identical short code, with different PN offset (delay) that is used for identification.

Forward synchronization channel transmits synchronization information to the STs at the *initialization state* to allow them to synchronize the codes they generate to the network. FSyncCh is transmitted at a 1/8 rate (1200 and 1800 in RS1, RS2, respectively) organized in an 80 ms super-frame.

Forward paging channels transmit system parameter information specific messages to STs paged. There is at least one, and max 7, PChs per sector. The transmission rate is 1/2 or full rate, organized in an 80 ms super-frame. The choice is communicated in the FSyncCh. STs are uniformly distributed among the FPChs by a hashing algorithm.

Forward traffic channels have a variable data rate: 1/8, 1/4, 1/2 and full rate – 9600 and 14,400 for RS1 and RS2 respectively. The output of the variable rate vocoder is fed to a half-rate convolutional encoder, followed by bit repetition for the lower voice rates to keep a constant bit rate transmission.

Power Control Subchannel (PCSCh) performs power control over the reverse link. It consists of one bit per control period. The 20 ms frame is composed of 16 *Power Control Groups* (PCG), 1.25 ms each. Within that period the BTS estimates the signal level received from each ST on the RTCh. A power control command bit is transmitted two PCGs later (2.5 ms later), consisting of a single bit. It is transmitted by puncturing the coded

traffic symbol, and replaces two consecutive bits in the FTCh. The location of the power control bit within the PCG is randomized.

2.2.3 Power Control

2.2.3.1 Reverse Link Power Control

The capacity of the CDMA cellular system is interference limited by transmissions of other users in the cell and others in adjacent cells. The transmission power of each ST is controlled to minimize this interference and maximize the capacity. The control parameter is the error rate in the link, measured per frame in the CDMA system (FER – *Frame Error Rate*) that has to be kept under a level commensurate with the service. The allowed FER for voice is 1%. The FER is mostly influenced by the received E_b/I_t, which depends on the level of transmitted power. The power control system thus consists of 3 layers: *open loop power control*, where the ST estimates its transmission power level based on measurement of total received power and preacquired BTS parameters, *closed loop power control* that corrects the ST estimates by measurements of the received signal at the BTS, and *outer loop power control* that adjusts the ST power to suit the required FER.

Open loop power control is an autonomous operation of the ST. It operates during the access phase, when acquiring the connection to the network, and while in the traffic state. The ST estimates the transmission gain to the BTS by measurement of the average total power received (S_{Tm}), which does not require any prior knowledge of timing and BTS ID. The transmit power P_{RACh} is then computed from S_{Tm} and BTS transmitted parameters including *Power Offset-K*. This parameter is obtained by equating the reverse link to the forward link

$$K \equiv \frac{(C/I)_{Set} \cdot N_0 W \cdot F_{BS} \cdot P_{BS}(1+\varsigma_N+\varsigma_{OC})}{1-\eta} \tag{2-1}$$

where C/I_{set} is the required level at the BTS receiver, N_0W is the thermal noise, F_{BS} is the BTS noise factor, P_{BS} is the BTS transmit power, ς_N, ς_{OC} are the ratio of the thermal noise and of interference from adjacent BTSs to the BTS power, respectively, and η is the load level in the BTS. The nominal level set for RS1 is at -73 [dBmWatt^2] for 850 MHz band and -76 [dBmWatt^2] for the PCS band, representing a 50% loaded cell, 7 dB set E_b/I_t, 5 dB noise figure and 43 dBm BTS power. The power of the access probe is then

$$P_{RACh}[dB] = -S_{Tm} + K + \sum C_i \tag{2-2}$$

where C_i are ascending and correction terms defined for the access sequence. There are a maximum of 16 ascending probes in a probe sequence. The same equation holds while in the traffic state. The ST continues to measure S_{Tm} and add up correction terms, to account for changes in the BTS power, load and interference.

The *open loop power control* acts as an inverse AGC. Its dynamic range is 80 dB – to cover the range of path-loss within a typical cell. Because the fading on the forward and on the reverse links are not correlated, its estimate of the reverse link is accurate only to within 4 to 8 dB. The time constant is a trade-off between the need for a very fast response to a fast fade, and becoming a major source of interference to the network, and is set to about 30 ms, which allows it to compensate for fading only to slow moving STs.

Closed loop power control is when in the traffic mode, the BTS measures the received E_b/I_t from each ST and issues a power control bit every 1.25 ms, which commands the ST to increase or decrease its power by one increment of 1 dB. Its dynamic range is 48 dB. The accuracy of the closed loop power control in matching the desired signal level at the BTS receiver is about 1.5 dB. The BTS counts the consecutive "down" commands, and if that exceeds a specified threshold value the BTS interprets it as a malfunction of the ST and sends a "lock" command that disables the ST.

In *outer loop power control* FER is mostly determined by the E_b/I_t, but also by other parameters, including ST speed and multipath environment. The *outer loop power control* is set to maintain the required FER. The FER is assessed per every frame at the BSC. If the FER target is not met, it instructs the BSC to raise the target E_b/I_t ("set point") by 3 to 5 dB. The BTS then decreases the *set point* by 0.3 dB after every consecutive frame until a new "up" message arrives from the BSC. This individual setting of E_b/I_t per ST increases the variability of E_b/I_t by up to 2.5 dB, thereby reducing the capacity respectively.

2.2.3.2 Forward Link Power Control

The *forward link power control* (FLPC) applies to the FTCh only. Its purpose is to guarantee a set FER level while reducing the total power transmitted by the BTS to the minimum. The latter is important for reducing interference to other cells, reducing in-cell interference due to multipath (non-orthogonality) and increasing the FWD link capacity when it is limited by the BTS power. The overall variation allowed is ± 3 dB to ± 4 dB. The power control is applied to the *digital gain* (DG) of each traffic channel. A preset DG is assigned to each channel based on assessment of the signal received from that ST (*open loop power control*). The digital gain is then reduced by 0.25 dB every predetermined period (up to 80 frames). The ST counts the frames received in error, and if their percentage (FER) exceeds a

predetermined level per required service, or the number of consecutive frames received in error exceeds a threshold, it issues a message (PMRM – power measurement report message). Upon receipt of the message, the digital gain is kicked up, typically 2 dB, and the process continues again.

2.2.4 Soft Handoff

2.2.4.1 Introduction

The *handoff* is a process whereby the communication of a ST to its party transitions from being relayed through one BTS to another BTS in a transparent way without interruption of the session. CDMA supports *Soft Handoff* (SHO) whereby the ST communicates with two or more BTSs simultaneously. This process is maintained as long as the communication with all the participating BTSs is satisfactory, and typically occurs over an area on the boundary of the coverage between these cells. *Softer Handoff* applies similarly between sectors belonging to the same BTS (and thus allowing for a coherent processing of all signals). The objective of the SHO is to guarantee a smooth handoff between cells. At the same time, the SHO serves to balance the transmission level of the STs across the network, reduce excessive interference between adjacent cells and balance the load between them. It also provides macro diversity for the ST, thus further reducing its transmission power. All participating BTSs transmit simultaneously during SHO. Their forward link power control compensates only partially for the excess transmission power from the participating BTSs.

2.2.4.2 Soft Handoff Process

The ST continuously scans the pilot code map for pilots that are strong enough to be considered for SHO. The rake receiver consists of 3 correlators ("fingers") for despreading the desired traffic and its delayed multipath replicas, and one pilot search correlator that performs the scan. The efficiency of this serial search requires a hierarchical structure in order to prioritize the search. This is built from the network planning and measurements and provided to the ST by the BTS. The pilots are divided into four groups:

Active set – Pilots associated with FTChs that are assigned to the ST and participate in the SHO. Also pilots associated with FPChs or FCCChs (in later versions of the standard) that are being monitored by the ST while in an idle state. The maximum number of pilots in the *active set* is 3. There are versions of STs with 6.

Candidate set – Pilots that are not currently in the *active set* but have been received by the ST with enough strength to indicate that the associated FTCh could be successfully demodulated. The maximum number is 10.

Neighbor set – Pilots that are not currently in the *active set* nor in the *candidate set*, but are likely candidates for handoff. The maximum number is 40.

Remaining set – The set of all possible pilots in the current system (SID) on the current CDMA frequency assignment, excluding the pilots in the *neighbor set*, the *candidate set* and the *active set*.

The SHO process is initiated by the ST. It is summarized in Fig. 2-3.When a pilot strength exceeds T_{ADD} (a level set by the system) it sends a *pilot strength measurement message* (PSMM) and transfers the pilot to the *candidate set* (1). The BTS responds by a *handoff direction message* (2), allowing the ST to transfer the pilot to the *active set*.

The ST performs and responds by a *handoff completion message* (3). When the pilot strength drops below T_{DROP} the ST starts the *handoff drop* timer (4). Once expired the ST sends a PSMM (5), the BTS sends a *handoff direction message* (6) and the ST removes the pilot from the *active set* to the *neighbor set* and sends a *handoff completion message* (7).

In case there are already 3 pilots in the active set, and a pilot in the candidate set exceeds any of them by T_{COMP} they interchange locations; the weaker goes to the candidate set and the new stronger goes to the active set.

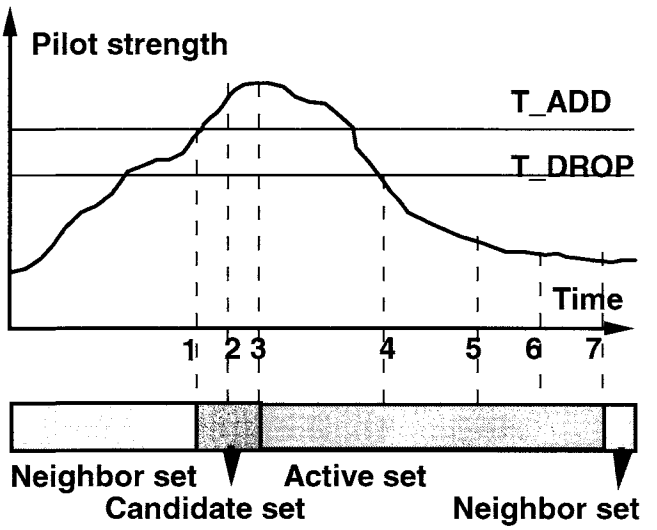

Figure 2-3. Soft Handoff sequence

2.3 Third Generation - 3G

2.3.1 The Motivation

The motivations for the third generation cellular are two-fold: technology drive and business push. The enormous success of the cellular service created a momentum for additional services, both by the technology leaders and manufacturers envisioning market saturation for the voice services, and by operators envisioning reduced profitability with increasing competition.

The efficiency of the cellular telephone transmission is limited by the nature of the service, requiring full duplex voice with low latency, and full mobility. High order modulation constellation is too sensitive to interference to sustain the multipath fading and the reuse requirements for high capacity.

Reaching to data services opens a new regime for both technology and business. Revenue is made of the information value of the bit, not the sheer air time. Latency, full duplex and full mobility are relaxed in lieu of higher data rates. A wide range of transmission modes, trading off SNIR, signal duration and spreading rate, is then open to suit the various needs of data and multimedia. Fig. 2-4 exemplifies the fact that the "volume" of transmission of a bit is fairly fixed, and its cost is optimized by service and environment-adaptive choice of its shape.

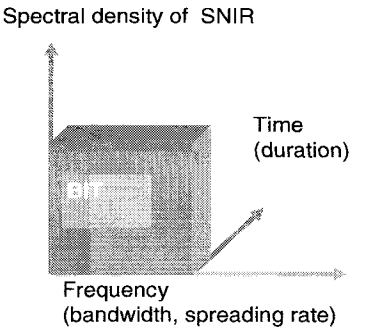

Figure 2-4. The cost of bit transmission

2.3.2 The Standardization

The ITU initiated a global standardization for 3G in a program named IMT2000 (International Mobile Telephone). The race of two major groups led

to the creation of two main standards: 3GPP (3rd generation partnership project) produced the WCDMA – UMTS standard, seeking an evolutionary process from the GSM and its infrastructure, while 3GPP2 produced the CDMA2000 standard, a fully evolutionary standard from IS 95. Both standards are based on CDMA technology and have similar structure and processes. The main differences are summarized in Table 2-2. The rationale for the choice of parameters in CDMA2000 is full backward compatibility with IS 95 and a simple upgrade of existing networks. UMTS opts for a wide band, having been given a virgin spectral allocation. The rationale for non synchronized BTSs is difficulties envisioned in GPS-based synchronization for micro and indoor BTSs.

2.3.3 The Features and Techniques

3G service objective is multimedia communications. Four traffic classes have been defined, each with its measure of Quality of Service (QoS), according to transmission constraints, and mainly the tolerance to latency:

Conversational – low end-to-end delay, symmetric traffic. Mainly circuit-switched voice services, and (circuit or packet-switched) video telephony. The QoS is strictly human perception.

Streaming – Transmission of data that can be processed as a steady continuous stream. Asymmetric, latency-tolerant. Typical services are web broadcast and video on demand.

Interactive – Request response pattern. Short round-trip delay. Typical applications are web browsing, video games, location-based services.

Background – Applications that do not require immediate attention. Starting from SMS, email services and to files transfer.

The techniques applied in response to these needs include:

Packet switching – the traditional circuit-switched allocation of a duplex channel continuously for the duration of a call is extremely inefficient for asymmetric data transfer and multiple data services. The data is packaged in addressed packets, dynamically allocated to users controlled by various scheduling preferences. Packet switching opens the infrastructure to a connectionless regime.

Variable spreading rate – high data rate uses lower spreading and applies protection by ARQ and longer codes (including turbo codes)/ longer frames.

Fast, complex channel control – with fast channel measurement and feedback.

Adaptive modulation and coding (AMC) – adapting the modulation and coding to the channel state and service.

Hybrid ARQ (HARQ) – (Hybrid Automatic Repeat Request) advanced message acknowledgement that expedites the transmission and verification.

Fast scheduling – scheduling transmissions according to channel conditions and "fairness criterion".

Fast FL power control – improvement of the FL channel and mitigation of multipath.

FL transmission diversity – (optional). Improvement of the FL.

Time multiplexing – Full power transmission to a channel-favorable designated user per each time slot ("water filling").

2.4 CDMA2000

2.4.1 Introduction

CDMA2000 is an extension of IS 95, designed for providing the service requirements of 3G. It supports both circuit-switched and packet data, and multiple supplementary and dedicated channels optimized for different multimedia applications. CDMA2000 is backward compatible with IS 95B, including most of the infrastructure, and its deployment constitutes a simple upgrade to IS 95 network. It requires CDMA2000-compatible ST.

CDMA2000 standard supports two spreading rates (SR):
SR1 spreads 1.2288 Mchips/s over 1.25 MHz band (CDMA2000-1x).

There are two versions of SR3: in SR3 DS (direct sequence), 3.6964 Mchip/s are spread over 3.75 MHz bandwidth, and SR3 MC (multicarrier) incorporates 3 1.25 MHz FL channels and one 3.75 MHz RL. SR3 has not yet been implemented commercially.

2.4.2 Forward Link

Six forward link *Radio Configurations* (RC) are defined for 1x, listed in Table 2-1. RC10 – EV-DV is discussed in section 2.9.

The main differences from IS 95 include:
- Different length Walsh codes, from 4 to 128 chips, to suit the application.
- QPSK modulation (and higher constellations in RC10 EV-DV).
- Turbo codes enhance the convolutional FEC codes in some configurations.
- Fast FL power control (800Hz) that assists in mitigating fading. There are 1, 0.5 and 0.25 dB steps that allow for a tighter control and reduce the ripple.
- Transmit diversity (OTD – orthogonal TD and/or STTD (Space Time TD).
- Additional channels to accommodate a variety of applications.
- Frame lengths – 20 ms for signaling and user information, 5 ms for control information.
- Forward Common Auxiliary Pilot Channel (FCAPiCh), and Forward.
- Dedicated Auxiliary Pilot Channel (FDAPiCh) to support smart antenna transmission.

Table 2-1. Forward link radio configurations for CDMA2000-1x

RC	Data rate (Kbps)	FEC Encoder rate	Modulation	TD
1	1.2; 2.4; 4.8; 9.6	1/2	BPSK	
2	1.8; 3.6; 7.2; 14.4	1/2	BPSK	
3	1.2; 1.35; 1.5; 2.4; 2.7; 4.8; 9.6; 19.2; 38.4; 76.8; 153.6	1/4	QPSK	+
4	1.2; 1.35; 1.5; 2.4; 2.7; 4.8; 9.6; 19.2; 38.4; 76.8; 153.6; 307.2	1/2	QPSK	+
5	1.8; 3.6; 7.2; 14.4; 28.8; 57.6; 115.2; 230.4	1/4	QPSK	+
10	81.6; 158.4; 163.2; 312.0; 316.8; 326.4; 465.6; 619.2; 624.0; 633.6; 772.8; 931.2; 1238.4; 1248.0; 1545.6; 1862.4; 2476.8; 3091.2	1/5	QPSK, 8-PSK, 16 QAM	

2.4.3 Reverse Link

The main differences from IS 95 include:

- Separate channels for different applications.
- Coherent reverse link with a continuous pilot per user.
- Continuous (not bursty) transmission.
- Forward power control information is time multiplexed with the pilot.
- Independent fundamental and supplemental channels.
- Frame lengths - 20 ms for signaling and user information, 5 ms for control information.
- Adaptive threshold Soft Handoff that reduces the SHO zone. Referring to Fig. 2-3 – once a pilot is reported crossing above T_{ADD} and being transferred to the *candidate set*, it is being measured and reported frequently, creating a pattern of its increase slope relative to the total energy detected and coherently combined from all pilots in the *active set*. It is transferred to the active set once it satisfies a criterion of ratio of powers and trend. Frequent power measurements of each pilot in the active set and in the candidate set establish the trends. When a pilot crosses down a ratio and trend criterion a timer is initiated, and upon its expiration it is moved to the *candidate set* or the *neighbor set* if it is above or below T_{DROP}. This process reduces the SHO zone, and the "ping pong" of pilots in and out of the SHO.

2.5 WCDMA UMTS

WCDMA for UMTS (Universal Mobile Telecommunication System) was released by 3GPP in December 1999. It is a standard responding to the requirements of IMT2000 for 3G cellular service.

Table 2-2. Major differences between WCDMA and CDMA2000 1x

	WCDMA	CDMA2000
Carrier spacing	5 MHz	1.25 MHz
Chip rate	3.84 Mcps	1.2288 Mcps
Power control frequency	1500 Hz	800 Hz
Base station synchronization	No	Yes
Frame length	10 ms	20 ms

2.6 CDMA Timeline

July 1993 *IS 95* - the first cellular CDMA standard, was published.
May 1995 IS 95A revision published.

Frequency-division duplex (FDD) system with 1.25 MHz channels. Primarily designed for voice services, but also provides circuit- switched data services at speed up to 14.4 Kbps. Fast power control (800 Hz) on RL, and slow power allocation on the FL (50 Hz). Supports soft handoff between base stations and softer handoff between sectors in the same base station.

1996 First commercial deployment in Hong Kong.

June 1997 IS 95B standard approved. Offers 64 Kbps packet switched data. FSCChs (*Forward Supplemental Code Channels*) are introduced, using Walsh codes from the traffic pool. Up to 7 FSCChs and one FTCh may be assigned to one user, reaching data rate of 115.2 Kbps. First commercial deployment in 1999.

July 1999 CDMA2000 (1x RTT) is approved. (1x stands for use of single 1.25 MHz channel. RTT – *Radio Transmission Technology*). First commercial deployment in Oct. 2000. Includes IS 95B as a subset. Voice capacity is increased on both FL and RL by 60% to 100%. Fast FL power control. QPSK modulation. Transmit diversity (optional) on FL. Coherent RL. Quick paging channel for increased standby time. Supplemental channels for packet data services at rates up to 153.6 Kbps on FL and RL.

December 1999 3GPP releases WCDMA-UMTS.

CDMA2000 Release A. New FL common channels to improve paging channel efficiency. Supports concurrent services (e. g. voice, packet data, circuit-switched data). Supplemental channel data rate increased to 307.2 Kbps.

CDMA2000 Release B. Rescue channel to reduce call drops.

CDMA2000 Release C (1xEV- DV FL). Time shared packet data channel on the FL. Time-division multiplexed. Fast scheduling with rate adaptation based on channel state feedback from the mobile. Hybrid ARQ. Forward link data rates up to 3.1 Mbps.

CDMA2000 Release D (1xEV- DV RL). Packet data channel on the reverse link. Autonomous rate adaptation by mobiles. Hybrid ARQ. RL rates up to 1.8 Mbps. Broadcast channel on the FL.

1xEV-DO. The different releases of CDMA2000 1x support circuit switched voice and data services on the same carrier. 1xEV- DO (1x EVolution –Data Optimized) is optimized for packet data services on a separate 1.25 MHz carrier.

October 2000 1xEV-DO Rev 0 standard approved. Commercial deployment in Korea, January 2002.

April 2004 1xEV-DO Rev A standard approved. 3.1 Mbps on forward link (2.45 Mbps in 1xEV-DO Release 0), 1.8 Mbps on reverse link (153.6 Kbps in 1xEV-DO Release 0).

2.7 Forward Link Time Multiplexing

The multipath channel conditions, and the respective SINR, vary across the coverage area and vary with time from one ST to another through their motion. While diversity techniques used in the CDMA regime smooth and "even out" the fluctuating channel, resources are sacrificed to serve the disadvantaged users via the power control on behalf of the total throughput of the BTS. Data applications that are not sensitive to latency can take advantage of slotted sequential transmissions to the users at times they enjoy the most favorable channel conditions. Full power transmission, "riding the crests of the multipath", as described in Fig. 2-5, renders much higher BTS throughput. Time slots are allocated by the *scheduler* to the Access Points (AP, an equivalent terminology to ST) according to their momentary channel conditions. A *fairness criterion* compromises between the maximum BTS throughput possible and a fair distribution of the service between APs. Mobility, that changes the multipath conditions differently to each AP, is expected to provide a fair statistical distribution of the channel conditions among them. Many users' activity offers more opportunities for signal peaks to the scheduler and increases the throughput.

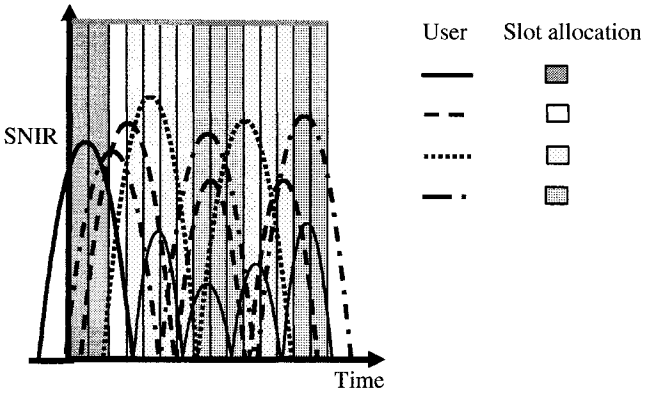

Figure 2-5. Multi-user diversity

This is "*user diversity*". Fading can actually improve the throughput with this scheme, and diversity techniques to "smooth" the channel are not employed, nor power control.

Each AP monitors all the accessible BTSs all the time, and reports an advisory with the desired data rate to the one with the best link, based on the measured SINR. These timely reports are processed by the scheduler to allocate the time slots. This time multiplexing scheme has been adopted by 1xEV-DO, 1xEV-DV and HSDPA for transmission of asymmetric high data rate.

2.8 1xEV-DO

1xEV-DO is an air interface optimized for packet data. It uses dedicated 1.25 MHz frequency allocations within the CDMA2000 allocated band.

The *forward link* is time multiplexed. It uses 1.67 ms time slots, full power, as shown in Fig. 2-6. Its coverage conforms to the coverage of IS 95 and CDMA2000 cells. The highest throughput is obtained in smaller cells, however. Data rate can change from slot to slot, from 38.4 Kbps to 2.4576 Mbps, and up to 3.1 Mbps in Rev A. All data transmissions are at the same power. Transmission in each slot is directed to only one mobile. It does not have soft handoff, only hard handoff. Adaptive Modulation and Coding (AMC) is used, together with Hybrid ARQ, to enhance throughput.

The scheduler at the base station chooses which mobile to transmit to in each slot.

Mobiles continuously transmit Data Rate Control (DRC) channel that indicates data rate and sector from which they want to be served. The scheduler uses channel feedback from mobiles to decide who to transmit to, and implement some fairness criterion.

The *reverse link* is coherent CDMA with data rates from 9.6 Kbps to 153.6 Kbps and up to 1.8 Mbps in Rev A. The rate assignment is dynamic, decentralized.

Schedule-to-Tx-when-channel-is-above-average reduces the interference to other BSs statistically. Revision A incorporates Hybrid ARQ on reverse link also.

2.9 1xEV-DV

1xEV-DV is an extension of 1xRTT (CDMA2000), incorporating 1xEV-DO time multiplexing for high data rates. It is backward compatible with CDMA2000, including handoff. Packet data CDMA is scheduled for best transfer.

High data rate is time multiplexed and transmitted to the user with the best momentary channel, with all the power unused by the CDMA channels – a technique called "*water filling*". The forward link transmission resource used is described in Fig. 2-7. The main features and differences from HSDPA are summarized in Table 2-3.

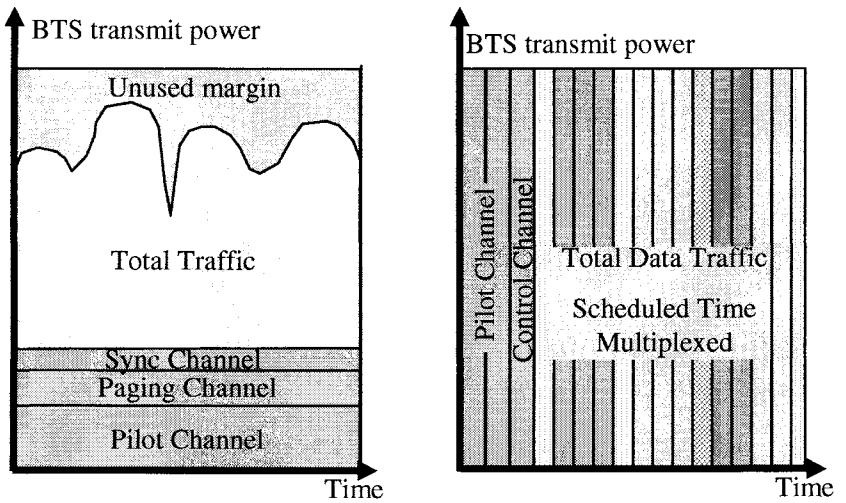

Figure 2-6. 1xEV-DO FL transmission

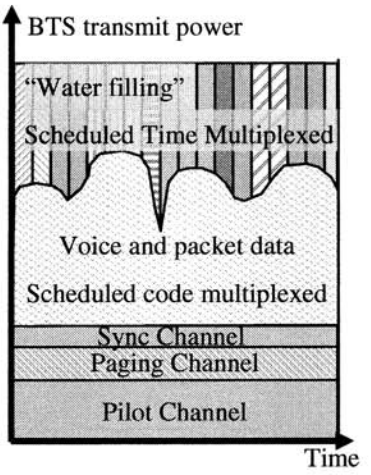

Figure 2-7. 1xEV-DV forward link transmission

2.10 HSDPA

HSDPA – *High Speed Downlink Packet Access,* is an extension of WCDMA and backward compatible with it. It is a downlink only multimedia optimized, transmitting up to 10.8 Mbps throughput (maximum specified by codes is 14.4 Mbps). It requires special ST. Its optimization rules are a bit different than those for UMTS. Table 2-3 summarizes the differences between HSDPA and 1xEV-DV .

Table 2-3. Main features and differences between HSDPA and 1xEV-DV

Feature	HSDPA	1xEV-DO
Forward Link Frame Size	2ms TTI (3 Slots)	1.25,2.5, 5, 10 ms Variable Frame Size (1.25 ms Slot Size)
Channel Feedback	Channel quality reported at 500 Hz rate (every 2 ms)	C/I feedback at 800 Hz (every 1.25 ms)
Data User Multiplexing	TDM/CDM	TDM/CDM (Variable frame)
Adaptive Modulation and Coding	QPSK & 16 QAM Mandatory	QPSK, 8 PSK & 16 QAM
Hybrid ARQ	Chase or incremental Redundancy (IR)	Async. Incremental Redundancy (IR)
Spreading Factor	SF=16 using UTRA OVSF Channelization Codes	Walsh Code Length 32
Control Channel Approach	Dedicated Channel pointing to Shared Channel	Common Control Channel

REFERENCES

[1] J. Shapira, and C.E. Wheatley, *Channel Based Optimum Bandwidth for Spread Spectrum Land Cellular Radio*, Proceedings of PIMRC 92, pp. 199-204, Boston, October 1992.
[2] A.J. Viterbi, *CDMA*, Addison-Wesley, 1995.
[3] R. Padovani, *Reverse Link Performance of IS-95 based Cellular Systems*, IEEE Personal Communications, pp. 28-34, Third Quarter 1994.
[4] J.S. Lee, and L.E. Miller, *CDMA Systems Engineering Handbook*, Artech House, 1998.
[5] V.K. Garg, *IS 95 CDMA and CDMA2000*, Prentice Hall, 2000.
[6] L. Korowajczuck, et. al., *Designing cdma2000 Systems*, John Wiley&Sons, 2004.
[7] H. Holma, and A. Toskala, *WCDMA for UMTS*, Wiley, 2001.

3

THE MOBILE RADIO PROPAGATION CHANNEL

3.1 Overview of the Mobile Wireless Channel

3.1.1 Introduction

The cellular land mobile radio is driven by requirements for high teletraffic capacity of many concurrent users in the same service area, and high transmission quality, reaching to wired telephone quality. The transmission environment in this service is demanding - excess propagation loss and heavy multipath, due to obstructions which are abundant in the urban environment, vary and fluctuate in time as the mobile user is in motion. Cellular telecommunication systems' architecture and signal design are designed to counter the impairments of the transmission by the channel. Simple statistical characterization of the channel, based on sample measurements or on otherwise generic statistical assumptions, is far from providing the spatial-time channel variations as required for description and analysis of its interaction with the communications system. An arsenal of physically-based canonical propagation models serve as a solid basis for an insight into the interaction process, while the statistical coating covers for the unknown exact behavior.

3.1.2 Channel Characteristics

The cellular mobile channel is characterized by the following:

3.1.2.1 Excessive loss. The mobile is to be serviced everywhere within the cell, and line of sight between the cell-site antenna and the mobile cannot always be maintained, nor is it desired. Highly populated areas, where capacity is at high demand, are congested with structures, man-made objects and sometimes trees that obstruct the transmission path. Use is made of the excess loss to achieve the required isolation from other cells.

3.1.2.2 Scattering and Reflections. The propagation within the relatively small, congested cells is dominated by scattering and reflections by the structures and objects surrounding both the cell-site and the mobile antennas. The flexibility required from the mobile or the handset dictates an omnidirectional antenna, which collects signals arriving from any direction. Most base station antennas have limited directivity also, thus allowing the whole terrestrial neighborhood to contribute multipath between the base station and the mobile ST, via scattering and reflection. The multipath scatter from objects in the vicinity of either antenna (e.g. buildings, poles, wires), or are reflected from large surface structures (e.g. large buildings, mountains) that might have a favorable path to both antennas.

3.1.2.3 Fading channel. The multipath formed by the scatterers and reflectors add up at the receive antenna to produce the received signal. In the absence of time discrimination, as is the case for a narrow band transmission, the signals sum coherently and produce a wave-interference pattern throughout the cell. A mobile traveling through such a pattern traverses signal strength peaks and dips - which constitute the well-known fading.

3.1.3 Path-Loss and Channel Fluctuations

The complex characteristics of the channel are conveniently classified into the following:

3.1.3.1 Path-loss. This describes the propagation of the total power – aggregate of the direct path and all forward scattered contributions that sum up with only slow phase changes between them. The path-loss changes slowly with frequency, and there is virtually no difference between narrow band and broadband path-loss for the same frequency band. The main processes the path-loss is undergoing are the geometrical spreading in free space (R^{-2} regression), the near grazing propagation along the interface between two media (grazing the earth, a series of fences or building roofs, or grazing the forest canopy) where the regression is essentially R^{-4}, and shadowing with typical Lognormal statistics.

3.1.3.2 Channel quality. The multiple wave paths on the way to the receiver, termed "multipath propagation", arrive at different times and from different directions, depending on the locality of the ST. These may coherently interfere with each other, creating the "flat fading" – for a narrow band receiver, or creating a time-dispersive signal, with a "delay spread", to broadband receivers, and exhibiting "Doppler spread". These variations are frequency, time and space dependent and their rate of change is within the time constants of the communication system – modulation, signal bit or frame, or control. The signal and its processing are designed to mitigate those channel impairments.

3.2 Path-Gain Physics

3.2.1 The Transmission Equation

The transmission of signals from one antenna to another is formulated by the Transmission Equation

$$\frac{P_R}{P_T} = T(R) \equiv G_T G_R PG(R) \tag{3-1}$$

where

P_R	is the power received at the receive antenna terminal,
P_T	is the power transmitted at the transmit antenna terminal,
$T(R)$	is defined as the Transmission Gain,
$PG(R)$	is the Path-Gain, which is the Transmission Gain between two isotropic antennas (The inverse is known as *Path-Loss*), and
G_R, G_T	are the gain of the receive and transmit antennas, respectively.

The underlying assumptions for the validity of this equation are:

- ✓ *Causality*. There is no interaction between the antennas. The receive antenna does not influence (the impedance of) the transmit antenna. This means that the antennas are far enough apart, and the wave radiated from the transmit antenna spreads out and only a small part thereof reaches the receive antenna, so that any return wave is negligible.
- ✓ *Reciprocity*. The same Transmission gain prevails if the role of the transmit and receive antennas interchange. (This pertains to an isotropic medium, which is the case for purpose of our discussion).
- ✓ *Far field*. The antennas are so far apart that they are seen as a point by each other, and the antenna radiation can be described as a product of radial function (power density decreasing as R^{-2}) and angular function (representing the "antenna radiation pattern").

When the antennas are in free space, the radiation spreads radially in straight lines, and is collected by the other antenna "effective receiving area" A_R

$$T = \frac{G_T A_R}{4\pi R^2} = G_T G_R \left(\frac{\lambda}{4\pi R} \right)^2 . \tag{3-2}$$

The effective receiving area relates to the antenna gain as

$$\frac{A_R}{\lambda^2} = \frac{G_R}{4\pi} \Rightarrow A_R = \frac{G_R \lambda^2}{4\pi}. \tag{3-3}$$

3.2.2 Wave Reflection from a Perfectly Conducting Plane

A wave impinging on a surface is reflected. A perfectly conducting planar surface creates an "image" of the source behind the surface, as depicted in Fig. 3-1.

The angle of incidence equals the angle of reflection. There is no loss in reflection from a perfectly conducting surface. The transmission equation for the reflected wave is

$$\frac{P_{reflected}}{P_T} = G_T(\vartheta_{Tref}) G_R(\vartheta_{Rref}) \left(\frac{\lambda}{4\pi(R_1 + R_2)} \right)^2 \tag{3-4}$$

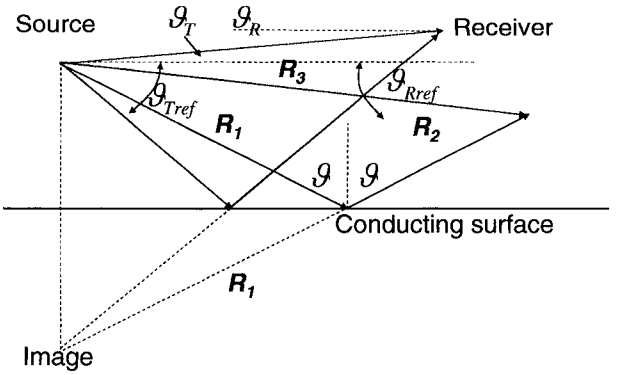

Figure 3-1. Reflection from a conducting surface

and the ratio of the reflected signal to the direct one is

$$\frac{P_{Reflected}}{P_{Direct}} = \frac{G_T(\vartheta_T) G_R(\vartheta_R)}{G_T(\vartheta_{Tref}) G_R(\vartheta_{Rref})} \left(\frac{R_3}{R_1 + R_2} \right)^2 \tag{3-5}$$

where $G(\vartheta)$ indicates the gain in the direction ϑ.

The propagation over ground at low grazing angles is derived directly from these rules: Fig. 3-2 describes propagation between one antenna at height H above the ground, and another antenna at height h.

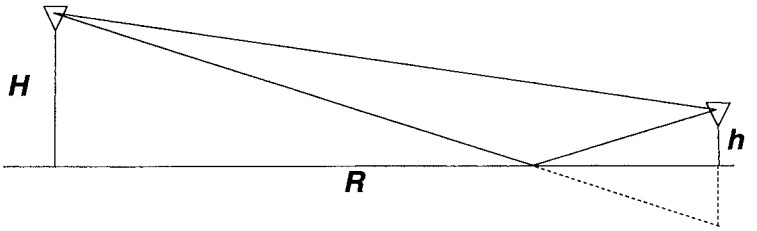

Figure 3-2. Low grazing angle propagation

The length of the direct ray is $L_D = \sqrt{(H-h)^2 + R^2}$, and that of the reflected ray is $L_R = \sqrt{(H+h)^2 + R^2}$. These paths differ only slightly, which impacts on the wave phase only. The transmission equation for the two-ray propagation is thus

$$\frac{P_R}{P_T} = G_T G_R \left(\frac{\lambda}{4\pi R}\right)^2 \left[\exp\left\{jk\sqrt{(H-h)^2+R^2}\right\} + \Gamma \exp\left\{jk\sqrt{(H+h)^2+R^2}\right\}\right]^2 = \cong G_T G_R \left(\frac{\lambda}{4\pi R}\right)^2 \left[\exp\left\{-jk\frac{Hh}{R}\right\} + \Gamma \exp\left\{ik\frac{Hh}{R}\right\}\right]^2 . \quad (3\text{-}6)$$

Γ is the reflection coefficient. Γ=1 for waves that are polarized with the electric field in a plane perpendicular to the surface (also called TM waves). It is Γ=-1 for waves polarized with the electric field parallel to the surface (TE waves).

The multipath interference of the direct and the reflected wave of TM waves at low grazing angles above a perfectly conducting surface becomes

$$P_R/P_T\big|_{TM} = G_T G_R (\lambda/4\pi R)^2 [2\cos(k\,Hh/R)]^2 . \quad (3\text{-}7)$$

The signal nullifies at

$$h_{n,TM} = (2n-1)R\lambda/4H . \quad (3\text{-}8)$$

The power of the multipath for TE waves at low grazing angles is

$$P_R/P_T\big|_{TE} = G_T G_R(\lambda/4\pi R)^2[2\sin(k\,Hh/R)]^2\,. \tag{3-9}$$

Nulls appear at

$$h_{n,TE} = n\,R\lambda/2H\,. \tag{3-10}$$

This effect, known as "lobing" in radar, is described in Fig. 3-3. As an example – for R=1000 m, H=10 m, λ=0.16 m, the first peak is at h=4 m.

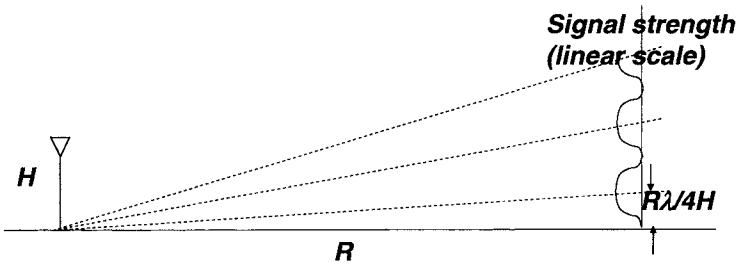

Figure 3-3. Propagation lobing, TE wave, low grazing angles

Here the first null is at grazing, and for low angles the propagation law becomes

$$P_R/P_T \cong G_T G_R\,(Hh)^2/R^4\,^2. \tag{3-11}$$

Note that the propagation regression law for low grazing angles is R^{-4}.

3.2.3 Reflection at the Interface between Dielectric Media

Wave impinging on a surface of a material with different electrical properties is partially reflected, the angle of the reflected wave being identical to that of the incident wave, and partially penetrates the surface into the second medium, as described in Fig. 3-4.

---

[2] The height-gain function for antennas lower than some 30 m has been found to be h^c due to surface roughness by typically man-made obstacles. A proposed expression in [2, 2.2.3] is c=h/20+1/2. It makes only a little difference from (3-11) for pedestrian and car users.

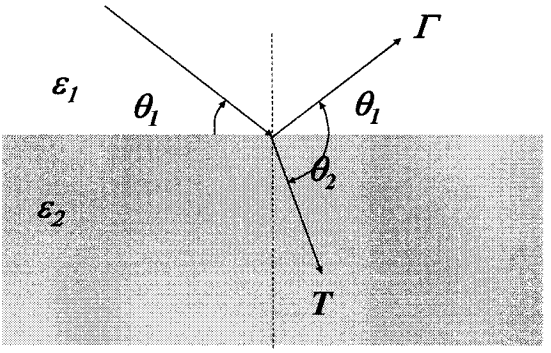

Figure 3-4. Reflection and transmission between two media

The projection of the phase velocity of the wave along the surface has to match on both sides. The direction of propagation of the waves is derived from this condition:

$$\cos\vartheta_1/\cos\vartheta_2 = \sqrt{\varepsilon_2/\varepsilon_1}\ . \tag{3-12}$$

Equation (3-12) is known as Snell's law of refraction. A critical angle ϑ_{2C} exists in the denser medium – the one with higher dielectric constant $\varepsilon = \varepsilon_2$, where the wave in the thinner medium ε_1 grazes the surface $\vartheta_1 \to 0$:

$$\cos\vartheta_{2C} = \sqrt{\varepsilon_1/\varepsilon_2}\ . \tag{3-13}$$

A wave incident on the surface from the denser medium at an angle smaller than the critical angle is trapped in the denser medium and is totally reflected.

The strength of the reflected wave depends on the polarization of the wave (see Section 3.5):

$$\Gamma_{TM} = \left(\sqrt{\varepsilon_2 - \cos^2\vartheta_1} - \varepsilon_2 \sin\vartheta_1\right) \Big/ \left(\sqrt{\varepsilon_2 - \cos^2\vartheta_1} + \varepsilon_2 \sin\vartheta_1\right) \tag{3-14a}$$

$$\Gamma_{TE} = \left(\sqrt{\varepsilon_2 - \cos^2\vartheta_1} - \varepsilon_1 \sin\vartheta_1\right) \Big/ \left(\sqrt{\varepsilon_2 - \cos^2\vartheta_1} + \varepsilon_1 \sin\vartheta_1\right). \tag{3-14b}$$

The TM wave has an angle ϑ_B where $\Gamma = 0$. There is no reflection for this incident angle and the signal penetrates the second medium with no loss. This angle, named after Brewster, is

$$\cos\vartheta_B = \sqrt{\varepsilon_2/(1+\varepsilon_2)}. \tag{3-15}$$

The reflection coefficient in the thinner medium, at the interface with the denser one, is plotted in Fig. 3-5. It nullifies at the Brewster angle, and reverses phase. Thus, at grazing angles lower than ϑ_B the reflection coefficient is negative for both TE and TM waves, and reaches $\Gamma \to -1$ as $\vartheta \to 0$. This explains why Eq. (3-11) holds for low grazing angles propagation over ground, for both polarizations.

The Brewster angle in the thinner medium, for various ε values of the denser medium, is depicted in Fig. 3-6.

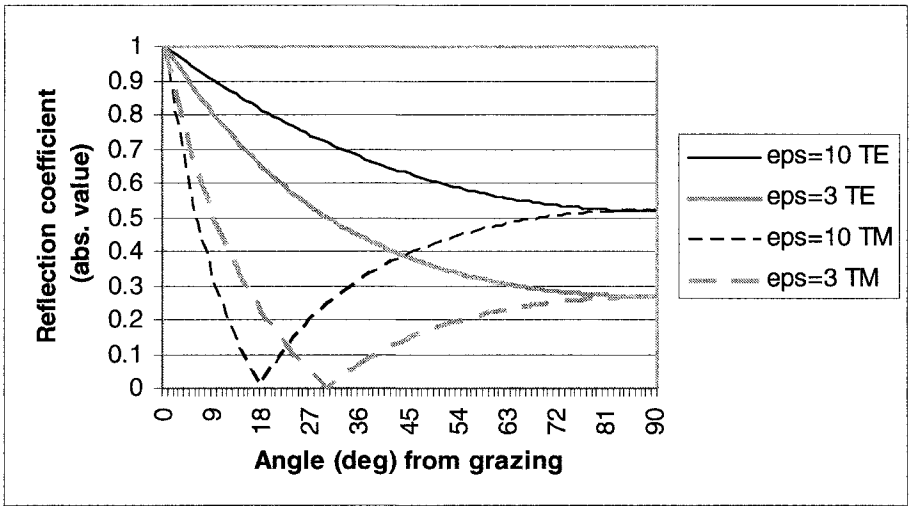

Figure 3-5. Reflection coefficient in the thinner medium ($\varepsilon_1 = 1$)

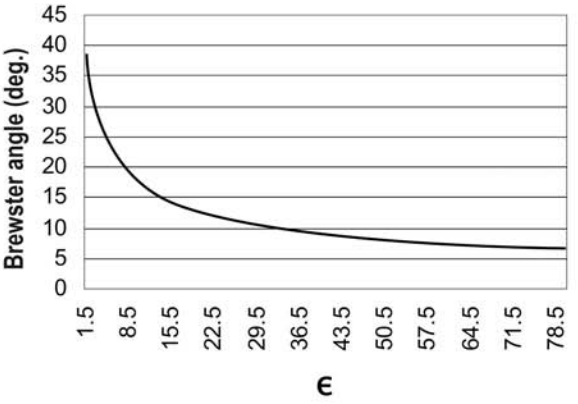

Figure 3-6. Brewster angle at the interface with medium ε

3.2.4 The Two-Ray, Flat Earth Propagation Model

The configuration of the basic terrestrial propagation is sketched in Fig. 3-7. The respective model is shown in Fig. 3-8. The two-ray multipath is presented by Eq. (3-6), and for low grazing angles $\Gamma \to -1$ and Eq. (3-9) holds, leading to Eq. (3-11). The grazing angle ϑ is related to the range R via $(H-h)/R = Tan\vartheta \cong \vartheta$. At a shorter range (and higher ϑ) the signal reaches the peak of the first lobe Eq. (3-10) at a distance R_b, called the break point distance $R_b=4Hh/\lambda$. Further lobes fluctuate around free-space propagation with average regression R^{-2}. At yet a shorter range the signal is attenuated by the slope of the beam of the antenna and then by the sidelobes' "skirt". This follows a trend of $1/sin^2\theta$ for a non-tapered aperture antenna (see Section 3.6.3).

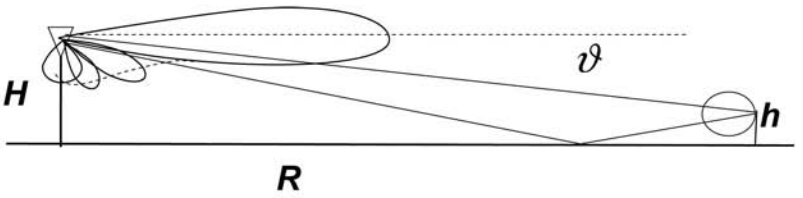

Figure 3-7. Two-ray propagation over flat earth

Figure 3-8 is a dB plot of the path-gain for isotropic antennas. Both the path-gain and the range are plotted on a Log scale. The far zone (zone 1) is characterized by a regression of R^{-4}, presented as a -40 dB/decade line in the plot. The break point is at $R_b=4Hh/\lambda$. The average trend of R^{-2} in zone 2 is represented by the -20 dB/ decade line. The crossing point, where the free-space regression equals the grazing multipath regression, is derived from Eqs. (3-2) and (3-11)

$$(\lambda/4\pi)^2/R^2=(Hh)^2/R^4 \rightarrow R_c=4kHh \tag{3-16}$$

where $k\equiv 2\pi/\lambda$ is the wave number.

Note that the multipath breakpoint depends on the antenna height and on the frequency. It extends further out at the 1800 – 1900 MHz bands than it is in the 800 - 900 MHz bands. Zone 3 starts closer to a lower antenna. The height of the antenna is thus a means of controlling the coverage.

The envelope of the sidelobes of a non-tapered directive antenna is described as

$$((\pi/\vartheta_{BW})\sin\vartheta)^{-2}\cong((\pi/\vartheta_{BW})(H-h)/R)^{-2} \tag{3-17}$$

where ϑ_{BW} is the antenna beamwidth in the elevation plane. The path-gain in zone 3 is then

$$L_{Iso3}=(2kR)^{-2}\left(\frac{\pi}{\vartheta_{BW}}\frac{H-h}{R}\right)^{-2}=\left(\frac{\vartheta_{BW}}{2k\pi(H-h)}\right)^2 \tag{3-18}$$

independent of the distance R. The path-gain in zone 3 increases vs. decreasing distance for antenna with illumination taper. The flattening of the path-gain slope in zone 3 limits the dynamic range of a link through the coverage – an important feature that enables the extension of the coverage.

The "roll-off breakpoint" R_{RO} is obtained by equating Eq. (3-17) to 1.

$$R_{RO}=(H-h)\pi/\vartheta_{BW} \tag{3-19}$$

A more compact and convenient representation of this model is achieved by subtracting the free-space regression curve from the path-gain (in dB), to obtain Fig. 3-9.

3.2.5 Lateral Waves at the Interface – Forest Propagation

Snell's law for the interaction between two space waves across an interface between two media is based on equating the phase velocity on both sides of the surface. There is no space wave solution for waves propagating along the surface. There is, however, a diffracted wave, called "lateral wave", whose propagation mechanism is depicted in Fig. 3-10. It carries its energy in the thinner medium, while continuously leaking into the denser medium at the critical angle. Its strength decays away from the surface in the thinner medium (Fig. 3-10).

Lateral waves are negligible compared to space waves. They become the dominant mechanism of propagation in the forested areas. These are characterized by a loss component (the dielectric coefficient is complex), that exponentially attenuates the direct wave, and the dominant wave is that reaching the canopy at the critical angel, traveling along the canopy and leaking back into the forested media along its path.

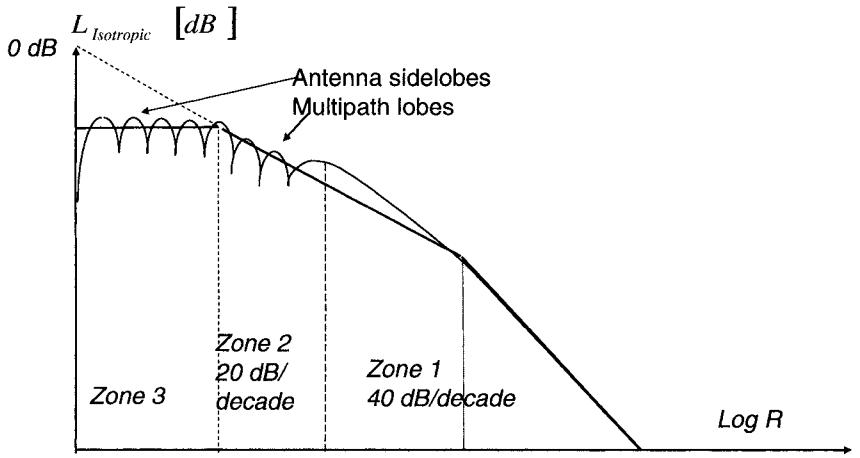

Figure 3-8. Flat earth propagation model

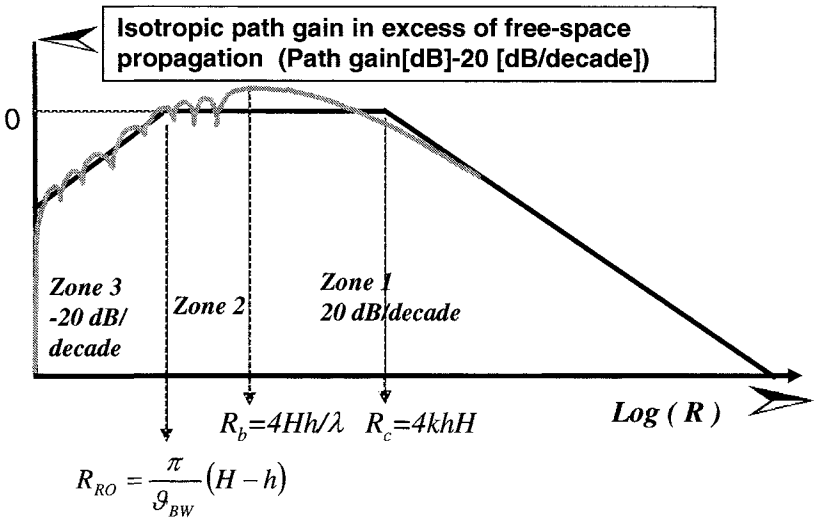

Figure 3-9. Flat earth propagation in excess of free-space regression

The path-gain between Tx and Rx within the lossy medium (case *a* in Fig. 3-11) is given by (following Bertoni [3e] (7-20)):

$$PG=\left(\frac{1}{|\varepsilon-1|}\right)^2\left(\frac{1}{kR}\right)^4\exp\left\{2\left((H_s-h_1)+(H_s-h_1)\right)k\,\mathrm{Im}\sqrt{\varepsilon-1}\right\} \qquad (3\text{-}20)$$

where the parameters are described in Fig. 3-11. The exponential terms account for the losses in the lossy medium ($\mathrm{Im}\sqrt{\varepsilon-1}$ is negative). Note that the regression exponent is R^{-4}.

The access node in case *b* is out of the forest, but below the height of the canopy H_c. The wave impinges on the forest edge and a lateral wave propagates there from along the canopy.

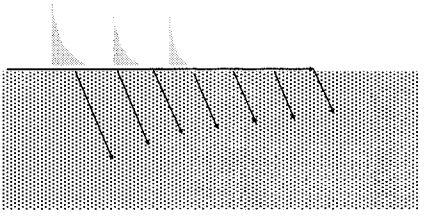

Figure 3-10. Lateral wave

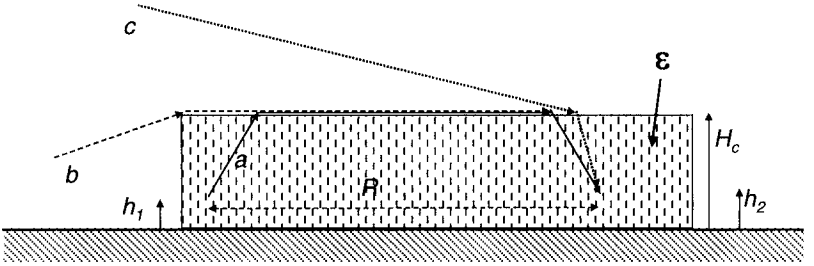

Figure 3-11. Propagation modes in the forest

Case *c* describes an access node out and above the canopy. Space waves dominate, according to Snell's law, Eq. (3-13).

3.2.6 Diffraction

Wave impinging on an edge is diffracted and spreads out of the diffraction edge in a plane perpendicular to the edge, as described by the "skirts" in Fig. 3-12, while being reflected along the edge as in the image rule in Fig. 3-1 (d_2 is the reflected ray from the impinging d_1 ray). The transmission gain through diffraction is

$$\frac{P_R}{P_T} = G_T G_R \left(\frac{\lambda}{4\pi}\right)^2 \frac{D^2 \lambda}{2\pi d_1 d_2 (d_1 + d_2)} \tag{3-21}$$

where the diffraction coefficient D represents the diffraction gain at a distance of one wavelength from the edge. It relates to σ_L, the line-scattering cross-section, as

$$\sigma_L[m] = D^2 \lambda \,. \tag{3-22}$$

Diffraction by a screen, to be discussed next, renders a simple expression and is used as a fair approximation for the cases of importance for the cellular channel.

3.2.6.1 Knife-Edge Diffraction

This representation approximates the diffraction near the shadow boundary, where interaction between the direct ray and the diffracted ray take place.

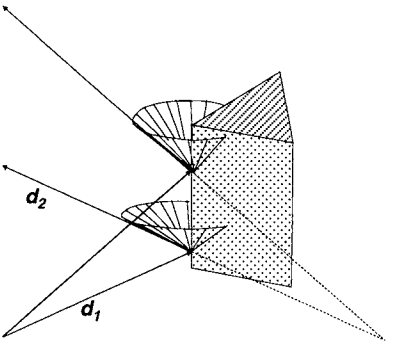

Figure 3-12. Edge diffraction

This is typical to propagation over hilly terrain. The governing parameter in Fig. 3-13b that describes the situation is $u \equiv 2x\sqrt{(1/R_1 + 1/R_2)/2\lambda}$. The respective gain within the transition zone is plotted in Fig. 3-14. P_D is the power through diffraction and P_F – through free-space, both at point P_2 relative to that at point P_1. The loss at the light-shadow boundary (u=0) is 6 dB.

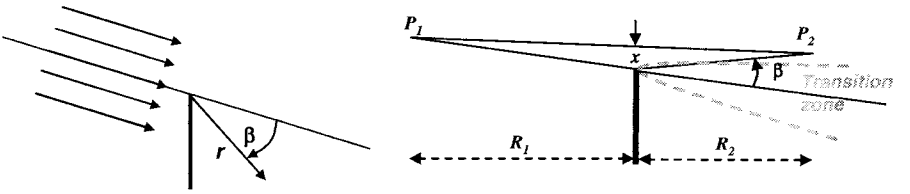

a. Screen diffraction

b. Knife-edge diffraction – transition zone

Figure 3-13. Screen diffraction

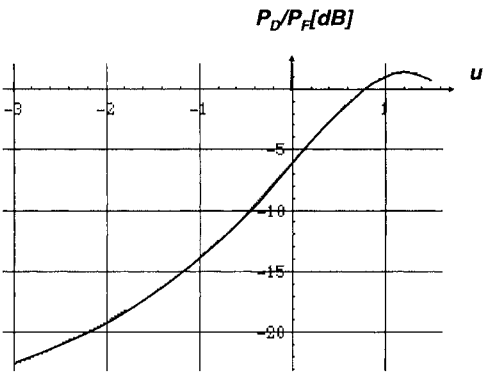

Figure 3-14. Knife edge diffraction gain

3.2.6.2 Corner Diffraction

Edge diffraction beyond the transition zone is expressed in terms of the angle of diffraction β into the shadow zone, as in Fig. 3-13a. The diffraction coefficient for an absorbing screen

$$D = \left[1/\beta - 1/(2\pi + \beta)\right]/2\pi \cong 1/2\pi\beta \tag{3-23}$$

represents approximately a wide range of edges and corners. The error in neglecting the second term is 1 dB for $\beta = \pi/2$. Here D is the diffraction coefficient. The diffraction coefficient for a metallic edge is

$$D_m = \frac{1}{4\pi}\left[\csc\left(\frac{\pi+\beta}{2}\right) - \sec\left(\frac{\pi+\beta}{2}\right)\right]. \tag{3-24}$$

The diffraction coefficient represents the diffraction gain at a distance of one wavelength from the edge. The diffraction loss at a distance r beyond the edge is

$$L[dB] = -20LogD + 10Log\left[\frac{r}{\lambda}\right]. \tag{3-25}$$

Figure 3-15 plots the diffraction loss for both absorbing screen and metallic screen.

3.2.6.3 Forward Scattering - the First Fresnel Zone

Waves that propagate through multiple paths interfere with each other and create interference fringes over their interaction space. These fringes are the cause of the fading of a signal for a mobile user that traverses them. The fringes are created by phase difference between the participating rays, relating to the electrical path they travel. A path difference of $\lambda/2$ creates a destructive interference, and so are differences of $(2n\text{-}1)\lambda/2$. These contours are called Fresnel zones. In a homogenous medium they draw concentric ellipses, the foci of which are the transmit and receive ends. These are depicted in Fig. 3-16.

All rays within the first Fresnel zone, which is encapsulated in an ellipse defined by a path difference $\Delta < \lambda/2$, interfere constructively and form the forward propagation path. The width s of the first Fresnel zone (the minor axis of the ellipse) is

$$s = \sqrt{2R\lambda} \,. \tag{3-26}$$

A clear first Fresnel zone guarantees no fading on this path. It will be shown to be a condition for ground clearance in radio links, and to define the low loss distance in propagation along streets, and penetration to buildings.

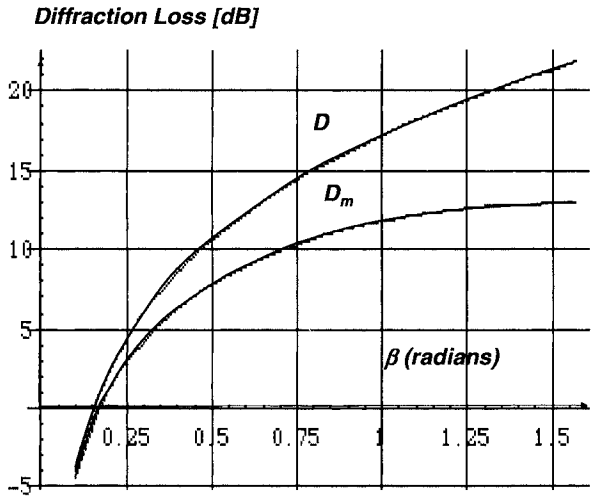

Figure 3-15. Diffraction loss for absorbing D and metallic D_m screens

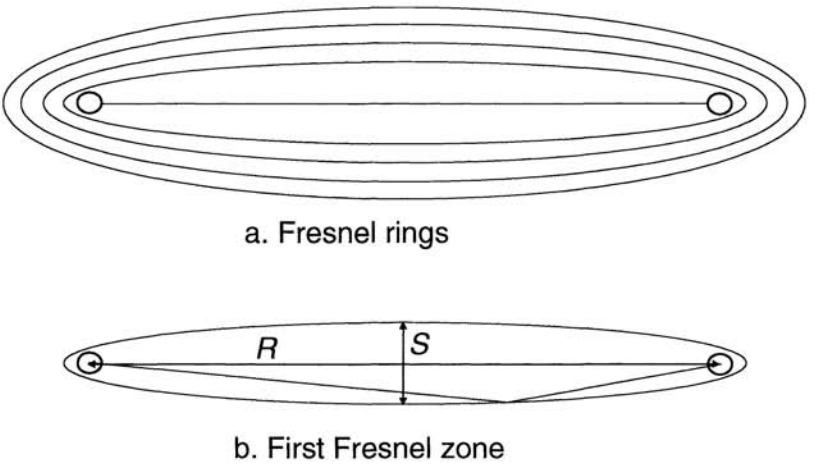

Figure 3-16. Fresnel zones

3.2.6.4 Multiple Screens Diffraction

Propagation at grazing angles over a series of rooftops is modeled by diffraction by a series of screens, as described in Fig. 3-17. The first Fresnel zone between the antenna and the last building edge is shown to capture a number of roofs (shown marked) that depends on the grazing angle θ. The sequential diffraction by the series of screens, all within the first Fresnel zone and constructively combining, determines the strength of the field at the edge where diffraction down takes place [3h].

The field settling coefficient is

$$Q \equiv 2.347\left[\sqrt{d/\lambda}\,(H-h)/R\right]^{0.9} \tag{3-27}$$

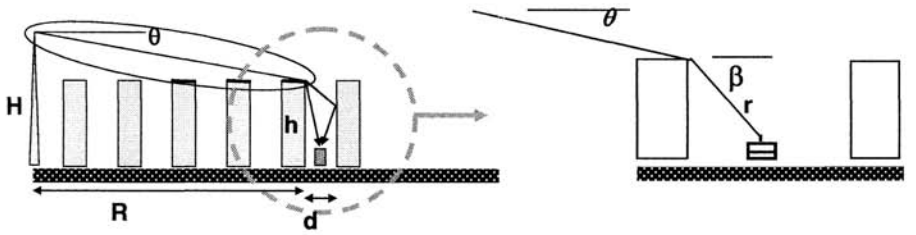

Figure 3-17. Grazing propagation over a series of roofs

within the range $0 < \sqrt{d/\lambda}(H-h)/R < 0.4$, beyond which it settles at $Q \to \approx 1$ and the overall transmission gain through diffraction is, from Eqs. (3-21) and (3-23),

$$\frac{P_R}{P_T} = G_T G_R \left(\frac{\lambda}{4\pi}\right)^2 \frac{Q^2 D^2 \lambda}{2\pi R^2 r} = \frac{11 G_T G_R}{2\pi R^2 r}\left(\frac{\lambda}{4\pi}\right)^3 \left(\frac{1}{2\pi\beta}\right)^2 \left(\frac{H-h}{R}\sqrt{\frac{d}{\lambda}}\right)^{1.8} . \quad (3\text{-}28)$$

The propagation model is presented in Fig. 3-18. The break point is derived by equating $Q=0.4$ in Eq. (3-27), R_{RO} is derived from Eq. (3-19) with the respective diffraction loss.

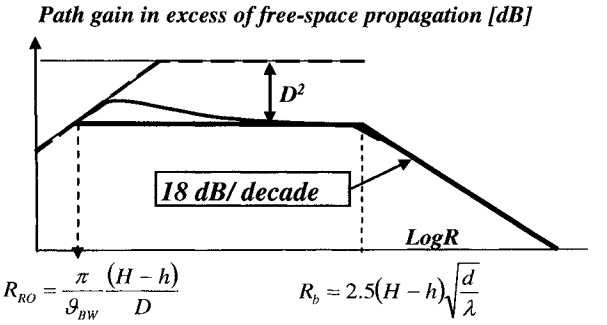

Figure 3-18. Over the roofs propagation model

3. 3 Path-Gain Prediction Models

3.3.1 The Role of Measurement and of Modeling in Channel Characterization and Prediction

The objective of channel characterization is its evaluation at any point within the region, at any time, in terms of its effect on the performance of the wireless communications system. Measurements, though being the measure of the truth, cannot answer this need by themselves, as they only sample the channel in space and in time. Models are used for this purpose. Models may be *heuristic* – mathematical interpolation and extrapolation of measurements, or best match of measurements to *solutions of related physical models* (also called "canonical problems"), or a combination thereof.

Heuristic models – these are statistical models, based on a series of measurement campaigns. They exercise some weighted averaging and

matching to a mathematically convenient model. Because of their statistical nature and the limited data ensemble used to generate them, they tend to best suit the areas where measurements were taken or those with similar structure (e.g. types of buildings and their community arrangement), and better suit large areas, where the statistical averaging suffices. Small areas and specific scenarios are not served well by these predictions. More over, the heuristic models fail to bring any insight, so much needed in analyzing field scenarios.

Canonical problems – these are basic, physically solvable models that aim at simulating a class of scenarios. The whole Section 3.2 is devoted to a selected group of canonical models. The main advantage of these physical models is the insight they provide, enabling parametric extrapolation and prediction. They enable adherence to the major effects in the assessment of the performance and situations.

Canonical models are too simple, however, to represent more complex scenarios. They need calibration by measurements to match parameters. A combination of a few canonical models is needed to interpret and to best predict certain scenarios.

Measurements – the nature of the cellular environment defies exact, repeatable measurement of the channel. The coverage may vary by 10 dB across the street. The complexity of traffic and its time variation brings about similar differences between consecutive measurements in built up areas. Furthermore, the cost of a measurement campaign is defying its frequent and comprehensive usage. Therefore, measurements have a statistical, not accurate, deterministic value. They are best used when serving to validate and to calibrate physically based models. The recent advent of sensors embedded in the mobile equipment, and the channel measurement and reporting inherent in the handsets of the third generation, offers the opportunity for a dynamic modeling of the channel, to serve for dynamic optimization of the service.

3.3.2 Physically Based Prediction Models

COST WI model - this is a model for urban environment, based on the multiple screens diffraction model (Section 3.2.6.4) originated by Walfisch and Bertoni [3h], and Ikegami's corrections for the street orientation. The dependence of diffraction coefficient on the street orientation has been developed by Ikegami and incorporated into the model.

Lee's model – is an extension of the flat earth model (Section 3.2.4) to hilly terrain. A concept of "effective antenna height" is introduced to account for the height of the antenna relative to the local slope of the ground at the mobile location. This is presented in Fig. 3-19. Note that the slopes are exaggerated in the picture – Eq. (3-11) holds for very shallow angles only. Higher angles are in the R^{-2} regime. This justifies the approximation of

measuring the antenna height in the vertical plane and not perpendicular to the ground slope at the mobile.

Urban areas over rolling terrain – Lee's model is extended to consider COST WI for the locality of the mobile. In essence, the terrain relief is elevated to the average roofs' height, and Lee's model is used to establish the effective height of the antenna. The environment around the mobile is taken as locally flat for exercising the COST WI model.

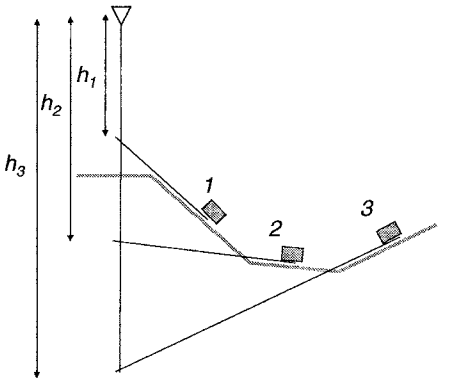

Figure 3-19. Lee's model

Forested area over rolling terrain – the same approach is used: the terrain relief is elevated to the average height of the canopy, and Lee's model used to determine the effective antenna height. The forest model (Section 3.2.5) is applied for the propagation over, and penetration into, the forest.

Ray tracing models – these are more complex models that need a detailed site map, and are therefore site-specific. Ray tracing is a compromise between the simple models and a yet more elaborate electromagnetic modeling. The choice of ray paths is not fully procedural and requires due expertise. Missing rays, or excess rays, may lead to major errors.

Propagation in the street canyon – this has been addressed by multiple ray tracing. Only a small number of rays, typically up to 6, are relevant. Multiple reflections are highly attenuated by the buildings and the interbuilding spacing. The width of Fresnel zone Eq. (3-27) serves to determine the length $R = s^2/2\lambda$ of wall-reflection free propagation. Further rays only modulate this path-gain. This is 1.25 km propagation at the PCS band for a street width (wall to wall) of 20 m. The effective ground level is elevated to the average traffic height in dense traffic situations.

3.3.3 Building Penetration and Indoors Propagation

The penetration to, and propagation inside buildings are complex mechanisms that depend on multiple, site-specific parameters. These may be classified to:

- ✓ Wall and window penetration
- ✓ Propagation within the floor
- ✓ Propagation between the floors

3.3.3.1 Wall Penetration

The building wall is a lossy, finite thickness, dielectric layer. The transmission through the wall depends on the wall dielectric coefficient, its loss and its thickness, and on the direction and polarization of the incident wave. The thickness of outer walls may vary from less than one, to a couple of wavelengths in the PCS band. The contribution of Snell's refraction loss is less than 10 dB for nonmetallic walls, and fluctuates with the incident angle according to the resonances of the wall thickness. It reaches over 20 dB at angles near grazing (propagation along the street). Horizontal polarization (TM waves) have better penetration at low grazing (along the street) because of Brewster angle (Fig. 3-5). Structured walls (e.g. hollow blocks, metal grid) further increase the transmission gain at frequencies above cutoff for the grid structure.

The Ohmic loss through the wall varies from a couple to over 10 dB, depending on the material and wetness.

3.3.3.2 Window Penetration

The window is considered as a receiving aperture, as in Fig. 3-20. Plane wave is incident on the window and penetrates without attenuation to a depth of $d = s^2/4\lambda$, which represents the first Fresnel zone (a parabola in this case of plane wave incidence).

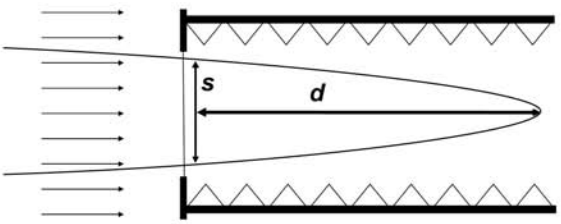

Figure 3-20. Window penetration

Beyond that distance the diffraction of the window edges start interfering with the penetrating plane wave and become dominant at about $d = s^2/\lambda$ (the far field criterion). Further penetration, if not disturbed by objects or walls, can be estimated by

$$w/w_i = (A/\lambda d)^2 (\lambda/2\pi h)^2 \qquad (3\text{-}29)$$

where w is the power density, w_i is the incident power density, A is the area of the window, and h is the distance off axis. The second term is the off-axis attenuation and holds only for $h > \lambda d/4s$, and equals 1 otherwise.

A few conclusions that come out of this analysis:

The window penetration dominates to a distance of $d = s^2/\lambda$. The wall penetration, that is not a diffraction process and does not have the D^{-2} loss, becomes dominant.

- ✓ Both wall and window penetration peak at normal incidence and degrade towards grazing (along the street).
- ✓ The window penetration is directional. Diffusion inside takes place by wave bouncing from the walls and diffracted by objects.

3.3.3.3 Indoors Propagation

The interior of buildings varies widely from large open spaces in malls to densely packed offices. Ray tracing is elaborate, and reliable only to within the contributions of smooth walls, ceilings and floors reflections. An efficient model that lumps all distributed scattering is presented in Fig. 3-21. [12h, Sec. 8.4]. Free-space propagation prevails for a distance $R = H^2/2\lambda$, where H is the height of the layer clear of dense obstructions.

Further out, the diffraction by the series of scatterers, following roughly: R^{-4}, becomes dominant, as per the model described in Section 3.2.6.4.

Additional walls and large obstructions penetrating the clear layer are accounted for by two-dimensional ray tracing.

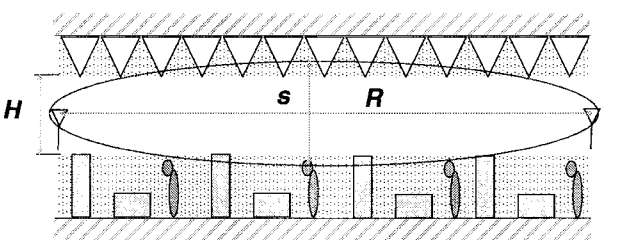

Figure 3-21. Indoors propagation and Fresnel zone clearance

3.3.3.4 Propagation between Floors

Floor penetration follows the discussion in Section 3.3.3.1. The Floor construction is heavier and is steel-grid reinforced, rendering typical loss of 10 to 20 dB per floor. Coupling through windows, of signals reflected from adjacent buildings, may dominate over penetration through multiple floors.

3.3.4 Heuristic Models

Many heuristic models have been proposed, each relating to a specific measurement campaign. They are, by their nature, large area models with a high local standard deviation in built-in areas. These are covered in detail in the reference literature.

Okamura-Hata – is based on a measurement campaign in Japan, in a flat residential area, with antenna high above the scenery. The model specifies a single regression curve $R^{-\gamma}$, γ being fitted to different environments, and antenna height-gain of 6 dB per octave. The near zone – closer than the break point, is not included and may be specified separately.

Ibrahim-Parsons – proposed parameters for the regression curve based on measurements in the UK. They also proposed multi-regression models, where γ varies from one radial section to another according to the clutter type.

Har S-T model – is a single regression curve model based on measurements in San Francisco traversing the city core in a zigzag. The resulting radial regression coefficient is 46 to 47 dB per decade.

3. 4 Multipath and Fading

3.4.1 Impulse Response

Multipath due to scattering events typifies the mobile cellular channel. Users move among other obstacles that scatter the transmitted signal and receive multiple replicas of the signal from different directions and with respective delays. The spatial and timely variations of the signal that influence the communications are therefore best characterized and interpreted by transmitting and observing the propagation of an impulse. Figure 3-22 represents sampled measurements from a campaign conducted by Qualcomm in 1990 [1]. It serves us well in observing certain features of the multipath propagation. The snapshots on the right show the impulse response along the same route, each showing more than one response. The first response is not always the highest, but is the longest in most cases. Stacking these snapshots, taken at 0.3 second intervals, is shown on the left in a "waterfall" display, where the delay is now on the vertical axis, while the base axis is the time march of the mobile along the streets. The "waterfall" reveals a structured

multipath, easily interpreted as emerging from reflections by major buildings en route. Smaller scatterers influence the neighborhood of the mobile and appear as extending the first response cluster.

A model of the scattering neighborhood is presented in Fig. 3-23. The concentric ellipses mark the delay of the response scattered from an object on the ellipse. A scattered contribution from an object diminishes with the square of its distance from either end of the path. The "scattering neighborhood" consists of scatterers within some 100 wavelengths from the mobile, and is responsible for the extended delay and the fast fading of the first response cluster. The shaded backside of the neighborhood comprises both small scatterers and longer delay and accounts for the statistical nature of the multipath, while the large reflectors constitute the structured multipath, as exhibited in Fig. 3-22.

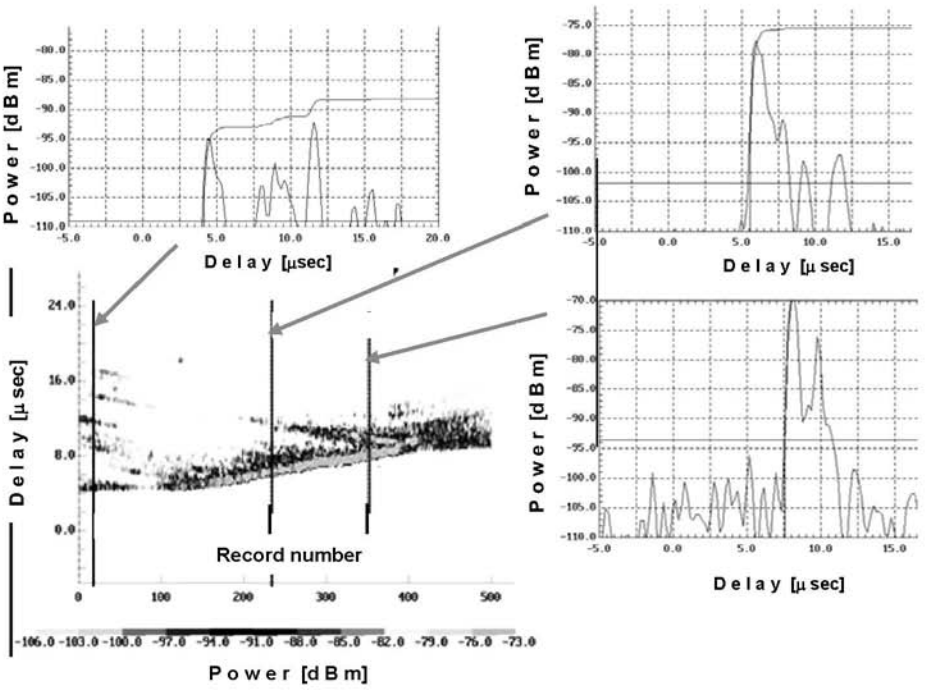

Figure 3-22. A series of Impulse response snapshots, taken by Qualcomm in a measurement campaign in San Diego (1990), and a "waterfall" display of a stack of snapshots along the road

It is important to note that only a small number of scatterers contribute to the "neighborhood", each having a significant scattering cross-section. The scattered contribution of a car, for example, whose typical scattering cross-

section is 5 m^2, positioned 10 m away from the mobile antenna, is 24 dB lower than the signal arriving directly.

It takes tens of such scatterers to build up a nullifying fading. Flat surfaces, on the other hand, are strong reflectors when specularly oriented. Their reflected beam stays collimated to about $R = 0.2d^2/\lambda$, where d is the size of the reflector. Thus, at the PCS band, a road sign 5 m wide beams out 31 m , a building 20 m wide – 500 m, and a large building 50 m wide – over 3 km.

Delay spread is the delay period over which significant returns arrive at the receiver. A conventional definition of the delay spread is the standard deviation of the delay profile.

Relating to Fig. 3-23 one observes that the scattering neighborhood creates a spread that decays roughly exponentially, while additional contributions come from longer delay reflectors. *Angle spread* is that angular extent over which the source is spread due to scatterers. Its conventional definition is the standard deviation of the profile, which for the scattering neighborhood takes a typical shape of Gaussian. Additional contributions arrive from large reflectors at wider angles. Typical values for suburban and rural environments are 1 to 2 μs and 6^0 to 10^0 [12e], respectively. Both increase considerably in dense urban areas and low antennas (see Section 3.6.8.2).

3.4.2 Coherent Time and Coherent Bandwidth

The extent to which a delayed signal adds coherently to create fading interference depends on the signal bandwidth; an impulse, received with an infinite bandwidth, totally resolves the multipath.

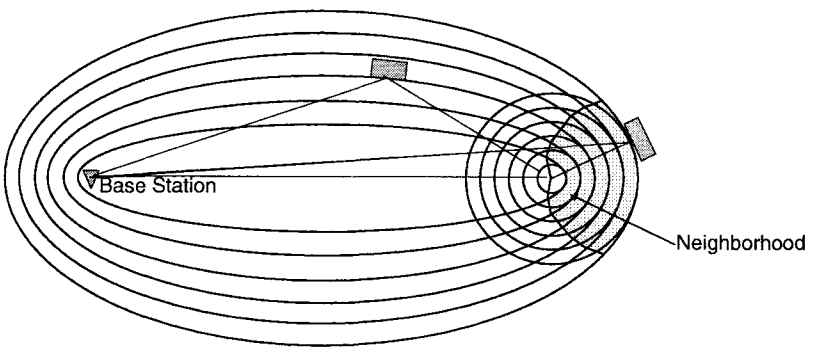

Figure 3-23. The multipath environment

For a CW signal, all these components add up to a single stationary phasor that changes only as the mobile (or the scatterers) move, producing flat fading. A signal with a finite bandwidth B has a time resolution associated with it - $\tau \approx 1/B$.

Signals arriving with a longer delay do not add coherently to the direct path, rather powerwise, thus bounding the depth of the fades of the coherently interfering signals (those within the time resolution window). The out-of-window signals are suppressed altogether in the CDMA correlation receivers ("fingers"), leaving only the coherently interfering constituents enclosed in the time window, and residual noise-like interference[3].

The channel is classified in respect to the signal into the categories described in Fig. 3-24. The dashed line bounds the impossible system zone $TB > 1/2$.

The *coherent bandwidth* of the channel - B_c, is defined by $B_c \tau_{\max} < 1$, where τ_{max} is the largest excess delay of the channel. A signal whose bandwidth is narrower than the coherence bandwidth is not spectrally distorted (no inter-symbol interference) but undergoes flat fading. The typical excess delay in outdoors propagation exceeds 3 μs, bounding the coherent bandwidth to <300 KHz. Excess delay in narrow alleys and small squares, on the other hand, may be limited to 300 ns, with a respective coherent bandwidth of 3 MHz. The excess delay indoors is still shorter, and the coherent bandwidth may exceed 30 MHz.

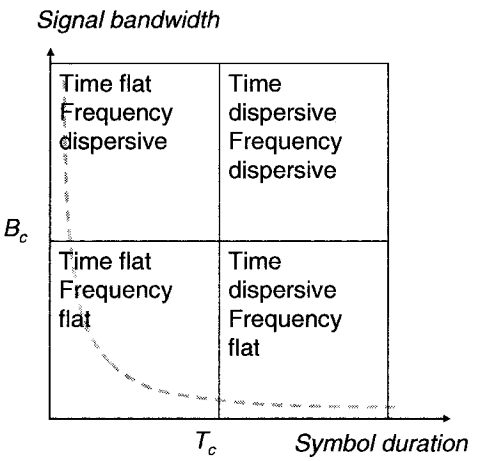

Figure 3-24. Characterization of the channel by dispersion

[3] The correlation receiver has a finite filtering gain. In the CDMA IS95 and CDMA2000 it is 21 dB. Noncorrelated signals appear as noise suppressed by this much.

Note the 1.25 MHz bandwidth of CDMA2000, optimized for the outdoors, while UMTS, 4.5 MHz, maintains shallow fading in more compact environments. The *coherent time* of the channel - T_c, is defined by $T_c f_{D\max} < 1$, where f_{Dmax} is the highest Doppler frequency in the channel. A symbol shorter than the coherence time is not time distorted or dispersed. The coherent time is an important criterion for multipath mitigation – the interleaver coder reorders the transmitted bits so as to spread each symbol over a period exceeding the coherent time, thus creating time diversity. The time limit on the interleaver frame sets a respective minimum Doppler (and rate of motion) below which it is ineffective. At the other end, the coherent time sets the limit on the time slot, and therefore rate of data transmission in scheduled time-multiplex mode (EV-DO, HSDPA).

3.4.3 Fading Statistics

Flat fading of a signal narrower than the coherent bandwidth of the channel is exhibited in Fig. 3-25. The *fast fading*, repeating as frequent as every $\lambda/2$, typically follows Rayleigh statistics for Non Line of Sight (NLOS) propagation. The flat fading is highly frequency dependent. Averaging the fast fading over a window of some 20 wavelengths results in the *sector average* that describes the forward propagation of the total power, and has only a mild dependence of the frequency (per discussion in Section 3.2). It is also called "slow fading", or "shadow fading". It typically follows statistics of Lognormal, with a standard deviation of 8 dB.

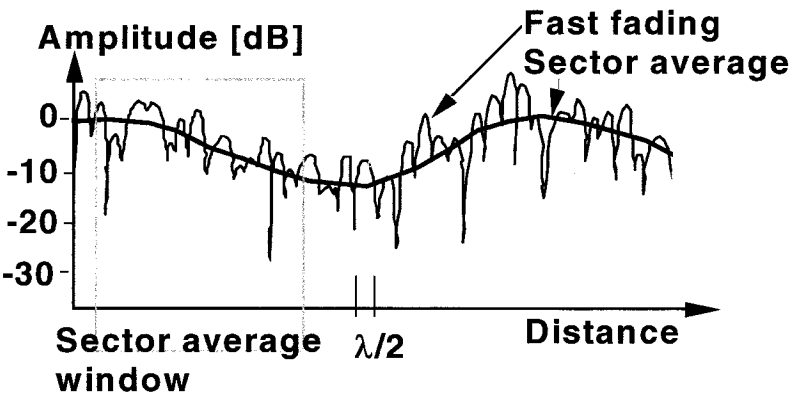

Figure 3-25. Flat fading

The Rayleigh statistics represents a homogeneous ensemble. Its PDF (Probability Density Function) of the signal envelope is

$$p_R(R) = 2R\exp\{-R^2\} \tag{3-30}$$

where R is the signal amplitude normalized to the RMS amplitude. The presence of a strong contributor, as is with a line of sight (LOS) component, is modeled by the Rice distribution. This distribution is nonrational, however. A close fit to the Rice distribution is obtained by the Nakagami-m distribution, which has a rational expression. It reduces to Rayleigh distribution for m=1.

$$p_N(r) = \frac{2}{\Gamma(m)}\left(\frac{m}{\Omega}\right)^m r^{2m-1}\exp\left\{-\frac{m}{\Omega}r^2\right\} \tag{3-31}$$

where $m = \dfrac{\langle r^2\rangle^2}{\left\langle\left(r^2 - \langle r^2\rangle\right)^2\right\rangle}$ and $\Omega = \langle r^2\rangle$.

A presentation of the CDF (Cumulative Distribution Function) of these statistics on a "Rayleigh paper" [11] renders Rayleigh a straight line and higher M in the Nakagami-m distribution – almost straight lines, with steeper slopes. This provides a clear presentation of measurement and analysis, as described in Fig. 3-26.

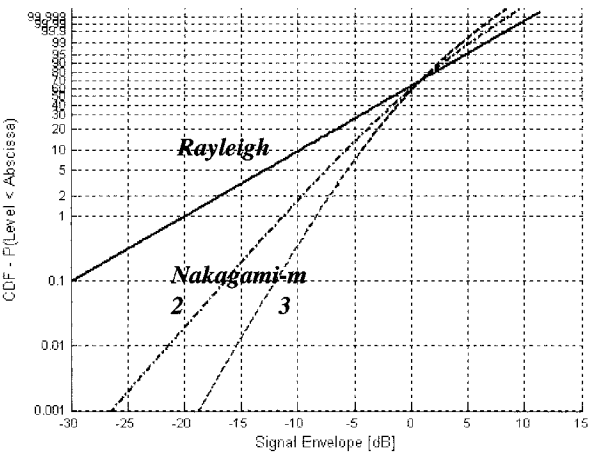

Figure 3-26. Rayleigh paper

This presentation is helpful in online recording and evaluating field measurements. It allows an easy extrapolation of the curve based on the sparse sampling in typical drive tests.

Steeper slopes indicate a dominant contribution – either LOS or strong reflection, and also measure the effect of diversity when the measurement incorporates diversity receivers.

3. 5 Polarization Effects

The difference between TM and TE waves in reflection, refraction and diffraction has been reviewed in previous sections. This section focuses on the depolarization of the wave through propagation, its fading and correlation between fading of waves polarized differently. These serve to evaluate the performance of polarization diversity.

3.5.1 Polarization of Electromagnetic Waves

The sources of electromagnetic radiation are *electrical dipole* and *magnetic dipole*. The radiation pattern of *electrical dipole* is depicted in Fig. 3-30d. It is materialized by a small (infinitesimal) linear oscillating current element, as shown.

The polarization of the wave is defined according to the direction of the electrical field vector, transversal to the direction of propagation. The wave radiates radially away from the dipole in homogeneous media, its flux (radiation density) decreases geometrically as $1/4\pi R^2$ and its polarization does not change. Traveling through nonhomogeneous media may change the direction of the wave propagation – rays are bending when traversing thinner or thicker media (lower or higher dielectric constant) according to Snell's law (Eq. (3-12)), but their polarization does not change.

Magnetic dipole is materialized by a small (infinitesimal) current loop around the virtual dipole. Its radiation pattern is identical to that of the *electrical dipole* but its polarization is orthogonal to that of the *electric dipole*. Antennas are modeled as an ensemble of electrical and magnetic dipoles according to the radiating current distribution, and their radiation is the sum of the radiation emerging from the elemental sources. The polarization of the wave radiated by an antenna depends on its design and excitation, and may be different in different directions, according to the phased combination of all the constituting sources. Reciprocal antennas maintain the same polarization characteristics in the receive mode as in the transmit mode.

A linearly polarized wave is one whose polarization does not change at any point with time. A phasor summation of two linearly polarized waves

creates a wave that is linearly polarized according to the vector summation rule, if the constituting waves have the same phase. In case there is a phase difference, the polarization of the wave at any point (for example – at the receiving end) changes periodically. It becomes *circular polarization* if the two constituents are orthogonal, having the same amplitude, and their phase difference is $\pi/2$ (they are *in quadrature*). The wave is *elliptically polarized* in any other case.

3.5.2 The Depolarization of Electromagnetic Waves

Wave impinging on an interface (as in Fig. 3-4) is partially reflected and partially transmitted through. The reflection coefficient depends on the polarization of the wave relative to the interface surface (TE or TM wave). If the incident wave is not purely either, then the reflected wave, and the transmitted wave, will have different composition of the constituent (TE and TM) waves, and their vector sum results in a different polarization. Diffraction by edges (as in Fig. 3-12) is also different for TE and TM waves. Waves undergoing multiple reflections and diffractions thus change their polarization, and the waves arriving at the receive antenna through multipath undergo fading by their interference, which is polarization dependent. This situation is sketched in Fig. 3-27. Both antennas are modeled as matched to linear polarization, slanted α and β on the transmit and receive sides, respectively. Note that the polarization matching of each antenna is over the angular span of the multipath rays (as described in Fig. 3-23). The depolarization is measured by decomposing the wave into the transmitted polarization and its orthogonal one, and the ratio of time-averaged power between these is termed XPD – cross polarization discrimination. The fading of these two orthogonally polarized components has been measured to be essentially uncorrelated [9a-e]. The histogram of the polarized signal at the receiving end is sketched in Fig. 3-27 as a gray rectangle around the polarization of the incoming signal (α). The ratio of length to width of this rectangle is a measure of the XPD. The area of the rectangle is visited by time-marching polarized signal.

The average signal transfer to the receiving antenna depends on the *polarization matching* (*PM*) between the transmit and receive antennas

$$PM = \cos^2(\beta - \alpha) \tag{3-32}$$

which multiplies the transmission equation (Eq. (3-1))

$$P_R/P_T = T = G_T \cdot G_R \cdot PG \cdot PM \ . \tag{3-33}$$

The cellular wireless environment is not isotropic: propagation is essentially in the horizontal plane, and most obstacles are oriented either horizontally or vertically. The XPD is therefore expected to be polarization-dependent, peaking for V-H polarization. Published reports on measured values for V-H XPD [9e] vary between about 4 dB for indoors to over 15 dB in rural outdoors, averaging between 8 and 12 dB for outdoors.

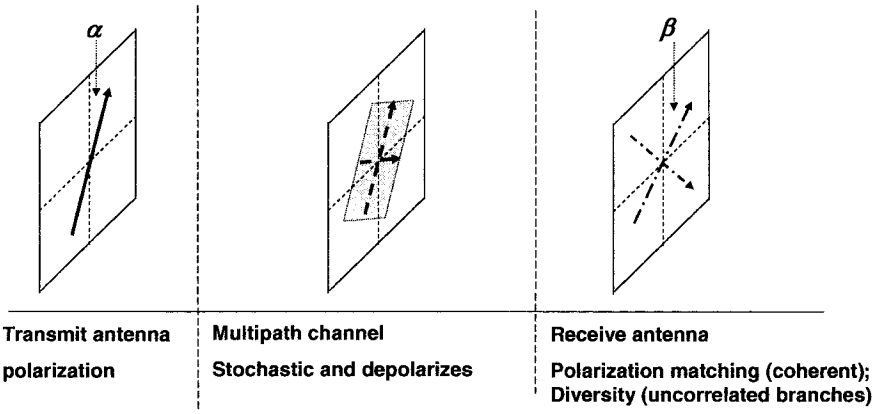

Figure 3-27. Signal transfer through a depolarizing medium

A dynamic measurement over the polarization circle ($0 < \alpha < 90^0$) is reported in [9f-h], showing high XPD values for all angles for suburban environment. It consisted of a dipole rotating in the vertical plane, mounted on a car, transmitting at 1900 and 2000 MHz, and received by V polarized and 45^0 slant polarized base station antenna. The XPD in the suburban environment averaged 9 to 10 dB at both frequencies.

3. 6 Antennas and Coverage

3.6.1 Introduction

The antenna is a linear, passive component in the wireless communications system. It is a transformer between the transmit/receive circuits, which constitutes a controlled environment, and the propagation channel – an environment that shares uncontrolled elements and parameters. As such, it is both a radiator into the propagation channel and a component in the RF circuitry. The antenna system is comprised of the elemental radiators,

that may be connected to an RF beam forming network to form an array, and the beam shaping structure consisting of reflectors or other beam guiding structure. Radome or antenna cover, whose purpose is environmental protection or concealing the antenna, influences both the radiation and the RF impedance of the antenna. Nearby structures also affect the directivity, and may affect the impedance of the antenna.

Its properties on the radiation side:

- ✓ It acts as a directional filter with low pass characteristics, and as a polarization filter. Its directional properties are characterized by the *radiation pattern* (or also termed *antenna pattern*), describing the strength of the radiated power density in each direction; its *directivity*, specifying the ratio of its radiated power density in a given direction to its average radiated power density; its *gain*, the product of the directivity with Ohmic losses within its circuits.
- ✓ Its directional properties are reciprocal when it is matched to the transmit/receive circuit (the same directivity on receive as on transmit). These are frequency dependent.

The RF network:

- ✓ Matches the radiating elements' impedance to the RF circuit.
- ✓ Forms the radiation beam by coherently connecting the elemental radiators with proper amplitude and phase weights (Beam Forming Network - BFN).

3.6.2 Antenna Parameters

Radiation pattern is a plot of the antenna flux density [Watts/ m^2] as measured on a large imaginary sphere with the antenna at its center, or over a circular cut of this sphere.

Beamwidth is the angular separation between the half-power points on the major lobe of the radiation pattern. It is an approximate representation of the radiation pattern by the shaded arc in Fig. 3-28. It is to be recognized that this approximation contains about 25% excess power in the higher 3 dB zone, but it does not account for the power out of the arc in the lower part and the side lobes, which is higher.

Beam area is the (Steradian) angular area that the half-power of the beam captures over the measurement sphere. This is approximated by the product of the beamwidths (*Radians*) in two cardinal planes, e.g. Az, El $B(Steradian) \approx B_{AZ} B_{EL}$.

Directivity is the ratio of the flux density in a given direction to its average over the whole radiation sphere. Maximum directivity – in the direction of the maximum flux density, is also called the directivity of the antenna

$$D(\vartheta,\varphi)=\frac{S(\vartheta,\varphi)}{P_{rad}/4\pi}=\frac{4\pi S(\vartheta,\varphi)}{\int_0^{2\pi}d\varphi\int_0^{\pi}S(\vartheta,\varphi)\sin(\vartheta)d\vartheta} \tag{3-34a}$$

$$D(\vartheta,\varphi)\big|_{\max}=\frac{S(\vartheta,\varphi)\big|_{\max}}{P_{rad}/4\pi}\cong\frac{4\pi K}{B(Steradian)} \tag{3-34b}$$

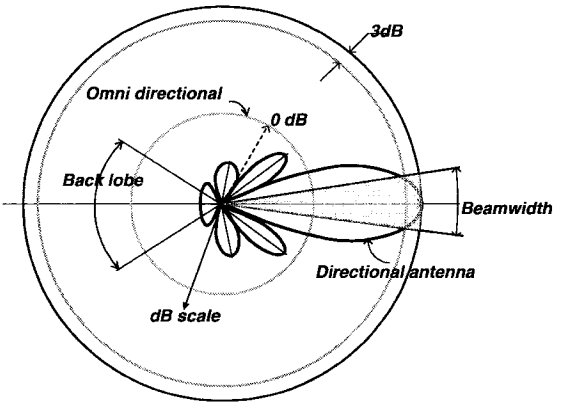

Figure 3-28. Radiation pattern

where $S[Watts/m^2]$ is the flux density and P_{rad} is the total radiated power. K is a correction factor to account for the power in the beam slopes and the sidelobes.

$0.63<K<0.85$ for different antenna practices. For an average $K=\pi/4=0.785$, the directivity of the antenna is

$$D=\frac{\pi^2}{B_xB_y}=\frac{32{,}400}{B_xB_y(Deg^2)} \tag{3-35a}$$

and for a circular beam it is

$$D=\frac{4\pi}{B^2}=\frac{41{,}253}{B^2(Deg^2)}. \tag{3-35b}$$

Gain - $G=\eta D$ where η is the power efficiency of the antenna, accounting for Ohmic losses $\eta=P_{rad}/P_{in}$, P_{in} being the power fed to the antenna terminals.

Isotropic antenna is an imaginary antenna that radiates with uniform intensity in all directions. Its directivity is D=1 (=0 dBi).

EIRP(θ,ϕ) – Effective Radiated Power, is the equivalent power that an isotropic antenna would have radiated to achieve the same flux density in a chosen direction

$$EIRP(\vartheta,\varphi) = P_{in}G(\vartheta,\varphi). \tag{3-36}$$

Boresight is the direction of the maximum directivity at the peak of the main beam. Antennas are aligned according to their boresight[4].

Front-to-back ratio is the ratio between the maximum gain of the antenna (peak of the main lobe) and the highest peak in the rear (usually taken over $180^0 \pm 30^0$).

Antenna phase center is the location in or near the antenna that constitutes a center for the measurement sphere, such that the phase of the measurements does not change over the main beam.

In *Antenna bandwidth*, the definition of bandwidth depends on the parameter of interest and the change specified: beam shape, input impedance, phase center, etc.

Antenna Polarization. The antenna is built to match one polarization state (e.g. linear vertical, linear slant, right-hand circular, elliptical, etc.). The degree of match (for a receive antenna – this is the match with the polarization state of the incident wave) is presented by the parameter *PM* (Eq. (3-32)).

3.6.3 Gain of an Aperture Antenna and the Sidelobe "Skirt"

The directivity of a uniformly illuminated aperture d is

$$D = kd\left(\frac{\sin(u)}{u}\right)^2 \tag{3-37}$$

where $u = 0.5kd\sin(\vartheta)$. The envelope of the sidelobe "skirt" is $Skirt = kd/u^2$. Other illuminations that have a faster decay "skirt" use the aperture less efficiently and render lower gain. Thus the trends for *cosine* and *cosine*^{2} illuminations are u^{-4} and u^{-6} respectively. The "skirt" for a uniformly illuminated aperture is shown in Fig. 3-29.

[4] The term "boresight" is borrowed from gunnery, where it defines the axis of the gun barrel.

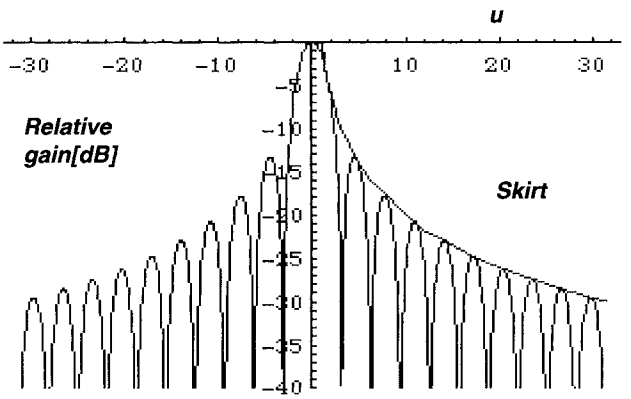

Figure 3-29. The sidelobe "skirt" for a uniformly illuminated aperture

3.6.4 Wave Field Regions

The transmission equation assumes that the antenna is a point source, and the radiation flux is described by a product of a radial function (the geometrical expansion R^{-2}) and the angular dependence, described by the radiation pattern. These conditions prevail far enough from the antenna. The field interaction with the antenna is more complex closer to the antenna.

Far field is the zone where the assumptions of the transmission equation prevail. The criterion for the far field is

$$r > \frac{2d^2}{\lambda} \tag{3-38}$$

where d is the largest dimension of the antenna aperture. This value is set so that the first null, between the main lobe and the first lobe, is 23 dB deep. Note that antennas with elliptical beam may have different far-field distance for each cardinal plane. Also note that the *electrical aperture* of the antenna extends beyond the physical structure for traveling wave antennas (e.g. Yagi antenna).

Fresnel zone – the geometrical near field is a transition zone where the beam that starts out of the antenna as a collimated beam up to about $r_c<0.2d^2/\lambda$, diverges to its radial lobes pattern in the *far field*. The phase center does not hold in this zone, as the phase fluctuates across the measurement sphere.

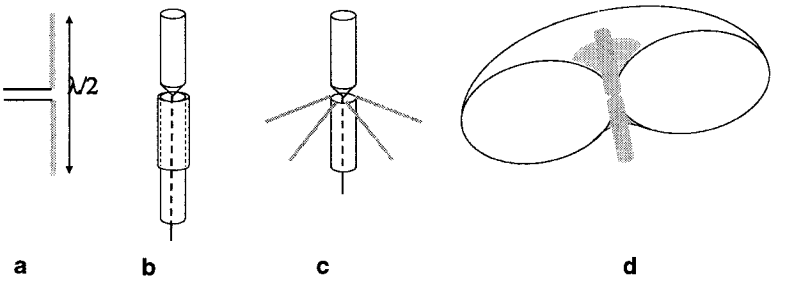

Figure 3-30. Dipole antenna embodiments and pattern. a. *Dipole* b. *Sleeved dipole* c. *Ground-planed monopole* d. *Radiation pattern*

Near (induction) field is the region close to the antenna where significant non radiating magnetic and/or electric fields prevail and may interact with other objects, and influence the antenna impedance and radiation pattern.

$$R<5\lambda \text{ for } d<4\lambda, \text{ and } r/d < 0.62\sqrt{d/\lambda} \text{ for } d > 4\lambda. \quad (3\text{-}39)$$

3.6.5 Dipole Antenna

3.6.5.1 Dipole Pattern

Dipole is the elemental radiator. Its radiation pattern is described in Fig. 3-30d. It is omnidirectional in a plane normal to the dipole, and nulls along the dipole axis. The directivity of a $\lambda/2$ dipole is 2.16 dBi.

3.6.5.2 Transmission Gain between two Dipoles

The transmission gain between two dipoles is of interest for assessing the coupling between handsets and access nodes, and for spurious coupling between antennas on the BTS tower. This is depicted in Fig. 3-31, and presented in Eq. (3-40):

$$T = \frac{G_1 G_2}{(d^2 + h^2)}\left(\frac{\lambda}{4\pi}\right)^2 = \left(\frac{3}{8\pi}\right)^2\left(\frac{\lambda}{R}\right)^2 \cos^3 \vartheta . \quad (3\text{-}40)$$

3.6.6 Colinear Arrays

A colinear array is a linear array of dipoles phased to radiate broadside omnidirectionally. The directivity of a colinear array is

$$D = 2d/\lambda \quad (3\text{-}41)$$

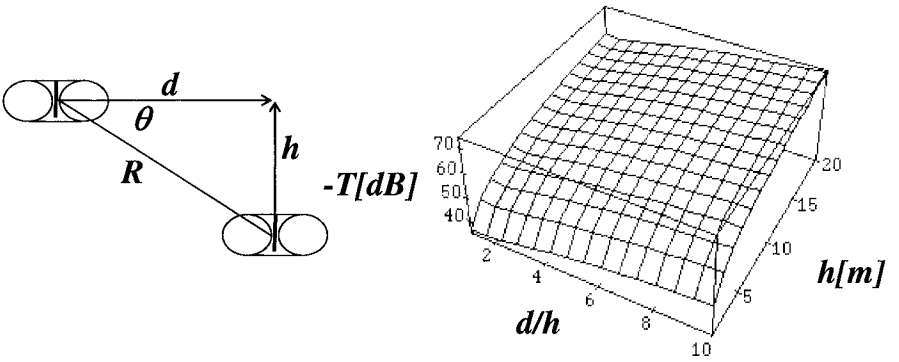

Figure 3-31. Coupling between two dipoles

where d is the array length. The directivity of a sector antenna whose azimuthal beamwidth is θ^0 is then

$$D = \frac{720}{\theta[\text{deg}]} d/\lambda \,. \tag{3-42}$$

3.6.7 Coverage Shaping

3.6.7.1 Introduction

The coverage is defined by the flux density over the service area. The coverage design is concerned about ample flux in the area dominated by the desired cell, limited overlap area for Soft Handoff between cells, and Softer Handoff between sectors, and high isolation thereafter. Similar considerations rule the coverage design of repeaters. The tools for coverage design are the antenna location, beam shape and orientation. Outdoor coveage is illuminated over a relatively small range of elevation angles from the horizon downwards, while the horizontal beamwidth is typically wide, omnidirectional or covering a sector. The following discussion treats first the range control that is governed by the antenna height, gain and beam tilt.

3.6.7.2 Antenna Height

The transmission gain for the flat earth model, Eq. (3-11), renders a trend $R \propto \sqrt{H}$.

The break point distance (Fig. 3-8) depends linearly on H, as from Eq. (3-8), $R = 4Hh/\lambda$, and on the frequency. The antenna height in this context is the "effective height" in Lee's model (Fig. 3-19). The relevant height for antennas covering clutter – buildings, or forested areas, as in Figs. 3-17 and 3-11, respectively, is the height over the average height of the clutter. Lee's model applies for clutter covered rolling terrain, with the height measured relative to the clutter.

A limited coverage and high isolation from adjacent cells is of interest in Microcell or an embedded repeater. A lower antenna height provides a limited coverage and also higher isolation, as the R^{-4} regression starts closer to the antenna. This scenario is illustrated in Fig. 6-7, showing that the steeper slope of the transmission gain creates a sharper boundary with the surrounding cell.

Directive antennas are used in advanced coverage design, as discussed later in this chapter. Their use depends on the antenna height above the clutter. The horizontal pattern of the antenna is diffused by the clutter. The scattering neighbhood (Fig. 3-23) around any point the wave impinges on the clutter is confined to some 100 wavelength. The smearing effect is thus negligible for antennas positioned high above the clutter, but becomes significant for antennas skimming the clutter, where the clutter is illuminated closer to the antenna. The benefit of high directivity, and pattern nulling, as in adaptive antennas, is diminished in these scenarios.

The footprint of the antenna is not sensitive to the exact location of the antenna, for antennas positioned high above the clutter, free of nearby major reflectors. The *antenna pattern and orientation* determine the footprint. The situation is different for antennas positioned in the street below the building height. The multiple reflections around the antenna determine the resulting footprint more than the antenna pattern. Moreover, the resulting pattern is highly sensitive to the interaction of the antenna with the nearby walls. The *location of the antenna* is the critical parameter in these cases.

3.6.7.3 Beam Tilting

The confinement of the footprint to the desired coverage is a prime objective in the cellular networks, where the reuse of the channel resources is the measure of capacity. A high transmission gain slope is a means for obtaining the isolation and constraining the Soft Handoff zone. The asymptotic slope in the outdoors is R^{-4}. Further control of the transmission gain slope is obtained by tilting the beam down to capture the desired coverage and increase the isolation further out.

The effect of tilting the beam is demonstrated in Fig. 3-32. A PCS band sector beam with elevation beamwidth of 6^0 is positioned 30 m above the ground. The curves are drawn over the peaks of the ripple ("lobing"). The transmission gain for beam tilt of half (3^0), full and 1.25 beamwidth are

shown to increase the slope for tilt up to one full beamwidth, where additional 20 dB/decade is achieved. A recession of the break point takes place along with the increase of the slope: 4 dB for half beamwidth and 6 dB for full beamwidth. The peak transmission gain increases by 12 dB for a full beam tilting, providing higher flux density within the coverage area. Over tilting beyond the full beamwidth creates a sharp null, but a much shallower slope outwards.

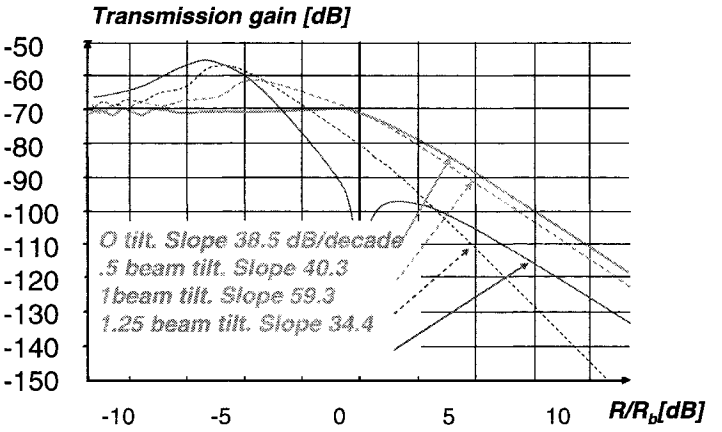

Figure 3-32. The effect of beam tilting on the transmission gain

Beam tilting can be applied either mechanically or electrically. Mechanical beam tilting does not change the antenna pattern, in its own coordinate reference. However, it changes its footprint on the ground, as the footprint is a cut in the radiation envelope by a plane that is tilted upwards from the equator plane. There is no resulting change at 90 degrees sideways off the boresight, while the gain at the boresight projection is reduced.

The main beam thus widens, and takes the form of a "bean" when the tilt exceeds full beamwidth, creating a dip on the boresight.

The backlobe shoots upward respectively. Electrical tilt, on the other hand, involves a change in the phasing of the vertical aperture, and thus the whole pattern tilts around the vertical axis of the antenna. Phasing the aperture may have adverse effects on the vertical cut of the antenna radiation envelope ("vertical pattern"), increased sidelobe level, and mainly – grating lobes rising at large vertical angles. These may be large enough to reduce the antenna

gain. These limit the range of applicable electrical tilt. Typical cellular access antennas are built with radiating element spacing of about 0.8 wavelengths, which limits the tilt to less than one beamwidth.

Beam tilting is a very effective means of coverage control. This is especially true for CDMA, where the cell boundary "breathes" and balancing is required to follow changes in the distribution of load throughout the network. Remotely controlled electrically tiltable antennas (RET) allow for controling the coverage and balance throughout the network at a minimal operatioal cost. Combined with means for remote field-probing of the network, emerging with the 3rd generation mobile units, this offers an opportuinity for responsive optimization of the network, as discussed in Section 4.9.

3.6.7.4 Beam Shaping and Steering

The capacity in a CDMA cell increases by narrowing the sector width, as this reduces the interference within the cell and allows for a higher density of users. Control over the sector width, controlling the EIRP in a nonuniform sector and matching the boundary with adjacent cells require more degrees of freedom, which are obtainable with multi-element, larger aperture antennas. These antenna arrays, together with their *beam forming network (BFN)* and associated control, fall into the generic category of *smart antennas*. These include *phased arrays, multibeam arrays, combination thereof, and adaptive beam-forming* that involve the detection process. The objective of the "smart antenna" in a CDMA cell is to minimize the interference by reducing the beamwidth (maximizing the gain) and reducing the sidelobes' level relative to the angular distribution of the interference sources. The size of the antenna array is found to be the limiting factor – for its appearance, weight and wind-load, and limits the level of the sidelobes' suppression. Four to eight-column arrays are the practical limit for the cellular frequencies, with minimum beamwidth of 30 and 15 degrees, respectively.

The schematics of beam steering, beam switching, multibeam and coverage shaping arrays are sketched in Fig. 3-33. The beam in Fig. 3-33a is steered during the coverage adjustment, or adaptively in conjunction with radio resource and network parameters, or in conjunction with the detection process in "smart antenna".

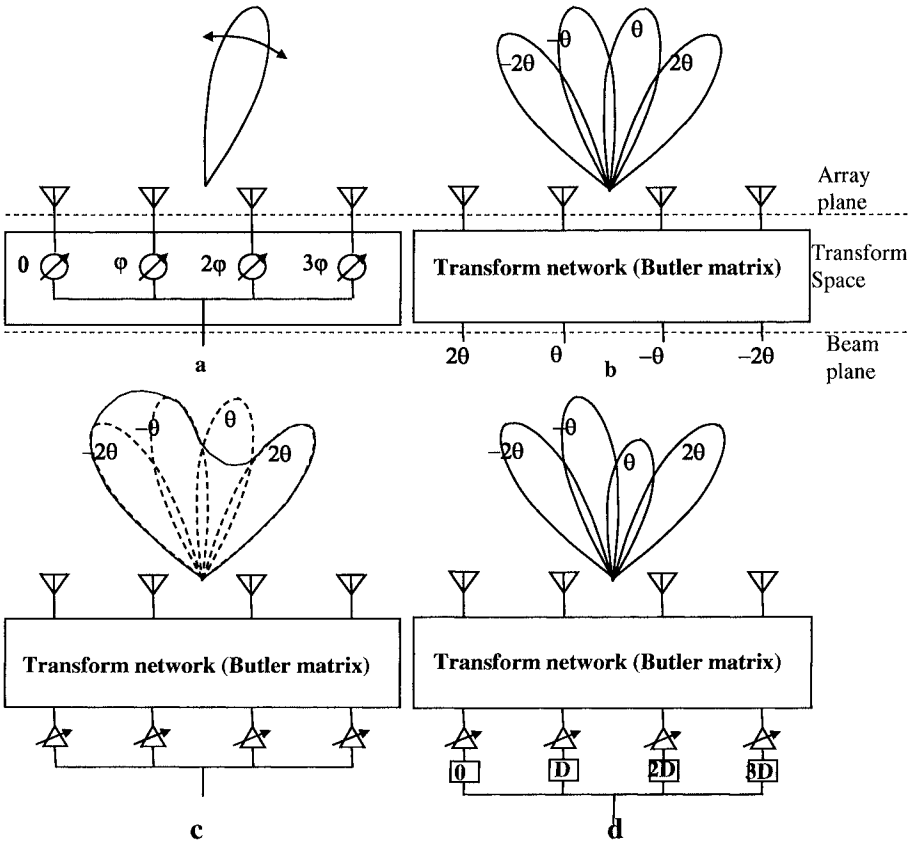

Figure 3-33. Coverage shaping antennas. a. Phased (beam steering) array b. Multibeam (or beam switching) array c. Coherent combined array - "sector shaper" d. Diversity combined array - "sector sculptor"

Each of the beam ports in the multibeam array in Fig. 3-33b is connected to a separate transceiver, in which case it forms a rosette of narrow sectors, or a single transceiver is switched between the beams, acting in a steering/ adaptive mode. Weighted coherent combining of the beams in the multibeam array (Fig. 3-33c) serves to shape the sector coverage [10a]. Beams' decorrelation is applied in Fig. 3-33d [10b] by introducing different delays in each of the beam ports, thus smoothing the coverage and introducing angle diversity between the beams.

A combination of two 60^0 steered beams, spaced to provide space diversity with a delay inserted between them [9c], enables both alignment and width adjustment of the sector coverage, while providing space diversity.

3.6.8 Antenna Diversity

3.6.8.1 Macro and Micro Diversity

The time and space variability of the channel is one of the greatest challenges of the wireless mobile communications. The service area and activity are neither controllable nor predictable to a degree enabling a structured smoothing of the channel over time and space. The system resorts to statistical mitigation means, by seeking alternative channels whose fading have as little correlation with one another as possibly achievable, and optimally combining them. The diversity gain depends on the decorrelation between the antennas, and the balance of the average level of signals received by them. The diversity techniques and processing are discussed in Chapter 5. Here we address the methods of creating diversity paths with antennas. Each of the diversity paths has to be differentiated by the system in order for diversity combining or selection to take place. Separate antennas, or antenna ports, are needed to receive or transmit diversity paths that rely on antenna characteristics. These pertain to direction of arrival and polarization, which involve phase (or equivalently short time delay) between the signals at the diversity antenna ports, and refers to *flat fading*. Time delay between paths is resolved by the rake receiver in the CDMA system when exceeding one or more signal chips. These are then diversity-combined. This process does not require separate antennas. The characterization of the mobile channel was discussed in earlier sections of this chapter.

It was categorized to path-loss (loosely called *slow fading*), and fast fading. The path-loss counts the forward scattering and direct propagation to measure the average signal, while averaging over the fast fading. This is typified by Lognormal statistics, with relatively long correlation distances and coherent time, and thus serves as a data base for planning. The fast fading, on the other hand, fluctuates over a period of half a wavelength and up to hundreds Hz.

The diversity means for *slow fading* is called Macrodiversity, and incorporates the capture of independent rays beyond the correlation distance. Macrodiversity is accomplished by linked remote access nodes: adjacent cells, remote sectors and repeaters. The signal combining depends on the nature of the link between the access nodes. It is selection diversity in most cases. Colocated diversity means are designed to mitigate fading created by coherent interference between multipath. These are highly dependent on the frequency and on the antenna configuration.

3.6.8.2 Space Diversity

Physical interpretation. Consider two antennas, spaced apart a distance d in the antennas' plane, as in Fig. 3-34. Multiple coherent sources impinging from different directions create at the antennas' plane an interference pattern between their respective wave fronts ("interference fringes"), which changes with time according to the motion of the sources. The signal received by each antenna depends on the amplitude of the interference pattern at the antenna location. The received signal fluctuates in time ("signal fading") according to the motion of the sources and the respective change in the interference pattern. Two such sources are depicted in Fig. 3-34, conveniently places at an angle ϕ around the line perpendicular to the antennas' plane, in which case the interference pattern creates periodic peaks and nulls across the antennas' plane. The correlation between the signals received by the antennas from this source pair decreases as the spacing d between the antennas grows to its optimal length $d = \lambda/2\varphi$, where the signal peaks at one antenna when it nulls at the other.

Further insight is gained by considering the antenna pair as forming a beam (phased array). The first null of this beam is at $\varphi = \lambda/2d$. This means that when the beam is pointing to a direction ϕ, the direction of one source, the null is at $-\phi$, the direction of the other source.

Correlation coefficient. While the two-source example illustrates the interference fringes, the scattering environment is more complex. It is portrayed in Fig. 3-34 by a neighborhood of scatterers encircling the source, which represents a typical environment for the diversity antennas of an elevated BTS (see Fig. 3-23) that views that distribution through a limited angle 2ϕ.

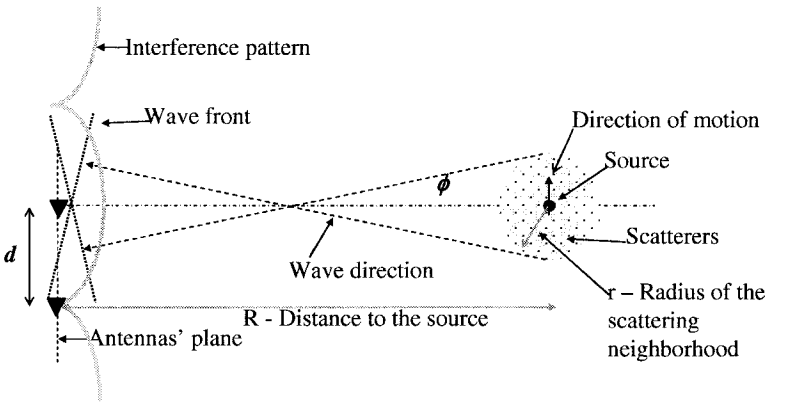

Figure 3-34. Interference pattern at the antenna plane form a distributed source

This angular distribution of sources, $S(\phi)$, is called the *angular spread.* The mobile, on the other hand, is surrounded by scatterers, and its *angular spread* is omnidirectional.
The correlation between two antennas spaced a distance d apart is

$$\rho \equiv \frac{1}{2\pi} \int \frac{G_1(\varphi)}{G_{1\max}} \frac{G_2^*(\varphi)}{G_{2\max}^*} S(\varphi) e^{jkd\sin\varphi} d\varphi . \tag{3-43}$$

Mobile unit (ST). This is evaluated now for G=1 (Omnidirectional antennas) and uniform angular distribution of sources. The correlation between antennas embedded in scatterers, as a mobile unit in urban environment, is represented by a uniform distribution encircling the antenna pair

$$\rho = \frac{1}{2\pi} \int_0^{2\pi} e^{jkd\sin\varphi} d\varphi = J_0(kd). \tag{3-44}$$

The Bessel function of zero order J_0 does not exceed 0.5 beyond $d/\lambda = 0.3$. It reaches its first null at $d/\lambda = 0.38$. Further away it behaves as $\rho \cong \frac{1}{\pi}\sqrt{\frac{\lambda}{d}}\cos(kd - \pi/4)$. The correlation distance in this fading environment is thus smaller than 0.3 wavelength.

Base station. The base station antennas view the neighboring scatterers around a source through a limited angle, as in Fig. 3-34. For a uniform distribution of sources over this angular range

$$\rho = \frac{1}{2\varphi} \int_{-\varphi}^{\varphi} e^{jkd\sin\varphi} d\varphi = \frac{\sin(kd\sin\varphi)}{kd\sin\varphi} \cong \frac{\sin(kd\varphi)}{kd\varphi} . \tag{3-45}$$

The *Sinc* function reduces to 0.5 for $d/\lambda = 0.6/2\varphi$ and reaches its first null at $d/\lambda = 1/2\varphi$. Now recall from Fig. 3-34 that $\varphi = r/R$ to obtain the relation for optimal spacing

$$R/2r \geq d/\lambda > 0.6\,R/2r . \tag{3-46}$$

Antenna height dependence. The optimal spacing d has been found experimentally to increase with the antenna height above the scenery [7a]. A linear relation $\eta \equiv h/d$ has been recorded experimentally over the practical range in urban and suburban areas, and the recommended value is $\eta = 11$. The

physical rational behind this is illustrated in Fig. 3-35. The scattering neighborhood around the mobile unit, which constitutes the bulk of the *angle spread*, consists of the surrounding structures. The lower the antenna is above these and closer to grazing their roofs, the broader is the illuminated scattering area. The linear relation is an approximation only. At near and below grazing (BTS antenna at or below the average roof tops) the propagation and scattering regime changes, as discussed in Section 3.2.6.4.

Ripple effect. So far we have considered omnidirectional antennas in Eq. (3-43). Gain difference between the antennas reduces the diversity gain, as the signal in the weaker antenna may not be able to recover a deep fade of the stronger one. Gain differences occur between antennas with different gain, between antennas pointing in different directions and between antennas closely coupled, enough to change their pattern. The impact of coupling between two side-by-side long colinear arrays is to create ripple in the omnidirectional pattern [8a, b]. This ripple is bound, for very long arrays, by

$$Ripple[dB] < 20Log\left|\left(1-\frac{1}{2\pi}\sqrt{\frac{\lambda}{d}}\right)\Big/\left(1+\frac{1}{2\pi}\sqrt{\frac{\lambda}{d}}\right)\right| \qquad (3\text{-}47)$$

which is plotted in Fig. 3-36, showing that at a spacing of 8λ the ripple is 1 dB. Diversity reception between two sector antennas is effective only over a limited zone, where the Softer Handoff is active, and the gain difference between the antennas is lower than about 6 *dB*.

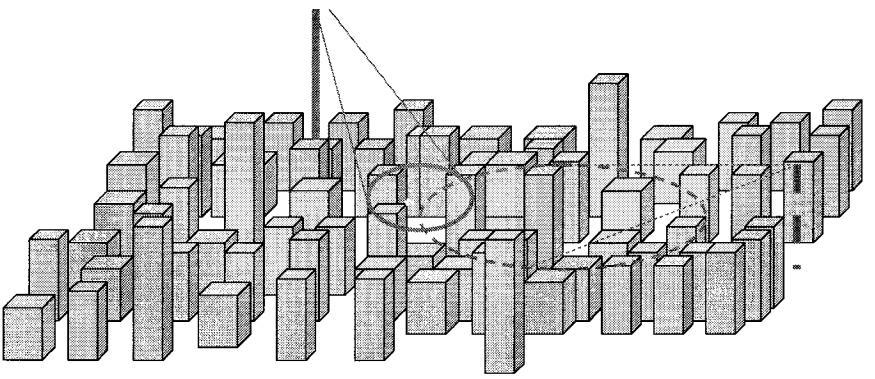

Figure 3-35. Scattering neighborhood vs. antenna height

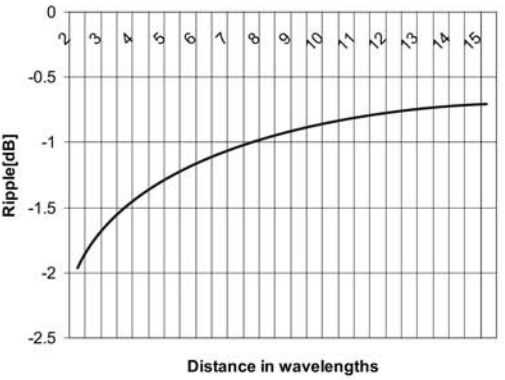

Figure 3-36. Pattern ripple in side-by-side omni antennas

Vertical spacing. Whereas vertical spacing is a common practice in long range Point-to-Point links, it is ineffective in the cellular regime. The angle spread in the PTP is vertical, resulting from atmospheric layering, and the corresponding space diversity is vertical. The scattering environment, as viewed by the BTS, is essentially horizontal. The horizontal angle spread is by far wider than the vertical one, as shown in Fig. 3-37. An example will serve: h=30 m; R=1000 m; r=100 m θ_H=200/1000=0.2 rad; θ_V=30/200-30/1000=1/200=0.005 rad; θ_H/θ_V=40.

An exception to this rule is a scenario of BTS below the average roof top, where the reflections from the building are highly directional. The same is true for the diversity at a mobile embedded between buildings, where the vertical angle spread is appreciable.

3.6.8.3 Angle Diversity

This technique originates from tropo-scatter communications, where highly directive antennas are used to focus on different sections of the scattering troposphere, thereby receiving an independently fading signal.

This situation is not typical to the outdoors cellular environment, however, where the angle spread of the scattering sources is much narrower than the beamwidth of a practical base station antenna. The best to be done in this situation is to match each of the branch beams to receive the angle spread over a different slope of its pattern, or to adaptively steer a beam to receive over a slope of its pattern that maximizes the signal. Two beam positions are compared for selection or combining. A "monopulse" beam forming, comparing sum and difference of two squinted beams that overlap at about half beamwidth, is one example of implementation. An equivalence to space diversity antenna pair is illuminating: equal-gain combining, as in Fig. 3-38,

forms a manifold of receiving beams. Minimum correlation between the antennas over this angle spread occurs when the angle spread spans from the peak of a beam to its null, $d = \lambda/2\varphi$, as shown in Fig. 3-34.

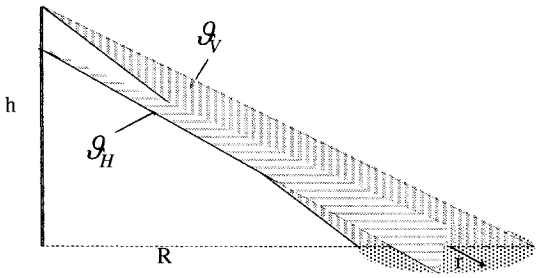

Figure 3-37. Vertical vs. horizontal spacing footprint

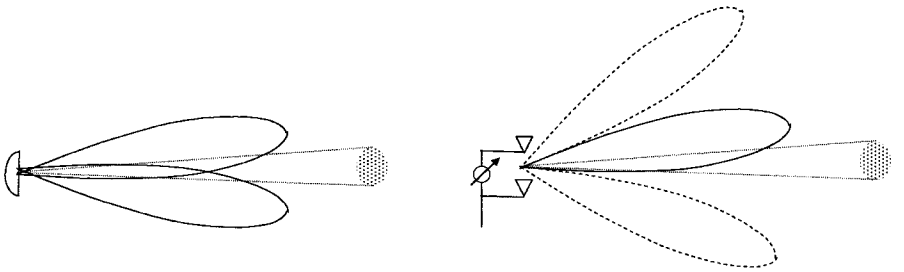

Figure 3-38. Equivalence of angle diversity to equal-gain combined space diversity pair

The aperture size to support such a beamwidth is $d = \lambda/\varphi$, twice the spacing between the antenna pair. The optimal aperture size is then

$$R/r \geq d/\lambda > 0.6R/r\,. \tag{3-48}$$

This sets a clear measure of the effectiveness of angle diversity in a cellular sector; any practical aperture is too small to provide an appreciable diversity gain. It does provide a high coherent gain, however.

3.6.8.4 Polarization Diversity

The transmission path has been shown in Section 3.5 to partially depolarize the wave, and the fading of multipath summation at the receiver are independent for the orthogonal polarizations. This triggers the concept of

polarization diversity: receiving (or transmitting) in two orthogonal polarizations, and diversity-combining the branches. The high XPD prevailing in many environments does not explain the resulting diversity gain that depends on the balance between the branches.

Experiments show [9f-h] that the diversity-combining circuits act effectively as polarization matching circuits in such cases, while operating as benign diversity combiners in low XPD situations. This draws a neat analogy to space diversity antennas, where a coherent gain is advantageous for angular spread smaller than the beamwidth formed between the diversity antenna pair, while uncorrelated diversity gain is higher for angular spread larger than the beamwidth.

Branch balancing has been discussed [9f-h] by electronically rotating the polarization of the antenna pair so that $\alpha - \beta = \pm 45^0$. While balancing the branches in this way, the correlation between the branches grows too. It has been shown not to exceed 0.7, however, which favorably trades-off this configuration for low XPD. Note that for a proper electronic rotation of the polarization, the two orthogonal antennas have to share the same phase center, otherwise generating elliptical polarization.

3.6.9 Antenna Noise Temperature

3.6.9.1 Antenna Temperature and G/T

Both natural and man-made sources emit electromagnetic radiation that interferes with the desired communications. The distributed interference radiation picked up by the receiving antenna is referred to as the noise contributed by the antenna to the receiving system. The source of the natural radiation is thermal and is measured in terms of temperature, and the antenna-contributed noise is therefore termed *antenna temperature* T_a.

$$T_a = \frac{1}{kB} \iint G(Az, El) \cdot n(Az, El) \cdot dAz \cdot dEl \tag{3-49}$$

where k is the Boltzmann constant, B is the receive bandwidth [Hz], the temperature is measured in Kelvin, and n is the noise flux density. Evidently, in case the noise flux is uniform, n=*const.*, the antenna temperature is independent of the antenna gain. With Eq. (3-32) one obtains:

$$T_a = (Beam - Area) \cdot G \cdot n / kB = 4\pi n / kB \,. \tag{3-50}$$

G/T is a term used for assessing the received signal to noise of a given antenna

$$S/N = (EIRP \cdot PG/kB) \cdot (G/T) \tag{3-51}$$

where *EIRP* is the EIRP of the desired signal source that the antenna is receiving, and *PG* is defined in Eq. (3-1).

3.6.9.2 System Noise in the Cellular Service

The antenna collects thermal noise and interference in addition to the desired signals. The ground temperature is 293^0K while the sky is 5^0K. Antennas in the cellular service that are directed horizontally and skim the clutter collect ground noise by the lower half of the antenna beam, and the antenna noise temperature is 146^0K (*NF*=-3 dB). This adds to the receiver noise.

$$NF_{System} = 10Log\left(10^{\frac{NF_{Receiver}}{10}} + 10^{\frac{NF_{Antenna}}{10}}\right) \tag{3-52}$$

Man-made interference in populated areas increases the background noise and the respective antenna temperature. Table 3-1 classifies the background interference and respective antenna temperature.

By tilting the receive beam one beamwidth down, the antenna temperature increases by about 3 dB. The effect on the systems noise of tilting the antenna one full beamwidth down depends on the antenna noise. This is plotted in Fig. 3-39 for a receiver with noise figure 5 dB. It shows that the effect of tilting reaches additional 3 dB only in a noisy urban environment.

Table 3-1. Man-made antenna noise classification

Zone	Antenna NF	Antenna temperature
Quiet (rural)	<5 dB	$<900^0$K
Mid (suburban)	<10 dB	$<3000^0$K
High (urban)	15 dB	9000^0K

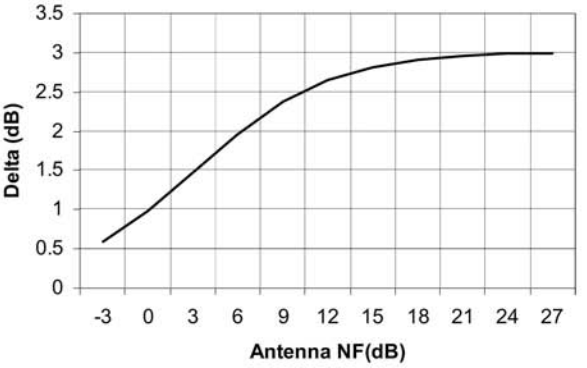

Figure 3-39. Effect of beam tilting on the systems noise

3.6.10 Coupling between On-Site Antennas

3.6.10.1 Introduction

RF repeaters amplify the signal received by one antenna and transmit the same through the other antenna. Excess coupling between the antennas results in oscillations (feedback of coherent signals) and added noise/ interference (feedback of incoherent signal within the band). A margin of about 15 dB is required to be maintained between the antenna coupling and the repeater gain. This limits the repeater gain and coverage in range extension applications. The analysis of the coupling and guidelines for its mitigation are reviewed. The coupling zones are portrayed in Fig. 3-40.

3.6.10.2 Coupling Model

Conductive coupling. These relate to grounding, shielding and filtering practices within the repeater unit and the installation practice, and can be avoided by good engineering.

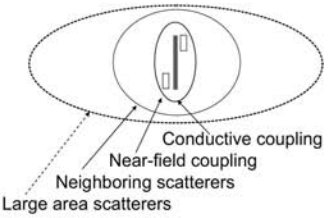

Figure 3-40. The antenna coupling categories

Near-field coupling. The term relates to electrical and magnetic fields that are inductive and capacitive (not pure radiation fields). These decay away from any source at a rate R^{-3} and higher.

Representative values for near-field (inductive) coupling between dipoles are: side-by-side dipoles T= -6 dB @0.8λ, colinear dipoles T= -9 dB @ 0.2λ, and staggered dipoles T= -9 dB @0.25λ (h=0.5λ). The inductive coupling dominates to a distance (see Eq. (3-41)) [12k, 4.4.2]

$$\frac{r}{\lambda} \le 0.2\left(\frac{2d}{\lambda}\right)^{3/2} = 0.2D^{3/2} \tag{3-53}$$

for side-by-side arrays, which for 10 dB omni antennas is 6 wavelengths.

Far-field coupling [6a]. This is covered by the transmission equation, except for the on-axis (colinear) coupling, which – for dipoles and colinear arrays, is

$$T[\text{dB}] = -21 - 40\ \text{Log}(R/\lambda), \tag{3-54}$$

which is plotted in Fig. 3-41 for 850 and 1900 MHz.

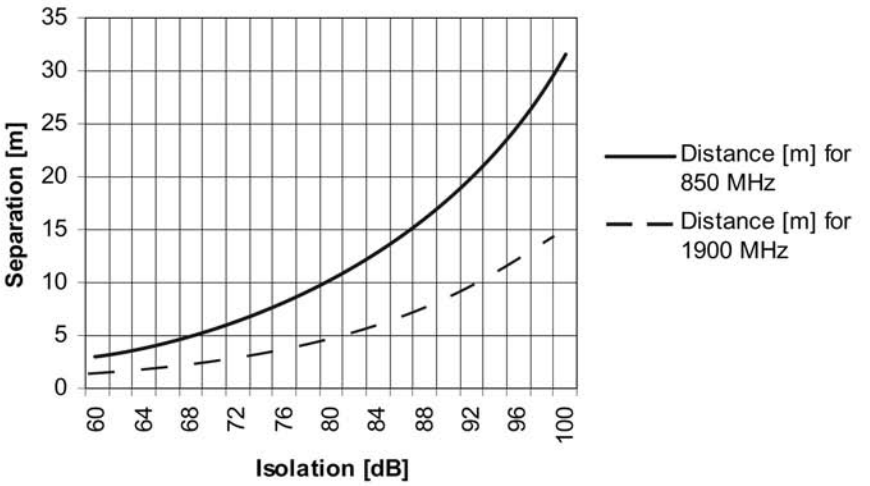

Figure 3-41. Isolation between colinear antenna on-axis per their separation

Neighboring scatterers. These depend on size and shape. The strongest contribution is reflection from flat surfaces (e.g. walls) which may be stronger than the direct coupling

$$\frac{T_{reflected}}{T_{direct}} = \frac{FG_{1scatterer}G_{2scatterer}R_{direct}^{\ 2}}{G_{1direct}G_{2direct}(R_1+R_2)^2} \tag{3-55}$$

where $F \cong 1$ for $R < 0.2d^2/\lambda$, d being the smaller dimension of the reflecting surface.

Note that the distance $R_{1,2}$ may be much larger than R_{direct}, yet when the gain of the antennas in the direction of the scatterer, $G_{scatterer}$, is much higher than G_{direct}, the scatterer may have a dominant coupling.

As an example, a specular return from a building 30 m away, within the main beam of the donor antenna (g=22 dB), and the backlobe of the distribution antenna (g=0 dB), equates to the direct coupling between the antennas separated by 5m, the gain of each near its axis being g=0 dB.

Large area scattering. Scattering from a large area of terrain, illuminated by both antennas, amounts to non-negligible contributions [5a-e]

$$\frac{T_{scattered}}{T_{direct}} = \frac{R_{direct}^{\ 2}}{G_{1direct}G_{2direct}} \int_{Area} dA \frac{G_{1scatterer}G_{2scatterer}\sigma^0}{4\pi(R_1R_2)^2} \tag{3-56}$$

where $\sigma^0[m^2/m^2]$ is the terrain scattering cross-section per unit area. This has been measured to average 0 dB in urban area, and -15 to -30 dB for rural area [5e]. The integration is performed over the area covered by both antennas. This is described in Fig. 3-42. The main beam encompasses most of the antenna power (see Eq. (3-34) and discussion of K) and integration over its footprint is accurate enough for this estimate. The regression rule in *zone 2* (see Fig. 3-9) is R^{-2}. There is no regression in *zone 3*. The integration over *zone 1* renders negligible contribution and is ignored.

$$\begin{aligned}\frac{T_{scattered}}{T_{direct}} &= \frac{R_{direct}^{\ 2}G_{1scatterer}G_{2scatterer}\sigma^0}{4\pi G_{1direct}G_{2direct}}\left\{\int_{R_{RO}}^{\infty} R^{-3}\varphi\, dR + \frac{\varphi}{2R_{RO}^{\ 2}}\right\} = \\ &= \frac{G_{1scatterer}G_{2scatterer}\sigma^0}{4\pi\, G_{1direct}G_{2direct}}\left(\frac{R_{direct}}{R_{RO}}\right)^2\varphi\end{aligned} \tag{3-57}$$

R_{RO} is defined in Eq. (3-19).

A numerical example will serve the insight: assume $G_{distribution}$=17 dB (6^0x90^0), backlobe gain is 0 dB, G_{donor}=29 dB (6^0x6^0), G_{direct}=0 dB, R_{direct}=5 m, H=20 m. In this case $T_{scattered}/T_{direct}[dB] = -4 + \sigma^0$. This is negligible in rural area, but becomes dominant at lower antenna height, urban area, and specifically when both donor and distribution antennas point in the same direction.

The large area scattering adds up over a large delay spread. The amount of coherent coupling depends on the bandwidth of the signal vs. the coherent bandwidth of this channel. The coherent delay for CDMA is ~0.8 μs, translated into 120 m range. The scattered contribution from terrain over this short range is small. The incoherent contribution that is picked up contributes to the noise/ interference.

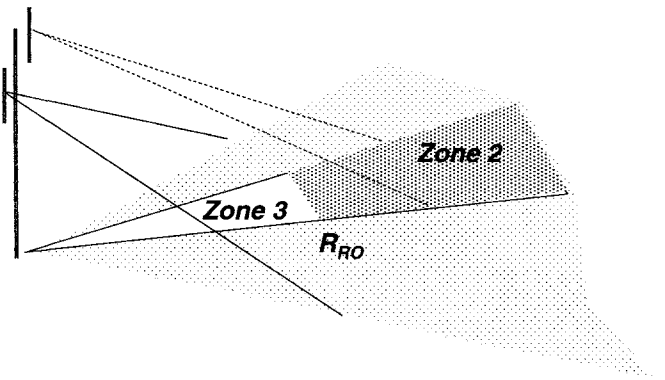

Figure 3-42. Large area scattering

REFERENCES

[1] J. Shapira, *Channel characteristics for Land Cellular Radio, and their systems implications*, IEEE Antennas and Propagation Magazine, Vol. 34, No. 4, pp. 7- 16, August 1992.

[2] H.L. Bertoni, S.A. Torrico, and G. Liang, *Predicting the Radio Channel Beyond Second-Generation Wireless Systems,* IEEE Antenna and Propagation Magazine, Vol. 47, No. 4, pp. 28-40, August 2005.

[3] Forest and Urban Propagation References:

a. H. Oraizi and S. Hosseinzadeh, *Determination of the Effect of Vegetation on Radiowave Propagation by the Parabolic Equation Method,* white paper, www.broadcastpapers.com., October 2003.

b. L.W. Li, T.S. Yeo, P.S. Kooi, M.S. Leong, and J.H. Koh, *Analysis of Electromagnetic Wave Propagation in Forest Environment Along Multiple Paths*, Journal of

electromagnetic waves and applications (J. electromagn. waves appl.), Vol. 13, No. 8, pp. 1057-1059, 1999.

c. Y. Chaiko, *Mathematical Models of Radio Wave Propagation in Woodland for Mobile Communication Systems*, Doctoral student of Computer Management, Information and Electronics systems of Transport (Student ID 001RED005), Riga, 2004.

d. K. Sarabandi, and I.-S. Koh, *Effect of Canopy–Air Interface Roughness on HF–VHF Wave Propagation in Forest*, IEEE Trans. AP S, pp.111-121, Feb. 2002.

e. H. Bertoni, *Radio Propagation for Modern Wireless Systems*, Sec. 7.3, Prentice Hall, 2000.

h. *ibid,* Chapter 6.

[4] Beam Tilt References:

a. H.-S. Cho, Y.-I. Kim, and D.K. Sung, *Protection Against Cochannel Interference from Neighboring Cells Using Down-Tilting of Antenna Beams,* in IEEE VTC, Spring, 2001.

b. W.C.Y. Lee, *Mobile Cellular Telecommunications*, Sec. 6.7.3, McGraw-Hill, 1995.

[5] Large Area Scattering References:

a. J. Shapira, *Characteristics of Surface Scatter Interference in Terrestrial Communications*, 23rd URSI General Assembly, 1990.

b. V.K. Prabbhu, *Simple Upper Bound on Microwave Terrestrial Interference Due to Terrain Scatter*, Globecom'88, 33.2.1, 1988.

c. J. Shapira, *TERSCAT – A Model for Prediction of Terrain Scattered Interference in Microwave Communications*, Proc. IEEE Conf. Israel, 1989.

d. W.E. Smith, P.L. Sulivan, A.J. Giger, and G.D. Alley, *Recent Advances in Microwave Interference Prediction*, ICC '87, 23.2, 1987.

e. A.J. Giger, and J. Shapira, *Interference Caused by Ground Scattering in Terrestrial Microwave Radio Systems*, in IEEE ICC '83, E2.8, 1983.

[6] Cosite Isolation References:

a. TIA/EIA, *Licensed PCS to PC S Interference*, TSB84-A, 8.1999.

[7] Space Diversity References:

a. W.C.Y. Lee, *Mobile Communications Design Fundamentals*, Sec. 6.2.2., Howard W. Sams &Co, 1986.

b. W.C.Y. Lee, *ibid* Sec. 6.3.4.

c. W.C.Y. Lee, *Mobile Cellular Telecommunications*, Sec. 5.4.5., 5.6.5, McGraw-Hill, 1995.

d. W.C.Y. Lee, *Angle Spread Versus BTS Antenna Height*, 4th Workshop on Smart Antennas in Wireless Mobile Communication, Stanford, 1997.

[8] Ripple Effect References:

a. W.C.Y. Lee, *Mobile Communications Design Fundamentals*, Sec. 6.3.5., Howard W. Sams &Co, 1986.

b. W.C.Y. Lee, *Mobile Cellular Telecommunications*, Sec. 5.5.2, McGraw-Hill, 1995.

[9] Polarization References:

a. W.C. Jakes (Ed.), *Microwave Mobile Communications*, Sec. 3.3. IEEE Press, 1974.

b. S. Kozono, H. Tsuruhata and M. Sakamoto, *Base Station Polarization Diversity Reception for Mobile Radio*, IEEE Trans. VT, Vol. VT-33, No. 4, pp. 310-306, 1984.

c. W.C.Y. Lee and Y.S. Yeh, *Polarization Diversity System for Mobile Radio*, IEEE Trans. Comm. Vol. Com-20, No. 5, 1972.

d. A.M.D. Turkmani, A.A. Arowojolu, P.A. Jefford, and C.J. Kellet, *An Experimental Evaluation of the Performance of Two-Branch Space and Polarization Diversity Schemes at 1800 MHz*, IEEE Trans. VT, Vol. 44, No. 2, pp. 318-326, May 1995.

e. R. Vaughan, *Polarization Diversity in Mobile Communications*, IEEE Trans. on VT, Vol. 39, No. 3, August 1990.

f. S. Miller and J. Shapira, *Transmission Considerations for Polarization Smart Antennas,* Proc. of IEEE 51st VTC, Rhodes, Greece, May 05-07, 2001.

g. J. Shapira and S. Miller, *A Novel Polarization Smart Antenna,* Proc. of IEEE 51st VTC, Rhodes, Greece, May 05-07, 2001.

h. J. Shapira and S. Miller, *On Polarization Transmit Diversity In CDMA Regimes,* 4TH EPMCC Conference, Vienna, February 20-22, 2001.

i. P.C.F. Eggers, I.Z. Kovacs, and K. Olesen: *Penetration Effects on XPD with GSM 1800 Handset Antennas, Relevant for BS Polarization Diversity for Indoor Coverage*, Proceedings of VTC, 1998.

j. H. Kuboyama, Y. Tanaka, K. Sato, K. Fujimoto and K. Hirasawa, *Experimental Results with Mobile Antennas Having Cross- Polarization Components in Urban and Rural Areas*, IEEE Trans. VT, Vol. 39, No. 2, pp. 150-160, May 1990.

k. D. Emmer, E. Humburg, P. Weber, and M. Weckerle, *Measurements of Base Station Two-Branch Space and Polarization Diversity Reception and a Comparison of the Diversity Gain Based on the CDF of Signal Level and Simulations of BER in a GSM System*, IEEE VTC'98, pp. 5-10, 1998.

l. J. Toftgard, and P.C.F. Eggers, *Experimental Characterization of the Polarization State Dynamics of Personal Communication Radio Channels*, 43rd IEEE VTC, 1993.

[10] Smart Antennas References:

a. J. Shapira, *Modular Active Antennas Technology for Intelligent Antennas*, 6th workshop on Smart Antennas in Wireless Mobile Communications, Stanford University, July 1999.

b. S. Gordon, and M. Feuerstein, *Evolution of Smart Antennas from 2G to 3G Air Interfaces*, 6th workshop on Smart Antennas in Wireless Mobile Communications, Stanford University, July 1999.

c. J. Shapira, *Dynamic Enhancement and Optimal Utilization of CDMA Networks*, PIMRC2004, Barcelona, Sept. 2004.

[11] P. Beckmann, *Amplitude-Probability Distribution of Atmospheric Radio Noise*, Radio Science Journal, Vol. 68D, No. 6, July 1964.

[12] Reference Books:

a. J.D. Parsons, *Mobile Radio Propagation Channel,* 2nd Edition, Wiley 2000.

b. K. Fujimoto, and J.R. James, *Mobile Antenna Systems Handbook*, 2nd Edition, Artech House, 2000.

c. M. Patzold, *Mobile Fading Channels*, Wiley, 2002.

d. J. Korhonen, *Introduction to 3G mobile Communications*, Artech House, 2001.

e. R. Vaughan and J.B. Andersen, *Channels, Propagation and Antennas for Mobile Communications*, IEE, 2003.

f. N. Blaunstein, *Radio Propagation in Cellular Networks*, Artech House, 2000.

g. N. Balauinstein and J.B. Andersen, *Multipath Phenomena*, Artech House, 2002.

h. H.L. Bertoni, *Radio Propagation for Modern Wireless Systems*, Prentice Hall, 2000.

i. A. Giger, *Low-Angle Microwave Propagation: Physics and Modeling*, Artech House, 1991.

j. M.L. Meeks, *Radar Propagation at Low Altitudes*, Artech House, 1982.

k. C. Balanis, *Antenna theory* , Harper & Row, 1982.

4

RADIO ACCESS RELATED PERFORMANCE OF CDMA CELLULAR NETWORKS

The cellular network is best utilized when providing maximum teletraffic capacity. The reverse link and the forward link capacity in a CDMA network are limited by base station resources (e.g. modems/channel elements, transmit power, Walsh codes) and by interference. The CDMA network is not naturally balanced and may be limited by only one of these parameters, thus not maximizing its utilization. The relations between users' distribution, coverage, orthogonality and diversity, and their impact on the forward link and reverse link capacities and performance are discussed in this chapter.

An extensive literature elaborates on the rationale and network-interactive performance of the IS 95-type systems and is sampled in the references. [1] is a basic introductory to the system, [2-6] develop the capacity-coverage relations, and [7] tips onto the rationale of the channel bandwidth and its relations to the ensuing multipath and number of "fingers". The interaction of microcells with larger cells is treated in [8], and an advanced method for balancing the links is proposed in [9]. [10-13] review system planning and performance, while [14-16] similarly evaluate the UMTS radio network. [17] is a supporting paper that formulates the diversity gain in a convenient form. [18-22] treat advanced cell shaping and "smart antennas" for CDMA, and [23] is an overall evaluation of enhancement and optimization techniques for CDMA. This chapter is supported by the above literature, and strives to present a coherent and comprehensive treatment based on the basic founding equations of this service and related propagation environment.

4.1 CDMA Forward and Reverse Links

The CDMA system achieves full reuse of the same frequency channel throughout the network by spreading the transmission over a long pseudo-random code, and filtering each user's link by an individual code. The residual interference caused by all other users accumulates as approximated noise at

the detector of each user in the receiver of the base station, and is minimized by the application of the power control to each transmitting user, equating the signal level received from each user to the minimum required for proper detection at the base station. The forward link is structured differently, however: the number of interference sources to a user is limited to the transmissions from the nearest base stations, and their strength compared to that of its own base station is significant only near the border of the cell. An orthogonal set of codes is thus used on the forward link, eliminating the trans-code interference, except for delayed multipath that impairs orthogonality.

The difference between the forward and reverse links affects their key measures, as summarized in Table 4-1. The links are not balanced automatically, and an optimization process needs to be applied.

4.2 Reverse Link Coverage-Capacity Assessment

The range of communications is bound by the *Link Budget*: the ratio between P_{mMAX}, the maximum power available from the ST transmitter, and S_B, the minimum signal level acceptable to the BTS receiver for maintaining the required quality of service, related by $P_m(r)T(r) = S_B$ and $P_{mMAX}T(r_{MAX}) = S_B$, where T is the transmission gain. While P_{mMAX} is set by the equipment manufacturer and its type approval, S_B depends on the interference in the system, that emerges from other users in the same cell, users in other cells and interference external to the CDMA network. The available capacity of the CDMA cell is also dependent on the same sources of accumulated interference. The coverage and the capacity of the CDMA cell are thus linked and traded-off for one another.

Table 4-1. Difference between forward and reverse links

	Reverse Link	Forward Link
Capacity limit	Other users' interference	BTS power
Coverage limit	User's power	BTS power
Power control	Controlled by aggregate interference to the BTS	Controlled by link budget and interference to the ST
Cell boundary	Shrinks when loaded	Expands when loaded

4.2.1 The Reverse Link Equation

$$\frac{E_B}{I_t} = \frac{W}{R_B} \frac{P_m(r)T(r)}{N_o W F_{BTS} + (n-1)P_m(r)T(r)\nu + I_{oc}W} \tag{4-1}$$

where

E_b/I_t is the energy per bit over the spectral density of interference plus noise. A target value of required E_b/I_t is set in the power control loop for a desired performance (Frame Error Rate).

P_m is the mobile transmit power,

T is the transmission gain,

G_{Base}, G_{Mobile} is the gain (over isotropic) of base station and ST antennas, Respectively,

PG is the path-gain between isotropic antennas (proportional to R^{-4} throughout the book unless otherwise stated),

L is the path-loss (the inverse of path-gain),

N_o is the spectral single-sided (thermal) noise density,

W is the transmission bandwidth,

R_B is the bit rate,

F is the system noise factor (for the BTS),

ν is the voice activity factor,

I_i is the spectral density interference by other in-cell users, and

I_{oc} is the spectral density of interference coming from other cells.

The modem errorless sensitivity E_b/I_t is bound by Shannon theory to a minimum excess energy of -1.6 dB for a wideband Gaussian additive noise channel with unlimited length coding. A two paths Rayleigh fading channel requires $E_b/I_t = 5(= 7dB)$ at the modem (1% FER) in the IS 95 system that is provided with an interleaver-enhanced convolutional error-correction code, and diversity combining of the paths [1, 4, 5]. Further enhancement of the modem in CDMA2000 by coherent detection reduces the reference required E_b/I_t to 5 dB. These modem requirements vary with the channel characteristics and affect the achievable capacity in the cell.

While the in-cell interference is controlled by the power control, that from the other cells is not. It is however bound by the Soft Handoff rule that brings under the cell control any ST whose signal, as received at the BTS, is equal to or stronger than that allocated to the ST within the cell. Assumption of a uniform distribution of the ST through the network, and uniform cells, allows to link the I_{oc} to I_i by

$$I_{oc}/I_i \equiv f = I_{oc}/(n-1)P_m(r)T(r)\nu \tag{4-2}$$

which takes a value of 0.55 for the above uniform distribution of users and identical cells assumptions, and a propagation law of r^{-4} with a Lognormal distribution (due to shadowing) and σ=8 dB.

The power received at the BTS from one ST, normalized to the BTS thermal noise, is solved from the signal-to-interference Eq. (4-1):

$$\frac{P_m(r)T(r)}{N_0WF_{BTS}} \equiv q = \frac{C/I}{1-(n-1)\nu(1+f)C/I} \equiv \frac{C/I}{1-\eta}. \tag{4-3}$$

Here $C/I \equiv (E_b/I_t)/(W/R_b)$ and

$$\eta \equiv (n-1)\nu(1+f)C/I \tag{4-4}$$

is the *load factor* of the cell. The signal (normalized to the self noise) q required to be received from each user - grows with the load, as depicted in Figure 4-1. At the pole of Eq. (4-3)

$$\eta = 1 \Rightarrow N \equiv \frac{1}{(1+f)\nu\, C/I} + 1 \tag{4-5}$$

where N is a reference number of active STs for η=1, called *pole capacity*. The RL capacity of a CDMA cell is now readily calculated from Eq. (4-4):

$$n_{MAX} \cong (n_{MAX} - 1) = \frac{\eta_0 (W/R_b)\zeta\, K}{(E_b/I_t)\nu(1+f)} \tag{4-6}$$

where $\zeta \cong 0.85$ accounts for the sectorization efficiency (in a sectorized cell) and $K \cong 0.85$ accounts for variability of the power control.

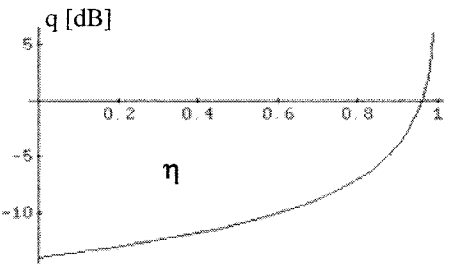

Figure 4-1. Signal received at the BTS from each user vs. load

Setting η_0=0.85; W/R_b=1,230/9.6=128 (=21 dB); v=0.45; f=0.55, we arrive at n_{MAX}=22. The capacity of RC2 (14,400 bps vocoder) is lower: W/R_b=1,230/14.4=85.4, and n_{MAX}=15. The different modes and data rates in CDMA2000 (Section 2.4) require also different E_b/I_t per the respective services, and their capacity (throughput) is calculated accordingly.

4.2.2 Capacity Limit and Noise Rise

The system may become unstable for high load; the power control reacts to small change in the load by a large change in the transmit power of all STs. A load limit is then set to a *nominal load factor* η_0, typically at 0.8 to 0.85.

An easy evaluation of the *pole capacity* of a cell is obtained by measuring the total received power at the BTS. Approximation is made $n-1 \cong n$ leading to

$$S_T \equiv \frac{P_{Total}}{N_o WF} = 1 + (n-1)\nu(1+f)q = \frac{1}{1-\eta} \quad . \tag{4-7}$$

This function, plotted in Fig. 4-2, is called *noise rise*, and is a measure of the load in the cell. A limit is set on the *noise rise* by the operator, typically at 7 to 8 dB.

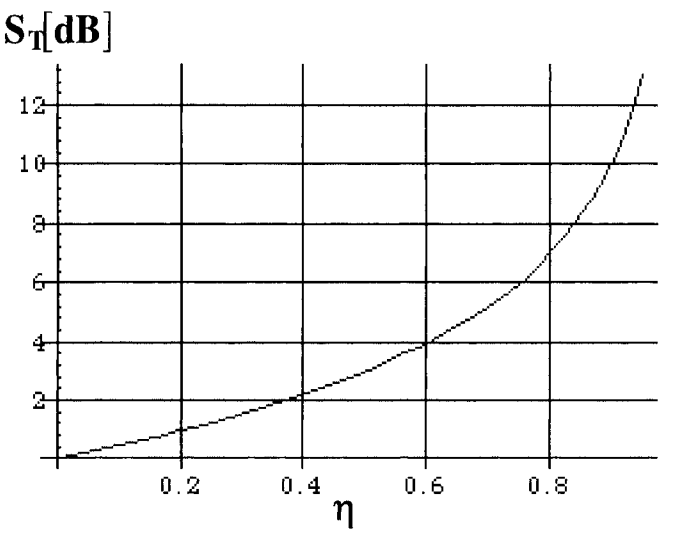

Figure 4-2. Total received power at the BTS (Noise rise)

Now

$$S_T = \frac{1}{1-\eta} = \frac{1}{1-\frac{(n-1)}{(N-1)}}$$

and

$$N-1 = \frac{n-1}{1-\frac{1}{S_T}} = \frac{n-1}{1-10^{-\frac{S_T[dB]}{10}}}. \qquad (4\text{-}8)$$

Equation (4-8) provides a simple measure for the cell *pole capacity*, based on a given number n of active users and a measurement of the *noise rise* S_T.

4.2.3 Impact of Tower-Top LNA (TTLNA) and of Diversity

Both Tower-Top LNA (TTLNA) and receive diversity are means to enhance the reverse link, but their impact is different. *TTLNA* reduces the noise figure of the BTS by amplifying the received signals prior to their attenuation by the cable leading from the antenna to the BTS receiver. As such they increase the available transmission gain T_{MAX} and the cell range. The TTLNA does not impact the cell capacity. *Diversity reception*, by applying two or more diversity antennas, smoothes the channel and reduces the required E_b/I_t for a given quality of service (e.g. FER). By so doing it increases both the cell range and its capacity, as implied from Eq. (4-3).

4.2.4 Cells with Different Size and Load

We now extend the reverse link equation to include cells of different size and different loads, as in a nonuniform network. The ratio of the load is defined (for cells of the same size) $x = \eta_{oc}/\eta_i$, which relates to different ST density near the common boundary, and thus to additional interference. An extension to cells with different size is $u \equiv (R_i/R_{oc})$; R_i and R_{oc} are the self-cell and the adjacent cell radii, respectively, which recognizes the relative density near the boundary between the two cells, each loaded with the same number of users[5]. Equations (4-3, 4-4) now become

[5] See Appendix A. u is accurate to within 20% for $0.3<(Roc/R_i)<3$. $\hat{u} = 1.06(R_i/R_{oc}) - 0.075$ is accurate to within 2% up to $(Roc/R_i)=6$.

$$q_i = \frac{C/I}{1-(n-1)v(1+uxf)C/I} \tag{4-9}$$

$$\eta_i \equiv (n-1)(1+uxf)v\frac{C}{I}. \tag{4-10}$$

This extended relation will serve us in analyzing capacity and cell boundaries for nonuniform networks, microcell-macrocell interaction and embedded repeaters.

4.3 Soft Handoff and the Definition of the Cell Boundary

4.3.1 The Reverse Link Cell Boundary

The power setting of STs in adjacent cells is interconnected via Soft Handoff (SHO). While in SHO mode, each ST is controlled by power control commands from all the cells involved (those in the *Active Set*) and its power level is always set to match the lower power requirement between these cells. The reverse link (virtual) boundary between the cells is thus defined by equal power requirements from the ST by the two least power-demanding cells.

By equating the normalized power received by both BTSs (Eq. 4-3):

$$\frac{q_1 F_1}{T_1} = \frac{q_2 F_2}{T_2} = \frac{P_m}{N_0 W} \tag{4-11}$$

where T_1, T_2 denote the transmission gain from the ST to each BTS, and P_m is the mobile transmission power. Though the relation between transmission gain and range depends on the local environment, a simple radial regression $T_i = A_i R_i^{\gamma_i}$ is a good approximation for average outdoors transmission gain trend. This is depicted in Fig. 4-3 (where $A_1 = A_2$; $\gamma_1 = \gamma_2$; $F_1 = F_2$ for simplicity).

Equation (4-11) is satisfied at the crossing of the P_m curves from the two cells. A change in the threshold setting of either cell (change in load or additional interference) causes the respective curve to shift (the dotted curve in Fig. 4-3) and the boundary (curve crossing) to shift. The cell with heavier load shrinks (cell #2 in Fig. 4-3) and sheds excessive load to neighboring cells. This effect is called "cell breathing".

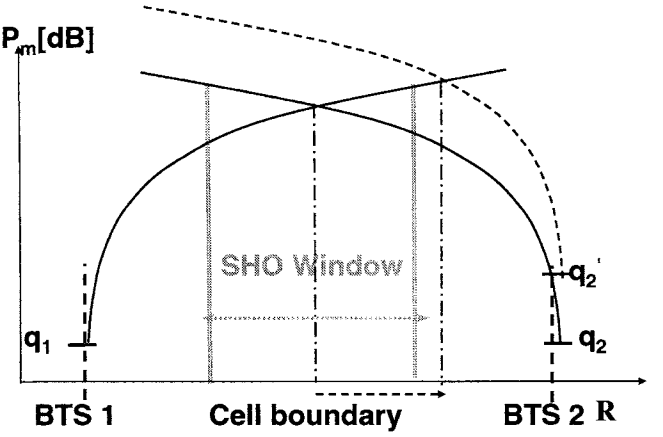

Figure 4-3. The cell boundary and its dynamics

4.3.2 Cell Coverage and "Cell Breathing"

4.3.2.1 Cell Range

The range of coverage is derived from the link budget Eq. (4-3)

$$T(R) = (N_0 W F_B / P_m) \cdot (C/I) / (1-\eta) = AR^{-\gamma} . \qquad (4\text{-}12)$$

A single exponential regression γ is conveniently assumed for the propagation law in our analysis to follow, where A is a constant defining the antenna location and directivity, and the environment. The first ratio in Eq. (4-12) relates the transmit power to the noise power and is a general link budget for any communications. The second ratio is CDMA-specific: $C/I = (E_b/I_t)/(W/R_b)$ is the level set for a specified data rate and service level in a given environment (Section 4.2.1), while η reflects the fractional load level with a given activity ratio and other cells' interference (Section 4.2.4).

R_0 is the range of a fully loaded cell $\eta = \eta_0$. Its prediction depends on propagation model, as surveyed in Chapter 3. We resort herein to the basic flat earth model (Eq. 3-11), based on R^{-4} propagation and dependence on the antenna height. This may prove optimistic in most environments, but its explicit dependence on the exponent and the antenna height serves well in further comparative analysis of changes in parameters.

$$R_0 = (G_B G_m)^{1/4} (Hh)^{1/2} (P_{mMax}/N_0 W F_B)^{1/4} ((1-\eta_0)/(C/I))^{1/4} FM^{1/4} \quad (4\text{-}13)$$

where P_{mMax} is the maximal transmit power of the ST, and H and h are the height of the BTS and ST antennas, respectively. FM is the fade margin, accounting for Lognormal shadowing.

In a typical large cell G_B=17 dBi; G_m=-5 dBi; H=30 m (=15 dB meter); h=1.5 m (1.76 dB meter); P_{mMax}=23 dBm; N_0WF_B=-108 dBm; C/I=-14 dB; 1-η_0=0.15 (=-8.2 dB), FM=-8 dB, which renders R_0= 22.6 km.

4.3.2.2 Cell Breathing

The receive threshold of the BTS changes with the load, as plotted in Fig. 4-1, and the range of the cell varies accordingly,

$$(R/R_0) = ((1-\eta)/(1-\eta_0))^{1/4}. \quad (4\text{-}14)$$

This change in coverage with load is called "cell breathing" and is plotted in Fig. 4-4.

The extent of breathing is exemplified for a single cell embedded within a uniform cluster of cells. The change in ST density implies change in x. From (4-11) and considering Eqs. (4-3, 4-9, 4-10, 4-14),

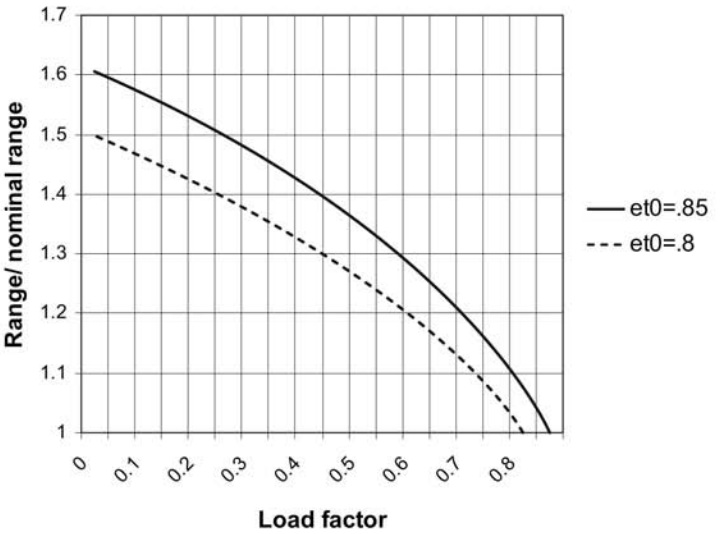

Figure 4-4. Dependence of the cell range on the load

$$\left(\frac{R_i}{R_o}\right)^{\gamma} = \frac{1-\eta_i\left(\frac{1+xf}{1+f}\right)}{1-\eta_o} \tag{4-15}$$

which is depicted in Fig. 4-5 for γ=4. The interference effect of the single cell on the surrounding cells is small and neglected.

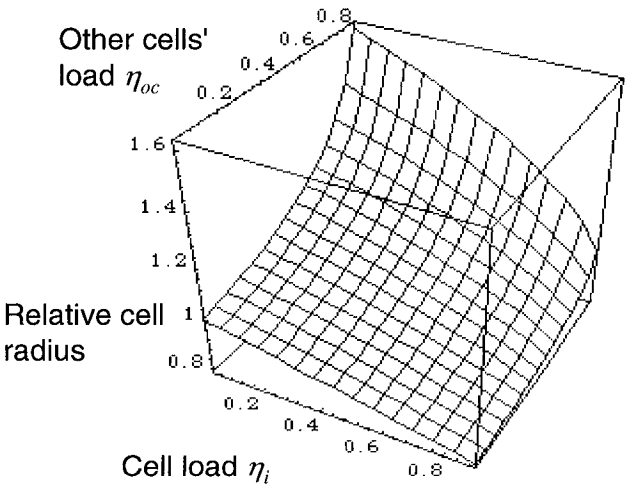

Figure 4-5. Cell breathing

4.3.2.3 Range Dependence on the User Density

Now consider a uniform distribution of users in the area, ρ users per unit area. The load η is related to the range as $\eta \equiv (n-1)v(1+f)C/I \cong kn = k\pi\rho R^2$. Let ρ_0 be defined as the density for fully loaded cell $k\pi\rho_0 R_0^{\ 2} = n_0$. Equation (4-14) now becomes $(R/R_0)^4 = \left(1-k\pi\rho_0 R_0^{\ 2}(\rho/\rho_0)(R/R_0)^2\right)/\left(1-k\pi\rho_0 R_0^{\ 2}\right)$, which is solved

$$\left(\frac{R}{R_0}\right)^2 = \frac{1}{2}\frac{\eta_0}{1-\eta_0}\left(\frac{\rho}{\rho_0}\right)\left[\sqrt{1+4\frac{1-\eta_0}{\eta_0^{\ 2}}\left(\frac{\rho_0}{\rho}\right)^2}-1\right] \tag{4-16}$$

and plotted in Fig. 4-6 for η_0=0.85. The cell is coverage-limited for densities lower than ρ_0. The coverage is shrinking as the density grows. The

cell is capacity-limited by $k\pi\rho_0 R_0^{\ 2} = n_0$, and higher densities are accommodated by range shrinkage $(R/R_0)^2 = \rho_0/\rho$.

Note that the load factor depends on the load within the cell as well as interference from other cells. The latter depends on the relative size of the adjacent cells and their relative load.

4.3.3 Cell Jamming

The limit on the *noise rise* at the BTS is set to match the system stability constraint. This is a tuning parameter of the network, set by the operator, denying access to additional users. Note that this measure of maximum load is typically set in reference to the BTS noise figure F_{BTS} and does not depend on outside interference (Jamming). The effect of the additional interference, not controlled by SHO of the CDMA network, is to raise the *noise rise* curve (the grey line in Fig. 4-7), and thus raise the required ST transmission power P_m.

Additional noise and/or interference external to the controlled network thus limit the *coverage* of the cell to the maximum P_{mMAX} available to the ST. If we consider jamming power J at the input to the BTS, normalized to self-noise of the BTS, then Eq. (4-16) becomes

$$S_{T+J} \equiv (P_{Total}/N_o WF) + J = 1 + J + (n-1)\nu(1+f)q(1+J) = (1+J)/(1-\eta) \qquad (4\text{-}17)$$

and the range of the cell for that load level η becomes $R_J/R = (1+J)^{-1/4}$.

Once the *noise rise limit* is set, the shift of the noise rise curve by additional interference brings it to meet the *noise rise limit* line at a lower *load factor*. This results in a de facto loss of capacity. A 3 dB additional noise, exemplified in Fig. 4-7, causes a regression of the *load factor* from 0.85 to 0.7 - a 17.5% loss of capacity.

Then $S_T = (1+J)/(1-\eta_J) = 1/(1-\eta_0)$ and

$$\eta_J = 1 - (1+J)/S_T \, . \qquad (4\text{-}18)$$

Note however that there is no loss of coverage – the cell coverage is commensurate with its original full load R_0. The reduced activity can now be spread over the original coverage.

A trade-off between capacity and coverage can be applied by matching the power limit to cross the new *noise rise* curve at the *right slope* (rather than the

set *noise rise limit*). Capacity is then maintained at the cost of higher transmission level (P_m) from the mobiles.

This strategy reduces the coverage if the required P_m exceeds the maximum available to the ST at the cell edge. Then $S_{TJ}/S_T = 1 + J$ and

$$R_J/R_0 = (1+J)^{-1/4} \tag{4-19}$$

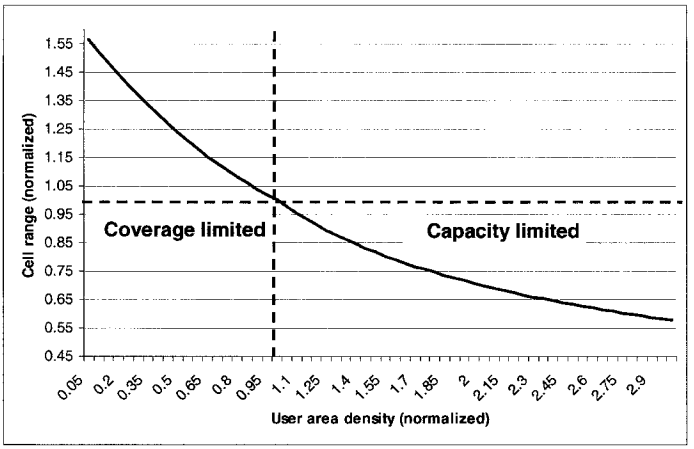

Figure 4-6. Cell range vs. user area density

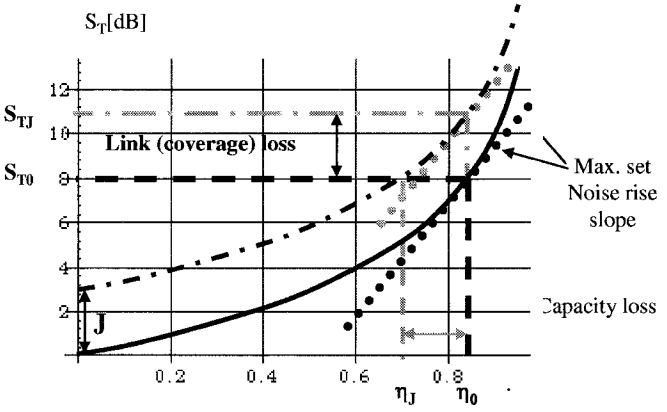

Figure 4-7. Total BTS received power vs. load ("noise rise").
The shift of the curve by 3 dB is caused by additional interference

where R_0 is the maximal range obtained by transmitting P_{mMAX}. It does not affect the cell, however, in a capacity-limited cell with a high density of users that do not reach to the cell edge to start with, and their maximal range $R_{\max} < R_j$. It is also applicable for optimizing the cell enhancement with repeaters, as will be discussed in Chapter 6.

4.3.4 The Forward Link Cell Boundary

The forward link cell boundary is determined by the measurement of *Ec/Io* and serves to initiate and terminate the Soft Handoff process. Note that *Ec/Io* of adjacent cells equate at a point that depends only on the pilot levels in these cells, and not on the relative loads of the cells. However, the SHO zone thresholds T_{ADD} and T_{DROP} do depend on the cells' relative loads and tend to extend the coverage of the loaded cell[6]. This creates an imbalance with the reverse link boundary that shrinks the loaded cell. The SHO "window" is shown in Fig. 4-3. In a balanced cell it should be about symmetrical around the reverse link boundary. Cell balancing is not an automatic process, however, and even if initially balanced, the forward and reverse links' boundaries drift apart upon changes in the relative loads of adjacent cells[7]. Cell imbalance reduces the capacity of both the forward and reverse links, and increases the outage. Simple fix – by increasing the width of the SHO window, reduces the outage but does not recover capacity.

4.4 Forward Link Assessment

4.4.1 Derivation of the Forward Link Equation

The BTS transmits a common pilot, synch, paging and n traffic codes – code multiplexed and in synchronism. The part of the transmission that stays synchronized through the multipath, designated by the orthogonality factor α, is detected by one "finger" in the ST receiver, while transmissions that are delayed by multipath by more than one chip are captured by other "fingers" that are searching in the delay space. The number of available "fingers" in the ST is 3 (IS 95). The rest of the transmission that is not captured by any "finger" does not contribute to the signal but appears as interference to all fingers. The "lost" transmission amounts to $(1-\delta)(1-\alpha)$. The ST detects each

---

[6] E_c/I_0 of the heavier loaded cell decays slower into the other cell then its counterpart from the lighter loaded cell, which shifts the TADD and TDROP toward the lighter loaded cell.

[7] See Section 4.5.3 for a scheme for automatically balancing the links, whereby the pilot power is adjusted according to load of the cell and that of the adjacent cells.

"finger" and then coherently combines the detected signals, typically by "maximal ratio combining" that exploits the diversity gain in combining the uncorrelated fingers. We conveniently adopt here the multiray model, where each ray is Rayleigh fading and E_b/I_t is improved by the diversity gain between multiple rays (thus forgoing Rician situations). The forward link traffic equation to ST_i for the leading "finger" is

$$\left.\frac{C}{I}\right|_{i1}(r_i)=\frac{\alpha_i P_{S_i}(r_i)T(r_i)}{N_o W F_m+(1-\alpha_i)P_{BTS}T(r_i)+I_{oc}W} \tag{4-20}$$

where

C/I is the Carrier-to-Interference value at the ST receiver,
F_m is the ST noise figure,
I_{oc} is the spectral density of interference coming from other cells,
P_s is the power transmitted per user #i,
α is the orthogonality factor. 1-α is the fraction of the transmitted power that is received by the ST with a delay longer than one chip, and is not orthogonal to signal code,
δ is the fraction of the nonorthogonal transmitted power, 1-α, that is captured by the rake receiver later "fingers" and is coherently detected,
g is the diversity gain due to the delayed multipath rays, and
P_{OH} is the power allocated to overhead.

Typically most of the signal energy is contained in the first two fingers, and we therefore simplify the discussion by treating two fingers. The equation for the second finger then becomes

$$\left.\frac{C}{I}\right|_{i2}(r_i)=\left(\frac{\delta_i(1-\alpha_i)P_{Si}(r)T(r_i)}{N_o W F_m+[1-\delta_i(1-\alpha_i)]P_{BTS}T(r_i)+I_{oc}W}\right). \tag{4-21}$$

Note that both Ps_i and C/I_i depend on the distance (or – more accurately, on the transmission gain to the location of the ST). This is because no power control rule has been defined yet.
The resulting C/I at the ST is then

$$\left.\frac{C}{I}\right|_{i}(r_i)=\left.\frac{C}{I}\right|_{i1}(r_i)\cdot g\left\{\left.\frac{C}{I}\right|_{i1},\left.\frac{C}{I}\right|_{i2}\right\}. \tag{4-22}$$

We now define $x_F = P_{otherBTS} / P_{BTS}$, the ratio of the transmission power of the interfering BTS to self. In the following analysis we relate to a single interfering BTS for sake of simplicity, though generalization is straightforward.
Now

$$P_{BTS} = \nu_F \sum_i^n P_{S_i}(r_i) + \left(P_P + P_{Sync} + P_{Page}\right) \equiv P_{Traffic} + P_{OH}\,, \tag{4-23}$$

then

$$\left.\frac{C}{I}\right|_i = \frac{P_{S_i}(r_i)\alpha_i g(\alpha_i, \delta_i; r_i)}{\frac{N_0 W F_m}{T(r_i)} + \left((1-\alpha_i) + x_F \frac{T_{oci}(r_{oci})}{T(r_i)}\right)\left(\nu_F \sum_1^n P_{S_j}(r_j) + P_{OH}\right)}. \tag{4-24}$$

4.4.2 The Orthogonality Function

The *orthogonality factor* α represents the fraction of the BTS power that arrives at the ST with delay smaller than a single chip in the CDMA network, and thus maintains the orthogonality between the transmitted codes. All the rest of the transmitted power appears as nonorthogonal interference to the receiver. Part of that is captured by later "fingers" and contributes to the diversity gain. Average orthogonality factor is referred to in relation to certain global cell features (e.g. capacity, power rise). However, the orthogonality depends on the locality of the ST and the environment in the cell, and is not uniform through the cell.

An estimate of the orthogonality factor throughout the cell is derived in Appendix C. Contributions delayed by more than a chip duration are shown to result from reflections from flat large obstacles (e.g. buildings, road signs, etc.) while those from scattering are negligible at these distances. The contribution of reflectors to the received power at the ST is compared with that of the direct path. This ratio is translated to the ratio of nonorthogonal to orthogonal power reaching the ST, for a given distribution of reflectors within the cell. The probability of Line of Sight (LOS) contribution from reflectors is diminished at large distances, where the grazing ground reflection changes the propagation regime (Section 3.2, and Eqs. (3-11), (3-16)). A "break point" in the function, depending on the antenna height above the clutter, is similar to the one in the respective propagation model. An intermediate zone model, where the direct path undergoes grazing reflection while the reflected paths are LOS, is bound between closely spaced transitions from near to intermediate, and from intermediate to far zone (See Appendix C for details).

The functional dependence of α on the ST distance from the access node is plotted in Fig. 4-8 per Eq. (4-25), covering the "near zone"

$$\alpha = (1+1/x)^2 / \left(S_N x + (1+1/x)^2\right) \tag{4-25}$$

and per Eq. (4-26) for the "far zone"

$$\alpha = (1+1/x)^4 / \left(S_N x + (1+1/x)^4\right); \tag{4-26}$$

and the "break point", where (4-25) and (4-26) equate, is

$$x = 2kHh/r_0 . \tag{4-27}$$

Here $x \equiv R/r_0$, the ratio of the ST distance from the access node to the distance the wave traverses during one CDMA chip time ($r_0 = \bar{c}\tau$, $\bar{c}$ being the speed of light and τ - the chip duration). The reflectors' density coefficient $\hat{S}_N$ is

$$\hat{S}_N = \hat{S}_0 r_0 \text{ where } \hat{S}_0 \propto \rho F^2 . \tag{4-28}$$

ρ is an area density factor for the reflectors, F is a reflection coefficient relating to the size of the reflectors, H, h are the BTS and the ST antenna heights, respectively, and k is the wave number. Figure 4-8 plots α for a range of values of $\hat{S}_N$.

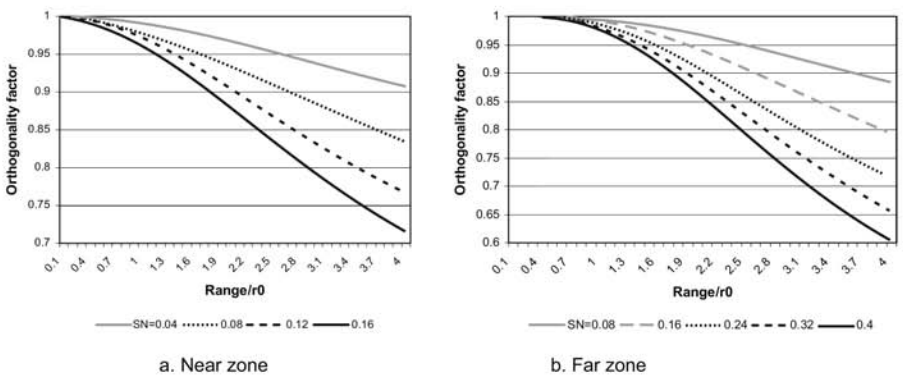

Figure 4-8. The orthogonality function vs. range

The distribution of the orthogonality throughout the cell affects the diversity gain and the capacity. Furthermore, it affects the throughput and the optimal scheduling in time-multiplexed data transmission (e.g. EV-DO and HSDPA).

4.4.3 Orthogonality and Diversity Gain

Part of the nonorthogonal power is received by the delayed "fingers" of the ST receiver, and optimally combined to produce diversity gain. The effect of orthogonality and diversity on the power rise is exemplified in Fig. 4-9. The relation between these depends on the nature of the delayed multipath (delay spread).

This determines the fraction of the nonorthogonal power that is intercepted by the delayed "fingers" of the ST receiver, and its distribution among them.

Typically the power is distributed among the fingers in a descending order (but this is not a rule, as discussed in Section 3.4.1, and examples reported in Fig. 3-22). The power is assumed to be intercepted by only two "fingers" in the model computed in the following figures, neglecting the diversity contribution of the third, presumed weak, finger. The rest of the transmitted power, $(1-\delta)(1-\alpha)$, contributes to the interference[8].

We follow an approximate expression derived from simulations and experiments (after Turkmani, et al. [4]) for the dependence of the (maximal ratio combined) diversity gain on the ratio between the two diversity branches

$$g[dB] = 7.14e^{-0.59\rho - 0.11\Delta}[dB] \ . \tag{4-29}$$

The ratio between the branches, Δ, is obtained from Eqs. (4-20), (4-21):

$$\begin{aligned}
\Delta[dB] &= 10Log\left\{\left.\frac{C}{I}\right|_{i1}(r_i) \Big/ \left.\frac{C}{I}\right|_{i2}(r_i)\right\} = \\
&= 10Log\left\{\frac{N_o W F_m / P_{BTS} T(r_i) + I_{oc} W / P_{BTS} T(r_i) + [1-\delta_i(1-\alpha_i)]}{N_o W F_m / P_{BTS} T(r_i) + I_{oc} W / P_{BTS} T(r_i) + (1-\alpha_i)} \cdot \frac{\alpha_i}{\delta_i(1-\alpha_i)}\right\} \\
&= 10Log\left\{\frac{\hat{N} + [1-\delta_i(1-\alpha_i)]}{\hat{N} + (1-\alpha_i)} \cdot \frac{\alpha_i}{\delta_i(1-\alpha_i)}\right\}
\end{aligned} \tag{4-30}$$

[8] The typical average orthogonality factor in 1.25MHz CDMA systems ranges between 0.95 to 0.6. Up to 30% of the transmitted power is sometimes delayed beyond the third "finger" and is not coherently detected. The typical orthogonality in 4.5 MHz CDMA systems (e.g. WCDMA) is lower – down to 0.4.

$$\hat{N} \equiv \left(N_0 W F_m + I_{oc} W\right) / P_{BTS}\, T\left(r_i\right) \tag{4-31}$$

$\hat{N}$ represents thermal noise and out-of-cell interference. Note that the ratio

$$G \equiv I_i / \left(N_0 + I_{oc}\right) = \left(1-\alpha\right) / \hat{N} \equiv \left(1-\alpha\right) P_{BTS} T\left(r_i\right) / \left(N_0 W F_m + I_{oc} W\right) \tag{4-32}$$

representing the ratio of interference due to its own cell's transmission to noise-plus other cells' transmission, is termed *the geometry factor G* in some publications [15, Section 2.5.1.11].

The impact of the orthogonality and the diversity is not uniform through the cell coverage. Their dependence on the distance from the access node, or rather on $T(r_i)$, influences the range of the cell and the dynamic range of the FLPC. Note that the term $\hat{N}$, representing thermal noise and interference from adjacent cells normalized to BTS power as received at the ST, is negligible near the cell center, and becomes dominant toward the cell edge. Thus for $\delta \to 1$

$$\Delta[dB] \cong 20 Log\left(\alpha / \left(1-\alpha\right)\right) \text{ for } r << R$$

$$\Delta[dB] \Rightarrow 10 Log\left(\alpha / \left(1-\alpha\right)\right) \text{ for } r \to R\,. \tag{4-33}$$

The multipath diversity gain (Eqs. (4-29), (4-30)) is shown in Fig. 4-9 for correlation coefficient ρ=0.3, showing the two distinct regions as in Eq. (4-33).

We now combine Eqs. (4-20), (4-22), and (4-30) to produce Fig. 4-10. A *flat C/I zone* is shown that depends on the orthogonality in the cell: high orthogonality renders a short-range high C/I near the center, but a faster decay toward the edge, while lower α extends the flat zone.

It is evident then that the loss of orthogonality reduces the SNR near the cell center but has only little impact near the cell edge. This is an important observation for time-multiplexed transmission, as in 1xEV-DO, where advantage is taken of the high SNR for transmission of high data rate.

The impact of diversity is significant near the cell edge, and it has the tendency to extend the cell boundary. These effects become most significant in evaluating the performance of time-delay transmit diversity, to be discussed in Chapter 5.

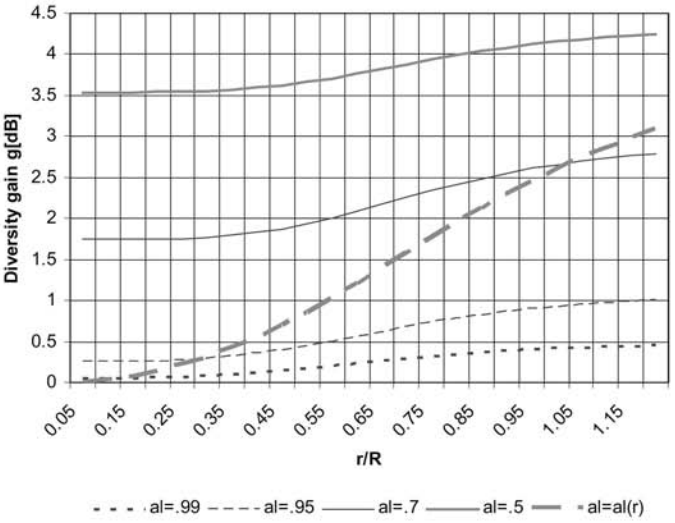

Figure 4-9. Multipath diversity gain vs. distance from the access node. ρ=0.3, δ=0.5; n=10, P_s=0.5W, P_{Otl}=2.5W, $T(R)$=-140 dB, F_m=8 dB

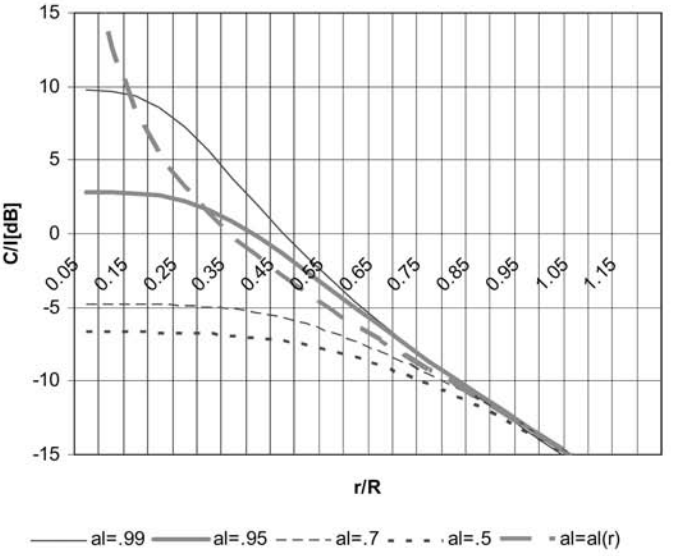

Figure 4-10. C/I vs. distance from BTS (effect of SHO not included) ρ=0.3, δ=0.5; n=10, P_s=0.5W, P_{Otl}=2.5W, $T(R)$=-140 dB, F_m=8 dB

4.4.4 Orthogonality and Forward Link Power Control

Nonorthogonal multipath of all other transmitted codes from the same BTS adds interference that is proportional to the BTS power. The *Forward Link Power Control* (FLPC) has a limited dynamic range for this reason: should a full dynamic range power control be applied, then the power transmitted by the BTS to STs near the center is very low, while the non-orthogonal interference to these STs is very strong, being part of the transmission to the furthest STs in the cell. This undesirable effect is an *inverse near-far effect.*

The power allocated to a traffic user under FLPC (Eq. (4-20) with set C/I) is:

$$P_{S_i}(r_i) = \frac{C}{I}\left\{\left(\frac{N_0 W F_m}{P_{BTS} T(r_i)} + x\frac{T_{oci}(r_{oci})}{T(r_i)}\right) + (1-\alpha)\right\}\frac{P_{BTS}}{\alpha g(\alpha; r_i)}. \qquad (4\text{-}34)$$

A flat zone is observed near the cell center due to the dominance of the term $(C/I)/g(\alpha)\cdot(1-\alpha)/\alpha \cdot P_{BTS}$, which constitutes jamming interference to the short-range users, otherwise requiring much lower power allocation. This *inverse near-far effect* is exhibited in Fig. 4-11. A limit is therefore set on the range of the FLPC to typically 10 dB.

4.4.5 Forward Link Capacity

Solving Eq. (4-24) for P_{Si} and summing up the total traffic power according to Eq. (4-23) renders

$$\nu_F \sum_{i=1}^{n} P_{S_i}(r_i) = \nu_F \{N_0 W F_m \sum_1^n \frac{(C/I)_i}{T(r_i)\alpha_i g(\alpha_i, \delta_i; r_i)} + \\ + \left(\sum_1^n \left(\frac{(C/I)_i}{\alpha_i g(\alpha_i, \delta_i; r_i)}\left(1 - \alpha_i + x_F \frac{T_{oci}(r_{oci})}{T(r_i)}\right)\right)\right)\left(\nu_F \sum_1^n P_{S_j}(r_j) + P_{OH}\right)\}$$

which is solved for P_{BTS} as follows:

$$P_{BTS} = \frac{\nu_F N_0 W F_m \sum_1^n \frac{(C/I)_i}{T(r_i)\alpha_i g(\alpha_i, \delta_i; r_i)} + P_{OH}}{1 - \nu_F \left(\sum_1^n \left(1 - \alpha_i + x_F \frac{T_{oci}(r_{oci})}{T(r_i)}\right)\frac{(C/I)_i}{\alpha_i g(\alpha_i, \delta_i; r_i)}\right)} \equiv \frac{N_{Thermal}(d) + P_{OH}}{1 - \eta_F(d)} \qquad (4\text{-}35)$$

This forward power equation has a pole, representing the nominal maximum capacity of the forward link in a cell [1].

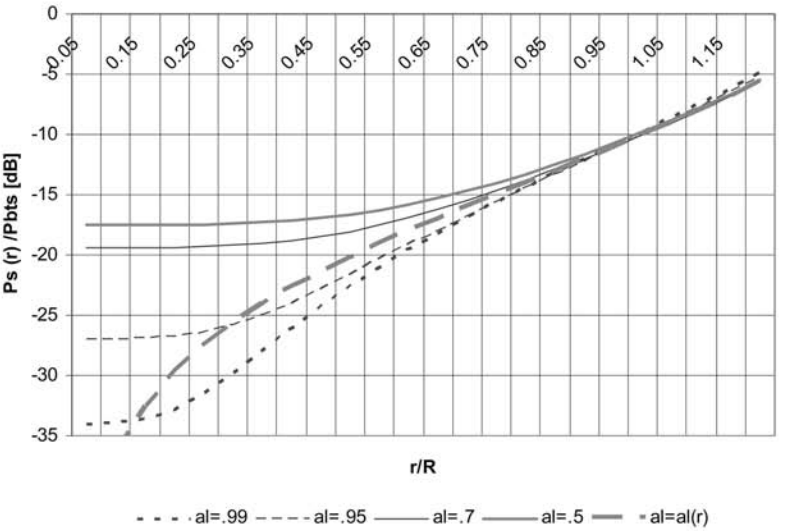

Figure 4-11. Power allocation (Ps/P_{BTS}, [dB]) under FLPC to a traffic channel vs. distance from BTS (effect of SHO not included). ρ=0.3, δ=0.5; n=10, *Av.* P_s=0.5W, P_{OH}=2.5W, $T(R)$=-140 dB, F_m=8 dB

Here (d) signifies dependence on the ST distribution in the cell.
The forward link load factor η_F is then defined as

$$\eta_F \equiv \nu_F \left(\sum_1^n \left(1 - \alpha_i + x_F \frac{T_{oci}(r_{oci})}{T(r_i)} \right) \frac{(C/I)_i}{\alpha_i g(\alpha_i, \delta_i; r_i)} \right). \tag{4-36}$$

Though the orthogonality α is location dependent and not uniform throughout the coverage, an *average* orthogonality value is nevertheless assumed for the cell in evaluating its gross features. Furthermore, by applying power control the same target C/I is reached for each user. Thus, extracting α and C/I out of the summation in Eq. (4-35), along with $g(\alpha,\delta)$, results in the *power rise* equation for (full range) forward link power control (FLPC):

$$P_{BTS} = \frac{\nu_F \dfrac{C/I}{\alpha g(\alpha,\delta)} N_0 W F_m \sum_1^n \dfrac{1}{T(r_i)} + P_{OH}}{1 - \nu_F \dfrac{C/I}{\alpha g(\alpha,\delta)} \left(n(1-\alpha) + \sum_1^n x_F \dfrac{T_{oci}(r_{oci})}{T(r_i)} \right)} \equiv \frac{N_{Thermal}(d) + P_{OH}}{1 - \eta_F(d)} \tag{4-37}$$

$$\eta_F \equiv \nu_F \frac{C/I}{\alpha g(\alpha,\delta)}\left(n(1-\alpha)+\sum_1^n x_F \frac{T_{oci}(r_{oci})}{T(r_i)}\right). \tag{4-38}$$

At the *capacity pole* η_F=1

$$N_{pole} \equiv \left(\frac{\alpha g(\alpha,\delta)}{\nu_F C/I} - x_F \sum_1^n \frac{T_{oci}(r_{oci})}{T(r_i)}\right) \Big/ (1-\alpha) \tag{4-39}$$

which sets the upper bound on the number of active users in the cell applying FLPC. Analyzing Eqs. (4-35), (4-37), (4-38) and (4-39) we observe:

The *capacity pole* depends on the nonorthogonal multipath, which adds interference to the forward link transmission, but also adds diversity. These two have opposite effects, to be shown in Fig. 4-12.

The *capacity pole* depends on the users' distribution within the cell; users closer to the BTS draw less power, while those near the edge consume more power resources, and are subject to higher other cells' interference. This is exhibited in Fig. 4-13.

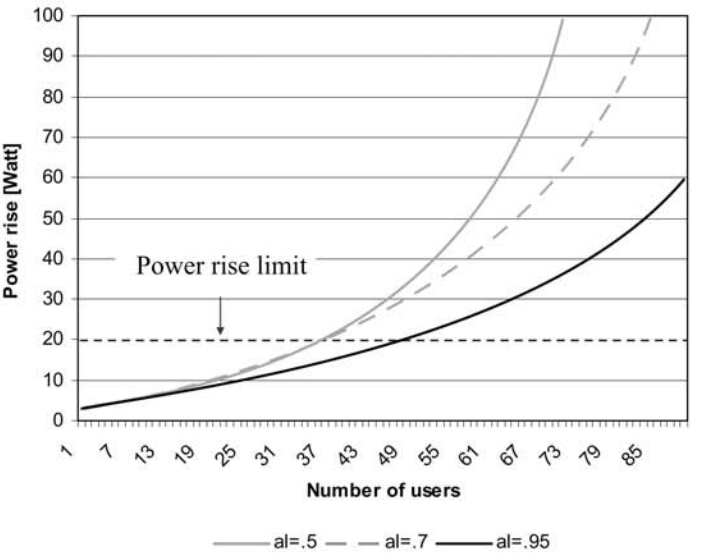

Figure 4-12. Power rise for different orthogonality and diversity values[9]

[9] Appendix B; Uniform distribution.

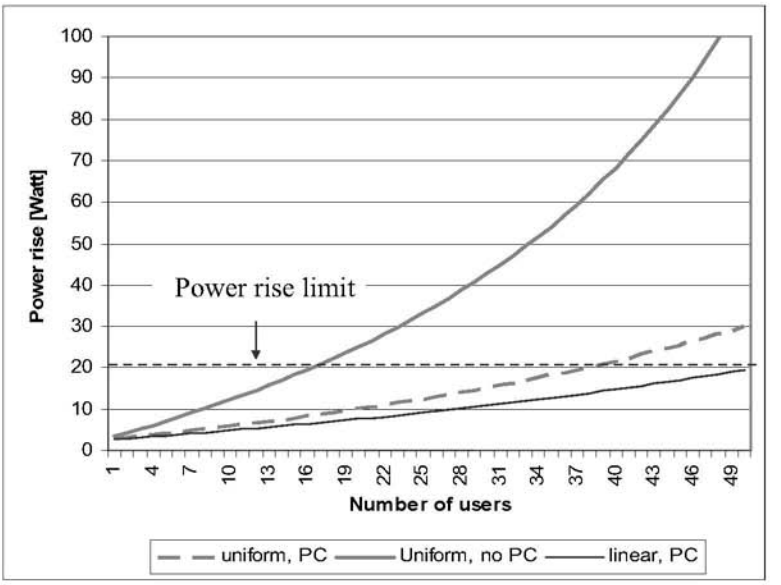

Figure 4-13. Power rise for different distributions of STs[10]

The FL *pole capacity* is much higher than the RL pole capacity for high values of α, which represent the orthogonality and lack of in-cell interference in the FL. The variability of the FL *pole capacity* is however very high, depending on the state of orthogonality, on availability of diversity (whether transmit diversity at the BTS or receive diversity at the ST) and on the users' distribution and link loss (e.g. building penetration).

The FL capacity is limited by the available power from its power amplifier. This *power rise limit* is designed to match the RL capacity.

The ST noise figure influences the level of power transmission but not the *power rise trend* or the *capacity pole*. It does influence the FL capacity by raising the *power rise* curve.

4.4.6 User Distribution

The user (radial) distribution (or, more precisely, the distribution of the path-loss) has a dominant effect on the required transmit power, and therefore on both coverage and capacity.

[10]Appendix B; α=0.7.

This is exemplified in Fig. 4-13 for three different distributions: area uniform with 10 dB FLPC, linear distribution (as along a highway) with 10 dB FLPC, and a distribution on the rim of the cell. The slope of the power rise is by far steeper and the capacity lower for users' concentration on the edge.

Admission control policies and respective algorithms are offered by different vendors that allow admission denial of users requiring high digital gain at times the cell is loaded to capacity. These are users at the edge or in *radio holes*.

4.4.7 Capacity Limit of the Forward Link

The nominal interference-limited capacity (*pole capacity*) of the forward link is typically much higher than that of the reverse link, and the forward link is then limited by the maximum available power of the BS power amplifier. The *power rise* at the BTS is therefore a practical measure of the forward link load. The situation of forward power limited capacity manifests itself in an abrupt rise in the blocking rate and rate of dropped calls.

We observe that the BTS power depends on the path-loss to each served user. As these are not known, the BTS power is considered a random number that depends on the users' distribution. As such, the *power rise* curves in Fig. 4-13 become the average values of a statistically distributed random variable. The probability of the *power rise* to cross the power limit is directly related to the blocking probability. A call blocking rate of 2% is typically considered the capacity-limiting parameter of the forward link.

4.4.8 Coverage and Capacity - Call Blocking and Dropped Calls

The coverage in the reverse link is limited by the transmit power of the furthest user. The power control levels out all signals arriving at the BTS receiver, and its *interference-limited capacity* is almost independent of the users' distribution within the cell. The coverage of the forward link, on the other hand, is limited by the BTS power that serves all users. *Coverage* and *capacity* are therefore linked together on the forward link, depend on the users' distribution, and are limited by the BTS power.

Call blocking and dropped calls on the forward link are two service impairments that are linked together. Dropped calls result when a user enters a shadowed area and the power required to sustain the call is higher than the power limit per user. The dropped call events relate directly to the limit on the dynamic range of the forward link power control (*digital gain*) and are *loss of coverage* events. The probability of dropped calls relates to the abundance of

"radio holes" within the coverage area[11]. On the other hand, the throughput of the BTS is limited by the total power available out of the power amplifier. Admission control and call blocking is a *capacity* event if blocked by the admission control, or a *coverage* event if the access attempt fails due to lack of allocated power, the latter being a result of a "radio hole". A *positive* consequence of dropped call events is that power is freed for the admission of new calls. This reduces the blocking rate and increases capacity.

The interrelationship of coverage and capacity in the forward link exerts a more stringent coverage design of the forward link than that of the reverse link. Planning and optimization incorporate coverage design to avoid "radio holes" and cell balancing to avoid serving extremely disadvantaged users.

4.4.9 Capacity Measurement

The capacity of the forward link is measured by observing the blocking rate exceeding the set value (e.g. 2%). This method does not allow assessing the level of load for a partially loaded cell. Other proposed methods are the "average power-per user" method, dividing the total traffic power during the busy hour (total power less the overhead power) by the number of active users, and the measurement of the slope of the "power rise" curve, which follows the total power and the number of active users during an activity cycle from quiescence to busy hour and extrapolates a straight line to meet the power limit line. The accuracy of both methods is limited, however, by the locality of users' distribution and multipath environment at the time the measurement is taken. The distribution in a populated area may vary appreciably during the day: during rush hours most of the users may be outdoors, and if on highway – may be in a clear view, and low path-loss. Evening activity may be more from the indoors, with slow moving users (slow flat fading) and high path-loss. The slope method further assumes that the *power rise* is a straight line. All three methods are in use and have been further developed, to take into account dynamic overload and admission control algorithms that are proprietarily applied by different vendors and modify the observations.

4.5 Link Balancing

The above analysis reveals that the reverse and forward links are not necessarily balanced. Coverage limit is measured by link budget to the farthest ST, and serves as a basis for balancing the links. However, the ST radial (path-loss) distribution within the coverage area has a dominant effect

[11] Note that building penetration may constitute the most prevalent "radio holes".

on the BTS transmit power requirement and on the blocking rate, while it has no effect on the blocking rate of the reverse link. The reverse link load level depends mainly on the angular distribution of the users relative to the BTS location, as the power control evens out the path-loss differences.

4.5.1 Coverage Balance

Balance between the forward and the reverse link at the cell/ sector boundary means the adjustment of the links' parameters so as to match the Soft HandOff conditions for both links for each user. In a balanced situation the reverse link balance (Eq. (4-11)) occurs about midway through the SHO "window" (between T_{ADD} and T_{DROP}). This is a *coverage balance* that optimizes the Soft Handoff zone. By equalizing the forward and reverse link coverage the SHO is well-defined and its boundaries can be minimized, resulting in minimizing the SHO channel cards overhead and forward link power overhead.

4.5.2 Capacity Balance

The best utilization of the resources of both reverse and forward links is obtained by balancing the links, thus attaining maximum capacity from the network. Consider a uniform distribution of users within the cell, $n = \rho\pi R^2$, where ρ is the user density. The reverse link coverage relates to the user density as $R \propto \rho^{-1/2}$ and is limited by the ST available power to R_r. The forward link range is limited by the BTS power and the transmission gain. If that is taken as R^{-4}, the number of users served relates to the cell range as $n \propto R^{-4}$, but also $\rho = (n/\pi)R^{-2}$. The forward link coverage therefore relates to the user density as $R \propto \rho^{-1/6}$. These limits are drawn in Fig. 4-14 on a Log-Log scale for convenience. The realizable zone is marked bold. Imbalance between the links exerts excessive resources without gaining capacity.

4.5.3 Balancing the Links by Controlling the Pilot Power

The forward and reverse links can be made to equate on the cell boundary by adjusting the pilot power of both cells to match the required conditions [7]. Let the pilot power be $P_p = \zeta P_{BTS}$. The equation for the pilot detection then becomes (see Eq. (4-24)):

$$\frac{E_C}{I_t} = \zeta\alpha g(\alpha) \Bigg/ \left(\frac{N_0 W F_m}{P_{BTS} T(r_i)} + \left((1-\alpha) + x \frac{T_{oci}(r_{oci})}{T(r_i)} \right) \right). \qquad (4\text{-}40)$$

Consider the first term of the denominator: $\zeta P_{BTS} T(r_1)/N_0 W F_m$ is the pilot power as received by an ST at the boundary, normalized to the thermal noise.

This has to meet the ST modem threshold:

$$\zeta P_{BTS} T(r_1)/N_0 W F_m \geq q_m \tag{4-41}$$

where r_1 is the range to the boundary of cell #1. At the forward link boundary

$$E_{C1}/I_0(r_1) = E_{C2}/I_0(r_2) \geq \tau_b \tag{4-42}$$

where τ_b is set to meet required reception performance. Naturally $\tau_b > \tau_{ADD}$, typically by 3 dB or more. Recall that I_0 is the spectral density of the total received power at that point, including self BTS, other BTSs and thermal noise, while I_t counts only the (spectral density of) the interference, including the nonorthogonal part of the self BTS transmission, other BTSs and thermal noise.

These may differ by 0.5 to about 1.5 dB at the cell boundary (3 to 10% error in cell range). Nevertheless, this approximation is used for sake of simplicity of the algorithm.

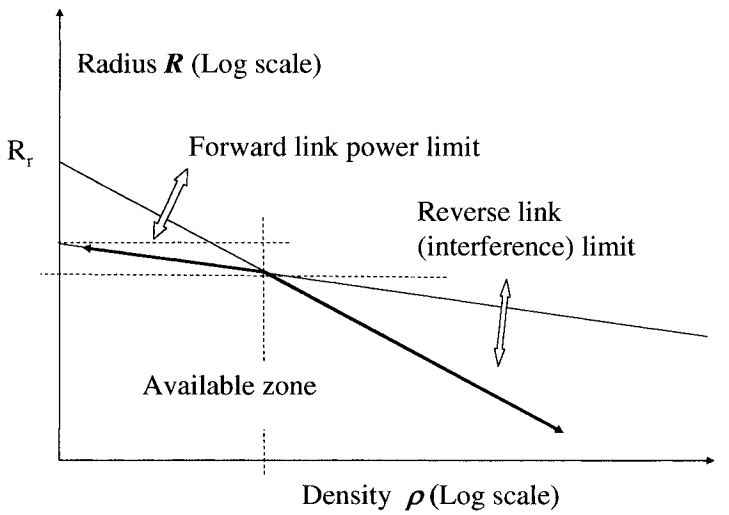

Figure 4-14. Link balancing zone

Now $E_{C1,2}(r_{1,2})W = P_{p1,2}T(r_{1,2})$ and $P_{p1}/P_{p2} = T(r_2)/T(r_1)$. This forward link condition is equated to the reverse link boundary condition Eq. (4-11) to render the relation between pilot power ratio and reverse link load ratio

$$P_{p1}/P_{p2} = (F_2/F_1)(1-\eta_1)/(1-\eta_2). \tag{4-43}$$

These are now incorporated in Eq. (4-40) to get the equation for the pilot ratio ζ.

$$\tau_b = \frac{\zeta \alpha g(\alpha)}{\frac{\zeta}{q_m} + \left((1-\alpha) + x\frac{F_2}{F_1}\frac{1-\eta_1}{1-\eta_2}\right)}$$

$$\zeta = \frac{\tau_b}{\alpha g}\frac{(1-\alpha) + x\frac{F_2}{F_1}\frac{1-\eta_1}{1-\eta_2}}{1-\frac{1}{\alpha g}\frac{\tau_b}{q_m}} = \frac{\tau_b}{\alpha g}\frac{(1-\alpha)+z}{1-\frac{1}{\alpha g}\frac{\tau_b}{q_m}} \tag{4-44}$$

Equation (4-44) interrelates the pilot setting with the self cell load (expressed through τ_b) and environment (expressed through α and diversity gain), and with the ratio of loads and power setting with adjacent cells (parameter z). The other cells' load parameter z

$$z \equiv x\frac{F_2}{F_1}\frac{1-\eta_1}{1-\eta_2} \tag{4-45}$$

is a product of the ratio of the FL transmit power of the other BTSs to self – x, the ratio of noise figure of the other BTSs to self, and the ratio of excess reverse link capacity of self to other cells. The total power is set by (4-41):

$$P_{BTS}T(r_b) \geq \frac{q_m N_0 W F_m}{\zeta}. \tag{4-46}$$

The fraction of BTS power allocated to the pilot ζ is plotted in Fig. 4-15 for the parameters α=0.7 and large cell (τ_b=q_m/2 for 50% load). The dependence of the z parameter on the ratio of loads of self and adjacent cells (Eq. (4-45)) is shown in Fig. 4-16 for x=1, F_1=F_2.

A dynamic adjustment of the balance requires online measurement of the network load parameters, and respective adjustment of the pilot. This balance condition at the boundary holds also for asymmetric links, as in data transmission, where the forward link may have a higher throughput than the reverse link. A similar method of dynamic balancing the links is proposed in [8].

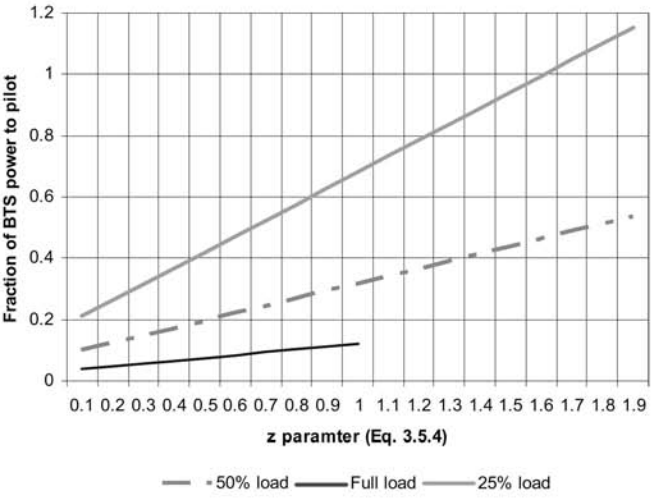

Figure 4-15. Fraction of power allocated to pilot (per Eq. (4-44))

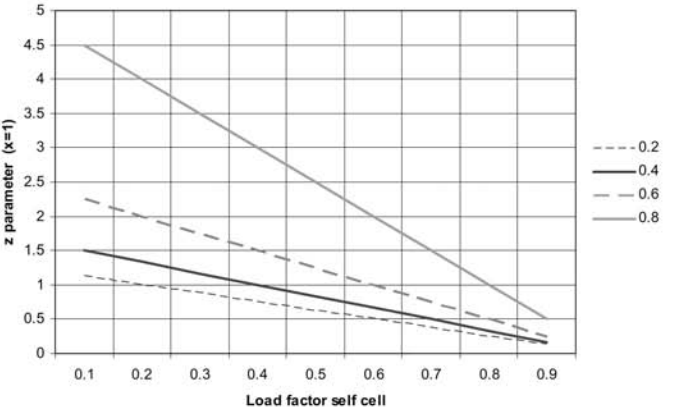

Figure 4-16. The *z* parameter (Eq. (4-45))

4.5.4 Link Balancing by Beam Control

An alternative/ complementary to controlling the pilot power is controlling the transmission gain $T(r_b)$. Equation (4-44) relies on equating the transmission gain on the forward and the reverse links. These can be controlled toward link balancing by separately adjusting the transmission and reception beams' parameters at the BTS.

Link equalizing at the *sector boundary* is applied by controlling the beamwidth of the reverse link antenna, and the forward link antenna, separately, for both adjacent sectors, as required. Link equalizing at the *cell boundary* is applied by controlling the tilt of the reverse link antenna, and that of the forward link antenna, separately, for both adjacent cells, as required. As much as the same can be achieved by controlling the transmit power it may not be desirable as it limits the capacity within the cell/ sector and the ability to serve users with high path-loss (e.g. indoors).

The usage of the same antenna for both forward and reverse links, and the beam shape and tilt control thereof, is a compromise and a suboptimum solution. Techniques for beam tilting and beam shaping are discussed in Chapter 3.

4.6 Load Balancing

It is important to clarify the terms *Load* , *Coverage* and *Balance.*

Load is the fraction of maximum *capacity* in the cell/ sector (in terms of ERLANG, MOU or throughput). There may be a difference between the reverse and the forward link capacity, which depends also on the user distribution.

Coverage is measured on a single link basis (e.g. the pilot).

Balance is between the loads in adjacent cells/ sectors. This is a *capacity balance*, aimed at equalizing the load margin for the relevant cells/ sectors.

Load balancing between sectors (that are angularly displaced around the BTS) and between cells (that are separated by radial distance between the BTSs) therefore require controls on both dimensions of the coverage - radial and angular. An uneven reverse link load in two adjacent sectors is balanced by moving the radial boundary between the sectors, so as to reduce the subscriber base and the interference from the loaded sector, and share load with the adjacent sector. This is achieved by controlling the beam width and orientation.

A cell/sector is most frequently forward link limited by power, which is exhibited in the blocking rate. This is a coverage-limited situation, where the radial domain has to be adjusted by control of the vertical profile of the beam, typically by tilting the beam.

4.7 Soft Handoff Search Window

The Soft HandOff process engages two or more BTSs in the active session. The selection of the active BTSs is based on repeated measurements performed by the ST searcher, that sequentially searches a designated pilot by shifting the pilot-tuned correlator in time over a preassigned *search window*. The detected pilots are then classified to the *active, candidate, neighbor* and *remaining sets* according to their strength and other SHO parameters. The search plan is a trade-off between maintaining the GoS by including the strongest pilots in the active set all the time, which requires frequent measurements of the *active* and *candidate sets*, and properly mapping the *neighbor* and *remaining sets*, keeping track of pilots that become candidates for the *active and candidate sets*. Such a time scheduled plan may have a simple hierarchical and cell-independent order in a uniform grid of identical cells, and direct, single path propagation. In a shadowed and multipath environment, and heterogeneous cell clusters in the network, this map becomes location-specific and less predictable. The most critical trade-off is the *active* and *candidate sets* window: the larger the window, the longer, and less frequent is the search. A short window may miss a candidate pilot coming out of the shadow. Typical CDMA2000 *active* and *candidate sets'* window is 10 to 20 chips, centered around the first arrival (pilot set time) or average previous strongest pilot arrival. The *neighbor set* is 14 to 28 chips, and the *remaining set* – 20 to 40 chips. Windows tend to be larger in clusters of large cells with long delayed multipath and high overlap between cells, and smaller in clusters of compact, highly isolated microcells.

4.8 Heterogeneous Cell Clustering

The environment, as well as the service requirements, may dictate different shapes and sizes to cells. The CDMA system operates on the same channel throughout the network, linked by the Soft HandOff between the cells. Clustering of different types of cells does not incorporate special frequency planning as in other systems, but it does require due consideration to interface matching and balancing by setting the coverage and the link parameters. The parameters involved in the engineering of a heterogeneous CDMA network are discussed in this section.

4.8.1 Cell Shaping

Coverage shaping of cells and sectors is an instrumental tool for the optimization of the network coverage, capacity and performance. Optimization of soft and softer handoff overhead requires proper boundary

matching and optimal overlap between the coverage of adjacent cells and sectors. Further, the dependence on the local distribution of users in the cell, and on interference from other cells' users near the cell boundary drives the shaping of the cell coverage to match the distribution and the environment.

4.8.1.1 Sector Beamwidth, Soft and Softer Handoff

Sector illumination is a trade-off of required gain and EIRP, sector coverage, adjacent sectors' and cells' interference, and SHO and SrHO overhead. A beamwidth of 120^0 (a crossover at –3 dB) is optimal for coverage of a 120^0 sector, but suffers from excessive overflow interference to the adjacent sector and a large softer handoff zone. A narrower beamwidth increases the variation of gain within the sector, but reduces the interference to adjacent sectors and the SrHO overhead. The dependence of FL capacity on the sector antenna beamwidth is plotted in Fig. 4-17 for a circular cell coverage (see Appendix G for derivation). 90^0 beamwidth is a common design compromise, with crossover of –6 dB between sectors.

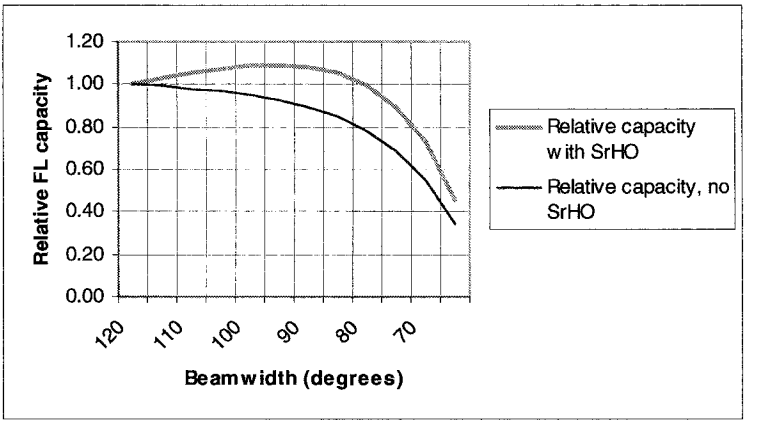

Figure 4-17. FL capacity vs. sector beamwidth, including SrHO overhead and diversity gain

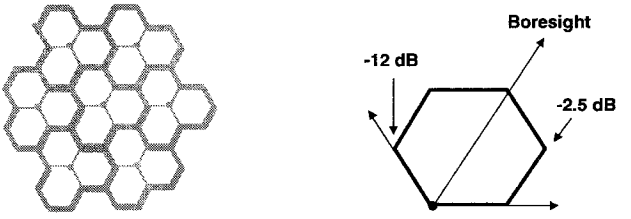

a: Cloverleaf cluster b: Sector and beam pattern

Figure 4-18. Cloverleaf cell and cells' cluster

Note that narrowing the sector beamwidth does not optimize the SHO overhead – the narrow beams create distinct lobes that overlap into the coverage of the adjacent cells. An alternative cellular grid is the *Cloverleaf pattern*, shown in Fig. 4-18, whereby the beam pattern is taken advantage of. The lobed cells interweave into a hexagonal grid, while reducing the coverage overlap and the SHO and SrHO overhead.

The optimal beamwidth for sector coverage, with R^{-4} propagation rule, is 68^0. The SHO and SrHO overhead are substantially smaller than in the *hexagonal cells' grid.*

4.8.1.2 Sector and Cell Shaping

Control over the sector width, controlling the EIRP in a nonuniform sector and matching the boundary with adjacent cells require more degrees of freedom, which are obtainable with multi-element, larger aperture antennas.

These arrays are loosely called "smart antennas" and are classified by their controllability and interaction with the network control and the BTS: controlled by fixed *beam forming networks* (BFN), by controllable radio resource and network performance parameters, or by direct adaptive interaction with the modems. These arrays are limited by size typically to maximum 8 elements in the cellular service, which also sets a minimum usable beamwidth commensurate with the angle spread in that environment (Chapter 3).

Steered beam and switched beam arrays (Fig. 3-33a, b, respectively), used with adaptive control for optimizing the communications with specific users, is a typical *smart antenna* application. These have not captured widespread use in CDMA networks because of excessive complexity and intimate interaction with the BTS circuitry, which inhibits add-on enhancement by operators. Sector coverage shaping by weighted combining of the beams of the multibeam array is described in Fig. 3-33c, 3-33d [10-12]. The steep slope of the 30^0 beam renders a reduced intersector overlap. Capacity increase by over 50% has been reported [11]. The shaping of the coverage is obtained by weighting of each beam. Smoothing of the pattern is obtained by coherent beam combining (c) or by diversity combining (d). Wide (60^0) beam steering is introduced in [10, 12]. The latter combines separate steering of two spaced antennas, with diversity transmission between them, to control both the combined beamwidth – from 60^0 to over 90^0, and its direction, and thereby control the adjacent sectors' widths and directions.

4.8.2 Microcells

4.8.2.1 *Microcell* Classification

Microcells are small-sized cells, typically built to be embedded within a cluster of larger cells. Microcells are classified by their use into the following:

Hot spot *microcell.* High density of users limits the size of the serving cell. A "hot spot" is a locality within the network with a high density that is served by a high capacity *microcell.*

Clustered urban *microcells.* A larger high density area, as in the core of urban areas, is covered by a cluster of high capacity *microcells.*

"Radio hole" *microcell* covers a locality with a poor coverage within the network.

Microcells are classified by the environment they are designed into and the solutions applied:

Indoors *microcells.* They are typified by a high isolation from the rest of the network, by virtue of the building walls, and by the special indoors propagation environment.

Street *microcells.* The coverage for antennas located below the height of neighboring buildings ("under the roof tops") is dictated by the streets structure. Propagation extends as line of sight or nearly so along the street, with little leakage to cross streets.

Outdoors embedded *microcell.* In the absence of isolating structures, the coverage is contained by lowering, tilting down and shaping the antenna pattern, and tuning the *Microcell* sensitivity.

4.8.2.2 Embedded *Microcell* - Coverage and Balancing

Embedded *microcells* are designed to have a defined coverage within the umbrella cell, in order to serve their designated purpose. Excess coverage overlap results in an oversized SHO zone (sometimes extending over most of the umbrella cell), pilot pollution and loss of BTS power. The containment of the *microcell* coverage is therefore a main design challenge.

Further, a highly loaded *hot spot microcell* creates excess *other cell interference* to the umbrella cell, reducing the effective reuse (increasing f in Eq. (4-2)) and the umbrella cell capacity. The isolation of the *microcell* load from the umbrella cell, by properly controlling the SHO zone around the high user density, constitutes the second design challenge.

Balancing the reverse and forward *microcell/* umbrella cell boundaries is the third design challenge.

The *microcell/* umbrella cell scenario is described in Fig. 4-19 [8]. The reverse link power-controlled ST "trumpet-shaped" power P_m has to be penetrated by the *microcells* in order to establish for it a coverage area. This has to be accomplished by either a steeper *transmission gain* slope from the

ST to the *microcell* than to the umbrella cell over that area, $d/dr(1/T_M(r)[dB]) > d/dr(1/T_C(r)[dB])$, or a higher reception threshold $q_M > q_C$ (see Eq. (4-3)), or both. Further, the extent of the SHO zone depends on the ratio of the *transmission gain* slopes around the "trumpets" crossover contour. The higher that ratio is – the narrower is the SHO zone. It is apparent from the figure that the SHO zone stretches out further in the outward direction from the BTS site than in the inward direction. This is evident from reviewing the respective *transmission gain* slopes – they have the same sign outward, but opposite signs in the inward direction. Inward directional antenna at the *microcell* assists in balancing these trends and reducing the SHO zone outwards.

At the *reverse link* boundary (see Eq. (4-11))

$$\frac{q_M}{q_C} = \frac{T_M(R_{MR})}{T_C(R_{CR})} \cdot \frac{F_C}{F_M} \tag{4-47}$$

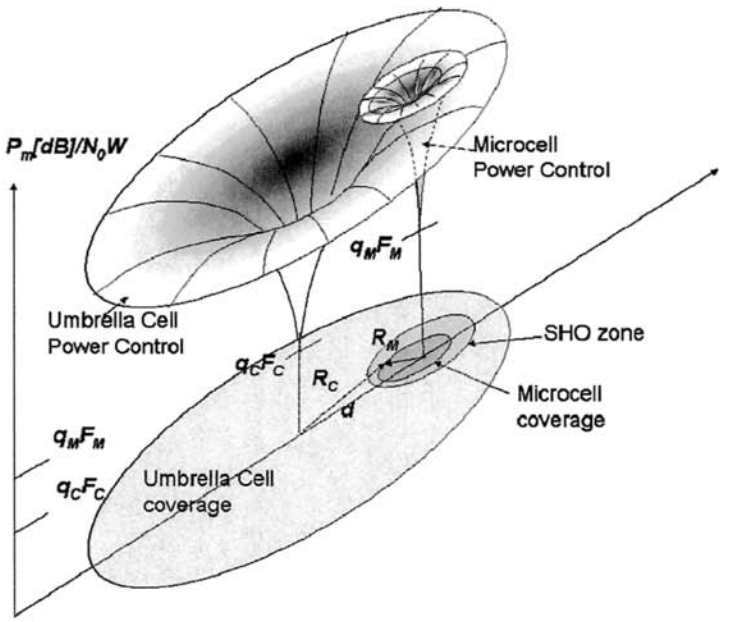

Figure 4-19. (© [1994] IEEE) Microcell embedded in an umbrella cell

The transmission gain is proportional to the antenna height (squared) and inversely proportional to the distance (to 4th power) $T(R)=H^2/R^4$ for a flat earth model (Eq. (3-11)), and thus

$$\frac{T_M}{T_C}=\left(\frac{H_M}{H_C}\right)^2\left(\frac{R_C}{R_M}\right)^4. \tag{4-48}$$

Combining this with Eq. (4-47) renders

$$\frac{R_{MR}}{R_{CR}}=\left(\frac{H_M}{H_C}\right)^{1/2}\left(\frac{F_C}{F_M}\cdot\frac{q_C}{q_M}\right)^{1/4} \tag{4-49}$$

which sets the height of the *microcell* antenna and its noise factor as tools in containing its coverage. Note that R_{CR} in Eq. (4-49) is the average distance from the umbrella BTS to the *microcell* boundary, $R_{CR}\cong d$, the distance to the *microcell* antenna. Antenna down tilting (Sec. 3.6.7.3) increases the slope of the transmission gain and further reduces the coverage of the *microcell.*
The forward link boundary is defined by Eq. (4-42) wherefrom

$$\frac{P_{PM}}{P_{PC}}=\frac{T_C(R_{CF})}{T_M(R_{MF})} \tag{4-50}$$

which sets the dependence of the *microcell* pilot on its distance (or rather its transmission gain) from the umbrella BTS antenna. Incorporating Eq. (4-48)

$$\frac{R_{MF}}{R_{CF}}=\left(\frac{H_M}{H_C}\right)^{1/2}\left(\frac{P_{PM}}{P_{CF}}\right)^{1/4} \tag{4-51}$$

and a reverse/ forward boundary balance is obtained by equating this with Eq. (4-49)

$$\frac{P_{PM}}{P_{PC}}=\frac{F_C}{F_M}\cdot\frac{q_C}{q_M}. \tag{4-52}$$

4.8.2.3 Embedded *Microcell* – Capacity

Microcells serve as "hot spot" capacity cells in localities with a high density of users. The boundary of an embedded microcell with the umbrella cell is a rim around which the user density, pertaining to the large cell, is much lower than that of the microcell. The outer interference that limits the *microcell* capacity is thus much lower than that of clustered cells, and its capacity is substantially higher.

The capacity of the umbrella cell is reduced accordingly due to the additional interference from the embedded microcell. The capacity penalty to the umbrella cell can be diminished by designing the *microcell* boundary to extend beyond the area occupied by high density of users, as demonstrated in Fig. 4-20. Limiting the population to a radius δR_m backs off the maximal power of the STs in the microcell by D dB, thus reducing the interference to the umbrella cell.

The interrelated capacity equations are analyzed in Appendix A, and results are plotted in Figs. 4-21, 4-22 and 4-23 for microcells' radii $1/5^{th}$ and $1/10^{th}$ the umbrella radius, and for power back off (D parameter) 0 to 10 dB.

The capacity of the microcell is 50% higher than that of a cell in a uniform network, and is almost that of an isolated cell. This is because of the major difference in the users' densities inside and around the boundary of the microcell.

It is interesting to note that the combined capacity of the umbrella and the embedded *microcell* is higher than that of two cells in a uniform network. This is caused by the local nature of the interference impact in the power controlled and soft handoff interconnected CDMA network. The advantage of the *microcell* that is almost isolated from outer interference, overcomes the additional interference to the umbrella cell.

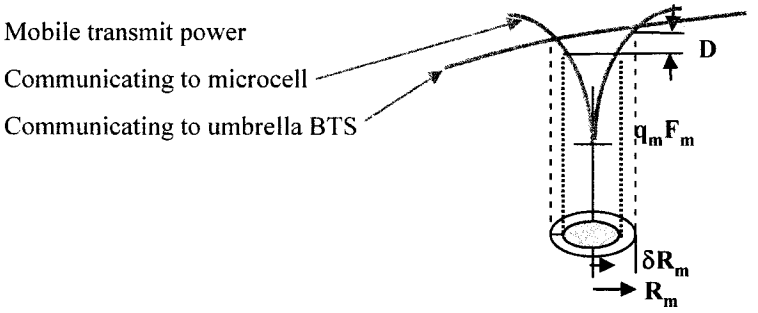

Figure 4-20. (© [1994] IEEE) Limiting the populated area in a microcell and power back off

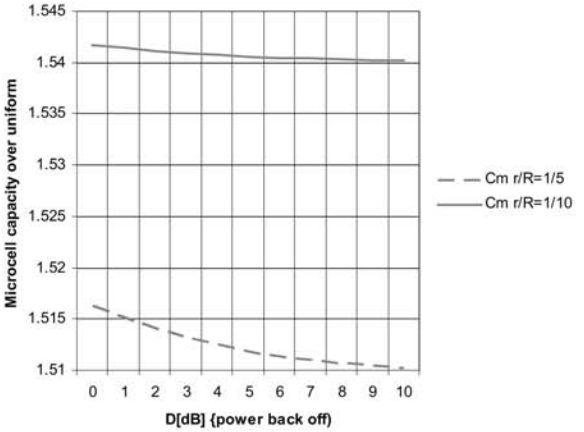

Figure 4-21. Capacity of an embedded microcell, relative to a cell in a uniform network

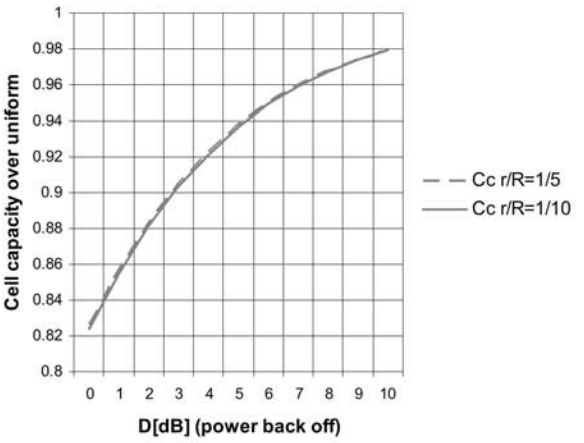

Figure 4-22. Capacity of the umbrella cell with embedded microcell, relative to a cell in a uniform network

4.8.3 Omni Cells

Omni cells refer to cells employing one PN code. These are designed for low cost, low capacity and optimized for coverage. Sometimes they cover the whole 360 degrees (as in rural areas) while other times their coverage is lobed so as to cover only designated areas. Two-lobe lineal cells are specifically designed for coverage along highways or streets.

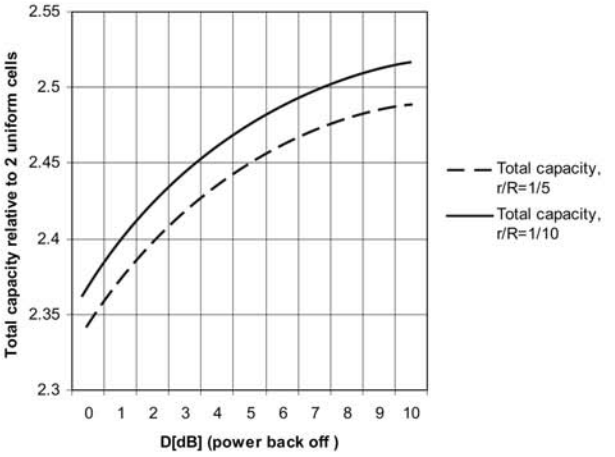

Figure 4-23. Combined capacity of the umbrella and the microcell, relative to a cell in a uniform network

4.8.3.1 Parameters Influencing Large Cells

Antenna gain and height trade-off. Omni cells in rural, flat area, are designed to maximize range. The transmission loss is proportional to R^4/GH^2 (see Eq. (3-11)), where G is the gain of the BTS antenna and H is its height. Considering the radar horizon (that takes into account standard atmosphere) is $R[km] << \sqrt{17H[m]}$ as maximal range for this propagation law, the trade-off sensitivity is $\frac{dR}{R} = \frac{1}{4}\frac{dG}{G} + \frac{1}{2}\frac{dH}{H}$. This means that the cost of increasing the range by 50% is either increasing antenna gain by 7 dB, or multiplying the antenna height by 2.25. Increasing antenna gain is the lower cost option in most cases. The gain obtained by limiting the beamwidth in elevation is $G_{EL}[dB] = 20.6 - 10\log \vartheta_{EL}{}^0$ and is limited to about 13 dB for omni-directional cell, as a beam narrower than about 6^0 may loose coverage for any terrain undulation or atmospheric fading. There is therefore an advantage to additional antenna gain by limiting the angular illuminated area to the desired one only. Multi-lobed illumination, for serving more than one designated area, involves further considerations, to be treated below.

Tower-top amplifiers. The height of the large cells' towers brings to focus a trade-off of relaying the RF signals to the antenna by cables, which incurs a power loss of 3 dB or more on transmit, and respective additional noise

figure, or placing the amplifiers at the top, where they are not as accessible and serviceable.

Diversity. Antenna diversity is applied in most BTSs for increasing the RL gain and range. Diversity means are not as effective in large omnidirectional cells, however.

The gain of the *space diversity* is at optimum for antenna spacing $d \cong \vartheta[rad]^{-1}$ where θ is the angle spread. The latter depends on local scatterers around the ST ("local neighborhood") that is not range dependent, but environment dependent. The angle spread thus shrinks with the distance, and the required antenna spacing increases accordingly. Effective space diversity requires very large antenna spacing in open, flat areas, which may not be practical for very high towers. For example – a 20 km range in near LOS, with a scattering neighborhood of 200 m, renders an angle spread of 1/100 rad, and a need for 15 m spacing in PCS and 35 m in cellular band. Note that space diversity is not omnidirectional by nature. Max gain is achieved at broadside (perpendicular to the antennas' baseline), decreasing to diminishing gain at end-fire.

The effect of *polarization diversity* depends on the characteristics of the ST: those that are handheld or otherwise tilted from vertical position may benefit from *polarization matching* more than diversity, as the XPD is expected to be very high in open, rural area and little scattering, so the net effect is that of matching.

4.8.3.2 Multi-Lobed Cells

These are the preferred solution to highway coverage, typically with two lobes, street coverage (sometimes called *street microcells*), and to rural area with clustered communities. Lobed illumination incorporates multiple directional antennas. All the lobes share the same transmitted signal, and the BTS receiver shares the incoming signals and interference from all lobes. This configuration is closely related to the application of repeaters, treated in Chapters 6 and 7. Two main considerations are involved in multi-lobing: *range profiling* and the *beams' distribution/ summation network.*

Range profiling. The transmission gain $T \propto G(\vartheta,\varphi)R^{-4}$ is limited by the system maximal link loss, bound between transmission power and maximum sensitivity. Range is then related to gain $R(\varphi_i) \propto G(\vartheta_i,\varphi_i)^{1/4}$, and $G(\vartheta_i,\varphi_i) \cong G_{EL}(\vartheta_i) \cdot G_{Az}(\varphi_i)$ (Cf. Section 3.6.2), where $_{EL,\ AZ}$ indicate elevation and azimuth, and θ_i, φ_i the elevation and azimuth angles of the i_{th} beam. While G_{EL} is typically limited by the vertical size of the antenna and elevation beamwidth is typically 6^0 to 15^0, coverage shaping relates to $G_{AZ}(\varphi_i) = 2\pi/BW(\varphi_i)$ and the range is inversely proportional to (fourth root of) the azimuthal beamwidth. Profiling is sought where long range is required for

covering remote users' clusters or a stretch of road along with coverage of neighboring communities in other directions. The profiling is different for the forward and the reverse link: FL is limited by total transmitted power, while the RL is limited by the ST power and the total noise power at the receiver.

Transmit power distribution. The range profile is determined by the gain and the power allocation to the beam, and the number of users n_i within the beam that are located at the extreme range. With FL power control most of the transmission power is allocated to users that are the extreme range, and then $P \propto \sum_i n_i / B_i R_i^4$ where P is the total transmitted power and B_i is the respective azimuthal beamwidth. The power is distributed to the antennas either at the output of the power amplifier (high-power distribution network), or in low power, prior to power amplification. Low power distribution allows for allocation of power according to the number of users served by each beam, by gain control of separate power amplifiers to each antenna. Placement of the power amplifiers at the tower-top also alleviates power loss in the lengthy cables. Each beam amplifier has to accommodate the peak power designed for that beam (see also 3.6.7.4 and Fig. 3-33c). Splitting the power at the output of a single power amplifier is not flexible and may involve losses in the high-power RF network.

Receive signals summation. Each user is power controlled to the right level at the entry to the BTS receiver after summation of all beams. The gain of each antenna influences the ST transmit power, and thus controls the maximal range for users exercising full power. The range profiling is derived $B_i R_i^4 \propto P_m / S_T$ utilizing Eqs. (4-3), (4-4) and (4-7). Here P_m is the maximal ST power and S_T is the BTS noise rise. Additional noise is contributed from the antenna temperature, which is independent of the antenna gain (Section 3.6.9), from the passive combining network and cables, and from the LNA. Amplifying the signals at each antenna output by a dedicated LNA (Low-Noise Amplifier, also called TMA – Tower Mounted Amplifier in this application) offers higher sensitivity at each beam and a flexibility in combining beams that are not evenly loaded.

Overlapping beams. The shape of the required coverage is not split into nonoverlapping beams in many cases, as where both long-range directional beams along the highway, and a wide beam covering the near zone community are needed, or where two overlapping directional, sector-like beams overlap. The respective antennas may not be colocated so as to have a common phase center. The signal transmitted through all antennas is the same coherent signal, and interference between the coherent beams in their overlap zone creates fringes which shadow strips of the footprint. Similarly, reception of signals from sources located at these overlapping zones creates fringes on the summation of the coherent signals received by both antennas. This is an issue in clutterless open areas, where there are not enough scatterers to diffuse

the footprint. Means to diffuse these fringes are beam jitter, phase jitter or delay that exceeds one CDMA chip. The jitter creates artificial fading at the rate of the jitter. The FEC decoder and deinterleaver in the receiver recover these fading if their frequency is tuned to within its effective range. Jitter within 50 to 100 Hz is typical. The decorrelation by delay is recovered by the rake receiver. However, the additional "finger" adds noise (discussed above in the context of multipath).

The nature of fringes. Fringes are created between two coherent antennas whose phase centers are spaced apart. Their dips are spaces by $\Delta\vartheta \cong (180/\pi)(\lambda/d)$[deg] where λ is the wavelength and d is the spacing. Thus for $d = 10\lambda$, $\Delta\vartheta \cong 6^0$ .These fringes create deep nulls where the strength of the two signals are about equal, namely – around the crossover between the lobes. The angle zone of concern is limited by the ripple that can be tolerated. Thus, for a 3 dB ripple this zone is bound between $-3\ dB < (G_1 - G_2) < 3\ dB$.

4.9 Network Optimization

4.9.1 Objectives

The radio resources of the cellular network are the equipment and infrastructure, the operations force and the allocated spectrum. Optimization means maximization of the benefit from these available resources: maximize the throughput (capacity), maximize the coverage – to provide the contiguous service area, and maximize the quality of service to strengthen the subscriber base, while minimizing required resources.

The radio resources require optimization at the planning and deployment of the network, at a time when the teletraffic activity and its distribution change appreciably, and when an upgrade takes place – by changing air interface standards and/ or changing infrastructure components. The fast evolution of standards and diversification of services disrupts the network balance and stability and is destined to require an online dynamic optimization based on timely measurements of the network parameters.

4.9.2 The Dimensions of Optimization

The controllable radio parameters that lend themselves to optimization are discussed in the following sections.

4.9.2.1 Channel Quality

The threshold average *Eb/It* required by the receiver determines the coverage, the power setting and the capacity. The fading in a scattering environment destabilizes the channel and a margin is required to guarantee

error free reception. This margin is traded-off by channel diversity on the receive side, transmit side or both.

4.9.2.2 Path-Loss Variability

The path-loss variation across a cell exceeds 80 dB. Subscribers in shadowed areas incur additional losses that drain the BTS power and increase the failure rate of access attempts. Moving in and out of these "radio holes" increases the rate of dropped calls and resources allocated to access attempts. Excess path-loss variability is treated by properly distributing the access radio points, by remote sectors and by repeaters. The variation caused by polarization mismatch of each subscriber can be mitigated by dynamic polarization matching at the BTS and/ or the ST.

4.9.2.3 Link Balancing

Link imbalance induces extended SHO zone, pilot pollution, dropped calls and access attempts failure. Methods of balancing the links include control of the pilot power, of the coverage and of the transmission gain slope. Network probing is required for proper balancing.

4.9.2.4 Pilot Pollution

This is the area where a large number of pilots, greater than the allowed active set, have a significant strength and are candidates for the active set. The large number of transmissions from different BTSs increases the total interference, thereby reducing the *Ec/Io* and creating an area with a high rate of dropped calls and unsuccessful access attempts.

Pilot pollution is caused by unbalanced, excessive pilot (and forward link) power from multiple cells. It hampers the performance and reduces the capacity of the system, both by draining excess power from the BTSs and by increasing the interference. Pilot pollution is cured by balancing the links – by adjusting the pilot power, and by increasing the transmission slope through antenna down tilt – between cells, and narrowing the antenna beam between sectors. The latter also helps in narrowing the Soft and Softer HandOff zones. Distribution of the access – by remote sectors or repeaters, is another means to enhance the transmission slope and reduce the SHO zone [9].

4.9.2.5 Load Balancing

The load is not uniform across the network, and varies among sectors and cells. Excess load from saturated cells can be shed to the neighbors by coverage control means – moving the cell boundary by controlling the beamwidth and tilt of BTS antennas in both cells.

4.9.3 Scope and Dynamics of Optimization

4.9.3.1 Factors Affecting the Rate and Scope of Optimization

Complexity. The number of interrelated access node and network parameters is high. A market level optimization is an insurmountable computational exercise, sensitive to huge errors relating to inaccuracies in the parameters' measurement and prediction, and to the inhomogeneity of the network and its optimization objectives. A market-level optimization serves only as initial scoping of the project and rough allocation of the infrastructure.

Cost. The dominant cost elements in the optimization process are the measurement and information gathering, and the implementation of the changes. The field measurement process involves lengthy drive tests over the area to be optimized, some of which have to be repeated during different activity periods, and for validation of the implemented changes. The implementation involves changes in antenna positioning – a process that needs more than one iteration in many cases, because the antenna patterns stored in the optimization tool do not reflect their footprint in the given environment.

Vendor-operator responsibility. The nature of the BTS vendor warrantee inhibits some operators from administrating any changes in the BTS and network setup, and leaves only the RF access to be optimized.

4.9.3.2 Evolution of Optimization

Cell optimization. The most intimate relations between parameters are at the cell level. Inhomogeneous distribution of activity and coverage are optimized locally by application of diversity, coverage shaping, distributed antenna and repeaters. Typical scenarios are penetration indoors and changes of activity from outdoors to indoors oriented. "Hot spots" and "radio holes" fall in this category. Adaptive beam steering and "smart antennas", which interact directly with the receiving process, have to be integrated into the BTS. Their dynamic interaction with adjacent cells disrupts the SHO zone, and a buffering control may be needed to separate the radial from the angular coverage control[12] .

The interactive cluster and optimization hierarchy. The effective neighborhood of a cell in a CDMA system, that interacts with it through the SHO process and affect its interference, is not larger than one to two tiers around the cell, amounting to a cluster of 10 to 15 cells (or 30 to 45 sectors). Incorporating a larger number of cells in the optimized cluster reduces the

[12] The "clever antenna" concept controls the angular beamwidth and direction, for its function as a "smart antenna", while controlling the EIRP at the cell edge for maintaining a stable SHO zone. The latter is applied by beam tilting.

accuracy, as it adds "noise" to the process. Moreover – clusters with homogeneous activity, and therefore unified optimization objectives, tend not to exceed this number anyhow. Optimization of a larger market is then best performed by optimizing the clusters of this size, and then mending the interfaces – in case these happen to fall on lower priority areas, or re-iterating the optimization in sliding manner over this cluster size, when the high priority cluster is larger.

Technology evolution. Means are becoming available and cost-competitive for performing both the network measurement and the antennas' control, so as to alleviate most of the cost of the optimization process. Remote Electrical Tilt (RET) antennas are a cost-effectiveness compromise between fully electronically tilt and steered antennas [8] and simple, mechanically manipulated ones. RET enable a dynamic optimization by reacting to the online field measurements and respective computations. Network probes, providing measurement of the pilot and forward signal strength and respective ST transmit power, are available embedded in selected commercial STs. Remotely controlled repeaters complement this arsenal, to enable the dynamic control and optimization of cell clusters ("smart clusters", Fig. 4-24). Their commercial introduction is expected with the increasing stress on the networks by multimedia services [24].

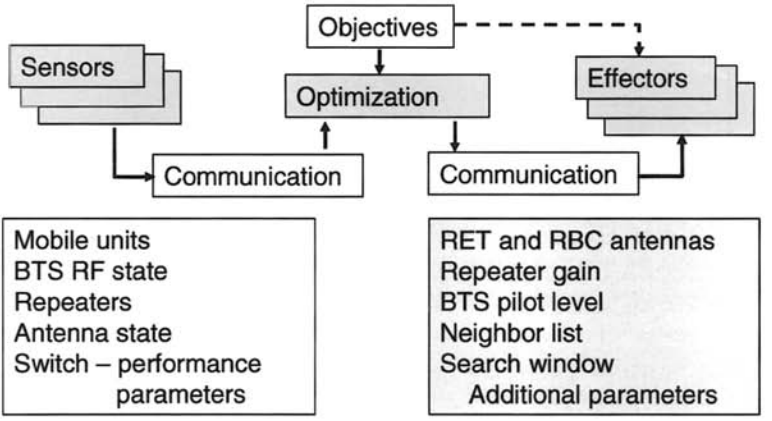

Figure 4-24. Dynamic optimization of a "Smart Cluster"

REFERENCES

[1] K.S. Gilhousen, I.M. Jacobs, R. Padovani, A.J. Viterbi, L.A. Weaver, Jr., and C.E. Wheatley, *On The Capacity of a Cellular CDMA System*, IEEE Trans. VT-40, pp. 303-312, May 1991.

[2] S. Soliman, C. Wheatley and R. Padovani, *CDMA Reverse Link Open Loop Power Control*, Proceedings of GLOBECOM 92,Vol. 1, pp. 69-73, Dec. 1992.

[3] J. Shapira, and R. Padovany, *Spacial Topology and dynamics in CDMA cellular Radio*, Proc. 42nd IEEE VTS Conf., Denver, CO, May 1992.

[4] *CDMA Network Engineering Handbook*, Qualcomm, 1992.

[5] A.J. Viterbi, *CDMA*, Chapter 6, Addison-Wesley, 1995.

[6] TIA/EIA Telecommunications Systems Bulletin TSB84-A, 1999.

[7] J. Shapira, and C.E. Wheatley, *Channel Based Optimum Bandwidth for Spread Spectrum Land Cellular Radio*, Proceedings of PIMRC 92, pp. 199-204, Boston, October 1992.

[8] J. Shapira, *Microcell Engineering in CDMA Cellular Networks*, IEEE Transactions on Vehicular Technology, Vol. 43, No. 4, pp. 817-825, November 1994.

[9] R. Padovani, L.A. Weaver, and P.E. Bender, *Method and Apparatus for Balancing the Forward Link Handoff Boundary to the Reverse Link Handoff Boundary in a Cellular Communications System*, US patent 5,722,044, 24.2.1998.

[10] J.S. Lee, and L.E. Miller, *CDMA Systems Engineering Handbook*, Artech House, 1998.

[11] S.C. Yang, *CDMA RF Systems Engineering*, Artech House, 1998.

[12] L. Korowajczuck, et. al., *Designing cdma2000 Systems*, Wiley, 2004.

[13] D. Li, J. Khoja, and V.K. Prabhu, *System Capacity in the Forward Link in CDMA Systems*, Proc. of IEEE Radio and Wireless Conference RAWCON'03, 2003.

[14] H. Holma, and A. Toskala, *WCDMA for UMTS*, Chapters 8, 9, Wiley, 2001.

[15] J. Laiho, A. Wacker, and T. Novosad, *Radio Network Planning and Optimization of UMTS*, Wiley, 2002.

[16] K. Sipita, Z.-C. Honkasalo, J. Laibo-Steffena, and A. Wacker, *Estimation of Capacity and Required Transmission Power of W CDMA Downlink Based on a Pole Equation*, Proc. of IEEE VTS Conf., Spring 2001.

[17] A.M.D. Turkmani, A.A. Arowojolu, P.A. Jefford, and C.J. Kellet, *An Experimental Evaluation of the Performance of Two-Branch Space and Polarization Diversity Schemes at 1800 MHz*, IEEE Trans. VT, Vol. 44, No. 2, pp. 318-326, May 1995.

[18] J. Shapira, *Active Antenna Array Configuration and Control for Cellular Communication Systems*, US Patent 6900775, May 31, 2005.

[19] W.C.Y. Lee, and D.J.Y. Lee, *The Impact of Repeaters on CDMA System Performance*, Proc. 51st IEEE Vehicular Technology Conference, Vol. 3, pp. 1763-1767, 2000.

[20] K. Fujimoto, and J.R. James, *Mobile Antenna Systems Handbook, Second Edition*, Chapter 5, Artech House, 2001.

[21] S. Gordon, and M. Feurstein, *Evolution of Smart Antennas from 2G to 3G Air interfaces – Capacity Increase and Performance Optimization*, Sixth workshop on Smart Antennas in Wireless Mobile Communications, Stanford University, July 1999.

[22] J. Shapira, *Modular Active Antennas Technology for Intelligent Antennas*, 6th workshop on Smart Antennas in Wireless Mobile Communications, Stanford University, July 1999.

[23] J. Shapira, *Dynamic Enhancement and Optimal Utilization of CDMA Networks*, PIMRC2004, Barcelona, 2004, also Chapter 6 in: *Emerging Location Aware Broadband Wireless Ad Hoc Networks,* Springer, 2005.

[24] G.I. Zysman, J.A. Tarallo, R.E. Howard, J. Friedenfelds, R.A. Valenzuela, and P.M. Mankiewich, *Technology Evolution for Mobile and Personal Communications*, Bell Labs Technical Journal, Jan-March 2000.

5

DIVERSITY IN TRANSMISSION AND RECEPTION

Mobile communications is characterized by fluctuating signal levels and additive interference from in-cell and outer-cells, which directly affect the communicated signals and result in time-varying signal quality (signal to interference plus noise power ratio - SINR) that requires special means to combat these effects and provide reliable communications. Among the most important means utilized are error-correcting codes, power control and diversity. When operating repeaters in a CDMA network, additional issues are introduced, including the application of diversity techniques to repeaters, the interaction of the repeater diversity operation with the BTS, the repeater backhaul support of diversity, and – on a different scale, the application of diversity to the repeater backhaul link. These issues are addressed in this chapter.

5.1 Overview of Diversity in Communications

5.1.1 Introduction

The wireless mobile communications channel is typified by location dependent characteristics, which turn into time-varying characteristics as the users move around (Chapter 3). The signal arriving at the receiver comprises of multiple rays, and each typically undergoes attenuation through shadowing, scattering by objects near the source or near the receiver, and reflections from large reflecting objects located anywhere in the illuminated path. These multiple rays, commonly termed *multipath*, interfere with each other at the receiver to form a fading signal. These interference fading are also called *small-scale fading*, or *fast fading*, to differentiate from signal shadowing, *slow fading* (also called *large-scale fading*), that extend over a larger area and longer time and are typically characterized by Lognormal statistical distribution. The statistics of the *fast fading* in a Non Line of Sight (NLOS) scenario is modeled well as a circularly symmetric complex

Gaussian (CSCG). The amplitude (absolute value of the complex envelope) is then Rayleigh distributed (Eq. 3-30) with phase uniformly distributed over 0 to 2π.

Diversity is a way to combat fading by providing the receiver with multiple *copies* of the transmitted information, with statistically independent fading. The different signal copies are applied to the multiple channel receiver through *diversity branches,* or *diversity channels*. The receiver operates on the multiple branch signals to extract the desired signal under an optimization criterion. The branches are physical entities, enabled by multiple antennas or antenna ports (in the *space* domain), multiple frequency allocations (in the *frequency* domain), or multiple delays of the signal replica (in the *time* domain), as examples. Diversity can be applied at the transmit side (Tx diversity), or at the receive side (Rx diversity), or both at transmit and receive sides (Tx and Rx diversity)[13]. When discussing diversity, it includes both the *methods* of generating independently fading copies, and the processing *algorithms* at the diversity receiver. Diversity methods and techniques have been reviewed extensively in the literature [1-4]. The improvement achieved by diversity processing is termed *diversity gain*. There are different definitions of diversity gain which depend on the application and nature of the communication system involved, that lead to different quantitative measures of the improvement. Within the context of the cellular wireless communications, the improvement sought is reduced BER (Bit Error Rate) for a given power level, or vice versa – reduced power level for the same BER. The channel impairment of main concern in this service is amplitude fading (Section 3.4). Diversity gain therefore relates to the envelope correlation between fading channels and its relation to the BER level for a given type of service (given data rate). Strictly speaking, the diversity gain refers to the reduced probability of signal outage, usually referred to a relative signal fade-depth, e.g. 10% of the power CDF (sometimes called "*reliability level*"). Appendix E indicates the close relation between the envelope correlation and power correlation for Rayleigh fading channels. Thus, one way to analyze diversity performance is by examining the short-term[14] power cumulative distribution functions (CDFs) per branch before and after diversity processing [2, 3][15]. The difference in their value stems from a shift

---

[13] Tx and Rx diversity is sometime referred to as MIMO Diversity, MIMO standing for *multi-input multi-output*, indicating usage of multiple antennas both at transmit and receive ends [5].

[14] "short-term" is measured over a period longer than the signal symbol, but shorter than the coherent time of the channel.

[15] Performance is evaluated by comparing the 10% points before and after applying diversity. The p% power outage value: $x_{p\%}$ is defined by: $P(x \le x_{p\%}) = p\%$, where x is the power random variable.

of the CDF curve, resulting from *coherent power summation*, and increased steepness of the slope of the curve. *Net diversity gain* is related to the steeper slope of the signal envelope (or power) CDF. The diversity gain is measured relative to the CDF of the strongest branch.

A related definition of diversity gain, interconnecting the BER with the SNR for a given data rate, is $d(R) = -\lim_{SNR\to\infty} \frac{\log[P_e(R,SNR)]}{\log SNR}$, where $P_e(R,SNR)$ is the BER at the given rate and SNR.

This means that the diversity gain is the magnitude of the slope of the log-log plot of BER as a function of SNR for low BER values. This relates to the previous definition by realizing that in this service the BER is proportional to the fraction of time the signal is in fade, and thus – to the CDF of the signal power.

Figure 5-1 shows an intuitive diversity processing where two input signal copies (denoted by dotted and striped lines) yield a less fluctuating signal (continuous line) as a result of diversity processing, riding on the top of the two independently fading signals. The threshold link quality line (measured in BER – Bit Error Rate, or similar), is surpassed appreciably, thus allowing for either saving of power while maintaining the same BER, or increasing the data rate.

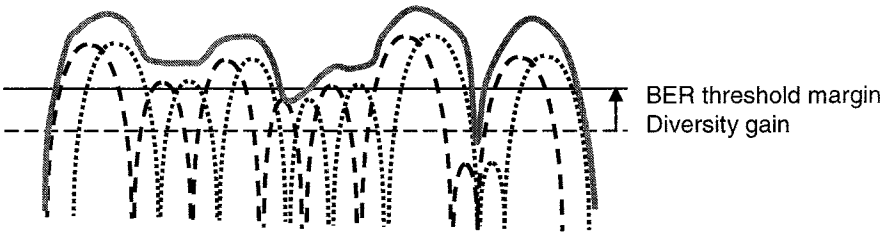

Figure 5-1. Two-branch diversity signal enhancement

It is important to distinguish between *diversity gain*, *power (coherent) gain* and *net diversity gain*. Power (coherent) gain stands for the gain in mean power when using multiple branches, which acts coherently as a single branch with enhanced power. The location of the signal dips, and their depth are not changed - only their width. Thus, with a fully correlated reception of two (identical) copies of the same signal as in Fig. 5-2, there is no *net diversity gain*, and the *power gain* is +3dB.

We adhere in the following to the conventional definition of *diversity gain* (in the broader sense) that incorporates *both* the *net diversity gain* and the *power (coherent) gain*. When receiving multiple copies of a signal there is

always *power gain* and possibly a positive *net diversity gain*. When transmitting multiple copies of a signal, there is no power gain at the receiver if the total Tx power is preserved, while in case the power per branch is preserved - the received power gain grows with the number of branches.

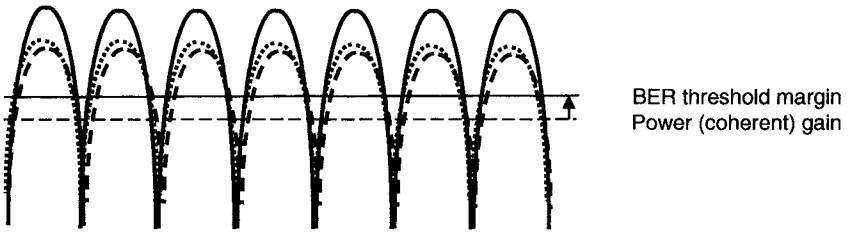

Figure 5-2. Two-branch power gain with correlated signal copies

Figure 5-3 sketches the CDF of a single fading channel, and then of coherently combined fading channels (power gain) and diversity-combined channels (diversity gain). The linear CDF scale renders a typical "S" curve.

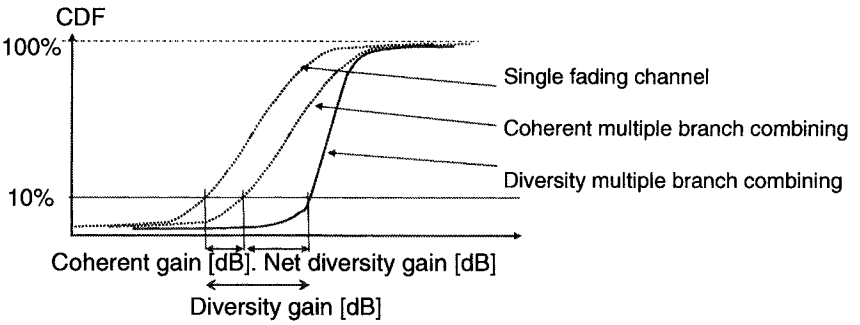

Figure 5-3. Cumulative Distribution Function (CDF) of fading signals showing diversity combining

An especially illuminating presentation of the CDF of Rayleigh statistics and alike is on the Rayleigh chart, plotted as $10Log[-Ln(1-CDF)]$ vs. the SNR[dB], shown in Fig. 3-26. A Rayleigh fading signal follows a slanted straight line. Diversity–combined signals (as multipath in the rake receiver) or

partially LOS (Rician statistics) are closely described by a Nakagami-m statistics (Eq. (3-31)) as nearly straight lines with steeper slopes. These are easy to follow and interpret in assembling field measurements.

The diversity branches are rarely fully independent and equal power. The two significant factors affecting the diversity gain are the branch correlation and the ratio of average power of the branches.

Correlation between fading channels. A key factor in achieving good diversity performance is the minimal correlation between the fading signal copies. Measurements show that a correlation of 0.7 is the highest applicable for obtaining a satisfactory diversity gain. This is supported by analysis of the Rayleigh statistics fading [6]. Lower correlation improves the diversity gain.

Power ratio. Branches of equal average power have the potential of nullifying each other by destructive interference, thus creating deep fades. Naturally, diversity is most effective in such situations, as it takes only a small perturbation in phase and/or in amplitude to defuse a deep fade. The higher the power ratio between the branches – the shallower is the fade, and the diversity gain is lower.

5.1.2 Diversity Dimensions

The dimensions along which diversity is discussed include the various types of diversity channels, diversity coloring schemes, and diversity order.

5.1.2.1 Fading Channels and Diversity Means

Fading channels are commonly modeled as a transmission being received with multiple reflected and scattered rays, the superposition of which resulting in a signal with unpredictable envelope and phase. The result is a time-varying distortion of the information signal, which depends on the speed, direction, frequency, waveform bandwidth and characteristics of the channel. When the *signal bandwidth* is narrower than the *coherence bandwidth* of the channel (Cf. Section 3.4.2) the signals' spectrum is not distorted, and the channel effect is reduced to *flat fading*, well described as a multiplicative Rayleigh random variable operating on the signal envelope, in addition to the introduction of a uniformly distributed random phase. A combination of a received direct (nonfading) ray and several (statistically independent) Rayleigh fading rays constitutes the channel model that is sufficient for treating most of the encountered scenarios with cellular environment. When the delays of the different rays are time-displaced by more than one-chip duration in the CDMA system, they appear as distinct fingers at the output of the rake receiver (Fig. 3-22).

Diversity conditions are formed between the channel and the signal design [7]. These may be categorized by physical dimensions space, polarization,

time, frequency, and combinations thereof in a certain logical order (codes). Ways of achieving separate channels with low fading correlation amongst them are presented, along with their limits, and methods that allow distinguishing between the various branches at the receiver to allow for proper diversity combining.

Space diversity: (Section 3.6.8.2) employing multiple spaced antennas for transmitting or receiving or both; by using large enough spacing it is possible to significantly decrease the fading correlation between different channels (see Sections 3.6.8.2-3). The underlying decorrelating feature is the *angle spread* (Fig. 3-34) over which the source plus its neighboring scatterers are seen by the receiving antennas. The distance $d = \lambda/2\varphi$ is considered the *aperture coherence* condition, where 2φ is the *angle spread.* Reception over a distance smaller than the coherent distance is increasingly coherent, with a reduced diversity gain. (The argument is the same in transmit diversity).

Polarization diversity: (Cf. Section 3.6.8.4) employing two orthogonally polarized antennas, e.g. V-H, or ±45° cross-polarized antennas, or RHC (right-hand circular) and LHC (left-hand circular) circularly polarized antennas. Two orthogonal paths are formed when linked to a similarly dual polarized antenna pair. When receiving signals from a singly polarized antenna, a diversity path is created by energy leaking from the transmitted polarization to the orthogonal one along the propagation path ("*polarization spread*") by scattering, and then received by the orthogonally polarized antenna pair. The scattering mechanisms for signals that are orthogonally polarized are different and their fading patterns are thus independent, which diminishes the correlation between the polarized received signals. There is an analogy between *angle spread* and *polarization spread* (or its inverse – XPR: cross polarization ratio). The higher the XPR is, the more coherent is the reception and the receive mechanism is described as *polarization matching* (similar to *beam steering* in the angle domain) rather than diversity gain.

Antenna pattern diversity/Angle diversity: (Cf. Section 3.6.8.3) employ different beams from the same site, which are pointed in different directions. *Angle diversity* is closely related to *space diversity*, and is related to the *angle spread* via the *aperture coherence* limit $\vartheta \cong \lambda/d = 2\varphi$, where ϑ is the beamwidth and d is the antenna aperture size.

Frequency diversity: (Cf. Section 3.4.2) employs different frequencies for transmission of multiple copies of the signal, or spreads the signal energy over a broad frequency band. If the frequencies are sufficiently displaced, beyond the *coherent bandwidth* of the channel, then channel fading is practically independent between the different branches. The CDMA transmission spreads over a band that is appreciably wider than the *coherent bandwidth* of the channel. The fading of each coherent band thereof interferes with the other independent fading, smoothes the received signal and does not

suffer from flat fading. The *coherent bandwidth* is inversely proportional to the *channel delay spread* (Section 3.4.1).

Time diversity: (Cf. Section 3.4.2) employs multiple transmissions of the information at significantly displaced times, beyond the *coherent time* of the channel, such that a transmission that falls into a deep fade is recovered at a later time. The *coherent time* is inversely proportional to the *Doppler spread* of the channel. *Time diversity* is employed in conjunction with the Forward error-correcting code (FEC), by scrambling the symbol and spreading it over a period much longer than the *coherent time* (*interleaving*). In the CDMA it is spread over a frame (20 ms in IS 95, for example) such that no whole code word falls into a fade, and successive symbols within each code word fade independently. The FEC is built to recover sparse random errors upon reception subsequent to the deinterleaver reordering of the received signal. Data transmission in 3G standards employs Automatic Repeat Request (ARQ) protocol that repeats the transmission of a frame that is erroneously received. When the retransmission is beyond the *coherent time* of the channel, it provides *time diversity*.

Delay diversity: (Cf. Section 3.4.1). The CDMA signal bandwidth is appreciably wider than the coherent bandwidth of the channel, and signals delayed by over a chip (which is about (channel-bandwidth)$^{-1}$) are already resolved by the rake receiver that consists of a set of time-searching correlators ("fingers") matched to the spreading code. Such delayed signals (Fig. 3-22) traverse different paths than the earlier arrivals, thus undergoing independent fading. The delayed signals captured by fingers are optimally combined to produce diversity gain. Note that delay diversity applies only to large delay spread (long delays) and not to flat fading. It is complementary to the antenna diversity that applies to flat fading.

Summarizing the fading channels and diversity means:

Flat fading are characterized by Rayleigh statistics for NLOS and by Rician statistics for mixed paths. These are well approximated by Nakagami-m statistics that have a rational expression (Eq. (3-31) and Fig. 3-26). Flat fading is mitigated by *antenna diversity*: space diversity, angle diversity, limited by the *angle spread* vs. *aperture coherence* (distance between space diversity antennas or aperture of the antenna in angle diversity), or polarization diversity, limited by the *polarization spread* of the channel. *Time diversity* does not require separate antennas, and is limited by the *coherent time* of the channel.

Frequency dispersive channels create long-delayed multipath (delay spread > (coherent bandwidth of the channel)$^{-1}$). These are characterized as multiple rays, each approximated by Nakagami-m statistics [Cf. Section 3.4.3]. A frequency dispersive channel is mitigated by the rake receiver in the

CDMA system, utilizing the *delay diversity*, or by *equalizers* in narrow band systems.

Some environments may not be suitable for diversity applications, mainly line of sight (LOS) characterized as a nonfading additive-white-Gaussian-noise channel (AWGN channel).

5.1.2.2 Signal Coloring

Signal coloring is part of the diversity processing means, and is required for transmit diversity, and by the rake receiver in multipath detection. The signal coloring applies to the signal copies and enables the receiver to operate on each of the signal copies to produce the enhanced signal.

Time delay: A signal delayed by one CDMA chip time or more is identifiable by the rake receiver. Artificial delay is employed in time-delay transmit diversity (TDTD) from diversity-spaced or diversity-polarized antennas, or ports of multibeam antennas, imitating artificial multipath to the receiver.

Phase sweeping: The transmission from the diversity antenna is phase modulated at a rate commensurate with the effective fading recovery rate of the coder-interleaver (less than about 100 Hz). The phase sweep is implemented by a slight frequency shift of the allocated carrier or by actual periodic phase modulation. The combined signal at the receiver is amplitude modulated at the sweep rate. It translates slow Rayleigh fading channels into fast Rayleigh fading channels that are recoverable by the coder-interleaver, and is effective for slow motion, long fades. Phase-Sweeping transmit diversity (PSTD) can be applied to space or polarization diversity.

Codes are used for marking the different copies used in diversity transmission so that the receiver may identify each separately and combine them effectively to produce diversity gain. A simple such example is the Alamouti [8] space-time block code (STBC). This technique does not expand bandwidth, does not require feedback from the receiver to the transmitter, requires low-complexity processing, and has similar performance to maximal ratio combining (MRC – see discussion below) at the receiver. We illustrate it in its simplest form for two Tx antennas: let the transmitted signal symbols be paired into blocks, denoting (we omit the continuous time dependence for simplification, and all waveforms are complex functions) one such block of 2-symbols duration as $[s_1\ s_2]$. Let one antenna transmit the sequence $t_1 = [s_1\ -s_2^*]$, where the asterisk denotes the complex conjugate operation, while the second (diversity) antenna transmits the sequence $t_2 = [s_2\ s_1^*]$ [16]. If the channel response from the Tx antennas to the receive antenna is h_1, h_2, respectively,

[16] This scheme is also termed space-time transmit diversity (STTD) in 3G CDMA systems.

(these are complex variables) and assuming that the channel response does not change over the two symbols duration, then, using the same notation, the receive signals block is:

$$r = [r_1 \; r_2] = [(h_1 s_1 + h_2 s_2 + n_1) \; (-h_1 s_2^* + h_2 s_1^* + n_2)] \tag{5-1}$$

where $[n_1 \, n_2]$ are the Rx additive noises over the two symbol durations, respectively[17]. We assume that the receiver knows the channel response (based on a dedicated pilot signal transmitted from each Tx antenna) up to a factor α, and performs the following linear processing on r:

$$\begin{aligned} \hat{s}_1 &= \alpha h_1^* r_1 + \alpha h_2 r_2^* = \alpha[(|h_1|^2 + |h_2|^2) \cdot s_1 + h_1^* n_1 + h_2 n_2^*] \\ \hat{s}_2 &= \alpha h_2^* r_1 - \alpha h_1 r_2^* = \alpha[(|h_1|^2 + |h_2|^2) \cdot s_2 - h_1 n_2^* + h_2^* n_1] \, . \end{aligned} \tag{5-2}$$

The result is that each symbol is received multiplied by the combined norms squared of the channel responses - which emphasizes the diversity combining operation. If h_1, h_2 do not fade simultaneously, the symbols are recovered.

Note that code coloring requires signal manipulation at the transmitter and is not applicable to RF repeaters.

5.1.2.3 Diversity Order

The diversity order is defined as the number of branches providing multiple copies of the signal that are statistically independent (or having low-correlation) between the fades. The diversity order may be any integer $N \geq 2$, but since the improvement diminishes with ascending N, the diversity order commonly employed is 2, and rarely beyond 4. Note that polarization diversity order is limited to 2 in the far field. Small antennas operating in the near field and receiving different field components may achieve higher diversity order. These are applicable for short-range, wide angle interaction.

5.1.3 Macro- and Micro-Diversity

Microdiversity alleviates signal small-scale fading whereas macro-diversity copes with shadowing as well as small-scale fading (see also 3.6.8.1). Thus, with microdiversity antennas are essentially colocated, only spaced enough for space diversity or dual polarized for polarization diversity.

---

[17] Another method termed orthogonal transmit diversity uses $t_1 = [s_1 \; s_2]$ and $t_2 = [s_1 \; -s_2]$, respectively.

The antennas in such cellular deployments may belong to one sector (usually a pair of antennas is used for reverse link diversity, per sector) or to neighboring sectors in the same cell, providing Softer Handoff (SrHO) in CDMA networks. With macrodiversity however, antennas belong to different cells or different radio access nodes of the same cell (repeaters) that have an overlapping coverage area, which are located hundreds and sometimes thousands of meters apart. The macrodiversity between cells in CDMA networks is achieved through the Soft Handoff (SHO) process between cells, where a mobile user is supported simultaneously by more than one cell. The overlap coverage area between a BTS and its repeater is served by the BTS via two remotely located access nodes providing macrodiversity gain.

5.2 Diversity Combining

The diversity processing of multiple branch signal copies has been investigated in great detail and applied in many wireless communication systems. The performance results for the main methods are briefly reviewed in the following. These methods are applied at the receiver end of the channel. Evaluation of the diversity-combining schemes is based on the following signal statistics model. In the general case of MIMO (Multiple In – Multiple Out) where M transmit antennas and N receivers are employed, the received signal x_i arrive through channel $c_{ij}\exp\{j\theta_{ij}\}$ from source s_j at antenna i is

$$x_i(t) = c_{ij}e^{j\theta_{i,j}}s_j(t) + n_{ij}(t), \qquad 0 \le t \le T;\ i = 1,2,\cdots,N;\ j = 1,2,...M\ . \tag{5-3}$$

In the sequel we limit the discussion on Rx diversity to the SIMO case, $M=1$, thus $c_{i1}(t) = c_i(t)$, $\theta_{i1} = \theta_i$. The long-term average of signal to noise power ratio is denoted by $E(s^2)/E(n^2) = \Gamma$. "Long-term" means averaging over a period longer than the coherent time of the channel (Cf. Section 3.4.2), and over multiple fading periods (equivalent to the "sector averaging" in path-loss measurements - Cf. Section 3.4.3). $n_i(t), 0 \le t \le T, i = 1,2,\cdots,N$, the additive noises, are assumed to be i.i.d.[18] zero-mean (per a given t), and have identical power spectral density. The channel states $c_i\exp\{j\theta_i\}, i = 1,2,\cdots,N$ are assumed to be i.i.d. random variables.

Equation (5-3) can be written in concise vector form as

$$x = c\cdot s + n \tag{5-4}$$

[18] i.i.d. stands for (statistically) independent and identically distributed (random variables).

where x denotes the received signal vector (its entries being the branch signals x_i), s is the desired signal, n is the additive noise vector (its entries being the branch noises n_i) and c is the channel state vector, with complex entries $c_i e^{j\theta_i}$.

5.2.1 Selection Diversity Processing

In this scheme a switch selects the branch with the momentary highest amplitude, and the received signal thus "rides over the peaks" of all branches. Selection diversity can be applied at the RF level (switching between antenna ports) or at the output of the branch receivers. With N copies of the signal as an input, the received signal y_N at the output of the diversity processor is given by:

$$y_N = \max(x_1, x_2, \ldots, x_k, \ldots, x_N) \,. \tag{5-5}$$

The Cumulative Distribution Function (CDF) of y_N is a product of the CDFs of each input signal x_k if these x_k random variables are statistically independent (thus uncorrelated): $\mathrm{CDF}(y_N)=\Pi^{N}_{k=1}\mathrm{CDF}_k(x)$ [9]. In case the random variables x_k are i.i.d, we have $\mathrm{CDF}(y_N)=[\mathrm{CDF}(x)]^N$. Now, the CDF is a monotonic non-decreasing function ranging between 0 and 1, and the resulting CDF of the output signal, $\mathrm{CDF}(y_N)$, being a product of the CDFs of the branches' signals, has a steeper ascent than that of each of the branches, if they are not correlated. Figure 5-3 demonstrates this result qualitatively.

The CDF plot on the left-hand side is that of each single branch signal. If the signal copies of both branches are correlated then the selection algorithm would pick any of the signals, and the resulting output signal CDF stays unchanged. If the branch signals were uncorrelated, then the selected momentary maximal signal would have the shape as the right-hand side CDF in the figure, which is steeper. The signal with a steeper CDF varies over a smaller power range, and is thus steadier. The diversity gain is defined relative to the strongest branch signal. Under the assumptions set forth at the beginning of this section the momentary ("short-term"[19]) output SNR is

$$SNR_{out} = \max_i \left(c_i^2\right)\Gamma \,. \tag{5-6}$$

[19] Momentary or "short-term" SNR is measured over a period longer than the signal symbol, but shorter than the coherent time of the channel.

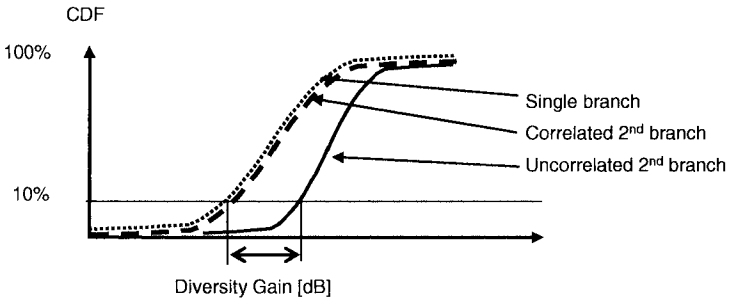

Figure 5-4. CDF plots of selection diversity processed signals

Note that when transmit diversity is considered (with N identical-power branches), it is assumed that the total transmitted power P is not changed, and each antenna transmits P/N. The diversity gain is then lower by the factor N (the *net diversity gain* is the same but the coherent power gain is removed).

An empirical equation for 2-branch selection diversity (SEL) gain with respect to the strongest branch signal, with cross-correlation ρ, and power ratio Δ [dB] between the stronger and weaker branch signals is [10]:

$$G_{SEL} \cong 5.7 e^{\{-0.87\rho - 0.16\Delta\}} \, [dB]. \tag{5-7}$$

Figure 5-5 graphically presents the empirical diversity gain G_{SEL} $[dB]$.

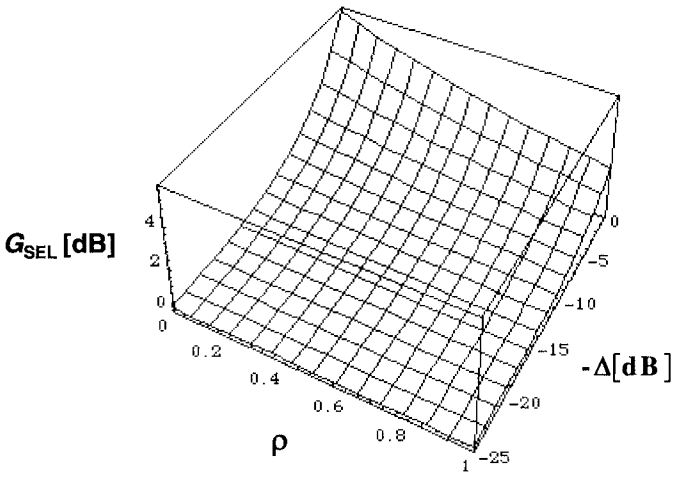

Figure 5-5. CDF plots of selection diversity processed signals

Example: Selection receive diversity is applied to two branch signals with correlation coefficient 0.7 and 2dB mean power difference between them. The selection power and diversity gain is:

$$G_{SEL} \cong 5.7\, e^{\{-0.87 \cdot 0.7 - 0.16 \cdot 2\}} = 2.25\,[dB]. \tag{5-8}$$

5.2.2 Equal-Gain Combining Diversity Processing

A better way than selection, if the braches' average signal to noise ratios are comparable, would be to exploit the multiple copies of the signal in the branches and perform some linear processing (i.e. weighted combing) that would not distort the signal and achieve signal coherent combining gain while the noises are combined incoherently. The improved signal to noise ratio (SNR) at the output would result in a diversity gain.

The equal-gain combining (EGC) scheme is composed of optimally co-phasing the desired signal copies in the multiple branches and then combining the resulting signal copies. Such a scheme may apply at the RF level or at the output of the receivers. The momentary ("short-term") output SNR is

$$SNR_{out} = \left(\sum_{i=1}^{N} c_i\right)^2 \frac{\Gamma}{N}. \tag{5-9}$$

In case the average SNRs are equal for all branches, this scheme may be shown to render the highest SNR_{out}. This is not the case for uneven branches, however. The branch with the low SNR contributes relatively more noise, to the extent that the diversity gain may become negative, as in Fig. 5-6. The degradation of the output signal to noise ratio may reach $10 \cdot \log_{10} N\ [dB]$. Indeed, Fig. 5-6 shows negative diversity gain for these values.

This scheme is not optimal for polarization diversity-combining, for example, where the branches are not equal. An optimal linear combining algorithm is discussed in the next section, which yields the maximum SNR (the MRC processor).

The detailed statistical analysis of the EGC processor is somewhat involved [11]. The improvement trend per the output signal CDF is similar to that for selection diversity, namely a right shift and ascending steeper slope.

An empirical equation [10] for 2-branch equal-gain combining power *and* diversity gain, with cross-correlation ρ, and power ratio Δ [dB] between the stronger and weaker branch signals is Eq. (5-10), plotted in Fig. 5-6:

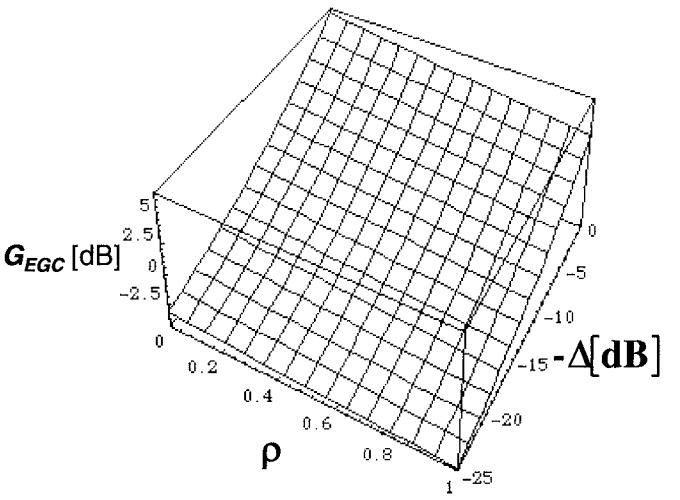

Figure 5-6. CDF plots of equal-gain combining diversity processed signals

$$G_{EGC} \cong -8.98 + 15.22 e^{\{-0.2\rho - 0.04\Delta\}} \, [dB]. \tag{5-10}$$

Example: Equal-gain combining receive diversity is applied to two branch signals with correlation coefficient 0.7 and 2 dB mean power difference between them. The power and diversity gain is:

$$G_{EGC} \cong -8.98 + 15.22 e^{\{-0.2 \cdot 0.7 - 0.04 \cdot 2\}} = 3.23 \, [dB].$$

5.2.3 Maximal Ratio Combining Diversity Processing

The Maximal Ratio Combining (MRC) processor aims at combining the copies coherently (in phase) using optimal weighting (making it a linear filter, in spatial domain rather than in time) to produce the maximum *momentary* signal to (mean) noise power ratio (SNR) at the output. For details see [1].

Denote the received signal vector (its entries being the branch signals) by x,

$$x = c \cdot s + n \tag{5-11}$$

where s is the desired signal, n the additive noise vector (its entries being the branch noises) and c the channel response, with complex entries. The MRC optimization problem is defined as follows: operate on x by a weight vector w,

$$y = w^{H} \cdot x = w^{H} \cdot c \cdot s + w^{H} \cdot n \tag{5-12}$$

such that the signal to noise ratio

$$SNR_{out} = E\left(\left|w^{*} \cdot c \cdot s\right|^{2}\right) \Big/ E\left(\left|w^{*} \cdot n\right|^{2}\right) \tag{5-13}$$

is maximized. An evaluation of the MRC processor weights and resulting SNR is provided in Appendix F. The analysis and performance of the MRC is well-established (see [2], [3]). A nice property of the MRC processor is that its output momentary SNR equals the sum of the input SNR's. By assuming independent fading between branches, it is possible to attain the statistical characteristics of the output SNR by convolving the probability density functions of the branches' SNRs.

Figure 5-7 demonstrates qualitatively the results for the 2-branch case.

The CDF on the left is that of each of the single branch signal. If both signal copies are correlated then the MRC algorithm would combine the signals and the CDF would preserve its shape but shift to the right by 3 dB – indicating a mere 3 dB power gain. If the branch signals were uncorrelated, then the selected momentary maximal signal would have the right-hand side CDF, which is steeper.

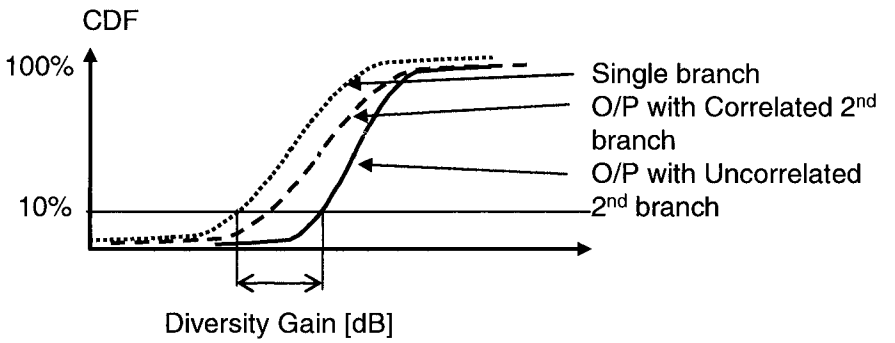

Figure 5-7. CDF plots of MRC diversity processed signals

The momentary output SNR is

$$SNR_{out} = \left(\sum_{i=1}^{N} c_i^2\right)\Gamma . \tag{5-14}$$

The single Rayleigh fading branch, two-branch selection diversity and MRC diversity output CDFs are shown for comparison in Fig. 5-8 (on a "Rayleigh paper", Fig. 3-36).

The resulting CDF of the output signal is right shifted and steeper, manifesting the achieved diversity gain.

Note that the analysis of the MRC optimal weighting and resulting expression for the output momentary SNR Eq. (5-14) is neither dependent on the fading statistical characteristics (e.g. Rayleigh pdf) nor on the correlation between the fade complex values $c_i \exp\{j\theta_i\}$. An empirical equation for 2-branch MRC diversity gain, with cross-correlation ρ, and power ratio Δ [dB] between the stronger and weaker branch signals is [10]:

$$G_{MRC} \cong 7.14 e^{\{-0.59\rho - 0.11\Delta\}} \left[dB\right]. \tag{5-15}$$

Figure 5-9 graphically presents the empirical diversity gain $G_{MRC}\ [dB]$.

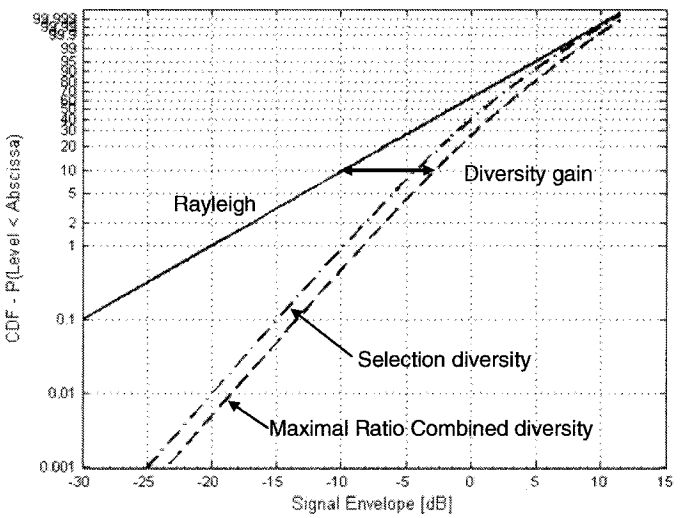

Figure 5-8. CDF of Rayleigh statistics on a "Rayleigh paper": one branch (reference), two-branch selection diversity, and two-branch MRC diversity

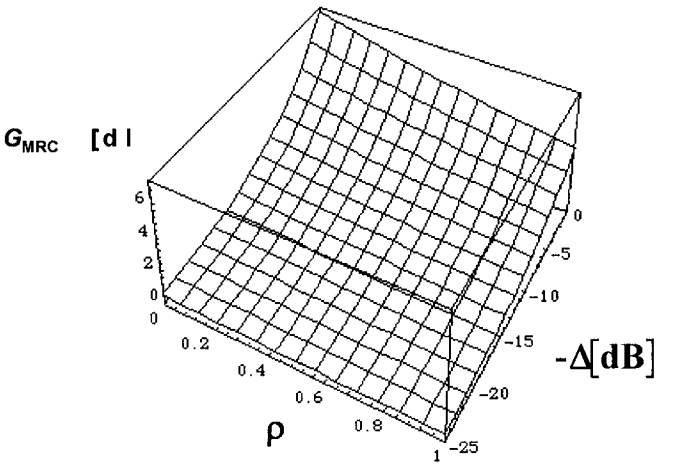

Figure 5-9. CDF plots of maximal ratio combining diversity processed signals

Example: MRC receive diversity is applied at the RAKE receiver to two fading fingers with correlation coefficient 0.7 and 3 dB mean power difference between them. The MRC power and diversity gain is:

$$G_{MRC} \cong 7.14 e^{\{-0.59 \cdot 0.7 - 0.11 \cdot 3\}} = 3.4 \,[dB].$$

The diversity gain is defined with respect to the stronger input signal branch. Figure 5-10 illustrates the diversity gain reduction with power mismatch between the branches with the 2-branch diversity methods. We assume in the depicted cases a cross-correlation coefficient value of 0.5.

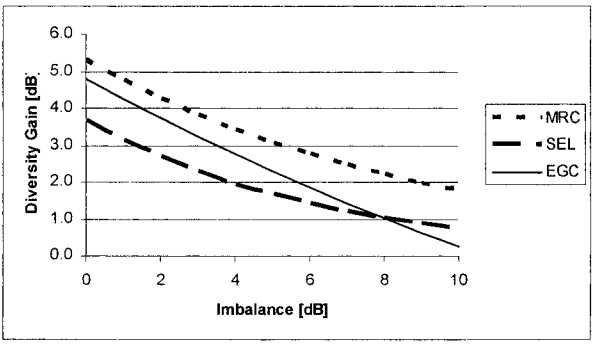

Figure 5-10. Effect of imbalance Δ [dB] on diversity gain ($\rho = 0.5$)

It may be concluded that in the range from full balance to 3 dB of imbalance, all methods (with $\rho = 0.5$) loose approximately 1.5 dB, or 0.5 dB/1 dB imbalance.

5.3 RF Diversity Methods in CDMA Cellular Systems

Mitigation of the fading channel by diversity means is applicable to both forward and reverse CDMA links. These are different, however, by the nature of the signals on these links, by the propagation and scattering environment as viewed from the radio access point and from the ST, and by cost-effectiveness considerations, differently applicable to the BTS and to the ST. These are reviewed in this section. Attention is focused on means that do not require modification of the signal processing in the BTS or the ST, and are thus suitable as add-on enhancements to operational networks and for application in remote access nodes and repeaters. This group comprises of antenna diversity means, coupled at the RF level.

5.3.1 Space Diversity

Space diversity utilizes the phase difference (or equivalently short delay) of a wave front arriving at two or more spaced antennas at an angle from broadside (Fig. 3-34). The signal, incoming from a source and scattered by a scattering neighborhood to form an *angle spread* 2φ over which signals are arriving, creates time replicas differing by the respective short delays. These replicas are not correlated when the antennas are spaced apart sufficiently, hence the name *space diversity*. The appropriate spacing is inversely proportional to the *angle spread* and is called *aperture coherence* (see Eq. (3-43)): a distance much shorter than the *aperture coherence limit* renders coherent reception of the signal, with respective aperture (power) gain. An insight to that is gained by considering the beamwidth $\vartheta \cong \lambda/d$ that is formed by coherently combining these antennas: if $\vartheta > 2\varphi$ then the *angle spread*, representing the whole cluster of radiating sources, is encapsulated within the beam and is coherently received with the array (power) gain. On the other hand, in case $\vartheta < 2\varphi$ the receive array does not capture all the signals, and those that "spill" beyond the beam are not correlated, thus achieving diversity. Any distance larger than the aperture coherence provides high de-correlation. However, by inspection of Eqs. (3-45) and (3-46) it is realized that there is a diminishing return in extending the distance beyond the *aperture coherence limit*: the correlation fluctuates while descending only slowly.

The BTS antennas are typically placed above the service area (Fig. 3-35), and the scattering neighborhood around the STs is mostly horizontally

projected. The horizontal angle spread is by far larger than the vertical one, which is the reason for horizontal displacement of the diversity antennas (Fig. 3-37). Optimal antenna spacing in BTS or other radio access nodes is between 10 and 30 wavelengths (2 to 5 m in 1900 MHz and 4 to 10 m in the 900 MHz bands), relating to angle spreads of 6^0 to 2^0, respectively, at broadside. The angle spread broadens as the antenna is lowered toward the height of the clutter (e.g. buildings. See Fig. 3-35). The required antenna spacing thus grows with the antenna height above the scenery. A linear relation $h/d \cong 11$ has been reported [12]. Note that the decorrelation is not omnidirectional, but relates to the projection of the aperture on the direction of arrival of the signal. The spacing for antennas covering a 120^0 sector has to consider a projection at 60^0 (sector border), which is half the broadside distance. The diversity gain in an omnidirectional coverage cell degrades to almost extinction toward the direction of the end-fire (direction of the line linking the antennas).

By utilizing antennas with equal gain, radiation pattern and polarization, one assures to have equal average strength of the received signal, which maximizes the diversity gain. This is only limited by the coupling between the antennas that induces a pattern ripple for small spacing (Eq. 3-47 and Fig. 3-36). The prevalent polarization of the BTS space diversity antennas is vertical. The space diversity antennas used with repeaters are generally of the same types as employed in BTS sites. In special applications, such as highway coverage, special antennas with narrower beamwidth ($\leq 30^0$) may be used, such as panel arrays or parabolic reflector antennas.

The use of diversity antennas on the ST has been limited for cost and size considerations. They find usage installed in cars and in larger terminals as laptop computers. The optimal spacing for the ST that is surrounded by scatterers is about $d/\lambda = 0.3$ (Eq. 3-44), namely 10 cm in 900 MHz and 5 cm in 1900 MHz.

5.3.2 Polarization Diversity

Reports on successful diversity-combining reception through two orthogonally polarized antennas at the BTS (see 3.6.8.4 and references in Chapter 3 and [3, 13-17]) yielding comparable diversity gain to space diversity in urban areas led to the increasing application of polarization diversity antennas in lieu of space diversity antennas, mainly in urban and suburban areas. The prime advantage of this method is compactness: a single antenna replaces two spaced antennas, each of a similar size. Only three antennas are required for a three-sectored cell, compactly packed together. Initial trials and commercial deployment applied antennas polarized in a V-H

polarization pair. Dual slant-polarized antennas $(\pm 45^0)$ are now preferred for superior performance.

The polarization diversity gain is composed of *polarization matching* gain (equivalent to the coherent power gain in antenna beam/ space diversity) and *net polarization diversity* gain (Fig. 5-3). The *polarization matching* gain relates to the distribution of polarization among the STs that is matched with this scheme [16, 17], while the polarization diversity gain relates to the depolarization of the wave on route through scattering and reflections, an effect measured by XPD (Cross Polarization Discrimination) or its inverse, *polarization spread.* XPD represents a power average ratio of orthogonal polarizations. The scattering events on route for the orthogonally polarized waves are different, and yield low correlation between their fading patterns. This is taken advantage of in the diversity-combining of the orthogonal branches.

The polarization of a handheld user antenna is typically slanted (held between the user's ear and mouth), and the polarization observed at the BTS site depends on the user orientation. A simple model assuming uniform distribution of the orientation of the users in the coverage yields 6.8 dB polarization mismatch loss with a vertically polarized BTS antenna (Eq. (3-33)), and only 3.3 dB loss (this time due to the directivity loss of a slanted dipole) with a polarization-matched antenna. Thus the 3.5 dB average gain of the dual-polarized BTS antenna, when diversity-combined, vs. a vertically polarized antenna, is a *polarization matching* gain, existing even in a LOS situation. The diversity combiner circuit also accomplishes the polarization matching and tracks the polarization of each user, which is a slow process relative to the fading mitigation, and is compared to the *slow fading* term that relates to shadowing effects. The polarization mismatch is therefore sometimes termed *polarization shadow* based on that analogy. Different than shadowing effects that are location dependent and tend to create radio holes, the polarization shadows are pretty uniformly distributed in the area and change in time. They are mitigated only with polarization diversity reception.

Typical XPD values run between 4 dB indoors and in compact environments, to over 12 dB in rural areas, averaging around 8 to 10 dB in suburban areas. XPD is higher between V-H polarizations than between slanted $(\pm 45^0)$, explained by the nature of the man-made structures whose surfaces and edges mostly align with V or H planes. By reviewing the diversity gain parameters (Section 5.1.1) and especially the diversity gain expression (Eq. (5-15)) it is noticeable that high XPD reduces the diversity gain appreciably vs. space diversity, where the branches are well-balanced. The way to explain the equitable results obtained by these methods is to incorporate the polarization loss that it built into the vertically polarized space diversity antennas. Polarization diversity is effective primarily in urban and

suburban areas that are richer in scattering events and where the polarization of the STs' antennas is spread wider.

The *antenna* radiation patterns of both orthogonal polarizations should track well over azimuth and elevation to enable good polarization diversity performance, and preferably have a common phase center. Notably, the polarization balance of the dual slant-polarized antennas, conveniently implemented as panel antenna arrays, deteriorates toward the sector border at 60^0 off boresight. The H polarization component is suppressed, while the V component prevails. Omnidirectional coverage requires at least three antennas around.

Polarization diversity is also suitable for the subscriber terminal for its compactness advantage.

5.3.3 Angle Diversity

Two or more beams, each much narrower than the observed angular spread and viewing a different part thereof, receive uncorrelated replicas of the signal and provide angle diversity. This is not the case with the outdoors cellular environment, where the angle spread is limited and beamwidth is typically wider because of limitations on the antenna size or antenna array spread (Section 3.6.8.3). Application of the angle diversity by receiving the angle spread signal over a slope of the beam, and then either tuning the beam direction or comparing two beams in a monopulse-like configuration, takes place in multibeam and steering antenna arrays, but with limited effectiveness [18]. This can be enlightened by Fig. 3-38, showing the analogy to equal-gain combining of a space diversity pair, and the respective limitation on the achievable decorrelation - $\vartheta \cong \lambda/d = 2\varphi$, which optimizes aperture size when comparable to space diversity spacing.

5.4 Transmit Diversity

The cellular service is founded on hubs – base stations that communicate in a Star architecture with subscriber terminals (ST) within its coverage. The subscriber units are built for small size, low-cost and long battery life. Antenna diversity is thus not widespread in STs. The burden of providing diversity to the forward link falls on the BTS and other Radio Access Nodes (RANs). Standards for incorporation of transmit diversity are included in 3G cellular (UMTS/CDMA2000), but not generally implemented. Transmit diversity is not standardized in 2G systems.

Transmit diversity is a challenging task in many ways. The signal is to be transmitted over multiple paths whose fading are uncorrelated upon reception at the receiver, and be identifiable by the receiver for properly diversity-

combining them. The FL and RL frequencies in the FDD systems are spaced further than the *coherent bandwidth* of the channel, and FL channel state information cannot be inferred from receiving the RL channel at the BTS. These roles: providing fading-uncorrelated replicas of the signal, providing "colors" for identifying the replicas and providing channel state information for either branch selection or coherent combining, are divided between the transmit and the receive sides in different ways, depending on the complexity allocated to each and the expected performance.

The simplest schemes rely on features existing in the STs and in the BTS and require no modifications in either end. These are *RF add-on schemes.* These are applicable to both 2G and 3G CDMA systems. The pilot transmission in the FL of the CDMA systems provides the channel state information, and the rake receiver produces the diversity combining. The channels are identified by artificial time delay introduced on transmission, which the rake receiver processes as multipath. PSTD (to be discussed below) applies also to TDMA-type 2G systems.

Blind coded schemes rely on the receive side to identify and combine the diversity channels received on a single antenna. The 3G STs are provided with the diversity code processing. The UMTS WCDMA standard provides TSTD (Time Switched Transmit Diversity) and STTD (Space-Time Transmit Diversity). The Alamouti [8] code is utilized in STTD. CDMA2000 provides STTD and OTD (Orthogonal Transmit Diversity, see Section 5.1.2.2).

Closed loop (side-information-enhanced) schemes. Feedback from the ST is provided to the transmitter on the channel state, which allows for presetting the transmit channel for optimal reception. UMTS WCDMA incorporates TSTD with a single bit feedback for selection diversity at the receiver. Only one antenna transmits at a time, according to the stronger channel at the receive end.

Remote RANs comprise of RF relay circuitry only. In order for a remote RAN to provide transmit diversity it needs to relay both channels from the BTS and retransmit to the service area, or apply RF add-on schemes. Both are discussed in the following sections.

5.4.1 Time-Delay Transmit Diversity (TDTD)

The channel diversity is provided by a space diversity antenna pair at the transmit side, spaced as needed for decorrelation, or by a dual-polarized, collocated antenna pair, or by multibeam array in angular diversity mode. The transmit signal is split, and one branch is delayed by a delay exceeding one chip of the spreading code (0.81 μs and 0.26 μs in CDMA2000 and WCDMA, respectively), and preferably several chips – to avoid the first multipath cluster (see for example Fig. 3-22). The receiver receives the

transmission from both antennas with the delay between them, that is processed by the rake receiver and combined as delayed multipath. Each finger is replicated, as exemplified in Fig. 5-11. The resolvable time delay provides the "coloring" that identifies the replica from the main signal and allows for the diversity-combining in the rake receiver.

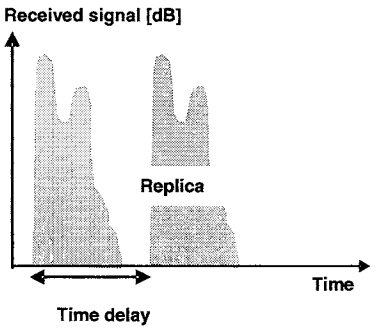

Figure 5-11. TDTD as received by the rake receiver

As much as benign diversity channels are provided by this scheme and the average power and SNR in the branches is controlled by the transmitters (and typically set to equality), the additional channel transmission also provides noise to the fingers of the main replica, and vice versa, reducing the average SNR of each finger to 0 dB.

This is a limitation of multiple delayed transmission, which is sometimes, but not always overcompensated by the diversity gain, as discussed further in Section 5.6. The limited number of fingers in the rake receiver poses an additional bound: multipath that is not captured by these fingers also adds to the receiver noise. Thus a three-fingered rake receiver picks up only the leading finger and its replica, and a second multipath finger if it exists, but not its replica or any further multipath fingers. All the rest of the signal is received as added noise. This is the reason that no more than two branches of TDTD are commonly implemented. TDTD can be implemented at the base-band, at the IF level or at the RF. The implementation of the split and delay is simplest at the base-band, but requires inherent modifications of the BTS. Only 3G systems have optional two transmit paths.

Implementation of IF delay is also straightforward, but – again, requires some modifications that are applicable only in case there is an access to the IF circuitry. Application at RF is an add-on modification, as shown in Fig. 5-12 [19, 20]. The RF delay is typically implemented by a SAW device. These are lossy devices, and have to apply at low power prior to the power amplification.

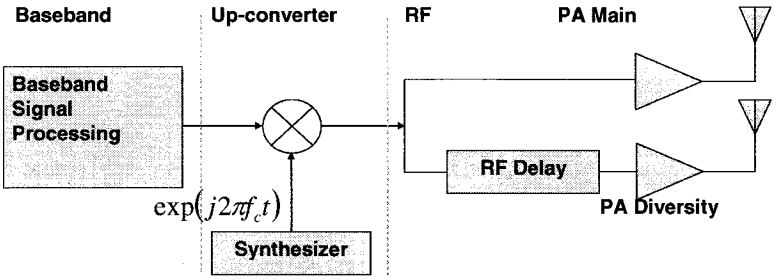

Figure 5-12. TDTD implementation at low level RF

Unlike baseband or IF implementation, the RF implementation applies to the whole band, not only to a single carrier (FA).

The physical implementation of add-on transmit diversity is sketched in Fig. 5-13. Typical BTS configuration encompasses one main antenna serving for both Tx and Rx via a duplexer, and an additional Rx diversity antenna. This antenna is enhanced by a duplexer to also serve the diversity transmission path that taps to the transmit path, provides the delay (or phase sweep) in the Transmit Diversity Unit (TDU), and amplifies in the diversity power amplifier. The main power amplifier is backed off 3 dB, and so is the diversity PA, to produce a total transmit power equal to the power before the add-on diversity.

TDTD is compatible with 2G CDMA and 3G systems with no modifications to the STs or to the RAN. It is applicable to BTSs, remote RANs or repeaters.

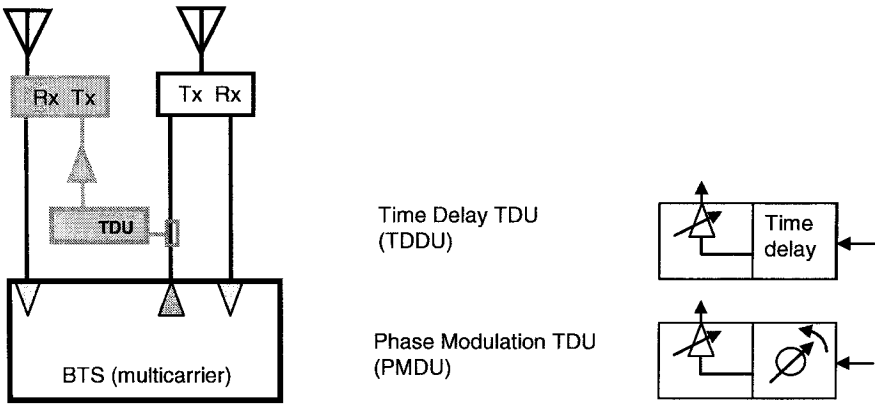

Figure 5-13. Physical implementation of add-on TDTD and PSTD

5.4.2 Phase-Sweep Transmit Diversity (PSTD)

This is an *implicit diversity* scheme [5, 21-26] that utilizes the FEC de-interleaver at the receiver. Two or more replicas of the signal are transmitted through antennas arranged for space, polarization or angular diversity. The phase on the diversity branch is swept at a peak rate of typically 30 to 100 Hz. The signal at the receive end is composed linearly of two branches that are independently fading. The phase sweep between them creates an amplitude-modulated signal at the phase sweep rate. The slow fading, typical of pedestrian and quasi-stationary ST, are thus shifted into fast fading that is recoverable by the FEC deinterleaver, built in STs of 2G and 3G.

The PSTD transforms a slowly single Rayleigh fading signal into a fast single Rayleigh fading signal. Its diversity gain, together with the FEC de-interleaver, falls but 1 dB short of benign diversity STTD scheme. It deteriorates, however, for multiple Rayleigh fading signals, and for signals having a dominating unfading component (Rician statistics). Not only does it loose the gain in these channels that have their inherent diversity, but it increases the fade depth in stable channels, and is deficient to a no-diversity channel by up to about 1 dB. Its diversity gain also diminishes at high speeds, where the fading rate is within the optimal range of the FEC deinterleaver in the first place.

No substantial difference in performance is observed between the application of linear phase sweep (implemented as a frequency shift), sinusoidal or stepwise phase shift, as long as the phase changes are smooth enough for the estimating function of the receiver and the Doppler spread is within the bounds of the receiver. This allows for a variety of implementation schemes. Figure 5-14 sketches an implementation at the up-converter phase modulator, whereby a frequency shift is applied by the synthesizer to the diversity branch.

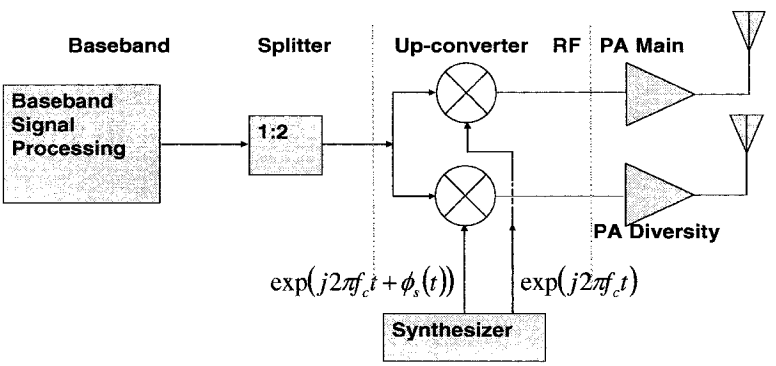

Figure 5-14. PSTD implemented at the up-conversion phase

This application requires a modification of the BTS. An add-on scheme is described in Fig. 5-15. The RF signal is split, and the diversity branch is phase modulated by an analog (sine modulation) or a multistate digital circuit.

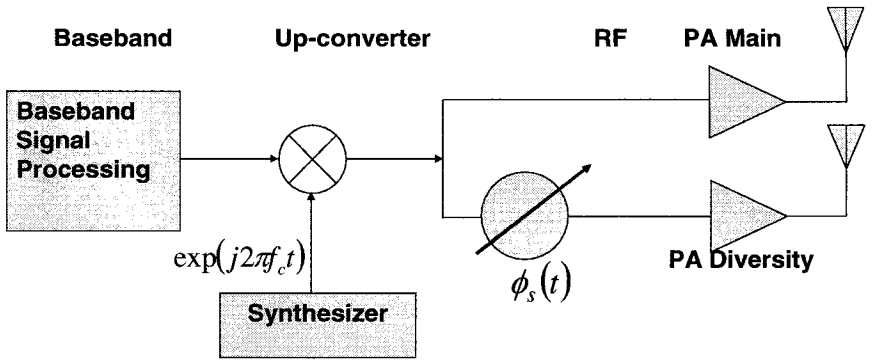

Figure 5-15. PSTD implemented at the RF level

5.5 Relaying and Cascading Diversity in Remote RANs

Remote RANs in the CDMA system only amplify the signal. The reception and diversity-combining of the RL is processed at the donor BTS. Similarly the generation of the transmit diversity "coloring" codes, or branch weighting in a closed loop transmit diversity, is processed at the donor BTS.

The application of diversity in a remote RAN requires a backhaul relay of the diversity branches between the donor BTS and the RAN, which implies additional costs for a dedicated diversity conduit. Alternatives for diversity relaying are discussed in this section, along with add-on transmit diversity generation at the RAN in the FL and pseudodiversity combining at the RAN for the RL.

5.5.1 Direct Diversity Relaying

Direct relay of diversity branches is applicable for optical fiber, FSO and microwave transmission conduits. These have ample bandwidth to accommodate the extra channels. The main cost element is the extra conversion/ multiplexing unit, at the donor unit and at the remote RAN unit. Multiplexing applies in IF, or by WDM (wavelength-division multiplexing) in optical fiber or FSO. Parallel and multi-hop repeaters relay each branch (main and diversity) on separate conduits [27-29] to the respective diversity branch at the donor BTS. All share the same diversity codes generated at the donor

BTS, as in Fig. 5-16. The same scheme applies for the RL: each diversity branch is separately cascaded.

Over the air backhaul, F1/F1 or F1/F2 may use dual-polarized link antennas [30, 31]. The orthogonally polarized branches are then relayed to a dual-polarized donor antenna. A high XPD is required along the link: the polarization has to be well aligned between the donor and the link antenna, and a high XPD channel designed.

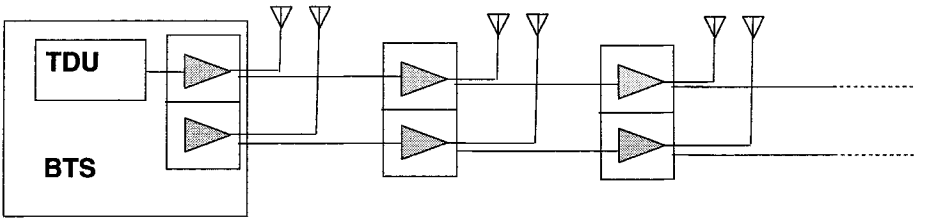

Figure 5-16. Multi-hop cascading of Tx diversity branches. *TDU is Transmit Diversity Unit, providing the weights and "coloring" codes*

Note that in case the donor applies polarization diversity in its coverage area the dual polarized F1/F1 backhaul links directly to the donor service antenna. Dual polarization backhaul also applies to multi-hop repeaters. Each branch is cascaded separately along all hops and relayed to the respective diversity branch at the donor. The same scheme applies for RL.

Note that the orthogonality of the polarized antennas is utilized in the backhaul application, not the polarization diversity. There is no similar application with spaced antenna pair, because the spacing required for de-correlation is beyond any practicality (Section 3.6.8).

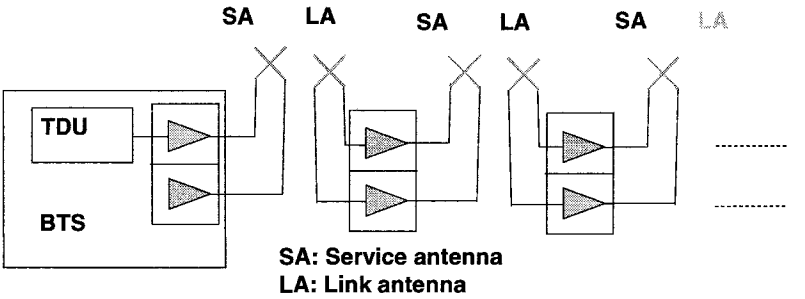

Figure 5-17. Multi-hop cascading of over-the-air F1/F1 Tx polarization diversity

Decorrelation condition $d_D/\lambda \cong R/d_R$, where d_D, d_R are the antenna separation at the donor and remote RAN, respectively, and R is the distance between them[20].

5.5.2 Remote Transmit Diversity

Add-on RF transmit diversity is applicable to remote RANs, as per Fig. 5-13. Either TDTD or PSTD is applicable. The single branch backhaul FL that relays the main branch only is split in the RAN, diversity applied and the two branches amplified and transmitted via space or polarization diversity antennas.

Note that TDTD doubles the number of delayed multipath. In case both branches are received by the remote RAN, as when linking to the service diversity antennas of the donor, TDTD applies to this input and the resulting RAN transmission further doubles the multipath, overflows the number of fingers at the ST receiver and saturates it with additional noise. A similar reasoning applies to PSTD. Repetitive application of PSTD broadens the Doppler spread into ranges that unnecessarily degrade the FEC deinterleaver performance. The same rule applies to any Tx diversity weight or code generation. Tx diversity generation has to apply only once along the link to the diversity-combining receiver. This is clarified in Fig. 5-18. The trade-off between Fig. 5-16 scheme and that of Fig. 5-18 is between an extra diversity conduit and a TDU in the RAN. Over-the-air F1/F1 can apply only with polarization diversity, as in Fig. 5-17, where the backhaul antenna is polarized to match only the main diversity branch of the donor service antenna.

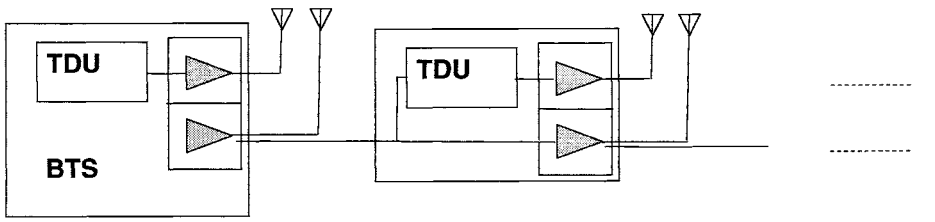

Figure 5-18. Generation of Tx diversity in remote RAN

[20] A heavily cluttered backhaul link may decorrelate between the branches, as in MIMO application, but such NLOS link is very lossy and not suitable for backhaul.

5.5.3 PseudoDiversity Combining (*PDC*) – Relaying RL Diversity

The application of a dedicated diversity backhaul conduit, as in Figs. 5-16 and 5-17, is circumvented by pseudodiversity combining (*PDC*) the RL diversity branches at the remote RAN, and relaying both branches on a single link to the donor receiver. Diversity branches are combined, weighted and "colored" at the remote RAN to be relayed on a single link to the donor receiver, as depicted in Fig. 5-19 [32-34].

Only RF techniques are applicable at the remote RAN. The diversity unit (DU) is a time-delay unit (*TD PDC*) or a phase modulation unit (*PS PDC*), as in Fig. 5-13. The purpose of the variable gain amplifier on the DU branch is to balance the diversity branches' average power. In addition to the uncorrelated branches, the link antenna also transmits the amplified noise of both LNAs, thus increasing the RAN noise figure by 3 dB. The impact of the RAN noise figure on the donor BTS depends on the net gain y of the RAN amplifier and the link to the donor. This is discussed in Chapter 6.

Cascading of multi-hop RL diversity is applied as in Figs. 5-16 and 5-17, where each diversity branch is separately concatenated to the respective branch at the donor receiver. Cascading multi-hop RANs on a single RL conduit is schematically presented in Fig. 5-20, where the combined signal is linked to the main branch of the preceding RAN. Concatenation has to apply on the main branch, as *PDC* has to apply only once along the diversity link to the diversity branch of the donor receiver, or else the delay spread multiplies and noise is added.

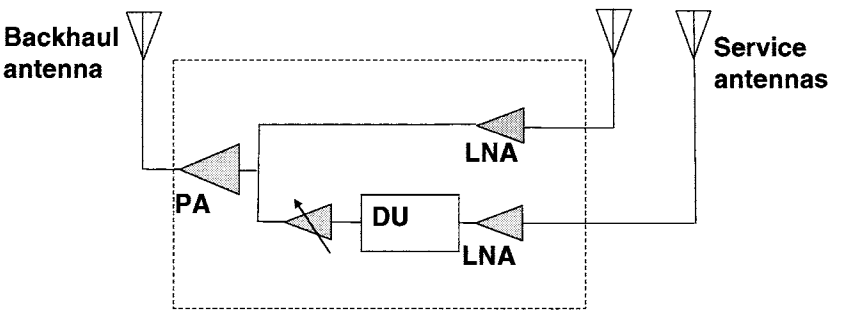

Figure 5-19. RL Pseudodiversity combining at the remote RAN. LNA – Low-noise amplifier. PA – Power amplifier. DU – Diversity unit

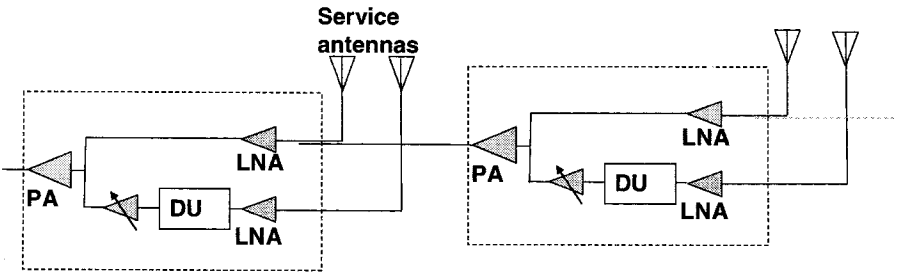

Figure 5-20. Cascading RL pseudodiversity combining

5.5.4 Diversity Reception of Relayed Diversity Branches

Each sector in a typical BTS has typically two receiver front ends for diversity reception from two antennas. The relayed diversity branches from the remote RANs link to each port via a dedicated conduit – optical fiber, FSO, microwave transmission or over-the-air orthogonally polarized transmission. *PDC* link requires a single antenna port, as the diversity reception utilizes the rake combining for *TD PDC*, and the *PS PDC* is processed at the FEC deinterleaver. The linkage to one antenna diversity port introduces additional noise to one branch, impairing the SNR balance between them, and thus reducing the diversity gain of the donor service antennas. A measure of this impairment is given in Fig. 5-10. The control of the noise linkage from the repeater chain to the donor is discussed in Chapter 6. An exception is F1/F1 over-the-air utilizing space diversity at the donor. Both donor service antennas receive the same signal and the same repeater noise, and it is coherently combined with a diversity gain of 3 dB.

5.6 The Impact of Diversity on the CDMA Cellular Network

The CDMA system relies on interference averaging of multiple users, each smoothed by spreading over the spectrum and applying multiple diversities and cumulatively controlled by power control and Soft Handoff. Its coverage, capacity and performance are sensitive to the channel state and the availability of ample diversity to optimize the performance of the modems. The system employs multiple built-in diversities: frequency diversity by spreading [7], delay diversity in the rake receiver, time diversity in the FEC interleaver, user diversity that smoothes the interference statistics, power control and Soft Handoff, and antenna diversity. The reverse and

forward links differ in structure and dependence on the channel and on the locality of the users. The impact of the inherent and additionally applied diversity means on the state of the system, differs between the FL and RL and depends on the environment, users' density and distribution, and cell clustering. The diversity state also affects the observed network probes' readings and measurements. These are analyzed in order to gain insight needed for network planning and control.

5.6.1 Diversity in the Reverse Link

The reverse link voice capacity is stated in Eq. (4-6), repeated here for convenience:

$n_{MAX} \cong \eta_0 (W/R_b)\zeta K/((E_b/I_t)\nu(1+f))$. Data transmission in 3G standards use different data rates R_b and the respective E_b/I_t depends on code and diversity means (e.g. HARQ, Cf. Chapter 2) applied to these modes. We focus on the salient parameters, common to all CDMA modes and influenced by the propagation and activity distribution: the power control, whose inefficiency due to inaccuracy and fluctuations is designated K, the other cells' relative interference, designated f and dependent on the Soft Handoff and intercell boundary, and the required E_b/I_t that depends on the channel fading conditions and on applied channel diversity.

The required E_b/I_t in the RL may vary from over 10 dB in flat fading to less than 3 dB in an LOS condition. The average of about 6 dB refers to a delay-diversity optimal combining of typically nonequal 2 to 3 fingers (Fig. 3-22 for example), together with two-branch antenna diversity that mitigate flat fading. Additional over 2 dB gain is reported [35] by application of 4-branch antenna diversity in a combination of space and polarization diversity. The reduced requirement on E_b/I_t enhances capacity. The enhanced sensitivity increases the coverage and penetration to radio holes and into buildings. It also extends the cell's boundary. The rapid changes of the RL power control in attempt to mitigate the fading of slow moving STs have reduced peaks due to the diversity smoothing, increasing the value of K.

The diversity gain of each of the diversity means is not uniform throughout the cell coverage and over the range of speed of the STs. The orthogonality function, discussed in Section 4.4.2 and in Appendix C, in the context of the FL, is a characteristic of the propagation channel and applies equally to the RL. Orthogonality relates to the delay spread, and is proportional to the coherent bandwidth of the channel. Figure 4-8 shows the general trend of the orthogonality, and therefore of the coherent bandwidth, to decrease away from the BTS. Flat fading is more abundant at short ranges. The gain of antenna diversity means, mitigating flat fading, is higher in these regimes, being the prime diversity. This is an important observation because

the angle spread is wider for such shorter distances, and the required spacing for space diversity – smaller. The rake receiver delay-diversity, on the other hand, applies for longer ranges, richer with long delayed multipath. Both the rake and the antenna diversities are prime diversity means for slow movers (along with the power control) while the FEC deinterleaver picks up for car speeds.

5.6.2 Transmit Diversity in the Forward Link

The forward link in the CDMA standards utilizes time diversity (also utilized in the reverse link) by FEC code-interleaving. The effectiveness of this scheme is limited by frame-length, which in IS 95 and CDMA2000 is 20 ms, and in WCDMA is 10 ms. Only fast fading are mitigated by these schemes, while pedestrian slow fading or quasi-stationary portable ST, whose fade length exceeds the frame time, do not enjoy diversity and require high E_b/I_t – over 10 dB, for satisfactory reception. The main impetus for application of transmit diversity is the improvement of communications for the slow moving subscribers in a Non Line of Sight, flat fading environment. The FL power control in IS 95 is slow – responding at a rate of 50 Hz, and is able to recover deep fades only at very slow speeds, leaving an improvement to be desired to the transmit diversity. The power control in CDMA2000 reacts at 800 Hz rate, and that in WCDMA is 1500 Hz – both designed to support the slow STs and bridge the gap to the optimal range of the FEC interleaver functions. The added value of the transmit diversity is thus diminished, and estimated by about 1 dB, accounting for further reduction of the required E_b/I_t and reduction of the variation of the transmit power and their spikes due to the power control during fades. This may be the prime reason that transmit diversity is not widely spread.

5.6.3 Time-Delay Transmit Diversity

In a TDTD the transmission of the RAN is split to two, preferably equal branches that are now fed to two antennas in a space diversity or polarization diversity configuration. The signal of one of the branches is delayed by more than one CDMA chip so that it is received by a separate "finger" at the ST receiver. Apart from the diversity gain thus achieved, the delayed signal appears as additional noise to the first "finger' and vice versa, which reduces the C/I of each "finger". The diversity gain of TDTD depends therefore on the channel orthogonality α and on the distance of the ST from the BTS. Reduced orthogonality implies natural multipath diversity, which reduces the added diversity gain provided by TDTD. The effect of TDTD on a highly orthogonal channel is to introduce noise and by that reduce the C/I, which –

in the area near the RAN, means a reduction from some 20 dB to 3 dB that is not compensated for by the diversity gain. This latter effect is detrimental to high data rate time-multiplexed transmission, as in EV-DO and HSDPA. It will be shown in the following that the main benefits of TDTD are in enhanced penetration to radio holes, range extension and reduction of interference fringes in multi-lobed coverage.

5.6.3.1 Derivation of the Diversity Gain

In the following analysis we assume only 2-ray multipath, plus additional multipath not captured by the rake receiver. This is a typical channel statistics. This can be extended to a higher number of rays. Further we assume only 3 fingers in the rake receiver. Reference is now made to Section 3.4. We refer to Eqs. (4-20) - (4-24) and Eqs. (4-29) - (4-31) and repeat the same process while introducing the TDTD. Recapitalizing on Eqs. (4-22) - (4-24), denoting $I_{oc}W = x_F P_{BTS} T_{oc}$ and assuming $T(r) \propto r^{-4}$, we reach $I_{oc}W/P_{BTS}T(r) = x_F (r/(2R-r))^4$ where $x_F = P_{otherBTS}/P_{BTS}$ is the ratio of the transmission power of the interfering BTS to self. This approximation is justified in Appendix B. Equations (4-20), (4-22) become

$$\left.\frac{C}{I}\right|_g (r) = \left(\frac{\alpha \frac{P_S(r)}{P_{BTS}}}{\frac{N_0 W F_M}{P_{BTS} T(R)} \left(\frac{r}{R}\right)^4 + (1-\alpha) + x_F \frac{(2R-r)^{-4}}{r^{-4}}} \right) g\left(\left.\frac{C}{I}\right|_1 (r); \left.\frac{C}{I}\right|_2 (r) \right) \qquad (5\text{-}16)$$

and Eq. (4-30) is then

$$\Delta[dB] = 10Log \left(\frac{\left(\hat{N}_{Th} + x_F \left(2 - \frac{r}{R}\right)^{-4} \right) \left(\frac{r}{R}\right)^4 + 1 - \delta(1-\alpha)}{\left(\hat{N}_{Th} + x_F \left(2 - \frac{r}{R}\right)^{-4} \right) \left(\frac{r}{R}\right)^4 + 1 - \alpha} \cdot \frac{\alpha}{\delta(1-\alpha)} \right) \qquad (5\text{-}17)$$

where

$$\hat{N}_{Th} \equiv N_0 W F_M / P_{BTS} T(R) \qquad (5\text{-}18)$$

represents the ratio of ST thermal noise to BTS power as received at the edge of coverage.

When applying TDTD, two rays are transmitted, each with half the baseline power. The result is two pairs of rays. We assume here that the power is split equally. We then have from Eq. (5-16)

$$\left.\frac{C}{I}\right|_g(r)=\left(\frac{\frac{1}{2}\alpha\frac{P_S(r)}{P_{BTS}}}{\left(\hat{N}_{Th}+x_F\left(2-\frac{r}{R}\right)^{-4}\right)\left(\frac{r}{R}\right)^4+\left(1-\frac{\alpha}{2}\right)}\right)g\left(\left.\frac{C}{I}\right|_1(r);\left.\frac{C}{I}\right|_2(r);\left.\frac{C}{I}\right|_3(r)\right) \tag{5-19}$$

The rake receiver detects only 3 "fingers". Therefore the "unused" signal is

$$(1-\delta')(1-\alpha)=\left(1-\frac{\delta}{2}\right)(1-\alpha). \tag{5-20}$$

We have assumed that each branch of the TDTD produces two rays. The signal power and interference power for each ray is summarized in Table 5-1.

Table 5-1. Signal and nonorthogonal interference in the multipath rays

Branch	Ray	Signal (x P_S/P_{BTS})	Interference
1	1	$\alpha/2$	$1-\alpha/2$
	2	$\delta(1-\alpha)/2$	$1-\delta(1-\alpha)/2$
2	3	$\alpha/2$	$1-\alpha/2$

The diversity combining of three rays is assumed to be performed in two steps, for simplicity of the analysis: first the rays 1 and 3 are combined. These have equal C/I and $\Delta[\delta B]_{1,3}=0$ (equal branches). The diversity gain is $g_3[dB]=7.14e^{-0.59\rho}$ [10].

Then the combined branch 1-3 is combined with ray 2. Revisiting Eq. (5-17) we have

$$\Delta[dB]_{1-3,2}=10Log\left(\frac{\left(\hat{N}_{Th}+x_F\left(2-\frac{r}{R}\right)^{-4}\right)\left(\frac{r}{R}\right)^4+1-\frac{1}{2}\delta(1-\alpha)}{\left(\hat{N}_{Th}+x_F\left(2-\frac{r}{R}\right)^{-4}\right)\left(\frac{r}{R}\right)^4+1-\frac{\alpha}{2}}\cdot\frac{\alpha}{\delta(1-\alpha)}\right)+7.14e^{-0.59\rho} \tag{5-21}$$

$$g_{TDTD}[dB]=g_{1,3}+g_{1-3,2}=7.14e^{-0.59\rho}\left(1+e^{-0.11\Delta_{1-3,2}}\right) \tag{5-22}$$

and the diversity gain is obtained by comparing Eq. (5-19) with Eq. (5-16), as shown in Fig. 5-21 for a range of values of the orthogonality factor α, and for variable orthogonality as per Section 4.4.2.

The effect of TDTD in extending the cell range is shown in Fig. 5-22, for α=0.7 and 0.95. C/I is drawn for the FL with fixed power-per-channel allocation (no power control). TDTD introduces additional noise by the second branch, which suppresses the high C/I near the cell center for highly orthogonal scenarios. It excels over the orthogonal, high α channel, away from the cell center where the other cells' interference and the ST noise become dominant. This becomes clear upon revisiting Eq. (5-19) with Eq. (4-31), to derive

$$\frac{(C/I)_{TDTD}}{(C/I)_{Multipath}} \propto \frac{g_{TDTD}}{g_{Multipath}} \cdot \frac{1}{2} \cdot \frac{1-\alpha+\hat{N}(r)}{1-\alpha/2+\hat{N}(r)} \tag{5-23}$$

Now, $\hat{N}(r)$ is negligible near the cell center and growing to dominance toward the edge (inversely proportional to the "geometry factor" *G*). Toward the edge the ratio is high in favor of TDTD for high α where the multipath-gain is low in the first place. Near the center the situation is reversed.

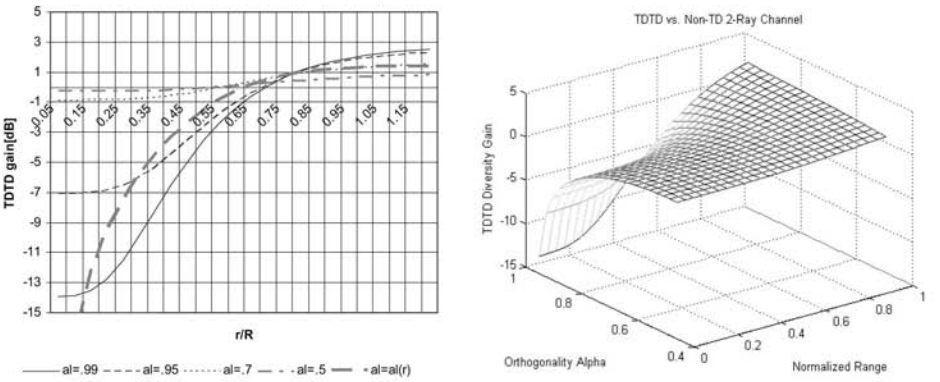

Figure 5-21. TDTD gain [dB]. ν=0.55, n=10, Av.P_s=0.5, P_{OH}=2.5, F_m=8 dB, T=140 dB, δ=0.5, ρ=0.3, x=1

TDTD with Uneven Branches

We now extend the discussion to unequal branches: the transmission power is split into *kP* in the first ray and *(1-k)P* in the second ray, where *k<1*.

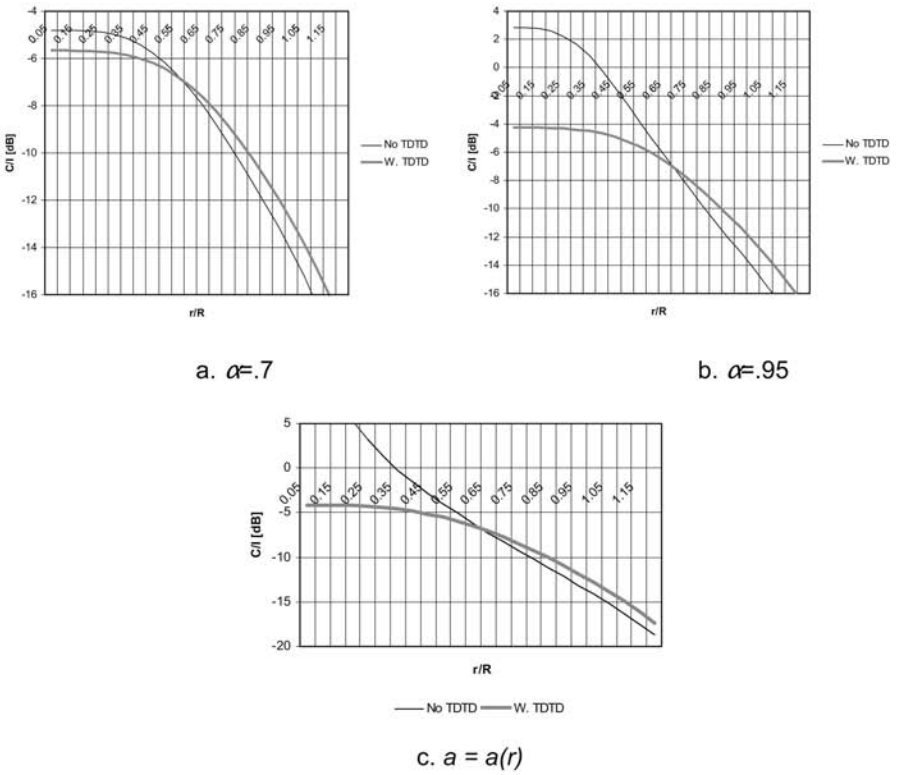

Figure 5-22. C/I vs. range for TDTD and non-TDTD
ν=0.55, n=10, P_s=0.5, P_{OH}=2.5, F_m=8 dB, T=140 dB, δ=0.5, ρ=0.3, x=1

Further we limit the discussion to $k > 0.5$, because part of the power of the second ray is lost to interference only.

Equation (5-19) now becomes

$$\left.\frac{C}{I}\right|_g (r) = \left(\frac{k\alpha \dfrac{P_S(r)}{P_{BTS}}}{\left(\hat{N}_{Th} + x_F \left(2 - \dfrac{r}{R}\right)^{-4} \right) \left(\dfrac{r}{R}\right)^4 + (1 - k\alpha)} \right) g\left(\left.\frac{C}{I}\right|_1 (r); \left.\frac{C}{I}\right|_2 (r); \left.\frac{C}{I}\right|_3 (r) \right). \quad (5\text{-}24)$$

The signal and interference for the respective rays is tabulated in Table 5-2.

Table 5-2. Signal and nonorthogonal interference in the multipath k, 1-k

Branch	Ray	Signal (x P_S/P_{BTS})	Interference
1	1 (k)	$k\alpha$	$1-k\alpha$
	2	$k\delta(1-\alpha)$	$1-k\delta(1-\alpha)$
2	3 (1-k)	$(1-k)\alpha$	$1-(1-k)\alpha$

The ratio of C/I of the respective rays is

$$\Delta[dB]_{1,3} = 10Log\left(\frac{\left(\hat{N}_{Th}+x_F\left(2-\frac{r}{R}\right)^{-4}\right)\left(\frac{r}{R}\right)^4+1-(1-k)\alpha}{\left(\hat{N}_{Th}+x_F\left(2-\frac{r}{R}\right)^{-4}\right)\left(\frac{r}{R}\right)^4+1-k\alpha}\cdot\frac{k\alpha}{(1-k)\alpha}\right) \tag{5-25}$$

$$\Delta[dB]_{1-3,2} = 10Log\left(\frac{\left(\hat{N}_{Th}+x_F\left(2-\frac{r}{R}\right)^{-4}\right)\left(\frac{r}{R}\right)^4+1-k\delta(1-\alpha)}{\left(\hat{N}_{Th}+x_F\left(2-\frac{r}{R}\right)^{-4}\right)\left(\frac{r}{R}\right)^4+1-k\alpha}\cdot\frac{k\alpha}{k\delta(1-\alpha)}\right)+ \tag{5-26}$$

$$+7.14e^{-0.59\rho}e^{-0.11\Delta_{1,3}}$$

and the diversity gain is obtained by Eq. (5-27). This is presented in Fig. 5-23 for k=1/2, 2/3, 3/4.

$$g_{TDTD}[dB] = 7.14e^{-0.59\rho}e^{-0.11\Delta_{1,3}}\left(1+e^{-0.11\Delta_{1-3,2}}\right) \tag{5-27}$$

5.6.4 Phase-Sweeping Transmit Diversity (PSTD)

Phase-sweeping transmit diversity attracts attention for its simplicity and independence of standards. Its principles and performance are reviewed by multiple analyses, simulations and test reports [5, 21-26]. Two or more branches are transmitted from the RAN whose antennas are arranged to provide channel diversity by spacing, polarization or angle. The branches are phased such that their phase difference varies at a pace that is slow enough not to affect a major change during a symbol, but fast enough to decorrelate over the interleaver frame. We presently consider two branches, the most typical case.

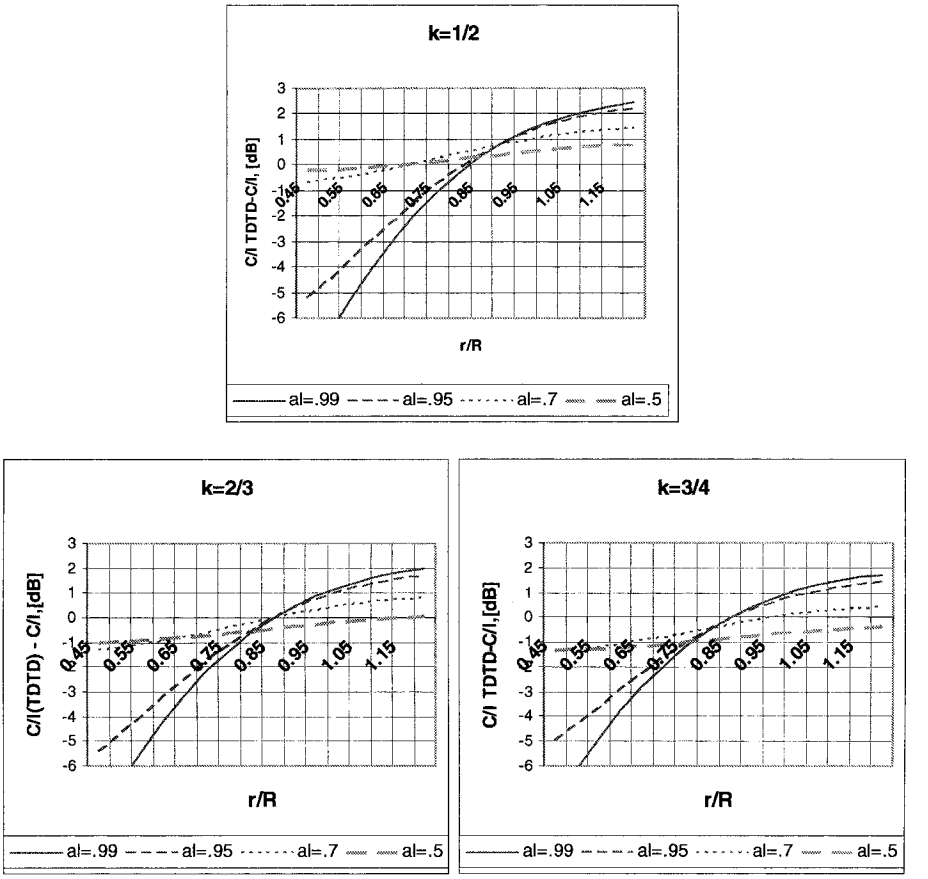

Figure 5-23. TDTD gain for uneven branches
ν=0.55, n=10, $Av.P_s$=0.5, P_{OH}=2.5, F_m=8 dB, T=140 dB, δ=0.5, ρ=0.3, x=1

The differential phasing creates alternations between sum and difference of the branches. In case that one branch is in a fade, these alternations maintain the strong branch, with just a small ripple on it. Thus, in case of uncorrelated flat fading branches the fading of each one is recovered, and deep fades appear at times when both branches have about equal strength. Modeling the branches statistics by Rayleigh leads to a resultant Rayleigh fading signal, because the sum of independent (complex) Gaussian signals is a Gaussian. The key to the diversity gain in this scheme is in shifting the slow fading rate to a rate where fading is recoverable by the FEC deinterleaver at the receiver, thus recovering slow fading.

Inasmuch as it only shifts the fading rate for uncorrelated flat fading branches into a convenient rate regime, PSTD does deteriorate stable signals

and creates a periodic deep fading outcome with a negative diversity gain. The diversity gain decreases for delayed multipath signals that create diversity gain in the rake receiver, and for signals with Rician statistics.

5.6.5 Comparative Evaluation

Both TDTD and PSTD are candidate techniques for add-on application in 2G and 3G BTSs and remote RANs. Both can be implemented at the RF level. The two methods differ, however, in their diversity mechanism, and their effect on the CDMA network is complementary, as shown in Fig. 5-24: PSTD is effective for highly orthogonal environments near the cell center and slow moving STs, while TDTD excels at the edge of coverage and radio holes. Both are mostly effective for slow users, where the FEC deinterleaver diversity is not effective. The fast FL power control provides fading mitigation for slow users, thus reducing the attractiveness of these Tx methods for 3G systems.

An important observation relates to the applicability of these methods for time-multiplexing high data rate systems: EV-DO and HSDPA. These systems operate on scheduled allocation of full power to the ST with momentary best channel.

The high C/I near the cell center that is evened out by the power control in the CDMA domain is the preferable zone for high data rate transmission. The TDTD suppresses this advantage by the additional nonorthogonal finger that reduces the C/I substantially, and it is not suitable for these types of transmissions.

PSTD, on the other hand, does not add noise. Its application to time multiplexed systems supports *user diversity*, by changing the channel state at a higher rate. These systems do not benefit from channel diversity proper, as the link is allocated to the ST whose channel is at the fading peak, reaching 3 dB above average, and the PSTD rate for this application may be chosen as appropriate to the scheduling routine, typically slower than in benign diversity application [36].

5.6.6 Impact of Diversity on Network Probes and Status Measurement

The application of diversity means to the CDMA network impacts its set-up and its performance, as discussed in the preceding sections. The RF diversity means are optional and may be applied and tested comparatively vs. a baseline system without these means. Within that, it is important to review the diversity effects on the network probes that are available to the field engineer and on the measurement parameters and interpret them correctly. These probes draw information that accumulates periodically at the switch,

relating to the BTS activity, RF parameter readings at the BTS, and information derived from designated STs in "drive tests" – traversing a pre-planned path under well-defined conditions that allow for repeatability. None of these probe or measurements' readings is a complete and repeatable status report of the network, because the network is in a continuously dynamic change due to its users' activity and location, and adaptive control algorithms that apply in each BTS in response to the network dynamics. Repetitive patterns of the network activity are therefore sought, to be considered *stationary statistical ensembles*, and used as reference scenarios for evaluation and comparative probing and measurements. Most important within these are the teletraffic patterns –daily, weekly and monthly.

Built into these are the assumptions that not only the intensity, but also the distribution pattern of the teletraffic activity is similarly repetitive, and so are the propagation conditions, including natural (e.g. seasonal) and vehicular traffic, etc. The application of diversity means modifies the communications links and with them – the network control parameters, including cells' boundaries, which disturbs the basic assumptions of stationarity, and requires due care in the interpretation.

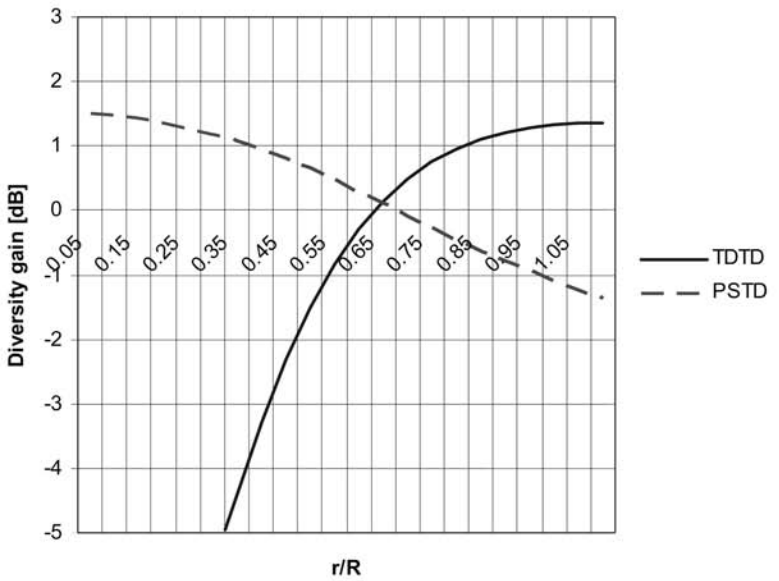

Figure 5-24. Diversity gain vs. range from the RAN, for TDTD and for PSTD. $\alpha=\alpha(r)$

5.6.6.1 Switch Data

The switch data reports overall sector activity statistics, and is a measure of capacity/ load and of performance indicators. The data is reported typically over 24 hours and busy hour reports. Relevant important parameters reported include:

RL RSSI (Received Signal Strength Indicator). This is the total power received, including users, interference and noise. The RSSI is measured at the quietest time (after midnight) to serve as a *noise rise reference,* and all measurements thereafter indicate the *noise rise.* RL diversity reduces the required E_b/I_t and thus the *noise rise* for the same level of activity, and thus allows for higher RL capacity.

MOU (Minutes Of Use). This is one measure of the RL load (another one is Erlang). It is expected to rise with RL diversity if the sector is RL limited. It rises with Tx diversity if the sector is FL limited.

Tx power (Total Tx power). The overhead power does not change with diversity, but the traffic per-link-power (also called *code domain power*) is affected by the Tx diversity. The total power is expected to reduce with Tx diversity. This is however not always the case: the improvement of the FL tends to extend the sector boundary and thus to capture users that have not been engaged before. These have inferior path-gain and draw more power per user. A benign comparison has to recognize the coverage difference and compensate for it either by computation or by retailoring the coverage, e.g. by beam down-tilting.

Digital Gain. The FL power control is applied to each traffic channel by applying a digital gain. The squared average of the digital gain is an indication of the total traffic power. This is affected by the Tx diversity.

Code Domain Power. Allows for a direct observation of the changes in the per-link-power for the same users before and after the change.

P_b (Power blocking rate). Blocking of access due to lack of power to serve them. A typical grade of service allows for 2%. The number of users served when the sector reaches this limit is a measure of the sector (FL) capacity. Tx diversity serves to lower P_b if the user population is not changed. There are proprietary algorithms to different BTS vendors that dynamically relieve the power blocking, by scaling power or balancing between loads in different FAs. These are to be consulted with.

P_d (Probability of dropped calls). This is not a direct indication of the capacity limit, rather of path-gain. Application of diversity may access users in deficient path-gain that have higher probability to be dropped. P_d does not necessarily diminish with application of diversity.

Soft Handoff (SHO) usage is reported. Also reported is 2, 3, 4 way SHO usage. These may change either way with application of diversity, as the diversity affects the sector boundary.

5.6.6.2 Drive Test Data

Drive test data measures performance indicators of one user over a sample road. Drive test is not a measure for cell capacity, nor any performance indicator, but a sample representing the drive test conditions. Comparative drive tests during the same traffic conditions provide an indication of location dependent performance. The driving speed is critical in comparative testing of Tx diversity. The ST receiver incorporates an interleaver decoder that serves to provide time-diversity. Its diversity gain is speed dependent: it increases from 0 dB at rest to over 4 dB at 10 kph. The diversity gain of the transmit diversity is complementary, and is highest at rest. A slow-speed drive test whose purpose is to measure the highest diversity gain has to be conducted at speeds lower than 3 kph (pedestrian pace).

RSSI is the total power received by the ST, including the BTS power and other BTSs' transmission. It is used as a reference for the ST for the power control. The RSSI changes with diversity only to within the change of the BTS power with diversity.

Received power. This is the traffic channel received power. It is a direct measure of the forward link. An increase in Rx power, for the same BTS transmit power, and the same location and drive and load conditions, indicate an improvement of the link. This is a direct measure of the Tx diversity gain along the route and under the specified conditions. Care has to be taken to measure the Rx power for the right PN, and to differentiate between non-SHO and SHO conditions.

*MTx.*The Mobile (ST) Tx power is a reverse link parameter, and depends on the BTS NF, the noise rise in the BTS (representing the RL load status) and the transmission loss (relating to the ST location). The MTx decreases for RL link that is enhanced by RL diversity, for the same traffic load. The MTx is not a measure of the transmit diversity or any forward link parameter. A proper measurement of the MTx requires that a controlled signal be transmitted by the ST. One convention for CDMA systems is a Markov sequence that simulates typical speech. MTx cannot be measured in an idle state.

E_C. This is a measure of the designated pilot power. It is used by the ST to estimate the channel for calculating the open loop power control and the MTx. The power measured by all usable fingers is summed up. There is no diversity gain. There is no impact of Tx diversity.

Ec/Io. The Ec/Io is measured for the strongest finger only, and it does not enjoy the diversity gain, but suffers from the additional interference transmitted in the TDTD mode. It is lower for TDTD because of the power split.

Ec/Io aggregate The power received in all usable fingers is summed up (powerwise) and normalized to energy per chip, and divided by the total (non-

despread) power spectral density in these fingers. There is no diversity gain and no direct effect of Tx diversity.

REFERENCES

[1] W.C. Jakes, Ed., *Microwave Mobile Communications*, Chapter 5, Wiley, 1974 (reprint IEEE Press, New York, 1993).

[2] J. Proakis, *Digital Communications*, Second edition, Chapter 7, McGraw-Hill, 1995.

[3] A. Goldsmith, *Wireless Communications*, Chapter 7, Cambridge University Press, 2005.

[4] J. Paulraj, *Diversity,* Chapter 12 in *The Mobile Communications Handbook*, Second Edition, CRC Press, 1999.

[5] A. Hottinen, O. Tirkkonen, and R. Wichman, *Multi-Antenna Transceiver Techniques for 3G and Beyond*, Chapter 3, Wiley, 2003.

[6] W.C.Y. Lee and Y.S. Yeh, *Polarization Diversity System for Mobile Radio*, IEEE Trans. On Communications, Vol. com-20, No. 5, pp. 912-923, October 1972.

[7] J. Shapira, and C.E. Wheatley, *Channel Based Optimum Bandwidth for Spread Spectrum Land Cellular Radio*, Proceedings of PIMRC 92, pp. 199-204, Boston, October 1992.

[8] S. Alamouti, and V. Tarokh, *Transmitter Diversity Technique for Wireless Communications*, US patent 6,185,258 B1 Feb. 6, 2001.

[9] A. Papoulis, *Probability, Random Variables, and Stochastic Processes.* McGraw-Hill, 1965.

[10] A.M.D. Turkmani, A.A. Arowogolu, P.A. Jefford, and C.J. Kellent, *An Experimental Evaluation of Performance of Two-Branch Space and Polarization Diversity Schemes at 1800 MHz*, IEEE Trans. Veh. Tech., Vol. 44, No. 2, pp. 318-326, May 1995.

[11] M.D. Yacoub, *Wireless technology: Protocols, Standards, and Techniques*, CRC Press LLC, Boca Raton, 2002.

[12] W.C.Y. Lee, *Mobile Communications Design Fundamentals*, Sec. 6.2.2, Howard W. Sams &Co, 1986.

[13] B. Dietrich, Jr., K. Dietze, J.R. Nealy, and W.L. Stutzman, *Spatial, Polarization, and Pattern Diversity for Wireless Handheld Terminals*, IEEE Trans. On Antennas and Propagation, accepted for publication.

[14] B. Dietrich, *Adaptive Arrays and Diversity Antenna Configurations for Handheld Wireless Communication Terminals*, PhD thesis, Virginia Polytechnic Institute and State University, 2000.

[15] R. Vaughan, and J.B. Andersen, *Channels, Propagation and Antennas for Mobile Communications*, IEE Press, 2003.

[16] C. Cox, *Antenna Diversity Performance in Mitigating the Effects of Portable Radiotelephone Orientation and Multipath Propagation,* IEEE Trans. on Communications, Vol. COM-31, No. 5, May 1983.

[17] J. Shapira and S. Miller, *On Polarization Transmit Diversity in CDMA Regimes,* 4^{TH} EPMCC Conference, Vienna, February 20-22, 2001.

[18] P.L. Perini, and C.L. Holloway: *Angle and Space Diversity Comparisons in Different Mobile Radio Environments,* IEEE Trans. on Antennas and Propagation, Vol. 46, No. 6, June 1998.

[19] J. Shapira, P. Lemson, and D. Levy, *Cellular Station Augmentation System and Method*, US patent 6,987,990 B2, Jan. 17, 2006.

[20] J. Shapira, S. Miller, and P. Lemson, *Time-Delay Transmit Diversity add-on to a Multicarrier Base Transceiver System*, US patent 6,957,050 B2 Oct. 18, 2005.

[21] J.S. Thompson, P.M. Grant and B. Mulgrew, *Down-link Transmit Diversity Schemes for CDMA Networks*, IEEE VTC'99, pp. 1382-86, 1999.

[22] J.S. Thompson, P.M. Grant and B. Mulgrew, *Downlink Transmit Diversity Schemes for CDMA Networks,* IEE Proc – Commun.,Vol. 147, No. 6, December 2000.

[23] B. Kirkland, J. Kubina and A. Smith, *Phase Swept and Time-Delay Transmit Diversity Performance Results for 1x RTT CDMA Systems*, IEEE VTC' 2000.

[24] A. Hiroike, F. Adachi, and N. Nakajima, *Combined Effects of Phase-Sweeping Transmitter Diversity and Channel Coding,* IEEE Trans. VT 41, No. 2, pp. 170-176, May 1992.

[25] W.-Y. Kuo, and M.P. Fitz, *Design and Analysis of Transmitter Diversity Using Intentional Frequency Offset for Wireless Communications,* IEEE Trans. on Vehicular Technology, Vol. 46, No. 4, pp. 871-881, November 1997.

[26] A. Gutierrez, J. Li, S. Baines, and D. Bevan, *An Introduction to PSTD for IS-95 and cdma2000,* Proc. of IEEE Wireless Communications and Networking Conference WCNC, Vol. 3, pp.1358-1362, 1999.

[27] K. Gilhousen, *CDMA Microcellular Telephone System and Distributed Antenna System Therefor,* US Patent 5,280,472, Jan. 18, 1994.

[28] R. Dean, *Dual Distributed Antenna System,* US Patent 5,513,176, Apr. 30, 1996.

[29] R. Dean, F.P. Antonio, K. Gilhousen, and C.E. Wheatley III, *Dual Distributed Antenna System,* US Patent 5,533,011, Jul. 2, 1996.

[30] K.R. Baker, *Polarization Enhanced CDMA Communication System,* US patent 6,061,336, May 9, 2000.

[31] J. Shapira, *Method and System for Improving Communication*, US patent 6,697,641 B1, Feb. 24, 2004.

[32] Y. Karasawa, and H. Iwai, *CDMA Communication System*, US patent 5,347,535, Sept. 13, 1994.

[33] J.R. Light, and C. Varsaro, *Method and Apparatus for Achieving Antenna Receive Diversity with Wireless Repeaters*, US patent 5,930,293, Jul. 27, 1999.

[34] M.P. Fuerter, *Delay Combiner System for CDMA Repeaters and Low-Noise Amplifiers*, US patent 6,125,109, Sept. 26, 2000.

[35] L. Aydin, E. Esteves and R. Padovani, *Reverse Link Capacity and Coverage Improvement for CDMA Cellular Systems Using Polarization and Spatial Diversity*, IEEE ICC'2002, pp. 1887-1892, 2002.

[36] U. Timor, S. Miller, *Forward-link Throughput Performance of 1xEVDO with Phase-Modulation Transmit Diversity (PMTD),* Proc. CIC2004, The 9th CDMA Inter. Conf., Seoul, Oct. 2004.

6

REPEATERS EMBEDDED IN THE CDMA RADIO ACCESS NETWORK

This chapter reviews and analyzes the interaction of the repeater with the CDMA radio access network and its impact on the repeater and on the network service parameters. Basic propagation and CDMA network rules are used for developing clear functional relations that provide insight and planning, control and optimization guidelines. Repeaters serve for coverage filling, indoors and in radio-shadowed areas, and for coverage extension beyond the donor cell's coverage, but also for capacity gain for "hot spot" repeaters. Coverage extension includes long, sometime weaving roads. Cascading repeaters in a multi-hop chain is analyzed and optimized.

Different aspects of this topic have been addressed in the literature: [1-3] are basic CDMA dynamics papers that build much of the foundations to the analysis, [4-7] treat microcells' interaction in a CDMA network. [8] describes a heuristic formula for calculating diversity gain, that is used in this chapter, and [9-17] treat the coverage and capacity of repeaters in the CDMA network.

6.1 Modeling of the Repeater in the CDMA Network

A repeater in a CDMA network is an RF access point for the user units. It is a bidirectional linear amplifier that conveys the transmissions between the user units and the BTS. As such, it is transparent to the network traffic, signaling and controls. The repeater interfaces to a base station (BTS) at the RF (or IF) level and shares the BTS resources with the BTS antennas and/or other repeaters. The users served by the repeater share the BTS resources with those served directly by the BTS and are controlled by the same BTS rules, including power control and Soft Handoff. These introduce inter-relations between repeater parameters and impose limiting factors. The interaction of the repeater with the donor cell is modeled in Fig. 6-1.

Both the repeater coverage and the donor coverage are affected by the set gain of the repeater G_{RR}. The net gain $y=G_{RR}T_D$ determines the link budget to

the repeater access and thus – the repeater coverage available for users with nominal power P_m. The amplification of the repeater self noise $-F_R G_{RR} T_D$, determines the additional noise that the repeater contributes to the base station, thus reducing the coverage available to the direct users of the donor cell.

Similarly, the forward link gain of the repeater G_{RF}, and the repeater available power, affect both repeater and donor coverage and capacity. The total repeater power retransmits the signals for all the donor users, not only those served by the repeater, and limits the repeater coverage and the number of users served in its coverage according to their location within the coverage (their power drainage according to their link gain T_{RF}), while the overall gain $T_{DF} G_{RF}$ determines the power drainage of the donor cell for the repeater users, and thus limits the donor cell coverage and capacity.

Noteworthy is the difference in the net gain between the RL and the FL. While the repeater noise is added at the input to the gain-chain $G_{RR} T_{DR} = y_R$, and its impact does not depend on the division of the net gain between the amplifier and the donor link, the situation is different in the FL: the repeater noise is being amplified by the repeater amplifier, but not by the donor link. A high donor link gain is thus emphasized in order to increase the signal to noise in the FL.

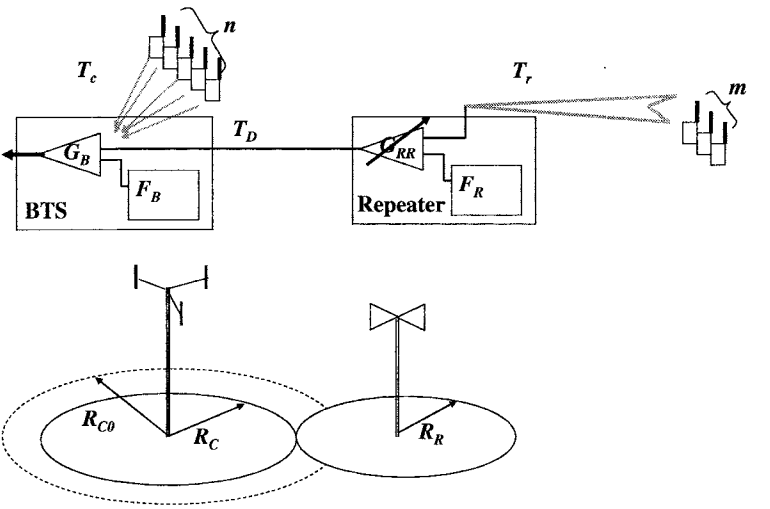

Figure 6-1a. Repeater in a CDMA cell – Reverse link

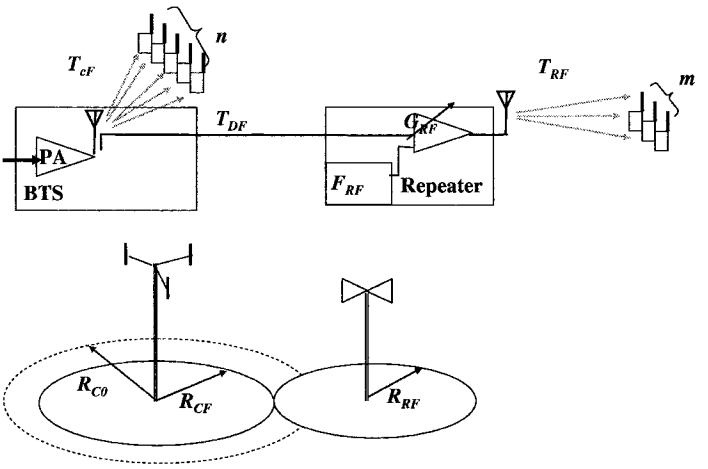

Figure 6-1b. Repeater in a CDMA cell – Forward link

Here

$T(r)$	is the transmission gain,
T_{RR}, T_{RF}	is the lowest transmission gain (maximal range) in the satellite coverage, where the user has to transmit its maximum nominal power,
F	stands for FL in all indices,
T_{DR}, T_{DF}	is the transmission gain for the donor link,
T_{cR}, T_{cF}	is the lowest transmission gain (maximal range) to a user in the cell, when loaded with the repeater,
R_{c0}, R_c, R_R	is the range of the baseline donor cell, of the donor cell loaded with the repeater, and of the repeater, respectively,
F_{RR}, F_{RF}	is the noise factor of the repeater at the satellite antenna terminal (on RL) and donor antenna terminal (FL) respectively,
F_B	is the noise factor of the BTS at the receive antenna terminal,
G_{RR}, G_{RF}	is the gain of the repeater in reverse and forward links,
P_{mMAX}	is the maximum nominal power transmitted from a user,
S_B	is the signal level from a user at the BTS terminal, as set by the power control for that load,
m, n	is the number of users served by the donor cell (n) and by the repeater (m),
n_{Tot}	$n_{Tot}=n+m$ is the total number of users served by the donor cell, and
y	is the net gain. $y=G_{RR}T_D$ net RL gain. $y_F=G_{RF}T_{DF}$ net FL gain.

6.2 Classification of Repeaters by their Interaction with the Donor Cell

The optimal choice of repeater parameters depends on the applications and the objectives they are to serve. Repeaters may be classified by their location and their purpose. Both affect their setting.

6.2.1 Embedded Repeaters

Embedded repeaters ((1) in Fig. 6-2) border their coverage within the donor cell. Their coverage is limited and controlled by their isolated location, antenna and gain setting. "Hot spots" are repeaters built for high capacity, short-range, and high isolation from the rest of the donor cell, in order to reduce interference. "Hole-filling repeaters" are those placed to cover shadowed areas within the donor cell, and are tuned to provide additional coverage. Indoors repeaters stand apart by virtue of their high isolation from the rest of the donor cell, and coverage design to suit the indoors propagation regime.

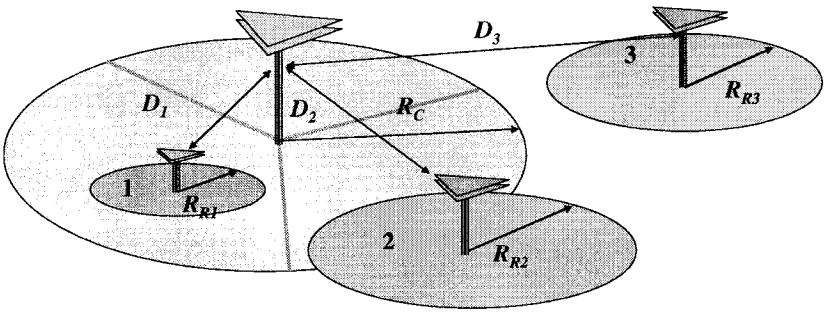

Figure 6-2. Classes of repeater interaction with the donor

6.2.2 Range Extension Repeaters

Range extension repeaters ((2) in Fig. 6-2) interface both with their own donor and with other cells. Extension repeaters are high gain, high-power repeaters for maximizing coverage. A chain of multi-hop cascaded repeaters is used for coverage of long stretches of roads or rural areas.

6.2.3 Cell boundary Repeaters

Lower gain, lower power repeaters duly placed near the cell edge provide a sharper boundary between cells, thus reducing pilot pollution and "radio holes" between cells and increasing the cell capacity [11].

6.2.4 Remote Repeaters

These are high gain, high-power repeaters ((3) in Fig. 6-2), in many cases replacing base stations. The repeater is beyond the coverage of the donor, and direct RF (over-the-air) linkage to the donor is replaced by optical fiber or a microwave link. Multi-lobed repeaters are often used to focus on the activity areas. A choice of parallel ("star") or series ("multi-hop") connection of the lobes depends on the configuration and relative coverage of the lobes.

The interaction of the repeater with the donor cell is clarified in Fig. 6-3. The signal strength is plotted vs. distance from the BTS, decaying as R^{-4}. The coverage of the repeater extends over the region where its signal exceeds that of the donor cell. This is controlled by setting the repeater gain y, and thus its transmitting power, and by its antenna height and directivity, which determine its transmission gain curve. Note that the net gain for hole filler repeaters and for hot spot repeaters is low, which limits their coverage to the desired areas and their impact on the donor cell.

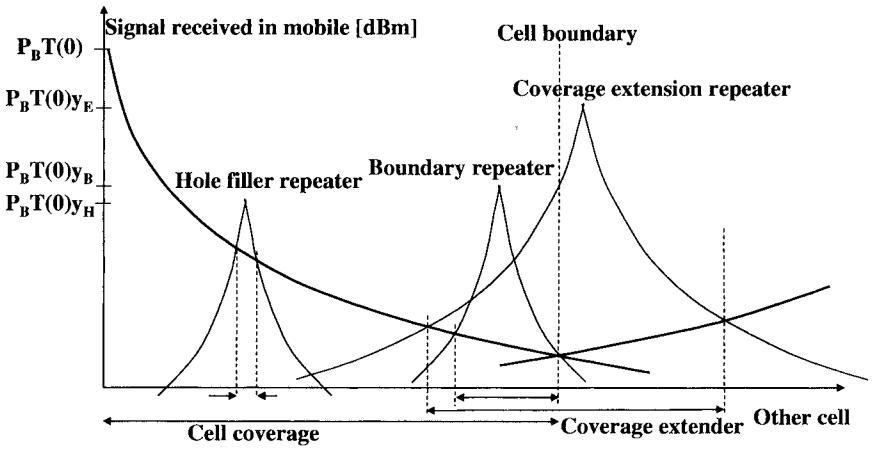

Figure 6-3. Repeater setting and coverage overlap per class

The key factor for boundary repeaters is the steep slope of their transmission gain that is achieved by beam tilting and directivity of their coverage inward. Extension repeaters, on the other hand, are built for maximum outward coverage. These have high net gain – approaching $y \to 1$, and their overlap with the donor cell is controlled by directing their antennas outward.

6.3 Interaction of the Repeater with the CDMA Network

The reverse link and the forward link capacity and coverage equations are derived in this section, and trade-off between the donor and the repeater is discussed. Capacity loss for the repeater apparent noise factor is derived, and a measure for compensating for that is proposed. Rules for repeater optimization are derived.

6.3.1 Repeater Modeling – Reverse Link

The *apparent noise factor* at the donor cell input due to the repeater self-noise is

$$F_R \cdot G_{RR} \cdot T_{DR} \equiv F_R y . \tag{6-1}$$

The *net repeater gain* **y** is the product of its gain and the transmission loss to the donor

$$y \equiv G_R \cdot T_D . \tag{6-2}$$

The *effective noise factor* of the repeater, when linked to the donor cell, is

$$F_{RE} = F_R + F_C / y . \tag{6-3a}$$

Similarly, the *effective donor cell noise factor*, when linked to the repeater, is

$$F_{CE} = F_C + yF_R . \tag{6-3b}$$

Normalized to the noise factor of the BTS these become: the *apparent repeater noise factor*

$$\hat{F} \equiv \hat{F}_R y \equiv \frac{F_R}{F_C} y . \tag{6-4a}$$

The *effective repeater noise factor* $\hat{F}_{RE} \equiv F_{RE}/F_C$ becomes

$$\hat{F}_{RE} = \left(1 + \hat{F}\right)\!/ y . \tag{6-4b}$$

The *effective donor cell noise factor* $\hat{F}_{CE} \equiv F_{CE}/F_C$ becomes

$$\hat{F}_{CE} = F_{CE}/F_C = 1 + \hat{F} . \tag{6-4c}$$

Note that $\hat{F}_{RE} > \hat{F}_R$ and is minimized for $y \to \infty$ (the *apparent repeater noise factor* dominates over the BTS self-noise), while $\hat{F}_{CE} > 1$ and is minimized for $y \to 0$ (the repeater is decoupled from the BTS). There is an inherent trade-off between the noise factors of the donor cell and the repeater, which translates into a trade-off between their coverage areas [16].

The donor cell coverage is limited by the maximum power available to the ST – P_{mmax}, and the required signal level S_B at the BTS input for a given load

$$T_C = S_B/P_m \Rightarrow R_{\max} \propto \left(P_{m\max}/S_B\right)^{1/\gamma} \tag{6-5}$$

where γ is the range regression exponent for the path-loss (refer to Section 3.3.4). Hereafter we resort to the physical propagation model (refer to Section 3.2.4. and Eq. (3-11)) throughout the chapter. Then

$$R_{\max} \propto \left(P_{m\max}/S_B\right)^{1/4}\left(G_m G_C\right)^{1/4}\left(H_m H_C\right)^{-1/2} \tag{6-6}$$

where H_m, H_C are the heights of the ST and the BTS antennas, and G_m, G_C are their gains, respectively. Note that the link budget P_m/S_B is proportional to g – the diversity gain in the link, which increases the effective signal to noise ratio (see Eq. (4-22) and Chapter 5). This is an important observation: most BTSs are equipped with diversity antennas on the RL, and some on the FL (FL transmit diversity is optional in CDMA2000 and WCDMA standards). Most repeaters, on the other hand, are not diversity-enhanced on either link and their respective coverage is thus smaller.

Now, the power control of the donor cell controls the power of both the donor users and the repeater user to reach the donor receiver with the required S_B

$$P_m \cdot T_R(R_R) \cdot G_{RR} \cdot T_{DR} = P_m \cdot T_{CR}(R_C). \tag{6-7}$$

Then the constraint on the repeater RL gain becomes

$$y_R \equiv G_{RR} \cdot T_{DR} = T_{CR}/T_{RR} = (G_C/G_R)(H_C/H_R)^2(g_{CR}/g_{RR})(R_R/R_C)^4 \tag{6-8}$$

which relates the repeater gain to the ratio of the coverage of the repeater and the donor cell. The repeater RL range relates to that of the donor as

$$R_R/R_C = y_R^{1/4}\left[(G_R/G_C)(H_R/H_C)^2(g_{RR}/g_{CR})\right]^{1/4} \equiv y_R^{1/4}U_R^{1/4}. \tag{6-9}$$

$\boldsymbol{U_R}$ defines the ratio of the gain and height of the repeater to the BTS antennas, and the ratio of diversity gain in the respective links.

6.3.2 Repeater Impact on Coverage and Capacity – Reverse Link

Equation (4-9) is revisited. The apparent repeater noise factor $\hat{F}$ is added to the noise term as a jamming term (Section 4.3.3)

$$C/I = q/\left(1+(n_{Tot}-1)q\nu(1+uxf)+\hat{F}\right) \tag{6-10}$$

where $q \equiv S_B/N_0WF_B$ is the user signal received at the BTS, normalized to the BTS thermal noise. This is solved to derive the pole equation

$$q = \left(1+\hat{F}\right)(C/I)/(1-\eta). \tag{6-11}$$

Here $\eta \equiv (n_{Tot}-1)\nu(1+uxf)$ is the load factor, n_{Tot} is the number of active users, ν is the voice activity factor (these are replaced by data throughput in data systems), and f represents the interference from cells in the same system that are adjacent to the donor cell and from those adjacent to the repeater. The cell range is reduced (Eq. (4-15)) to $R_C/R_{C0} = \left(1+\hat{F}\right)^{-1/4}$ and the repeater range relates to the (undisturbed) donor cell range as

$$R_R/R_{C0} = \left(y_R/\left(1+\hat{F}\right)\right)^{1/4}U_R^{1/4} = \hat{F}_{ER}^{-1/4}U_R^{1/4}. \tag{6-12}$$

The total received power at the BTS (compare with Eqs. (4-7), (4-13)) is

$$S_T \equiv P_{Total}/N_o WF = \left(1+\hat{F}\right)/\left(1-\eta\right). \tag{6-13}$$

The RL *pole capacity* N_{Tot} is easily derived from

$$S_T = \frac{1+\hat{F}}{1-\eta} = \frac{1+\hat{F}}{1-\frac{\left(n_{Tot}-1\right)}{\left(N_{Tot}-1\right)}} \quad \text{(compare to Eq. (4-8))}$$

$$N_{Tot} - 1 = \frac{n_{Tot}-1}{1-\frac{1+\hat{F}}{S_T}} = \frac{n_{Tot}-1}{1-\left(1+\hat{F}\right)\cdot 10^{-\frac{S_T[dB]}{10}}}. \tag{6-14}$$

With a set limit S_{T0} on the BTS *noise rise* the repeater noise decreases the donor cell allowable load from η_0 to η_F and thus its capacity. This is demonstrated in Fig. 6-4 – the *apparent repeater noise factor* $\hat{F}$ causes the noise rise curve to shift up and to cut the S_{T0} limit at a lower load factor. From Eq. (6-13) (and also Eq. (4-14))

$$S_{T0} = \left(1+\hat{F}\right)/\left(1-\eta_{F0}\right) = 1/\left(1-\eta_0\right) \Rightarrow \eta_{F0}/\eta_0 = 1-\hat{F}\left(1/\eta_0 - 1\right). \tag{6-15}$$

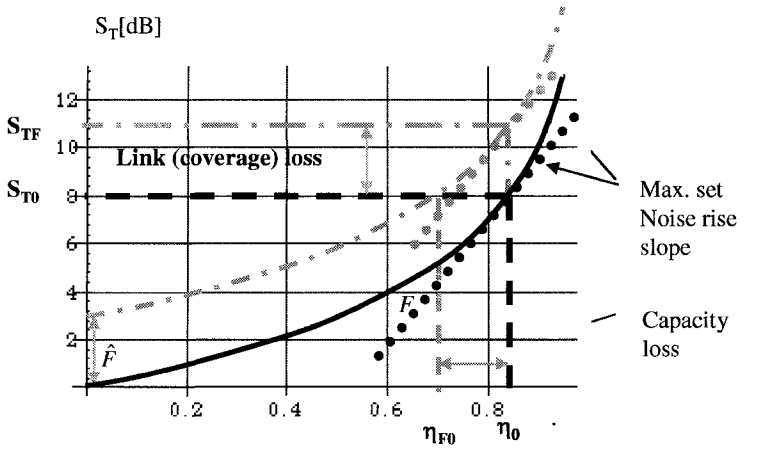

Figure 6-4. The impact of the repeater apparent noise figure on the noise rise, and trade-off of coverage for capacity

The capacity loss of the donor cell is plotted in Fig. 6-5 (Eq. (6-15) with *noise rise*=8 dB, η_0=0.85). This establishes a clear link between the repeater coverage, which increases proportionally to (square root of) the net repeater gain, and the loss of capacity of the donor cell. Note that the noise rise limit sets a limit on the donor cell coverage when in full load, and this full load coverage is not affected.

This approach suits urban embedded repeaters, where the repeater has a limited range and limited link loss that can be accommodated by minimizing y – the net repeater gain, and thus minimizing the repeater effect on the donor cell capacity. It is obvious that this limits the benefit of the repeater as a coverage extender, where high net gain is required, to donor cells that are not heavily loaded (and do not reach their load limit by the introduction of the repeater).

An alternative approach that considers the integrated performance of the donor with the repeater offers a trade-off between capacity gain and coverage gain. By tracking the *noise rise* maximal slope in Fig. 6-4, the donor capacity is preserved on behalf of its coverage by setting $\eta = \eta_0$ in Eq. (6-15)

$$S_{T\hat{F}} = \left(1+\hat{F}\right) \Big/ \left(1-\eta_0\right) \tag{6-16}$$

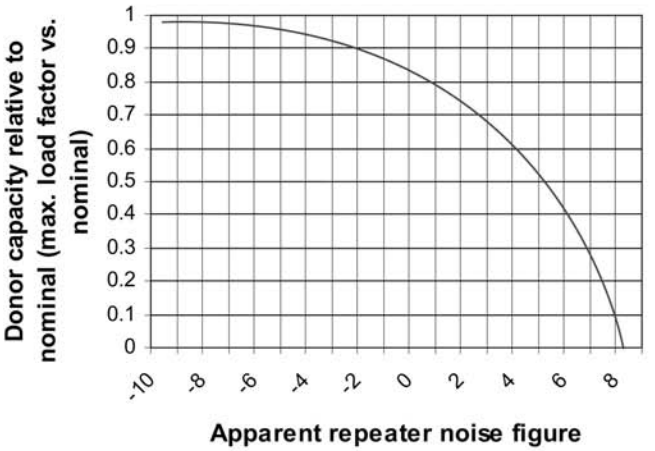

Figure 6-5. Capacity loss in the donor cell vs. Apparent Repeater Noise Figure $\hat{F}$. Fixed noise rise (S_T) (fixed coverage)

as shown in Figs. 6-6a and 6-6b. This process suits a high user density, low path-loss donor cell, where coverage extends beyond the user concentration, as in "hot spot microcell". It is detrimental for a loaded cell with a uniform user density, where the shrinkage of coverage entails a reduction in the user population. However, the added repeater coverage overcompensates for the loss of coverage in the donor cell in an integrated donor-repeater design.

Note that a common practice for setting the noise rise limit is resetting the noise rise to zero at the no-activity time (night time). This procedure does incorporate any outside noise (including repeater noise), and effectively raises the noise rise limit and reduces the coverage without affecting the capacity η_0.

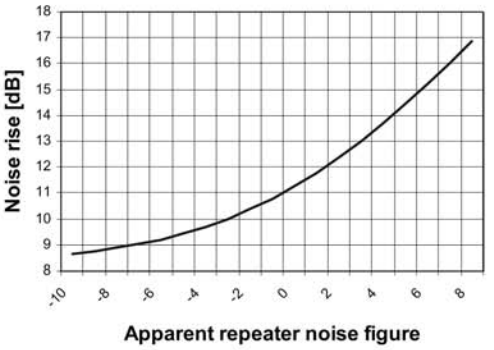

Figure 6-6a. Rise of noise rise limit (S_{TF}) (reduced coverage) for (S_{TF}) maintaining the capacity vs. $\hat{F}$

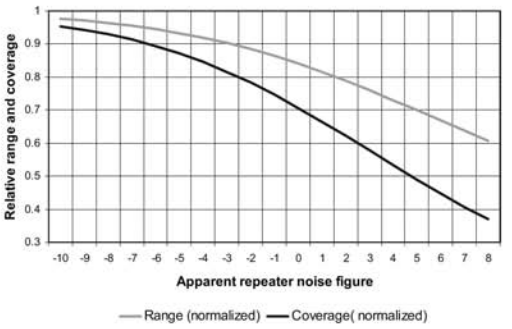

Figure 6-6b. Range and coverage of donor cell vs. apparent repeater noise figure $\hat{F}$, for fixed capacity

6.3.3 Forward Link Analysis

We follow the footsteps of Section 4.4.1 in analyzing the forward link equation for the repeater. The donor link is assumed to be orthogonal by design. Referring to Eqs. (4-20), (4-21), (4-30), and (4-31) we derive the expressions for the leading and the second finger in the repeater coverage, and the respective diversity gain between them. The allocated power $P_{SRi}(r_{Ri})$ is split between the multipath rays that are recombined by the diversity combiner at the ST according to their relative C/I . The power allocation $P_{SRi}(r_{Ri})$ is then determined according to the set C/I at the ST by the FLPC (Forward Link Power Control):

$$\left.\frac{C}{I}\right|_{i1}(r_{Ri}) = \frac{\alpha_{Ri} P_{SRi}(r_{Ri}) y_F T_{RF}(r_{Ri})}{N_o W\left(F_m + F_{RF} G_{RF} T_{RF}(r_i)\right) + (1-\alpha_{Ri}) P_{BTS}\, y_F T_{RF}(r_{Ri}) + I_{ocR} W}$$

$$\left.\frac{C}{I}\right|_{i2}(r_{Ri}) = \left(\frac{\delta_{Ri}(1-\alpha_{Ri}) P_{SRi}(r_{Ri}) y_F T_{RF}(r_{Ri})}{N_o W\left(F_m + F_{RF} G_{RF} T_{RF}(r_i)\right) + \left[1-\delta_{Ri}(1-\alpha_{Ri})\right] P_{BTS}\, y_F T_{RF}(r_{Ri}) + I_{ocR} W} \right).$$

The diversity gain expression follows [8]: $g[dB] = 7.14 Exp\{-0.59\rho - 0.11\Delta\}$ where

$$\Delta[dB] = 10Log\left\{ \left.\frac{C}{I}\right|_{i1}(r_i) \Big/ \left.\frac{C}{I}\right|_{i2}(r_i) \right\} = 10Log\left\{ \frac{\hat{N}_R + \left[1-\delta_{Ri}(1-\alpha_{Ri})\right]}{\hat{N}_R + (1-\alpha_{Ri})} \bullet \frac{\alpha_{Ri}}{\delta_{Ri}(1-\alpha_{Ri})} \right\} \tag{6-17}$$

$$\hat{N}_R \equiv \left(N_0 W\left(F_m + F_{RF} G_{RF} T_{RF}(r_i)\right) + I_{ocR} W\right) / y_F P_{BTS}\, T_{RF}(r_{Ri}) . \tag{6-18}$$

Here

P_{SR} is the power allocated to repeater user R_i, transmitted from the BTS,
C/I is the set level by the FLPC, received by both repeater users and donor cell users,
F_{RF} is the repeater FL noise figure,
I_{ocR} is the other BTSs' FL interference to an ST in the repeater coverage,
α_R is the fraction of the transmitted power from the repeater to the user that is orthogonal,
y_F is the net gain of the BTS transmission to the terminal of the distribution antenna of the repeater, and
$\hat{N}_R$ is the noise and interference power at the ST input from thermal and other BTSs, normalized to the power received from the donor BTS.

We develop Eq. (6-18) by referring to Fig. 6-2, and normalizing the donor cell range to 1, the distance to the next BTS – to 2, and the location of the repeater on the axis between them to *d*.

Note that $T_{RF}(r_{Ri}) = T_{RF}(r_i - d) = y^{-1}T_C(r_i - d)$. Then

$$\hat{N}_R = \frac{N_0 W F_m}{P_{BTS} T_C(1)} y_F^{-1} U_F^{-1} \left\{ \left(T_C(1) G_{RF} \frac{F_{RF}}{F_M} \right) + (r_i - d)^4 + x_F \left(\frac{2 - r_i + d}{r_i - d} \right)^{-4} \right\}. \quad (6\text{-}19)$$

Here U_F defines the ratio of the gain and height of the repeater to the BTS antennas, and the ratio of diversity gain in the respective forward links, similar to the U_R definition in Eq. (6-9).

This is now solved for P_{SR} under the required C/I (forward link power control applied) and then compared with P_S, the power allocated by the BTS to the user in the cell at the same location (see Eq. (4-34))

$$P_{SRi}(r_{Ri}) = \frac{C}{I}\bigg|_{set} \frac{\hat{N}_R + 1 - \alpha_{Ri}}{\alpha_{Ri} g_R(r_{Ri})}; P_{Si}(r_i) = \frac{C}{I}\bigg|_{set} \frac{\hat{N} + 1 - \alpha_i}{\alpha_i g(r_i)} \text{ to render}$$

$$\frac{P_{SRi}(r_{Ri})}{P_{Si}(r_j)} = \frac{\hat{N}_R + 1 - \alpha_{Ri}}{\hat{N} + 1 - \alpha_i} \frac{\alpha_i g(r_i)}{\alpha_{Ri} g_R(r_{Ri})}. \quad (6\text{-}20)$$

The noise and other cell interference term $\hat{N}$ (Eq. (6-19)), which is equated to the level of the BTS power at the edge of the donor cell, is negligible near the radio access point (the BTS antenna for $\hat{N}$, and the repeater antenna for $\hat{N}_R$) and grows toward the edge of coverage. The repeater noise term (the first term in the parentheses), however, is amplified along with the signal and maintains its value through the coverage. It is therefore desirable to limit the repeater gain G_{RF} and apply high gain in the donor link by using directive antennas and a line of sight link. The FL signal amplification $y_F = T_{DF} G_{RF}$ is thus maximized without overamplifying the repeater noise. A minimum of 20 dB SNR at the input to the repeater is desired.

Different settings of *y* and of *U* are required for achieving the coverage objectives of different repeaters in Fig. 6-2. Note that the diversity gain is a multiplier in the power equation, and its application increases both the range (the maximal link loss) and the capacity (the total available power). The following parameters are used in the examples:

$F_m = 8dB;\ F_R = F_m / y_F;\ P_B = 43dBm;\ T_C = 140dB;\ G_{RF} = 80dB;\ \delta = 0.5;\ \rho = 0.3;\ s = 0.01.$

6.3.3.1 Embedded Repeater

The repeater is located at 0.3 of the cell range. U=0.1, y=-10 dB. The ratio of power allocated by the BTS to a repeater user, to that allocated to a cell user at the same place, is plotted in Fig. 6-7. The repeater coverage is well contained within the cell.

6.3.3.2 Border Repeater

Figure 6-8. The repeater is at 0.7 of the cell range. Its purpose is to enhance the coverage near the boundary while reducing the SHO zone by providing a steep attenuation curve beyond the donor's boundary [11]. The repeater is positioned with lower antennas, sometimes directional toward the donor. U=0.1, y=-10dB.

6.3.3.3 Coverage Extension Repeater

Figure 6-9. The repeater is located at 1.15 of the cell range. Maximal extension outwards is sought. Repeater location is determined to overlap the donor coverage near the boundary, with no radio holes. Antennas are located and designed for maximal coverage. U=1, y=0 dB. No next cell in the example demonstrated.

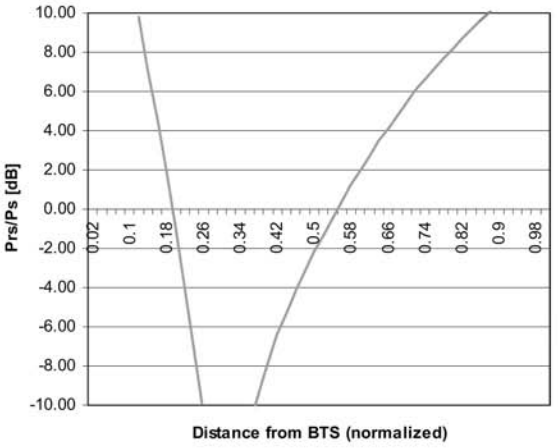

Figure 6-7. Ratio of power allocated to the repeater to that allocated to a cell user, embedded repeater

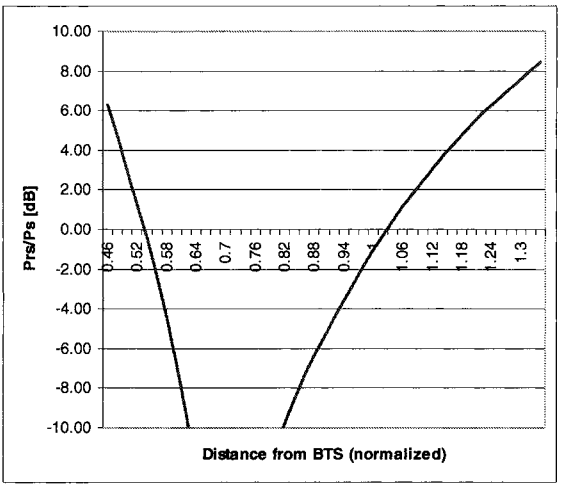

Figure 6-8. Ratio of power allocated to the repeater to that allocated to a cell user, border repeater

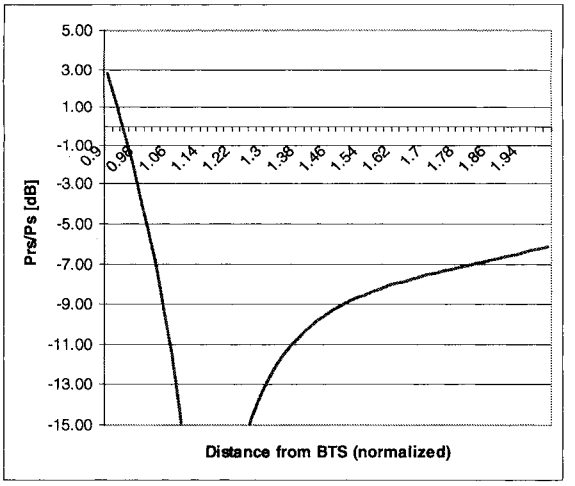

Figure 6-9. Ratio of power allocated to the repeater to that allocated to a cell user, cell extension repeater

6.3.4 Repeater Links Balancing

The optimization of the repeater usage involves maximal utilization of its resources – transmit power and gain, serving the expected coverage with

smooth transition to the donor coverage and minimizing noise and interference impact on the donor and neighboring cells. These objectives entail balancing the RL and FL coverage of the repeater and matching the balance to that of the overlapping donor, and maximizing the resource utilization under the constraints of spurious feedback coupling in both RL and FL.

6.3.4.1 Gain Balance

The purpose of the gain balance is to equate the coverage of the FL with that of the RL. Equating the forward link budget for the cell with that for the repeater

$$\begin{aligned} & P_B T_{CF} = P_B T_{DF} G_{RF} T_{RF} \\ & \therefore \frac{T_{CF}}{T_{RF}} = T_{DF} G_{RF} = y_F \ . \end{aligned} \tag{6-21}$$

Similar to Eq. (4-51), one derives

$$R_{RF}/R_{CF} = y_F^{1/4}\left[(G_{RF}/G_{CF})(H_{RF}/H_{CF})^2(g_{RF}/g_{CF})\right]^{1/4} \equiv y_F^{1/4} U_F^{1/4} \ . \tag{6-22}$$

Equating the FL to the RL

$$\frac{R_{RR}}{R_{RF}} = (R_{CR}/R_{CF})\left(y_R^{1/4} U_R^{1/4} / y_F^{1/4} U_F^{1/4}\right).$$

Assuming that the donor cell is balanced, $R_{CR} = R_{CF}$, the condition for balancing the repeater gain and achieving $R_{RR} = R_{RF}$ is then

$$\frac{y_R}{y_L} = \frac{U_L}{U_R} \ . \tag{6-23}$$

This balancing condition matches the repeater link balancing with that of the interfacing donor coverage. A consistent estimate of the open-loop balancing condition (see Section 2.2.3.1) through the interface between the respective coverage areas is a measure of proper balancing. This is a probe provided in IS 95 and CDMA2000-based systems.

6.3.4.2 Isolation Balance

The coupling between the receiving and the transmitting antennas in the "over-the-air" F_1/F_1 repeater creates a spurious feedback loop that deteriorates the repeater functioning. It replicates the signal with the delay through the repeater, creating a "ringing" series of repeated signals at the receive end, as depicted in Fig. 6-10. These ringing signals, delayed by the repeater loop delay (delay of the signal through the repeater and the spurious coupling loop), attenuate at the ratio of the isolation to the gain of the repeater.

Furthermore, the spurious coupling loop may bring the repeater to oscillations and transmission of noise through its bandwidth. A limit is set on the amplifier gain in order to avoid these effects

$$G_{RF}C_F < M; G_{RR}C_R < M \tag{6-24}$$

where C_F; C_R are the coupling coefficients between the transmit and the receive antennas, in the forward and in the reverse links, respectively, and M is a set margin, typically 1/30 (-15 dB) or lower. The scenario is depicted in Fig. 6-11. F_F, FR represent the forward and reverse link frequencies.

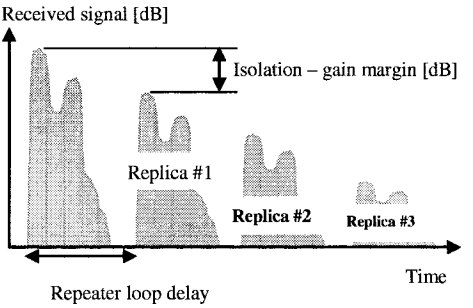

Figure 6-10. Repeater ringing

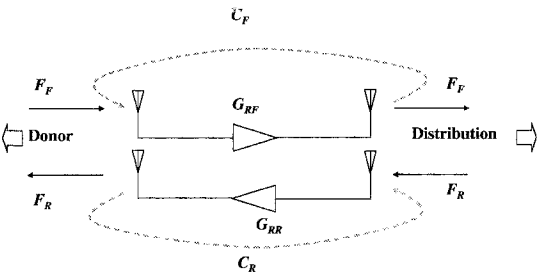

Figure 6-11. Spurious coupling in a repeater

6.3.4.3 Repeater Resources Balancing

The spurious coupling in the RL and the FL paths are equal, $C_F=C_R$ in case the backhaul and the service antennas serve for both transmission and reception. This leads to equating the maximal gain on both links, and also equating the gain of the FL and RL donor links that use the same antennas – $y_L=y_R$. The link balancing condition Eq. (6-23) is thus satisfied, with an optimal utilization of the repeater resources, if $U_L=U_R$.

In case separate antennas are used for transmission and for reception (or additional antennas are used for diversity) the coupling coefficients may differ. The higher coupling coefficient among C_F; C_R sets the limit on the respective gain, and the gain in the other link has to be limited by the link balancing condition. This is a situation of underutilization of the repeater resources.

6.3.4.4 Diversity Gain Balancing

Note that U comprise of antenna parameters – Eq. (6-22), which equate when the same antennas serve for RL and FL, but also diversity gain relations between the donor coverage and the repeater coverage. The diversity gain balance condition then implies similar diversity gain rations between FL and RL in the repeater coverage as in the donor coverage.

$$U_L = U_R \rightarrow g_{RF}/g_{RR} = g_{CF}/g_{CR} \tag{6-25}$$

Unbalanced diversity gain sets the limit on the respective repeater gain and diminishes the diversity advantage of the stronger link.

There is therefore an advantage for applying RL diversity in the repeater, as most donor cells do, and applying transmit diversity in repeaters when the serving donor cell does.

6.3.4.5 AMLC – Automatic Maximum Level Control

AMLC is an automatic guard system against oscillations. It reduces the amplifier gain so as to meet Eq. (6-24). It is usually implemented in the FL. A Tx PWR limit is set according to the required margin. This is the AMLC power. Whenever the actual Tx power exceeds the AMLC power the gain is reduced by steps of 1 dB, until it gets below AMLC. A periodical check is made for the condition Eq. (6-24) and if OK the gain is increased again in 1 dB steps. On top of all this there is a fast reduction of the gain in case of detected oscillations.

The imbalance between FL and RL that is created by the application of the AMLC is recovered by the RL power control loop. Advanced methods for balancing the repeater, and for stabilizing the compound FL and RL gain through the donor link, are discussed in Chapter 10.

6.4 Optimization of the Reverse Link

The objectives of the repeater coverage design differ for different situations, and the optimization constraints and process vary accordingly. There are three main classes of constraints driving the optimization:

Coverage-limited cells. The coverage of the donor cells is predetermined, and the repeater is designed for adding coverage while minimizing the shrinkage of the coverage of the donor cell. The baseline donor cell is not loaded to maximal capacity, and further decrease of its capacity is acceptable. This is a typical situation for an existing network seeking enhancement by repeaters for coverage of radio holes and indoors without disturbing the network plan. It is also a case for a Greenfield design of a rural area, where the cells' and the repeaters' coverage is designed as a whole, and capacity is a secondary consideration.

Capacity-limited cells. Cells that are loaded to capacity, preferably concentrated within a range shorter than their coverage, and need repeater enhancement for coverage of radio holes or additional, light load, coverage. Cell coverage is sacrificed for the repeater coverage.

User-density-limited cells. The area density of the users is predetermined, either by planning or by existing service. The cell area is interlinked to its load by the area density of the users. This is a realistic planning for service. The density within the donor cell coverage, and that within the repeater coverage, are the constraints for the optimization.

6.4.1 Derivation of the Optimization Equation

The apparent noise factor of the repeater shifts the noise rise curve in the donor cell, as in Fig. 6-4. The new curve intercepts the noise rise limit S_{TO} at a load level

$$\eta_{F0} = \eta_0[1 - \hat{F}(1/\eta_0 - 1)] = \eta_0 - \hat{F}(1 - \eta_0). \tag{6-26}$$

The repeater draws capacity from the donor cell. η_C, η_R are the loads due to users in the cell's and the repeater's areas, respectively, and $\eta_F = \eta_C + \eta_R \le \eta_0$. This is the *capacity equation*, relating the *apparent repeater noise figure* to the setting of the noise rise S_{TF} for reaching a capacity η_F. The ratio of the new setting of the noise rise to the nominal is

$$S_{TF}/S_{T0} = (1 + \hat{F})(1 - \eta_0)/(1 - \eta_F). \tag{6-27}$$

Note that for $S_{TF} = S_{T0}$ (baseline noise rise limit, preserving the cell's range) $\eta_{F0} = 1 - (1+\hat{F})/S_{T0}$, and for $\eta_F = \eta_0$ (baseline cell's capacity) $S_{TF}/S_{T0} = 1+\hat{F}$ .The respective cell range is

$$\left(\frac{R_C}{R_{C0}}\right) = \left(\frac{S_T}{S_{TF}}\right)^{1/\gamma} = \left(\frac{1}{1+\hat{F}}\frac{1-\eta_F}{1-\eta_{C0}}\right)^{1/\gamma} \tag{6-28}$$

where γ is the propagation exponent, and S_T is the noise rise for the baseline load η_{C0}. $S_T < S_{T0}$ if the baseline load $\eta_{C0} < \eta_0$.

6.4.2 User-Density-Limited Cells

6.4.2.1 Derivation of the Design Equation

A uniform area distribution of users is assumed, where ρ_C is the area density of users for the donor cell, and ρ_R - for the repeater. The load is thus proportional to R^2. The number of users in each coverage area is $n = \rho\pi R^2$. Rewriting Eq. (4-10), $\eta \equiv \frac{C}{I}(n-1)(1+uxf)\nu \cong kn$ renders $\eta = kn = k\rho\pi R^2$, where k represents the cell's activity and interference environment

$$k \equiv (C/I)(1+uxf)\nu . \tag{6-29}$$

Then $\eta_C = \eta_{C0}(R_C/R_{C0})^2$, which sets another (density) condition on the cell range, in addition to (6-28), and

$$\eta_F = \eta_C + \eta_R = \eta_{C0}\left(\frac{R_C}{R_{C0}}\right)^2\left(1+\frac{\eta_R}{\eta_C}\right) = \eta_{C0}\left(\frac{R_C}{R_{C0}}\right)^2\left(1+\frac{k_R\rho_R}{k_C\rho_C}\left(\frac{R_R}{R_C}\right)^2\right) \tag{6-30}$$

where η_R is the additional load in the donor cell by the repeater users. This is further developed, using Eqs. (6-29), (6-9)

$$\eta_F = \eta_C + \eta_R = \eta_{C0}\left(\frac{R_C}{R_{C0}}\right)^2\left(1+\frac{k_R\rho_R}{k_C\rho_C}y^{1/2}U^{1/2}\right) = \eta_{C0}\left(\frac{R_C}{R_{C0}}\right)^2\left(1+s_{RC}y^{1/2}U^{1/2}\right). \tag{6-31}$$

Here $s_{RC} \equiv k_R\rho_R/k_C\rho_C$ (6-32)

is the ratio of the load area density between the repeater and the donor cell.

From Eqs. (6-28), (6-31) and for γ=4

$$\left(\frac{R_C}{R_{C0}}\right)^2 = \left(\frac{1}{1+\hat{F}} \frac{1-\eta_{C0}\left(\frac{R_C}{R_{C0}}\right)^2 \left(1+s_{RC}y^{1/2}U^{1/2}\right)}{1-\eta_{C0}} \right)^{1/2} . \quad (6\text{-}33)$$

The capacity limit is $\eta_C + \eta_R \le \eta_F$, which limits Eq. (6-33) by Eq. (6-27) to

$$\left(R_C/R_{C0}\right)^2 \le \left((1-\eta_0)/(1-\eta_{C0})\right)^{1/2} . \quad (6\text{-}34)$$

η_F, η_0 are the maximum allowable load for S_{TF}, S_{T0}, respectively, and η_{C0} is the cell baseline load without the repeater.
This is readily solved:

$$\left(\frac{R_C}{R_{C0}}\right)^2 = \frac{\sqrt{\eta_{C0}{}^2\left(1+s_{RC}\sqrt{yU}\right)^2 + 4(1-\eta_{C0})\left(1+\hat{F}_R y\right)} - \eta_{C0}\left(1+s_{RC}\sqrt{yU}\right)}{2(1-\eta_{C0})\left(1+\hat{F}_R y\right)} \quad (6\text{-}35)$$

which relates all the design parameters to the resulting coverage and capacity. The optimization process is then an iterative solution of Eq. (6-35), conditioned by (6-34) with the set of the desired parameters' values.

6.4.2.2 The Optimization Process

Baseline parameters:
R_{C0} Baseline donor cell range
η_{C0} Baseline donor cell load
ρ_{C0} Donor cell user density (extracted from R_{C0}, η_{C0})
S_{T0} Baseline noise rise limit in the donor cell
η_0 Maximal load setting in the system (derived from S_{T0})

Input parameters:
$\hat{F}_R$ Ratio of noise factors of the repeater and the BTS
$G_{RR,\,max}$ Max. repeater gain allowed (isolation constraint)
T_D Donor-repeater link gain
y_{max} Constraint on y (derived from $G_{RR,\,max}$, T_D)
S_{RC} Ratio of user densities, and of interference environments for the repeater and for the donor cell (note Eq. (6-29)).

6.4.2.3 Optimization Examples

1) Rural area – range extension – Fig. 6-12. Donor load is low - $\eta_{C0}=0.3$. Repeater's density and interference are lower: $s_{RC}=0.7$. Antenna height and gain - similar to the BTS - $U=1$. Coverage is maximized for $y=0$ dB, with 35% overall coverage gain, donor coverage decreasing to 65% and about equating to repeater coverage. Capacity increase is 15% for $y=-7$ dB, and 5% for $y=0$ dB. The capacity increase is a result of capturing more users in the added area. The cell is far from its capacity limit. Working point is to be set according to the respective densities and the importance of maintaining the baseline donor coverage.

2) Radio hole in a dense area - Fig. 6-13. $\eta_{C0}=0.7$. Repeater's density and interference are much lower: $s_{RC}=0.2$. Coverage is maximized for $y=-3$ dB, but donor coverage is reduced to 90%, and capacity is reduced to 95% for $y=-9$ dB, and coverage gain of 19% for that point may be a right compromise between the coverage gain and the donor coverage and capacity loss. Note that a "radio hole filler" is not seeking to maximize coverage but to cover a well-defined shadowed area.

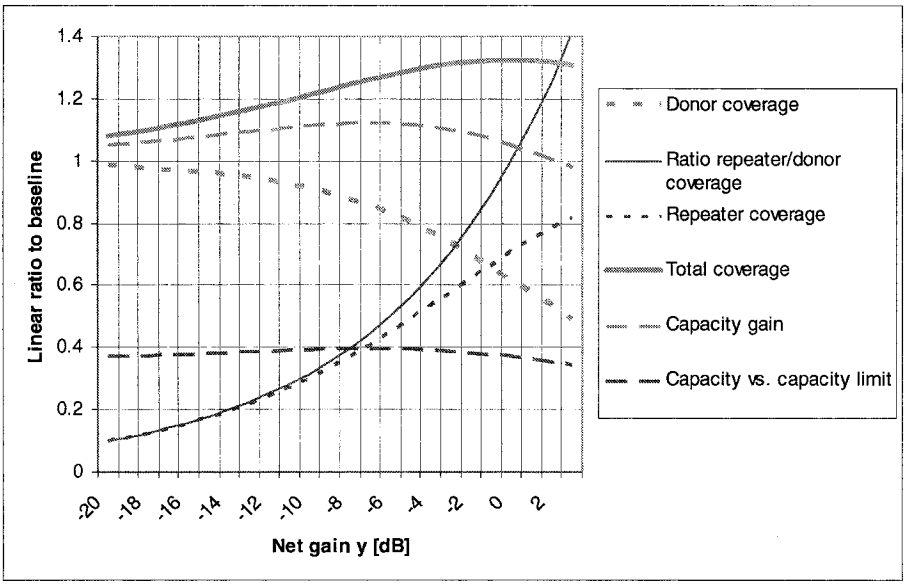

Figure 6-12. Coverage-capacity trade-off, rural area

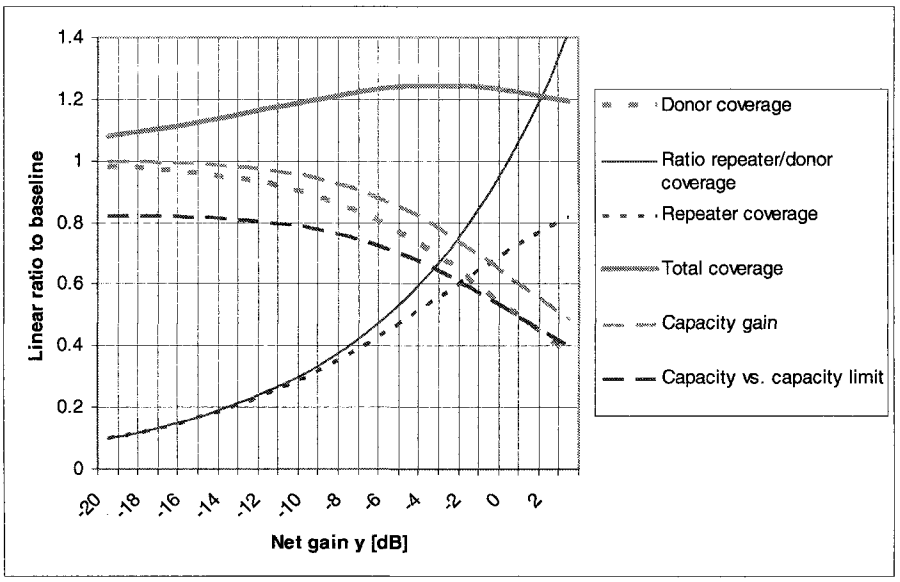

Figure 6-13. Coverage- capacity trade-off , "radio hole"

3) Hot spot - Fig. 6-14. η_{C0}=0.25. Repeater's density is much higher ("hot spot"): s_{RC}=4. Note the bracketed zone, where the capacity limit is exceeded. "Hot spot" repeater is typically designed for a small coverage. U is the parameter representing the ratio of antenna gain and height between the repeater and the donor. Its impact is demonstrated in Figs. 6-14a and 6-14b.

6.4.3 Capacity-Limited Cells

Many urban donor cells are capacity-limited. The link loss is low and the users do not reach their maximum power, and have a margin h transmission power, which means that the coverage of the cell R_{C0} is larger than the area occupied by active users $R_{C0active}$ by

$$\left(R_{C0}/R_{C0active}\right)=h^{\frac{1}{\gamma}}. \tag{6-36}$$

This margin may reach 40 dB in urban microcells.

Reverting to Eq. (6-27), a repeater feeding on a capacity-limited cell does not affect its active coverage as long as $h>1+\hat{F}$ or

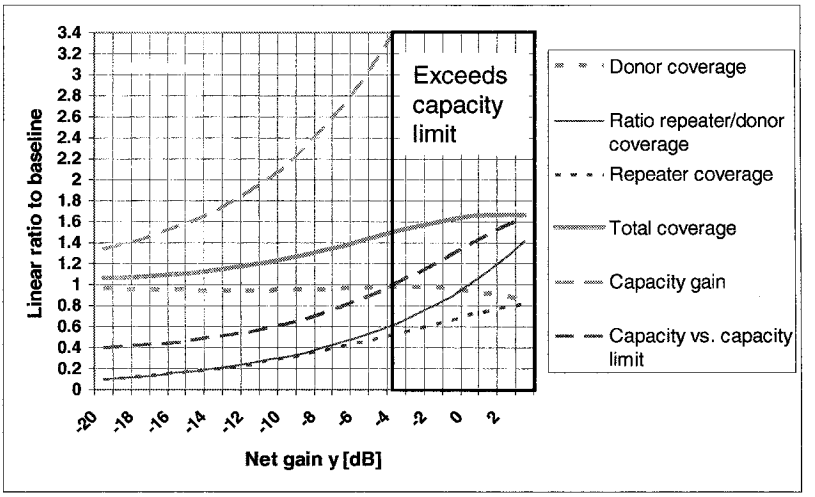

a. U=1

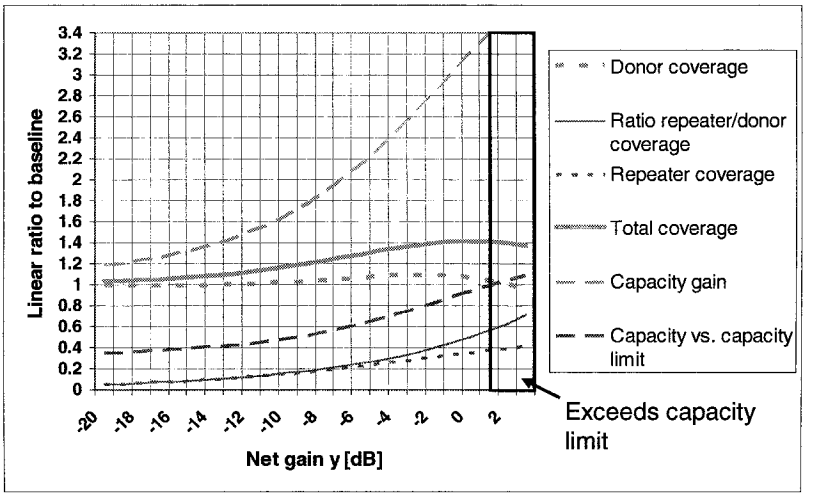

b. U=0.25 (Lower antenna gain/height for the repeater)

Figure 6-14. Coverage-capacity trade-off, "hot spot". η_{C0}=0.25; s_{RC} =4

$$y < (h-1)/\hat{F}_R \,. \tag{6-37}$$

Beyond that the cell is coverage-limited.

The added capacity by the repeater, η_R, is limited by $\eta_C + \eta_R \le \eta_0$.

6.5 Repeater Coverage Overlap with the Donor Cell

A repeater fully embedded in a donor cell, as in Fig. 6-15, or partially overlapping with the cell coverage, affects both forward and reverse links. On the reverse link, the additional path for the signal provides additional (micro and macro) diversity (and additional interference, in case the number of delayed "fingers" exceed those in the BTS receiver). The additional multipath on the forward link provides both additional diversity and additional interference by reducing the orthogonality. The latter is detrimental for time-multiplexed data links (e.g. EV-DO, HSDPA) that are taking advantage of the high SNR in the high-orthogonality areas of the cell core. An assessment of the overlap effects follows [7].

6.5.1 Coverage Overlap Analysis

Revisiting Eq. (6-10) we note that in the overlap zone both paths contribute to RL signal S arriving at the BTS

$$S = S_c + S_R = P_m(T_c + T_R y) = P_m T_c(1 + (T_R/T_c)y) = S_c(1 + S_R/S_c) \quad (6\text{-}38)$$

where

S_c is the signal received at the BTS through the cell path, and

S_R is the signal received at the BTS from the repeater path.

We are concerned with 3 regions of the cell: 1) Repeater coverage dominance $S_R/S_c \equiv (T_R/T_c)y >> 1$; 2) The virtual boundary zone (the overlap zone) where $(T_R/T_c)y \cong 1$; and 3) Donor cell dominance $(T_R/T_c)y << 1$.

The repeater signal is delayed and appears as a new set of fingers, adding both additional noise and diversity. The relative gain/loss depends on the amount of multipath available in the donor cell path. α, the orthogonality factor, represents here the multipath scenario. The diversity gain in the donor-cell path $g_c = g_c(\alpha_c)$ and in the compound path $g_{C+R} = g(\alpha_c S_c/S + \alpha_R S_R/S)$. The diversity gain depends on the number of available fingers for diversity pick up, and the average power ratio between the diversity branches, which equates at the virtual coverage boundary between the repeater and the cell.

Figure 6-15 illustrates the coverage overlap, determined by the cell power control. The (normalized) received signal at the BTS, set by the power control, is $q(\eta)$, and that received from the user at the repeater is $q(\eta)/y$. Evidently, y determines the coverage by setting the level of the signal to be received at the repeater. Now, the virtual boundary between the repeater and the cell coverage is (Eq. (6-9)) $y = U^{-1}(R_R/R_C)^4$, where R_C, R_R are the respective distances from the user to the BTS and the repeater.

A simplifying scenario $R_R << R_c$ and $R_R << d$ helps clarify the dominant processes. Referring to Fig. 6-15:

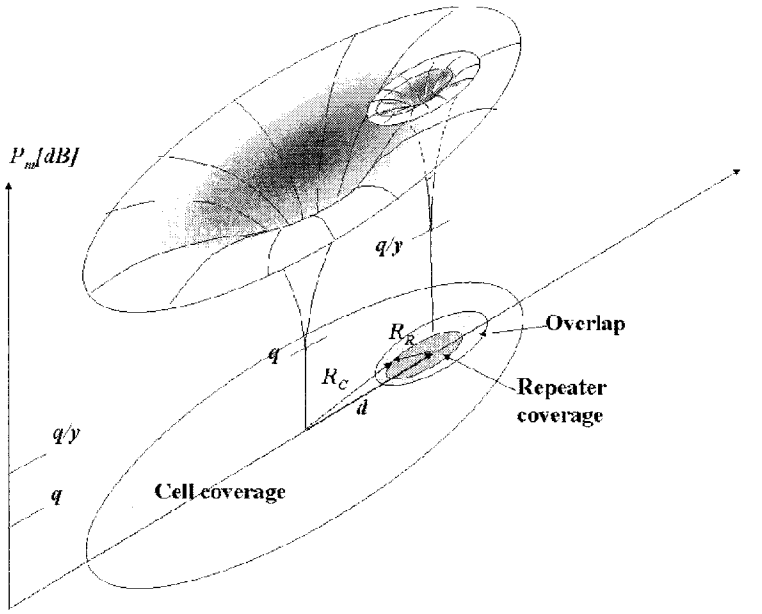

Figure 6-15. Repeater embedded in a donor cell – footprint and reverse link power

$R_C^4 = \left(d^2 + R_R^2 + 2dR_R\cos\vartheta\right)^2 \cong d^4\left(1+4\left(R_R/d\right)\cos\vartheta+...\right)$ where d is the distance of the repeater antenna from the BTS, and

$$T_R/T_C \cong U_R\left(d/R_R\right)^4\left(1+4\left(R_R/d\right)\cos\vartheta\right). \qquad (6\text{-}39)$$

Equating (6-39) to 1 (virtual boundary), to 4 (=6 dB – for repeater coverage dominance) and to 1/4 for cell dominance, produces non-concentric ovals, as in Fig. 6-15, that diverge away from the BTS.

6.5.2 Coverage Overlap Control

The virtual boundary zone has important effects on the signal quality and repeater transmit power. Control over the coverage overlap for different applications is reviewed.

6.5.2.1 Antenna Control

The transmission gain slope becomes steeper by lowering the antenna and by down tilting its beam, both affecting the parameter U in Eq. (6-39). This is further discussed in Chapter 3.

6.5.2.2 Limiting the Outwards Spread (following [7])

The largest overlap area is spread outwards, as shown in Fig. 6-15. The most effective means of limiting this spread is by directing the repeater antenna toward the BTS, which attributes angular dependence to the parameter U in Eq. (6-39). The gain outwards is thus reduced substantially, and the transmission gain slope is steeper, with a respective shrinkage of the outward coverage overlap. Care should be taken for the isolation between the donor and distribution antennas, both looking to the same direction in this case.

6.5.2.3 Isolation of the User Population

"Hot spot" repeaters cover an area with a higher user density. It is desired to avoid exposing this population to the overlap region, where high power may be drawn from both the BTS and the repeater. Tuning the repeater for a higher net gain y increases its coverage beyond the high density population and reduces its exposure to the cell (Fig. 6-15, [7]). Avoidance of the additional multipath in the overlap area is also important for the time-multiplex transmissions (EV-DO, HSDPA), and containment of the high density under the repeater control is an advantage.

6.6 Multiple Repeaters

Multiple repeaters can feed on the same donor cell, serving for multiple "radio holes" or for coverage extension – for rural area coverage, multi-lobe remote access, or covering a length of highway or tunnel. Their feed architecture can be parallel feed – star network, where each repeater has its own donor link and all are connected in parallel; or series feed – multi-hop network, where each repeater is fed from its predecessor. The latter saves on feed infrastructure when fed by microwave links or fiber, and may be the only option for over-the-air feeding in the absence of line of sight to the successive repeaters.

6.6.1 "Star" Architecture – Parallel Repeaters

This architecture is schematically portrayed in Fig. 6-16. The signals arriving from all repeaters sum up at the BTS, each with its own net gain y_i.

They are all RL power-controlled at the users, to arrive with the same signal level. The self-noise of each repeater $\hat{F}_{Ri} y_i$ also sum up at the BTS

$$\hat{F}_n = \sum_{i=1}^{n} \hat{F}_{Ri} y_i . \tag{6-40}$$

The impact of the accumulated noise on the system capacity and coverage is evaluated in the following.

6.6.1.1 Set *noise rise limit* S_{T0} – Undisturbed Coverage for the Donor

Note that the trade-off in this case is the reduction of the density of users within the donor coverage area in order to allow for capacity loading by the repeater (see discussion in Section 6.4.1).

This is viable when the baseline coverage of the donor cell is designed to accommodate a target density higher than the baseline density, and the repeater coverage trades off on this margin.

The capacity reduction is derived from Eq. (6-15):

$$\eta/\eta_0 = 1 - \hat{F}\left((1/\eta_0) - 1\right) = 1 - \left(\sum_{i=1}^{n} \hat{F}_{Ri} y_i\right)\left((1/\eta_0) - 1\right) \tag{6-41}$$

which is demonstrated in Fig. 6-5. In case all repeaters have $\hat{F}_{Ri} = \hat{F}_R; y_i = y$, the capacity loss is 18% for 3 repeaters with $\hat{F}_R = 1; y = 1/3\ (-5dB)$, while for y=1(0 dB) it becomes 53%.

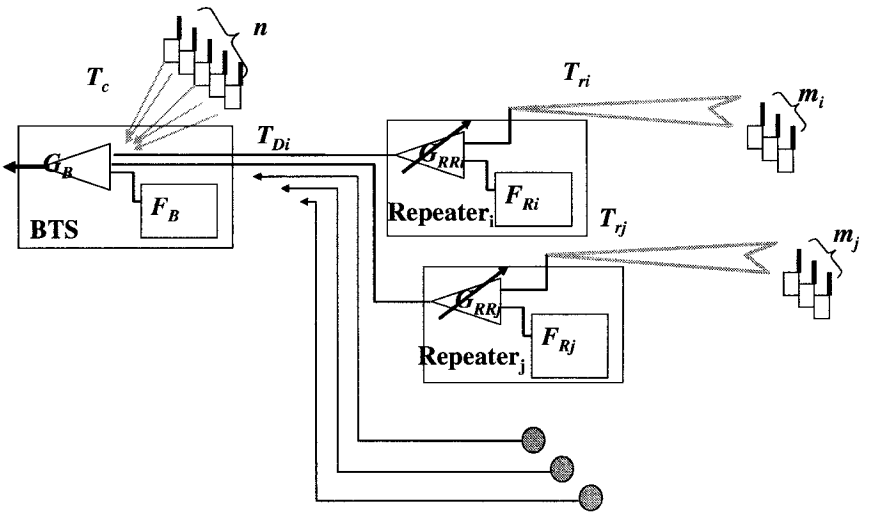

Figure 6-16. Star architecture of multiple repeaters

The total normalized coverage, from Eq. (6-9), is

$$Coverage/R_{C0}{}^{2} = 1 + \sum_{i=1}^{n} y_i^{1/2} U_i^{1/2}, \qquad (6\text{-}42)$$

the total normalized coverage of the cell and 3 identical coverage repeaters, with $U=1$; y=-5dB is 1.73, and for y=0 dB it is 4. Note, however that U=1 is an optimistic assumption that implies the same diversity gain in the repeater coverage as in the donor's. The resulting user density that can be served is notably low – only 12% of full density: 47% capacity is spread over 4 times the coverage area.

6.6.1.2 Capacity-Limited System

From Eqs. (6-9), (6-28)

$$\frac{Coverage}{R_{C0}{}^{2}} = \left(\frac{R_C}{R_{C0}}\right)^{2}\left[1+\sum_{i=1}^{n}\left(\frac{R_{Ri}}{R_C}\right)^{2}\right] = \left(1+\sum_{i=1}^{n} y_i^{1/2} U_i^{1/2}\right)\left(1+\sum_{i=1}^{n}\hat{F}_{Ri} y_i\right)^{-1/2}. \qquad (6\text{-}43)$$

This is plotted in Fig. 6-17 for identical repeaters, and U=1.

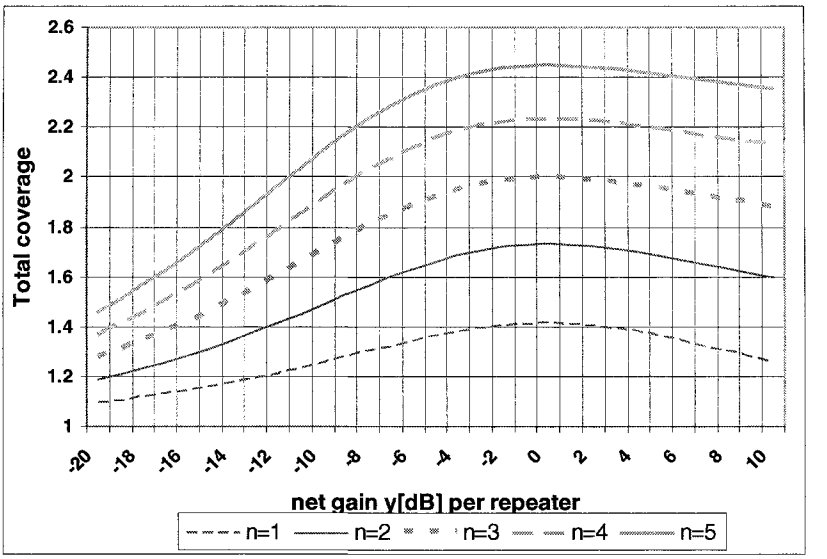

Figure 6-17. Total coverage of donor and repeaters in star arrangement for max capacity

Note that as much as the achievable total coverage is lower than in the coverage-limited strategy (2 vs. 4 for y=0 dB, 3 repeaters), the system enjoys full capacity, which is now shared with the repeaters. The density in the donor cell is respectively lowered.

The trade-off between the strategies is accomplished by setting the limit on the noise rise according to Eq. (6-27).

6.6.1.3 Density Constrained Design

A realistic design that considers the user density over the area as given, and thus ties up the cell load to its coverage, is discussed in Section 6.4. Expansion of the respective design constraints, Eq. (6-35), to the parallel connection of multiple repeaters – is straightforward. Equation (6-31) is modified to

$$\eta_F = \eta_C + \sum_i \eta_{Ri} = \eta_{C0}\left(R_C / R_{C0}\right)^2 \left(1 + \sum_i s_{RCi} y_i^{1/2} U_i^{1/2}\right), \tag{6-44}$$

and Eq. (6-35) becomes

$$\left(\frac{R_C}{R_{C0}}\right)^2 = \frac{\sqrt{\eta_{C0}{}^2\left(1+\sum_i s_{RCi}\sqrt{y_i U_i}\right)^2 + 4\left(1-\eta_{C0}\right)\left(1+\sum_i \hat{F}_{Ri} y_i\right)} - \eta_{C0}\left(1+\sum_i s_{RCi}\sqrt{y_i U_i}\right)}{2\left(1-\eta_{C0}\right)\left(1+\sum_i \hat{F}_{Ri} y_i\right)} . \tag{6-45}$$

The relative coverage of each repeater is obtained from Eq. (6-9), and the respective load – from Eq. (6-44). The case of multiple repeaters with identical parameters is amply covered by the examples in Section 6.4.3 by summing up the respective parameters to an equivalent single repeater.

6.6.2 Multi-hop Repeater Architecture

The multi-hop architecture is depicted in Fig. 6-18. Cascading (or "Daisy-chain linking) repeaters is an option when coverage of length of a strip (e.g. road, a tunnel, a chain of villages) is required. It is the only option for an "over-the-air" repeater chain when line of sight is not available over the whole chain. The effect of the cascaded repeaters on the donor and their total coverage and length covered is evaluated in the following, and then compared to the "star constellation".

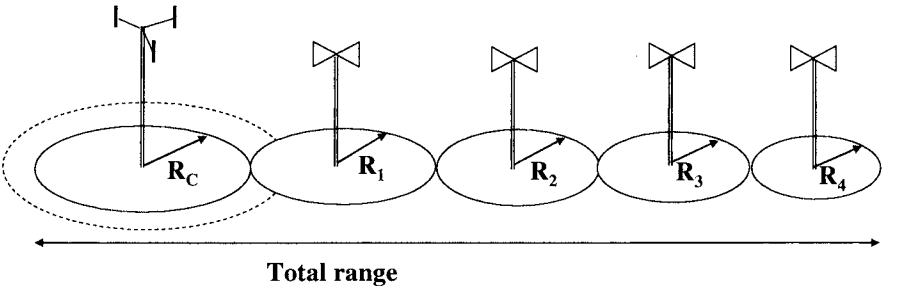

Figure 6-18. Multi-hop repeaters configuration

6.6.2.1 Multi-hop Repeater Analysis

The repeaters are feeding on one another in the chain, and their coverage is decreasing even for identical net gain y. The characteristic parameters of all the repeaters in the chain – $\hat{F}$ and y, are assumed to be the same. The *noise rise* at the donor is derived in Eq. (6-1) and plotted in Fig. 6-19. Note that this additive noise reduces the cell's available capacity and/or coverage, depending on the strategy. Apparent noise figure $\hat{F} = 8\ dB$ nullifies the cell capacity (Fig. 6-5) under fixed donor coverage conditions.

$$\hat{F}_n = \hat{F}_R y\left(1 + y\left(1 + y\left(1 + y\left(\cdots\right)\right)\right)\right) = \hat{F}_R\left(y + y^2 + y^3 + \cdots\right) = \hat{F}_R y\left(1 - y^n\right)/\left(1 - y\right) \quad (6\text{-}46)$$

6.6.2.2 Maximizing Capacity Strategy

Here maximum load is assumed (Fig. 6-19) $\eta_{\hat{F}} = \eta_{\hat{F}=0} = \eta_0$. The range of each repeater depends on its effective noise figure (Eq. (6-4b)) which incorporates the apparent noise figure of the whole cascade and its overall net gain. Thus for the i th repeater in a chain of n repeaters

$$\left(R_i/R_{C0}\right)^\gamma = y_i U_i/\left(1 + \hat{F}_n\right) \quad (6\text{-}47)$$

where $y_i = y^i$ and R_{C0} is the donor cell radius with no repeaters load. The total coverage area of all repeaters and donor (disregarding overlap) is

$$\frac{Coverage_T}{R_{C0}^{\ 2}} = \frac{1}{R_{C0}^{\ 2}} \sum_{i=0}^{n} R_i^{\ 2} = \left(1 + \hat{F}_n\right)^{-2/\gamma} \left(1 + U^{2/\gamma} x \frac{\left(1 - x^n\right)}{1 - x}\right) = \quad (6\text{-}48)$$

$$= \left(1 + \hat{F}_R \frac{y\left(1 - y^n\right)}{1 - y}\right)^{-2/\gamma} \left(1 + U^{2/\gamma} x \frac{\left(1 - x^n\right)}{1 - x}\right)$$

where $x \equiv y^{2/\gamma}$, U is assumed to be the same for all repeaters, and the total length covered is

$$\frac{L_{Total}}{2R_{C0}} = \frac{1}{R_{C0}}\sum_{i=0}^{n} R_i = \left(1+\hat{F}_n\right)^{1/\gamma}\left(1+U^{1/\gamma}z\frac{\left(1-z^n\right)}{1-z}\right) = \tag{6-49}$$
$$= \left(1+\hat{F}_R\frac{y\left(1-y^n\right)}{1-y}\right)^{-1/\gamma}\left(1+U^{1/\gamma}z\frac{\left(1-z^n\right)}{1-z}\right)$$

where $z \equiv x^{1/2} = y^{1/\gamma}$. These are evaluated for $\hat{F}_R = 1$, $\gamma = 4$ and U=1 and are shown in Figs. 6-20, 6-21 and 6-22. The coverage peaks for apparent noise figure 0 dB $\left(y = 0dB; \hat{F}_R = 0dB\right)$ at 2.5 the baseline coverage with 5 repeaters (the same as with "star" connection, Fig. 6-17), and the total length reaches 4 times the baseline.

It is important to observe that the coverage of consecutive repeaters decreases sequentially for y<0 dB, increases for y>0 dB (Fig. 6-23) and equals for y=0 dB.

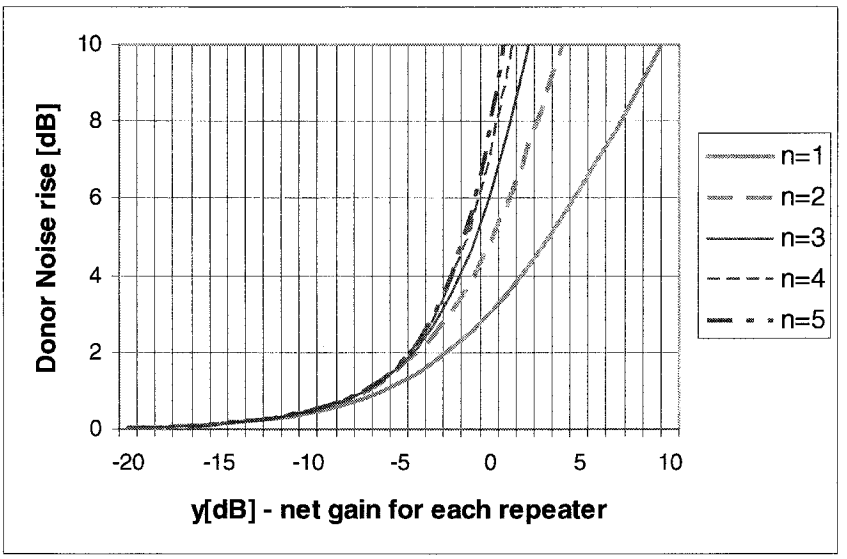

Figure 6-19. Noise rise $10Log\left(\hat{F}_n+1\right)$ at donor - Eq. (6-46)

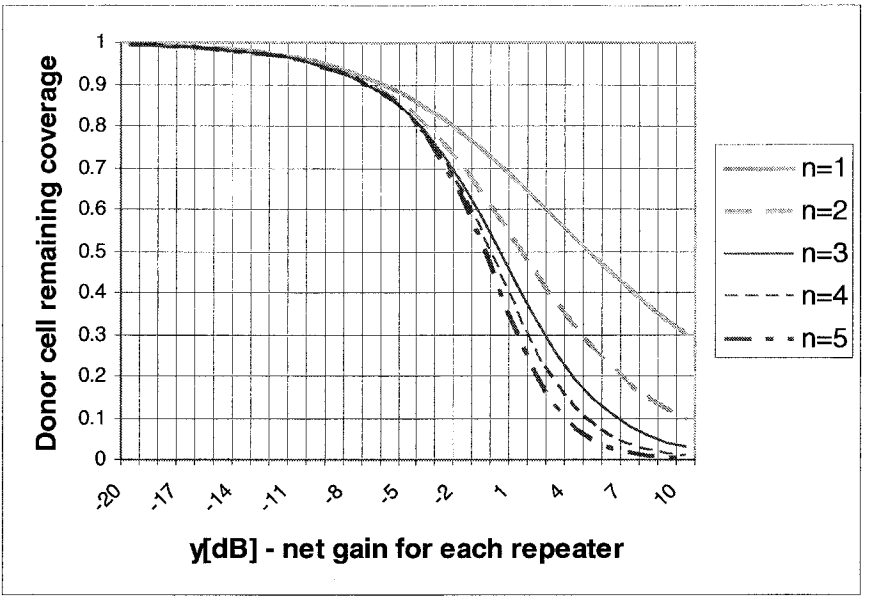

Figure 6-20. Donor cell coverage shrinkage by multi-hop repeaters

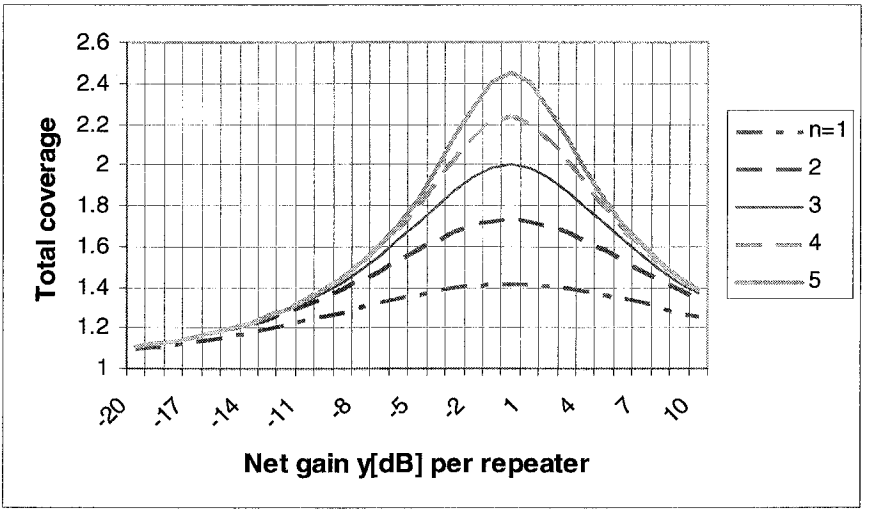

Figure 6-21. Total coverage of the repeater chain for maximizing capacity

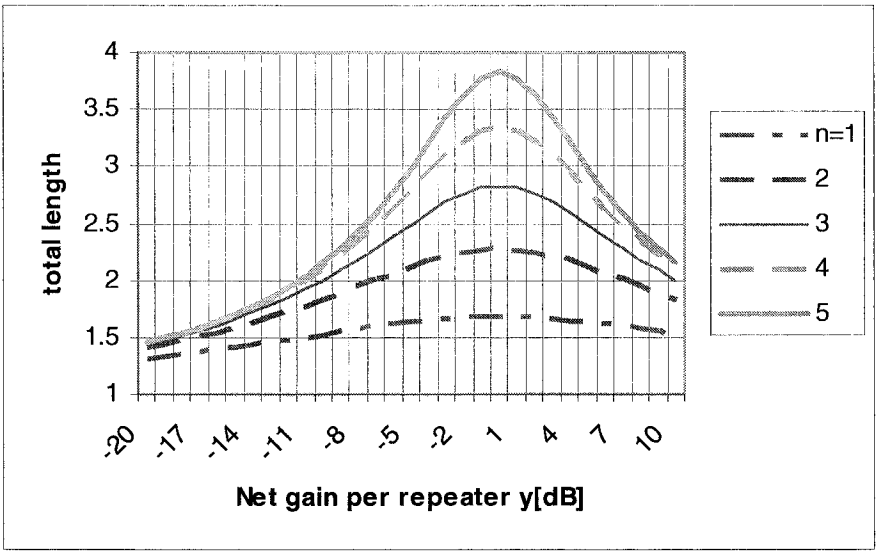

Figure 6-22. Total length covered by a repeater chain for max. capacity

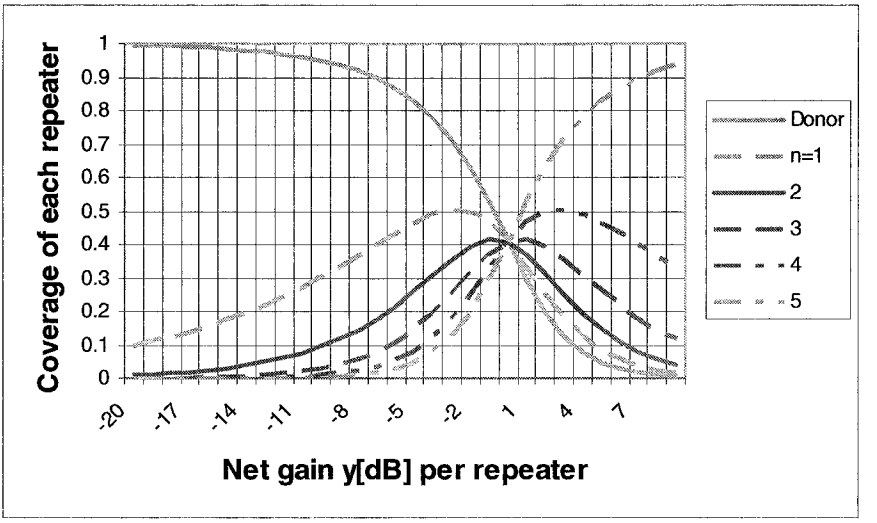

Figure 6-23. Coverage of the donor and of each repeater in a chain of 5 repeaters, capacity-limited, $\hat{F}_R = 1$, U=1

6.6.2.3 Maximizing Coverage Strategy

$S_{T0} = 1/(1-\eta_0)$. When the limit on S_T is set for the maximum capacity of a cell with no repeaters, S_{T0}, the additional noise rise $\hat{F}$ trades-off for capacity, but does not change the link budget. Equations (6-42) and (6-43) thus become

$$\frac{Coverage_T}{R_{C0}^2} = \frac{1}{R_{C0}^2}\sum_{i=0}^{n} R_{Ri}^2 = \left(1 + U^{2/\gamma} x \frac{(1-x^n)}{1-x}\right) \tag{6-50}$$

$$\frac{L_{Total}}{2R_{C0}} = \frac{1}{R_{C0}}\sum_{i=0}^{n} R_i = \left(1 + U^{1/\gamma} z \frac{(1-z^n)}{1-z}\right). \tag{6-51}$$

The remaining capacity, relative to the capacity set to the cell by S_T, is derived in Eq. (6-52) (from Eq. (6-26)) and plotted in Fig. 6-24:

$$\frac{\eta_{\hat{F}}}{\eta_{\hat{F}=0}} = 1 - \frac{1-\eta_{\hat{F}=0}}{\eta_{\hat{F}=0}} \hat{F} \frac{y(1-y^n)}{1-y} = 1 - \frac{1}{S_T - 1} \hat{F} \frac{y(1-y^n)}{1-y} \tag{6-52}$$

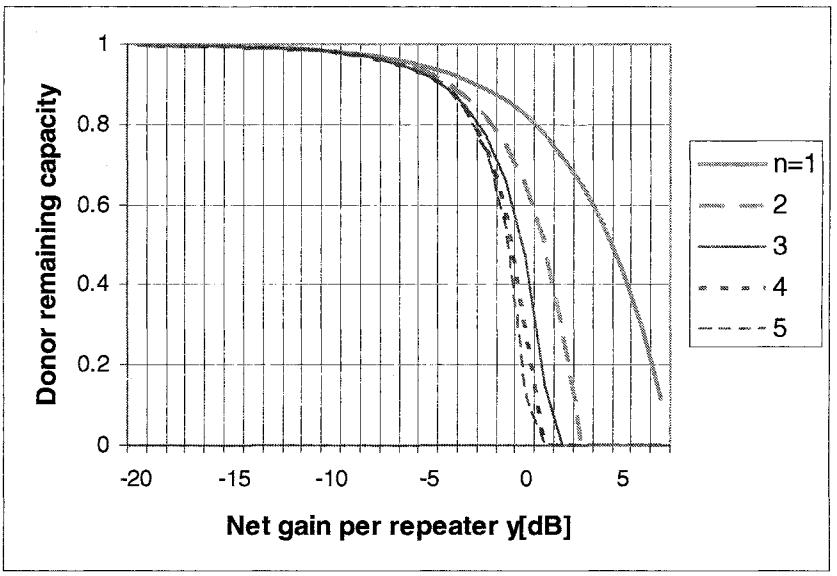

Figure 6-24. Remaining capacity for the donor cell and repeater chain, η_0=0.85 (Eq. (6-52). Plot extends to $\eta_F > 0.1$ remaining capacity

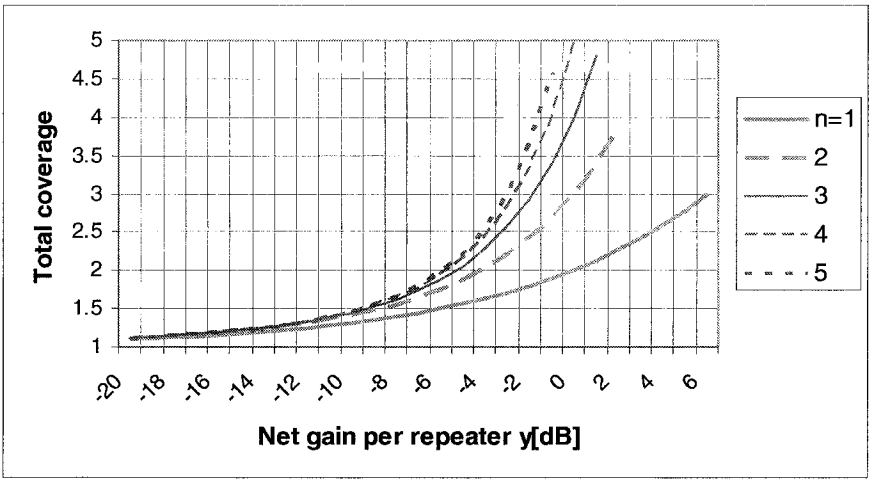

Figure 6-25. Total coverage of a repeater chain, with limit on S_T at η_0=0.85 (Eq. (6-50)). Plot extends to $\eta_F > 0.1$ remaining capacity

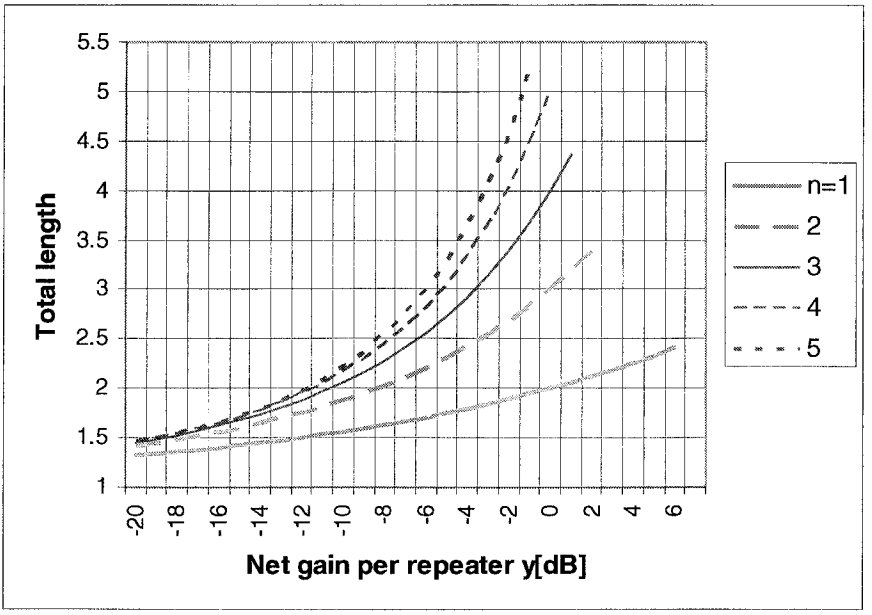

Figure 6-26. Total length of a repeater chain, with limit on S_T at η_0=0.85 (Eq. (6-51)). Plots extend to $\eta_F > 0.1$ remaining capacity

6.6.2.4 Density constrained design

Expansion of the respective design constraints, Eq. (6-35), to the cascade connection of multiple repeaters is straightforward. Equation (6-31) is modified to

$$\eta_F = \eta_C + \sum_i \hat{\eta}_{Ri} = \eta_{C0}\left(R_C / R_{C0}\right)^2 \left(1 + s_{RC} U^{2/\gamma} x \left(1 - x^n\right)/\left(1 - x\right)\right) \qquad (6\text{-}53)$$

and Eq. (6-35) becomes

$$\left(\frac{R_C}{R_{C0}}\right)^2 = \frac{\sqrt{\eta_{C0}{}^2\left(1 + s_{RC} U^{2/\gamma} x \frac{\left(1 - x^n\right)}{1 - x}\right)^2 + 4\left(1 - \eta_{C0}\right)\left(1 + \hat{F}_R \frac{y\left(1 - y^n\right)}{1 - y}\right)} - \eta_{C0}\left(1 + s_{RC} U^{2/\gamma} x \frac{\left(1 - x^n\right)}{1 - x}\right)}{2\left(1 - \eta_{C0}\right)\left(1 + \hat{F}_R \frac{y\left(1 - y^n\right)}{1 - y}\right)} \; . \qquad (6\text{-}54)$$

The total relative coverage of the repeaters is obtained from Eq. (6-50), the total length from Eq. (6-51), and the respective load – from Eq. (6-52). The case of multiple repeaters with identical parameters is amply covered by the examples in Section 6.4.3 by using the compound respective parameters $\hat{F}_n; y_n; x_n$ to an equivalent single repeater.

6.6.3 Comparison of Star and Cascade Repeater Linking

The "star" and multi-hop connection of multiple repeaters serve a similar purpose, and the distinction between them may be cost and/ or complexity. The comparison of their performance serves the design trade-off.

Noise rise $\left(1 + \hat{F}\right)$ ratio between multi-hop and star is displayed in Fig. 6-27 (Eqs. (6-44) and (6-40)). These equate for y=0 dB.

Capacity-limited design. The star system excels. They match at y=0 dB.

Conclusions. In order for the multi-hop chain to have identical coverage for all repeaters, which is the optimal design, their respective net gain has to be y=0 dB. The tuning of the apparent noise figure is then administered by the control of the net gain *of the first repeater.* In such a case Eqs. (6-48), (6-49) reduce to

$$C_{overageT} / R_{C0}{}^2 = \left(1/R_{C0}{}^2\right)\sum_{i=0}^{n} R_i^2 = \left(1 + n\hat{F}_R y_1\right)^{-2/\gamma}\left(1 + nU^{2/\gamma} x_1\right) \qquad (6\text{-}55)$$

$$L_{Total} / 2R_{C0} = \left(1/R_{C0}\right)\sum_{i=0}^{n} R_i = \left(1 + n\hat{F}_R y_1\right)^{-1/\gamma}\left(1 + nU^{1/\gamma} z_1\right) \qquad (6\text{-}56)$$

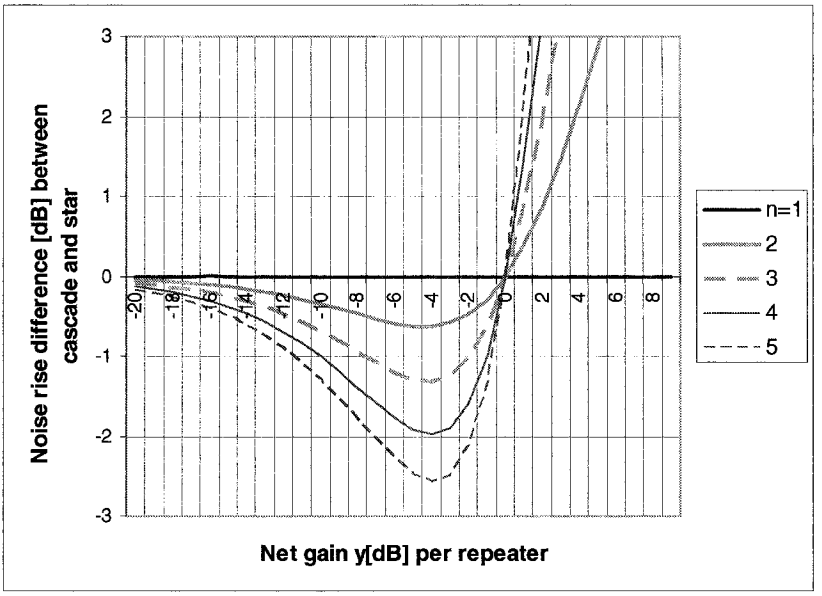

Figure 6-27. Comparison of the noise rise of a cascade chain to star constellation

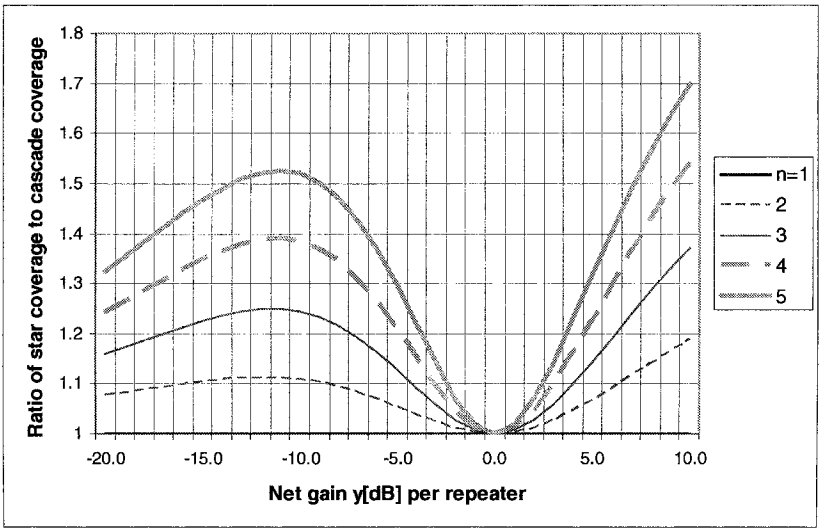

Figure 6-28. Comparison of the total coverage of star to multi-hop systems, in capacity-limited design

and the chain is represented by a single equivalent repeater (or n repeaters in a star connection). This is the proper process for repeater chains indoors and in tunnels, where relatively low coverage is required from each repeater.

Under these terms there is an equivalence of performance between the star and the multi-hop chain.

6.6.4 RF Distribution Network and the Distributed Antenna

Coverage of compact, complex environments such as indoors or campus may require the distribution of multiple RF access points (nodes). This is typically accomplished by an RF distribution network. Passive networks are schematically described in Figs. 6-29a, b. L_i is the loss to the i_{th} element, C_i – its coupling coefficient, and F_i – its noise factor. Note that the passive distribution networks act as parallel multiple access points, both in Figs. 6-29a and b. The apparent noise factor at the entry to the BDA for scheme a is $\hat{F}_i = F_i C_i \prod_i \Delta L_i$, while for scheme b it is $\hat{F}_i = F_i L_i$. The overall apparent noise factor at the entry to the BDA is $\hat{F} = \sum_i \hat{F}_i$. The coupling C_i is designed to compensate for the accumulated loss from the access #i to the BDA. Scheme c is a cascade of multi-hop repeaters (Eq. (6-41)), while scheme d is a "star" (Eq. (6-40)). Active distributed networks, incorporating sequential delay between the access elements, is termed "distributed antenna". The delay is conceived for adding transmit and receive diversity between the elements, thus providing an artificial delay diversity for indoor and compact neighborhoods [10].

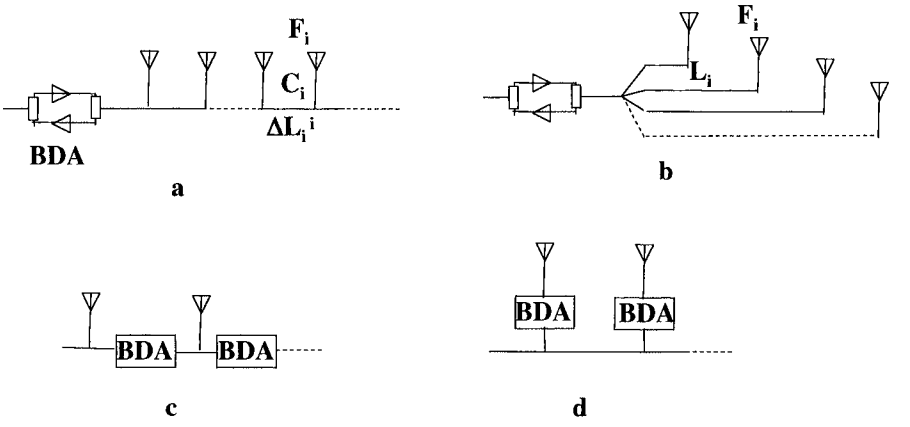

Figure 6-29. RF distribution network. a - passive serial ("leaky cable"); b - passive parallel ("star"); c - active serial; d - active parallel

6.7 Search Windows

All BTSs in the IS 95 and CDMA2000-based networks are synchronized to a common clock, through atomic clocks and/ or GPS. This is needed for identifying the pilots of each BTS, all of which have the same *short code* of 2^{15} chips but are time-phased (offset) in steps of 64 chips (51.2 μs).

The initial pilot sets provided to an ST upon access is a single pilot, and a neighbor list and remaining list. The ST searches for the pilot within its *active set search window*, which has to match its expected maximum delay. The additional delay incurred by the repeater path has to be accounted for in the *active set search window* of the STs served by the repeater and the donor cell feeding the repeater. This allows an ST to access when in the repeater coverage, and to move smoothly between the repeater and the donor coverage without loosing the pilot. The difference in delay between the donor reception and the repeater reception *should be less than half the search window for the active set.*

The signal received at the ST through the repeater is delayed by the repeater delay, typically 6 μs (this delay depends on the channel and band filters), then additional path delay from the donor to the repeater and then to the ST- according to the additional range, and the donor fiber additional delay, in case the repeater is linked to the donor by fiber.

The wave velocity in the fiber is 2/3rd that of free space, which adds 50% more delay to the actual fiber length. These delays are significant compared with the donor cell coverage delay, which requires due consideration in setting the search windows for donor cells serving respective repeaters. A simple formula calculates these relations [17]:

$$Cable\_length \le \left(\tau_{Cu} - \tau_{Ru} - \tau_{R} + W_A/2\right)\beta \qquad (6\text{-}57)$$

where

τ_{Cu} is the propagation delay from the BTS to the ST at the transition point between the repeater coverage and the donor coverage,

τ_{Ru} is the propagation delay from the repeater to the ST at the transition point between the repeater coverage and the donor coverage,

τ_R is the delay through the repeater,

W_A is the *search window* for the active set, and

β is the phase velocity in the cable.

REFERENCES

[1] K.S. Gilhousen, I.M. Jacobs, R. Padovani, A.J. Viterbi, L.A. Weaver, Jr., and C.E. Wheatley, *On The Capacity of a Cellular CDMA System*, IEEE Trans. VT-40, pp. 303-312, May 1991.

[2] J. Shapira and R. Padovani, *Spatial Topology and Dynamics in CDMA Cellular Radio*, Proceedings of the 42nd IEEE VTS Conference, pp. 213-216, Denver, CO, May 1992.

[3] S. Soliman, C. Wheatley and R. Padovani, *CDMA Reverse Link Open Loop Power Control*, Proceedings of GLOBECOM 92,Vol. 1, pp. 69-73, Dec. 1992.

[4] T.-S. Chu and M.J. Gans, *Fiber optic Microcellular Radio*, Proceedings of the 41st IEEE VTS Conference, pp. 339-344, St. Louis, MI, May 1991.

[5] L.J. Greenstein, N. Amitai, T.S. Chu, and L.J. Climini, Jr., *Microcells in Personal Communications Systems*, IEEE Communication Magazine, Vol. 30, No. 12, pp. 76-88, December 1992.

[6] W.C.Y. Lee, *Efficiency of a New Microcell System*, Proceedings of the 42 nd IEEE VTS Conference, pp. 37-42, Denver, CO, May 1992.

[7] J. Shapira, *Microcell engineering in CDMA Cellular Networks*, IEEE Trans. VT, Vol. 43, No. 4, pp. 817-825, Nov. 1994.

[8] A.M.D. Turkmani, A.A. Arowojolu, P.A. Jefford, and C.J. Kellet, *An Experimental Evaluation of the Performance of Two-Branch Space and Polarization Diversity Schemes at 1800 MHz*, IEEE Trans. VT, Vol. 44, No. 2, pp. 318-326, May 1995.

[9] M.R. Bavafa, and H.H. Xia, *Repeaters for CDMA Systems*, IEEE VTC'98, pp. 1161-65, 1998.

[10] K.S. Gilhousen, and F. Antonio, *CDMA Microcellular Telephone System and Distributed Antenna System Therefor*, US Patent 5,280,472, 1994.

[11] W.C.Y. Lee, and D.J.Y. Lee, *The Impact of Repeaters on CDMA System Performance*, in *Proc. 51st IEEE Vehicular Technology Conference*, Vol. 3, pp. 1763–1767, 2000.

[12] K.S. Jeong, J.M. Cheong, T.H. Park, T.G. Kim, and S. Park, *Performance Analysis of DS-CDMA Reverse Link with Fiber-Optic Repeaters*, in Proc. 51st IEEE Vehicular Technology Conference, Vol. 3, pp. 2439–2443, 2000.

[13] S.-J. Park, W.W. Kim, and B. Kwon, *An Analysis of Effect of Wireless Network by a Repeater in CDMA System*, in Proc. 53rd IEEE VTC, Vol. 4, pp. 2781–2785, 2001.

[14] T.W. Ban, B.Y. Cho, W. Choi, and H.-S. Cho, *On the Capacity of a DS/CDMA System with Automatic On-Off Switching Repeaters*, in Proc. IEEE VTC, pp. 780-4, 2001.

[15] H.-C. Jeon, Y.-S. Jung, B. Kwon and J.-T. Ihm, *Analysis on Coverage and Capacity in Adoption of Repeater Systems in CDMA2000*, 2002 International Zurich Seminar on Broadband Communications, ETH Zurich, pp. 33-1-6, February 19-21, 2002.

[16] *Repeaters for Indoor Coverage in CDMA networks*, Qualcomm White paper 80-31576-1 Rev B, 2003.

[17] *Relating Search Window Sizes to Fiber Delay in a Repeater*, Qualcomm White paper 80-31550-1 Rev B, 2003.

7

REPEATERS DESIGN AND TUNING IN CDMA NETWORKS

This chapter discusses CDMA repeaters. Having set the foundation of the CDMA network radio characteristics in Chapter 4, and the subtleties of interaction between repeaters and the CDMA radio network in Chapter 6, this chapter covers the repeater system design considerations including specifications, tuning and operation of the repeaters, and highlights of repeaters type approval. Repeater RF engineering is elaborated upon, and its impact on the repeater performance, interface with the backhaul systems and the network is enlightened.

7.1 RF Repeaters

This section introduces the reader to the basic repeater architecture, its interfaces with the BTS, and critical signal paths.

7.1.1 The Role of RF Repeaters

RF repeaters operate at the RF level on CDMA FDD transmissions, and serve to enhance coverage, capacity and the network quality of service. Repeaters in the CDMA network serve as bidirectional signal boosters, with very few parameters to tune. The gain and power, together with the antenna position and radiation pattern, are the fundamental parameters that determine the repeater performance (once the frequency allocation and bandwidth have been set).

7.1.2 Network Diagram and Signal Flow

We start with the high level model that is common to all types of RF repeaters and shows the basic RF signal flow, as presented in Fig. 7-1.

The repeater may include two distinct units, a *donor unit* at the donor BTS side, and a *remote unit*, which is the repeater unit that provides service to

mobile subscribers. In the case of F1/F1 repeaters (OFR), the donor unit is excluded, and the remote repeater unit operates directly on the radio transmission off the BTS service antenna. Other types of repeaters rely on a *backhaul* for communicating the FL and RL signals between the donor and the remote units. The types and characteristics of the backhaul systems that are commonly used in repeater applications are treated in Chapter 8.

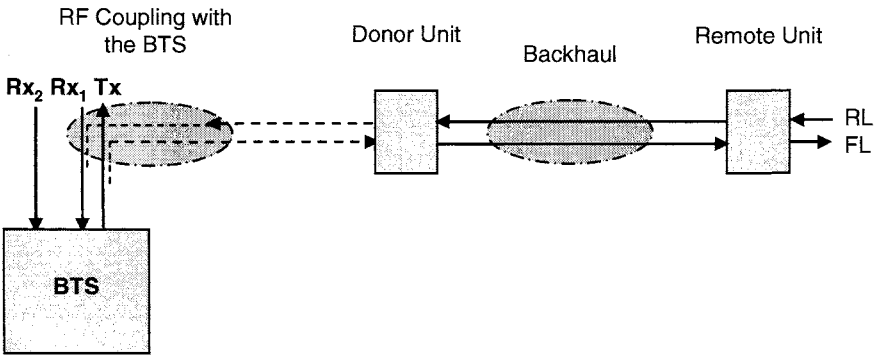

Figure 7-1. Repeater model and signal flow diagram

The main signal paths in FL and RL, as depicted in Fig. 7-1, include: interfacing properly with the donor BTS, providing the conditioned signals that go through the backhaul, processing the service signals and interfacing over-the-air with the subscriber terminals in the repeater coverage area.

7.1.3 Repeater Generic Diagram

The generic diagram of a repeater is presented in Fig. 7-2 and includes the main elements constituting a remote unit [1]. The donor unit is composed of similar elements and thus is not detailed at this preliminary description.

The RF repeater includes two separate RF chains for amplifying the FL and RL signals. Each chain begins (*C,* or *A* and *B*) with wide band-pass filtering (WBPF) followed by low-noise amplification (LNA), then additional amplification with optional narrow band-pass filtering (NBPF), filters *F* and *G*, that select a single carrier (in a channelized repeater) or a group of carriers (in a band repeater), and a transmission stage of power amplifier. These are commonly classified by the repeater power level as high-power amplifier (HPA) when specified for more than a few watts, or medium-power amplifier (MPA - *D*) when in the range of 1 watt.

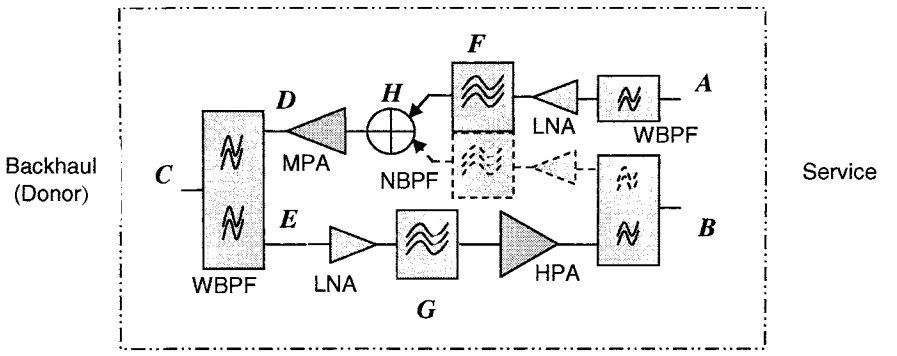

Figure 7-2. Repeater generic diagram

Finally, a repeater may provide pseudodiversity combining, demonstrated in Fig. 7-2 (*F, H* in the RL). In this case the repeater provides two receive branches (Cf. Chapter 5) in RL and pseudo-combines (combiner *H*) the signals from two antennas into one backhaul output.

7.1.4 BTS Interface

A typical BTS comprises 3 sectors. Each sector employs two antennas, one for Tx/Rx and the other for Rx diversity[21]. The Tx/Rx antenna is connected to the sector radio section via a duplexer, whereas the diversity (receive only) antenna is connected via an Rx filter. The repeater backhaul to the BTS may be realized by an over-the-air RF transmission or by a physical conduit that carries the backhaul. The latter is either optical (fiber or free space), coaxial cable or a point-to-point microwave backhaul. The repeater is coupled to the BTS at the RF level using RF directional couplers (typically via 30 dB-coupling loss), or over-the-air coupling as in the case of the OFR. The FL samples the transmitted signal of one BTS port. (BTS-generated transmit diversity is optional in 3G systems and necessitates two transmission branches to be relayed to the repeater). The RL is coupled to one of the two diversity Rx ports of the BTS, except for OFR where both BTS antennas receive the signal. The diversity branches of repeaters employing RL diversity are linked to both diversity branches in the BTS respectively.

The couplers are connected at the BTS antenna ports. These have to sustain the high Tx power. Coupling at low power level is preferable wherever the BTS structure allows an access to the low-power Tx ports of the

[21] This description is simplistic, and there may be cases where the two antennas are used for both Tx and Rx, when several carriers are commissioned, and must be transmitted with minimum combining losses.

BTS (prior to the BTS power amplifier)[22]. A -10 dB coupler may suffice in that case. The RF sampling in this case may be on a per-carrier basis, and the sampled carriers are combined at low power for further repeater processing. This is necessary in case the repeater is intended to enhance only a subset of the active BTS carriers (e.g. attend the 1xRTT or WCDMA carriers, but not the 1xEV-DO or HSDPA carrier(s)). Figure 7-3 illustrates the directional coupler connections. The RL is simply coupled to the BTS multicarrier antenna ports.

The main considerations in determining the coupling in FL are: (a) The required power level at the input to the repeater donor unit. For example, if the maximum allowed input power is -20 dBm, and the BTS Tx power is +42 dBm, then the coupling should be -62 dB (realizable by a -30 dB coupler and a series low-power attenuator of 32 dB); (b) The insertion loss added to the BTS Tx path must to be kept minimal, to avoid loss of transmit power. A -30 dB coupling induces ~0.25 dB loss, with minimal effect on the BTS EIRP; and (c) The signal dynamic range. The level of the coupled Tx signal is reduced and thus comes closer to the noise floor.

The coupled signal power must have enough power-margin to comply with the emission mask requirements, and an extra margin has to be allowed to account for the repeater added noise.

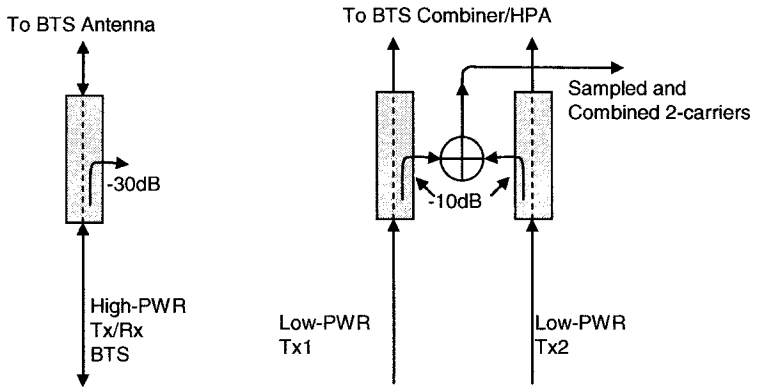

(a) High-power (multicarrier) RF coupling

(b) Low-power (single carrier) RF coupling

Figure 7-3. RF coupling with BTS

[22] Note that the PA may have power control loops that have to be considered in such a case.

Coupling at high-power is well above the noise floor and does not endanger the emission mask clearance. This is illustrated in Fig. 7-4, where a BTS Tx signal that complies with the emission mask requirements with ample margin is sampled at a lower level.

Example: Assume a CDMA2000 BTS single carrier (1.25 MHz) low-power port at a level of –20 dBm. Let the BTS noise floor be the –80 dBc, or –100 dBm/1.25 MHz. Using a –10 dB coupler would result in a –30 dBm sampled signal. A repeater with 5 dB noise figure presents an equivalent input thermal noise floor of 5 dB + (–113 dBm/1.25 MHz) = – 108 dBm/1.25 MHz. Thus the repeater's signal clearance above the noise will be –30 – (– 108) = 78 dB, as compared to the 80 dB of the BTS signal. Employing instead a -30 dB coupler yields a mere clearance of 58 dB, which may be marginal.

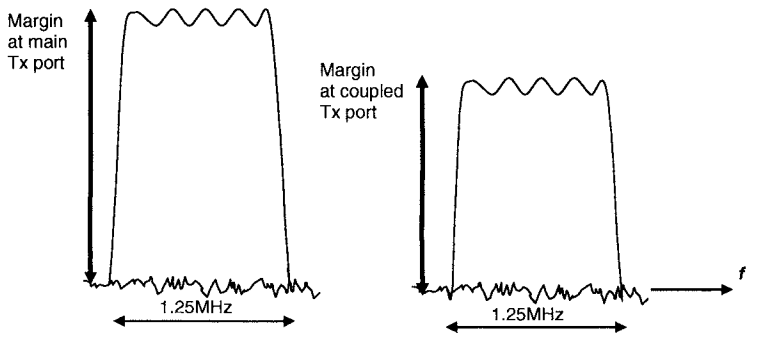

Figure 7-4. FL RF sampling and emission mask

7.1.5 Critical Signal Paths and Parasitic Coupling

Repeater systems process RF signals over an extremely high amplitude range between its ports (reaching to 90 and up to 120 dB), and proper isolation within the repeater and between its external ports is a key to its performance. We briefly survey the critical signal paths in a typical repeater system, considering both the FL and RL RF chains, as per Fig. 7-5. The paths considered are circle-numbered for reference.

Internal isolation between the amplification stages: Sufficient internal isolation between the electronic blocks has to be designed for and achieved, commensurate with the high gain.

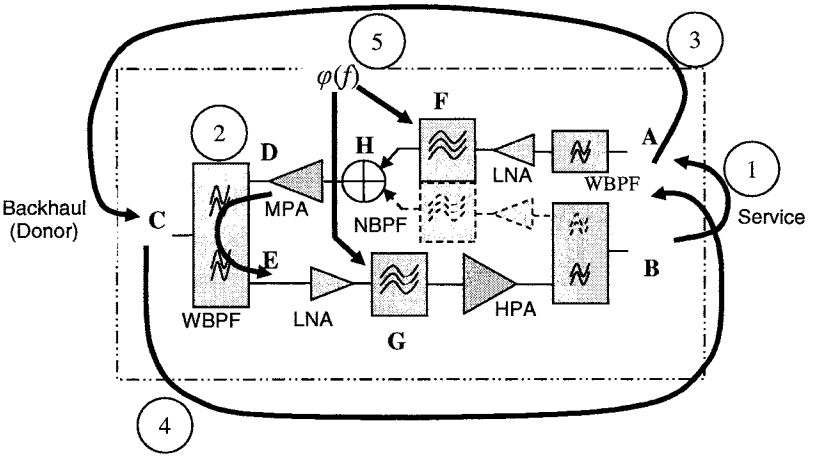

Figure 7-5. Critical signal coupling paths

Paths 1 and 2: Duplex isolation between the Tx and Rx paths. The duplexers should provide adequate attenuation to avoid Tx noise in Rx band, and avoid Rx desensitization by the high power Tx signal.

Paths 3 and 4: Isolation between the Tx and Rx antenna ports, for the FL and RL. Coupling between the service and backhaul antennas, typically co-located on the tower (as with OFR and FSR systems) has to be controlled (Cf. Chapter 3). The effects of this coupling are discussed in more depth below.

Path 5: The narrow band filtering operations include selective filters that may cause some signal distortion. If a heterodyne realization is chosen for the NBPF, then phase noise and frequency errors may cause additional signal distortion. Thus, any signal path through a selective subsystem involves a distortion function $\varphi(f)$, which must be designed for and achieved.

7.1.6 Signal Distortions

The repeater is expected to behave as a linear system, reproducing the CDMA signals with high fidelity. In practice there are several undesirable sources for signal distortion, including frequency error, error-vector magnitude (EVM) and Rho (decorrelation measure), to be explained in the next section.

Distortion sources include: additive thermal noise, nonlinear distortions that must be controlled for signals within a specified dynamic range (see Appendix D), oscillator phase noise and narrowband filtering with phase (delay) and amplitude ripple over the pass band, which cause parasitic modulation of the desired signals. These distortion effects on the CDMA

signals are addressed in detail in the next section, and must be carefully controlled to guarantee an overall acceptable performance.

7.2 Repeater Architecture

The repeater systems design considerations are treated next. Parameters that are used to characterize repeater requirements and performance, repeater architectures, repeater supporting functions and repeater chain design are reviewed. Then the repeater impact on the network is considered, at the radio network engineering level. For further in-depth analysis of repeater interaction with the CDMA network, consult Chapter 6.

7.2.1 Governing Parameters and Design Principles

We divide the basic parameters that are used to characterize repeater systems requirements into several categories. Our main focus is on the radio parameters, with a brief review of auxiliary parameters including energy, mechanics and management.

7.2.1.1 RF Parameters

The RF parameters define the repeater functionality within the CDMA network, and the effects on the relayed signals.

RF Gain: The FL and RL gain are independently controlled parameters, with respective maximum value G_{max}, range G, and step size ΔG (usually specified as 1 dB). The RL and FL gain are linked by the balancing requirement. The gain accuracy (defined as an uncertainty range $\pm\delta G$, e.g. from ±1.5 dB and up to ±3 dB) is defined as the difference between the set gain value and the actual RF gain. Gain may vary with temperature and frequency. Figure 7-6 illustrates the gain parameters in frequency domain.

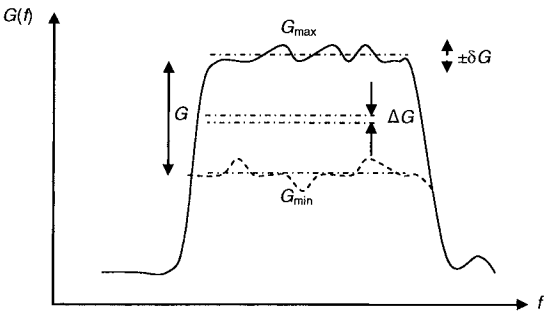

Figure 7-6. Gain parameter definitions

Gain flatness and small variations over the band may be achieved by careful use of RF components within the required tolerances, well-controlled impedance matching, and careful shielding, since RF leakage may impair the achieved gain and introduce gain ripple. The RF parameters' variations in production over component lots are compensated and calibrated as part of the production process. The gain is stabilized over temperature by employing digitally controlled attenuators that are set according to built-in correction tables – a standard procedure in RF calibrated amplification chain realizations. Repeater units may have gain from 50 dB to 120 dB, and the control range is from 30 dB to 60 dB below the maximum gain, depending on the repeater type and application (Section 7.3).

The implementation of very high gain (> 70 dB) at the same frequency requires careful design, prudent implementation and expensive shielding. High gain repeaters tend to employ heterodyning techniques where the system gain is divided between RF and IF frequency domains.

In designing RF chains, the gain distribution must consider the levels of the signal and expected interference along the chain, providing for adequate linearity and noise performance of the RF stages. The bandwidth along the repeater chain affects these variables as well, with filter stages incorporated for suppression of unwanted interference (Section 7.2.4).

Bandwidth: The bandwidth specification of a repeater is determined by the service band, or the required channel bandwidth (in the case of a channel-selective repeater). Additional requirements may introduce selectivity constraints, which translate into filter *attenuation slopes* and *ultimate rejection* requirements (Section 7.2.3). The repeater utilizes several filter technologies, including duplexers and cavity band-pass filters, dielectric and SAW filters. Figure 7-7 illustrates typical filter characteristics including selectivity and rejection, applicable to any of the filters that are incorporated in the repeater, and to their end-to-end equivalent response.

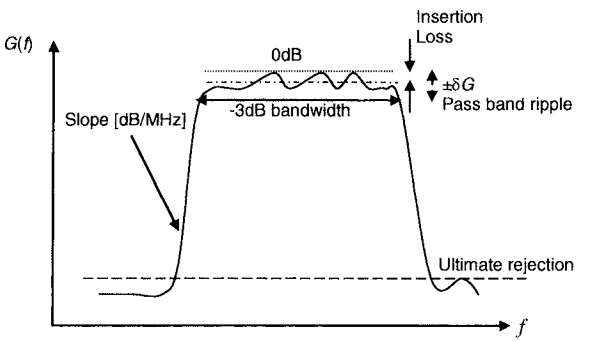

Figure 7-7. Filter response characterization

The bandwidth is usually defined at the half-power (–3 dB) frequency response points, in addition to the –1 dB points' bandwidth that signifies the amplitude distortion of the CDMA carrier caused by the filter.

The insertion loss of the duplexers should be very low across the bandwidth (typically around 0.4 dB in the Tx path, and 0.6 dB in the Rx path) to minimize the Tx power and sensitivity losses. Filters that are part of the repeater active RF chain may incorporate higher insertion loss, with negligible consequence on the noise figure. Dielectric and SAW filters may have insertion losses in the range of 3 dB to 20 dB, respectively. The overall response of sequential multiple filtering determines the distortion level of the desired signals, and must be specified and implemented carefully along the RF chain. Any pass band slope in the frequency response is included in the pass band ripple specification[23].

RF Power: The FL maximum Tx power of a repeater is determined according to the expected coverage range. The repeater transmitted power is related to the traffic load of the donor BTS. The RL Tx power is linearly related to the FL Tx power, and it rises with the total noise rise at the donor BTS. Repeaters may be classified as low-power, emitting 100 mW to 1 W, medium-power, ranging from 1 to 5 W, and high-power, exceeding 10 W.

The RL Tx power is determined by backhaul balance and noise level considerations with a predictable power-margin relative to the output thermal noise level (Section 7.3.1).

Noise Figure: The noise figure (NF) determines the relative noise contribution of the repeater circuitry (Appendix D). The FL noise considerations are dictated by the emission regulations and in RL by the required repeater sensitivity and the donor BTS sensitivity, as expressed by the effective noise factors (Eqs. (6-4)). Typical NF values in commercial repeaters are 6 dB in FL and 4 dB in RL.

Linearity: The repeater must amplify the RF modulated signals linearly, with a specified limit on the level of generated spurii and out-of-band interference. Linearization of multicarrier amplification needs more attention. The RF linearity is defined by the intercept points (3^{rd} and 2^{nd} order, and so on (see Appendix D)), usually measured in a two-tone test. The relation between the output 2-tone intercept points and the maximum CDMA power under emission mask constraints is nontrivial; thus direct tests with CDMA generated signals composed of multiple codes are required in order to establish the system linearity. The critical elements that set the limits on the repeater linearity are the power amplifiers in FL and RL (Section 7.3.1). Another nonlinear affect is caused by external signals that may be received by

[23] In channelized repeater systems, it is possible to add gain compensation as a function of the FA setting; this reduces the flatness constraints on the filters.

any of the repeater antennas, and arrive at the output of the power amplifier. The output stages of the power amplifier may cause parasitic mixing between the so-called *reverse injected* signals and the desired transmitted signals, resulting in emission of additional unwanted spurii. It is common to employ isolators at each power amplifier output to minimize this effect.

Delay: The repeater hardware delay is an important parameter that is taken into account towards operating the repeater in the CDMA network (Section 6.7). The repeater is a pass band system, thus it induces delay in the relayed signals that grows inversely with the repeater bandwidth and directly with its frequency attenuation sharpness (related to the selective filter number of poles). The delay of the repeater adds to the propagation delay and must be specified (usually in the range of 0.5 to 16 μsec depending on the repeater type) to allow for proper setting of the search window.

Fidelity - Distortion Definitions: In addition to nonlinearity distortions that affect the out-of-band spectrum, in-band distortions of the desired signal are discussed next. The fidelity of the CDMA signal past the repeater is characterized by a few parameters that quantify the modulation distortion caused by the repeater. These may then be translated into RF design constraints (e.g. group delay variations, phase noise, and frequency error. See below).

EVM: The *erro- vector magnitude* (EVM) signifies distortion in the signal constellation. The CDMA signal out of the repeater is despread and its constellation compared with a perfect reference despread signal. Generating the difference constellation over time (termed *error-vector*), then taking the absolute value of the error vector produces the EVM. The RMS and peak values of the EVM define the signal distortion. RMS EVM requirements range from 8% to 13%.

Image rejection: This parameter relates to nonlinearity (e.g. AM/AM and AM/PM distortions in amplifiers) and the fidelity of modulators and demodulators. A modulator is depicted in Fig. 7-8. It is important to keep the *I*-path and *Q*-path balanced from the baseband generator all the way to the output, both possessing equal gain and phase shift. A single sideband baseband signal is introduced to the up-converter.

The ideally expected output SSB signal is the frequency-shifted signal $A\cos[2\pi(\pm f_m + f_c)\,t]$. Another in-band image signal may appear in case of imperfect SSB modulation given by $B\cos[2\pi(\mp f_m + f_c)\,t + \vartheta]$ (as caused by I/Q imbalance). This imperfection is quantified by the image rejection (*I.R.*) parameter, defined as

$$I.R. = 10 \cdot \log_{10}\left[(A/B)^2\right][dB]. \qquad (7\text{-}1)$$

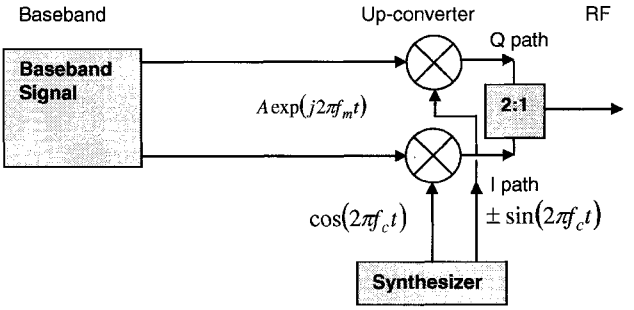

Figure 7-8. Modulator scheme

The image rejection is directly related to the EVM caused by the modulator imbalance as follows:

$$I.R. = 20 \cdot \log_{10}\left[EVM\,\%/100\right][dB]. \tag{7-2}$$

The EVM measure suffices to define this type of distortion, thus *I.R.* is rarely used in conjunction with repeaters.

Rho (PCDE): The distorted CDMA signal out of the repeater is correlated with a perfect reference CDMA signal (the input signal); the correlation coefficient defines the Rho parameter, and should be kept close enough to unity (Rho values above 0.98 are considered acceptable). A related measure is the peak code domain error (PCDE) where the difference between the perfect reference and a modified version of the measured waveform is projected onto the reference CDMA signal; this should be a small value (close to zero in absolute value) and is usually expressed in dB (PCDE values below –35dB are usually considered acceptable). We have

$$PCDE = 10 \cdot \log_{10}\left[(1 - Rho)^2\right][dB]. \tag{7-3}$$

The relationship between the Rho and PCDE parameters is illustrated geometrically in Fig. 7-9.

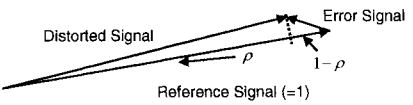

Figure 7-9. Signal distortion measures

The evaluation of Rho may be performed in frequency domain by dividing the CDMA waveform into frequency bins f_i, and invoking Parseval's relation[24]. If the reference signal has values X_i and the distorted signal has values Y_i, both at f_i, then the Rho factor is given by

$$Rho = \frac{\sum_i X_i Y_i}{\sqrt{\sum_i X_i^2}\sqrt{\sum_i Y_i^2}} \tag{7-4}$$

Measurement of RF parameters: The measurement of the repeater RF parameters constitutes a discipline by itself and is based on clear definitions of the required performance as well as the measurement procedure [2], [3]. Consult [4], [5] for many relevant measurement techniques. Subtleties encountered in RF measurements are addressed in Section 7.4.5. Two examples will serve to demonstrate the nature of RF parameter measurements:

1) IM performance in a 2-tone test: the setup is illustrated in Fig. 7-10. Two signal generators produce two continuous wave signals (CW) at frequencies f_1 and f_2. Each signal passes through an attenuator L and is applied to a power combiner. The attenuators L increase the isolation between the two signal generators (the isolation equals the combiner isolation between its input ports in dB, plus $2L$ dB).

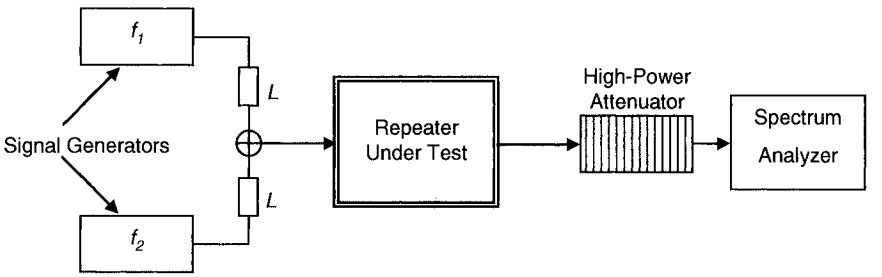

Figure 7-10. Two-tone RF test

---

[24] $\int_{-\infty}^{\infty} x_1(t)x_2(t)dt = \int_{-\infty}^{\infty} X_1(f)X_2(-f)df$; Also – a real signal in time domain has an even spectrum. We limit the discussion to real waveforms in time and frequency domains. The extension to complex waveforms is straightforward.

A typical value of L is 10 dB. This arrangement ensures generation of a clean two-tone signal without parasitic reverse IM_3 products that may have been generated by the signal generators. The repeater amplifies the two-tone signal and its high power output is applied to a high-power attenuator (e.g. 50 dB).

The output spectrum is then examined using a spectrum analyzer with sufficient dynamic range, and the two tones and any IM products are measured to determine the intercept point of the repeater.

2) Noise figure: the setup is illustrated in Fig. 7-11. Noise figure may be evaluated using dedicated noise figure test equipment that includes a calibrated noise source, and can measure the output system noise for two instances of different input noise level. This enables automatic evaluation of the system noise figure. We emphasize here a special noise figure test of an FDD repeater that includes active transmission of the repeater in the opposite duplex direction so that any leakage from the high-power transmission that may enter the low-power measured path is included in the test.

Since the high-power output must not enter into the noise figure meter, an auxiliary duplexer is employed off the repeater port to decouple the high-power output signal from the noise figure meter that tests the other band. A high-power load, that absorbs and heat dissipates the Tx signal, terminates the duplexer output. The noise figure meter measures the noise figure while the duplex band is active and produces out-of-band noise.

Note that it is possible to measure the noise figure with a high-power signal transmitted in the duplex band, but this requires a similar arrangement with an additional duplexer at the other port of the repeater; one port of the duplexer would connect to a CDMA signal generator, while the other is fed back (possibly via an attenuator) to the noise figure meter.

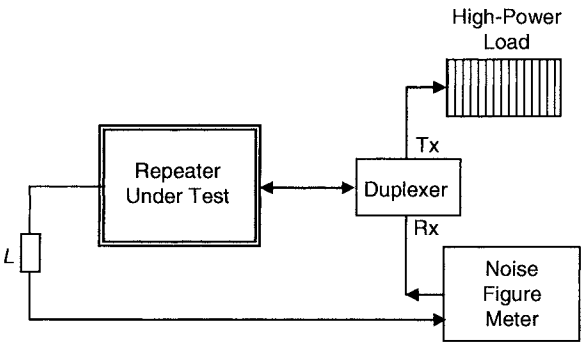

Figure 7-11. Noise figure RF test

7.2.1.2 Mechanics and Energy Sources

The mechanical and electrical considerations in repeaters follow common engineering practice. Energy is provided from AC or DC sources, with backup batteries employed for uninterrupted power supply. The low efficiency of the high-power amplifiers (typically less than 10%) results in much heat that must be dissipated using conduction fins, heat pipes, with possible use of fans.

Use of fans is not considered reliable enough and is typically avoided in outdoors repeaters that are not accessible for easy maintenance. Convection-cooled repeaters have limits on the Tx power that may be supported by a constrained size enclosure. A fan-less unit that weighs less than 50 kg may be expected to support less than 30 Watts of RF transmitted power.

7.2.1.3 Management Capabilities

Once installed and commissioned, the repeater is an unattended node and the operator needs to monitor the repeater radio performance analysis, verify the well-being of the repeater, and alarm/report failures. The management system provides the operator with the capability to routinely communicate with the repeater and assure its proper operation. The repeater network management system RNMS provides the operator with management capability of a fleet of repeaters.

Local C&M: Local control and monitoring (C&M) unit (usually a PC) is directly connected to the repeater, and used during set up and commissioning of the repeater, and during local test and repair. Physical wireline (e.g. via RS232, RS485 connections) or wireless (e.g. Bluetooth, or Wi-Fi) connections facilitate the local communication. It is advantageous to control the whole repeater system from any backhaul end, which simplifies the set up process. This is enabled by installation of an internal modem in the repeater for such communication.

Remote C&M: Once installed, the repeater must be managed from remote locations. This is usually provided for by a CDMA wireless modem that operates as a registered subscriber in the repeater cellular network. There are few possible modes of operation, including connection-oriented (circuit switched) or connectionless (packet). The protocol used for remote management of the repeaters may be proprietary or an open standard, e.g. SNMP over IP. The wireless modem integration into the repeater has to be on a service port, with adequate isolation (attenuation) to avoid saturation of the wireless modem (in FL) or the repeater (in RL). See Section 10.2 for more details.

RNMS: Cellular operators construct a network management center to monitor and control the entire network operation, including the repeater network elements (NEs, may be viewed as leafs in a network management tree, see

[6]), which are part of such a network. The repeater network management system (RNMS) may be operated using a dedicated *repeaters server*, which is linked to the network operations center (NOC) management system, or be fully integrated into the NOC management system, which then communicates directly with each repeater NE. The RNMS routinely collects data on the operational repeaters, monitors alarm messages, and pages the relevant personnel in case of a severe alarm. An important capability within the RNMS is to monitor the RF performance of the repeaters via their performance reports based on the readings of the wireless modem. See Section 10.2 for more details.

Alarms: In case of failure the repeater may generate alarm messages that specify the failure. This important information allows identifying the nature of the failure, and the best way to perform a corrective maintenance action.

7.2.2 Distributed and Unified Repeater Architectures

Repeaters may be constructed as a single unit or composed of several units. The purpose of separating repeater parts is to settle the PA and the LNA right at the antenna (TTE- Tower-Top Electronics) and thus avoid power loss between the PA and the antenna, and loss of sensitivity by the cable attenuation. The low power processing and the backhaul transmission are kept near the backhaul antenna or the backhaul transducer (backhaul remote unit), keeping low losses on this side. The linkage between these is low power, where losses have no effect. There is a trade-off in performance, cost and operational convenience between unified and distributed architecture options.

7.2.2.1 Unified Architecture

The unified architecture is the common way repeaters are designed and offered, with all functions integrated into a single box. In many cases the repeaters are installed at floor level for operational convenience, despite the losses incurred by the long antenna RF cables (Fig. 7-12).

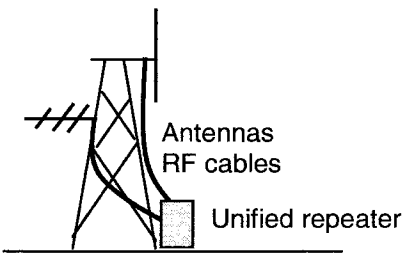

Figure 7-12. Ground mount unified repeater

In tower-top installation the unit is placed close to the service antenna, with longer cables to the backhaul antenna, placing the emphasis on the improved performance on the service side. Microwave backhaul requires its transducer unit (outdoor unit - ODU) to be placed right at the backhaul antenna, and the unified-built repeater still comprises two enclosures (Section 7.3.7). The main drive for the unified architecture is cost, both in capital expenses and operational maintenance cost of the system.

7.2.2.2 Distributed Architecture

The distributed repeater architecture aims at minimizing transmission losses, thus improving the FL and RL performance by a few dB relative to the unified approach (~3 dB with 40 m towers in the 850 MHz band). A high-power tower mount front-end (booster) unit is placed near the service antenna. Another unit encompassing the low-power RF circuitry, including selective filtering, power-supply, controller and wireless modem may be located conveniently at ground level. This unit is termed *facilities unit*. In extreme cases, with over-the-air repeaters (OFR or FSR), it may yet be advantageous to provide another 'backhaul unit' that is mounted next to the backhaul antenna, for improved backhaul transmission gain, as described in Fig. 7-13. The cables between the repeater units need not be low loss, heavy weight cables as in the unified case, as losses are readily compensated for by the low-power (and low-cost) amplifiers in the units. The cost per cable is thus reduced, as well as the tower load. The wind load due to the tower-top unit may not be significant if the unit is shaped to fit behind the antenna. This distributed architecture has clear RF performance advantage but is logistically cumbersome and expensive.

Table 7-1 summarizes the advantages and disadvantages of the two repeater architectures.

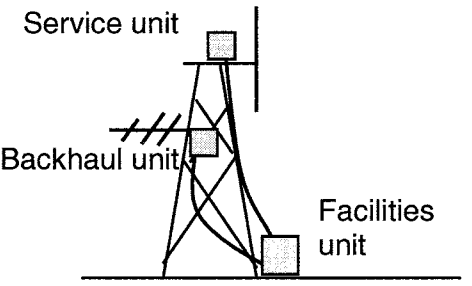

Figure 7-13. Distributed repeater

Table 7-1. Comparison of Unified and Distributed Repeater Architectures

Attribute	Distributed Repeater	Unified Repeater
Effective System RF Performance	Excellent	Good
Individual Unit Size	Small	Large
Overall Size/Weight	Large	Moderate
Wind Load Cross-section	Smallest	Moderate
Installation	Complex	Simple
Operational Handling	Involved	Simple
RF Antenna/Interbox Cables	Thin	Thick
Product Cost	High	Moderate

7.2.3 Band-Filtered and Channel-Filtered Repeaters

Repeaters may be classified according to their frequency pass band characteristics. The two common types are *band* and *channel* filtered repeaters (see Fig. 7-14). A band repeater operates over the full operators' allocated band, e.g. 10 MHz or 15 MHz, even if only part of the band is occupied. Theoretically this should not cause any problems if all the transmitters in the served area operate under strict conformance to the radio emission standards. Logistically it is advantageous for the operator to be ready for future addition of carriers, provided that the maximum repeater Tx power is sufficient to support additional carriers, and that all carriers require the same coverage profiles. Note that with the recently emerging data services (1xEV-DO, HSDPA, etc.) it may happen that separate planning and service areas are targeted for the data network, and channel filtering may then be required.

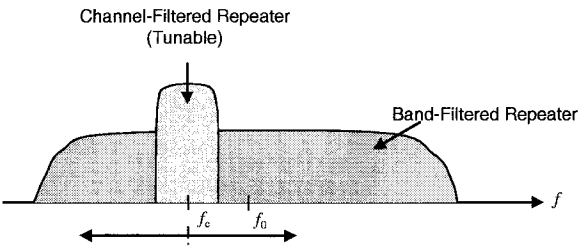

Figure 7-14. Band and channel-filtered repeaters (FL or RL response)

The other approach (channel-filtered) defines the repeater bandwidth according to the operationally deployed network, with selective filtering that corresponds to the number of serving carriers in the repeater area. Such repeaters may, typically, support 1 to 4 CDMA2000, or 1 to 2 WCDMA carriers. Note that even if the CDMA network is operating in dense urban areas with more carriers, it may well be the case that over a highway, or some rural neighborhood, much lower demand results in operating just a single CDMA carrier and the repeaters in such areas may be channel-filtered accordingly.

The band repeaters are usually not tunable, and are preset to operate over the prescribed band. The channel selective repeaters are tunable, and channel setting is provided as part of the management capabilities[25].

Typical selectivity (attenuation slopes and ultimate rejection) of filters that are useable in repeaters is illustrated in Table 7-2 [7, 8].

Table 7-2. Typical selectivity of filters

Filter Technology	Selectivity Attenuation Slope	Ultimate Rejection
Cavity Resonator (Duplexer)	80 dB/15 MHz to 70 dB/2.5 MHz	90 dB
SAW (Channel)	40 dB/2 MHz	50 dB
Dielectric, Ceramic	25 dB/20 MHz	25 dB

7.2.4 Signal and Interference Budget

The desired signal levels in FL and RL are evaluated using standard gain and power budgets calculations. Admissible levels of interference must be defined and incorporated in the detailed design. Ignoring interference issues may result in generation of unwanted spurii, and even desensitization of the repeater, in which case the sensitivity and specified Tx power may not be achievable.

[25] Channel index and center frequency relations are defined by FCC and ETSI standards. See Appendix H for definitions of the common channel grids.

The two underlying principles for handling interference are:

1) Assure the *linearity* of the system for the sum of desired signal *and* interference, along the RF chain up to the point where the interference is effectively suppressed.

2) Employ *distributed* filtering along the RF chain to suppress interference.

Application of these rules is performed on the FL and the RL, and the interplay of gain and filtering is discussed in Section 7.2.5.

It is possible to distinguish 3 regions in frequency domain that require separate consideration of interference as depicted in Fig. 7-15.

First is the out-of-band region (*A*) that falls outside the band filter. The duplexer or Rx filter pass band defines this region, and the filtering is performed at the repeater input. The second region (*B*) is within the pass band of the repeater, but outside the channel filter pass band. Finally, region (*C*) is within the channel filter pass band, and is the most vulnerable, since the desired signals exist in this band, and the repeater exhibits there its highest gain.

The gain and 1dB compression points (referred to input) of paths through region *A* (in case of a band repeater), and *B* (in case of a channel repeater), define the immunity of the repeater to interference.

Two types of interference must be considered. One is interference that is generated by the repeater and may affect the operation of other networks (when co-sited or adjacently located), and the other is external interference that could degrade the repeaters' functioning[26].

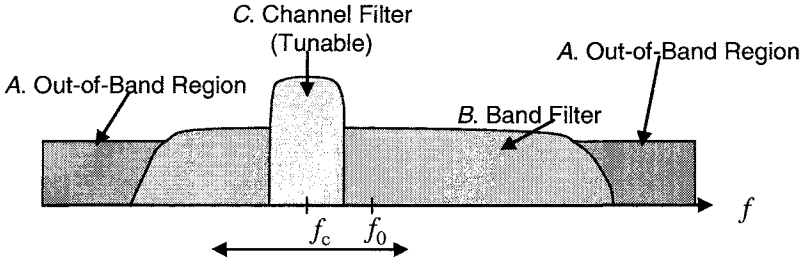

Figure 7-15. Regions for interference analysis (FL or RL response)

[26] In considering interference we assume that all the minimum emission and out-of-band filtering requirements are fulfilled. The considerations discussed here go beyond these requirements, and are typical to colocation scenarios.

Repeater generated interference: the repeater may generate noise and adjacent channel power (ACP) that affects colocated systems, e.g. FL interference from 850 MHz band repeaters into colocated 900 MHz GSM BTS receivers. This out-of-band noise and ACP may be reduced by sharper attenuation of the repeater Tx filter in the service duplexer.

External impinging interference: strong interference that enters the repeater in 850 MHz band *A* or *B*, may cause desensitization, e.g. interference from colocated transmissions at neighbor frequencies such as ESMR transmissions near at 850 MHz interfering with cellular band RL receptions. Such interference may be attenuated by steeper frequency response of the repeater Rx filter in the service duplexer. Many more colocation cases are considered in [2].

7.2.5 Gain and Filtering Chain

The repeater gain is obtained by cascading its building blocks' gain values

$$G = \prod_{n \le k} G_n \cdot \tag{7-5}$$

Equation (7-5) is valid as long as the power along the chain satisfies the linearity condition of Eq. (7-6), for input power P_r and stage k output 1 dB compression power P_k^1 (maximum linear range output power),

$$P_k = P_r \cdot \prod_{n \le k} G_n < P_k^1 . \tag{7-6}$$

The values of G_k may be greater than 1 for amplifiers, or positive and less than 1 for passive devices including attenuators, filters, splitters and combiners, etc.. The RF chain noise figure of a cascade of k stages $F_{(k)}$, with the k^{th} stage noise figure denoted by F_k, is given by (See Appendix D):

$$F_{(k)} = \begin{cases} F_{(1)} = F_1, k = 1 \\ F_{(k-1)} + \dfrac{F_k - 1}{\prod_{n=1}^{k-1} G_n}, \quad k > 1 \end{cases} \tag{7-7}$$

The noise density at the output of block k is

$$N_k = (kT_0) \cdot F_{(k)} \cdot G \tag{7-8}$$

where G is defined in Eq. (7-5) and the input noise thermal density assumes the value $(kT_0) = 10^{-11.4}[mW/MHz]$.

The filtering is incorporated into the RF chain at several critical points along the chain, as illustrated in Fig. 7-16. We consider next the filtering functions along the RF chain according to the 4 distinct sections, per Fig. 7-16.

Section A: this is the front-end, composed of a band-pass filter that may be part of the duplexer, a low-noise amplifier for low system noise figure, possibly followed by another band-pass filter. The first Rx filter is low-loss and attenuates out-of-band unwanted signals, as well as the repeater high-power Tx duplex signal. The additional band-pass filter (BPF) provides post-LNA attenuation of unwanted residual out-of-band signals, including any image frequency signals prior to heterodyning. Thus, a broadband front-end amplifier must sustain a predefined interference level in addition to the desired signal that passes through the front-end filters[27].

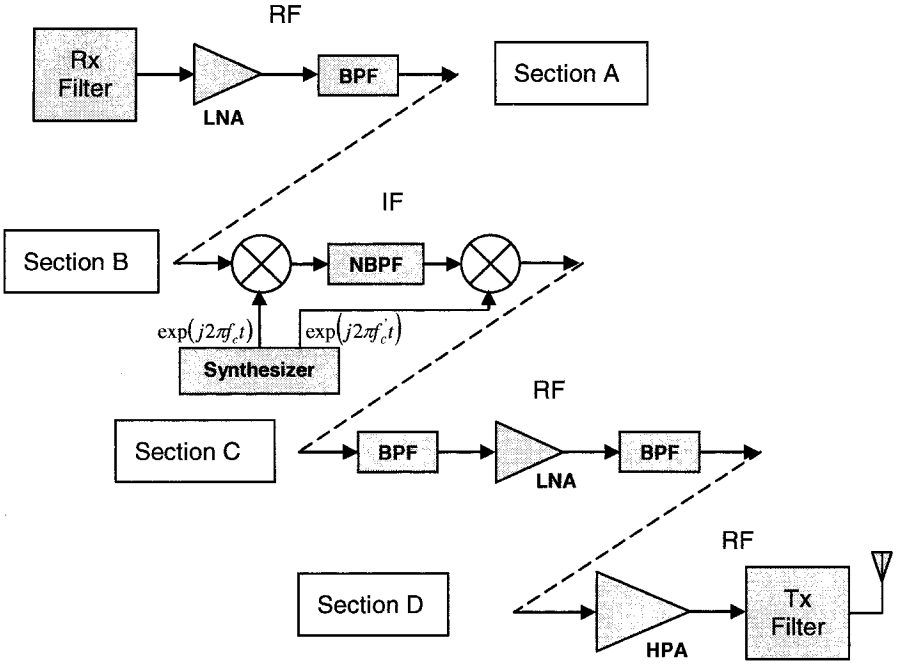

Figure 7-16. Example of an RF chain

[27] Thus, the 1 dB compression levels along the RF chain must be higher than the expected maximum level by approximately 10 to 15 dB. This is a necessary but not sufficient condition to guarantee the linearity specifications of the system, which must be evaluated using more accurate tools such as IP_3 calculations, or an RF simulator tool that incorporates nonlinear models of the RF components.

The front-end filters provide a mild out-of-band attenuation slope that may reach 100dB beyond several tens of MHz off the operational band.

Section B: IF filtering is applied using sharp surface-acoustic wave (SAW) devices for selective channel repeaters, or in-band repeaters requiring steep out-of-band rejection. The sharp narrow band-pass filtering (NBPF) is frequency tunable by varying the local oscillator frequency. In case of an F1/F1 repeater, a common synthesizer frequency is employed: $f_c = f_c^{'}$, whereas for F1/F2 repeaters, $f_c \neq f_c^{'}$. The IF NBPF is responsible for the repeater's ultimate selectivity, but its operation must be augmented by the filters in Section *A* to avoid saturation due to strong interference at previous stages, or unwanted generation of intermodulation products in the IF bandwidth prior to the NBPF stage.

Section C: having attenuated the out-of-band signals in Section *B*, the repeater amplifies the desired signals to be retransmitted. This section employs BPFs to attenuate out-of-band noise that is boosted together with the desired signals. One concern is to limit the Rx duplex band noise level at the antenna port. The other (if required) is to limit the adjacent band noise that may jam a neighbor site. These BPFs (e.g. dielectric filters) keep the out-of-band noise at a low level as the desired signal is amplified along the chain. The amount of attenuation is determined according to the ACPR of the HPA, such that the noise is negligible relative to the ACP.

Example: A CDMA2000 single-carrier +40 dBm HPA (with F=7 dB, G=50 dB) has ACPR of 50 dBc. This means that the amplifier's self-noise output spectral power density is –114+7+50= –57 dBm/MHz, while the 3rd order spurii are at power spectral density of –10 dBm/1.25 MHz = –11 dBm/MHz. Thus, the HPA self-noise is negligible relative to the IM products.

Assuming that the low-power amplification prior to the HPA (Section *C*) is +20 dB, and its noise figure is 6 dB, we have then for the out-of-band noise at the HPA output: –114+6+20+50 = –38 dBm/MHz. (We assume that the channel filter eliminates the out-of-band noise, and it starts to build-up at the thermal noise level out of Section *B*).

If the HPA-generated IM products are of negligible power in the Rx duplex band, then effective attenuation of the post NBPF noise by BPFs may alleviate the requirement of the duplexer Tx filter. The Tx noise coupled to the Rx port should not significantly affect the Rx sensitivity, e.g. 10 dB below the Rx noise referred to the input. Figure 7-17 illustrates the noise and spurii at the repeater's output. The transmitted signal, along with intermodulation products, and the output noise contributions from the HPA and the low-power amplifiers in Section *C* are all indicated separately.

If the Tx coupled noise at the Rx port is required to be less than –118 dBm/MHz, then the Tx duplexer attenuation at Rx must be –38-(-118)=80 dB, whereas if the BPF in Section *C* attenuates the noise in the Rx band by 30

dB, the only remaining noise at the Rx band would be due to the HPA (-57 dBm/MHz), thus the duplexer attenuation requirement will render into -57-(-118)=61 dB. Such a duplexer with reduced selectivity incurs lower Tx band loss.

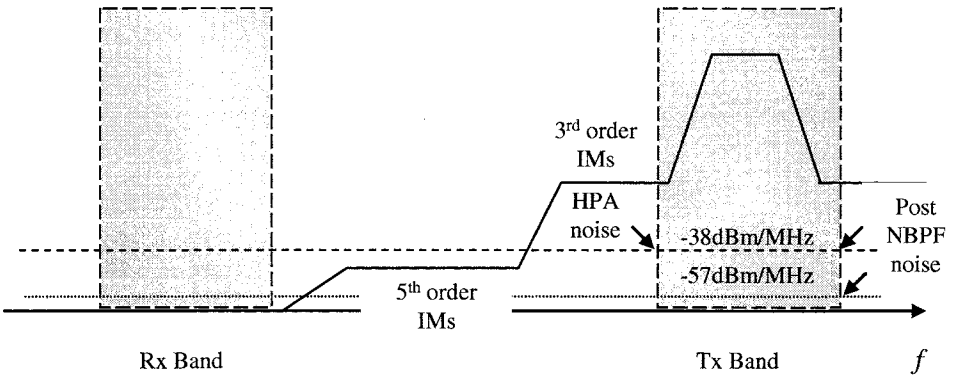

Figure 7-17. Example of noise and spurii out of the repeater

Section D: this is the high-power part of the RF chain including the Tx filter that is usually part of the duplexer. The Tx filter attenuates the out-of-band noise and spurii, and minimizes the cross interference from the transmitter to the duplex receiver.

Finally, the variable repeater gain is achieved by employing controllable attenuators. These attenuators must be carefully placed along the RF chain to guarantee the low-noise figure and adequate linearity over the attenuation range (of minimum 30 dB) from the maximum to minimum gain settings.

Filter selectivity constraints result from the above considerations and translate into filter *attenuation slopes* and *ultimate rejection* requirements (Section 7.2.3).

7.2.6 Level and Gain Control

The repeater FL and RL gain is set during commissioning based on the actual backhaul transmission gain. See Section 7.3 for more details. There is a need for automatic adjustment of the repeater gain due to uncontrollable changes over time, e.g. the backhaul conditions, the isolation between repeater antennas, or the RF power into the repeater.

An increase in input power, or decrease in isolation that may lead to oscillations, could result in over-power shut-down of the repeater power

amplifier. This undesirable service cutoff may be avoided by an Automatic Maximum Level Control (AMLC) loop, that reduces the repeater gain automatically to avoid an over-power situation. An active AMLC loop may interfere with the CDMA network power control process and is thus undesirable. Entering an AMLC state must trigger an alarm reporting, and update of the repeater setting.

Changes in the backhaul transmission gain affect the repeater performance and its coverage area. The Automatic Gain Control (AGC) loop varies the repeater gain in a way that compensates for the transmission gain change. The AGC equalizes the backhaul transmission gain with no interference with the network. Both the AMLC and AGC loops are operated independently in FL and RL.

Radio optimization by automatic gain corrections was devised for backhaul balancing [9].

7.2.6.1 AMLC

Automatic Maximum Level Control (AMLC) is defined as automatic transmit gain changes with the Tx power level as the objective parameter.

Figure 7-18 presents a schematic diagram of the AMLC loop. The RF power level out of the HPA is measured by a detector, and smoothed by a low-pass filter. The detected level is compared with a reference level (corresponding to the maximum Tx power out of the HPA). If the level exceeds the maximum power, the variable attenuation is increased at a rate determined by the loop gain parameter μ. The correction halts when the detected Tx power matches the reference level. Note that the AMLC operates only on attenuation values $L \geq L_{SET}$, where L_{SET} is the attenuation value set during commissioning.

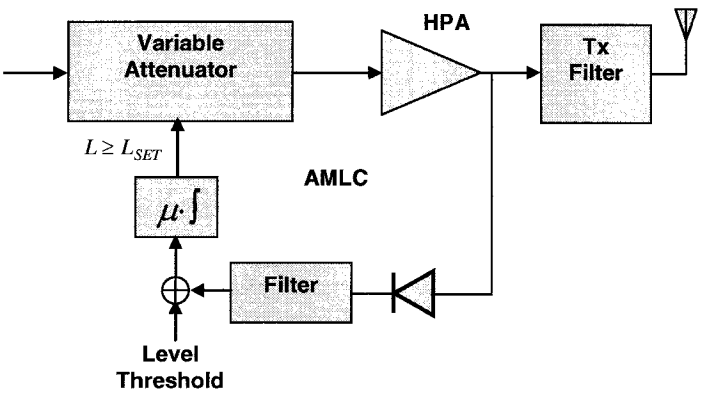

Figure 7-18. AMLC block diagram

The dynamic range of the AMLC may be anywhere from 15 dB and up to 30 dB, with time constants ranging from 10 ms to 100 ms. The AMLC level is commonly set a few dB above the maximum *linear* Tx power.

7.2.6.2 AGC

Automatic gain control (AGC) is defined as automatic receive gain changes with the received power level as the objective parameter.

Figure 7-19 is a schematic diagram of the AGC loop. The AGC stabilizes the backhaul transmission gain variations. To that end a dedicated signal termed pilot-signal (not related to the CDMA pilot) is transmitted at a fixed level from one end of the backhaul, independently of the CDMA traffic. The received pilot-signal level is detected and used to correct for any changes in the backhaul transmission gain.

The received pilot-signal is filtered by the BPF and then detected and smoothed by a low-pass filter. The detected level is compared with a reference level that is determined during the repeater commissioning (the *set level*).

The difference value is used to correct for backhaul dynamics at a rate determined by the loop gain parameter μ. The correction stops when the detected Tx power matches the reference level. Note that the AGC responds to positive or negative level changes.

The dynamic range of the AGC may be anywhere from 15 dB to 30 dB, with time constants from seconds to minutes.

The AGC may be used to simplify the commissioning process. By applying a desirable *set level*, the AGC will automatically strive to position the repeater gain at the appropriate setting.

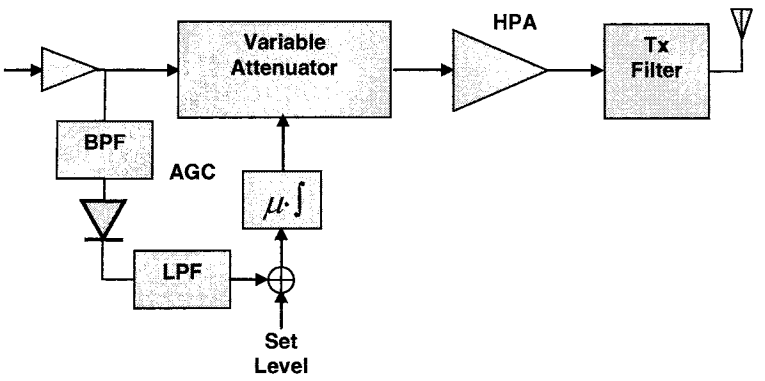

Figure 7-19. AGC block diagram

7.2.7 Antennas in Repeater Systems

The antenna theory pertinent to repeater applications was presented in Chapter 3. In this section we briefly introduce the reader to antenna types that are employed in outdoor repeater applications.

The antennas that serve in repeater applications may be classified according to their function, backhaul or service antennas, and by frequency bands. Table 7-3 presents typical antenna types and gain in dBi according to this classification.

Table 7-3. Repeater antenna types

Antenna Type (Gain [dBi])	Frequency Band	
	Cellular	PCS/MW
Function Service	Panel (15.5) (Dipole array)	Panel (17.5) (Dipole array)
Backhaul	Panel (17) Yagi (19) Grid dish (17)	Dish (24/30+)

✓ Service antennas: Outdoor repeaters employ service antennas that are available and common in BTS installations. Panel arrays are applied in sector and highway coverage, with H-plane beamwidth from 30° to 105°. Parabolic reflector ('dish') antennas may also serve for highway coverage. Vertically polarized colinear arrays that are omnidirectional in H-plane are used for omni coverage. Multi-band antennas are applied in multi-band repeater applications, simplifying the installation and zoning problems.

✓ Backhaul antennas: The backhaul antennas are compromised based on several constraints:

Size/shape: minimal size is sought for reduced tower wind load, tower rental cost and zoning objections. It is possible to maintain high gain (thus larger size) antennas with good wind load performance by employing wire-like structures, including Yagi and grid dish backhaul antennas.

Gain: high antenna gain improves the backhaul transmission gain budget. The benefit is two-fold: a) the remote unit gain may be reduced; and b) the isolation requirement between the service and backhaul antennas at the remote site is reduced. This is particularly important with OFR and in-band F1/F2 repeaters.

Sidelobes: the sidelobe level (SLL) affects isolation between the service and backhaul antennas at the remote site. Low SLL antennas are advantageous with OFR and in-band FSR repeaters.

7.3 Repeater Design

The repeater gain and power design is based on transmission gain (Cf. Chapter 6) and backhaul engineering (Cf. Chapter 8) considerations. Simplistically stated, any RF repeater operates within two power constraints imposed at its donor BTS and service ends; The repeater coverage requirement, number of served carriers and the donor BTS traffic load translate into a maximum Tx power specification for the repeater. On the other end, the BTS RF characteristics, including maximum Tx power per carrier and Rx sensitivity, are quite standard and allow for definition of the RF interface with the repeater, including the required power levels.

The transmission gain budget implemented in the repeater units depends on the specific repeater type, the backhaul characteristics, and the number of CDMA carriers. The backhaul budget considerations are further addressed in Chapter 8.

In this section we review the FL and RL design rules that lead to required gain and power values for different types of repeaters. Classic RF chain design rules for gain, noise and linearity performance are augmented by CDMA radio network considerations, including preservation of signal integrity under heterodyning, filtering and antenna coupling operations.

7.3.1 Basic Design Rules

7.3.1.1 Link Design Rules

FL design

The repeater FL objectives are to deliver the CDMA FL signals to the mobile users, at an adequate level, while complying with the FL emission mask and signal fidelity requirements. The FL design is dominated by emission mask considerations (Section 7.4). The unwanted emission results from intermodulation products (IMs) that are generated mainly by the high-power amplifier, and thermal noise. The system linearity is critical to emission mask compliance for small frequency offsets. IM products decay fast with frequency offset from the desired carriers, and become negligible for 5th and higher orders, leaving the far-out noise to become the design constraint. The spillover noise into an adjacent band may be further restricted by colocation requirements.

The CDMA repeater FL maximal Tx power is determined according to the coverage, the number of carriers and per-carrier traffic level.

The per-carrier pilot power in FL is a measurable reference level parameter that is independent of traffic. Thus it is convenient to base the FL analysis on pilot power, and then correct for the traffic additional load. The pilot power is preset at the BTS at about 10% to 15% of the maximum total carrier Tx power (-10 dB to -8.24 dB off the carrier maximum power)[28]. In the sequel we use an average value of -9 dB (corresponding to pilot set level P_p of 12.6% of the full BTS Tx power P_T), which may be corrected in specific cases according to the actual pilot set level.

The maximum repeater service Tx power $P_{S(Total)}$ with K carriers is thus (Eq. (7-9)):

$$P_{S(Total)} = Pp + 9 + 10 \cdot \log_{10} K\,[dBm] \tag{7-9}$$

where P_p denotes the repeater pilot Tx power. In some cases the pilot level at the repeater may not be available. In such cases assume that the measured total RF power per carrier is directly proportional to its relative traffic load (in % of the maximum traffic at full BTS power P_T)[29]. Using the definitions above for the BTS pilot power and full power, we define *headroom* as the ratio between the maximum and actual power at a given traffic load, expressed in dB, Eq. (7-10):

$$Headroom = -10 \cdot LOG_{10}[P_p/P_T + (Traffic\%/100) \cdot (1 - P_p/P_T)],\,[dB]. \tag{7-10}$$

This defines the dB-margin by which the FL power may rise for higher traffic.

The paging and synch channels were ignored, and uniform power was assumed for the traffic channels. Table 7-4 summarizes the headroom for several traffic loads. The FL emission mask requirements (Section 7.4.6) enter into the FL design by careful control of linearity and noise performance.

Linearity: the HPA linearity is critical to emission mask compliance. The HPA Tx power is defined at a higher level than the specified output due to the duplexer Tx filter loss. The performance depends on the number of carriers and the number of codes.

---

[28] Green-field networks experiencing low traffic loads are typically set with pilot level at ~15%, while heavily loaded networks employ reduced pilot levels of ~10% of the maximum power.

[29] The actual BTS FL Tx power depends on the users' distribution and radio location (indoor or outdoors) within the cell.

Table 7-4. RF repeater FL power headroom for gain setting at known load Tx_{Max} for single-carrier. For K carriers replace Tx_{Max} by $Tx_{Max} - 10 \cdot \log_{10} K\,[dBm]$

Traffic %	Headroom [dBm]	Tx Power [dBm]
0%	9.0 dB	$Tx_{Max} - 9.0$
10%	6.7 dB	$Tx_{Max} - 6.7$
25%	4.6 dB	$Tx_{Max} - 4.6$
50%	2.5 dB	$Tx_{Max} - 2.5$
100%	0.0 dB	Tx_{Max}

The monotonic linearity must be verified at maximum Tx power, and down by at least -10 dB. The linearity performance of the repeater low-power FL RF circuitry must be guaranteed to produce negligible spurii relative to the HPA.

Noise: the output noise density must be low enough by the emission mask clearance requirements. The out-of-band noise becomes the dominant contributor to out-of-band emission at far-out frequency offsets, including adjacent bands and the repeater RL FAs. By applying band-pass filtering prior to the HPA it is possible to control the output noise spillover to acceptable levels (see Section 7.2.5). For example: assume a required mask clearance of 50 dB at frequency offsets with negligible IM products, and a +43 dBm CDMA2000 single carrier transmission. The output noise may be as high as -7 dBm in one carrier bandwidth. Assuming a broadband repeater with 6 dB FL noise figure, the equivalent input noise density is then –113+6 = –107 dBm/1.25 MHz. Thus the repeater maximal gain may be -7 – (–107) = +100 dB! The input minimal signal level is then +43 – 100 dB = –57 dBm. With a channel selective repeater the out-of-band noise is attenuated, making higher gain values possible.

RL design

The RL repeater set gain is determined primarily by the desired BTS noise rise. The RL sensitivity is defined as the minimum RL input signal power required to produce an acceptable E_b/N_0 (or equivalently a FER) value, and is related to the effective noise factor at that port. Given the cell and repeater noise factors it follows from Eq. (6-4) that the net gain y of the repeater determines the RL sensitivities of the donor cell and the repeater. The two extreme cases are $y \to \infty$ and $y \to 0$ representing the dedicated donor cell (serving only repeater traffic) and decoupled repeater (from donor cell) cases, respectively. Setting the net gain y solely determines the relative contribution of the repeater noise to the donor cell thermal noise (see Eqs. (6-3b) and (6-

4c)). Also, fixing the RL gain of the repeater defines the relative coverage of the donor cell and the repeater (Cf. Eq. (6-9)). Thus, RL noise and sensitivity are key to the repeater RL design and tuning. A common setting practice is to measure the donor cell noise rise level during low traffic hours, such as at night or early morning, with and without the repeater, and set the gain y such that a desired noise rise change is achieved with the repeater (e.g. a value of +1 or +2 dB for coverage applications).

In addition to the RL gain and noise considerations, the Tx power specifications of the remote unit must be set, with the RL power amplifier characteristics. RL transmissions are affected by the *dynamics* of the CDMA signals, leading to the following arguments:

1) In applications with $y<1$ the repeater has limited effect on the donor cell coverage. The resulting small thermal noise rise at the donor cell due to the repeater, e.g. $\delta = +0.7\ dB$, translates into a repeater coupled noise level that is low, relative to that of the BTS, namely: $10\log_{10}\left(10^{0.1\delta}-1\right) dB$, or $-7.6\ dB$ with above rise of 0.7 dB. The RL Tx power of the STs in the repeater served area is determined according to the fast power control commands from the donor cell. The STs are received at the BTS at equal average power, relative to the BTS noise floor and total number of active STs (Cf. Eq. (4-3) and Fig. 4-1). The signal-to-noise power ratio of the repeater transmitted signal must be higher than that at the BTS by $[\delta - 10\log_{10}\left(10^{0.1\delta}-1\right)]\ dB$, e.g. 8.3 dB in above example; another example is illustrated in Fig. 7-20. Thus, based on a planned y value, a margin may be defined relative to the repeater noise. We round up this margin to +10 dB.

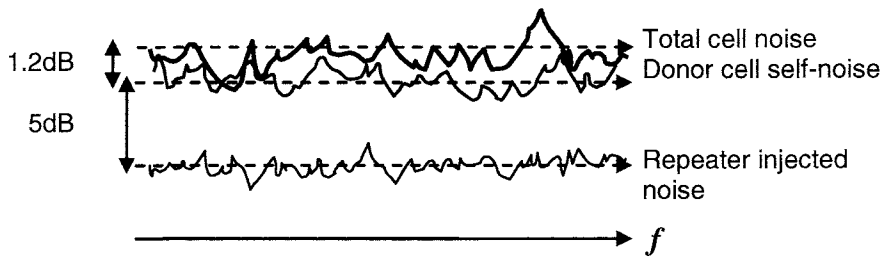

Figure 7-20. BTS thermal noise components

2) The RL donor cell total *average* input power rises with the overall donor cell traffic by up to ~8.5 dB[30] above the thermal noise level, as shown in Fig. 4-2. This is due to the interference from other users whose spread spectrum transmissions are uncorrelated (Cf. Fig. 2-2). The repeater RL maximum Tx power must account for this load dependent power rise, rounded to ~9 dB. Note that the Tx power of the repeater-served STs increases according to the donor cell traffic rather than that carried by the repeater.

3) The accuracy of the RL open-loop power control is ~8 dB, mainly due to the *uncorrelated* fading in FL and RL. The response time of the open-loop is ~30 ms and it compensates for fading at slow speed. The RL closed-loop power control is a fast loop, responding at $\leq$ 1 dB/1.25 ms (CDMA2000). Thus, there may be short over-power bursts by accessing users at times their FL is fading more than their RL. These are corrected for within less than 10 milliseconds by the closed-loop power control. These bursts are higher at the repeater whose net gain is lower than unity ($y < 1$), and even more – when the repeater RL and FL gain is not properly balanced. These "spikes" are most noticeable during periods of low traffic activity, when a change in the power level of a single user affects the noise rise appreciably, but diminishes when traffic load is high. As an example, with 30 users an 8 dB rise per single user amounts to a total power increase of 6/30, or ~1 dB. Moreover, their effect is further diminished in a multicarrier transmission through the repeater. Thus, as much as these "spikes" are noticeable at the repeater RL, their impact on its peak power is no more than about 2 dB.

In view of the above arguments, we summarize for the repeater's RL RF chain that it should provide for *undistorted* power P_R which is ~10+9+2 = 21 dB above the thermal noise level, or

$$P_R = -114 + 10 \cdot \log_{10}(B\ [MHz]) + F_R[dB] + G_R[dB] + 21,\ [dBm]. \qquad (7\text{-}11)$$

Example: Let the repeater net gain y be set such that the repeater's RL noise at the donor cell is 5 dB below the cell thermal noise floor (the donor cell thermal noise rise will thus be 1.2 dB). The repeater RL transmissions' SNR will be 6.2 dB more than the SNR of the transmissions at the donor cell. Figure 7-20 illustrates the donor cell thermal noise components.

The CDMA signals and the combined donor cell noise are illustrated in Fig. 7-21, including rise due to traffic and access probe overshoots.

Continuing the example, the repeater RL RF chain must accommodate a maximal Tx power level of ~6.2+9+2 = 17.2 dB above thermal noise level.

---

[30] This is a limit set by the operator.

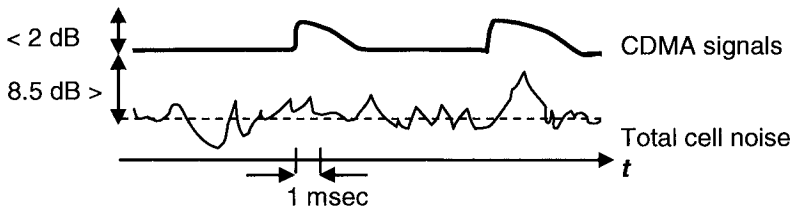

Figure 7-21. Levels of RL CDMA signals relative to the noise

We adopt the following rule for the repeater RL minimum Tx power specification:

$$P_{RR} = -113 + F_{RR} + G_{RR\_\max} + 10 \cdot \log_{10} K + 21[dBm] \tag{7-12}$$

where the variables $P_{RR}, F_{RR}, G_{RR\_\max}, K$ denote the RL *linear* maximum Tx power [*dBm*] , RL noise figure [*dB*], RL maximum gain [*dB*], and number of carriers, respectively. Note that with WCDMA carriers the bandwidth dependent constant –113 should be replaced by –108. The power-margin beyond the noise level was set to +21 dB.

Note: The above discussion assumed a *balanced repeater* setting. FL - RL imbalance may result in even higher power overshoots, due to wrong transmit adjust setting. These are further discussed in Section 10.3.

7.3.1.2 RF Chain Design

The RF chain design is based on the following main requirements: frequency band and bandwidth, number of carriers, definition of backhaul conduit characteristics (frequency band and bandwidth, length, transmission maximum and minimum gain, interference), input signal power range, interference input levels and frequency bands, output power (maximum, range, and gain step size), unwanted emission constraints (including special coexistence constraints), RL sensitivity, distortion limits, power supply voltage and range, and environmental conditions (indoor/outdoor deployment, temperature range, etc.).

RF chain design is a well-established art. We highlight the main issues that enter into a repeater RF design:

1) Well-controlled chain design G, NF, 1 dB headroom, IP3. Variable attenuator location and control sequence for optimized noise and linearity performance (this involves a cut and try process).

2) Frequency plan, image rejection, image attenuation, and avoiding end-to-end spectral mirroring.

3) Synthesizers' frequency range and step size, phase noise, and frequency jitter (average, RMS, peak errors).

4) Filters' specifications (rejection, insertion loss and pass band ripple, attenuation slope, ultimate rejection), filter technology, location along the RF chain, through levels and power rating.

5) Controlled leakage and isolation between high-gain modules, diversity branches, and FL/RL signal paths.

6) RF monitoring ports.

The positive difference between the compression point and expected actual maximum signal levels defines the *headroom.* The headroom is a *backoff* measure (from saturation) that is defined along the RF chain and enables the linear system operation. An important constituent of any repeater is the high-power amplifier. Efficient power amplifiers employ advanced linearization techniques (e.g. predistortion, bias modulation, or feedback) to achieve clean high-power signals at reasonable efficiencies (~10%).

Definitions of the radio requirements from a repeater, and corresponding test definitions are specified in type-approval standards (e.g. [2], [3]).

7.3.1.3 Distortions Control

The parameters that quantify signal distortion were introduced in Section 7.2.1.1. Distortion may be caused by selective filtering, heterodyning and additive noise. An ideal system that exhibits constant gain and linear phase over a frequency pass band is distortion free. We consider in the sequel deviations from this ideal behavior as manifested in the distortion measures, including gain ripple, group delay variations, phase noise, and frequency error.

Group delay

Linear phase (over the frequency pass band) corresponds to a fixed group delay. This parameter affects the signals that pass through the repeater and requires adjustment of the search window (Section 6.7) to allow for service by the repeater. The group delay is a direct function of the repeater selectivity, and increases with filtering attenuation slope. The group delay may vary from several hundreds of nsec and up to 16 μsec, depending on the repeater type (band or channel selective, F1/F1 or F1/F2, etc.) and the number of selective filters along the RF chain. The propagation delay (over-the-air or in a fiber conduit) is usually not specified as part of the repeater equipment, but it should be accounted for when adjusting the search window.

Group Delay Variations (GDV)

The nominally fixed delay exhibits a delay ripple (or - equivalently, deviations from linear phase) over the frequency pass band of the repeater, which contributes to the signal distortion.

The phase is related to the group delay as[31]

$$\phi = 360 \cdot \int \tau \, df, \quad [^\circ] \tag{7-13}$$

and for a delay step $\Delta\tau$ (as a function of frequency), the phase change is

$$\Delta\phi = 360 \cdot f \cdot \Delta\tau, \quad [^\circ]. \tag{7-14}$$

A step delay variation of 100 nsec (from "zero" reference, in frequency domain) results in a linear phase variation at a rate of 36°/1 MHz. Filters do not assume delay variation steps, but rather wavy delay variations that wiggle about the fixed average delay (in frequency domain). A narrow band filter may exhibit several delay variation cycles over the carrier bandwidth, as illustrated in Fig. 7-22. Modeling the delay variations by a sinusoidal waveform $\tau = \Delta\tau \cdot \sin\left(2\pi f / (4f_0)\right) = \Delta\tau \cdot \sin\left(\pi f / (2f_0)\right)$ we get

$$\begin{aligned} \Delta\phi &= 8 \cdot \Delta\tau \cdot f_0 \cdot \sin^2\left(\frac{\pi f}{4f_0}\right), \quad [radian] = \\ &= \left(\frac{1440}{\pi}\right) \cdot \Delta\tau \cdot f_0 \cdot \sin^2\left(\frac{\pi f}{4f_0}\right), \quad [^\circ]. \end{aligned} \tag{7-15}$$

In the above example, the maximum phase deviation occurs at $2f_0$, and it is 36° for the stepped delay variation, and 22.9° for the sinusoidal delay variation.

The phase deviation with frequency causes a reduced correlation value, due to the phase mismatches over the frequency bins, and consequently Rho (Eq. (7-4)) may be expressed as

$$Rho = \frac{\sum_i \cos(\Delta\phi_i)}{\sum_i 1}. \tag{7-16}$$

---

[31] The group delay is $\tau = d\phi/d\omega$, thus $\phi = \int \tau \, d\omega = 2\pi \int \tau \, df$ $[radians]$.

A numerical evaluation of Rho for the sinusoidal delay variation in Fig. 7-23 yields Rho=0.9703. If f_0 is reduced 10-fold, with the same GDV (100 nsec), then Rho becomes 0.9997.

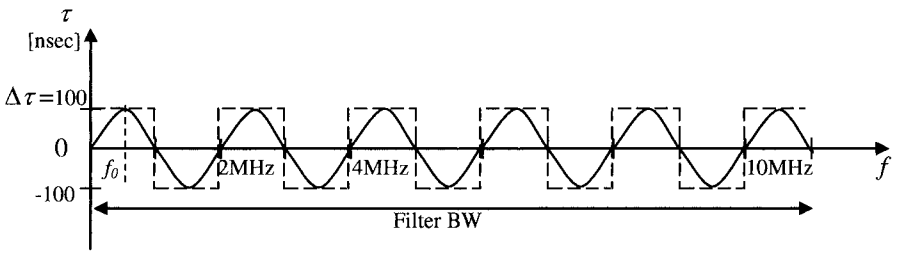

Figure 7-22. Cycles of group delay variations over a frequency band

Gain ripple

A reference CDMA signal $X(f)$ with an amplitude ripple function $\alpha(f)$ (assume no phase ripple) produces an output value $\alpha_i X_i$ for an input signal value X_i at frequency f_i. The Rho factor (Eq. (7-4)) then assumes the form

$$Rho = \frac{\sum_i X_i \cdot \alpha_i X_i}{\sqrt{\sum_i X_i^2}\sqrt{\sum_i \alpha_i^2 X_i^2}} = \frac{\sum_i \alpha_i X_i^2}{\sqrt{\sum_i X_i^2}\sqrt{\sum_i \alpha_i^2 X_i^2}} \,. \tag{7-17}$$

With small gain ripple, let $\alpha_i = 1+\varepsilon_i$, where the amplitude ripple ε_i may assume positive or negative values (e.g. a ripple of ±0.75 dB corresponds to $|\varepsilon_i| < 0.1$). Substitution in Eq. (7-17) yields

$$Rho = \frac{\sum_i (1+\varepsilon_i) X_i^2}{\sqrt{\sum_i X_i^2}\sqrt{\sum_i (1+\varepsilon_i)^2 X_i^2}} \,. \tag{7-18}$$

If $X_i = 1$ for all i (a flat reference signal spectrum), then

$$Rho = \sum_i (1+\varepsilon_i) \Big/ \left(\left(\sum_i 1 \right) \left(\sum_i (1+\varepsilon_i)^2 \right) \right) \,. \tag{7-19}$$

For ε_i uniformly distributed in ±0.08 (linear scale), Rho assumes values around 0.999.

Frequency offset

Frequency offset results from instantaneous frequency shifts within the heterodyne repeater. Both *average* and *peak* frequency errors must be specified for quality and uninterrupted service[32]. Narrow band filtering at IF that relies on frequency heterodyning, with the same LO serving for down and up conversion, results in nil frequency offset. A band RF repeater (or booster) that performs filtering and amplification with no heterodyning operations, or an optical fiber repeater with optical intensity modulation and detection, do not cause frequency offsets.

FSR type repeaters that rely on two distant units, with frequency shifting operations performed in each unit, require special attention regarding frequency offsets.

When the oscillators are realized employing synthesizer techniques [10], the accuracy hinges upon the reference clock accuracy $\lambda = \delta f / f_0$, where f_0 is the clock nominal frequency and δf denotes its frequency instability. A frequency shift operation that is based on synthesizers employing a common reference clock, results in an error Δf :

$$\Delta f = \lambda \cdot (f - f') \tag{7-20}$$

where $(f - f')$ is the frequency shift. Thus, in-band FSR that performs relatively small frequency shifts (e.g. < 25 MHz) requires a reference clock with accuracy of the order of

$$\lambda = \Delta f / (f - f') \approx 40/25 \cdot 10^6 = 1.6 \ ppm. \tag{7-21}$$

In contrast, an out-of-band FSR executes frequency shifts of hundreds or thousands of MHz, and requires very stable reference clocks (atomic, or GPS-based sources). As an example, a 900 MHz to 1900 MHz FSR requires a reference clock (Eq. (7-21)) of $\lambda \approx 40/10^9 = 0.04 ppm$. With independent reference clocks employed in the donor and remote units, the overall worst-case service frequency error Δf is the sum of frequency errors of the units. Repeaters that incorporate a dedicated modem function between the donor and remote units may employ automatic frequency locking (AFL), with the remote unit locking onto the donor unit clock. This slow control loop is used to correct for long-term drifts in the clocks. If the backhaul frequency accuracy is relatively relaxed (as with MW backhauls), the AFL reduces the end-to-end frequency error to minimum (practically a few Hz). In case the backhaul frequency error must be accurately controlled as well, then one

[32] A frequency error < 40 Hz is considered an acceptable value.

accurate reference clock is required in the system, preferably located at the donor unit.

Phase error

The repeater synthesizers are non-ideal frequency sources, incorporating phase noise that causes parasitic modulation of the relayed signals [11]. To preserve the fidelity of the relayed signals, the synthesizers' phase noise must be low enough to cause less than an acceptable level of distortion (including EVM and Rho) of the desired signals.

The oscillator phase noise is observed in frequency domain as the spectral regrowth around the carrier frequency, and its spectral density is measured as a function of the offset and relative to the carrier frequency in dBc/Hz. Phase noise for a fixed-frequency synthesizer ('non-hopping') can be made very low, and depends mostly on the VCO performance (Fig. 7-23).

For illustration, a reasonably good 900 MHz band synthesizer phase noise performance is: –90 dBc/Hz @10 KHz, –113 dBc/Hz @100 KHz and –125 dBc/Hz @1 MHz offsets.

The RMS phase noise is calculated by integration of the power spectral density of the synthesizer signal [12]. The integrated phase shift enters the evaluation of Rho, as in Eq. 7-16. The effects of the phase noise on Rho are negligible; if the RMS phase noise is $\sigma°$, then by a Normal approximation, the 67% confidence level phase is $\pm\sigma°$, and $\pm 3\sigma°$ for 95% confidence. For a typical value of phase error $\sigma° = 3°$, $3\sigma° = 9°$. Thus, from Eq. 7-16, the Rho factor is lower bounded (with probability 95%) by cos (9°) = 0.9877.

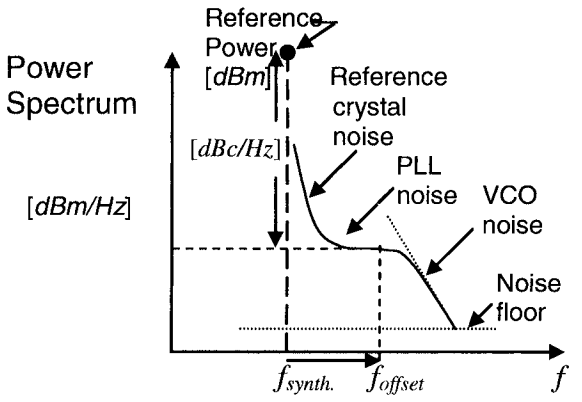

Figure 7-23. Phase noise of a synthesizer

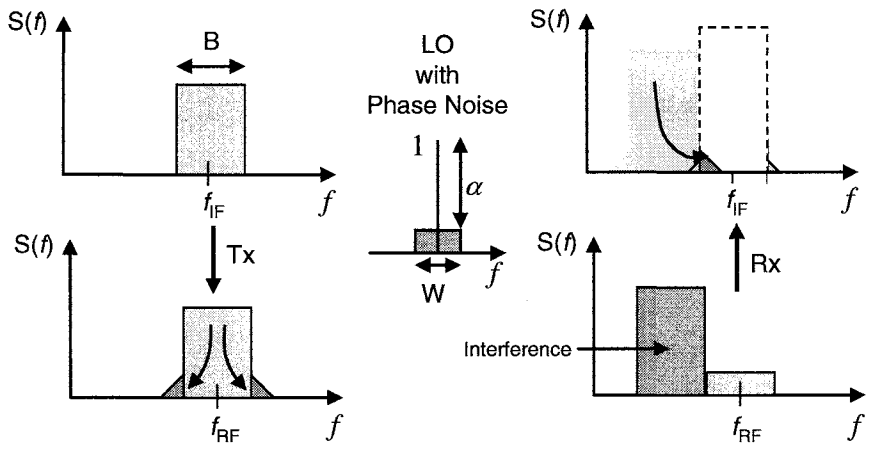

(a) Emission mask (b) Selectivity

Figure 7-24. Synthesizer phase noise degradation of emission mask and selectivity

The main reasons for keeping the phase noise of the synthesizers low are borrowed from those applied in radio transmitters and receivers' design. Figure 7-24 demonstrates the phase noise distortions in the Tx and Rx paths. A non-perfect local oscillator (LO) with phase noise that is modeled as a rectangular pedestal of level α $[Hz^{-1}]$ relative to the LO, and of bandwidth W, is depicted at the center of the figure. With the pass bandwidth denoted as B, we have W << B. The undesirable anomalies in Tx and Rx are readily explained by viewing mixing (which is multiplication in time-domain) as convolution in frequency domain. In Tx (Fig. 7-24a, from top downwards) the non-perfect heterodyning introduces adjacent out-of-band spillover that must be controlled for emission mask compliance. In Rx (Fig. 7-24b, from bottom upwards) the adjacent channel interference must be rejected while serving the desired weak signal at f_{RF}. Due to the LO phase noise, some residual power leaks into the IF bandwidth prior to the selective filtering operation. Thus, the LO phase noise interferes with the selectivity of the down-conversion operation.

7.3.1.4 Interlink Chain Effects

The FL and RL operate simultaneously on separate frequency bands. This helps in minimizing parasitic coupling effects between the links within the repeater unit. The duplexer couples the two links with a single antenna, and constitutes an interlink junction. The spatial coupling between antennas in F1/F1 and F1/F2 repeaters is another source for interlink effects.

The Tx and Rx interactions on each end of the repeater are borrowed from common radio transceiver design as follows:

✓ Tx channel signal leakage into Rx input: The high-power Tx signal at the Tx FA is attenuated by the Rx filter of the duplexer. A strong enough residual Tx signal at the Rx input may saturate the Rx LNAs and desensitize the RF receive chain. Thus, the duplexer Rx filter must attenuate the Tx signal to a level that is less than the Rx input 1 dB compression point. This guarantees unsaturated linear processing by the front-end up to a selective filter that further attenuates the residual Tx signal.

Conclusion: Knowing the transmitter maximum power *into* the duplexer, then the Rx input compression level *and* the duplexer Rx filter attenuation at the Tx frequency must be *jointly* specified.

✓ Tx noise and spurii (IMs') leakage into Rx input: The wideband Tx noise at the Rx FA is attenuated by the Tx filter of the duplexer. The residual noise appears at the Rx input and adds to the Rx effective noise; this noise leakage must be well controlled to avoid degradation of the Rx channel sensitivity. Thus, the Tx filter of the duplexer must attenuate the noise at the Rx frequency to a level that is negligible relative to the front-end effective noise of the Rx channel (-10 dB leakage relative to the Rx effective noise would increase the noise figure by approximately 0.4 dB).

Conclusion: Knowing the Rx input effective noise level (includes the Rx noise figure), then the transmitter wideband noise and IM's power at Rx frequency *into* the duplexer *and* the duplexer Tx filter attenuation at the Rx FA are *jointly* specified such that the Rx front-end sensitivity degradation will be less than a specified value (e.g. 0.4 dB).

The coupling between backhaul and service antennas yields additional effects. In OFR systems, the main effect is oscillations (Cf. Chapter 6) that occur on each link separately, thus this by itself is not an interlink phenomenon. However, oscillations cause saturation of the link RF chain; as a result, the uncontrolled out-of-band spurii may overwhelm the other link as well.

A high enough power of an out-of-band residual Tx signal of one link may affect the opposite link in a case where the combined antennae isolation and the duplexer Tx-Rx attenuation is not sufficiently high. Such interlink effects may render the repeater ineffective. These effects become evident with in-band F1/F2 repeaters, particularly with small frequency shifts, and even more so due to the very high gain employed. These issues are discussed below (Section 7.3.5).

7.3.2 RF F1/F1 Repeater

The RF repeater constitutes an approximated linear RF network that performs bidirectional filtering and amplification with minimal signal distortion, additive noise put aside. The architecture is based on a full-duplex RF chain as depicted in Fig. 7-25.

The repeater is connected to antennas on both ends. As the FL and RL paths have a similar structure, we review just *one* of them. The antenna is connected to a Tx/Rx port of a duplexer, with suitable filtering characteristics and RF power rating. The Rx port of the duplexer feeds an LNA that pre-amplifies the weak received signal. A selective band-pass filter, of appropriate bandwidth, selectivity, group delay ripple and sufficient ultimate attenuation, filters the preamplified signal. The filter bandwidth is determined according to the type of repeater – band or channel selective.

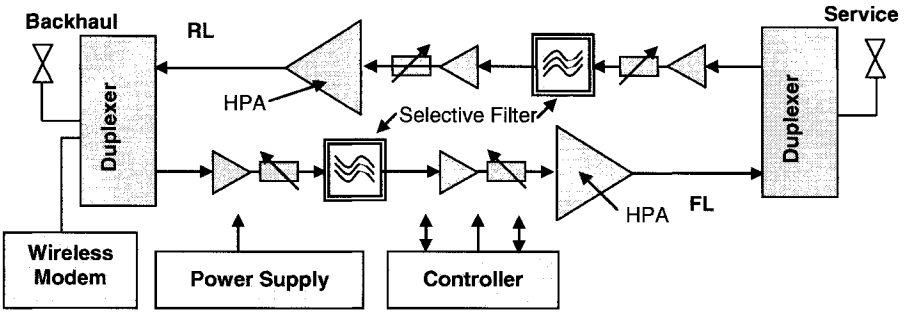

Figure 7-25. RF repeater architecture

The selective filter may be realized using a heterodyne approach as depicted in Fig. 7-26, with filtering performance advantage and flexibility. The RF signal that has been filtered by the duplexer and any additional broadband filter (e.g. ceramic or dielectric) is frequency shifted into a lower intermediate frequency (IF) using a local oscillator (LO). The IF signal is filtered by a selective (e.g. SAW) filter, and possibly amplified at the IF level, then shifted back to the original RF frequency using the same LO. Employing a common LO, as shown in Fig. 7-26, eliminates frequency errors. The selective filter channel is determined by the LO frequency, and may be varied over a specified frequency band.

Further amplification at RF frequencies may be employed past the selective filter in Fig. 7-26, accompanied by additional filtering (e.g. ceramic) that attenuate wideband noise out of the channel band.

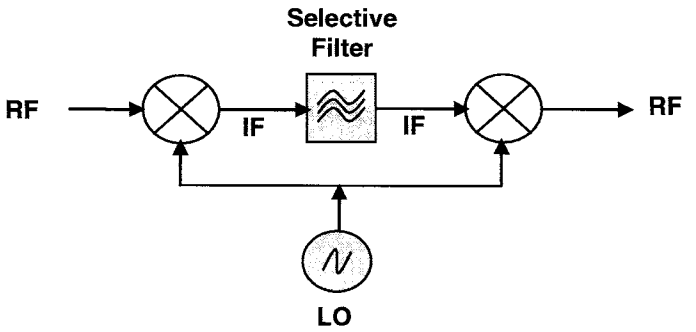

Figure 7-26. OFR selective filter heterodyne realization

Residual noise at the output, after duplexer attenuation, may couple into the opposite link input and deteriorate its noise figure.

Sufficient suppression of the wideband noise therefore has to be provided. Finally, a high-power amplifier is reached, which boosts the RF signal to the required Tx power; this signal is fed to the Tx port of a duplexer and reaches the antenna through the common (Tx/Rx) port of the duplexer.

The controller handles all the repeater management functions, including control of programmable hardware (e.g. digital attenuators, synthesizers, switches, etc.), generation of alarms, performing various automatic functions (such as AMLC, monitoring and processing, etc.), and communicates with the wireless modem and the RNMS center (via the wireless modem).

It is possible in specific realizations to separate the functions among several controllers, e.g. one handling all the communication functions while another performs the repeater internal management tasks. The reader is directed to Sections 7.2.1.2 and 10.2.1 for additional discussion on network management.

Figure 7-27 presents a block diagram of the RF repeater to illustrate the gain and power analysis. The arguments to follow are per Section 7.3.1.1. Denoting by:

P_T	the BTS Tx power per carrier
K	the number of carriers
kT_0BF	the equivalent system thermal noise in bandwidth B and noise factor F
$G(\theta_R)$	the BTS antenna gain (relative to isotropic) in the repeater direction
$T_I(d_R)$	the transmission gain between the BTS and the repeater separated by distance d_R

G_B	the gain of the repeater backhaul antenna (relative to isotropic)
P_{RF}, P_{RR}	the repeater FL, RL total Tx power
G_{RF}, G_{RR}	the repeater FL, RL gain
$G_{F\max}, G_{R\max}$	the repeater FL, RL maximal gain
$P_{F\max}, P_{R\max}$	the RL Tx power margin relative to noise
M	the repeater maximal Tx power

The repeater FL gain-power budget is

$$P_{RF} = P_T K\ T_I(d_R) G_{RF} \tag{7-22}$$

subject to

$$G_{RF} \le G_{F\max} \text{ and } P_{RF} \le P_{F\max}\ . \tag{7-23}$$

Similarly, the repeater RL gain-power budget is

$$P_{RR} = (kT_0 BF) K G_{RR} T_I(d_R) M \tag{7-24}$$

subject to

$$G_{RR} \le G_{R\max} \text{ and } P_{RR} \le P_{R\max}\ . \tag{7-25}$$

Note that the repeater transmits in FL the full BTS traffic, and in RL the ST's power is adjusted according the BTS noise rise (including the BTS full traffic) and not just the repeater traffic and noise floor. These affect the maximum specified power (Eqs. (7-23), (7-25)).

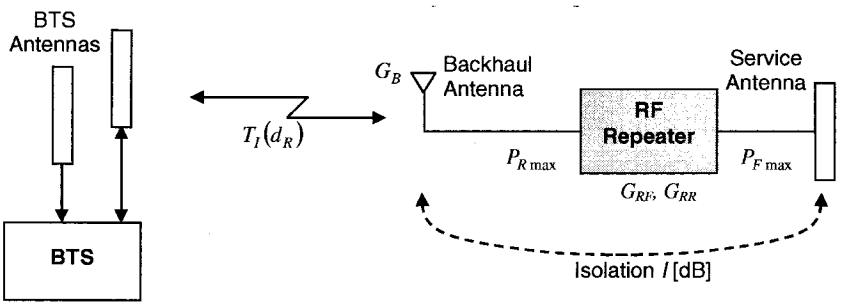

Figure 7-27. RF repeater gain-budget block diagram

The repeater FL and RL gain is practically limited to $G_{\max} \approx 95$ dB due to the following reasons:

✓ Oscillations (see Chapter 6). The isolation constraint is:

$$I > G + 15\,[dB]. \tag{7-26}$$

Higher gain values impose isolation values that require excessive separation of antennas. This is problematic in tower mount installations and undesirable operationally.

✓ Emission mask (see Section 7.4.6). Very high gain translates into lower input signal level. Also the higher repeater gain results in high out-of-band noise density that must be attenuated by the repeater filters. These make very high gain band OFR's less attractive.

✓ Adjacent channel interference is a major operational parameter in co-located networks. The repeater out-of-band gain is required to be suppressed so as to meet these requirements. The repeater selectivity and maximum in-band gain determine the out-of-band gain. This constrains the maximum in-band gain.

Example: Assume a 1900 MHz BTS with maximum Tx power per carrier of +42 dBm, and perform the calculations for maximum power levels. Let the BTS employ a 60° sector antenna with gain of 17 dBi. Let a 10 W single-carrier repeater be located at 15° off the sector boresight, 6.6 km away from the donor BTS. The repeater backhaul antenna gain is 24 dBi. We estimate first $G(\theta_R)$ using a parabolic approximation to the main lobe dB-pattern (Cf. Chapters 3 and 4):

$17dBi - 3 \cdot \left(2 \cdot 15° / 60°\right)^2 = 16.25dBi$. For a free-space[33] unobstructed path between the BTS and the repeater, the transmission gain is then[34]:

$T_I(d_R) = 16.25 - [32.45 + 20\log(1900\text{MHz}) + 20\log(6.6\text{Km})] + 24 = -74.166$ dB.

Finally by Eq. (7-22): $+40 = +42 - 74.17 + G_{RF}$, or $G_{RF} = 72.17dB$. Thus, the repeater gain setting in FL should be ~72 dB.

---

[33] In case of ground propagation the expression for $T(d_R)$ should be modified, see Section 3.2.4. Note that the knee point between R^2 and R^4 propagation is *4 kHh*. With the repeater antenna raised, say H=30 m, that means 20 times the knee distance for the user on the ground. It is safe to assume that the donor antenna in the repeater is in the R2 range in most cases.

[34] The path geometric free-space attenuation L between isotropic antennas is $(4\pi d/\lambda)^2$ or, invoking $\lambda[m] = c/f \approx 300/f[MHz]$, the dB-scale result is:

$L[dB] = 32.45 + 20\log(f\ \text{MHz}) + 20\log(d\ \text{Km})$.

The *minimum* repeater gain is typically 30 dB to 40 dB below its maximum gain, and provides some flexibility in operating the repeater over shorter ranges, or lower power levels.

The RL gain is expected to be roughly the same as the FL gain, Eq. (7-24), from balanced link considerations. There are deviations from this rule, however; the repeater RL noise figure and noise coupling ratio at the BTS affect the RL gain. Diversity employed at the repeater may also shift the gain by a few dB.

The achievable RL noise figure of the repeater is less than 4 dB for the higher gain setting. The RL Tx power analysis for a repeater with maximum gain of 95 dB is demonstrated per Eq. (7-11). The RL in-band noise density for a CDMA2000 carrier at maximum gain is –113 + 4 + 95 = –14 dBm/1.25 MHz.

Thus, $P_{RR} = -14 + 21 + 10 \cdot \log_{10} K = 7 + 10 \cdot \log_{10} K [dBm]$.

7.3.3 Optical Fiber Repeater

The optical fiber RF repeaters operate over a dark optical fiber conduit, with backhaul characteristics summarized in Chapter 8. A block diagram of the optical fiber repeater is depicted in Fig. 7-28.

The system incorporates a pair of backhaul converters (RF-optical and Optical-RF), with an average RF power limit into the converter of ≈ 0 dBm, and RF noise spectral density out of the receiver converter of the order of: ≈ -68 dBm/1.25 MHz. Fiber loss is negligible. Two basic constraints dictate the satisfactory performance in FL over the optical backhaul (Cf. Section 8.4.3):

1) adequate backhaul transmission gain budget. This depends on the laser Tx power and sensitivity of the optical photo detector, providing a Tx-Rx margin that can recover the fiber losses.

2) the backhaul must present an adequate signal-to-noise ratio and dynamic range for the supported CDMA carriers, according to the emission restrictions.

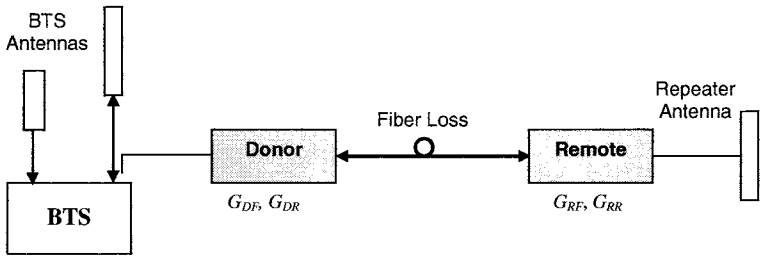

Figure 7-28. Optical fiber repeater gain-budget block diagram

The RF gain-budget, for the donor and remote units, is derived following a round-trip, starting with the FL and then the RL.

Donor Unit - FL

The donor unit employs a RF directional coupler interface with each donor BTS sector, and may be coupled to a single sector, or several sectors – e.g. 3 sectors if extending a full donor cell. Using a 30 dB coupler for sampling, the BTS RF output results in +13 dBm/carrier into the donor unit (assuming the macro BTS produces a maximum Tx power of +43 dBm/carrier). With a maximum total RF power into the optical converter kept at 0 dBm, the FL gain of the donor unit for the best signal-to-noise ratio at the input to the remote repeater unit is

$$G_{DF} \le 0-13-10\cdot\log_{10} K\ [dB]. \tag{7-27}$$

Here the carriers count K encompasses all of the extended sectors. A *maximum* gain of –5 dB is assumed here in order to compensate for additional possible losses between the BTS and donor unit (jumper cables, splitter/combiner if provisions are made for adding carriers, etc.).

The *minimum* gain applies to a case of multicarriers and multiple sectors that are transported over the RF-optical fiber backhaul. Assuming 4 carriers and 3 sectors - a total of 12 carriers results in a gain reduction by 11 dB (with a respective per-carrier power reduction into the converter). With an additional 1 dB, the minimal donor FL gain assumed here is:

$$G_{DF} \ge -13-12=-25\,[dB]. \tag{7-28}$$

In summary, we conclude a FL gain range for the donor unit as

$$-5 \ge G_{DF} \ge -25\ [dB]. \tag{7-29}$$

Remote Unit - FL

The RF input signal to the remote (repeater) unit, produced at the output of the remote optical converter, is delayed on its way, attenuated due to the backhaul loss (≤24 dB for backhaul distance ≤12 Km) and immersed in white noise. The power spectral density of the noise depends on the optical transmitter and receiver noise factors, and the backhaul length (Cf. Section 8.4.3). Thus, the RF signal power at the input and output of the remote unit is given by

$$P_{RF_{in}} = P_{DO}T_O(l_R) \tag{7-30}$$

$$P_{RF} = P_{RF_{in}} G_{RF} \tag{7-31}$$

where

P_{DO} is the RF power into the donor optical converter[35],

$T_O(l_R)$ is the backhaul transmission gain for fiber length,

$P_{RF_{in}}$ is the RF power into the remote unit (FL),

P_{RF} is the RF power out of the remote unit (FL),

G_{RF} is the FL repeater (remote unit) gain, and

$T_O(l_R)$ depends linearly (in dB) on the fiber length (see Chapter 8 for more details).

We may approximate the backhaul transmission gain (assuming 12 dB optical attenuation per 20 km of backhaul) by

$$T_O(l_R) \approx -2 \cdot (12/20) \cdot (l_R\ [Km])\ [dB] = 1.2 \cdot (l_R\ [Km])\ [dB]\ . \tag{7-32}$$

The FL gain of the remote unit can now be derived, depending on the repeater output service power. For $P_{\max} = +43\ dBm$ the maximum gain (estimated for the minimum input signal, with 12 carriers) is

$$G_{\max} = +43 - (-12 - 24) = +79\ [dB]. \tag{7-33}$$

Thus we assume

$$G_{RF} \le 80\ [dB]. \tag{7-34}$$

The minimum gain occurs with a single-carrier at maximal input power and minimum backhaul loss; the gain is reduced by 12+24=36 dB, thus (round up the change to 40 dB) we have

$$G_{RF} \ge 40\ [dB]. \tag{7-35}$$

An AMLC may be incorporated off the service high-power output, with considerations similar to those presented for the OFR.

---

[35] The RF power intensity modulates the laser optical transmitter using a very low modulation index (a few %) due to linearity considerations. The *optical* gain, loss (or attenuation) and power are signified by adding the abbreviated letter '*O* ', e.g. 4 mW*O*=+6 dBm*O*. Every additional dB of optical loss results in detected 2 dB of RF loss.

The backhaul dynamic range (signal-to-noise power ratio) of 61 dB for a 20 km fiber length (Cf. Section 8.4.3) provides for transmission of CDMA carriers in compliance with the emission restrictions. Addition of carriers reduces this per-carrier SNR by the total number of carriers expressed in dB. The RL direction does not require this wide range, and is discussed next.

Remote Unit - RL

Following similar noise considerations as for the OFR, and using a RL noise figure of 4 dB for the repeater unit, the RL gain is determined such that the noise level into the backhaul optical converter dominates the noise floor of the optical backhaul. This guarantees that the overall system noise figure will remain close to 4 dB rather than deteriorated by the backhaul noise floor.

The RL noise figure is

$$F_R = F_{RR} + (F_{LR} - 1)/G_{RR} \tag{7-36}$$

where

F_R is the total RL noise figure,

F_{RR} is the remote unit RL noise figure,

G_{RR} is the remote unit RL gain, and

F_{LR} is the backhaul RL noise figure.

The RL noise figure is plotted in Fig. 7-29 as a function of G_{RR}, assuming $F_{RR} = 4dB$ and $F_{LR} = 48dB$.

It can be concluded that a RL gain of at least 60 dB of the repeater unit guarantees the low system noise figure.

Assuming the above noise figure and RL gain, the noise level at the RL input to the converter is thus: –113+4+60 = –49 dBm/1.25 MHz, and adding the headroom of 21 dB brings the maximum RL power to –22 dBm/1.25 MHz. This level is well below the 0 dBm average power limit into the optical converter. The RL gain may thus be allowed to go even higher, e.g. 75 dB, applicable with longer fiber backhauls[36].

The minimal RL gain is set to 35 dB, and can be used with a very short backhaul and in cases where limited repeater coverage is desired.

In summary:

$$35 \le G_{RR} \le 75\ [dB]. \tag{7-37}$$

[36] For RF link losses of more than 20 dB the receiver photo detector's noise (which is not dependent on the link loss) becomes the limiting factor of the attenuated signal SNR.

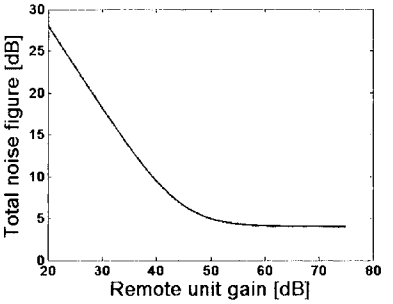

Figure 7-29. RL noise figure as a function of the repeater RL gain

Donor Unit - RL

The donor unit is coupled to the BTS via a directional coupler (a standard value is 30 dB coupling) to one of the two receive ports of the donor sector, as in Fig. 7-28. The RL noise injected through the coupler by the donor unit determines the noise rise due to the repeater in that port.

Since the second port is not affected by the donor unit noise, the overall degradation of the BTS sensitivity is limited to 3 dB in an AWGN sensitivity test[37]. Denoting the donor injected noise level relative to that of the BTS port by η, the BTS sensitivity degradation ΔS $[dB]$ is

$$\Delta S = 10 \cdot \log_{10}\left[\frac{2\,S/N}{S/N + S/(N+\eta \cdot N)}\right] = 10 \cdot \log_{10}\frac{2 \cdot (1+\eta)}{2+\eta} \quad [dB]. \tag{7-38}$$

The BTS sensitivity degradation is plotted in Fig. 7-30, and is a monotonic function of the relative injected noise level.

It is thus seen that for a donor BTS sensitivity degradation of 0.5 dB the injected noise may be ~5.5 dB below the BTS noise.

We consider next the RL gain range of the donor unit.

As an illustration, a BTS with noise figure of 4 dB has an input equivalent noise level of –109 dBm/1.25 MHz. For 0.5 dB degradation, the injected repeater noise may be –114 dBm/1.25 MHz. This translates at the coupler's input into a noise level of –84 dBm/1.25 MHz. A remote unit with RL gain of 60 dB and noise figure of 4 dB produces –49 dBm/1.25 MHz of noise into the backhaul. A backhaul of minimal (0 dB) loss results in a donor unit that is required to attenuate the noise into the coupler by 35 dB. In practice we allow

[37] Additive White Gaussian Noise (AWGN) test is performed on the BTS ports with no fading.

for a few extra dBs reaching a low donor unit gain value of –40 dB. Similarly, the maximum gain is for a case with high backhaul loss, and requiring a noise level into the coupler of –65 dBm/1.25 MHz; in this case the repeater noise dominates the BTS noise (on a single input port) resulting in maximum repeater sensitivity at the cost of 3 dB degradation of the BTS (AWGN) sensitivity.

Assuming a 20 Km backhaul, the backhaul noise is decreased by 16 dB, decreasing to –49–16 = – 65 dBm/1.25 MHz. Thus, in this case the required donor unit gain is 0 dB.

In summary:

$$-40 \le G_{DR} \le 0 \ [dB]. \tag{7-39}$$

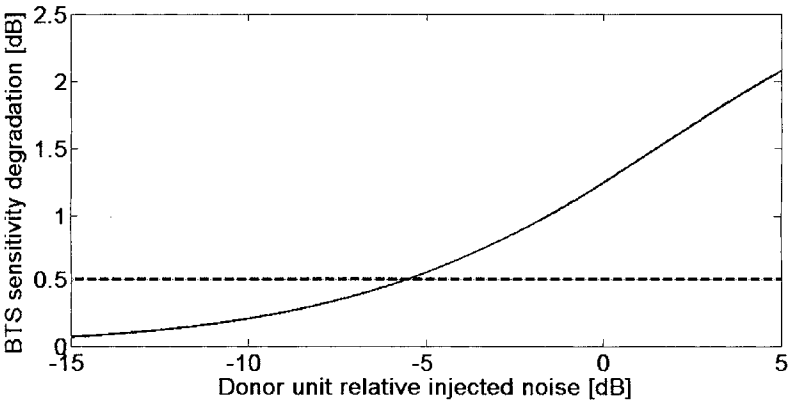

Figure 7-30. Donor BTS sensitivity degradation as a function of the injected noise relative to BTS noise on one port

7.3.4 Free-Space Optic Repeater

The free-space optical backhaul is a relatively low-cost means for transporting RF modulated signals over short distances (~200 to 2000 m). For more details on the FSO backhaul see Section 8.4.4. The block diagram of an FSO repeater is presented in Fig. 7-31.

The outdoor units (ODUs) perform the function of the optical converters in the optical fiber backhaul. The functional breakdown of an ODU is illustrated in Fig. 7-32. The transmitter levels and detector sensitivity are similar to those employed with optical fiber, thus the RF analysis of the fiber repeater may be replicated here.

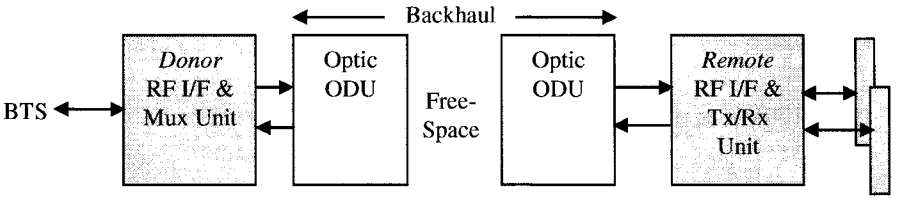

Figure 7-31. Block diagram of an FSO system

The operation and characteristics of the donor and remote units are as described in Section 7.3.3; the units perform signal level conditioning and possibly filtering. The remote (repeater) unit includes high-power amplification of the signals transmitted by the service antenna. Figure 7-33 displays the gain-budget block diagram for the FSO repeater.

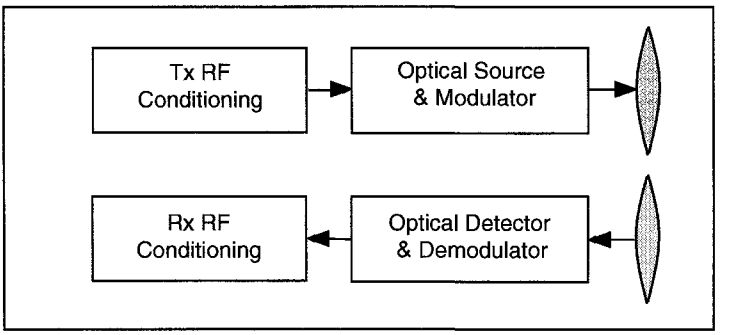

Figure 7-32. Block diagram of an optic ODU

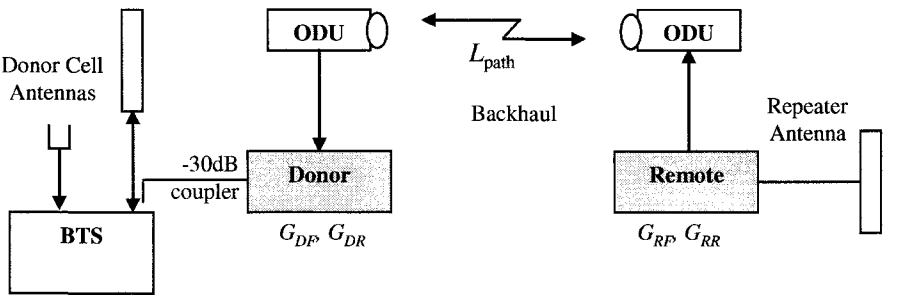

Figure 7-33. FSO repeater gain-budget block diagram

We conclude the gain ranges for the donor and remote unit by similarity to the optical fiber repeater. Based on Eqs. (7-29), (7-34), (7-35), (7-37), and (7-39) and under the same assumptions:

$$-25 \le G_{DF} \le -5 \,[dB] \tag{7-40a}$$

$$-40 \le G_{DR} \le 0 \,[dB] \tag{7-40b}$$

$$40 \le G_{RF} \le 80 \,[dB] \tag{7-40c}$$

$$35 \le G_{RR} \le 75 \,[dB]. \tag{7-40d}$$

7.3.5 In-Band F1/F2 Repeater

The F1/F2 (FSR) repeaters operate over free-space, with a point-to-point radio backhaul of characteristics addressed in Chapter 8. A block diagram of the FSR is presented in Fig. 7-34.

The frequency shift repeater employs two units. The donor unit performs frequency shifting between the service and backhaul channels, and the required power amplification in FL.

The remote unit performs the opposite frequency shifts to result in service transmission and reception at the BTS service FAs. The donor unit is an RF heterodyne unit, and interfaces the BTS via directional couplers. The frequency shifting is performed using a single synthesizer in each direction. Frequency shifting may cause spectrum mirroring depending on the LO frequency relative to the output frequency. The backhaul spectrum may be mirrored as long as the complementary unit performs a complementary mirroring operation. Thus, the frequency plan for the FSR system LOs must be carefully selected.

The remote unit operates using a backhaul antenna and a service antenna. In addition to frequency shifting the signals, the remote unit must filter them selectively in both FL and RL, and power amplify in FL and RL directions. The frequency shift and selective filtering is performed in the remote unit as shown in Fig. 7-35. Two LOs are employed, one for down-conversion into a convenient IF frequency, where the selective filter performs the narrow band filtering, and another LO for up-conversion into the required backhaul frequency. Since the frequency accuracy is dictated by the reference clock used at the remote unit, the overall frequency accuracy may suffer some degradation; E.g. with a shift of 10 MHz and frequency stability of 10^{-8} the frequency error would be only 0.1 Hz. Larger frequency shifts result in proportional increase in frequency error.

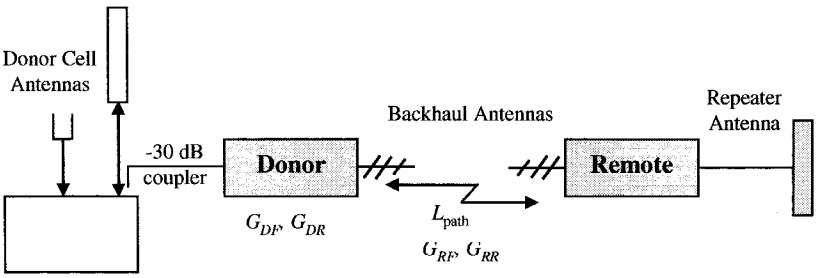

Figure 7-34. Frequency shifted repeater gain-budget block diagram

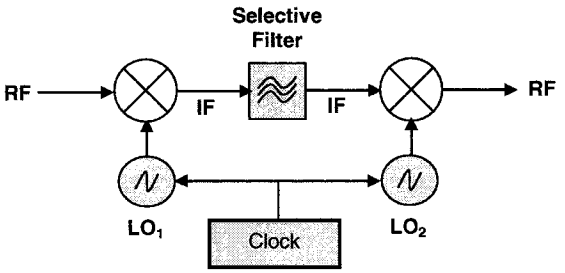

Figure 7-35. Selective filter heterodyne realization

Although the use of different frequencies for service and the backhaul eliminates the possibility of oscillations, there are several other pitfalls that deserve attention when attempt is made at operating the remote unit with limited antenna isolation, yet at very high gain. The previous discussion on RF repeaters and antenna isolation is now extended for the FSR remote unit.

Assume a finite isolation between the backhaul and service antennas denoted as I [dB]. Assume for simplicity similar duplexers on both ends of the repeater (the general case is straightforward to derive), and attenuating L [dB] the opposite backhaul signal[38]. Assume also the channel filter to have ultimate attenuation A [dB] and a sharp but finite transition slope from the pass band to the stop band. Then:

1) The duplexers' cross band suppression of Tx high-power signals and Tx broadband noise at the Rx band must be well-defined as was with the RF repeater (see above). These rules are applied to both the service and backhaul duplexers.

[38] The Tx filter attenuates the Rx signal and the Rx filter attenuates the Tx signal by L [dB].

2) The high-power FL service signal is coupled back via antenna coupling to the backhaul side input. The duplexer must further attenuate the coupled signal to assure linear operation of the front-end and avoid desensitization. A similar argument applies to the RL transmission. Thus, with receive 1 dB compression point referred to input P_{1dBin} [dBm], and transmit power P_{Tx} [dBm], (calculated similarly for the FL and RL) we get

$$P_{Tx} - I - L << P_{1dBin}. \tag{7-41}$$

3) The FL transmitted wideband noise and IMs is coupled back via antenna isolation to the backhaul side input. This Tx duplexer filter must attenuate sufficiently the coupled signal (prior to the antenna coupling) to prevent an increase of the link noise figure. Thus, with receiver noise figure F [dB], and transmitter noise plus IMs at the backhaul FL frequency N_{Tx} [dB] relative to the room temperature thermal noise floor (-114 dBm/1 MHz), (calculated separately for FL and RL) we get

$$N_{Tx} - I - L << F. \tag{7-42}$$

4) The FL high-power signal P_{Tx} [dBm] per CDMA carrier, is coupled back to the backhaul FL input, and reamplified by the repeater (assume the set gain to be G_{FL} [dB]), attenuated by the highest rejection of the channel filter at this frequency shift. This phenomenon loops itself, and may prevent compliance with the emission mask requirements. Note that this is an extension of the oscillations phenomenon to the frequency shifted case. Assume that representative emission mask requirements at large frequency offsets are < -12 dBm/1.25 MHz and the transmitted carrier bandwidth is 1.25 MHz, the following is required

$$P_{Tx} - I + G_{FL} - A < -12. \tag{7-43}$$

As an example, if the Tx power equals 40 dBm and the isolation between antennas is 70 dB, then at FL gain of 110 dB, the requirement on the channel filter ultimate rejection (actually on the repeater overall off-channel ultimate rejection) is $A > 92$ dB. This requires special filtering means within the repeater. It is nevertheless easier to implement good filters than to spatially suppress oscillations, as is the case with the OFR.

5) Finally, there is one additional effect to be noted, when attempting operation at very small frequency shifts (less than a carrier bandwidth). In such a case the channel filter may not reach its ultimate rejection, and attenuate the signal by less than A [dB]. Even if the precautions of '4' above

are met, the shifted signal that is coupled back goes on a second pass through the repeater. Figure 7-36 illustrates the effective frequency response for such very small shifts.

The output signal is coupled back and attenuated according to the antenna isolation; the duplexer may provides only a small suppression L' [dB] due to the small frequency shift, and the channel filter attenuation at the crossover point provides suppression A' [dB].

The round-trip gain at the crossover frequency is then

$$G' = -I - L' + G - A' \text{ [dB]} \tag{7-44}$$

For example: with 70 dB isolation, 5 dB duplexer attenuation, 110 dB FL gain and A' of 50 dB, the round-trip gain is -15 dB! This relatively small attenuation will cause a one-sided spectral peak that violates the required emission mask.

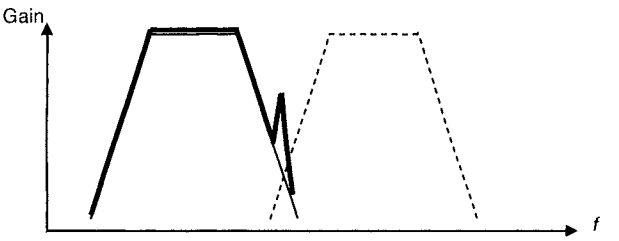

Figure 7-36. Channel filter effective response at tight shifts and finite isolation

Sharper channel filters (at the expense of increased delay) are required in such a case.

The RF gain-budget for the donor and remote units is next derived following a round-trip, starting with the FL and then the RL.

Donor Unit - FL

The FL coupled RF level into the donor unit is taken as +13 dBm/carrier maximum, less the jumper cable loss (see Section 7.3.3). Denoting the donor maximum Tx power by $P_{D(Total)}$, the number of carrier K, we have:

$$G_{DF} = P_{D(Total)} - 10 \cdot \log_{10} K - 13[dB]. \tag{7-45}$$

In case the sampled power is less than the maximum due to partial traffic, the FL gain will stay as in Eq. (7-45), and allow for the headroom margin if

and when the traffic increases. The headroom margin is a function of the relative traffic load (see Eq. (7-10)).

If the donor unit input pilot power is measured rather than total carrier power (we assume the pilot is 9 dB below the maximum power), then the FL donor unit gain equation is (for a -30 dBm coupler off a donor cell with +43 dBm/carrier, with 0 dB jumper cable loss):

$$G_{DF} = P_{D(Total)} - 10 \cdot \log_{10} K - 13 - 9 = P_{D(Total)} - 10 \cdot \log_{10} K - 22 [dB]. \qquad (7\text{-}46)$$

The total FL power transmitted by the backhaul is of the order of 2 to 10 W per carrier with FSR systems that employ a backhaul operating below 3 GHz. This translates into a minimum donor FL gain of +33 dBm –13 dBm –3 dB =17 dB (assuming 2 carriers), and a maximum gain of +40 dBm –(13 dBm – 8 dB) =+35 dB (we assumed connection losses of 8 dB). A reasonable range is then

$$15 \le G_{DF} \le 35 \, [dB]. \qquad (7\text{-}47)$$

Remote Unit - FL

Let the backhaul transmission gain be denoted by $T(R)$ $[dB]$, then the total maximum power into the remote unit is given by $P_{D(Total)} - T(R)$ $[dBm]$. If the service Tx power at full traffic of the remote unit is $P_{S(Total)}$ then its DL set gain is given by:

$$G_{RF} = P_{S(Total)} - P_{D(Total)} - T(R) [dB]. \qquad (7\text{-}48)$$

The conclusion is that the nominal remote unit FL gain setting is well-defined by the *required backhaul transmission gain.*

The maximum gain depends on the emission mask clearance (Cf. Section 7.3.1.1), and may be as high as 110 dB. Thus we may conclude that

$$70 \le G_{RF} \le 110 \, [dB]. \qquad (7\text{-}49)$$

Depending on the FSR design and the service - backhaul frequency shift, minimum antenna isolation may be required, in particular with aggressive gain values employed with FSR systems, as discussed below. Care must be taken in the positioning and orientation of the remote unit antennas in such cases.

Example: A single-carrier FSR repeater is designed for +35 dBm maximum donor unit backhaul Tx power and +40 dBm remote unit service

Tx power. Let the 15 km backhaul operate in PCS block B at channel 430 (see Appendix F). This corresponds to a FL center frequency of 1951.5 MHz. The free-space path-loss is: $32.5+20\log_{10}15+20\log_{10}1951.5=121.8[dB]$. The backhaul antennas are 3' parabolic reflector antennas, each providing a gain of 24 dBi. The backhaul transmission gain is then: $T(R)=24-121.8+24=-73.8[dB]$. Using Eq. (7-45), the donor unit FL gain should be set at: $G_{DF}=+35-13=+22[dB]$. The required remote unit FL gain is: $G_{RF}=+40-35-(-73.8)=+78.8[dB]$. Note that from the discussion on FL design in Section 7.3.1.1, G_{RF} may reach values near 110 dB. The 'unused' gain in the above example can be utilized in an AGC function for backhaul fading compensation (see Section 7.2.6.2).

During commissioning of the repeater (remote unit), extra care must be exercised in setting the FL gain such that the FL actual Tx power is below its maximum value by (at least) the headroom (in dB), which is also the actual donor BTS power relative to its maximum.

Remote Unit - RL

The achievable donor unit RL noise figure is less than 10 dB. The remote unit RL noise power must dominate the donor unit noise if a low system noise figure is required. Thus the remote unit transmitted noise should reach the donor unit by at least 20 dB above the thermal noise floor. We assume here backhaul transmission gain in the range of –60 dB to –90 dB, as in the FL analysis of the FSR, and maximal RL noise transmitted by the remote unit up to ~(110+F_{RR}) dB above the thermal noise floor. A few dB are contributed by the remote unit self-noise (possibly F_{RR} =4 dB). The minimal RL gain serves cases such as short backhaul, or a service area of reduced coverage. We define a RL gain control range of 40 dB, which is adequate for most applications. Thus

$$70 \le G_{RR} \le 110\ [dB]. \tag{7-50}$$

The RL Tx power is deduced from the output thermal noise by adding the 21 dB overhead (Eq. 7-11). Assuming a noise figure of 4 dB, and maximum RL gain the output average noise power spectral density is:

-113+4+110 = +1 dBm/1.25 MHz.

Thus the backhaul amplifier of the remote unit should be able to produce +1+21 = +22 dBm/1.25 MHz.

Donor Unit - RL

The donor unit was assumed to receive a noise level that dominates its self-noise by at least 10 dB. In practice the input noise level may be much higher, depending on the backhaul actual transmission gain, and the set RL gain of the remote unit.

The RL noise level out of the donor unit into the 30 dB coupler may vary from –85 to –65 dBm/1.25 MHz, similar to the discussion for the optical fiber repeater. Assume the backhaul transmission gain varies from –60 to –95 dB. Then, with noise level of +1 dBm/1.25 MHz out of the remote unit (see above example) the noise arrives at the donor unit at –59 to -94 dBm/1.25 MHz. Note that these levels dominate the donor unit self-noise as required. The donor unit RL gain must then range from –26 dB to +29 dB. Thus, with some margin, we have

$$-25 \le G_{DR} \le 35\,[dB]. \tag{7-51}$$

The power level that should be handled in the donor RL is 21 dB above the noise floor. The noise floor at the input to the RL donor unit is bounded by the upper limit noise level at the input to the -30 dB coupler, which is -65 dBm/1.25 MHz. Going back the through the gain-chain of the RL donor unit, for the worst-case of G_{DR}= -25 dB, the input signal level becomes –65 +25 +21 = –19 dBm/1.25 MHz. The max input power level then becomes: $-19+10\cdot\log_{10} K\,[dBm]$, with K the number of CDMA2000 carriers.

7.3.6 Out-of-Band F1/F2 Repeater

The out-of-band FSR is similar to the in-band FSR discussed in Section 7.3.5. Due to the large frequency separation, the duplexers provide effective out-of-band filtering that alleviates the slope and ultimate rejection requirements off the selective filters.

The gain values are similar to those presented for the in-band FSR.

It may be noted that this system resembles the optical fiber repeater, with the low backhaul loss and high noise floor of the optical fiber backhaul replaced here by a high loss and low noise floor free-space backhaul. This dictates the increased backhaul Tx power (preceding the lossy backhaul) and high gain at the remote unit, for extended backhaul ranges.

There may be cases where the role of the backhaul FL and RL are preferably interchanged, i.e. RL FA in F2 serves for FL backhaul and vice versa. This is to avoid accidental access attempts by STs roaming along the backhaul propagation path. These attempts are bound to fail, but nonetheless

interfere with the service. These apply for band separation that enables sufficient filtering between the service and backhaul bands.

Finally, it is noted that the larger frequency shifts result in increased frequency errors unless special precautions are taken, including a stable reference oscillator at the remote unit, or other means, such as an automatic frequency locking (AFL) loop (Cf. Section 7.3.1.3).

7.3.7 MW F1/F2 Repeater

The MW repeater presents an extension of the FSR case, with two functional units on each end of the backhaul (Fig. 7-37). One unit is operating at the service band and another outdoor unit (ODU) that is part of the MW backhaul. The remote unit is required to provide high RL gain to guarantee a low system noise figure set by the remote unit front-end. The gain for the various blocks may be defined once an RF interface level between the ODUs and repeater or donor units is set, e.g. anywhere between -20 to 0 dBm. The headroom margin of 21 dB above the noise level is applied in the RL analysis as explained in Section 7.3.1.1.

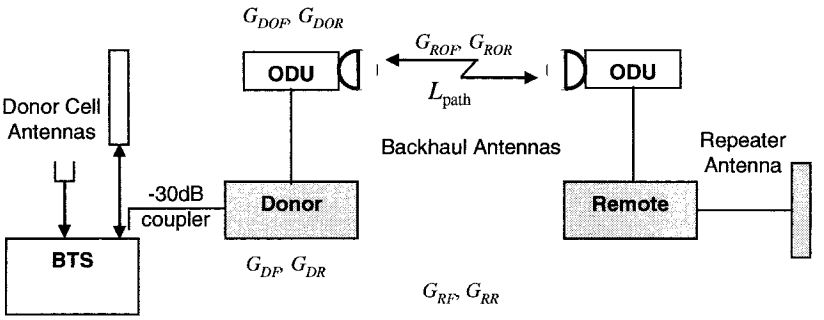

Figure 7-37. Gain-power budget of a microwave repeater

Finally, we assume a backhaul transmission gain ranging from –90 dB and up to –60 dB (Cf. Chapter 8), and a backhaul ODU maximum Tx power of +30dBm.

We briefly indicate the arguments for establishing the gain ranges of the MW repeater units using the above assumptions, and by numerical examples.

Remote ODU and Repeater Unit

FL ODU gain: The weakest input signal is +30 - 90 = -60 dBm. This is total power and may include several carriers, at full traffic. Using a -5 dBm output level, the ODU maximum gain is 55 dB. For links of -60 dB transmission gain the minimum ODU FL gain is 25 dB.

FL repeater gain: The weakest input signal from the ODU for a minimal output of -20 dBm, including 10 dB loss of an RF jumper connection, is: -20 - 10 = -30 dBm. For a service maximal Tx power of +45 dBm the FL gain of the unit is +75 dB.

RL repeater gain: Assuming an output signal level of -10 dBm per carrier (demonstrated here for a 1.25 MHz CDMA2000 carrier) into the ODU yields an output noise density of -10-21=-31 dBm (by the signal-to-noise RL power-margin rule). A repeater noise figure of 4 dB represents an equivalent input noise of -113+4 = -109 dBm/1.25 MHz. Thus the repeater RL gain is -31-(-109) = +78 dB, rounded up to 80 dB. The minimal gain may be set 25 dB below, thus +55 dB.

RL ODU gain: Similar backhaul considerations as for the FL yield the same gain range for the RL.

In summary, we have for the remote units the gain range as in Eqs. (7-52):

$$55 \le G_{RF} \le 75\,[dB] \tag{7-52a}$$

$$25 \le G_{ROF} \le 55\,[dB] \tag{7-52b}$$

$$25 \le G_{ROR} \le 55\,[dB] \tag{7-52c}$$

$$55 \le G_{RR} \le 80\,[dB]. \tag{7-52d}$$

Donor Cell ODU and Donor Unit

FL donor gain: The weakest FL input signal past the directional coupler is taken at +10 dBm, assuming a minimal number of carriers. If the level out of the donor unit is assumed at -20 dBm (as a compromise between high noise margin and linearity) then the maximal FL gain is -30 dB. This allows for up to 5 dB of additional cable loss to the ODU, to reach the ODU at -25 dBm. The ODU can then still produce a full power backhaul transmission. The minimum gain is set 25 dB below the maximum at -55 dB.

FL and RL ODU gain: Similar backhaul considerations as for the FL yield the same gain range for the RL. We assume that the remote ODU transmits +10 dBm per carrier (exemplified for a 1.25 MHz CDMA2000 carrier), the received level ranges from +10 -60 = -50 dBm to -80 dBm.

RL repeater gain: Let the donor ODU produce each carrier into the donor unit at +10 dBm maximum, and -10 dBm minimum (these assumptions may vary per design and shift the gain range). Recalling the noise is 21 dB below the maximum carrier power, we arrive at an input noise level range from -11

dBm to -31 dBm. The injected RL noise level range into the coupler is assumed to be from -65 to -85 dBm/1.25 MHz. Thus the donor unit RL gain should vary between -34 dB and -74 dB. Due to the flexibility in setting the ODU gain, the donor unit gain range may be shifted by a few dB as prescribed below.

In summary, we have for the donor cell units the gain range as in Eqs. (7-53):

$$-55 \le G_{DF} \le -30\,[dB] \tag{7-53a}$$

$$25 \le G_{DOF} \le 55\,[dB] \tag{7-53b}$$

$$25 \le G_{DOR} \le 55\,[dB] \tag{7-53c}$$

$$-75 \le G_{DR} \le -35\,[dB]. \tag{7-53d}$$

7.3.8 Repeater Tuning

7.3.8.1 Frequency Channel Setting

The frequency related information is usually set via a local connection using a personal computer (PC). Band repeaters that are designed to operate over a preassigned band (or sub-band covering several CDMA carriers owned by an operator) are either settable over a wider frequency range[39] or fixed with no frequency setting options for the end user.

In case of frequency shifted repeaters (including MW repeaters) the frequency channel setting involves two separate parameters; the user sets the service channel and the backhaul channel, while the repeater performs the correct frequency conversions by directing its local oscillators to the required frequencies. For the rest of this chapter it is assumed that frequency tuning of the repeater was already performed.

7.3.8.2 Repeater System Tuning Methodology

Repeater tuning is based on a preliminary radio design that defines the application objective (capacity, coverage), the interaction with the donor BTS (by defining the *y* parameter), and additional relevant considerations including backhaul budget, neighbor cells, coverage area, number of carriers, and so on.

The tuning involves several key elements:

Power: The maximal Tx power as derived from the expected coverage.

[39] But not too wide, limited by the selectivity characteristics of the repeater duplexers.

Noise: The repeater interaction with the donor BTS, i.e. the y parameter defining the planned thermal noise rise at the BTS RL with the repeater.
Balance: The repeater must provide balanced FL and RL coverage.

We consider repeater tuning in two instances (Cf. Chapter 6):

- ✓ Add-on to an existing CDMA network. In this case the repeaters complement the network by extending coverage, hole-filling, and providing radio access at hot spots. A typical selection is y <<1, to incur minimal shrinkage of the donor cell.
- ✓ Cluster optimization of a mixture of BTSs and repeaters. Here the optimized design may rely on a range of y values including y >1.

FL setting: The BTS maximum Tx power is denoted as P_{BTS_max} while the repeater maximum planned Tx power is $P_{Repeater\_max}$ (possibly different from that of the donor BTS). Let the actual BTS power be Δ [dB] below its maximum power, due to the actual traffic load. The repeater FL gain setting should be such that its Tx power is Δ [dB] below its maximum planned power. We use for Δ [dB] the term *margin*. The BTS and repeater FL power relationship is depicted in Fig. 7-38.

Note that the repeater maximum planned Tx power may be well below its rated maximum Tx power!

RL setting: The RL gain setting of the repeater is derived directly from the planned y and is verified by monitoring the donor cell noise rise reports.

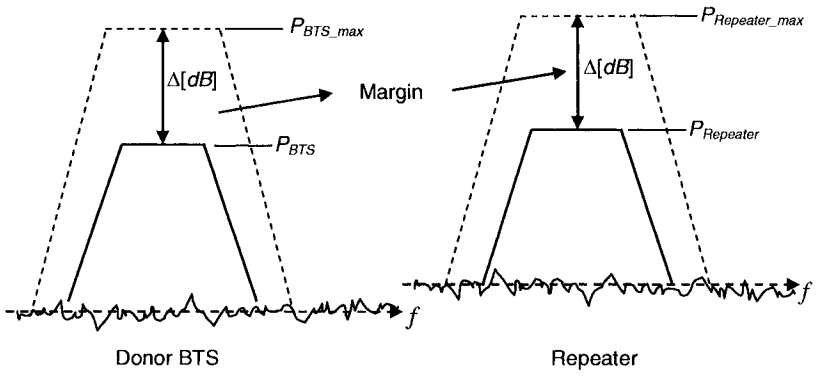

Figure 7-38. FL gain setting of a repeater

Theoretically, the repeater gain may be set in 'open-loop' according to the planned y value. This is close to reality with fiber backhaul repeaters.

Over-the-air repeaters have less predictable transmission gain values and must be tweaked following the initial setting.

The coarse setting is thus followed by a fine-tuning process. The FL set gain values are corrected according to the power readings, taking into account the required power-margin under the traffic load at the time of commissioning. This is true for any repeater type, and is performed at each unit FL output, if the repeater comprises several cascaded units.

The RL gain is fine-tuned to arrive at the required donor cell thermal noise rise; this process is performed during low traffic to allow for actual measurement of the donor cell thermal noise.

Finally - the balance is checked in drive tests, moving to the outskirts of the required coverage area, and fine-tuning the FL gain to match the RL already optimized setting. The balance performance is deduced from the drive test STs, including RSSI, *Ec/Io*, mobile Tx power, and the Tx gain adjust values. Proper balancing is manifested in minimal power overshoots by the STs, and gain adjust values in the range of 0±10 dB.

7.4 Regulation and Type Approval

7.4.1 Regulatory Constraints

Repeaters are transmitters and as such must operate under strict constraints to minimize interference, and not distort the desired signals that go through the repeaters in the operator's network. They are also specified to have minimal affect on adjacent channels belonging to other operators. The transmission regulatory rules set respective constraints on repeater parameters including out-of-band emissions and in-band signal distortions.

In addition, there are type approval certificates (e.g. UL, CE) related to environmental and safety provisions that apply to any electronic equipment, and may be required also from repeaters, depending on their operational use, mainly – if deployed indoors.

Regulatory bodies are national governmental bodies. These set the frequency allocations for services, the allowed emission levels, and the licenses for operators. They also approve the type of radiating equipment. The US body is FCC [13]; in the European Union it is CEPT. ITU is an international coordinating union for the participating nations [14]. Standardization bodies for systems and services are national, as TIA/EIA in the US [15], [16], and ETSI in Europe [17]. ITU is also an international standardization body [18]. Its project IMT2000 is an umbrella for the UMTS WCDMA standard formed by the 3GPP group [19], and the CDMA2000 standard formed by the 3GPP2 group. Users' groups, e.g. GSM, CDG, are lobbing and technical reference bodies.

7.4.2 Type Approval

The repeater systems must undergo type approval certification as any ordinary radio transmission equipment. The requirements depend on the specific CDMA standard (CDMA2000, WCDMA). The definitions of requirements for type approval constitute the following two parts: (a) requirement specifications, and (b) definitions of tests. The requirements specify the various parameters and their required limit values for approval, whereas the definitions of tests specify the exact procedures for performing the equipment tests for type approval. One good example of such specifications is the 3GPP pair of documents [2], [3].

7.4.3 Type Classification

The repeaters (similar to BTS transmitters) are classified according to their maximum average Tx power. The tolerances on the rated power, as well as the mask constraints, vary over the classes. Classes encountered are typically separated by the levels 43 dBm, 39 dBm, 33 dBm, and 31 dBm. In some cases the repeater gain is also restricted according to the class, with lower maximal gain specified for lower power class repeaters.

7.4.4 Test Parameters

Typical radio requirements and tests that are usually applied in type approval of repeaters include:
Tx power: The maximum Tx power is checked over the repeater operating band, within predefined tolerance limits (ripple over the band included).
Frequency error: The frequency error (*static* meaning average, and *peak*) must be less than a few tens of Hz, the limit being typically 0.05 ppm.
Selectivity: The repeater must present adequate out-of-band rejection, so that its effect on out-of-band signals is minimal. Additional requirements may define the maximum repeater out-of-band gain as a function of the frequency offset, in addition to the filtering selectivity.
Emission mask: The frequency domain maximum emission constraints out of the pass band of the repeater, when transmitting at full power, are defined and tested (see details in the following section).
Electromagnetic compatibility: The emission limits over a very broad frequency range are defined and tested according to indoor or outdoor equipment categories.
Emission suppression and coexistence: Special tests are defined for co-existence requirements between different types of transmission systems. As

an example, the coexistence of 850 MHz CDMA and 900 MHz GSM require restricted emission of CDMA into the GSM band.
Signal fidelity: Tests of fidelity parameters such as EVM, Rho, and PCDE ensure the signal fidelity having passed through a repeater.
System linearity: Emission mask tests cover the linearity tests, however, some-times additional two-tone tests may be required to confirm the linearity performance of the system.
Reverse interference: The repeater is checked for robustness against reverse injected interference (otherwise producing intermodulation spurii and polluting the spectrum).

7.4.5 Test Subtleties

In defining the tests' set-up, and actual interpretation of the specification requirements, there are many issues that need to be considered, a few of which are now illustrated:
Test equipment errors: since any test equipment (even if calibrated) exhibits some uncertainty, the equipment error must be subtracted from the measurements results.
Reference level definition: many emission tests are defined in dBc relative to a certain full power reference. Since the reference value is crucial for determining the emission level compliance, this definition must be well understood. Examples of misinterpretations include peak power vs. average power, single-carrier vs. multiple-carrier power, and center-carrier vs. edge-carrier power.
Resolution bandwidth: the emission measured power is proportional to the test resolution bandwidth, as long as the emission bandwidth is broader than the resolution bandwidth. Thus, the resolution bandwidth must be specified both for setting the reference and for the emission tests.
Number of codes: the CDMA signal peak-to-average power ratio depends on the number of codes (per given standard, and raised-cosine shaping factor). Thus, it is important to specify the number of codes, mainly in power and emission mask tests. In CDMA2000 the two commonly utilized numbers are 9 and 32 codes, whereas in WCDMA, 16, 32 or 64 codes are specified (with specified timing offsets and relative levels).
Dynamic range: the test equipment dynamic range is limited and cannot allow in some cases measurement of emission while the system under test emits a high-power signal (which is required for the emission tests). In such cases special filtering (in the form of duplexers, high-pass or low-pass or band-stop filters, etc.) must be exercised for attenuating the strong signal prior to the sensitive test equipment. The test equipment may then be used for measuring

the out-of-band emission while taking into account the calibrated filtering equipment.

Duplex operation: since repeater units are operated in full duplex, it is imperative to test them in FL or RL while the other link is active. Some coupling through duplexers (or other elements of the repeater) may cause interference from one backhaul to the opposite backhaul[40].

7.4.6 Emission Requirements

The emission requirements are composed of several parts; one is termed *emission mask* requirements and consists of certain *relative* attenuation requirements from the emitted signal spectrum as demonstrated here for the major CDMA standards. Then there are the *emission limits* that apply to out-of-band frequencies (below and above the operating range of the repeater) and are measured in absolute power units, in predefined resolution bandwidths. Presented are CDMA at cellular and PCS bands, and WCDMA\FDD.

The emission mask for the CDMA2000 cellular (850 MHz) and PCS transmissions is shown in Figs. 7-39 and 7-40, respectively.

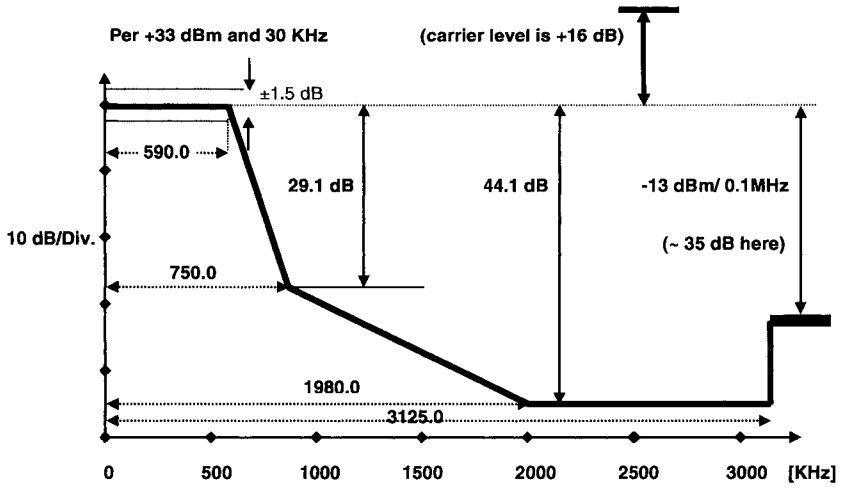

Figure 7-39. Emission characteristics for cellular (850 MHz) CDMA

[40] In remote repeater units the antenna isolation plays an important part in the operability and performance of the repeater. These aspects are not checked in type approval tests, but should be tested by equipment manufacturers as part of the equipment qualification tests.

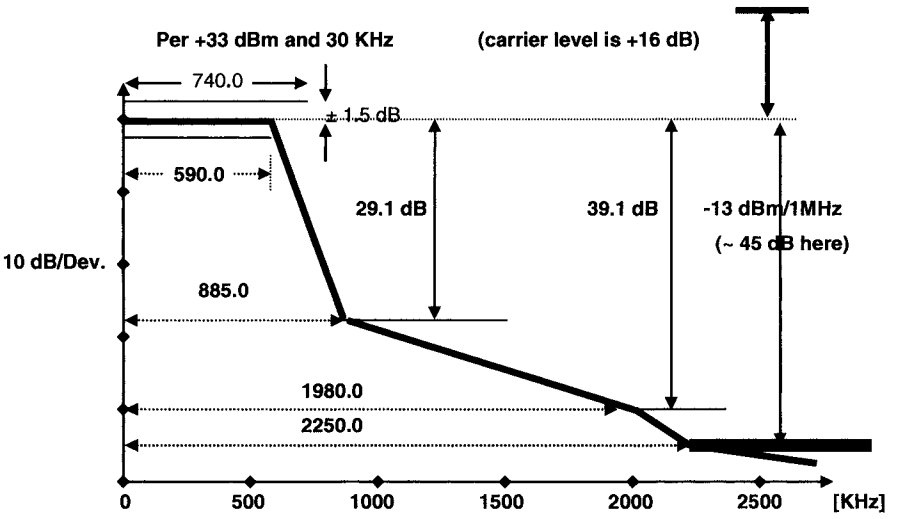

Figure 7-40. Emission characteristics for PCS (1900 MHz) CDMA

The emission mask for the WCDMA transmission is presented in Fig. 7-41.

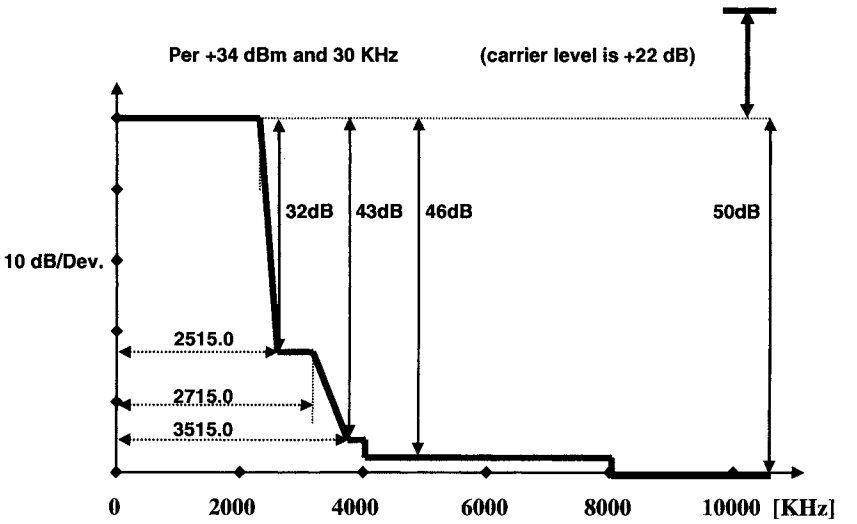

Figure 7-41. Emission characteristics for WCDMA

In each of the above emission masks, the relative attenuation is measured in a narrow resolution bandwidth (this is sometimes termed 'marker to marker' measurement) and at specified frequency offsets from the carrier center. In a multicarrier measurement, these tests are performed on the band-edge carriers.

The out-of-band emission limits vary and are –13 dBm per 100 KHz in the cellular band and 10 dB lower in the PCS band. Note that some standards (ETSI) may require that emissions are less than –30 dBm in 1 MHz.

REFERENCES

[1] N.J. Boucher, *Cellular Radio Engineering Handbook*, Fourth Edition, Chapter 11, Wiley-Interscience, 2001.

[2] ETSI (3GPP) TS 25.106 v6.2.0 *UTRA repeater radio transmission and reception* (release 6).

[3] 3GPP TS 25.143 v6.2.0 *UTRA repeater conformance testing* (release 6).

[4] Application notes in:
http://www.home.agilent.com/agilent/facet.jspx?c=79396.i.1&to=80030.k.1&cc=US&lc=eng&sm=g.

[5] Application note in: http://www.rsd.de/ .

[6] Telecommunications Management Network (TMN), International Engineering Consortium, *Web ProForum Tutorials*, http://www.iec.org .

[7] Filter examples: http://www.toko.com/passives/filters/ .

[8] Filter examples: http://www.filtro.net/images/products/filters/sawfilter.pdf .

[9] RepeaterOne (Qualcomm) *white papers* in: www.repeaterone.com
   a. 80 W0836-1 Rev A
   b. 80 H2657-1 Rev A
   c. 80 W0838-1 Rev A
   d. 80 W0013-1 Rev A
   e. 80-31550-1 Rev B.

[10] B.G. Goldberg, *Digital techniques in frequency synthesis*, McGraw-Hill, 1996.

[11] A. Lackpour, *Designing and Simulating a PCS Band CDMA Cellular Network Repeater*, EE596 Independent Study Final Report, EE Department, Pennsylvania State University, Spring 2002.

[12] U.L. Rohde, *Digital PLL frequency synthesizers: Theory and design*, Prentice-Hall, Englewood Cliffs, NJ, 1983.

[13] FCC: http://wireless.fcc.gov/rules.html .

[14] ITU: http://www.itu.int/home/ .

[15] CTIA: http://www.ctia.org/ .

[16] TIA: http://www.tiaonline.org/ .

[17] ETSI: http://www.etsi.org/sitemap_a.htm .

[18] ITU-RADIO SECTION: http://www.itu.int/ITU-R/ (for the radio section) .

[19] 3GPP Organization: http://www.3gpp.org/specs/specs.htm .

8

BACKHAUL FOR RF DISTRIBUTED RADIO ACCESS NODES

The outset for distributed RF radio access as presented in Chapter 1 included several types of repeaters, classified by their radio interaction with the donor cell, and by the connections (or backhaul, borrowing the term commonly used in digital links) between their donor and remote units. The backhaul thus constitutes part of the repeater system.

This chapter presents the linking types that are commonly employed with *dedicated conduit* repeaters, including the underlying characteristics of the backhaul, and the main considerations for employing a specific type of conduit.

8.1 Analog and Digital Backhauls

Repeater backhauls may be classified by the nature of the signals carried over the backhaul; we consider here only RF modulated signals, in contrast to payload data that requires a dedicated modem stack at the remote site (this type of site is termed a *remote sector*). The RF signals that are communicated between the repeater remote and donor units have the same PN as that of the donor sector, and thus serve to extend the donor sector coverage.

8.1.1 Analog Backhaul

The RF signals are transported over the full-duplex backhaul under linear processing operations, including amplification, filtering, heterodyning and linear modulation-demodulation. The noise that is generated along the backhaul chain is modeled as additive white noise, and is a controlled parameter in the design process.

8.1.2 Digital Backhaul

The RF signals are sampled by a fast A/D, digitized and backhauled over a suitable conduit. The digital backhaul allows for limited noise accumulation along the link as well as interference rejection. Out-of-band transmissions (transmitted by the repeater in FL, or those received by the repeater in RL) may be filtered using digital filtering techniques. The analog front-ends preceding the A/D converter and the converter itself share the same considerations typical to analog backhauls, such as noise, linearity and dynamic range performance. The focus in this chapter is on analog backhauls.

8.2 Classification of Backhauls

The backhauls are classified according to the type of conduit used, including tethered (coax, fiber) or tetherless (free-space optical or wireless radio transmissions), as follows,

8.2.1 Coax

Coaxial cables are mainly used for indoor and short outdoors distributed coverage. The coax serves indoor RF distribution amongst floors, and may require bidirectional boosters to compensate for the accumulated losses. In rooftop or tower installations, the coax serves a repeater that is coupled off a colocated BTS to provide service to an area that is not covered adequately by the donor site antennas.

8.2.2 Optical Fiber (OF)

Optical fiber is another means for extending RF between the donor and remote units of a repeater, with well-predictable performance. The RF signal must be modulated onto an optical carrier to be transported over the fiber with small losses; the modulated optical signal is then demodulated to yield back the RF signal. The low-losses of the OF (compared to coax) make it ideal for RF distribution in high-rise buildings and over long hauls up to 20 km. The broad bandwidth of the OF is used to remote multicarrier and multiple sector transmissions, using frequency-division multiplexing (FDM) and dense wavelength-division multiplexing (DWDM). By employing optical couplers it is possible to run the OF along multiple-repeater remote sites in star or chain connections [1], and distribute different sectors and carriers to repeaters. This facilitates BTS hotelling applications.

8.2.3 Free-Space Optics (FSO)

Free-space optics employs light as an optical carrier of RF signals similarly to that in the OF, but relies on line of sight transmission in free-space using transmit and receive lenses. By avoiding the need to run fibers between the sites the FSO enables fast and low-cost installations [2]. It also preserves the wide bandwidth, interference immunity, and security attributes of the OF, but cannot guarantee the low-loss and reliable communications to a distance of more than a few hundreds of meters. Fog, dust and sun radiation adversely affect the backhaul transmission gain and render the FSO installations limited to non-foggy regions and short distances, mostly in dense urban applications.

8.2.4 In-Band FSR

This class of repeater systems relies on a wireless backhaul operating over unused FAs that constitute part of the allocated spectrum for the operator's cellular service. The backhaul employs directional antennas that are connected to the donor and remote units, and located at sufficient height to establish a free line of sight between them. The CDMA RF signals are relayed by the backhaul, shifted to the backhaul FAs, but otherwise unchanged. Distortions in the remote unit are minimized by adequate frequency guard band and antenna isolation, as discussed in Section 7.3.5. The backhaul operates in any of the standard CDMA cellular bands.

8.2.5 Out-of-Band FSR

The FSR systems in this case employ larger frequency shifts from the service to the backhauls FAs. This is accomplished if unused allocated spectrum is available at a band that is different from the service band. The backhaul in this case is similar to that of the in-band FSR, and may be in any of the standard CDMA cellular bands, as well as other bands, e.g. the 2.5-2.7 GHz MMDS band.

8.2.6 MW FSR

The class of MW FSR systems is similar to the out-of-band FSR except that the wireless backhaul is operating in the MW frequency band (e.g. in licensed 7 GHz, 15 GHz, 18 GHz, 23 GHz, etc., or unlicensed 5.8 MHz band [3]). The backhaul antennas may be smaller relative to similar gain cellular backhaul antennas due to shorter wavelengths. The wider available bandwidth with the MW backhaul may be used to remote multicarrier and multiple

sector CDMA transmissions, using frequency-division multiplexing (FDM). The MW backhaul may extend over long distances, similarly to classical digital backhauls [4]. Its sensitivity to environmental and geographical conditions will be reviewed subsequently.

8.3 Repeater Backhaul Parameters

The backhaul constitutes part of the repeater and its performance affects the overall repeater system. The basic parameters of the backhaul are reviewed next, from the perspective of relaying cellular CDMA transmissions. Characterization of backhaul properties allows for circumvention of pitfalls by proper design (AGC being one example, Section 7.2.6), and optimal parameter setting during commissioning.

8.3.1 Introduction

There are several characteristics of the backhaul that are related to the transport of CDMA radio signals: frequency pass band and bandwidth, transmission gain values (mean, peak), delay, noise related performance, and distortions - including multipath, fading, dispersion, and nonlinearity effects. The nonlinearity and noise limits define the backhaul dynamic range and its capability to relay the required number of CDMA carriers.

Any backhaul RF performance is thus simplistically reduced (in RL and FL) to a few basic parameters over its operation band: backhaul gain G [dB], backhaul noise figure F_0 [dB], backhaul delay τ [sec], and backhaul dynamic range[41] Δ [dB]. The qualitative review in this section serves as an introduction to the quantitative details in subsequent sections.

8.3.1.1 Frequency Band and Bandwidth

The backhaul frequency band may be in cellular (800 – 900 MHz) or PCS/WCDMA (1800-2200 MHz) bands for OFR, and in-band and out-of-band FSRs, or at optical wavelengths with a fiber and FSO backhaul, or in a MW band.

The backhaul bandwidth determines the number of frequency multiplexed carriers times the number of sectors that can be transported over the backhaul (with guard bands for spurii-free recovery of the signals) and the optional service diversity channels.

[41] Dynamic range is defined here as the ratio between the combined (total) signal power, which generates spurii equal to the noise power (measured over a predefined bandwidth), to the minimum acceptable signal power, in dB.

The definition of bandwidth includes the –1 dB and –3 dB points that relate to the distortion of the in-band CDMA signals, and –40 dB, –50 dB points etc., that relate to the out-of-band gain and relaying of undesired signals. The channelized OFR and FSR repeaters usually employ tight band-pass filtering, whereas the optical and MW backhauls use more relaxed selectivity. Tight filtering is the main cause for bandwidth distortions, and results in deterioration of the Rho, PCDE or EVM (Section 7.2.1.1).

8.3.1.2 Frequency and Phase Error

The backhaul should pass the CDMA signals transparently end-to-end, with minimal frequency error. The repeater frequency error is strictly limited (Section 7.3.1.3) to several tens of Hertz, with the backhaul contribution included. Both average and peak errors must be well controlled, including the accumulated phase noise [5]. This is why special means for frequency stability are employed with backhauls (including stable reference clocks and AFL). Out-of-band and MW frequency shifted backhauls may cause the largest frequency errors. In-band FSR and frequency multiplexed optical backhauls employ small frequency shifts, resulting in reduced frequency errors.

8.3.1.3 Backhaul Delay

The backhaul delay is the sum of equipment and propagation delay. The propagation delay in wireless backhauls is $\tau_C = L/c$ (with L the length and c the speed of light), and in coax and optical fiber backhauls approximately $\tau_c^{'} = L/(0.67 \cdot c) = 1.5\tau_C$ (τ_C is the free-space delay over the same length). The backhaul equipment delay results mostly from band-pass filters (including duplexers, cavity and ceramic band-pass filters, or SAW filters) that are used in the donor and remote backhaul ends; FDM of multiple-sector transmissions requires filtering that contributes to the incurred delay. Although CDMA communications tolerates different delays in FL and RL, it is common to design for equal backhaul delay in FL and RL; the unit equipment delay may be distributed differently in the donor and remote units in FL and RL, as long as the total delay sum is equal.

Group delay variations (GDV) affect the CDMA signal fidelity and must be observed (Section 7.3.1.3). The backhaul is usually broadband with GDV values negligible relative to those caused by the selective repeater filters.

8.3.1.4 Noise

The backhaul contributes noise that contributes to the repeater system noise performance. The backhaul noise factor is equal to or higher than the backhaul loss. Wireless free-space backhaul noise results from the equipment

(modulator-demodulator) noise, sky noise and any additional terrestrial noise. Optical fiber backhaul noise results mainly from the transducers' noise. Characterization of the backhaul noise properties is an important parameter in two respects:

(a) The backhaul noise floor determines the dynamic range of the backhaul together with the maximum composite signal level that can pass undistorted through the backhaul (see below).

(b) Note that even if the backhaul noise is very high (such as with optical transducers), it is possible to reduce its effect by proper RF chain design (Appendix D) for a given dynamic range.

8.3.1.5 Dynamic Range

The dynamic range of the backhaul is related to its linearity and noise performance. The minimum signal level depends on the noise floor (albeit under different considerations in FL and RL – cf. Section 7.3.1.1), whereas the maximum combined signal level is determined according to the output power compression level. The higher dynamic range is typically required in FL for compliance with emission mask constraints; this sets a limit on the number of multiplexed carriers and sectors that can be served by the backhaul.

8.3.1.6 Backhaul Dynamics and Reliability

The transmission gain of backhauls that rely on tethered conduit (coax or optical fiber) is well-defined and stable. Over-the-air backhauls may suffer significant changes in the channel loss over short durations (minutes to hours), most notably for FSO and higher-frequency MW backhauls. Proper modeling of the link physics that is used in the backhaul planning, and compensation means incorporated in the equipment (e.g. pilot-aided AGC, Section 7.2.6) can alleviate most of the undesired variations in backhaul gain over time. The percentile of time with the backhaul transmission gain below a specified minimum value is defined as *backhaul outage*. The backhaul reliability is (100 - *backhaul outage%*), and is specified in 'number of nines' (e.g. '3 nines' correspond to 99.9%).

8.4 Repeater Backhaul Engineering

Basic design rules are summarized, followed by an overview of the main characteristics of the backhaul types.

8.4.1 Design Rules

The backhaul RF design is divided into two parts: the FL and RL. Since the backhaul constitutes part of the repeater, the underlying principles are

similar to those of repeater design (Section 7.3.1). Recall that the governing theory employed in the RF chain analysis is summarized in Appendix D.

8.4.1.1 FL Design

The donor unit serves as the repeater interface with the BTS and produces the FL signals into the backhaul. The backhaul is typified by the frequency band, bandwidth, and the maximum input power. The donor unit transforms the BTS sampled signals accordingly into frequencies and levels appropriate for the backhaul.

The major backhaul FL performance considerations include the following:

a) In CDMA transmission the power is proportional to the traffic. The backhaul is required to support the full FL BTS traffic in the relayed sectors, and not just the traffic served by the repeater.

b) The backhaul link should meet the emission mask requirements per employed standard, with a margin.

c) The BTS search window should incorporate the backhaul and the repeater delay in order to serve the repeater coverage area.

d) The backhaul link must preserve the CDMA signal quality, measured in Rho-factor or error-vector magnitude (EVM).

e) The backhaul must possess an adequate transmission gain margin and an AGC utility to accommodate channel variability.

f) Additional requirements apply to the backhaul pertaining to isolation and interference avoidance when colocated with spectrally-adjacent systems. Examples include colocation of several MW backhauls, or a cellular B band (880–890 MHz) backhaul operated next to a GSM BTS. The backhaul system must then be equipped with sharp filters and good structural isolation. Directional low side lobe antennas should link the radio backhauls, etc.

8.4.1.2 RL Design

The RL link may vary independently of the FL, and the backhaul design has to consider independently similar concerns to those for the FL. These include the following:

a) The backhaul should provide adequate dynamic range, defined by the number of serving carriers, traffic, BTS RL noise loading and RL power overshoots of ST access probes (Cf. Section 7.3.1.1).

b) The backhaul should comply with the minimum emission mask requirements per employed standard, with a margin.

c) The backhaul should preserve the CDMA signal quality, measured in Rho-factor or error-vector magnitude (EVM).

d) The backhaul delay must be accounted for at the BTS by extending the search window parameter. This is the same as for the FL.

e) The backhaul must possess an adequate transmission gain margin and an AGC utility to accommodate the channel variability. The RL transmission gain may vary independently of that of the FL.

f) The RL backhaul should allow for the specified noise rise range at the BTS; this tuning function is performed at the donor unit, and should have the backhaul noise included.

g) Additional requirements, such as colocation interference susceptibility (when applicable). As an example consider a backhaul operating in the cellular B band (835–845 MHz) next to an iDEN BTS transmitting in the 850 MHz frequency range. The backhaul must then be equipped with a sharp duplexer Rx filter, possibly directional low side lobe antennas, and so on.

8.4.1.3 Backhaul Dynamics

A time-varying backhaul transmission gain (Section 8.3.1.6) calls for special attention in the design process. The general approach for the backhaul power budget analysis is based on the following steps:

a) Establish (per RL and FL) the nominal (or mean) backhaul transmission gain.

b) Establish (per RL and FL) the repeater equipment *sensitivity*, i.e. the minimum signal level required at the output of the backhaul.

c) Calculate the mean received value for a given effective transmit power into the backhaul (per RL and FL) and compare to the required sensitivity (this value must exceed the required sensitivity). The difference in dB establishes the fade margin. It is possible to evaluate the backhaul outage probability, based on the statistical backhaul loss model. This equals the fraction of time the backhaul output signal is below the required sensitivity. The procedure is reversed if outage % is the design goal; then this serves to establish the required nominal transmit power into the backhaul.

8.4.2 Coax Backhaul

The coax performance is accurately predictable, with the following available specifications per conduit type:

- ✓ *Impedance*: The characteristic impedance of the cable (typically 50Ω).
- ✓ *Attenuation*: The coax attenuation is specified in dB/m (or dB/feet) and varies linearly (in dB) with length. Also, attenuation is specified per frequency, and increases with frequency. Examples: ⅜" heliax cable may

have a loss of 0.17dB/m, whereas a ⅝" heliax cable has 0.0807 dB/m at 900 MHz.

✓ *Resistance*: The ohmic DC resistance is important in applications where active repeater units are DC fed through the coax. DC resistance reduces with the coax diameter, e.g.: 0.00348 Ω/m for a ⅜" heliax cable, and 0.00137 Ω/m for a ⅝" heliax cable. The resistance of the inner and outer conductor may differ.

The coax backhauls are associated with passive elements that interface the backhaul and the end-units (BTS or donor and remote units), including RF couplers, splitters/combiners and attenuators. There are no special issues with RF power ratings of the cables for power levels of less than 100 Watts.

8.4.3 Optical Fiber Backhaul

Optical fibers are another type of well-controlled conduit for extending RF off the donor BTS. The optical fiber is a low-loss platform for transporting electromagnetic waves over long distances. The operation and properties of fibers may be found in numerous references [1], [6], [7].

Electro-optical transducers are used to modulate the RF signal onto an optical conduit and detect the RF signal off the optical conduit. The RF signal is intensity modulated on a laser light and is carried over the optical fiber with losses of less than 0.3 dBO/Km[42]. A photo detector is used at the remote end to recover the RF signal. Different wavelengths are duplexed to transport the FL and RL signals over a single fiber. Single wavelength suffices with simplex transmissions over several fibers. The main elements are summarized next:

✓ *Delay*: The optical fiber delay is roughly 1.5 times the free-space delay for the same distance. The converters that support the optical communications through the optical fiber include the following,

✓ *Transmitter*: The light produced by a laser diode (Fabry-Perot (FP) or distributed feedback (DFB) laser diodes (LDs)) serves as a carrier to the RF information. The two wavelengths mostly used with RF optical backhauls are 1550nm and 1310nm[43]. The dispersion is negligible at 1550 nm, and fiber losses are slightly higher for 1310 nm than 1550 nm (by ~0.1 dB/Km). Peak RF input into commercial converters is typically +10 dBm. Typical IIP_3 is +28 dBm.

---

[42] The optical attenuation A [dBO] results in an RF attenuation of $2A$ [dB], with transducers' loss included.

[43] $1\text{nm} = 10^{-9}$, $\text{m} = 10$ Å.

- ✓ *Modulator*: Amplitude modulation is employed by direct intensity modulation of the laser transmitter (Mach-Zehnder optical modulator – MZM, or electro-absorption modulator – EAM, are available external modulator techniques). A low modulation index is used to assure linearity. The modulated signal includes transmitter noise.
- ✓ *Receiver*: A photodiode is employed at the receive end to detect the incoming light photons. The detector (PIN, or avalanche photodiode - APD) produces a current proportional to the light intensity [1]. The detector noise adds to the attenuated transmitter noise.
- ✓ *Demodulator*: The light intensity detected into an analog current is filtered and amplified to yield a demodulated RF waveform.
- ✓ *Backhaul power and loss budget*: A typical list of parameters that serve for evaluation of the backhaul budget is presented in the Table 8-1 [8].

The accumulated loss is linearly proportional to the fiber length (up to small deviations that depend on the connectors and splices count).

The link budget in Table 8-2 is based on the parameters in Table 8-1.

Table 8-1. Optical backhaul budget parameters

#	Parameters	Typical losses and power levels
1	Typical connector pair loss	0.75 dB
2	Typical single-mode fiber attenuation	0.4 dB/km
3	Typical splice attenuation	0.1 dB/splice
4	Typical distance between splices	6.0 km
5	Typical power budget safety margin	3.0 dB
6	Transmit power (nominal)	6.0 dBm
7	Transmit power ≥	3.0 dBm
8	Receive power ≥	-12.0 dBm
9	Tx-Rx loss range	15.0 dB

Table 8-2. Optical backhaul budget example

Optical parameters	Loss and Margin
Fiber loss (20 km)	8.0 dB
Connector pair loss (assuming 2 pairs)	1.5 dB
Splicing loss (assuming 4 splices)	0.4 dB
Other losses (repairs)	1.0 dB
Total losses	10.9 dB
Tx-Rx loss range	15.0 dB
Operational margin	4.1 dB

- ✓ *Noise floor*: The end-to-end RF backhaul produces a noise floor additive to the demodulated RF signal. With 0 dB transmission gain it is approximately –68 dBm/1.25 MHz (with commercial off-the-shelf equipment), which amounts to a noise figure of ~45 dB.
- ✓ *Dynamic range*: The span from the maximum power to noise floor of the backhaul determines its dynamic range. This determines the number of carriers and sectors that may be transported over the backhaul.
- ✓ *Duplexer*: An optical duplexer couples the two wavelengths' transmissions (transmit and receive) to the single optical fiber.
- ✓ *Splicing*: Optical fibers are packed in standard length wheels (e.g. 6 km). Longer stretches of fiber require interconnection of two or more fibers by a delicate 'optical-soldering' splicing process. Splicing adds loss to the backhaul transmission gain.
- ✓ *Interface connectors*: There are several standard connectors in use (most notably FP-APC and FP-FPC) [8]. Care must be exerted to use matching connectors when fitting an optical fiber with a converter unit. Connectors add loss to the backhaul transmission gain.

Commercial RF-optical converters tolerate a maximum (no-damage) RF level of +10 dBm. The average RF total power into a converter is thus limited to ~0 dBm, allowing for peak-to-average overshoots of up to 10 dB. The average power is split between all the CDMA carriers through the backhaul.

The laser transmitter generates most of the RF backhaul noise. This is the reason why the RF signal-to-noise power ratio is not degraded over short backhaul distances (<5 km) with an optical fiber commercial backhaul. The receiver photo detector noise contribution is ~17 dB below the optical transmitter noise (at the backhaul output).

The output SNR is

$$\left(\frac{S}{N}\right)_{out} = \frac{\frac{S}{l_R}}{\frac{N_D}{l_R} + N_R} = \frac{S}{N_D + l_R \cdot N_R} = \frac{S/N_D}{1 + l_R \cdot \left(N_R/N_D\right)} \tag{8-1}$$

where

S is the RF signal power into the backhaul,

N_D is the donor optical transmitter RF equivalent output noise,

N_R is the remote optical receiver RF equivalent output noise, and

l_R^{-1} is the backhaul gain.

The ratio N_R/N_D allows for estimation of the SNR degradation (Eq. (8-2)), as a function of the backhaul loss l_R, with respect to the irreducible transmitter SNR:

$$SNR_{relative} = 1 + l_R \cdot (N_R/N_D). \tag{8-2}$$

The resulting signal-to-noise ratio degradation with backhaul loss is depicted in Fig. 8-1 for the above transmitter-detector noise ratio.

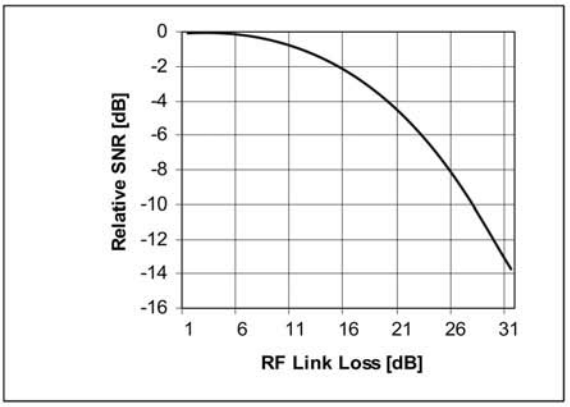

Figure 8-1. SNR degradation with optical backhaul loss

The figure illustrates a typical behavior of the SNR with backhaul loss, and should be evaluated similarly for different transmitter and receiver noise characteristics.

A simple procedure for estimation of the transmitter and receiver noise is possible using the laboratory setup depicted in Fig. 8-2.

The optical converters are connected via a variable optical attenuator, and a spectrum analyzer monitors the remote converter RF output. The RF signal generator produces a signal (modulated or continuous wave - CW) of known power at the backhaul operable frequency band, which is used to measure both the RF gain through the chain at any attenuator setting, and $(S/N)_{out}$. With a minimal fiber length, it is possible to observe an overall gain of approximately 0 dB (denote this backhaul gain as G_1) and a noise floor

measured in a fixed resolution bandwidth (this backhaul noise power is denoted N_1). Inserting an optical attenuation l_R results in gain G_2 and respective noise power N_2 for the same resolution bandwidth as before. With linear scale units we have:

$$N_i = N_D \cdot G_i + N_R, \; i = 1, 2 \tag{8-3}$$

where

N_D is the donor optical transmitter RF equivalent noise,

N_R is the remote optical receiver RF equivalent noise, and

N_i is the total backhaul noise, $i = 1, 2$.

Thus,

$$N_D = (N_1 - N_2)/(G_1 - G_2) \tag{8-4a}$$

$$N_R = (N_2 G_1 - N_1 G_2)/(G_1 - G_2). \tag{8-4b}$$

The RF dynamic range is determined by the backhaul noise floor and IP_3. The backhaul input IP_3 is of the order of +28 dBm. Thus, with a total input RF average power at 0 dBm, the 2-tone intermodulation products will be below -65 dBm each (referred to the input). This enables transmission of multiple CDMA carriers with enough clearance as imposed by emission mask requirements (see Section 7.4).

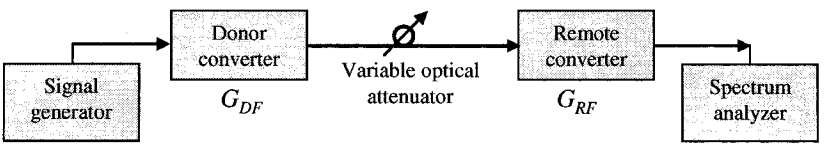

Figure 8-2. Laboratory setup for measuring the optical fiber noise budget

Recall the noise floor at the output with 0 dB backhaul loss of -68 dBm/1.25 MHz. The SNR is 68 dB for one CDMA2000 carrier at 0 dBm in

FL, and it reduces for backhaul loss of 24 dB (per Fig. 8-1) to 61 dB. Addition of carriers reduces this per-carrier SNR by the total number of carriers, expressed in dB. The RL direction needs a smaller dynamic range (Section 7.3.1).

8.4.4 Free-Space Optic Backhaul (FSO)

The free-space optical backhaul is a relatively low-cost means for transporting RF modulated signals over short distances (~200 to 2000 m). It may be simple to install and establish an operational backhaul within hours, in contrast to fiber that requires lengthy and costly preparations [2].

The RF is intensity modulated onto the light wave and detected by photodiode or phototransistor similar to the optical fiber repeater. Lenses perform the backhaul actual transmission through free space. A typical FSO repeater system including the backhaul is illustrated in Fig. 8-3.

The FSO backhaul is composed of a pair of converters in outdoor units (ODUs) that are similar to those of the optical fiber backhaul (Section 8.4.3). Similar near-infrared (near-IR) wavelengths and power levels are used, with the option to raise the optical power up to +24 dBm*O*. The converters are optically coupled to lenses; it is common that the full-duplex backhaul employs a pair of lenses on each ODU, separate for transmit and receive.

The beam divergence $\theta_D\,[Rad]$ and finite size receive lens $A_{Rx}\,[m^2]$ lead to a geometric loss L_G at distance d:

$$L_G = \frac{A_{Rx}}{(\theta_D \cdot d)^2}. \tag{8-5}$$

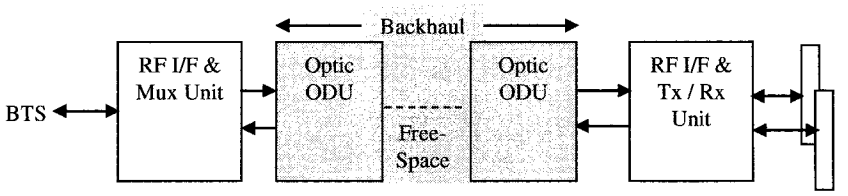

Figure 8-3. Block diagram of an FSO system

The FSO relies on free-space optical wave propagation [9], [10]. The free-space channel affects the optical signals of wavelength λ through scattering

(*Rayleigh*, *Mie* and *non-selective* (wavelength independent) scattering occur for particle size $2\pi r << \lambda$, $2\pi r \approx \lambda$, and $2\pi r >> \lambda$, respectively) and absorption.

The channel transmittance decays exponentially with distance d (Beer's law), thus the attenuation (on top of L_G) in dB grows linearly with distance:

$$T(d) = e^{-(\beta_{abs}+\beta_{scat})d} \tag{8-6}$$

where β_{abs} and β_{scat} are the absorption and scattering coefficients, respectively. The region from 0.7–2.0 μm is dominated by water vapor absorption, with dependence on wavelength. The transmittance varies abruptly with wavelength with several wavelength windows of fine transmittance, including the commonly employed wavelength of 0.85 μm or 1.55 μm.

Rayleigh scattering is negligible for the wavelengths employed (0.85 μm or 1.55 μm). Mie scattering becomes the dominant contributor to the scattering coefficient and attenuation of the IR signal, when the density of fog, haze, and aerosol particles in the atmosphere increases. Rain and snow give rise to non-selective scattering (raindrops have a radius between 100 and 10000 μm >> FSO light wavelength, and snowflakes tend to be even larger than raindrops) with minor contribution to attenuation of the order of 6 dB/km at rainfall of 25 mm/hour.

A related average and less quantitative measure is *visibility* (distance at which the eye can still detect a minimum level of contrast [11]). It was found experimentally that visibility correlates with IR path attenuation. Table 8-3 summarizes the free-space attenuation as a function of visibility.

Table 8-3. Near-IR attenuation as a function of visibility

Weather Condition	Visibility	Attenuation
Dense fog	40-70 m	392-220 dB/km
Thick fog	70-250 m	220-58 dB/km
Moderate fog	250-500 m	58-28 dB/km
Light fog	500-1000 m	28-13.4 dB/km
Thin fog	1-2 km	13.4-6.3 dB/km
Haze	2-4 km	6.3-2.9 dB/km
Light haze	4-10 km	2.9-1.03 dB/km
Clear	10-20 km	1.03-0.45 dB/km
Very clear	20-50 km	0.45-0.144 dB/km
Extremely clear	50-150 km	0.144-0.03 dB/km

It may be concluded that a clear to light hazy weather enables FSO communications with attenuation lower than 10 dB/km. Fog has a detrimental effect on path attenuation and limits the usable distance, which is directly related to the visibility. Another characteristic of the channel is fading, caused by air turbulence in warm climate regions. The received light intensity may vary at rates between 1Hz and 1 KHz due to *beam wander*, *scintillations*, and *beam spreading*, and is modeled as a log normal distributed random variable (for >500 m links; the rates are even higher for shorter links and strong wind gusts).

Diversity may be employed to combat fading, both by aperture averaging (employing large lenses or multiple lenses) and multiple transmitters, with lenses set ~0.2 m apart.

When the FSO backhaul is installed behind a window (preferably a few degrees off the normal to the window) there may be a few dB of loss due to the window coating.

A backhaul path budget analysis is demonstrated for a 500 m distance, in a clear environment, operating the ODUs behind windows. Assuming a 10 mW transmitter and receiver sensitivity of –16 dBm yields a loss range of 26 dB. With 0.5 mRad beam divergence and a 20 cm receiving lens the geometric loss (Eq. (8-3)) is 3 dB.

The path budget is summarized in Table 8-4. There is an operation margin of 14.5 dB that is used to overcome some fog and fading. The link can withstand thin fog, but thicker fog would call for a much shorter backhaul distance (or higher power transmitter, etc.).

In general, areas with severe fog peaks require significant margins if high backhaul reliability is required. Three-nines attenuation margins (based on surface visibility) range from 5 dB/km (Phoenix), through 50 dB/km (New York), 100 dB/km (Madrid), 150 dB/km (Chicago), and over 250 dB/km (London).

Table 8-4. Optical backhaul path budget example

Optical parameters	Loss and Margin
Geometric loss (0.5 km)	3.0 dB
Window attenuation	2x3.5 dB
Free-space attenuation (hazy)	0.5x1.0 dB
Pointing loss	1.0 dB
Total losses	11.5 dB
Tx-Rx loss range	26.0 dB
Operational margin	14.5 dB

The FSO backhaul includes RF elements that control the overall backhaul transmission gain to a desirable level, e.g. 0 dB, and may employ AGC for path dynamics compensation (Section 7.2.6.2).

8.4.5 Radio Point-to-Point Backhauls

The radio point-to-point (PTP) backhaul is used with FSR (in-band and out-of-band) and microwave (MW) RF repeaters. The discussion to follow encompasses all cases, differing merely by the radio backhaul frequency allocation.

Radio PTP backhauls are a well-established discipline, with widespread applications in the microwave (MW) bands [4], [12], [13]. Any radio PTP backhaul employs a transmitter feeding a transmit antenna, and a receive antenna feeding a receiver. A full-duplex backhaul uses on each end a transmitter-receiver pair coupled to the antenna via a duplexer. Typically radio backhauls are installed with free line of sight (LOS) between the backhaul antennas, and (at least) 1st Fresnel zone clearance (see Section 3.2.6.3). The free-space equation governing the nominal backhaul budget is determined by the Friis transmission equation (Eq. (3-2)):

$$P_r[dBm] = P_T[dBm] + G_T[dBi] - L_p[dB] + G_r[dBi] \tag{8-7}$$

where P_T, P_r, G_T, G_r, L_p denote the transmit and receive power, transmit and receive antenna gain, and free-space path-loss, respectively.

✓ *Geometric attenuation*: The path-loss is (Eq. (3-1)):

$$L_p[dB] = 32.5 + 20\log_{10} D[Km] + 20\log_{10} f[MHz]. \tag{8-8}$$

✓ *Backhaul antennas*: The antenna gain basic performance is governed by its shape and size (in wavelengths at the backhaul frequency):

$$G[dBi] = 4\pi \frac{A_{eff}}{\lambda^2} \approx \varsigma \cdot \frac{41000}{\theta_E \theta_H} \tag{8-9}$$

where A_{eff} is the effective area of the antenna, $\lambda[m] = 300/f[MHz]$ is the wavelength, θ_E and θ_H the E-plane and H-plane half-power beamwidth, respectively, and ς is a correction factor that depends on the type of antenna (see Section 3.6 and Table 7-3).

High transmit and receive antenna gain G_T, $G_r[dBi]$, respectively, are key contributors to the backhaul budget, and are limited primarily by size (zoning

and cost) considerations. From $G \propto f^2$ and path-loss $l_p = 10^{0.1 \cdot L_p} \propto f^2$, we have $G_T G_r / l_p \propto f^2$, thus the free-space backhaul budget with fixed-size antennas improves as the backhaul frequency gets higher.

In cellular bands (850 MHz) the antennas employed are flat panel arrays (typically 15 to 18 dBi), Yagi (typically 17 to 19 dBi), or dish (grid reflector is popular, with gain of 19-22 dBi). In the PCS bands, parabolic dish antennas are the preferred solution (23-25 dBi), as in higher (MW) bands with gains exceeding 30 dBi.

- ✓ *Fresnel zone clearance*: The Fresnel zone clearance is crucial for acceptable backhaul performance, since reflections at low grazing angles degrade the backhaul gain budget significantly (Cf. Section 3.2.6.3). For this reason, special care must be exerted when aiming at operating a backhaul over water.
- ✓ *Gaseous absorption*: Atmospheric gasses (mainly water vapor) exert an attenuation (expressed in dB/km) that grows monotonically with frequency, with several peaks at specific MW bands. The contribution of water vapor is less than 0.2 dB/km at 20 GHz, and less than 0.01 dB/km below 12 GHz [14].
- ✓ *Rain*: The effect of rain increases monotonically with frequency and the rainfall intensity. At 100 mm/hour the attenuation at 20 GHz is ~10 dB/km, and falls off exponentially to ~1dB/km at 6.5 GHz [14]. Rain attenuation is considered as fading, adding (in dB) to the backhaul path-loss. Standard climate maps divide the world into 15 rain zones and allow prediction of the losses per region, as well as the percentage of time for which a given rain intensity is attained. Horizontal polarization results in higher attenuation than with vertical polarization. To maintain a backhaul at a desired reliability, a fade margin must be provided (depending on the specific climate zone and link distance).
- ✓ *Vegetation*: Backhauls with a path through vegetation incur additional attenuation that may amount to 10 to 30 dB even with a few meters of trees with leaves for frequencies under 20 GHz. The losses in dB may double in the millimeter wave band. Thus, operation of a backhaul through vegetation must be avoided.
- ✓ *Receiver sensitivity*: The minimum acceptable power level received at the remote end of the backhaul defines the sensitivity. Repeater backhauls operate with different sensitivity values in FL and RL.
- ✓ *Fade margin*: This is the excess received signal level (in dB) relative to the receiver sensitivity as required to sustain communications in fading. The fade margin is required to maintain the backhaul quality with multipath fading (flat and frequency selective), rain fading and

atmospheric fading that may occur due to atmospheric affects on the refraction index [12].

- ✓ *Bandwidth*: The bandwidth required of the backhaul equals the number of CDMA carriers plus some guard band. The guard band depends on the filtering that is employed on the backhaul end to separate between different sector transmissions, and relocate each sector transmission onto its assigned service FAs. The guard band may occupy ~20% of the service payload bandwidth.
- ✓ *Frequency planning*: When several backhauls are colocated (on any end), care must be exerted in assigning backhaul frequencies (FA and bandwidth) to avoid interference. The FL and RL signals use separate bands on the backhaul, termed *high* and *low* duplex bands. To avoid interference between colocated 'high' (or 'low') transmitter and receiver, all colocated backhauls are assigned 'high' transmission and 'low' reception, or vice versa. The standard frequency planning tools employed with digital MW backhauls are applicable for the repeater backhaul design.
- ✓ *Quality and availability*: The fade margin is used to cope with statistical variations in the backhaul transmission gain. It is possible to transmit at the maximum available power and employ automatic gain control (AGC) to maintain a steady backhaul transmission gain (Section 7.2.6, and Chapter 10). The backhaul downtime due to fading is then shortened and availability increased [14]. Assuming a lognormal fading probability (with parameter σ [dB]) density function, and a nominal design for 50% availability, the 90% availability requires an additional 1.26σ [dB] on the budget; 2-nines require 2.3σ [dB], 3-nines require 3.09σ [dB] and 4-nines require 3.74σ [dB].

The PTP radio backhaul includes RF elements that control the overall backhaul transmission gain to a desirable level, e.g. 0dB, and may employ AGC for path dynamics compensation (Section 7.2.6.2). It is advantageous to employ a dedicated 'maintenance' modem link over the backhaul for communications between field technicians, or remote monitoring and control of the back haul and repeater units.

8.4.6 Backhaul Enhancement by Diversity

PTP backhauls may employ diversity to enhance their performance. Techniques such as space, angle and frequency diversity have been applied to digital backhauls [12]. Cost considerations usually rule out the option of diversity with radio repeater backhauls. Note that applying backhaul diversity to the backhaul link is different from supporting the diversity in the repeater service area by relaying the diversity branches through the backhaul. The

objective with backhaul diversity is to stabilize the backhaul link by providing multiple backhaul diversity branches. Both receive diversity and transmit diversity techniques are applicable, according to the modulation schemes of the backhaul link. Diversity and coloring are discussed in Chapter 5. The nature of atmospheric fading is different than that of scattering fading: the delay spreads over less than 10 ns, and the respective coherent bandwidth is over 100 MHz. A substantially wider bandwidth is required for frequency diversity. The (vertical) angle spread through the atmosphere is a small fraction of the degree, and the vertical spacing required is very large (per Eq. (3-46)) $d/\lambda > 0.6/\vartheta$. Pilot coloring: pilot aided combining enables optimal (maximal ratio combining) processing at the remote end. Since some of the losses (e.g. absorption) may occur on both branches, applying AGC in addition to diversity combining would yield a stabilized backhaul transmission gain.

8.5 Backhaul Cost Considerations

When applying repeaters to a cellular network the cost of the backhaul becomes part of the repeater cost. It is important to analyze the backhaul cost constituents and appreciate its share of the repeater cost. For additional considerations and the repeater economics, see Chapter 9.

8.5.1 Cost Contributors

The backhaul system comprises two units, one on each end. The complexity of the units however, varies as well as the size from one type of backhaul to another. All the backhaul types can transport several multicarrier sectors, except for the FSR that is usually limited to 2 CDMA2000 carriers. In the case of optical fiber, the units may be indoors. With FSO backhaul the unit is generally outdoors, unless installed behind a window; FSR in any of the cellular bands employs antennas for the backhaul, but the equipment is installed indoors for operational convenience. MW backhaul equipment is outdoors (ODUs) next to the antennas due to the high losses of the antenna transmission line. Table 8-5 summarizes the backhaul constituents.

The cost is related to the radio or optical transmit power, to supplementary elements (e.g. antennas), to supporting functions (e.g. backhaul transmission gain stabilization, frequency stabilization), and to the number of carriers and radio frequency (high-frequency MW electronics cost more than 1-2 GHz electronics).

Table 8-5. Backhaul constituents

Index	Backhaul	Main blocks	Tx Power	Carriers
1	Optical Fiber	Transducers, low-power RF, DC, C&M	6 dBmO	12
2	FSO	Transducers, Lenses, low-power RF, DC, C&M, AGC	14 dBmO	12
3	PTP Cellular	Heterodyne low/high-power RF, Antennas, DC, C&M	40 dBm	2
4	PTP MW	Heterodyne low/high-power RF, Dishes, DC, C&M, AGC	27 dBm	12

8.5.2 Cost

Based on the review of the various backhauls in the previous sections, and not counting the optical fiber cost as part of the equipment cost, Table 8-6 lists the complexity and relative cost of the backhaul types.

The optical fiber is the simplest since it operates at low power, relies on a conduit with stable characteristics, and does not involve a wide range of frequency translations.

Table 8-6. Backhaul constituents

Index	Backhaul	Complexity	Cost
1	Optical Fiber	Simple	X$
2	FSO	Medium	2X$
3	PTP Cellular	Complex	3X$
4	PTP MW	Very complex	4X$

The FSO backhaul is more complex than the optical fiber since it requires higher transmit power, lenses, and outdoor enclosure.

The FSR is even more complex than the FSO due to the frequency shifts (in out-of-band FSR the frequency stabilization contributes to cost relative to the optical backhauls), extensive filtering, high-power transmission and AGC functions, and antennas.

Finally, the MW backhaul inherits all of the FSR challenges, with the additional need to frequency translate into and from MW frequencies with

additional emphasis on frequency stability, directional antennas, and outdoor enclosure.

REFERENCES

[1] A.-R. Hamed, and S. Komati, Eds., *Radio over Fiber Technologies for Mobile Communication Networks*, Artech House, Boston, 2002.

[2] H.A. Willerbrand and B.S. Ghuman, *Fiber Optics without Fiber*, IEEE Spectrum, pp. 41-45, August 2001.

[3] L. Alexander, *Designing and simulating a PCS Band CDMA cellular network repeater*, Independent Study Final Report, EE Dept., Univ. of Pennsylvania, Spring 2002.

[4] *Transmission Systems for Communications*, Fifth ed., Bell Telephone Laboratories, 1982.

[5] R.P. Gilmore, *Specifying local oscillator phase noise performance: How good is good enough*, IEEE Symposium on Personal, Indoor and Mobile Radio Communications (PIMRC), 23-25 Sept. 1991, pp. 166-172.

[6] G.P. Agraval, *Fiber-optic communication systems*, 3rd Ed., Wiley-Interscience, 2002.

[7] G.P. Agraval, *Nonlinear optics*, 3rd Ed., Academic Press, London, 2001.

[8] W. Goralski, *Optical Networking and WDM*, Tata McGraw-Hill, New-Delhi, 2001.

[9] E. Korevaar, I.I. Kim and B. McArthur, *Atmospheric propagation characteristics of highest importance to commercial free space optics*, MRV Communications, San Diego, CA, Jan. 2003.

[10] I.I. Kim and E. Korevaar, *Availability of free-space optics (FSO) and hybrid FSO/RF systems*, Optical Access Inc., San-Diego, CA, 2001.

[11] M. Achour, *Simulating atmospheric free-space optical propagation: Part I, rainfall attenuation*, UlmTech, Inc., San-Diego, CA, Aug. 2001.

[12] A.J. Giger, *Low-Angle Microwave Propagation: Physics and Modeling*, Artech House, 1991.

[13] G. Hyde, *Microwave Propagation*, Chapter 45 in: Richard C. Johnson, Ed.: *Antenna Engineering Handbook*, 3rd Ed., McGraw-Hill, 1993.

[14] ITU-R Records:

a. P.672-2, *Attenuation by atmospheric gases*, ITU-R Recommendations, 1995 P Series, Radiowave propagation, International Telecommunication Union, Geneva, Switzerland, 1996.

b. PN.838, *Specific attenuation model for rain for use in prediction methods*, 1994 PN Series Volume, Propagation in non-ionized media, International Telecommunication Union, Geneva, 1995.

c. P.530-6, *Propagation data and prediction methods required for the design of terrestrial line-of-sight systems*, ITU-R Recommendations, 1995 P Series Fascicle, Radiowave propagation, International Telecommunication Union, Geneva, Switzerland, 1996.

d. See also ITU-T Recommendations G.801, G821 and G.826 on availability.

9

REPEATER ECONOMICS

The repeaters in the CDMA networks are non-regenerative and serve as transparent remote radio access nodes, offering the donor cell resources in their coverage area. Repeaters are thus a low-cost replacement for BTSs, and their use is justified on their cost-saving value. While a detailed cost analysis of the CDMA network is by far too complex and market specific, there are valuable lessons to be learned from certain cost-performance rules and their parametric analysis. The theme guiding this book – providing insight by analyzing the underlying basic process, is pursued in this chapter also. Cost constituents are evaluated against their performance value, and trends are shown [1]. Actual costing is not within the scope of the book, and is left to be evaluated based on specific data.

9.1 Baseline Networks

The cellular network, schematically portrayed in Fig. 9-1, comprises of a multitude of radio access nodes – BTSs (also called Node B in the UMTS system) that maintain the air interface with the subscriber in their coverage area, and a backbone network consisting of switches and backhaul conduits (dashed lines in Fig. 9-1). The cost of the BTSs constitutes over 70% of the total network cost, and is the largest upfront CAPEX (capital expenditure). Furthermore, these nodes require operational attention and management that amount to the majority of the OPEX (operational expenditure) of the network.

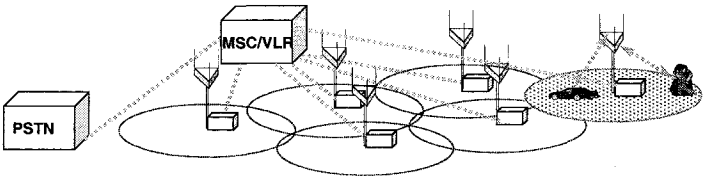

Figure 9-1. Schematics of a cellular network

Cost saving by minimizing the capital and operational cost of each BTS and their number within the service area is one of the prime objectives and continuing concerns of the network operators.

Cost-aware network planning considers the short-term expected teletraffic activity, allowing for growth in coverage and in capacity commensurate with the demand. This may include partial coverage of the denser areas and of main roads only, and incorporating equipment to support only a few channels (FAs) in the sparser areas. Readjustment is then called for as the demand grows.

9.1.1 Network Distribution in Typical Markets

The cellular market is steadily growing, at an ever increasing rate. The major bulk of green-field deployment is taking place in developing countries, while enhancement and transition to 3rd generation constitute the main effort in the developed part. Most of the networks deployed or enhanced are CDMA, whether CDMA2000 or WCDMA UMTS. The cost-aware deployment in the developing countries does not meet the rate of growing demand, and the networks soon undergo enhancement cycles. The fast development of technology and respective rate of revisions of the standards influence the upgrade in the established networks. The overall market is dynamically changing, and expected to stay this way for a while.

The distribution of the cellular network in the US market may serve as a base model for an operational market. Figure 9-2 describes the US network by the end of 2000. It clearly shows that the network is highly inhomogeneous – a small part of the population is crowded in urban areas, where the cells are very small, while the rest of the area is coverage-limited, serving a sparse population. The majority of the cells are coverage-limited.

A typical operating market may be segmented to 5 zones:

Zone 1 – urban. About 10% of the network. The highest density cells/ cell clusters. Average cell radius about half km. Both density and zoning rules out additional BTSs (except for indoors).

Zone 2 – dense suburban. About 25% of the network. Average cell radius about 1 to 2 km. There is still room for addition of cells.

Zone 3 – light suburban. About 25% of the network. Room for additional cells to accommodate capacity and fill in coverage holes.

Zone 4 – rural. About 30% of the network. Patches of coverage (villages, communities) and coverage of main roads.

Zone 5 – sparse rural. About 10% of the network. Very large cells for marginal service of vast areas.

Further segmentation shows that out of the cells that are considered capacity-limited, all three sectors are saturated in only 11%, while 38% have

two fully loaded sectors, and 51% - only one loaded sector. This characteristic, showing the diversity both on the large scale and in the small scale of the network, is common to most markets. The design objectives therefore vary over a wide range. In the following we address the different scenarios and build coverage-capacity cost models for each, and then repeat the same with the incorporation of repeaters.

9.1.2 Coverage – Capacity Model

The reverse link coverage – capacity relations as a function of the users' density, is provided by Eq. (4-16) and Fig. 4-6, and repeated in Fig. 9-3a for clarity. The cell radius is up to 60% larger when unloaded than when fully loaded, and decreasing with the load, limited by the ST power. When fully loaded, the radius continues to shrink at a rate $R \propto \rho^{-1/2}$ as the density increases, limited by the maximal noise rise allowed.

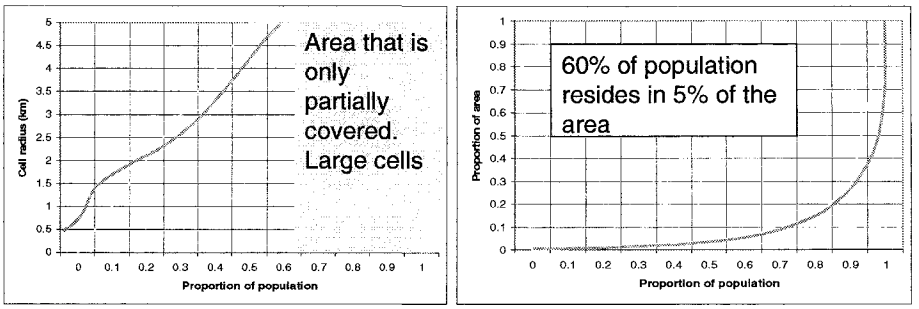

Figure 9-2. Cellular network in the US. (a) Cell radius distribution, (b) Distribution of the population

The forward link coverage (Cf. Section 4.5.2) relates to the user density as $R \propto \rho^{-1/6}$ limited by the available power to the access node PA. Figure 4-14 is repeated in Fig. 9-3b for clarity. The coverage area of lightly loaded cells is then limited by the power available to the access node, while coverage of high density cells is limited by RL interference (noise rise).

Road-covering cells are modeled by a lineal density function. These are two-lobed cells where $n = \rho_l 2R \equiv \rho_l l$. Thus the capacity-limited range $l \propto \rho_l^{-1}$ and power limited range - $l \propto \rho_l^{-1/5}$.

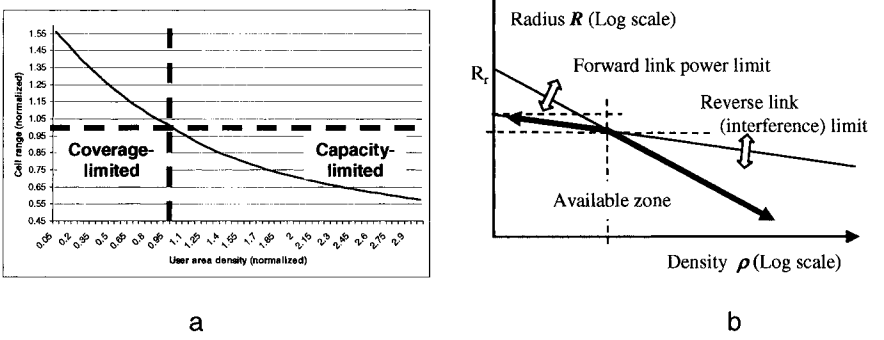

Figure 9-3. Coverage – capacity limits for a uniform area density of users. (a) Reverse link limits (Noise rise limit to capacity, ST power limit to coverage), (b) RL-FL balancing (PA limit to range at low densities)

The following analysis utilizes Eq. (3-11) for the power-height coverage relations for large-scale cellular deployment

$$T = P_r / P_t = G_t G_r (Hh)^2 R^{-4} \tag{9-1}$$

where T is the transmission gain, P_r, P_t are the receive and transmit power at the respective antenna ports, G_r, G_t are the gain of the respective antennas, H is the height of the radio access node antenna, and h is the ST antenna height. For the purpose of the present discussion we assume h=1.5 m, G_r=1. Focusing on the FL and on the BTS parameters, we assume P_r as given. This equation is modified in the case that the area is clutter-covered by woods or by building distribution. In such a case we refer to Section 3.2.5, and modify Eq. (9-1) to

$$T = P_r / P_t = G_t G_r L h^2 (H - H_C)^2 R^{-4} \tag{9-2}$$

where H_C is the average height of the clutter, and L accounts for the loss through the clutter from the canopy to the ST. We will use a value of L=1/30 (=-15 dB) representing typical scenarios. It follows that the covered area is

$$A_C \propto R^2 \propto (P \cdot G \cdot H^2)^{1/2} \propto P^{1/2} \cdot G^{1/2} \cdot H \,. \tag{9-3}$$

The differential change in coverage brings an insight about the sensitivity to the governing parameters:

$$dA/A = 1/2 \cdot dP/P + 1/2 \cdot dG/G + dH/H \ . \tag{9-4}$$

Thus, a 10% increase in coverage requires 20% more power, or 1 dB increase in antenna gain, or 10% increase in antenna height on the tower. Each one of these parameters has its limitations, to be considered together with the cost involved. *Power* has to be balanced with the RL, which sets a limit to the EIRP too. *Antenna gain* is limited by the elevation beamwidth, as a beam narrower than about 6^0 ($\pm 3^0$) may loose coverage for any terrain undulation or atmospheric fading, and horizontal beamwidth is inversely proportional to the coverage angle. *Height* will be shown to be a major cost factor.

9.2 Repeater Embedded Networks

9.2.1 Constituting Relations

Repeaters draw their resources from the donor cell/sector. The same link budget is maintained between the donor and the STs served within the donor coverage as with those STs served through the repeater coverage (Cf. Chapter 6). The repeater's served coverage depends on the net gain $y \equiv T_D G_R$ between the repeater and the donor cell. Its transmission gain is (consult Eq. (6-21))

$$T_R = T_C / (T_D G_R) = T_C / y \tag{9-5}$$

where T_R, T_C, T_D are the transmission gain of the repeater, the donor cell and the donor backhaul link, respectively, and G_R is the repeater gain. The fundamental RL coverage analysis and tradeoffs with repeaters hinges upon the *apparent repeater noise factor* (see Section 6.3 and Eq. (6-4a))

$$\hat{F} \equiv \hat{F}_R y \equiv \frac{F_R}{F_C} y \tag{9-6}$$

where F_R, F_C are the noise factors of the repeater and the donor cell, respectively. The repeater-added noise to the BTS RL results in an upward shift of the noise rise curve that affects the donor capacity, coverage or both, depending on the control of the noise rise limit (Cf. Section 6.3). The parameter y thus becomes the key tuning parameter, controlling the relations between the undisturbed donor coverage A_{C0}, its coverage when loaded by the repeater A_C and the repeater coverage A_R. Those relations are discussed in detail in Chapter 6 for various scenarios, including the optimization thereof.

We will draw examples from those relations further on. We are concerned with the area of the cluster $A_{CC} = A_C + \sum A_{Ri}$ and its relation to the baseline (undisturbed) A_{C0}. We will also seek similar relations between the length covered by the baseline cell l_{C0} and that obtained by the combination of the donor with repeaters, in case of a lineal coverage (as in covering roads) $l_{CC} = l_C + \sum l_{Ri}$.

9.2.2 Relevant Scenarios

Scenarios to be considered relate to the range of deployment densities reviewed above and to different phases in the life of a network.

Coverage maximization. The model assumes a uniform, low user density distribution.

Flat area model limits the cell size by network parameters only.

Flat cluttered area model imposes other propagation rules, as in Eq. (9-2).

Limited range model limits the cell range by major screening obstacles, as in undulating terrain, indoors, etc.

Lineal model is where a stretch of road is covered by the donor plus a chain of repeaters.

Supplemental coverage model. These accommodate small-scale non-uniformities, on a cell size level.

Radio hole. One or more dark holes that are of relatively small area but are critical to cover (a small neighborhood, mall, etc.). In many cases this need does not justify the installation of another BTS, and particularly if the donor BTS is far off its capacity limit. This is a classical repeater application, applied with hilly/valley terrains, indoor dark spots, etc.

Hot spot. A nonuniform user distribution over a sector, such that a major part of the cell's load is concentrated in a relatively small part of the cell area (Cf. Sec. 6.4.2.3). This may drain the donor power resources if located away from the donor antenna. A repeater that is close to the hot spot greatly alleviates this stress.

Site specific optimization. This is an example of fine-tuning a cell for optimizing cost and performance.

9.3 Cost Constituents

The cellular radio network economics involves up-front investments in the installation of a green-field network, and follow-up investments as the network matures. In addition to these capital expenditures (CAPEX) there are immediate and ongoing operational expenditures (OPEX) in operating, maintaining and optimizing the network. Our interest is in a comparative

evaluation of the cost of a BTSs-only network vs. the cost of a hybrid BTSs and repeaters network, and we focus on the differentiating cost elements. The following highlights the network related expense items:

CAPEX	
C_{BS}	Site cost
C_T	Tower cost, including cables and antennas
C_{BLP}	BTS low-power RF and IF equipment
$C_{BT\text{-}BB}$	BTS baseband equipment (channel elements, processing and control)
C_{PA}	Power amplifier cost
C_{DBH}	Backhaul/Backbone E1/T1/T3-ATM cost (if owned)
C_{Sh}	Shelter cost, including air-conditioning, etc.
C_{RS}	Repeater site cost
C_{RLP}	Repeater low-power RF and IF equipment
OPEX	
C_{BTO}	BTS operation and maintenance
C_{BHO}	Backhaul/Backbone leasing and maintenance cost
C_{TO}	Tower leasing cost
C_I	Installation cost

9.3.1 Tower Cost

The height of the tower above the clutter is a main factor determining the coverage (Eq. (9-3)). The tower carries the antennas, tower-top electronics (TTE) and cables. The most influential factor for its strength and cost is the *wind-load* that exerts a bending torque proportional *to its height cubed*[44]. The cost factor for the tower ranges between $C_T \propto H^{1.5}$ (guyed masts) to $C_T \propto H^3$ (high towers) [2]. Notably, the weight of TTE is less of a factor than the wind-load due to its surface area and the antennas' and cables surface area.

Another important cost factor with repeaters relates to the required isolation between backhaul and service antennas. In many cases the tower cost is per tower floor (sections) occupied, with more than one antenna at the same tower level costing much less than antennas placed at different tower levels. As a consequence, F1/F1 repeaters are the most expensive on tower cost, F1/F2 and MW repeaters with vertical separation in the range of 0 to 5 meters cost less, and the optical fiber repeater (with just a service antenna) cost least.

[44] This is the case for a harnessed tower. The cost factor for a guyed mast is linear, but is estimated as cubed considering the cost of the area captured between the guys.

Coverage repeaters, destined to replace BTS coverage, transmit from the same tower height. However, when considering supplementary coverage that is much smaller than that of the donor BTS, the tower height required may be significantly lower.

The coverage over a cluttered area depends on the height *above the clutter* (Eq. (9-2)). The cost of the ground based tower becomes even higher relative to the area covered. It is to be noted that over half the BTSs in urban areas in the US are roof mounted, with a low tower on top, which alleviates much of this issue. Most of the BTSs in the rural areas are tower mounted, however.

9.3.2 Tx Power Cost

The power amplifiers employed for CDMA transmission must be highly linear to preserve the clean emission mask, thus they employ various linearization techniques and are quite inefficient (current off-the-shelf amplifiers exhibit efficiencies in the range of 6% - 16%). The BTS provides maximum Tx power in the range of 16 to 20 Watt per carrier. Repeaters for medium and high-power applications produce from 5 to 20 Watt per carrier. The RF power cost ascends as $C_{PA} \propto P^{0.7}$, mainly due to the linearizer cost that impacts the lower power PAs more. The exponent is expected to drop, with the increasing application of digital linearization techniques. The cost estimate extends to the amplifier cost plus power supply cost plus cooling cost (either larger fins area in convection cooling, or extended heat pipes, etc.).

TTE (Tower-Top Electronics) encase the PA with the LNA on the tower in a weatherproof case, which saves on heavy cables and their loss. TTE is convection cooled by large fins for reliability, which limits the available RF power to about 20 Watt. Higher power units are air-conditioned in shelters. This splits the cost model into low carrier (FAs) count (3 to max. 4 in CDMA2000, 2 in WCDMA), and high capacity stations. Repeaters typically belong to the outdoors group.

9.3.3 Backhaul Cost

The backhaul may be based on an optical fiber conduit or a MW backhaul (rarely employing an FSO over short ranges). The BTS backhaul is digital, carrying the data. Leased cost is directly related to bandwidth (measured in E1s or T1s. etc.) and distance and may be a few thousands of dollars monthly, per BTS. Repeater backhaul carries the modulated RF over analog conduits (dark fiber or microwave transmission), except for on-frequency over-the-air that utilizes the cellular service resources. The backhaul cost is therefore evened out in the following comparison between BTS and repeater cost.

9.3.4 BTS and Repeater Cost

The site cost consists of:

BTS site $$C_{BS} = C_{BTS-BB} + C_{BLP} + C_{PA} + C_T + C_{Sh} + C_{DBH} = C_{BE} + C_T$$

Repeater site $$C_{RS} = \ldots\ldots\ldots\ldots C_{RLP} + C_{PA} + C_T + (C_{Sh}) + C_{BH} = C_{RE} + C_T$$

which shows commonality elements between the BTS and the repeater costs.

9.4 Cost Model for Area Coverage

9.4.1 Optimal Coverage of a Flat Area

Deployment of a network of radio access nodes over a large area constitutes a major undertaking. The cost constituents are the equipment, the shelter, the backhaul and the tower, all of these multiplied by the number of BTSs required. Hilly terrain limits the size of each cell and dictates more access points than needed in a flat rural case. An optimal size of a cell exists in such rural areas, depending on the cost constituents, which vary from developed to developing countries.

The cost of the BTS site, C_{BS}, consists of the cost of equipment C_{BE}, encompassing the radio, processing, shelter and backhaul equipment, and the cost of the tower, cables and antennas C_T. In order to maximize coverage it is assumed that all BTSs transmit the same power. While C_{BE} does not depend on the coverage of the BTS, the cost of the tower ascends exponentially with the tower height, $C_T = c_T H^a$, where c_T is the "specific cost" (cost per m^a) of the tower complex, and a is the cost exponent ($1.5<a<3$). Referring to Eq. (9-1) – T, the transmission gain is determined by the link budget for the required load and given transmission power, and is an input parameter, not a variable. We can thus extract an expression for $H = \left(T/\left(G_B G_m h^2 L\right)\right)^{1/2} R^2 = KA_C$ where $K \equiv \pi^{-1}\left(T/\left(G_B G_m h^2 L\right)\right)^{1/2}\left[m^{-1}\right]$ and A_C is the cell coverage. L is a loss factor (see Eq. (9-2)). In this case L=1. The cell coverage is circular and the BTS antenna is omnidirectional, which sets a limit to its gain at 12 dB. K is therefore a set parameter for the analysis. The cost of covering an area $A=nA_C$ by n access nodes is thus

$$\begin{aligned} C_{Area} &= nC_{BE} + nC_T = nC_{BE} + nc_T H^a = \\ &= n\left\{C_{BE} + c_T\left(KA_C\right)^a\right\} = n\left\{C_{BE} + c_T\left(KA\right)^a n^{-a}\right\}. \end{aligned} \tag{9-7}$$

This is now differentiated to seek the minimum number of nodes:

$$\frac{\partial C_{Area}}{\partial n} = C_{BE} - (a-1)c_T (KA)^a n^{-a} = 0, \; n = \left(\frac{(a-1)c_T}{C_{BE}} \right)^{1/a} (KA) \tag{9-8}$$

which clearly demonstrates the dependence on the ratio between the specific cost of the tower and that of the equipment. The difference in the equipment cost between BTS and repeater will be explored next to show different optimum points.

The respective coverage expression for cluttered area is Eq. (9-2). Repeating the same process yields

$$H = \left(\frac{T}{G_B G_m h^2 L} \right)^{1/2} R^2 + H_C = (KA) n^{-1} + H_C \text{. Here L<1. Then}$$

$$C_{Area} = n \left\{ C_{BE} + c_T \left((KA) n^{-1} + H_C \right)^a \right\}. \tag{9-9}$$

Seeking a minimum by differentiating and equating to zero renders a third order equation for a=3:

$$x^3 + \frac{3H_C}{2} x^2 - \frac{c + H_C^3}{2} = 0 \tag{9-10}$$

where $x \equiv KA/n = H - H_C$ and $c \equiv C_{BE}/c_T$. This reduces for H_C=0 to

$$H = (c/2)^{1/3} \tag{9-11a}$$

$$n = KA(2/c)^{1/3}, \tag{9-11b}$$

the same as in Eq. (9-8), as expected.

The trends are shown in Fig. 9-4. 50% nodes have to be added to account for complete overlap coverage.

The cost factor $c_T(a)$ is calculated to match the cost of a 40 m tower to \$45,000. Thus $c_T(1.5)=178[\$/m^{1.5}]$; $c_T(2)=28[\$/m^2]$; $c_T(2.5)=4.5[\$/m^{2.5}]$; $c_T(3)=0.7[\$/m^3]$.

The optimal number of nodes for the flat area, and relative cost, depends only weakly on the tower cost exponent (Fig. 9-4a). The situation is different with cluttered area: propagation over a forested area or over the roofs in an urban area (Fig. 9-4b). The cost of coverage of a flat cluttered area is

substantially higher. However, roof mounted masts in an urban area pertain to the flat area model (Fig. 9-4a) and relieve this excess cost.

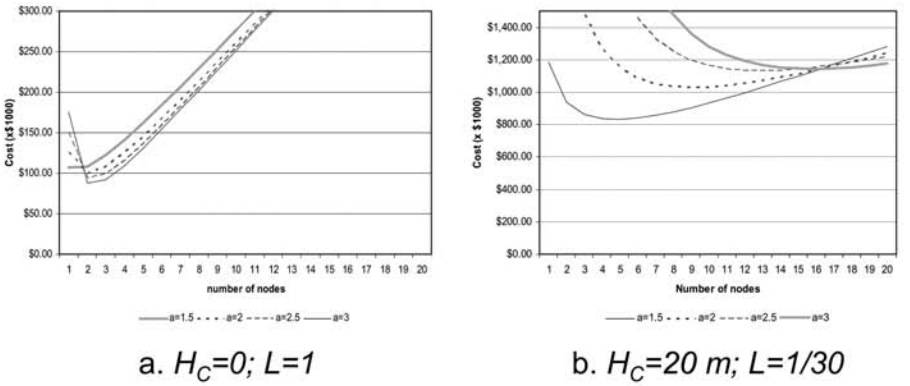

Figure 9-4. Cost of coverage of a flat area. T=-145 dB; G_B=12 dB; G_m=0 dB; h=1.5 m; C_B=$25,000; A=20,000 km^2

The dependence of the area coverage cost on the cost of the BTS is shown in Fig. 9-5 for cost height exponent a=2.5. The optimal cost varies from $916,000 to $1,646,000.

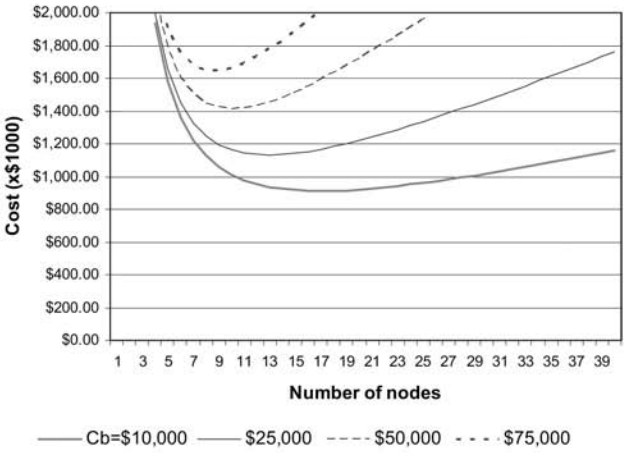

Figure 9-5. Cost of coverage of a flat cluttered area vs. cost of BTS. *T=-145 dB; G_B=12 dB; G_m=0 dB; h=1.5 m; A=20,000 km^2; H_C=20 m; L=1/30; a=2.5*

The model can now be further expanded to explicitly consider the cost of the power amplifier. Referring to Section 9.3.4, $C_{BE} = C_{BB} + C_{LP} + C_{PA} = C_B + C_{PA}$ where C_B lumps all the BTS equipment that is not high-power related. We set the ratio between C_{PA} to C_B to $C_{PA}/C_B \equiv r$ for nominal BTS power P=20 Watt. This conforms with a transmission gain T_0=*-145 dB*. Then $C_{PA}(T) = C_B r(T_0/T)^{0.7}$ (Section 9.3.2). This is now incorporated in Eq. (9-9) to yield

$$C_{Area} = n\left\{C_B\left(1 + r(T_0/T)^{0.7}\right) + c_T\left((KA)n^{-1} + H_C\right)^a\right\}. \qquad (9\text{-}12)$$

Figure 9-6 demonstrates the cost dependence on the transmission power for tower exponent factor a=2 (compare with Fig. 9-4a, b). There is a cost advantage to high power, which is understandable when considering that the cost power exponent is lower than the cost height exponent.

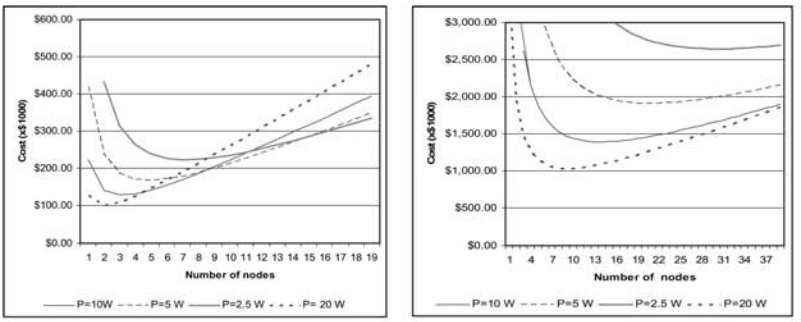

a. H_C=0; L=1 b. H_C=20 m; L=1/30

Figure 9-6. Dependence of cost on the transmission power. *a=2*

9.4.2 Optimal Coverage of a Length of Road

A similar analysis for lineal cells yields

$$H = \left(\frac{T}{G_B G_m h^2 L}\right)^{1/2} R^2 + H_C = \pi K\left(\frac{l}{2}\right)^2 n^{-2} + H_C \quad \text{where} \quad l=2nR= \text{ total length.}$$

Then

$$C_l = nC_{BE} + nc_T\left(\pi K(l/2)^2 n^{-2} + H_C\right)^a \qquad (9\text{-}13)$$

and the minimum number of nodes for a=3 is obtained by solving the equation

$$5H^3 - 6H_C H^2 - c = 0 \tag{9-14}$$

where $c \equiv C_{BE}/c_T$. For H_C=0 this reduces to

$$H = (c/5)^{1/3} \tag{9-15a}$$

$$n = (l/2)\pi^{1/2} K^{1/2} (5/c)^{1/6} . \tag{9-15b}$$

The cost of coverage of a length of road is plotted in Fig. 9-7, (a) for a flat road and (b) for road cluttered by forested or built area. The node antenna is directional, G_B=20 dB.

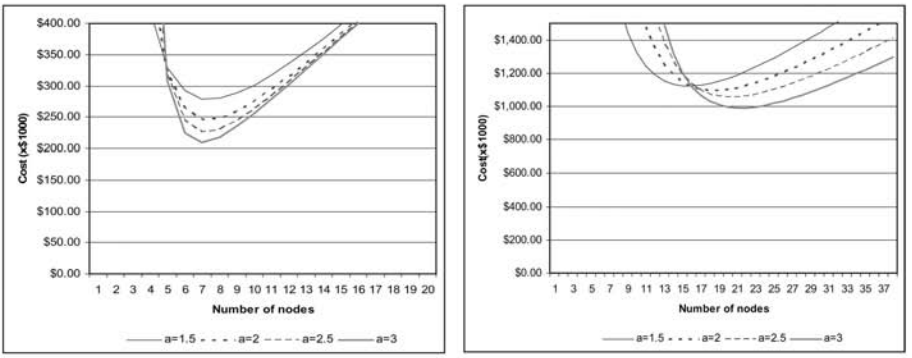

a. H_C=0; L=1 b. H_C=20 m; L=1/30

Figure 9-7. Cost of coverage of a length of road. T=-145 dB; G_B=20 dB; G_m=0 dB; h=1.5 m; C_B=$25,000; l=1,000 km

9.5 Cost Model for Area Coverage by a Cluster of BTSs and Satellite Repeaters

9.5.1 Large Area Coverage

The area of a cluster of a cell with m satellite repeaters is larger than that of the undisturbed cell when properly designed, but smaller than that of m+1 cells, because of the repeater loading to the cell:

$A_{C0} < A_{CC} = A_C + \sum_{i=1}^{m} A_{Ri} < (m+1)A_{C0}$. The design parameters of each of the nodes: height, power, gain, are the same as for the baseline cell, when designing for maximal coverage. With this in mind one can equate the cost of a cluster with that of an alternative cluster of baseline cells covering the same area. The ratio $k_m = A_{CC}(m)/A_{C0}$ is to be derived from respective scenarios in Chapter 6. The cost of a BTS plus m repeaters cluster, covering an area $A_{CC,}$ is then compared with the cost of k_m baseline BTSs. The cost ratio is

$$\frac{C_{Cluster}}{C_{Baseline}} = \frac{C_{BE} + mC_{RE} + (m+1)C_T}{k_m(C_{BE} + C_T)}. \tag{9-16}$$

It is important to differentiate two separate scenarios:

Lightly loaded cells. Cells encompassing only 4 carriers or less (CDMA2000) or 2 carriers (WCDMA). These cells may be encapsulated in outdoor cases (microcells) and not require shelters. In such a case, resorting to Section 9.3.4, $C_{BE} \cong C_{BT-BB} + C_{RE}$ and Eq. (9-16) becomes

$$\frac{C_{Cluster}}{C_{Baseline}} = \frac{(m+1)(C_{BE} + C_T) - mC_{BT-BB}}{k_m(C_{BE} + C_T)} = \frac{m+1}{k_m} - \frac{m}{k_m}\frac{C_{BT-BB}}{C_{BE} + C_T}. \tag{9-17}$$

Sheltered cells. The shelter cost is an additional element to be added to the right-hand side denominator of Eq. (9-16), which increases the attractiveness of repeater clusters.

9.5.2 Supplementary Coverage

Repeaters in supplementary coverage, that are not designed for comparable coverage to that of the donor cell - rather a limited smaller area, are optimized with different access parameters, as per Eq. (9-4). The height may be substantially lower, and so may the power. The trade-off in such a case is not between additional BTSs and repeaters, rather changing the BTS parameters (increasing height and/or power) [3].

9.6 Summary

The cost of the radio access nodes constitutes the bulk of the cellular network CAPEX. It is an up-front expenditure, and a cost-aware green-field deployment with optional flexibility to intensify the network per market growth is a desired business strategy.

The cost constituents of the access nodes can be classified into coverage-related costs and capacity-related costs. It is noteworthy that most of the

coverage-related costs pertain to towers and RF equipment, and are subject to local manufacturing – a major consideration for developing countries.

The differentiating cost factors between BTSs and repeater nodes pertain mainly to the digital part – modem stack (channel elements) and processing. The cost of the digital part of the BTS is continuously decreasing, along with the reduction of the operating costs due to enhanced automation of the BTS.

Much of the cost consideration of the network is attributed to its non-uniformity – both in terms of uneven coverage due to topography or man-made clutter, and uneven subscriber density and teletraffic activity. The coverage-related cost decreases significantly under such circumstances (e.g. radio holes, hilly terrain, dense urban environment) and repeaters are clearly a preferable choice.

REFERENCES

[1] J. Shapira, *Cost-Effective Mobile Communications for Developing Economies*, to appear in Indian Journal of Radio Science, Spring 2007.

[2] N.J. Boucher, *Cellular Radio Engineering Handbook*, Fourth Edition, Chapter 25, Wiley, 2001.

[3] D.J. Shyy, C.J. Stanziano, and P. Lemson, *CDMA2000 Network Repeater Deployment Experience*, IEEE 802.16 Session #40, Vancouver, BC, Canada, Nov. 2005.

10

ADVANCES IN CDMA REPEATERS

10.1 Introduction

Repeaters are transparent remote radio access nodes in the CDMA network, serving as a low-cost replacement to the base stations. As such they are basically frequency selective bidirectional amplifiers with a RF backhaul to the donor BTS and a service antenna. Improvements upon this basic function are sought, which reflect on both the repeater and the network performance. These include:

Repeater stability. The stability of the coverage of both the repeater and the donor cell, and the capacity of the donor cell, are linked to the stability of the repeater gain and link to the donor – the net gain y. This may be affected by equipment and propagation characteristics.

Repeater robustness. Performance degradation due to oscillations is being attended to by proper installation. Adaptive cancellation methods improve upon these, help in cost reduction and guard against timely changes in the isolation. Angular filtering of alien sources in the backhaul antenna prevents these from "stealing the repeater resources".

Repeater performance. One of the advantages of the donor service link over that of the repeater is the receive diversity offered by antenna diversity in the BTS. The lack of diversity reduces the repeater coverage and increases the relative load of the repeater-served subscribers in the donor.

Repeater monitoring and control. Alarms and status reporting are essential for the system reliability. Further control functions add flexibility in optimizing the network (e.g. gain control, antenna control).

Network reporting and control. Resource management and other performance parameters require knowledge of the activity served by the repeater, starting with the throughput, number of active subscribers and to their locations.

These advanced features emerge into the repeater domain. Their applicability is a cost-benefit trade-off. Introduction of digital processing to the repeaters enables multiple advanced features.

10.2 Performance Monitoring and Control

The repeater is an element in the CDMA network. Its monitoring is required for reliability, which is covered by failure identification and reporting, discussed in Chapter 7, and performance evaluation related to network parameters. Control over repeater parameters is an inherent part of network control and optimization, and adds dimensionality to the network flexibility and controllability. These control functions are all RF related. The repeater is not equipped with reporting and control communication protocols of the network, and a separate communication means has to be provided, along with Repeater Network Management System - RNMS. This is preferably colocated and interfaces with the network NMS. This separate signaling network is advantageous for the flexibility of the network, as repeaters are add-on elements to operational networks in many cases, and the independent RNMS allows for the needed augmentation and adjustment. A flexible communications agent is a CDMA modem installed in the repeater, operating on the same network. This provides both the communications channel and additional valuable network probing and reporting.

10.2.1 Application of a CDMA Modem in the Repeater

A CDMA modem operating on the same network and served by the repeater is an optimal probing, reporting and communications element. Being positioned with the repeater, at its service side, it periodically reports a selection of network related parameters, as a bona fide ST, and at the same time reports repeater parameters and optionally serves to relay control commands to the repeater. Examples of the main repeater functions that are monitored include Rx sensitivity, transmit power, backhaul transmission gain variations, FL/RL imbalance and the RL traffic carried by the repeater[45].

The test ST may be placed within the repeater remote unit or outside the repeater at a selected fixed location, coupled to the common (Tx/Rx) service terminal, and operating via the service side of the repeater as any commercially served ST [1a, b]. Figure 10-1 presents four tapping configurations of the repeater wireless modem. In all cases the wireless modem is connected such that it operates at the service FAs, as a regular ST. The four configurations are as follows:

[45] The repeater carries all the donor traffic on the FL, and only its own traffic on the RL.

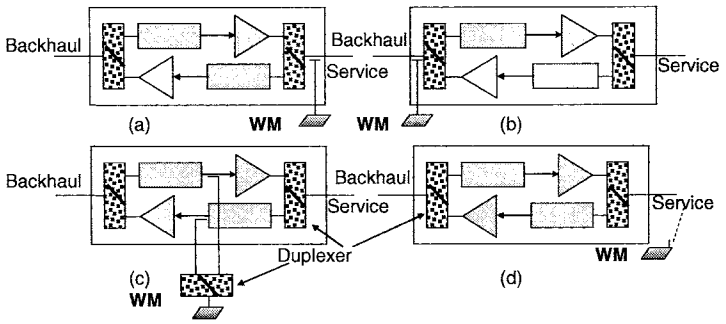

Figure 10-1. Tapping of the repeater wireless modem

(a) Service common Tx/Rx port: This option fits all types of repeaters. The tapping port may be supplied as part of the duplexer, e.g. –30 dB off both Tx and Rx levels. The modem requires yet additional adjustment of levels to simulate reasonable path-loss attenuation within the repeater coverage, e.g. additional 60 dB results in an overall -90 dB. The wireless modem must be screened well enough relative to the implemented coupling attenuation if it is used for performance measurements, since parasitic leakage may affect its receive versus transmit balance and render in erroneous reporting.

(b) Backhaul common Tx/Rx port: This option fits only the F1/F1 repeater (OFR). It is used only for communications and reporting to the RNMS in case of repeater malfunction, since performance measurements will not include signals that have passed through the repeater. The remote site may be out of the service coverage of the donor. The wireless modem employs the repeater backhaul directional antenna to establish the link. The coupling of the wireless modem has to be properly tuned to cover for the loss of repeater gain. Both the antenna directivity and its elevation should provide enough link margins for communication. A switching circuit between configuration (a) and (b), to switch automatically to (b) in case of repeater failure, may serve to report failures, while serving in configuration (a) for repeater and network monitoring during normal operation.

(c) Internal coupling: This configuration fits all types of repeaters and is similar to (a) with different coupling off the Tx and Rx paths [1a, b]. The RF levels are shifted by gain offsets, which are determined by the FL and RL active parts of the repeater between the wireless modem coupling points and the service port. This configuration enables reducing the value of the 60 dB attenuator of (a), but does not alleviate the careful isolation requirements in the performance measurement application.

(d) Employs an external wireless modem. The modem may be placed anywhere in the repeater service area, using its own antenna. This configuration is not suitable for monitoring and control of the repeater operational status unless it is interfaced with the repeater via a physical (e.g. RS485) or wireless (e.g. Bluetooth) connection. The remote connection can however be used to probe the performance in the repeater service area and report it [2].

In case of employing a multiple carrier CDMA repeater, the test ST would be assigned to one of the carriers, expecting the channel to be flat across the band. Monitoring all the carriers (FAs) however is desired. This information may be used to analyze the CDMA network operation at the donor BTS and repeater area, including traffic management and carriers' traffic loading. It is possible to assign the ST to the carriers one by one, but this requires special control SW that is programmed into the ST controller [2].

10.3 Stabilization by Gain Control

The net gain y of the repeater backhaul (Eq. (6-2)) has a direct effect on the repeater coverage (Eq. (6-12)), donor cell coverage (Eq. (6-9)) and donor cell load level (Cf. Section 6.3.2). A change of 1 dB in y, for example, changes the repeater coverage by up to 25%. Such variations occur both in the backhaul conduit and in the repeater gain itself. We reviewed various types of backhauls (Chapter 8), including optical fiber, free-space optics, RF in-band and out-of-band, and microwave. The backhaul FL and RL transmission gain may vary independently and affect the link balance. Backhaul failure and total cutoff are classified as a maintenance issue. Here we consider gain variations over time. The variations in the fiber backhaul losses may result from temperature changes and amplification drifts in the converters, and are limited to a few dBs, and vary slowly over time (weeks to months), whereas the radio transmission backhaul over large distances may suffer larger variations through atmospheric fading (up to 20 - 30 dB), over periods of minutes, and smaller variations due to rain attenuation. Tower sway may modulate the boresight of the high gain antenna, and thus the link, in high winds.

The system stability is recovered by automatically varying the repeater gain in the respective direction. This may be applied either at the transmit end of the backhaul link, at the receiving end or at both ends. The choice of the alternative varies between the RL and the FL chains, and between the different types of backhaul conduits. These are discussed in detail in Chapter 7. OFR over-the-air repeaters have control in the repeater side only – controlling the Rx gain on the FL and the Tx gain on the RL. The wireless modem, operating as a normal ST, detects E_c/I_0 and RSSI to extract E_c and

activates a gain control in the repeater FL to keep the pilot level steady. This stabilizes the repeater coverage. The control of the repeater RL gain is based on link balancing and repeater coverage balancing [1b]. Referring to Section 2.2.3.1, Eq. (2-1) calculates the value of K sent from the BTS to the ST, estimating the balance required between the FL and the RL links. This serves to set the ST transmit power (Eq. (2-2), repeated here):

$$P_m[dB] = -RSSI + K + \sum P.C.corrections\,. \tag{10-1}$$

In a balanced system, the average sum of the P.C. corrections (also called *transmit adjusts*) should even out. In case the RL gain of the repeater is not balanced with that of the FL, corrections will be applied by the system P.C. to the wireless modem to modify its transmission P_m. The reading of the average sum of the corrections is available from the wireless modem, and is applied to the repeater gain to even them out.

Note that this scheme is limited by the repeater RL power limit, and may not suffice for long haul links that may encounter deep atmospheric fades.

10.4 Interference Suppression

The repeater is modeled as a linear, transparent, frequency selective bidirectional amplifier. Its implementation is subject to deterioration of each of these required features:

Linearity is compromised when the amplifiers reach saturation, either due to overload, spurious interference or oscillations.

Adjacent channel and out-of-band interference may leak through the repeater filters.

Oscillations are the result of insufficient isolation between the backhaul and service antennas.

Alien BTS transmission is received and amplified in the repeater, "stealing" repeater capacity and causing pilot pollution and excessive SHO within the repeater coverage area due to servicing multiple pilots.

These issues require due attention. Means of their mitigation are offered in advanced repeaters.

10.4.1 Digital Repeaters

The term "digital repeaters" refers in this context to heterodyne repeaters that down-convert the signal to the IF, sample and digitally process the signal envelope before up-converting back to the RF for retransmission. The digital processing offers numerous advantages.

Digital filtering enables superior filtering performance, in sharpness and thus superior rejection of out-of-band signals both in out-of-band rejection, in amplitude flatness and phase linearity. On top of that, the filters are remotely tunable to choose the FA or a selection of FAs, not necessarily grouped together – a valuable flexibility to the operator.

Amplifier linearization. Predistortion linearization modules are now available to linearize low-cost power amplifiers [3].

Adaptive interference cancellation is discussed next.

10.4.2 Enhancing Isolation between the Backhaul and Service Antennas by Adaptive Interference Cancellation

The backhaul and service antennas of OFR repeaters are typically co-located on the same tower. Coupling between these antennas (Cf. Section 3.6.10) may generate feedback loops in the amplification chain of the repeater (Cf. Section 6.3.4.2), as portrayed in Fig. 10-2. These have to be kept at least 15 dB lower than the gain in that link in order to avoid oscillations and increased noise: $C_F[dB] < G_{RF}[dB] - 15$ and $C_R[dB] < G_{RR}[dB] - 15$. This is also a consideration for in-band FSR repeaters, where the adjacent band filtering may not suffice and further antenna isolation is required. Isolation is achieved by proper antenna design, with low sidelobes, and proper cosite installation on the tower. The distance required between the antennas for sufficient isolation is appreciable (see Fig. 3-41) and takes its toll in tower cost. Moreover, adjacent structures on and around the tower, and nearby buildings and other scatterers, do contribute to the coupling (consult Figs. 3-40 and 3-42) and compromise the available repeater gain. It is desired to relieve the installation requirements and preferably mount the antennas at the same level (on different sides of the tower), where an isolation of about 60 dB (850 MHz) to 70 dB (1900 MHz) is achievable, and to complement the isolation required by adaptive interference cancellation techniques.

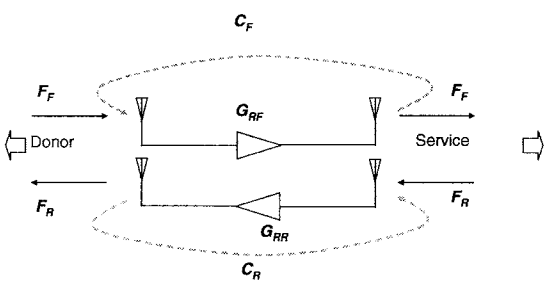

Figure 10-2. Spurious coupling in the repeater (reproduced from Fig. 6-11)

10.4.3 Adaptive Interference Cancellation

Adaptive cancellation techniques are based on resolving the feedback signal out of the compound primary-plus-feedback, and subtracting it adaptively from the signal stream. The feedback is resolved by recognizing that the delay through the repeater is much longer than the delay through the feedback, which allows for correlating between the signal sampled from the input to the repeater and the signal sampled from the output (Fig. 10-3). The latter is adaptively delayed to match the delay through the feedback path. The output of the complex correlators (see Fig. 10-3) is then weighted and subtracted from the signal stream. The same technique is applicable for the RL signal path and the FL signal path.

Adaptive processing is a mature technology [4] that has become useful in multiple applications: in adaptive antennas [4b], in amplifier linearization [4f], etc. Its application to repeaters is tailored to its specific requirements:

Signal design. The CDMA signal is wideband, with a short time correlation – 0.812 μs for CDMA2000 and 0.26 μs for UMTS.

Repeater delay. The repeater filters delay the signal through the repeater by about 6 μs as a minimum.

Coupling delay spread. The feedback signal is spread over a large delay, with most of the contributions delayed by less than 100 ns, and the rest diminished by 1.5 μs.

The spread of the delay together with the signal bandwidth leads to a complex design [5]. The process incorporates signals over a wide dynamic range, a range of delay and frequencies.

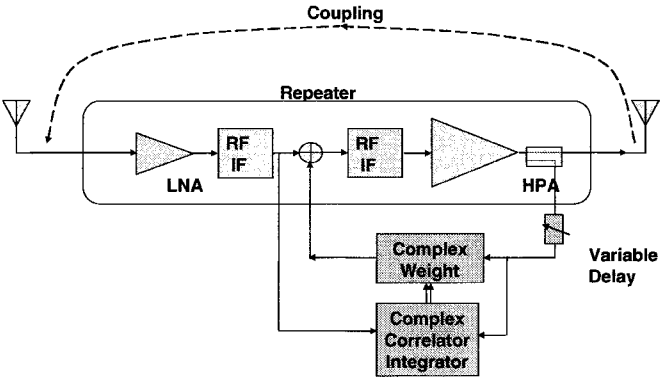

Figure 10-3. Adaptive cancellation at the remote unit

Practical considerations relate to high internal isolation within the canceller, and choice of components with properly frequency-flat response. The bulk of the advanced interference cancellation technology relates to overcoming these issues. Interference cancellers for CDMA repeaters [6] claim for over 35 dB cancellation.

10.4.4 Adaptive Cancellation of Radiated Interference

The backhaul antenna of an RF repeater is subject to illumination by alien BTSs, and is therefore liable to amplify and distribute these signals along with the desired signals. This is of a major business concern to operators, reluctant to relay competitor signals, but also a major source of interference – by saturating the repeater or by relaying the wrong BTS coverage. Frequency filtering of such interfering signals is only a partial solution to the problem and does not help at all in cases of a CDMA network, where the BTSs differ by pilot codes and not by frequency. Spatial filtering is therefore proposed.

Adaptive nulling is a known technique in communications and radar. It relies on comparing the signals received by two antennas with different radiation patterns, and weighting them in a way that suppresses the unwanted signal. The desired radiation patterns for the main (backhaul) antenna and the reference antenna are described in Fig. 10-4.

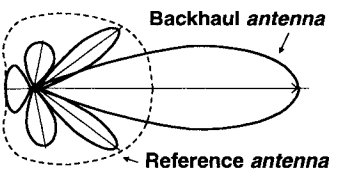

Figure 10-4. Main antenna and reference antenna for adaptive nulling

Signals received over the main beam of the main antenna are duly amplified by the antenna gain, while those received out of the main beam are weaker than those received through the reference, wider beam antenna. Alternative schemes utilize directional antennas for both the main and reference antennas, directing the reference antenna to a known interference source. This scheme, though yielding higher gain differentiation, requires the knowledge of the direction of the interfering signal, and the application of a larger size reference antenna, and is limited to a small number of interfering sources.

The adaptive processing scheme is sketched in Fig. 10-5. The interferer $i(t)$, assumed to be uncorrelated with the desired signal, is received

by the repeater antenna on the left-hand side, together with the desired signal. The additional *reference* antenna intercepts the interferer and, possibly, not the desired signal.

The adaptive canceller strives at producing at the error output a signal that has a minimum residual of signals correlated with those from the reference antenna that have been received by the repeater antenna. In case the interference is generated by a nearby source (e.g. a colocated transmitter on the same tower), it is possible to directly sample the interfering antenna terminal and use a coaxial cable connection as a 'reference' input to the adaptive canceller, instead of a reference antenna. In this case the pointing direction of the interference with respect to that of the desired signal is immaterial.

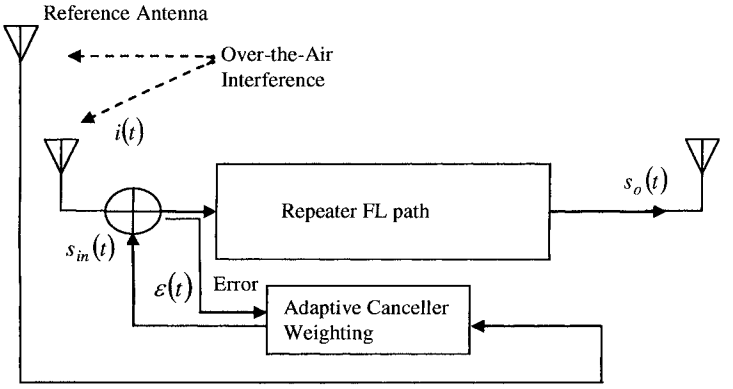

Figure 10-5. Adaptive cancellation of radiated interference

10.5 Receive Diversity in Repeaters

Diversity reception reduces the FER by reducing the probability of the signal to sink to low SNR values during fades. This allows the CDMA to reduce the required power for a set FER level and increase the capacity. The lack of diversity reception in the repeater service area reduces its coverage and the capacity of the donor cell. Application of diversity reception in the repeater is therefore desired, but comes with a cost. The repeater has to have an additional diversity antenna on the service side, and two channels of amplification and backhaul to the donor diversity inputs. A suboptimal implementation is pseudodiversity combining the diversity branches, and linking to the donor via a single backhaul link. This technique may also apply to a chain of repeaters in multi-hop arrangement. These are discussed in Chapter 5 in detail.

10.6 Transmit Diversity in Repeaters

Transmit diversity is an effective means to enhance the forward link, reduce the required power and enhance coverage and capacity. Its application is optional in the 3G systems. Transmit diversity requires two branches for transmission of the same signal, but with a different "color" to allow for the receiver to differentiate between the branches for proper diversity-combining. These colors may be codes, modulations or delay, and are described in detail in Chapter 5, where a full discussion of these techniques takes place. Coded diversity means have to be generated at the donor BTS and conveyed to the repeater via two separate links, which are then separately amplified by two amplification chains and transmitted by two service antennas. Alternative add-on diversity techniques generate the "color" by processing the RF signal, either delay (TDTD – time-delay transmit diversity) or phase-sweep transmit diversity (PSTD). These are applied at the repeater and do not require diversity backhaul.

10.7 Network Parameters Readout from the Wireless Modem

The test ST, serving as a wireless modem in the repeater, is a source of valuable information on the network in the service area of the repeater. Multiple parameters are extractable from the latest models of STs. The main parameters are:

RSSI. The RSSI measures the total power received by the ST over the carrier bandwidth, including noise and interference from other BTSs. All the FL BTS traffic and overhead goes through the repeater, and the RSSI varies accordingly.

Ec/Io provides indication on the FL channel quality for each pilot passing through the repeater, and an indication of the existence of rouge pilots. The level of the pilot signal *Ec* is calculated from *Ec/Io* and RSSI, and used for stabilizing the FL.

MTx. The ST transmit power is a measure of the RL. It is used for RL link balancing (Section 10.3) in conjunction with the *transmit adjust* [1b].

Transmit adjust (Eq. (10-1)) provides indications on imbalance between FL and RL, and serves in an automatic adjustment ([1b] and Section 10.3). It provides an alarm on any deterioration in the repeater performance, when exceeding an acceptable value.

10.8 Antenna Control

Coverage control, network load balancing and optimization are affected by antenna beam tilting, steering and shaping (Cf. Sections 4.8.1 and 3.6.7.3-4). This is a tedious process starting with planning and simulation, coverage measurements by drive testing, then antenna alignment and then repeated drive testing. The introduction of remotely controlled antennas alleviates most of this burden and shortens the process to the point that it can be dynamically controlled in response to the network state. Electronically controlled antenna arrays [7], incorporating separate beam control on the FL and on the RL, have proven their effectiveness in dynamic link balancing and load balancing. Electronic multibeam arrays [7, 8], for coverage shaping and load balancing between sectors, have proven significant capacity enhancement, but failed to capture appreciable market due to their excessive cost. The introduction of affordable electromechanical beam-tilting antennas made this option cost-effective. Furthermore there is an open standard for antenna control and monitoring (RET – Remote Electrical Tilt) defined by the Antenna Interface Standardization Group (AISG) [9]. Using antennas that are remotely controlled allows for easy and dynamic changes in tilt and steering [10]. Remote control of the repeater service antennas is feasible through the repeater control functions, thus enabling the dynamic tuning and optimization of the repeater within the CDMA network.

10.9 Tagging of Repeater-Served STs

The tagging of the STs served by the repeater is valuable information for evaluation of the state of the network and for other services, including ST location, counting of the ongoing traffic calls, the origination of failures and call drop events. The designation of the STs is called "water marking" and is accomplished by "coloring" the RL or the FL signal that goes through the repeater, in a way that is recognizable by the BTS (if RL) or the ST (if FL) without interfering with the intended transmission. Tone modulation *water marking* is reported by [1d]. The cooperation of the receiver at the BTS or the ST is required.

10.10 Location

The determination of the location of mobile subscribers is requested by emergency services (e.g. E911 in the US) and is also a basis for multiple commercial applications that leverage on the ST location. Location measurement techniques have been incorporated at the BTS level. The

location methods are satellite-based (GPS, incorporated in some STs) and network-based, utilizing Time-Of-Arrival (TOA), also called AFLT – Advanced FL Triangulation techniques, where the location processing is performed by the network. The triangulation techniques rely on the time-of-flight of the signal from the ST, equating it to distance by assuming a direct path. The delay incurred by the repeater, which amounts to 0.5 – 16 μsec (including the repeater and the backhaul delays) causes errors in location readings for STs served by the repeater. This may be recovered by providing the network with means for tagging the STs according to the repeater they are served by, in addition to a priori information on the repeater location and its excess delay. A method incorporating tone modulation *water marking* is reported [1d].

10.11 Measurement of Traffic Load through the Repeater

The traffic load through the repeater is an important network control parameter. It can be assessed by measurement of the repeater noise rise [1c]. The net gain through the repeater – y (Eq. (6-2) and Section 6.4) is lower than unity in most applications, and the level of signal reaching the repeater from a served ST is higher than the set level required by the BTS for that load level. The noise rise at the repeater input is therefore higher than the noise rise at the BTS and its reading is a sensitive indicator for the activity through the repeater. The sensitivity of this method is high for loosely coupled repeaters, where $y<<1$. The measurement for coverage extension repeaters, linked by high net gain $y \to 1$, is not as sensitive.

10.12 Load Balancing between Cells and Sectors

The loads' distribution throughout the network is typically uneven (Cf. Section 9.1.1), and changes with time – periodically during the day and during the week, and on occasional events. The network is then stressed by peaks in a number of sectors while other, frequently adjacent sectors, are lightly loaded. Load balancing by changing the direction and beamwidth of the sector antennas have been proposed (Cf. Sections 4.6, 4.8). This angular distribution of the load is only a partial remedy and situations arise where "hot spots" are local and situated away from the BTS. Load control by remote Radio Access Nodes (RAN) have been proposed [11, 12] and are described in Fig. 10-6.

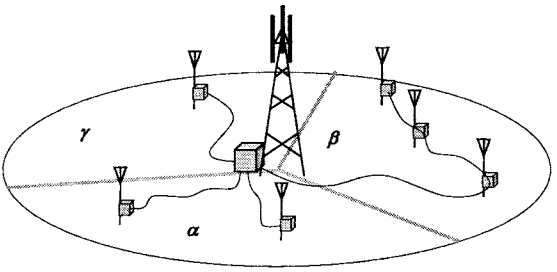

Figure 10-6. Load control by distributed repeaters and a control center

Repeaters are placed at potentially high density locations. They are fed by dedicated backhauls (e.g. fiber, FSO, microwaves) – all concentrated at a switching matrix that controls their allocation to the lightly loaded sectors (Fig. 10-7). Multi-hop cascading is optional as per the coverage requirements. The allocation of repeaters to other sectors entails due care to avoid excessive SHO and SrHO. Coverage has to be tailored accordingly, as discussed in Section 6.3.3.

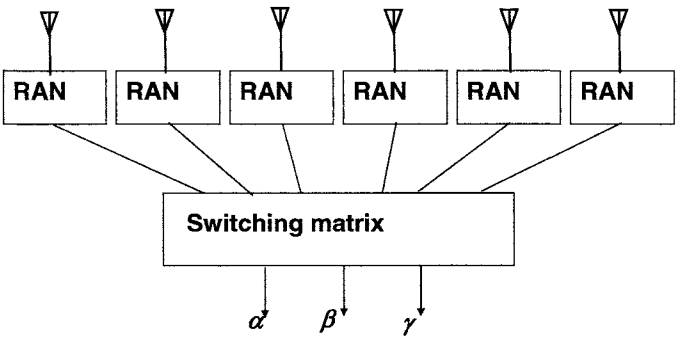

Figure 10-7. Switching and control matrix for load balancing

10.13 High Data Rate Systems

The high data rate versions of the 3G systems differ from the basic CDMA in two major ways:

The wave form is a scheduled time-slotted transmission, each addressed to specific subscribers.

Advantage is taken of the differentiation of channel states between subscribers, preference being given to those enjoying momentary high SNR.

This different paradigm also changes the rules for application of channel control schemes. Power control and SHO are not incorporated in the FL of these systems. The range dependence of the channel's orthogonality (Cf. Section 3.4.2) and of the available SNR (Cf. Fig. 1-10) lead to respective range-dependent availability of highest throughput and preference of smaller, more orthogonal coverage areas. Repeaters may have new functionality and justification beyond cost saving in this realm. The time-scheduled transmission opens signal relaying options through properly scheduled time-switched repeaters. Multi-hop repeater chain becomes a viable architecture for intensifying the throughput of high data rate networks, and its study captures an increasing interest [13, 14].

The impact of repeaters on their donor and neighbor cells is different for the CDMA and for the time-multiplexed regime, which should be carefully noted during planning and optimization. The macrodiversity provided by the repeater over the overlapping coverage area reduces the orthogonality in that area, and may drastically reduce the available SNR if applied over a highly orthogonal area near the adjacent access point. Application of coverage isolation techniques (e.g. choice of location, antenna tilt, etc.) deem important. Application of TDTD ruins the orthogonality and destroys the high SNR region around the access node, and is to be avoided. PSTD, on the other hand, continuously changes the fading structure over the coverage area. A slow PSTD may serve as a "mode mixer", distributing the opportunities among the subscribers. Furthermore, adaptive modulation may apply for actual subscriber allocation control [15].

OFDMA-based transmission standards proposed for the next generation enjoy a similar flexibility. These systems enjoy a very wide band that is divided through the network between the BTSs and the relaying repeaters in a scheduling process. The path control through multi-hop relays in these standards is obtained by the timely switched control of the frequency clusters allocated for that path [15, 16].

REFERENCES

[1] RepeaterOne (Qualcomm) white papers in: www.repeaterone.com
   a. 80 W0836-1 Rev A
   b. 80 H2657-1 Rev A
   c. 80 W0838-1 Rev A
   d. 80 W0013-1 Rev A
   e. 80-31550-1 Rev B.

[2] S.-W. Park, *System and method for supervising repeater by using wireless mobile*, US Patent 6,941,137 B2 Sept. 6, 2005.

[3] PMC-Sierra, *Digital correction signal processor* PM7815, 2004.

[4] Adaptive processing
   a. B. Widrow, J. McCool, and M. Ball, *The complex LMS Algorithm*, Proc. IEEE, 63, No. 4, p. 719, 1975.
   b. R.T. Compton, Jr., *Adaptive Antennas*, Prentice Hall, 1988.
   c. R.A. Monzingo, and T.W. Miller, *Introduction to Adaptive Arrays*, Wiley, 1980.
   d. O. Macchi, *Adaptive Processing*, Wiley, 1995.
   e. S.J. Orfanidis, *Optimum Signal Processing - An Introduction*, 2nd Ed., Chapter 7, McGraw-Hill, 1996.
   f. P. Kenington, *Mobile Transmitter Linearization for Spectrum-Efficient Modulation Formats*, Proc. COMSPHERE 99, URSI, Jan. 1999.

[5] S.J. Kim, J.Y. Lee, J.C. Lee, J.H. Kim, B. Lee, and N.Y. Kim, *Adaptive Feedback Interference Cancellation System*, IEEE MTT-S, Vol. 1, pp. 627-630, June 2003.

[6] M. Kurk, *Innovative Solutions in 3G Networks*, Andrew Corp, Technologies Hi-Tec show, Tel Aviv, May 2005.

[7] J. Shapira, *Networking 3-Dimensional Intelligent Antennas for Capacity Maximization of the Cellular System,* CDG Technical Forum, Vancouver, April 2001.

[8] S. Gordon, and M. Feuerstein, *Evolution of Smart Antennas from 2G to 3G Air Interfaces,* Sixth Workshop on Smart Antennas in Wireless Mobile Communications, Stanford University, July 1999.

[9] Antenna Interface Standards Group - AISG. www.aisg.org.uk .

[10] Beam shaping: *Adjustable Beam Control Antenna*, in www.kmwinc.com .

[11] J. Shapira, *Distributed Cell Balancing*, PCT-WO 2005/041348 A2.

[12] H. Wu, C. Qiao, S. De, and O. Tonguz, *Integrated Cellular and Ad Hoc Relaying Systems: iCAR*, IEEE Journal on Selected Areas in Communications, Vol. 19, No. 10, October 2001.

[13] A.N. Zadeh, and B. Jabbari, *Throughput of a Multihop Packet CDMA Network with Power Control*, in Proc. 51st IEEE VTC, Vol. 1, pp. 31–35, 2000.

[14] J. Cho, and Z.J. Haas, *On the Throughput Enhancement of the Downstream-Channel in Cellular Radio Networks Through-Multihop Relaying*, IEEE journal on Selected Areas in Communications, Vol. 22, No. 7, pp. 1206-1219, Sept. 2004.

[15] U. Timor, and S. Miller, *Forward-link Throughput Performance of 1xEVDO with Phase-Modulation Transmit Diversity (PMTD)*, Proc. CIC2004, The 9th CDMA International Conference, Seoul, Korea, Oct. 2004.

[16] B.H. Walke, and R. Pabst (Eds.), *Relay Based Deployment Concepts for Wireless and Mobile Broadband Cellular Radio*, WWRF/WG4 Relaying Subgroup, September 2003.

EPILOG

The CDMA network, now dominating the 3rd generation of cellular networks, is highly reconfigurable due to its flexible interaction rules, headed by the power control and the Soft Handoff. This allows for a flexible application and optimization by additional RF access nodes that enhance coverage, performance, cell and network capacity utilization.

The increasing dynamics of the service demands from the network requires a tighter and more dynamic control of the radio resources. All RF building blocks of the network will have to be dynamically controllable. This includes antenna beam and orientation control, power and pilots' control and repeater parameters control.

The locality of the network interaction allows to dynamically control relatively small cell clusters in response to the local environment and teletraffic demands. These *smart clusters* utilize prevailing network probes and apply controls over predominantly RF parameters, e.g. antenna tilt (RET antennas) and possibly orientation, power level and gain in repeaters, etc.

The mobile multiple access is escalating - high data rates, diversity of services and of products. Data throughput density (Mb/sq.km) is growing.

The underlying physical propagation medium does not change, and the rationale for distributing the radio access is becoming ever stronger.

The RF repeaters enhance the CDMA network as a cost reduction means for distributing the radio access. Their incorporation in the network is eased by the network flexibility and adaptation.

The CDMA repeaters fall short, however, of providing full controllability of the radio resources. This is due to the inherent nature of the CDMA – the need to despread and decode each session.

Other modulation/ multiple access schemes have hierarchical filtering to the session: frequency (OFDMA), time slots (TDMA), and a compromise of complexity/ cost and performance is more comfortable there. Such regenerative repeaters may indeed fulfill the promise for distributed access with full RRM. These are pursued with the 4th generation.

The BTSs of the 3rd generation are by themselves controllable regenerative repeaters. Within that, and with the advent of broadband wireless distribution (e.g. WiMAX), the network may strip off their wired fixed network ("backbone") that supports the BTSs, and BTSs may become the "of the air" repeaters of tomorrow.

MIMO (multiple in – multiple out) communication utilizes multiple antennas at both ends for transmission of multiple, uncorrelated signals. The scattering environment is expected to defuse the transmitted signals so as not

to be correlated upon joint detection at the multiple receivers. The ultimate goal of this concept is achieving capacity equal to that of a mesh wireline, where each transmission point is connected to each one of the receiving points by an independent conduit. Not every scattering environment lends itself to such full decorrelation of the MIMO system. The application of repeaters as active, controllable scatterers and scattering environment conditioners, brings a whole new dimension to this exciting development. The richness of configurations, control parameters and their dynamics is far from being fully explored and is an open field for research and opportunities for the industry.

APPENDIX A

REVERSE LINK INTERFERENCE IN HETEROGENEOUS CELL CLUSTERS

A.1 The Ring Model for Other Cells' Interference

A.1.1 Introduction

The reverse link interference from users in adjacent cells loads the BTS receiver. The Soft Handoff between cells in the same network links the other cells' interference to the controlled level of the users' transmission within the cell. The ratio of the "other cells" to self-interference, termed f, (see Eq. (4-2))

$$I_{oc}/I_i \equiv f = I_{oc}/(n-1)P_m(r)T(r)\nu \tag{A-1}$$

is introduced to the load Eq. (4-3)

$$\frac{P_m(r)T(r)}{N_0WF_{BTS}} \equiv q = \frac{C/I}{1-(n-1)\nu(1+f)C/I} \equiv \frac{C/I}{1-\eta} \tag{A-2}$$

and in the load factor (Eq. (4-4))

$$\eta \equiv (n-1)\nu(1+f)C/I\,. \tag{A-3}$$

The value of f has been approximated by models representing specific users' distributions, cell clustering configurations and propagation conditions. A model based on uniform-size hexagonal cells, uniform distribution of users and $r^{-4}10^{-\zeta/10}$ propagation rule, ζ being a dB attenuation LogNormal random variable with σ=8 dB [1], [4], renders f=0.55, and is acceptable as a reference approximation in the load equation.

A simpler model was presented in [3] that enables parametric calculations, and the assessment of the dynamics of the power control – soft handoff loops through the network. This model, also used in [4, 5], is applied here for

assessing the interference in heterogeneous cell clustering. The model assumes a set of rings of cells around the cell of interest, as described in Fig. A-1, which allows for the separation of the radial and angular variables and then simple, analytical integrations.

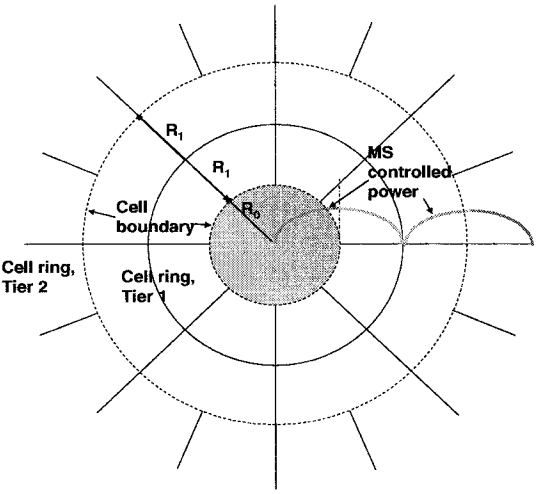

Figure A-1. Ring model of cell cluster

A simple extension of the load factor expression to heterogeneous cell clusters is provided in Eq. (4-10)

$$\eta_i \equiv \frac{C}{I}(n-1)(1+uxf)v \qquad \text{(A-4)}$$

where $u \equiv (R_i/R_{oc})$ represents the user density factor, and $x = \eta_{oc}/\eta_i$ the users' power factor. These factors are now examined through the model for their accuracy and domain of validity.

A.1.2 The Ring Model

The cells encircling the cell of interest are arrayed in rings, and their bases are stretched along the rings. Inasmuch as this configuration does not accurately duplicate the hexagonal cluster, the latter is also an artificial approximation of any practical deployment. The object of this model is to assess the integrated effect of the surrounding cells on the cell of concern.

This model, tested for approximately similar parametric behavior as the hexagonal one, serves its purpose well.

A uniform distribution of users within each cell ring is assumed. Generalization to radial dependence of the distribution in each ring is straightforward, but not necessary for the present purpose. The radius of the center cell is R_0, and will be normalized to 1 without loosing generality. The radius of the cells in the j_{th} tier is R_j, normalized to the radius of the central cell. Propagation law r^{-4} is assumed. Note that for $R_0=R_1$ the area of the first ring is 8 times that of the center cell, accommodating 8 wedge-shaped cells, 45^0 each, while the second ring comprises 16 cells with the same area, 22.5^0 each, and so on.

The total power received at the BTS from within the cell is

$$P_0 = n_0 P_m T(R_0) \tag{A-5}$$

where n_0 is the number of users in the cell, and P_m is the ST transmission power at the boundary $T(R_0)=A_0R_0^{-4}$. The total power received at the BTS from the j_{th} tier, each cell loaded to n_j, is

$$P_j = \frac{8jn_jP_mA_0}{\left((D_j+R_j)^2-(D_j-R_j)^2\right)}\cdot 2\pi\int_{D_j-R_j}^{D_j+R_j}\left(\frac{D_j-r}{R_jr}\right)^4 rdr = \\ = \frac{4jn_jP_mA_0}{D_jR_j^5}\left[-\frac{D_j^4}{2r^2}+\frac{4D_j^3}{r}+6D_j^2Ln(r)-4D_jr+.5r^2\right]_{D_j-R_j}^{D_j+R_j} \tag{A-6}$$

where

$$D_j = R_0 + R_j + \sum_{k=1}^{j-1} 2R_k \tag{A-7}$$

is the distance to the j_{th} BTS ring.

Now, $\hat{f} \equiv \sum_{j=1}^{m} P_j \Big/ P_0$. This is evaluated for $R_j=R_0$, $n_j=n_0$ and compared in Table A-1 with the respective tiers in the hexagonal grid [4].

The relative contributions of the respective tiers in the ring and the hexagon grids are very similar (compare lines 2 and 3 in the table). A correction factor 1.2585 is applied to line 3.

Table A-1. Outer cells' interference - f parameter

	Tier 1	Tier 2	Tier 3	Sum	%Tier 1	%Tier 2	%Tier 3
Ring	0.2889	0.0163	0.0042	0.3094	93.3852	5.2673	1.3475
Hexagon	0.3600	0.0240	0.0054	0.3894	92.4499	6.1633	1.3867
Correction to hex	0.3636	0.0205	0.0052				
Correction to 0.55	0.5136	0.0290	0.0074				

The inclusion of the LogNormal variation in the path-gain brings the total outer cell contribution to 0.55 [1]. Correction factor 1.7776 is applied in line 4. The contribution of tier 1 is about 93 %. Tier 3 is negligible altogether.

Having established the model, we now apply it to a heterogeneous cluster and examine the relative contributions of the tiers as a function of R_j/R_0, $R_1=R_2=R_3$ in Fig. A-2. The local nature of the power controlled, SHO CDMA system becomes clear. The smaller and denser the surrounding cells are, the higher is the contribution of further tiers, and vice versa.

Next we examine the u factor in Eq. A-4. Figure A-3 plots the ratio $0.55u/\hat{f}$ in a cell cluster where the central cell radius is R_0, and that of all surrounding tiers is R_j, each cell loaded with n users. The linear factor u is accurate to within 20% for cells' radii ratio between 0.3 to 3. The residual error when applying a correction factor $\hat{u}=1.06(R_0/R_j)-0.075$ is less than 2% up to R_j/R_0=6, as shown in Fig. A-4.

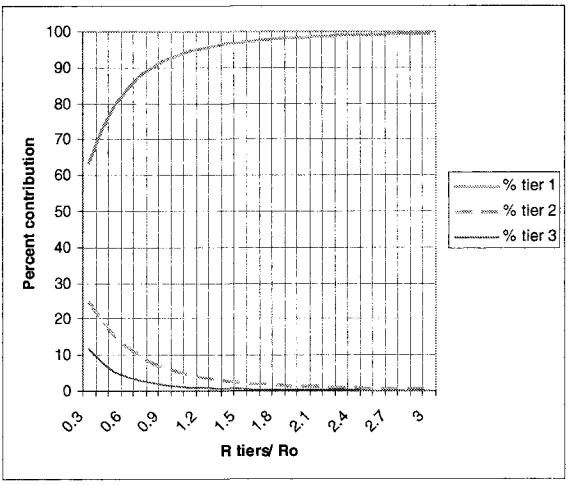

Figure A-2. Relative contributions of tiers vs. relative cell size

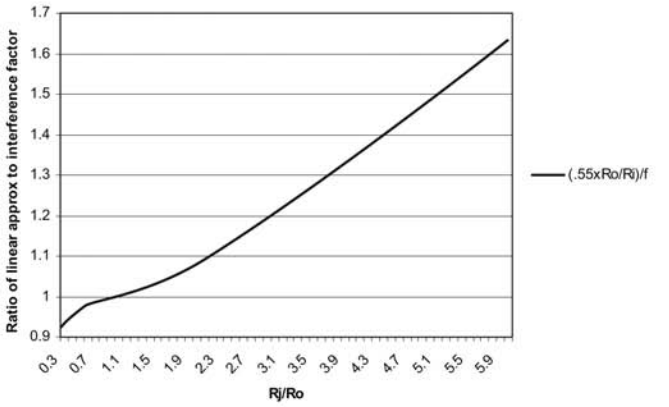

Figure A-3. The error of the linear approximation u

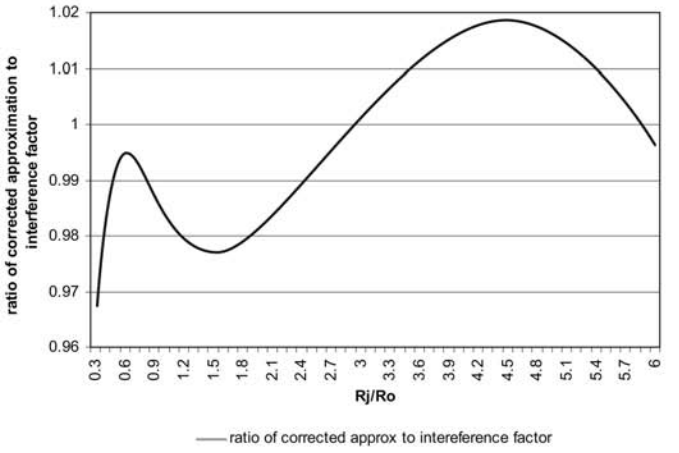

Figure A-4. The residual error of the corrected $\hat{u}$ factor

A.2 The Embedded Microcell Model

The analysis follows [6].

The small microcell is embedded in a much larger cell, as described in Fig. 4-19 and in Fig. A-5. The size of the microcell is much smaller than that

of the umbrella cell, $R_c/R_m>>1$. The ST power at the interface, P_m, is assumed the same around the microcell boundary rim. The users are uniformly distributed within a radius δR_m as in Fig. A-6. The interference from the microcell to the umbrella cell is

$$P_{cm} = \frac{N}{D(1+I_m)\pi R_m^{\,2}} \cdot 2\pi \int_0^{\delta R_m} \left(\frac{r_m}{R_m}\right)^4 r_m dr_m = \frac{N}{3D(1+I_m)}. \qquad \text{(A-8)}$$

The interfering power of the umbrella cell to the microcell is

$$P_{mc} = \frac{N}{(1+I_c)\pi\left(R_c^{\,2} - R_m^{\,2}\right)} \cdot 2\pi \int_{R_m}^{\infty} \left(\frac{R_m}{r_m}\right)^4 r_m dr_m = \frac{1}{A} \cdot \frac{N}{(1+I_c)} \qquad \text{(A-9)}$$

where $I_m = P_m/N$, $I_c = P_c/N$ are the ratio of the outer interference to the microcell and to the umbrella cell, respectively, to their self-interference. N is the pole capacity of an isolated cell (I_c=0), and $A \equiv (R_c/R_m)^2 - 1$.

The size of the umbrella cell is so much larger than that of the microcell that the power level in the umbrella cell around the rim of the microcell boundary is about constant through the integration.

We now solve for the capacity of microcell and of the umbrella cell.

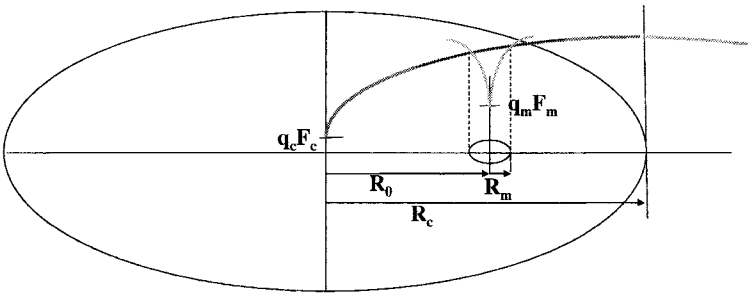

Figure A-5. Embedded microcell configuration

Define

$$C_0 = \frac{N}{1+I_0} \equiv \frac{N}{x_0}, \quad C_c = \frac{N}{1+I_{co}+I_{cm}} \equiv \frac{N}{x_c}, \quad C_m = \frac{N}{1+I_{mc}} \equiv \frac{N}{x_m} \qquad \text{(A-10)}$$

where C_0, C_c, C_m are the capacity of a cell in a uniform cluster, the umbrella cell and the microcell, respectively. From Eqs. (A-8) – (A-10)

$$x_c - x_{co} = \frac{1}{3Dx_m} \quad , \quad x_m = 1 + \frac{1}{Ax_c} \tag{A-11}$$

where $x_{co} \equiv 1 + I_{co}$.

This is solved as

$$x_c = B\left(1 \pm \sqrt{1 + \frac{x_{co}}{B^2 A}}\right) \tag{A-12}$$

where $B \equiv \frac{1}{2}\left(x_{co} + \frac{1}{3D} - \frac{1}{A}\right)$.

Only the first root (+) is positive and valid.

$$\frac{C_{umbrella}}{C_0} = \frac{1 + I_0}{x_c} \tag{A-13}$$

$$\frac{C_m}{C_0} = \frac{1 + I_0}{x_m}. \tag{A-14}$$

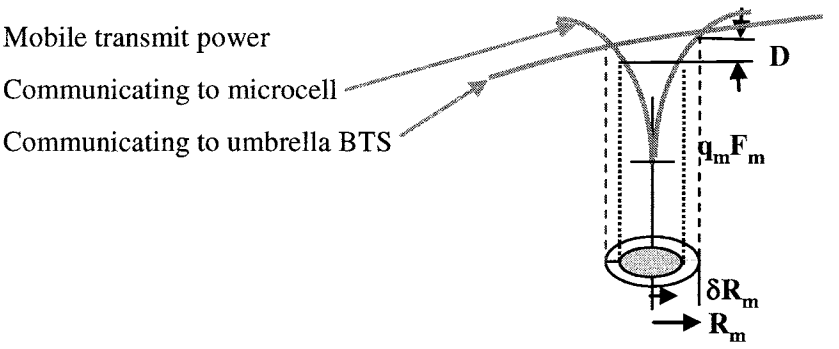

Figure A-6. Distribution of users in an embedded microcell

Note that $x_{co}=x_0$ in case the umbrella cell is surrounded by identical cells, loaded as the umbrella cell without the microcell.

The capacity of the microcell, shown in Fig. A-7, is higher than that in a uniform cluster, as its outer cell interference is lower. The capacity of the umbrella cell, shown in Fig. A-8, is lower because of the additional interference by the embedded cell. This additional interference is reduced by limiting the high density user population to a smaller area, and thus backing off the maximum power of the ST in the microcell.

Interesting to note (Fig. A-9) that the total capacity of the umbrella plus the embedded microcell is higher than that of 2 cells in a uniform cluster. This is because the effect of the outer interference is very local in the CDMA network, and the microcell is embedded in a sparse density in its close neighborhood.

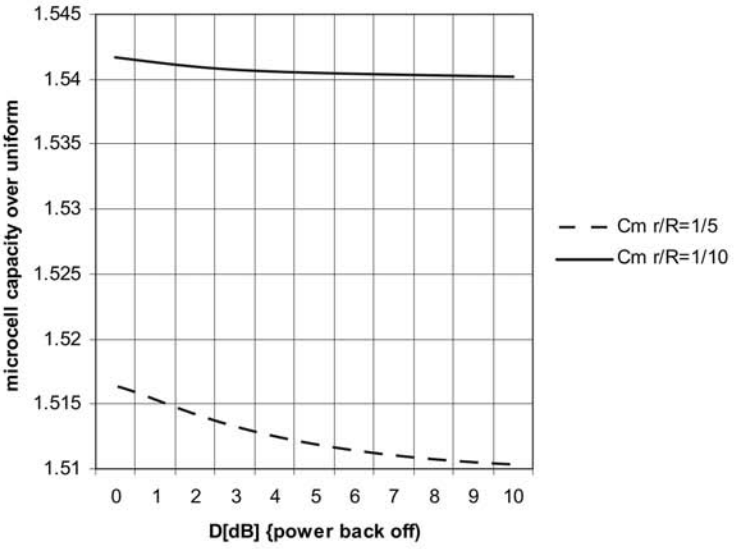

Figure A-7. Microcell capacity relative to uniform cluster

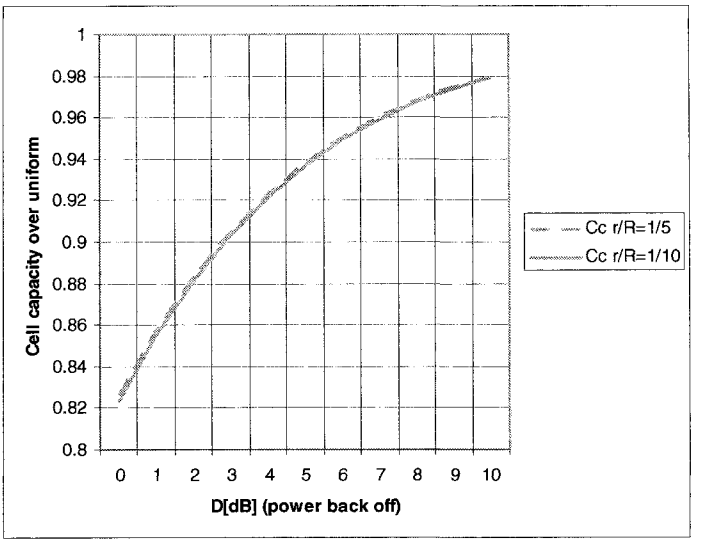

Figure A-8. Umbrella cell capacity relative to uniform cluster

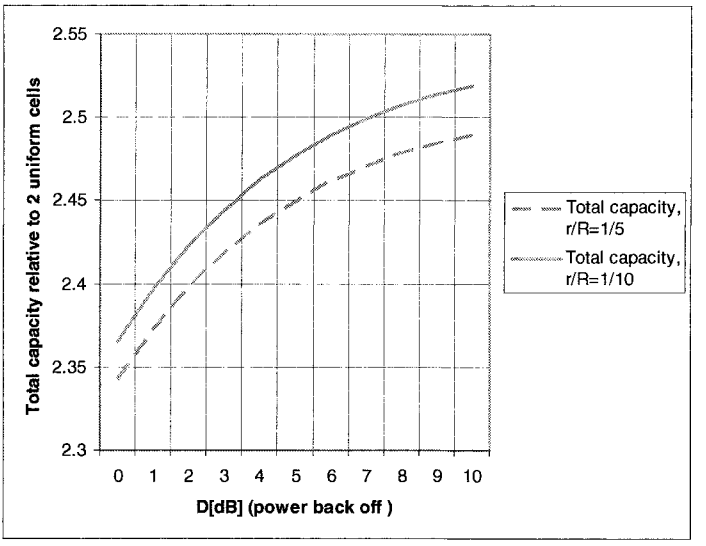

Figure A-9. Total capacity relative to 2 cells in a uniform cluster

REFERENCES

[1] A.J. Viterbi, *CDMA*, Chapter 6, Addison-Wesley, 1995.

[2] J. Shapira, *Effect of Spurious Intermod Transmission Interference on Cellular Radio Systems*, Qualcomm internal memo, 1991.

[3] J. Shapira, *A Model for Power Dynamics in CDMA Cell Cluster*, Qualcomm internal memo, 1991.

[4] *CDMA Network Engineering Handbook*, Qualcomm, 1992.

[5] T.S. Rappaport, *Wireless communications*, Chapter 8, Prentice Hall, 1996.

[6] J. Shapira, *Microcell Engineering in CDMA Cellular Networks*, IEEE Trans. Vehicular Technology, Vol. 43, No. 4, pp. 817-825, November 1994.

APPENDIX B

EVALUATION OF THE POWER RISE EQUATION

Resorting to Eq. (4-35)

$$P_{BTS} = \frac{\nu_F \dfrac{C/I}{\alpha g(\alpha,\delta)} N_0 W F_m \sum_1^n \dfrac{1}{T(r_i)} + P_{OH}}{1 - \nu_F \dfrac{C/I}{\alpha g(\alpha,\delta)} \left(n(1-\alpha) + \sum_1^n x_F \dfrac{T_{oci}(r_{oci})}{T(r_i)} \right)} \equiv \frac{N_{Thermal}(d) + P_{OH}}{1 - \eta_F(d)} \quad \text{(B-1)}$$

The ST distribution is modeled as continuous area-density ρ. The number of users is $n = \iint \rho(\varphi; r) r dr d\varphi$. Cell radius is normalized to 1. Considering a sectorized cell, interference contributions are expected from one (on axis), two (median) or three cells. These are computed respectively as

$$\left(\frac{r}{2-r}\right)^4 ; 2\left(\frac{r}{\sqrt{r^2 - 3.464r + 4}}\right)^4 ; \left(\frac{r}{2-r}\right)^4 + 2\left(\frac{r}{\sqrt{r^2 - 2r + 4}}\right)^4$$

and compared in Fig. B-1.

The difference is small enough to justify the model of a single cell and calibrate the power by x_F.

Consider the cases:

1) Users uniformly (area) distributed. Power control limited to 10 dB.

It follows $1/T(r)$ over $10^{-1/4} = 0.56 < r < 1$ and $10^{-3/2}$ over $0 < r < 0.56$, $\rho = n/\pi$

$$\sum_{1}^{n}\frac{1}{T(r_i)}=\frac{2\pi\rho}{T(1)}\left(\int_{0.56}^{1}r^5dr+\frac{1}{10}\int_{0}^{0.56}rdr\right)=\frac{n}{3T(1)}\left(1+2\cdot10^{-3/2}\right)=\frac{0.354n}{T(1)}. \qquad \text{(B-2)}$$

This differs from integration over a full range power control by 6.3%

$$\sum_{1}^{n}\frac{T_{oci}(r_{oci})}{T(r_i)}=2\pi\rho\int_{0}^{1}\frac{r^5}{(2-r)^4}dr=2n\cdot0.107=0.214\cdot n. \qquad \text{(B-3)}$$

2) No power control. The BTS transmits maximum power.

$$\sum\frac{1}{T(r_i)}=\frac{n}{T(1)} \qquad \text{(B-4)}$$

$$\sum_{1}^{n}\frac{T_{oci}(r_{oci})}{T(r_i)}=2\pi\rho\int_{0}^{1}\frac{r}{(2-r)^4}dr=5/12\cdot n. \qquad \text{(B-5)}$$

3) Linear distribution along the radial, with power control.

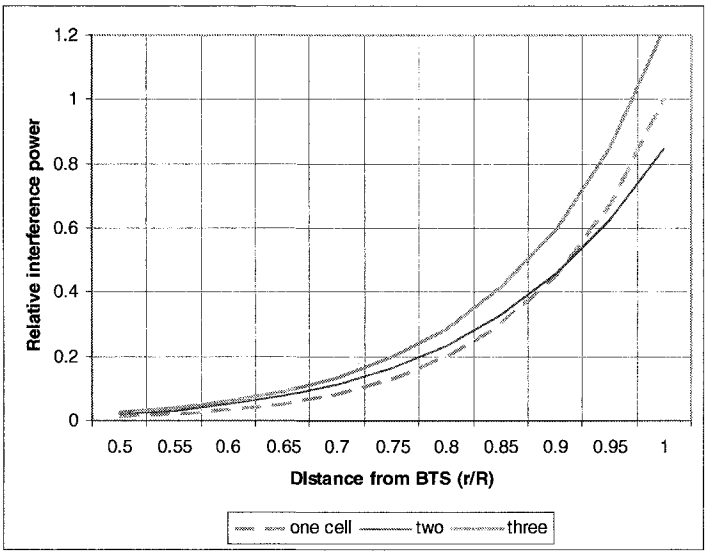

Figure B-1. Other cells' interference

$$n = \rho \int_0^1 dr = \rho \sum \frac{1}{T(r_i)} = \frac{n}{T(1)} \left(\int_{0.56}^{1} r^4 dr + \frac{1}{10} \int_0^{0.56} dr \right) = \\ = \frac{n}{5 \cdot T(1)} \left(1 + 4 \cdot 10^{-5/4}\right) = \frac{0.245n}{T(1)} \quad \text{(B-6)}$$

This differs from integration over a full range power control by 22%.

Parametric evaluation

$T(r) = T(1)r^{-4}$, $T(1) = -122$ dB, $\rho = 0.5$, $\delta = 0.8$, $C/I = 0.04$ (= -14 dB), $N_0WF_m = -105$ dBm, $x_F = 1$, $P_{OH} = 2.5$ Watt (39.8 dBm), $\nu = 0.55$.

Table B-1. Integration elements in (B-1)

Distribution	Uniform, no P.C.	Uniform, P.C.	On the rim	Linear
$\sum_i^n \frac{1}{T(r_i)}$	$\frac{n}{T(1)}$	$\frac{0.354n}{T(1)}$	$\frac{n}{T(1)}$	$\frac{0.245n}{T(1)}$
$\sum_i^n \frac{T_{oci}(r_{oci})}{T(r_i)}$	$0.417n$	$0.214n$	n	$0.1215n$

Table B-2. Multipath diversity gain (r = 0.5, high end. Fig. 4-8)

α	0.5	0.7	0.95	0.99
g[dB]	4.63	2.76	0.87	0.39
g	2.9	1.89	1.22	1.09

Table B-3. Expressions for (B-1) for different distributions

Uniform, PC	Uniform, no PC
$\dfrac{\frac{0.389n}{\alpha g}+2.5}{1-\frac{0.022}{\alpha g}(1-\alpha+x_F 0.214)n}$	$\dfrac{\frac{1.1n}{\alpha g}+2.5}{1-\frac{0.022}{\alpha g}(1-\alpha+x_F 0.417)n}$
On the rim	**Linear**
$\dfrac{\frac{1.1n}{\alpha g}+2.5}{1-\frac{0.022}{\alpha g}(1-\alpha+x_F)n}$	$\dfrac{\frac{0.269n}{\alpha g}+2.5}{1-\frac{0.022}{\alpha g}(1-\alpha+x_F 0.1215)n}$

APPENDIX C

ORTHOGONALITY FACTOR THROUGH THE CELL

ABSTRACT: The orthogonality factor α represents the fraction of the BTS power that arrives at the ST with delay smaller than a single chip in the CDMA network, and is thus captured in the "finger" of the despreader correlator. All the rest appears as nonorthogonal interference to the receiver. Part of that is captured by later "fingers" and contributes to the diversity gain. The orthogonality depends on the locality of the ST and the environment in the cell, and is not uniform through the cell. Contributions delayed by over a chip time have to be reflection events with an advantageous propagation path, or they are negligible. The estimate of orthogonality is based on the distribution of such events.

C.1 Scattering and Reflections

The multipath arriving at the ST undergoes scattering or reflections. We are interested in multipath contributions whose delays are longer than the CDMA chip time. Scattering contribution to the multipath diminishes with the square of the distance between the scatterer and the ST, and are negligible for distances commensurate with the chip delay time. The only surviving contributions are reflection events that have a line of sight (LOS) or near LOS to the BTS, to the ST or to both, as presented in Fig. C-1.

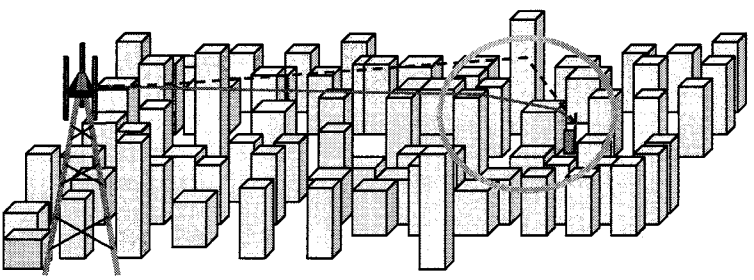

Figure C-1. Long delay reflection event

C.1.1 The Reflection Coefficient *F*

The reflection scenario is depicted in Fig. C-2. The ray is reflected by reflector D. The length of the ray is $r_1 + r_2 = a$ (the long axis of the reflection-delay ellipse) and is equal to $\hat{c}$ (distance between foci) in the 1st Fresnel ellipse (Fig. C-3). The reflection coefficient F is then expressed as:

$$F \equiv D\cos\varphi/(2\hat{y}). \tag{C-1}$$

Now, the 1st Fresnel ellipse is defined by $2(\hat{a}-\hat{c}) = \lambda/2$. By definition

$$\hat{b}^2 = \hat{a}^2 - \hat{c}^2 = (\hat{a}+\hat{c})(\hat{a}-\hat{c}) \cong 2\hat{c}\cdot\lambda/4 = \hat{c}\lambda/2$$

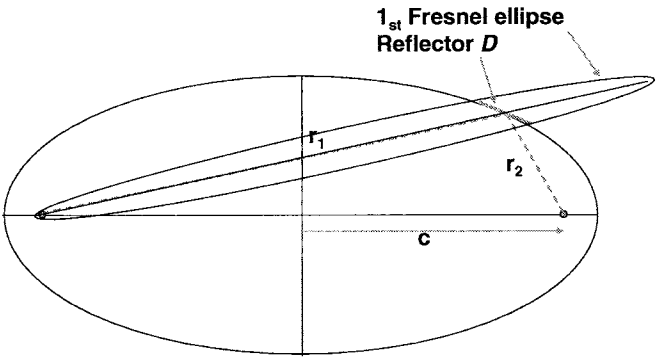

Figure C-2. The reflection ellipse

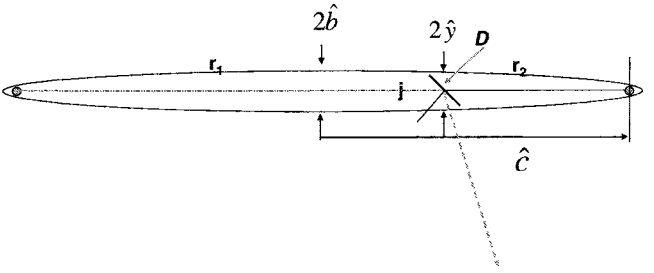

Figure C-3. The 1st Fresnel ellipse

where $\hat{a},\hat{b},\hat{c}$ are the Fresnel ellipse parameters $(\hat{x}/\hat{a})^2+(\hat{y}/\hat{b})^2=1$; $\hat{c}^2=\hat{a}^2-\hat{b}^2$. Then

$$|\hat{y}|=\hat{b}\sqrt{1-(\hat{x}/\hat{a})^2}\cong\sqrt{\frac{\lambda}{2}\cdot\frac{\hat{c}^2-\hat{x}^2}{\hat{c}}}= \\ =\sqrt{\frac{\lambda}{2}\cdot\frac{(\hat{c}+\hat{x})(\hat{c}-\hat{x})}{\hat{c}}}=\sqrt{\frac{\lambda}{2}\cdot\frac{r_1r_2}{\hat{c}}}=\sqrt{\frac{\lambda r_1(2\hat{c}-r_1)}{2\hat{c}}}\ . \tag{C-2}$$

Returning to the reflection ellipse, the angle between r_1 and the normal to the reflector is φ, and $tg\varphi=\frac{cy}{b^2}$. Then

$$\cos\varphi=\frac{1}{\sqrt{1+tg^2\varphi}}=\frac{1}{\sqrt{1+(c/b)^2(1-(x/a)^2)}}.$$

The parameters of the model are:

$R=2c$ is the distance between the BTS and ST. $r_0=\bar{c}\,\tau=2(a-c)=(r_1+r_2)-R$ is the minimum ray distance for a resolvable "finger", and $\bar{c}$ is the speed of light; a, b, c are the parameters of the reflection ellipse, and r_1 is the distance to the reflection point and is a running variable. Its maximal value (on axis) is $r_{1\max}=a+c=R+r_0/2$.

We seek to express F in terms of these constituents.

In the ellipse $r_1=a+cx/a\Rightarrow x=(r_1-a)(a/c)$. Then

$$1+(c/b)^2(1-(x/a)^2)=1+\frac{c^2}{a^2-c^2}\left(1-\frac{(r_1-a)^2}{c^2}\right)=\frac{a^2-(r_1-a)^2}{a^2-c^2}\text{, and}$$

$$\cos\varphi=\sqrt{\frac{a^2-c^2}{a^2-(r_1-a)^2}}\ . \tag{C-3}$$

Insertion of Eqs. (C-2) and (C-3) to Eq. (C-1) yields

$$F = \frac{D\cos\varphi}{2\hat{y}} = \frac{D}{2}\sqrt{\frac{a^2-c^2}{a^2-(r_1-a)^2}}\cdot\sqrt{\frac{2a}{\lambda r_1(2a-r_1)}} =$$

$$= \frac{D}{2\sqrt{\lambda r_0}}\cdot\sqrt{\frac{(\hat{R}+1)^2-\hat{R}^2}{(\hat{R}+1)^2-(2r(\hat{R}+1/2)-\hat{R}-1)^2}\cdot\frac{\hat{R}+1}{r(\hat{R}+1/2)(\hat{R}+1-r(\hat{R}+1/2))}} \qquad \text{(C-4)}$$

where

$$\hat{R} \equiv R/r_0\ ,\ r \equiv r_1/(R+r_0/2).$$

This is plotted in Fig. C-4, showing that the main contribution of reflectors emanates from a region surrounding the ST.

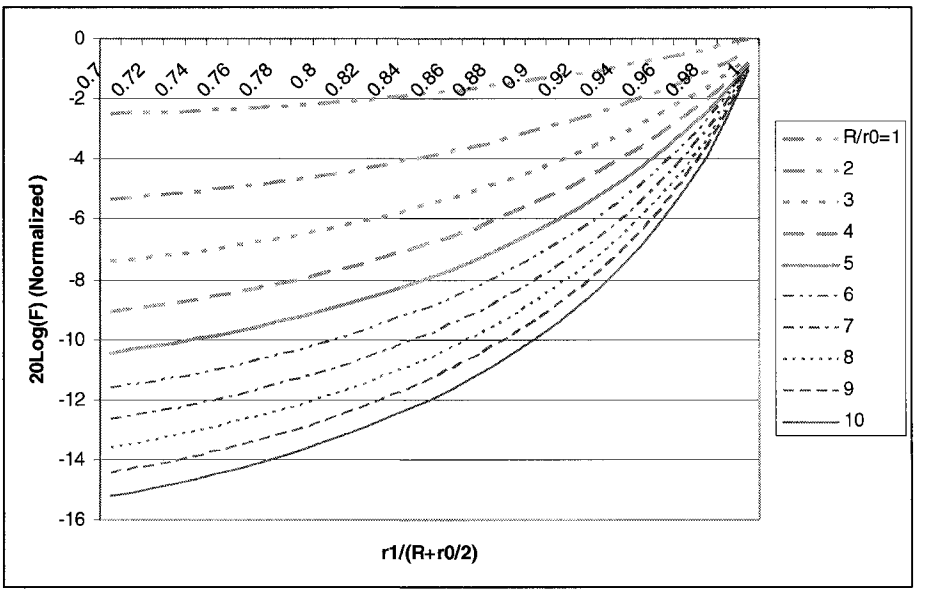

Figure C-4. Reflection coefficient along the ellipse

C.1.2 The Population of Contributing Reflectors

Reflectors are assumed to be uniformly distributed in the area, and their orientation distributed uniformly. The number of reflectors contributing rays that are delayed by τ is derived from the area between the ellipses

characterized by $r_0 = \bar{c}\,\tau$ and $r_0 + \Delta r_0$: the area of an ellipse is $S = \pi a\sqrt{r_0(a - r_0/4)}$ and the differential area is

$$\frac{dS}{dr_0} = \frac{\pi r_0(\hat{R}+1)\hat{R}}{4\sqrt{2\hat{R}+1}} \qquad \text{(C-5)}$$

where $\hat{R} \equiv R/r_0$. This is plotted in Fig. C-5, normalized to $R=r_0$. Now, the cumulative reflection contribution is $\hat{S} = \rho\int F^2(R, r_1)\, ds$ where ρ is the area density of reflectors. The contributing differential area is asymptotically proportional to $\hat{R}^{3/2}$. Coupled with the function F that exhibits a steeper descent for larger ranges, it is fair to assume within the accuracy required from the model, that $\hat{S} \propto R$ and is represented as $\hat{S} = \hat{S}_0 R$ where $\hat{S}_0 \propto \rho F^2$.

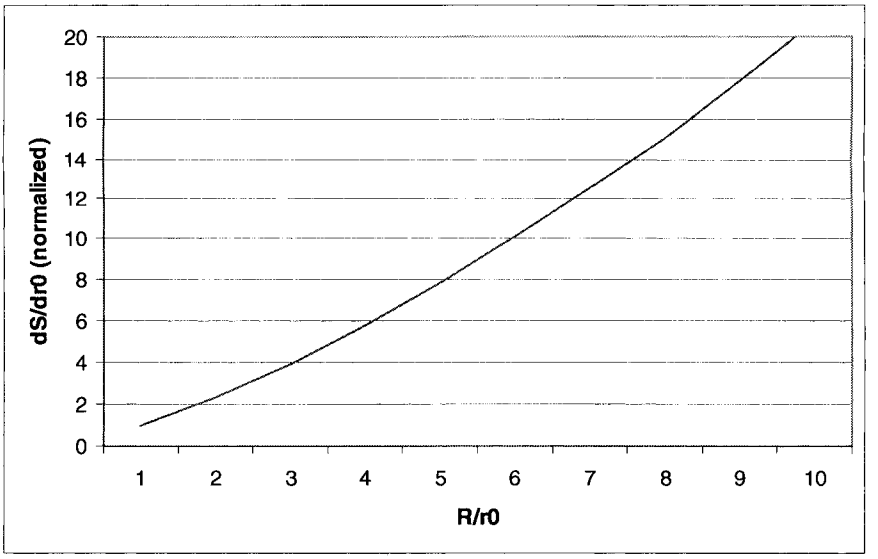

Figure C-5. Differential ellipse area for differential delay

C.1.3 The Reflection Contributions

The transmission equation

$$\frac{P_d}{P_t} = \left(\frac{\lambda}{4\pi}\right)^2 \frac{G_t G_r}{R^2} \tag{C-6}$$

where

P_d is the received power by direct path (LOS),
p_{gr} is the power received through flat earth propagation,
P_R is the received power through reflection,
P_t is the transmitted power,
G_t, G_r are the transmit and receive antennas' gain,
λ is the wavelength,
R is the distance between the BTS and the ST, and
D is the larger dimension of the reflector (and assuming specular reflection).

The transmission equation for flat earth propagation (Eq. 3-11)

$$\frac{P_{gr}}{P_t} = (hH)^2 \frac{G_t G_r}{R^4} \tag{C-7}$$

where H, h are the antenna heights.
The reflection equation

$$\frac{P_R}{P_t} = \left(\frac{\lambda}{4\pi}\right)^2 G_t G_r \frac{F^2}{(R + r_0)^2} \tag{C-8}$$

$$\frac{\sum P_R}{P_d} = \frac{\hat{S}}{(1 + r_0/R)^2} \cong \frac{\hat{S}_0 R}{(1 + r_0/R)^2} \tag{C-9}$$

$$\frac{\sum P_R}{P_{gr}} \cong \left(\frac{\lambda}{4\pi Hh}\right)^2 \frac{\hat{S}_0 R^3}{(1 + r_0/R)^2}. \tag{C-10}$$

Further away, when the reflected contribution also undergoes flat earth grazing reflection, Eq. (C-5) becomes, with Eq. (C-2)

$$\frac{\sum P_{Rgr}}{P_{gr}} = \frac{\hat{S}_0 R}{(1 + r_0/R)^4}. \tag{C-11}$$

C.2 Orthogonality Factor

The orthogonality factor represents the ratio of energy arriving at the ST with a delay shorter than one CDMA chip, to that arriving with a longer delay. We propose to set the ratio of contributions delayed between τ and $\tau+\Delta\tau$ to the direct contribution as an upper bound on the orthogonality. Equation (C-9) is called for the expression of orthogonality in the near zone, where the ST may be exposed to LOS:

$$\frac{\sum P_R}{P_d} = \frac{\hat{S}}{(1+r_0/R)^2} \cong \frac{\hat{S}_0 R}{(1+r_0/R)^2} = \frac{1-\alpha}{\alpha}$$

$$\alpha_N = \frac{(1+1/x)^2}{S_N x+(1+1/x)^2} \tag{C-12}$$

where S_N represents a cumulative near zone reflection contribution, $S_N = \hat{S}_0 r_0$, and $x \equiv R/r_0$. The expression for the intermediate zone, where the direct contribution undergoes grazing ground reflection while the reflection contributions are LOS, is extracted from Eq. (C-10) in a similar way

$$\alpha_I = \frac{(1+1/x)^2}{S_I x^3+(1+1/x)^2} \tag{C-13}$$

and $S_I = \left(\frac{\lambda}{4\pi Hh}\right)^2 \hat{S}_0 r_0^3$. The orthogonality factor for the far zone is derived from Eq. (C-11)

$$\alpha_F = \frac{(1+1/x)^4}{S_N x+(1+1/x)^4}. \tag{C-14}$$

These are plotted in Figs. C-6 to C-8 for near, intermediate and far zone, respectively.

Figure C-6 evaluates α for a range of the parameter $\hat{s}$, for the following: $\lambda = 0.36m$; H=25m; h=1.5m; F=1; r_0=120m ($r_0 = 0.5c\tau; \tau \cong 0.8\mu s$ in CDMA2000).

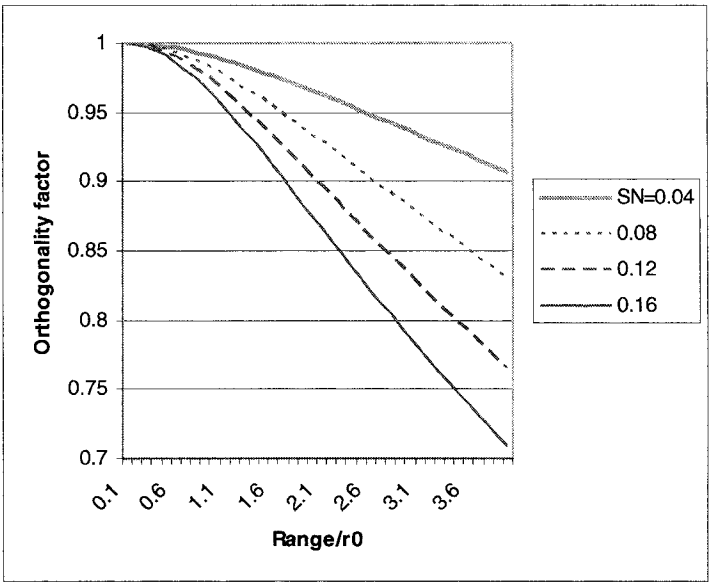

Figure C-6. Near zone (LOS) Orthogonality factor vs. normalized range

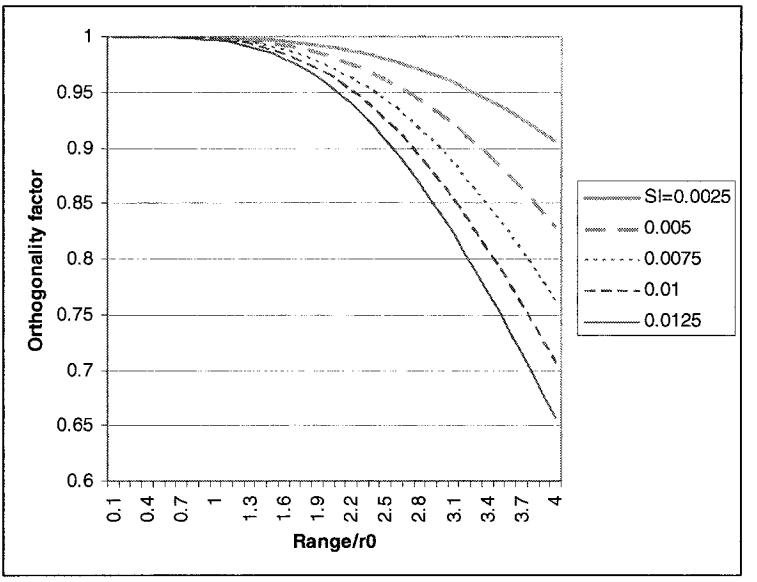

Figure C-7. Orthogonality function, intermediate zone. Reflectors - LOS, direct path - grazing ground reflection

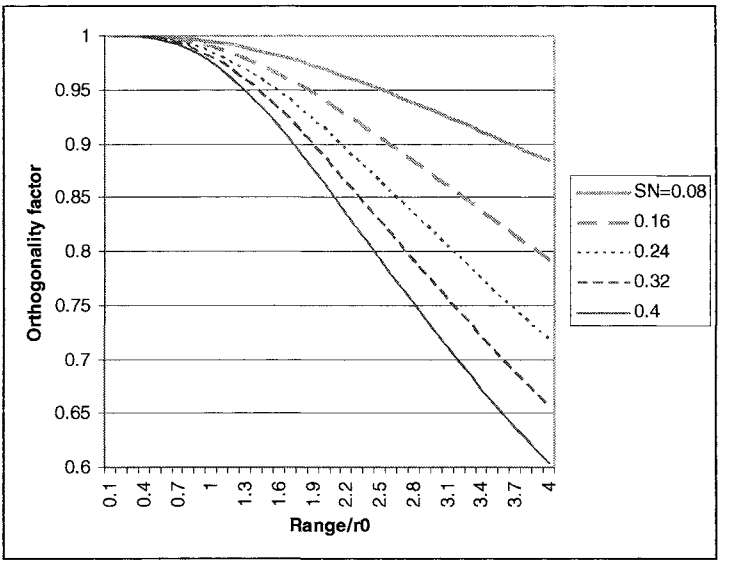

Figure C-8. Orthogonality factor, far zone. *Both reflectors and direct path – via grazing ground reflection*

C.3 Unified Factor – Transitions

C.3.1 Transition Near-Intermediate Zones

$$\frac{(1+1/x)^2}{S_I x^3+(1+1/x)^2}=\frac{(1+1/x)^2}{S_N x+(1+1/x)^2}.$$

This is readily solved by defining $u=1+1/x$, $x=1/(u-1)$ to render

$$R=2kHh \tag{C-15}$$

where k is the wave number $k=2\pi/\lambda$, which is not surprising. This is similar to the break point in the flat earth propagation model. A typical set of parameters for CDMA2000 is $\lambda=0.36m$; H=25 m; h=1.5 m; r_0=240 m. For this set of values we have R=1,309 m.

C.3.2 Transition Intermediate-Far Zones

$$\frac{(1+1/x)^2}{S_I x^3+(1+1/x)^2}=\frac{(1+1/x)^4}{S_N x+(1+1/x)^4}.$$

Now define $u=1+1/x$, $x=1/(u-1)$ to yield

$(s-1)u^2+2u-1=0$ where $s\equiv S_I/S_N=\left(\frac{\lambda r_0}{4\pi Hh}\right)^2$. This is solved for

$$u_{1,2}=\frac{1\pm\sqrt{s}}{1-s} \text{ and } x=R/r_0=\frac{1-s}{\sqrt{s}-s}=\frac{\left(\frac{4\pi Hh}{\lambda r_0}\right)^2-1}{\left(\frac{4\pi Hh}{\lambda r_0}\right)-1}\cong \quad \text{(C-16)}$$

$$=\frac{(2kHh-r_0)(2kHh+r_0)}{(2kHh-r_0)}=\frac{2kHh+r_0}{r_0}.$$

The second root is negative, because $s<<1$. This is not surprising. The delayed path through the reflectors is longer than the direct path by r_0, which is the difference between the near-intermediate transition point, Eq. (C-15) and the intermediate-far one, Eq. (C-16). For the same set of values s=0.034, x=6.45, R=1,550 m.

APPENDIX D

SYSTEM NOISE AND DYNAMIC RANGE

This Appendix reviews the basic theory governing the system noise and dynamic range aspects. These engineering key concepts are commonly used in any transmission system design, and thus form an essential basis for analysis and comparison of system performance.

D.1 Noise Figure

D.1.1 Definitions

Consider a linear system perfectly matched on its ports (e.g. 50Ω impedance) and having power gain G.

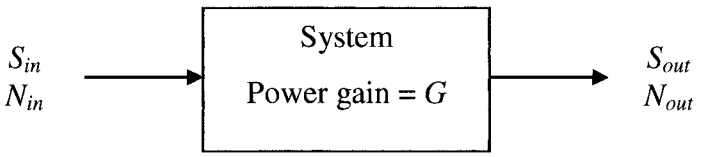

Figure D-1. Linear system definitions

The average signal power at input and output and average noise power at input and output are denoted by S_{in}, S_{out}, N_{in}, and N_{out}, respectively.
Recall that noise average power in the white noise case (fixed noise spectral power density) is

$$N = S_N \cdot B = kTB \qquad \text{(D-1)}$$

where $k = 1.24 \cdot 10^{-23}$ *Watt/Hz/°K* is the Boltzmann constant, T is the thermal noise temperature in °K and B is the bandwidth in *Hz*. S_N stands for the noise

spectral power density in *Watt/Hz*. Thus noise spectral power density may be characterized by either S_N or by the noise temperature T.
We have

$$S_{out} = G \cdot S_{in} \tag{D-2}$$

$$N_{out} > G \cdot N_{in} . \tag{D-3}$$

The first equality assumes linear system response (relating the input and out desired signals' power), whereas the second inequality assumes the system contributes some additional amount of noise to the external noise entering the system. It is assumed that the system noise and external input noise are statistically independent zero-mean random processes.
Define the *system noise factor* as:

$$F = \frac{N_{out}}{G \cdot N_{in}} . \tag{D-4}$$

Define also the *system noise figure* (in dB) as:

$$\mathrm{F} = 10 \cdot \log_{10}(F) . \tag{D-5}$$

Since any physical system contributes noise that is generated internally, we always have $F > 1$ or F>0 [dB].
An equivalent noise model that is commonly used, where the system internal contributed noise is represented by an equivalent internal additive input noise source (again, statistically independent of the external input noise, and both of zero mean) with the system becoming now an ideal noiseless linear block with power gain G, is presented in Fig. D-2.

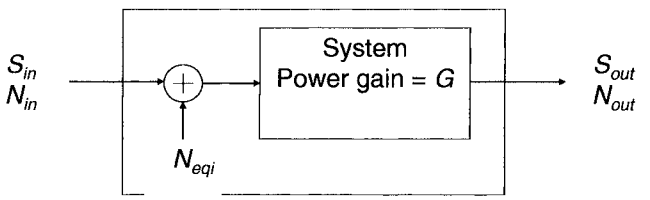

Figure D-2. Equivalent noise system model

The model of Fig. D-2 implies by independence of the zero-mean noise sources:

$$N_{out} = G \cdot (N_{in} + N_{eqi}) . \tag{D-6}$$

Using Eq. (D-6) in Eq. (D-4) we get an alternative form for the noise factor F

$$F = \frac{N_{out}}{G \cdot N_{in}} = \frac{G \cdot (N_{in} + N_{eqi})}{G \cdot N_{in}} = 1 + \frac{N_{eqi}}{N_{in}} = 1 + \frac{T_{eqi}}{T_{in}} . \tag{D-7}$$

Thus, a second definition of the noise factor is related to the ratio of internal equivalent noise power to the input power.
It is worth noting that the equivalent internal additive input noise may be expressed as follows

$$N_{eqi} = (F-1) \cdot N_{in} \tag{D-8a}$$

$$T_{eqi} = (F-1) \cdot T_{in} . \tag{D-8b}$$

Note that both definitions of Eqs. (D-4) and (D-7) relate F to N_{in}. Thus, F will vary for a given system with different levels of N_{in}.
A third definition may be derived by inserting G from Eq. (D-2) into Eq. (D-4), resulting in

$$F = \frac{N_{out}}{\frac{S_{out}}{S_{in}} \cdot N_{in}} = \frac{S_{in} \cdot N_{out}}{S_{out} \cdot N_{in}} = \frac{\frac{S_{in}}{N_{in}}}{\frac{S_{out}}{N_{out}}} = \frac{SNR_{in}}{SNR_{out}} \tag{D-9}$$

where *SNR* denotes the signal-to-noise power ratio. Thus F signifies the factor by which the *SNR* is degraded by a system, due to its internal noise contribution, per specified input noise level N_{in}.

Usually vendors specify noise factor (or noise figure in dB) referred to $N_{in}=N_0$, where the so-called *room temperature* noise density equals –174 dBm/Hz, or –114 dBm/MHz, etc.; the thermal noise temperature T_0 corresponding to N_0 may be found to equal 290°*K* or 17°*C*.

One important issue is the conversion of a predefined system noise factor F_0 (that matches an input noise temperature T_0) into a noise factor F (that matches an actual input noise temperature T). To this end, express T_{eqi} (corresponding to N_{eqi}) in the following two ways, using Eq. (D-8),

$$T_{eqi} = (F-1)\cdot T_{in} = (F_0 - 1)\cdot T_0 . \qquad \text{(D-10)}$$

The above invariance of T_{eqi} (and similarly for N_{eqi}) is a characteristic of the system, in that its internal noise spectral power density does not depend on the externally injected noise. From Eq. (D-10) the relation follows immediately,

$$F = 1 + (F_0 - 1)\cdot \frac{T_0}{T_{in}} = 1 + (F_0 - 1)\cdot \frac{N_0}{N_{in}} . \qquad \text{(D-11)}$$

One result is that the effective noise factor F for $T_{in} > T_0$ is *less* than F_0. This means that for higher input noise the relative increase of noise due to the internal system noise is reduced, rather than that we have a better system with absolute less noise power.

D.1.2 System Noise

An important conclusion resulting from Eq. (D-11) is the following interpretation: The *effective system noise referred to input* (and including the combined external and internal system noises) is defined as N_{sys} and given by

$$N_{sys} = F \cdot N_{in} . \qquad \text{(D-12a)}$$

Note that F here is defined relative to N_{in}. Similarly

$$T_{sys} = F \cdot T_{in} . \qquad \text{(D-12b)}$$

Now multiply Eq. (D-11) on both sides by T_{in} to get

$$F \cdot T_{in} = T_{in} + (F_0 - 1)\cdot T_0 = F_0 \cdot T_0 + T_{in} - T_0 . \qquad \text{(D-13)}$$

Thus, in a case where the input noise is higher than T_0 the effective system noise is composed of two contributions: the thermal 'noise floor' T_0 is multiplied by the noise factor F_0 and the surplus power T_{in} - T_0 is just added (as is usual for independent additive zero-mean random processes). The output noise power will then be given by

$$\begin{aligned} N_{out} &= G \cdot (F_0 \cdot N_0 + N_{in} - N_0) = \\ &= G \cdot [N_{in} + (F_0 - 1)\cdot N_0] \end{aligned} . \qquad \text{(D-14)}$$

Systems are generally composed of several building blocks, interconnected in series (cascade) and in parallel, in various combinations. Assuming the individual blocks are linear and cascaded, the system may be presented as in Fig. D-3.

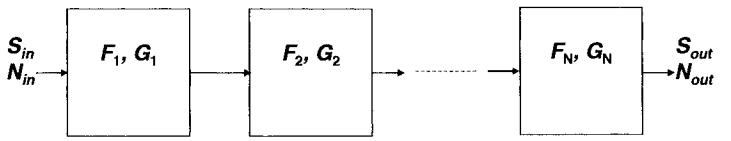

Figure D-3. Block diagram of a cascaded system

To find the system noise figure as a function of the parameters of the individual blocks, we adhere to Eq. (D-4) and calculate the output noise power N_{out}.

Each block is represented as in Fig. (D-2) and the noise sources (input noise and equivalent noises per block) are assumed zero-mean and statistically independent.

The power sum of the individual noises as they appear at the output constitutes N_{out}:

$$N_{out} = (N_{in} + N_{eqi1}) \cdot G_1 \cdot G_2 \cdot \cdots \cdot G_N + N_{eqi2} \cdot G_2 \cdot \cdots \cdot G_N + \cdots + N_{eqiN} \cdot G_N . \quad \text{(D-15)}$$

Dividing by $G_1 \cdot G_2 \cdot \cdots \cdot G_N \cdot N_{in}$ the result is

$$F = \frac{N_{in} + N_{eqi1}}{N_{in}} + \frac{N_{eqi2}}{N_{in}} \cdot \frac{1}{G_1} + \cdots + \frac{N_{eqiN}}{N_{in}} \cdot \frac{1}{G_1 \cdot G_2 \cdot \cdots \cdot G_{N-1}} . \quad \text{(D-16)}$$

Another popular form results by employing Eq. (D-8) in Eq. (D-16) for each term in the sum

$$F = F_1 + \frac{F_2 - 1}{G_1} + \cdots + \frac{F_N - 1}{G_1 \cdot G_2 \cdot \cdots \cdot G_{N-1}} . \quad \text{(D-17)}$$

There are a few important conclusions that can be summarized based on Eq. (D-17):

a) The noise figure of the first block F_1 fully contributes to the cascade noise figure F.

b) The noise figure contribution of any particular block in the chain (following the first block) is dependent on the inverse of the total gain of *all*

the blocks preceding the particular block. The physical explanation is that by amplifying (if the total preceding gain is greater than 1) the preceding noise into a particular block, the relative effect of the noise added by the particular block becomes smaller.

c) To minimize the cascade total noise figure, it is important to employ a first block with minimal noise figure F_1 and preserve an aggregate gain of >10 (as a simple rule of thumb) after any block in the chain; this would minimize the accumulation of noise figure along the chain. Of course, this also imposes some restrictions on the noise figures of the blocks with respect to the gains. Finally, this rule does not replace a precise optimization based on additional considerations (see next section) and limitations imposed by availability of components, target cost, etc.

D.1.3 System Sensitivity

The system noise is additive to the desired signal, and sets a limit as to the minimum signal level that may be demodulated successfully. It is possible to characterize the minimum required signal level by a parameter $(S/N)_{out}$ that defines the minimum signal-to-noise power ratio that enables demodulation at a predefined sufficient quality (for example, error-rate below a specified value, etc.). Given such a required output signal-to-noise (SNR) ratio, we define the sensitivity of the system as follows: sensitivity is the minimal input signal power that yields an output signal-to-noise power ratio of $(S/N)_{out}$.

The sensitivity may be found using Eq. (D-9):

$$\left(\frac{S}{N}\right)_{in} = F_r\left(\frac{S}{N}\right)_{out}. \tag{D-18}$$

The noise factor F_r is defined per input noise N_{in}. Also,

$$\left(\frac{S}{N}\right)_{in} = \frac{S_{in}}{kT_{in}B}. \tag{D-19}$$

Thus, the system sensitivity S_{in} is:

$$S_{in} = kT_{in}BF_r\left(\frac{S}{N}\right)_{out} = kT_{sys}B\left(\frac{S}{N}\right)_{out}. \tag{D-20}$$

In logarithmic scale this becomes:

$$S_{in}[dBm] = -174[dBm/Hz] + 10\log_{10}\left(\frac{T_{in}}{T_0}\right) + \\ + 10\log_{10}(B[Hz]) + 10\log_{10}(F_r) + \left(\frac{S}{N}\right)_{out}[dB]. \quad \text{(D-21)}$$

These results define the minimum detectable signal power as determined by the noise floor of a linear system, with known bandwidth, noise factor and detector specifications.

D.2 Dynamic Range

The results of the previous section indicated that noise figure may be well controlled and bounded by the noise figure of the first block in a cascade, given that the products of gains: $G_1 \cdot G_2 \cdots G_K$, $K = 1,2,N-1$ are large, beyond any bound. This is physically impossible since any realizable system operates off some power supply, and would saturate if the signal levels or power would start to increase beyond some limit. This section presents a model and parameters that are widely used to characterize the system nonlinearity in simple terms. As it would turn out, the actual RF system design involves both noise and linearity considerations, and a trade-off between the two.

D.2.1 Basic NonLinear Model

Any physical system, which is basically designed as a linear system (amplifier, attenuator, filter, etc.) may be described by its power transfer characteristic, as in Fig. D-4.

A linear region is usually identified for power levels that are below some limit (including the origin with 0 input resulting in 0 output power); above a limit (referred to input or output power) the transfer characteristic bends and starts to saturate. One definition of the nonlinear region is the power at which the linear extrapolated transfer characteristic deviates by 1dB (0.8 or 1.2 in linear power scale) from the actual characteristic. This level indicates the saturation limit and is termed 1 dB compression point, or P_{1dB}. It may be referred to input or output, as denoted in Fig. D-4.

This measure is coarse, and cannot be used to quantitatively analyze any nonlinearity effects.

A more fruitful approach [1] is based on a series approximation to the power transfer characteristic $v = g(z)$:

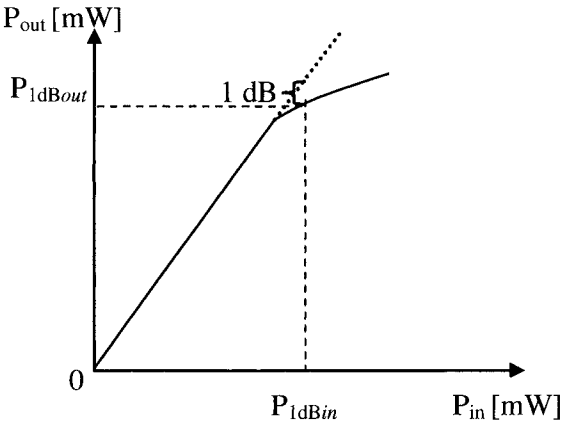

Figure D-4. Power transfer characteristic of a system

$$v = g(z) = a_1 z + a_2 z^2 + a_3 z^3 + \ldots \quad . \tag{D-22}$$

We assume that the 3rd order approximation of Eq. (D-22) is reasonably accurate in the characteristic transition region from linear to nonlinear. Higher-order terms may be included if a more accurate model is required. The coefficient a_1 stands for the linear power gain, whereas a_2 and a_3 signify the nonlinear part of the characteristic. An ideal linear system would be represented just by the first (linear) term.

D.2.2 Intermodulation Products

As a first evaluation of the effects of the nonlinear behavior, we analyze a two-tone signal that enters the block, thus:

$$z = A_1 \sin \omega_1 t + A_2 \sin \omega_2 t \, . \tag{D-23}$$

A linear system should present at its output two harmonics waveforms at ω_1 and ω_2 *only* – thus our focus will be on any *additional* frequency component that may appear at the output as a result of the nonlinear effects.

Substituting Eq. (D-23) in Eq. (D-22) and using trigonometric identities we get:

$$
\begin{aligned}
v = {} & a_1 A_1 \sin\omega_1 t + a_1 A_2 \sin\omega_2 t + \\
& + \frac{1}{2} a_2 {A_1}^2 (1 - \cos 2\omega_1 t) + \frac{1}{2} a_2 {A_2}^2 (1 - \cos 2\omega_2 t) + \\
& - a_2 A_1 A_2 \cos[(\omega_1 + \omega_2)t] + a_2 A_1 A_2 \cos[(\omega_1 - \omega_2)t] + \\
& + \frac{1}{4} a_3 {A_1}^3 (3\sin\omega_1 t - \sin 3\omega_1 t) + \frac{1}{4} a_3 {A_2}^3 (3\sin\omega_2 t - \sin 3\omega_2 t) + \\
& + \frac{3}{2} a_3 {A_1}^2 A_2 (1 - \cos 2\omega_1 t)\sin\omega_2 t + \frac{3}{2} a_3 A_1 {A_2}^2 \sin\omega_1 t (1 - \cos 2\omega_2 t).
\end{aligned}
\tag{D-24}
$$

Rearranging and collecting terms, results in:

$$
\begin{aligned}
v = {} & \frac{1}{2} a_2 {A_1}^2 + \frac{1}{2} a_2 {A_2}^2 + \\
& + \left[a_1 A_1 + \frac{3}{2} a_3 A_1 {A_2}^2 + \frac{3}{4} a_3 {A_1}^3 \right] \sin\omega_1 t + \\
& + \left[a_1 A_2 + \frac{3}{2} a_3 {A_1}^2 A_2 + \frac{3}{4} a_3 {A_2}^3 \right] \sin\omega_2 t \\
& + \frac{3}{4} a_3 {A_1}^2 A_2 \{\sin[(2\omega_1 - \omega_2)t] - \sin[(2\omega_1 + \omega_2)t]\} + \\
& + \frac{3}{4} a_3 A_1 {A_2}^2 \{\sin[(2\omega_2 - \omega_1)t] - \sin[(\omega_1 + 2\omega_2)t]\} + \\
& - a_2 A_1 A_2 \cos[(\omega_1 + \omega_2)t] + a_2 A_1 A_2 \cos[(\omega_1 - \omega_2)t] + \\
& - \frac{1}{2} a_2 {A_1}^2 \cos 2\omega_1 t - \frac{1}{2} a_2 {A_2}^2 \cos 2\omega_2 t + \\
& - \frac{1}{4} a_3 {A_1}^3 \sin 3\omega_1 t - \frac{1}{4} a_3 {A_2}^3 \sin 3\omega_2 t \ .
\end{aligned}
\tag{D-25}
$$

In addition to the input frequencies ω_1 and ω_2 several terms may be identified of 'new' frequencies that did not appear at the input: these include a DC term, $|2\omega_1-\omega_2|$, $2\omega_1+\omega_2$, $|2\omega_2-\omega_1|$, $2\omega_2+\omega_1$, $|\omega_1+\omega_2|$, $|\omega_1-\omega_2|$, $2\omega_1$, $2\omega_2$, $3\omega_1$, $3\omega_2$. The frequencies $|m\omega_1+n\omega_2|$ with m, $n \neq 0$ are termed $(m+n)^{th}$ order *intermodulation products*[46], or IM_{m+n}. Thus, 2nd order intermodulation terms include the frequencies $\omega_1+\omega_2$, $|\omega_1-\omega_2|$, and are denoted as IM_2 terms, and 3rd order intermodulation terms include the frequencies $|2\omega_1-\omega_2|$, $2\omega_1+\omega_2$, $|2\omega_2-\omega_1|$, $2\omega_2+\omega_1$, and are denoted as IM_3 terms. When m or $n = 0$ those frequency

[46] Sometimes abbreviated as *intermods.*

terms are referred to as *harmonics* of the fundamental frequency ω_1, or ω_2. Thus, $2\omega_1$, $2\omega_2$ are second order, and $3\omega_1$, $3\omega_2$ are third order harmonics.

When designing an RF transmission system, special care must be exerted to the linear performance of the system, and possible consequences of nonlinear effects.

Examples: (a) The third order intermodulation terms $|2\omega_1-\omega_2|$ and $|2\omega_2-\omega_1|$ are always important to consider since any bandwidth the system may occupy (however small) could eventually contain some IM_3 terms, if $|\omega_2-\omega_1|$ is small enough.

Note that for $\omega_2 > \omega_1$ the frequencies $2\omega_1-\omega_2$, ω_1, ω_2, and $2\omega_2-\omega_1$ appear in that order and are equally spaced.

(b) The second order intermodulation terms $\omega_1+\omega_2$, $|\omega_1-\omega_2|$ are of significance in any system design that should occupy at least an octave band. Second order harmonics should be examined as well in this case. As a specific case consider a system that covers the GSM900 band as well as the DCS1800 and PCS1900 bands. The second order IM products and harmonics of the 900 MHz band may cause interference to the 1800 and 1900 MHz signals. In addition, the $|\omega_1-\omega_2|$ terms of 1800 and 900 MHz signals may cause interference to the 900 MHz signals.

To obtain quantitative results, the relative power levels of the various frequencies will be considered next. Note that the levels of the fundamental frequency terms depend on their respective input levels but include a term that reflects an influence of one signal on the level of the other signal. These terms $(3/2)a_3A_1A_2^2$ for ω_1 and $(3/2)a_3A_1^2A_2$ for ω_2 signify a phenomenon known as *cross-modulation.*

The results of Eq. (D-25) present the amplitudes of the various frequency terms, and allow for a quantitative analysis of the spectrum resulting as a result of applying a two-tone input waveform to a third order nonlinear system.

The average power of each of the input signals is $(1/2)A_1^2$ and $(1/2)A_2^2$, respectively. The average power of the second order intermods is $(1/2)a_2^2A_1^2A_2^2$ each. The average power of the third order intermods is $(9/16)a_3^2A_1^4A_2^2/2$ and $(9/16)a_3^2A_1^2A_2^4/2$, and similarly for the harmonics, etc.; this enables an estimation of the resulting power spectrum, once the system is well-characterized by the coefficients a_1, a_2, a_3.

It so happens that the radio components and systems industry do not directly specify the above series coefficients, but instead present per each product a different set of parameters that is uniquely linked with the above coefficients, and is easier to measure in the lab, as well as use in power-level calculations. The equivalent set of parameters also has an appealing engineering

significance and became a de facto standard of characterizing the nonlinear behavior of RF components and systems.

The *linear* power gain G of the specified block is simply $a_1{}^2$. We next present the characterization of nonlinearity using the term *intercept-point* (*IP*), and its relation with the series coefficients. The *IP* is a theoretical power level at which the fundamental (first order) terms at the output and the *IM* terms have equal power[47]. Note that the power level at which the second order term equals that of the first order term need not necessarily be the same as the power at which the third order term equals that of the first order term. Thus we get generally two *IP* values – second order IP_2 and third order IP_3. In effect – instead of specifying the coefficients a_1, a_2, a_3, we use G, IP_2 and IP_3. We next find how these parameters are interrelated.
To this end one has to equate the *extrapolated* power of the first order and higher-order terms.

To further simplify the derivations, and get some basic (however powerful) insight into the effects encountered due to the nonlinearity, assume that $A_1=A_2=A$. Equation (D-25) may then be rewritten as:

$$
\begin{aligned}
v = & \frac{1}{2}a_2A^2 + \frac{1}{2}a_2A^2 + \\
& + \left[a_1A + \frac{9}{4}a_3A^3\right]\sin\omega_1 t + \\
& + \left[a_1A + \frac{9}{4}a_3A^3\right]\sin\omega_2 t \\
& + \frac{3}{4}a_3A^3\{\sin[(2\omega_1 - \omega_2)t] - \sin[(2\omega_1 + \omega_2)t]\} + \\
& + \frac{3}{4}a_3A^3\{\sin[(2\omega_2 - \omega_1)t] - \sin[(\omega_1 + 2\omega_2)t]\} + \\
& - a_2A^2\cos[(\omega_1 + \omega_2)t] + a_2A^2\cos[(\omega_1 - \omega_2)t] + \\
& - \frac{1}{2}a_2A^2\cos 2\omega_1 t - \frac{1}{2}a_2A^2\cos 2\omega_2 t + \\
& - \frac{1}{4}a_3A^3\sin 3\omega_1 t - \frac{1}{4}a_3A^3\sin 3\omega_2 t.
\end{aligned}
\qquad \text{(D-26)}
$$

[47] This is not an actual operating point (practically one never even reaches close to this situation, and would it be the case, the series approximation would not have been valid – many more higher-power terms should have been added and specified, and even then it is not guaranteed that such a situation could actually be reached, where first order and higher-order terms appear with equal power).

The cross-modulation terms are imbedded in this special case in the amplitudes of the two fundamental frequency terms.
Denoting the average power as S we can write the input power of *any* one of the two tones as:

$$S_{in} = \frac{A^2}{2}. \tag{D-27}$$

The output power of a fundamental frequency *if* the system were ideally linear can be written as:

$$S_1 = a_1^2 \frac{A^2}{2} = a_1^2 S_{in}. \tag{D-28}$$

And the output power of the 2nd and 3rd order intermods as:

$$S_2 = a_2^2 \frac{A^4}{2} = 2a_2^2 S_{in}^2 \tag{D-29a}$$

$$S_3 = \frac{9}{16} a_3^2 \frac{A^6}{2} = \frac{9}{4} a_3^2 S_{in}^3. \tag{D-29b}$$

The second order intercept-point is defined as the (extrapolated) power at which $S_1 = S_2$, or

$$a_1^2 S_{in} = 2a_2^2 S_{in}^2. \tag{D-30}$$

Thus,

$$S_{in}^{(2)} = \frac{a_1^2}{2a_2^2}, \text{ or referred to output: } S_o^{(2)} \equiv IP_2 = \frac{a_1^4}{2a_2^2}. \tag{D-31}$$

Similarly for the third order intercept-point

$$a_1^2 S_{in} = \frac{9}{4} a_3^2 S_{in}^3. \tag{D-32}$$

Thus,

$$S_{in}^{(3)} = \sqrt{\frac{4}{9}\frac{a_1^2}{a_3^2}} = \frac{2}{3}\frac{a_1}{a_3}, \text{ and referred to output: } S_o^{(3)} \equiv IP_3 = \frac{2}{3}\frac{a_1^3}{a_3}. \quad \text{(D-33)}$$

Figure D-5 illustrates graphically the above definitions and results.

It is possible to straightforwardly derive from the above relations the following results for output power of intermodulation products:

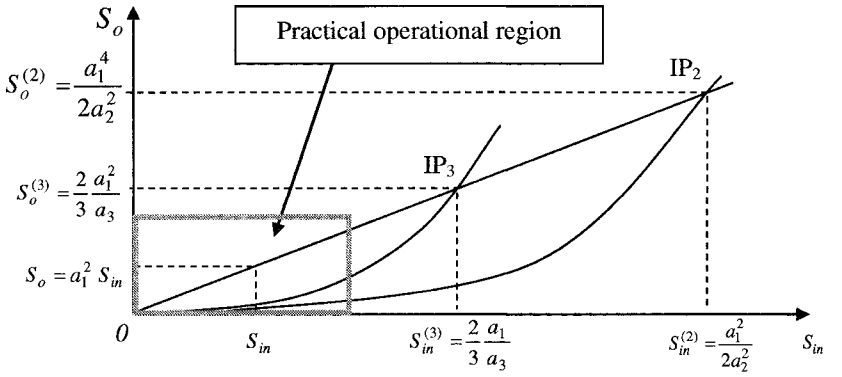

Figure D-5. Power of intermodulation products and intercept point

$$S_2 = \frac{S_1^2}{IP_2} \quad \text{(D-34a)}$$

$$S_3 = \frac{S_1^3}{IP_3^2}. \quad \text{(D-34b)}$$

It is convenient to present the above results in logarithmic (dB) scale. Denote logarithmic power (e.g. dBm) by P. Then we have, using notations that correspond to those used above, the following results for output *logarithmic* power levels, per input power P_{in}: from Eq. (D-29) the fundamental (first order) output power per frequency term is:

$$P_1 = G + P_{in}. \quad \text{(D-35)}$$

From Eqs. (D-29a) and (D-31) we get for the second order intermod output power:

$$P_2 = 2P_{in} - IP_2 + 2G\,. \tag{D-36}$$

See also Eq. (D-34a). Similarly from Eqs. (D-29b) and (D-33)

$$P_3 = 3P_{in} - 2IP_3 + 3G\,. \tag{D-37}$$

See also Eq. (D-34b). It is also useful to evaluate the intermod power relative to that of the fundamental frequency power, in dB:

$$\Delta P_2 = P_1 - P_2 = IP_2 - P_1 = \frac{1}{2}\left(IP_2 - P_2\right) \tag{D-38a}$$

$$\Delta P_3 = P_1 - P_3 = 2\left(IP_3 - P_1\right) = \frac{2}{3}\left(IP_3 - P_3\right). \tag{D-38b}$$

Figure D-6 illustrates graphically these definitions and results.

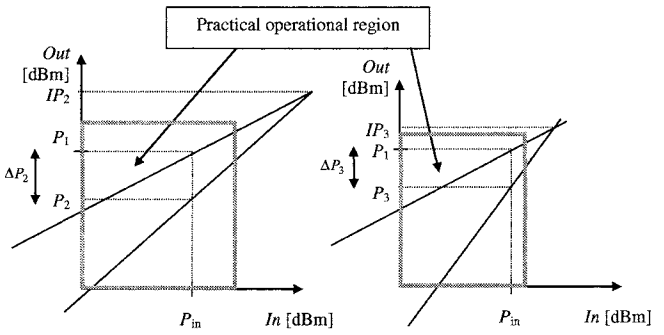

Figure D-6. Logarithmic scale intermodulation products and intercept point power

Since the slope of the output power of the fundamental component vs. input power is 1 dBm/dBm, that of the 2nd order intermod power is 2 dBm/dBm, and that of the 3rd order intermod power is 3dBm/dBm, it is possible (given the intercept points IP_2 and IP_3, which is specified by vendors of components and systems) to calculate the various power levels geometrically, using plots as in Fig. D-6.

D.2.3 System Intercept Point

Systems are generally composed of several building blocks, interconnected in series (cascade) and in parallel, in various combinations.

Assuming the individual blocks are linear and cascaded, the system may be presented as in Fig. D-7. Similar to having found the system equivalent noise figure, it is important to be able to calculate the effective system nonlinear performance, namely the system intercept-point.

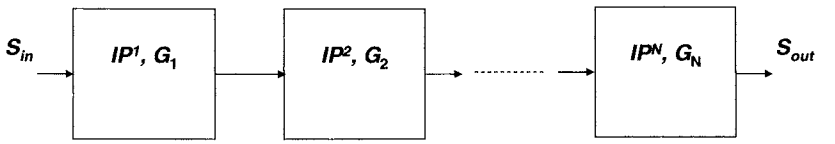

Figure D-7. Block diagram of a cascaded system

To find the system *IP* as a function of the parameters of the individual blocks, separately for 2nd order and 3rd order intermods we use the equal-power two-tone model and the expressions of Eq. (D-34). The underlying assumptions we make are that each block generates the intermodulation products due to the dominant two-tones, and passes linearly the intermods generated in preceding blocks (if any). The second assumption relates to the summation of all the accumulated intermodulation products at the output: these signals (or tones) may add coherently assuming they arrive at the output co-phased (this is a worst-case assumption, and quite unrealistic), or may add destructively, or assuming random uniformly distributed and independent phases between the tones of the same frequency; the last assumption results in incoherent combining, with total mean power equal to the power sum of all tones at the intermod frequency. We will use hereafter the assumption of incoherent summation.

Starting with the 2nd order IM product, we carry all generated IM_2 products to the output and sum the respective powers. Using Eq. (D-34a) we get:

$$S_2 = \frac{(S_{in}G_1)^2}{IP_2^{(1)}}G_2G_3\cdots G_N + \frac{(S_{in}G_1G_2)^2}{IP_2^{(2)}}G_3\cdots G_N + \\ + \frac{(S_{in}G_1G_2\cdots G_N)^2}{IP_2^{(N)}} = \qquad \text{(D-39)}$$

$$= S_{in}^2\left(\prod_{k=1}^{N}G_k\right)\left[\frac{G_1}{IP_2^{(1)}} + \frac{G_1G_2}{IP_2^{(2)}} + \frac{G_1G_2G_3}{IP_2^{(3)}} + \cdots + \frac{G_1G_2\cdots G_N}{IP_2^{(N)}}\right] =$$

$$= S_{in}^2\left(\prod_{k=1}^{N}G_k\right)^2\left[\frac{1}{G_2\cdots G_N IP_2^{(1)}} + \frac{1}{G_3\cdots G_N IP_2^{(2)}} + \right.$$

$$\left. + \frac{1}{G_4\cdots G_N IP_2^{(3)}} + \cdots + \frac{1}{IP_2^{(N)}}\right] .$$

Applying the total system gain $G_T = \left(\prod_{k=1}^{N} G_k \right)$, Eq. (D-39) maybe rewritten as:

$$S_2 = S_{in}^2 (G_T)^2 \left[\frac{G_T}{G_1 IP_2^{(1)}} + \frac{G_T}{G_1 G_2 IP_2^{(2)}} + \frac{G_T}{G_1 G_2 G_3 IP_2^{(3)}} + \cdots + \frac{G_T}{G_T IP_2^{(N)}} \right]. \quad \text{(D-40)}$$

Finally, the cascaded system IP_2 may be found using Eq. (D-34a):

$$IP_2^{Sys} = \frac{S_{1,Sys}^2}{S_2} = \frac{S_{in}^2 (G_T)^2}{S_2} = \\ = \left[\frac{G_T}{G_1 IP_2^{(1)}} + \frac{G_T}{G_1 G_2 IP_2^{(2)}} + \frac{G_T}{G_1 G_2 G_3 IP_2^{(3)}} + \cdots + \frac{G_T}{G_T IP_2^{(N)}} \right]^{-1}. \quad \text{(D-41)}$$

This may also be written symmetrically as

$$\frac{1}{G_T IP_2^{Sys}} = \frac{1}{G_1 IP_2^{(1)}} + \frac{1}{G_1 G_2 IP_2^{(2)}} + \frac{1}{G_1 G_2 G_3 IP_2^{(3)}} + \cdots + \frac{1}{G_T IP_2^{(N)}} = \\ = \sum_{k=1}^{N} \frac{1}{\left(\prod_{l=1}^{k} G_l \right) IP_2^{(k)}}. \quad \text{(D-42)}$$

A similar derivation for the system IP_3 using Eq. (D-34b) yields:

$$S_3 = \frac{(S_{in} G_1)^3}{\left(IP_3^{(1)}\right)^2} G_2 G_3 \cdots G_N + \frac{(S_{in} G_1 G_2)^3}{\left(IP_3^{(2)}\right)^2} G_3 \cdots G_N + \\ + \frac{(S_{in} G_1 G_2 \cdots G_N)^3}{\left(IP_3^{(N)}\right)^2} = \\ = S_{in}^3 \left(\prod_{k=1}^{N} G_k \right) \frac{G_1^2}{\left(IP_3^{(1)}\right)^2} + \frac{G_1^2 G_2^2}{\left(IP_3^{(2)}\right)^2} + \frac{G_1^2 G_2^2 G_3^2}{\left(IP_3^{(3)}\right)^2} + \cdots \\ + \frac{G_1^2 G_2^2 \cdots G_N^2}{\left(IP_3^{(N)}\right)^2} = \\ = S_{in}^3 \left(\prod_{k=1}^{N} G_k \right)^3 \frac{1}{\left(G_2 \cdots G_N IP_3^{(1)}\right)^2} + \frac{1}{\left(G_3 \cdots G_N IP_3^{(2)}\right)^2} + \cdots \\ + \frac{1}{\left(IP_3^{(N)}\right)^2}. \quad \text{(D-43)}$$

Finally, the cascaded system IP_3 may be found using Eq. (D-34b):

$$\left(IP_3^{Sys}\right)^2 = \frac{S_{1Sys}^3}{S_3} = \frac{S_{in}^3 \left(G_T\right)^3}{S_3} = \\ = \left[\frac{G_T^2}{\left(G_1 IP_3^{(1)}\right)^2} + \frac{G_T^2}{\left(G_1 G_2 IP_3^{(2)}\right)^2} + \cdots + \frac{G_T^2}{\left(G_T IP_3^{(N)}\right)^2}\right]^{-1} . \tag{D-44}$$

Again, rewritten symmetrically we have

$$\frac{1}{\left(G_T IP_3^{Sys}\right)^2} = \frac{1}{\left(G_1 IP_3^{(1)}\right)^2} + \frac{1}{\left(G_1 G_2 IP_3^{(2)}\right)^2} + \cdots + \frac{1}{\left(G_T IP_3^{(N)}\right)^2} = \\ = \sum_{k=1}^{N} \frac{1}{\left[\left(\prod_{l=1}^{k} G_l\right) IP_3^{(k)}\right]^2} . \tag{D-45}$$

There are a few important conclusions that may be summarized based on the results of Eqs. (D-42) and (D-45):
a) The intercept point of the last block $IP^{(N)}$ fully contributes to the cascade intercept point IP^{Sys}.
b) The contribution of any particular block in the chain to the IP^{Sys} is dependent on the inverse of the total gain of *all* the blocks following the particular block. The physical explanation is that by amplifying (with a total gain greater than 1) the output signal off a particular block, per given output level, the signal level out of the block is reduced and its contribution to the nonlinear performance becomes smaller.
c) To minimize the cascade total IP^{Sys}, it is important to employ a last block with maximal *IP* (e.g. a high-power amplifier) and preserve an aggregate gain of >10 (as a simple rule of thumb) past any block in the chain; this would minimize the accumulation of contributed *IMs* along the chain. Of course, the actual characteristics of the blocks are important, with low-*IP* blocks used with the low-signal level parts of the chain, and high- *IP* blocks towards the high-signal level parts of the chain. Finally, these rules do not replace a precise optimization and limitations imposed by availability of components, target cost, etc.

D.2.4 Dynamic Range

The noise-related results established a *minimum* signal level that a system can handle. The nonlinear system analysis yielded expressions for the wanted and unwanted (spurious) frequency components at the output of the system. For a pair of equal power signals at two frequencies (as in Eq. (D-26) and on), define the *maximum* signal level (any one of the two input signals) at which the output level of the strongest unwanted frequency would be at the noise

levels (i.e. equal to the output noise power at the signal bandwidth). If there is more than one strongest spurious component, we refer to just any one of them.

The dynamic range of a system is defined as the ratio of above maximal to minimal input signal levels, usually expressed in [dB].

We demonstrate the calculation of the dynamic range for a strongest 3rd order intermodulation product.

The 3rd order IM product is assumed to be at the output noise level:

$$N_{out} = N_{in} F_r G = kT_{in} B F_r G = IM_3; \quad P_3 = 10\log_{10}(IM_3). \tag{D-46}$$

The maximum signal level with respect to the 3rd order IM product is determined from Eq. (D-38b),

$$\Delta P_3 = P_1 - P_3 = 2(IP_3 - P_1) = \frac{2}{3}(IP_3 - P_3) \tag{D-47}$$

or

$$P_1 = P_3 + \frac{2}{3}(IP_3 - P_3) = \frac{1}{3}(2IP_3 + P_3). \tag{D-48}$$

The minimum signal level is determined according to the sensitivity expressions above: Eqs. (D-20) and (D-21).

$$S_{in} = kT_{in} B F_r \left(\frac{S}{N}\right)_{out} = kT_{sys} B \left(\frac{S}{N}\right)_{out}; \quad P_{in} = 10\log_{10} S_{in}. \tag{D-49}$$

For the dynamic range definition we use here $(S/N)_{out} = 1$ [48]. The conclusion is that the minimum signal level (that equals the noise occupied in bandwidth B) equals the level of the 3rd order IM product with maximum signal (see above), thus the dynamic range is:

$$DR = P_1 - GP_{in} = P_1 - P_3 = \frac{2}{3}(IP_3 - P_3) = \frac{2}{3}[IP_3 - 10\log_{10}(IM_3)] \tag{D-50}$$

and finally:

[48] Any other value may be chosen for the definition of dynamic range.

$$DR = \frac{2}{3}\left[IP_3 - 10\log_{10}\left(kT_{in}BF_rG\right)\right] \text{ [dB]} . \tag{D-51}$$

D.3 Beamforming and Combiners

One important RF systems discipline involves formation of antenna beams using basic antenna elements and splitters or combiners (depending on the direction transmission – Tx or Rx, respectively). Using several basic antenna *elements* provides flexibility in shaping the synthesized beam, employing *N*-1 complex weights (degrees of freedom) with *N* elements. The complex weights entail attenuation and/or phase shift per antenna (port), and the linear weighted combination of the element patterns results in the equivalent beam [2].
Equation (D-52) describes the beamforming operation:

$$y(t) = \sum_{k=1}^{N} w_k x_k(t) = \sum_{k=1}^{N} |w_k| e^{j\arg(w_k)} x_k(t). \tag{D-52}$$

Let the input signals per branch be the sum of a coherent signal and incoherent noise as in Eq. (D-53):

$$x_k = \alpha_k e^{j\beta_k} s + n_k . \tag{D-53}$$

Note that *s* is common to all branches up to a magnitude factor and phase shift. The beamforming operation is performed by a *combiner* in RVS link (Rx) or by a *splitter* (sometimes termed a *divider*) in FWD link (Tx).
The splitter operation is relatively trivial, and is governed by Eq. (D-54):

$$x_k(t) = \frac{1}{\sqrt{Nl}} y(t), \; \exists k \in 1,2,\ldots,N \tag{D-54}$$

where l is the insertion loss, expressed in dB as L: $L = 10 \cdot \log_{10} l$. All outputs are of the same value, and decrease with *N*.
The combiner operation is governed Eq. (D-55):

$$y(t) = \frac{1}{\sqrt{Nl}} \sum_{k=1}^{N} x_k(t). \tag{D-55}$$

Thus the combiner realizes the summation operation, up to a fixed factor, that depends on the number of ports and the insertion loss. Note that both the combiner and splitter are assumed to be matched on all ports (e.g. to 50Ω) and

passive[49]. The combiner includes an internal load that is required to satisfy the above physical assumptions.

Examples: Two simple cases are demonstrated for an ideal 2:1 combiner: we have $l = 1$.

Let the two identical input signals be: $x_k(t) = s(t), k = 1,2$. Then $y(t) = \frac{2}{\sqrt{2}} s(t) = \sqrt{2}\, s(t)$. In this case the output power equals the total input power $2\overline{s^2(t)}$, and the power dissipated on the internal load is 0.

Let the two input signals be: $x_k(t) = (-1)^k s(t), k = 1, 2$. Then $y(t) = 0$. The power dissipated on the internal loads is $2\overline{s^2(t)}$ in this case.

The general analysis of the combiner average output power in relation to its input power depends on the correlation between its input signals.

In the coherent signal case, assume all N inputs are equal to $s(t)$. Then the output signal is $y(t) = \frac{N}{\sqrt{Nl}} s(t) = \sqrt{\frac{N}{l}}\, s(t)$ and the output power is (Eq. (D-56)):

$$\overline{y_c^2(t)} = \frac{N}{l}\overline{s^2(t)}. \qquad \text{(D-56)}$$

In the incoherent signal case, assume all N inputs are zero-mean, statistically independent, and of equal power σ^2 . Then the output signal power is:

$\overline{y_n^2(t)} = \overline{\left(\frac{1}{\sqrt{Nl}} \sum_{k=1}^{N} x_k(t)\right)^2} = \frac{1}{Nl} \sum_{k=1}^{N} \overline{x_k^2(t)} = \frac{N}{Nl}\sigma^2 = \frac{\sigma^2}{l}$[50]. Thus, with N inputs all of independent zero-mean and equal power noises, the output noise power is fixed (independent of N). The output signal-to-noise power ratio is then $\frac{N}{\sigma^2}\overline{s^2(t)}$, reflecting the combining 'gain' N. If the desired signal appears at only one input port of the combiner then the output signal is $y(t) = \frac{1}{\sqrt{Nl}} s(t)$, and the output signal mean power is $\overline{y^2(t)} = \frac{1}{Nl}\overline{s^2(t)}$. Thus, the signal suffers in this case an N-fold attenuation in addition to the insertion loss l.

---

[49] The realization of these devices may be lumped or distributed, with the same underlying physical assumptions and the same governing equations.

[50] The power dissipated on the internal load with incoherent zero-mean and equal power independent inputs is $(N-1)\cdot\sigma^2$.

REFERENCES

[1] F.F. Fulton, *Two tone nonlinearity testing - the Intercept Point Pi*, Microwave Symposium Digest, G-MTT International, Vol. 73, Issue 1, June 1973.

[2] S.J. Orfanidis, *Optimum Signal Processing - An Introduction*, 2nd Ed., Chapter 7, McGraw-Hill, 1996.

APPENDIX E

ENVELOPE CORRELATION AND POWER CORRELATION IN FADING CHANNELS

Diversity methods are based on the low correlation between fades of multiple branch copies of a communicated desired signal. The degree of correlation between branch signals, as quantified by the correlation coefficient, is important for determining the diversity gain [1]. In this Appendix we identify several correlation coefficients related to random variables that characterize fading, the most notable being the Rayleigh distributed random variables. Care must be exercised in the definition of the correlation coefficient.

In general, the *envelope cross-correlation* is defined as

$$\rho_{r_1 r_2} = E(r_1, r_2) / \sqrt{\mathrm{var}(r_1)\mathrm{var}(r_2)}\,. \tag{E-1}$$

The *envelope correlation coefficient* is defined as

$$\rho_1 = E[r_1 - E(r_1), r_2 - E(r_2)] / \sqrt{\mathrm{var}(r_1)\mathrm{var}(r_2)}\,. \tag{E-2}$$

The *power correlation coefficient* is defined as

$$\rho_2 = E[r_1^2 - E(r_1^2), r_2^2 - E(r_2^2)] / \sqrt{\mathrm{var}(r_1^2)\mathrm{var}(r_2^2)}\,. \tag{E-3}$$

We have,

$$0 < \rho_{r_1 r_2}, \rho_1, \rho_2 < 1\,. \tag{E-4}$$

Practically it can be assumed for Rayleigh random variables that [2]

$$\rho_1 \approx \rho_2\,. \tag{E-5}$$

The Rayleigh random variable r is derived from an underlying *complex normal* random variable x, with $r = |x|$. The correlation coefficient of two *complex normal* variables x_1, x_2 is defined by (the asterisk * denotes complex conjugation)

$$\rho_{x_1 x_2} = \frac{0.5 \cdot E\left\{ \left(x_1 - \overline{x_1}\right)\left(x_2 - \overline{x_2}\right)^* \right\}}{\sqrt{\text{var}\, x_1 \cdot \text{var}\, x_2}},$$
$$\text{var}\, x_i = 0.5 \cdot E\left\{ \left(x_i - \overline{x_i}\right)\left(x_i - \overline{x_i}\right)^* \right\},\ i = 1,2\ . \tag{E-6}$$

The power correlation coefficient ρ_2 , of two Rayleigh distributed envelopes, r_1, r_2 is related to the correlation coefficient $\rho_{x_1 x_2}$ of the respective underlying complex normal variables by

$$\rho_2 = \left|\rho_{x_1 x_2}\right|^2 . \tag{E-7}$$

For additional information consult [3].

REFERENCES

[1] A.M.D. Turkmani, A.A. Arowogolu, P.A. Jefford, and C.J. Kellent, *An Experimental Evaluation of Performance of Two-Branch Space and Polarization Diversity Schemes at 1800 MHz*, IEEE Trans. Veh. Tech., Vol. 44, No. 2, pp. 318-326, May 1995.

[2] J.N. Pierce and S. Stein, *Multiple Diversity with Nonindependent Fading,* Proc. IRE, Vol. 48, pp. 89–104, January 1960.

[3] M.K. Simon and M.-S. Alouini, *Digital Communication Over Fading Channels: A Unified Approach to Performance Analysis*, 2nd Ed., Wiley, 2005.

APPENDIX F

EIGENVALUE ANALYSIS OF MRC

An illuminating analysis of MRC schemes is via the eigenfilter approach [1], [2]. Discrete-time SNR at the output of a linear MRC operation may be shown to have a Rayleigh quotient form, and its maximization equivalent to finding the maximal eigenvalue and corresponding eigenvector of a correlation matrix.

Denoting the channel correlation matrix as $C=E\{\boldsymbol{c}\cdot\boldsymbol{c}^H\}$, the noise correlation matrix as $N = E\{n\cdot n^H\}$, and the signal reference power as $S = E\{|s|^2\}$, the *SNR* may be written as

$$SNR_{out} = S\cdot\frac{\mathrm{w}^{\mathrm{H}}\cdot\mathrm{C}\cdot\mathrm{w}}{\mathrm{w}^{\mathrm{H}}\cdot\mathrm{N}\cdot\mathrm{w}} = S\cdot\lambda\,. \tag{F-1}$$

This form (a ratio of two quadratic forms in w) is known as the *Rayleigh Quotient*. The solution w_{opt} that maximizes the signal-to-noise ratio SNR_{opt} is related to the largest eigenvalue $\lambda_{\max}$ and the corresponding eigenvector $\boldsymbol{c}$ of the matrix $N^{-1}\cdot C$ as follows:

$$w_{\mathrm{opt}} = k\cdot\boldsymbol{c}^H = k\cdot N^{-1}\cdot\boldsymbol{c}, \text{ for arbitrary } k\neq 0, \tag{F-2}$$

$$SNR_{opt} = S\cdot\lambda_{\max} = S\cdot\boldsymbol{c}^H\cdot N^{-1}\cdot\boldsymbol{c}\,. \tag{F-3}$$

A nice property of the MRC processor is regarding the output *momentary* SNR, as a function of the input SNRs:

$$SNR_{out} = \sum_{k=1}^{N} SNR_k\,. \tag{F-4}$$

For the special case of equal power i.i.d. noise random processes additive to the k branch signal copies, the output signal power becomes the *sum* of all branches' powers. In this special case we have:

$$w_{\text{opt}} = k \cdot \boldsymbol{c}, \text{ for arbitrary } k \neq 0, \tag{F-5}$$

$$SNR_{opt} = S \cdot \lambda_{\max} = \frac{S}{\sigma^2} \cdot \boldsymbol{c}^H \cdot \boldsymbol{c} = \frac{S}{\sigma^2} \cdot \left| \boldsymbol{c} \right|^2 . \tag{F-6}$$

The above result is the same as in Eq. (5-14).

Note that all the above derivations did *not* assume any statistical properties, except for stationarity. No specific distribution function was assumed for the noise vector or channel transfer matrix.

REFERENCES

[1] J. Makhoul, *On the eigenvectors of symmetric Toeplitz matrices*, IEEE Trans. Acoust., Speech, Signal Processing, Vol. ASSP-29, August 1981.

[2] B. Holter and G.E. Øien, *The Optimal Weights of a Maximum Ratio Combiner Using an Eigenfilter Approach*, Proc. 5th IEEE Nordic Signal Processing Symposium (NORSIG-2002), Hurtigruten, Norway, October 2002.

APPENDIX G

OPTIMAL SECTOR BEAMWIDTH

ABSTRACT: The forward link capacity is power-limited for a given cell shape and other cells' environment. Users in the softer handoff (SrHO) draw twice the power (both sectors transmitting), except for the transmit diversity advantage over part thereof. The effect of the sector antenna beamwidth on the total power transmitted in the forward link is evaluated. No intercell interaction is considered here (circular cell is considered). Highest capacity is shown for 90^0 antenna beamwidth, with a substantial degradation for 60^0. (Note that 60^0 beamwidth is optimal for Cloverleaf cell, Fig. 4-18). Capacity loss due to Softer Handoff overhead is 20 to 40%.

G.1 Model

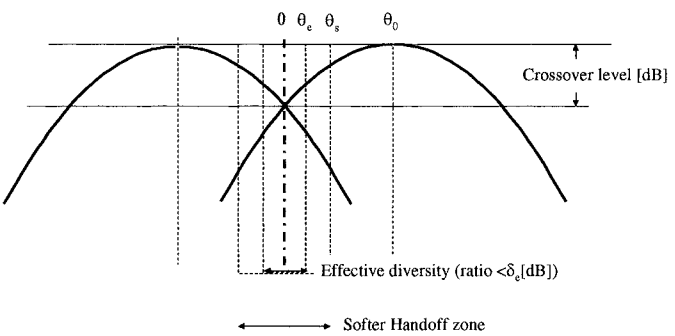

Figure G-1. Sector beam with softer handoff

$G(\theta)$	Gain of the sector beam
$G(0)/G(\theta_0)$	Gain at the crossover point between the sectors (relative to peak)
θ_s	Softer handoff zone boundary ($-\delta_s$[dB]$<G_1/G_2<\delta_s$[dB])
θ_e	Boundary of effective diversity zone ($-\delta_e$[dB]$<G_1/G_2<\delta_e$[dB])
S_{min}	Minimum signal level required at mobile user

ρ Area density of users
g_d Diversity gain between sectors
$\Delta_e \equiv 10^{\delta_e/10}$ Linear expression for the boundary δ_e
$\Delta s \equiv 10^{\delta_s/10}$ Linear expression for the boundary δ_s
Traffic - with power control (no bound assumed)
Power required per user

$$P_u = S_{\min} r^4 / G(\vartheta). \tag{G-1}$$

A uniform network with 3 equal sectors and a given other cells' interference (I_{0C}). A uniform user density ρ is assumed over the BTS circular coverage area. The total forward link traffic power (fixed OH power not counted) computed for the sector centered at angle $-\theta_0$ ($=-\pi/3$) is given by

$$P = \rho S_{\min} \int_0^1 r^5 dr \left\{ \int_{-\vartheta_0}^{\vartheta_0} \frac{d\vartheta}{G_1(\vartheta)} - \left(1 - \frac{1}{g_d}\right) \int_{-\vartheta_e}^{\vartheta_e} \frac{d\vartheta}{G_1(\vartheta)} \right\}. \tag{G-2}$$

The diversity gain is assumed to be fixed throughout the diversity zone. This is an underestimate of the overhead power.

G.2 Choice of Antenna Gain Function

The parabolic gain function is realistic only within the beamwidth. Its slope is too steep and the gain becomes negative. A Sinc^2 function is desired, but not integrable analytically. A cosine^2 is therefore exercised:

$$G(\vartheta) = G_0 Cos^2(k\vartheta) \tag{G-3}$$

where $k \equiv \dfrac{\pi}{4\vartheta_b}$, ϑ_b is half beamwidth, and G_0 is normalized over the sector

$$G_0 \int_0^{\vartheta_0} Cos^2(k\vartheta) d\vartheta = \int_0^{\vartheta_0} d\vartheta$$
$$G_0 = \frac{2}{1 + \dfrac{Sin(2k\vartheta_0)}{2k\vartheta_0}} \quad . \tag{G-4}$$

The half beamwidth is approximated via $\cos^2(k\vartheta_b) = 1/2 \cong 1 - (k\vartheta_b)^2/2$

$$\vartheta_b = 1/k \tag{G-5}$$

and the beam-crossing level at the sector boundary is

$$C = \cos^2(k\vartheta_0) = \cos^2(\vartheta_0/\vartheta_b). \tag{G-6}$$

The limit on this representation is that the first null is beyond the SHO and the effective diversity zones

$$\vartheta_s, \vartheta_e < \pi\left(\frac{1}{2k} - \frac{1}{3}\right). \tag{G-7}$$

G.3 Total Sector Traffic Power

From (G-2), (G-3), (G-4)

$$P = \frac{\rho S_{\min}}{6}\frac{1+\dfrac{Sin(2k\vartheta_0)}{2k\vartheta_0}}{2}\left\{\int_0^{\vartheta_0+\vartheta_s}\frac{d\vartheta}{Cos^2(k\vartheta)} - \left(1-\frac{1}{g_d}\right)\int_{\vartheta_0-\vartheta_e}^{\vartheta_0+\vartheta_e}\frac{d\vartheta}{Cos^2(k\vartheta)}\right\} \tag{G-8}$$
$$= \frac{\rho S_{\min}}{6}\frac{1+\dfrac{Sin(2k\vartheta_0)}{2k\vartheta_0}}{2k}\left\{tg(k(\vartheta_0+\vartheta_s)) - \left(1-\frac{1}{g_d}\right)(tg(k(\vartheta_0+\vartheta_e)) - tg(k(\vartheta_0-\vartheta_e)))\right\}.$$

G.4 Softer Handoff Boundary

$Cos^2(k(\vartheta_0 - \vartheta_s)) = \Delta Cos^2(k(\vartheta_0 + \vartheta_s))$. Cosine is positive through the range of interest. If $\vartheta_s < \vartheta_0$ we can use the approximate formula $\cos(a+b) \cong \cos(a) - b\sin(a)$ to get

$$\vartheta_s = \frac{1}{k \cdot tg(k\vartheta_0)}\left(\frac{\sqrt{\Delta_s}-1}{\sqrt{\Delta_s}+1}\right), \tag{G-9}$$

and in a similar way

$$\vartheta_s = \frac{1}{k \cdot tg(k\vartheta_0)}\left(\frac{\sqrt{\Delta_e}-1}{\sqrt{\Delta_e}+1}\right). \tag{G-10}$$

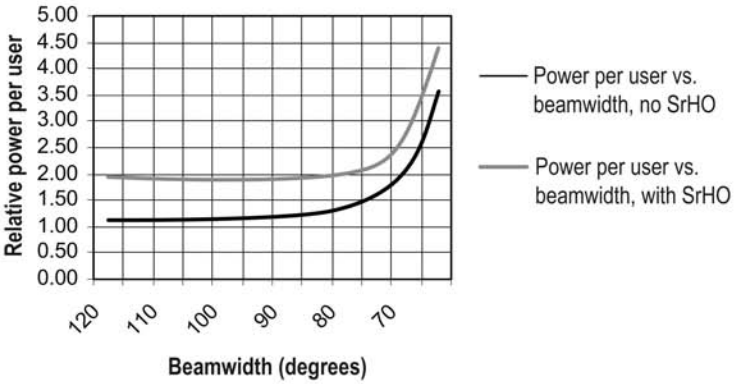

Figure G-2. Relative power per user vs. beamwidth, with and without SrHO overhead. Traffic only

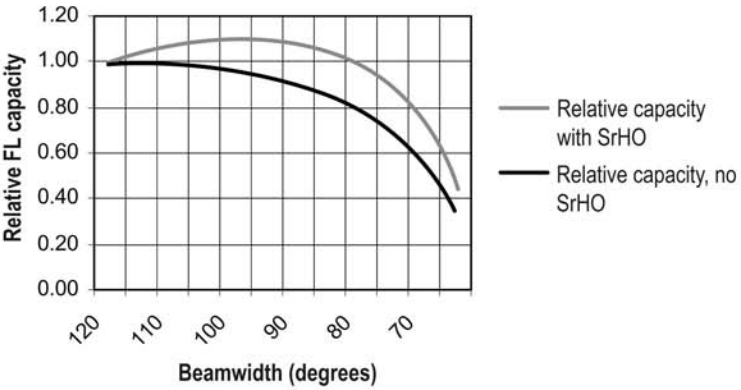

Figure G-3. Relative capacity with and without Softer Handoff, with power control, traffic only (no overhead), cosine^2 sector beam

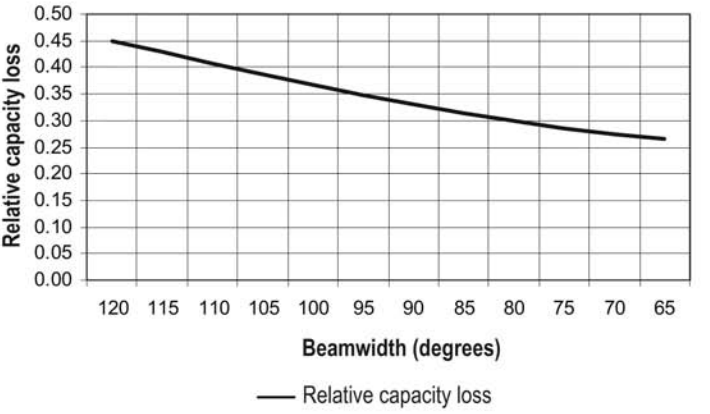

Figure G-4. Relative capacity loss due to Softer Handoff overhead, with power control, traffic only (no overhead), cosine^2 sector beam

G.5 Discussion

G.5.1 Limits on the Analysis

No pilot is considered. The effect of the pilot is two-fold:
-It adds overhead.
-The pilot is not power-controlled, and there is no compensation for the fall-off of the beam. The pilot becomes the actual limiter of the coverage in the areas between the sectors, and thus a limit on the capacity in case the cell cluster is designed for circular coverage.

The environment is considered to encircle a round cell (the effect of the other cells is angularly uniform around the cell).

G.5.2 Optimal Beamwidth

The optimal beamwidth for the forward link is 90^0. There is a capacity degradation for narrower beams.

G.5.3 Effect of the SrHO

The net effect of the SrHO is a power overhead that reduces the available power, and then the capacity. The capacity reduction due to the SrHO is between 40 to 20%.

APPENDIX H

CELLULAR BANDS AND FREQUENCY ALLOCATIONS

The following information briefly summarizes the major frequency bands, and the associated channel FA's definitions. See [1] for a complete list.

All frequencies f_n are in MHz.

- ✓ Only FL frequencies are presented.
- ✓ RL frequencies are readily calculated using the duplex separation.

Cellular ('850') Band
Duplex separation = 45 MHz

$$f_n = 870.00 + 0.030 \cdot n, \quad 1 \le n \le 799$$
$$f_n = 870.00 + 0.030 \cdot (n - 1023), \quad 990 \le n \le 1023$$

PCS Band
Duplex separation = 80 MHz

$$f_n = 1930.00 + 0.050 \cdot n, \quad 0 \le n \le 1199$$

DCS Band
Duplex separation = 95 MHz

$$f_n = 1805.00 + 0.050 \cdot n, \quad 0 \le n \le 1499$$

WCDMA Band
Duplex separation = 190 MHz

$$f_n = 2110.00 + 0.050 \cdot n, \quad 0 \le n \le 1199$$

MHz

850	Band A 870 - 880
	Band A' 890 - 891.5
	Band A"869 - 870
	Band B 880 - 890
	Band B' 891.5-894

PCS	Block A 1930-1945
	Block B 1950-1965
	Block C 1975-1990
	Block D 1945-1950
	Block E 1965-1970
	Block F 1970-1975

REFERENCES

[1] Technical Specification Group C, *cdma2000 High Rate Packet Data Air Interface Specifications*, 3GPP2 C.S0024, Version 4.0, pp. 9-6 – 9-27, 3GPP2, October 2002.

ABOUT THE AUTHORS

JOSEPH SHAPIRA is the president of Comm&Sens Ltd., a strategic consulting and initiatives company in wireless communications, remote sensing and imaging systems. He is also a N.T. Alexander Chair Professor for Telecommunications in IIT (Indian Institute of Technology) Madras. He is cofounder and past CEO and chairman of Celletra Ltd. – a cellular enhancement solutions company. During his tenure at Qualcomm he played a major part in the development of the CDMA standard and the radio engineering for the network. He then founded and was the President of Qualcomm Israel. Before joining Qualcomm, Dr. Shapira held a broad spectrum of research, management and staff positions in the largest government R&D organization in Israel, including establishment and leadership of the Electromagnetics lab. He also served on the advisory committee to the minister of telecommunications.

Dr. Shapira received his B.Sc. and M.Sc. in Electrical Engineering from the Technion - Israel Institute of Technology, and obtained a Ph.D. degree in Electrophysics from the Polytechnic University. He holds over 30 patents and patent-filing on cellular systems technology and optimization, chapters in 4 books and over 80 journal and technical symposia papers. He was awarded *best paper award* from IEEE AP-S in 1974, and the *Bergman award* by the president of Israel in 1980 for developing Electromagnetics in Israel. He is a *Life Fellow of the IEEE*, and served 6 years as a *Vice President of URSI* – the *International Union for Radio Sciences*. He is a member of *Club 100* – the forum of influential alumni of the Technion – Israel Institute of Technology.

SHMUEL Y. MILLER is executive vice president of systems & solutions of Celletra Ltd., a company that provides advanced radio coverage and capacity enhancements for cellular networks. He also holds an Adjunct Lecturer position at OBC (Ort Braude College) EE Department, Karmiel, Israel. His special areas of interest are adaptive signal processing, radio transmission systems, single and multi-user digital communications, space-time processing, diversity, antenna systems and tracking loops. During the past fifteen years his main activities have been on analysis and design of enhancements for cellular radio networks, linearization technologies and radio distribution systems.

Dr. Miller received his B.Sc. and M.Sc. in Electrical Engineering from the Technion - Israel Institute of Technology, and a Ph.D. degree in Information Sciences and Systems (EE Dept.) from Princeton University. He is a coauthor of over 20 patents and patent-filing on a proprietary frequency-hopping multiple access cellular standard and on cellular systems radio technologies, signal processing and optimization.

INDEX

1900 MHz band, 12, 415
1xEV-DO, 25, 39-42, 118
1xEV-DV, 40, 42
3G, 25, 34-36, 38, 156, 169-170, 187
3GPP, 35, 38, 296
3GPP2, 35, 296
Absorption, 320
Access node, 7, 118-119, 144, 158, 166, 167, 325, 327, 333, 354
Access probe, 28
Active set, 32
Adaptive
  beam-forming, 84
  interference cancellation, 346
  nulling, 348
Adjacent channel power (ACP), 254, 256
  ACPR, 256
Admission control, 124, 125
AGC, 31, 258-259, 308
Alarm, 249
AMPS, 2, 10, 24
Angle
  diversity, 154
  spread, 69
Antenna
  bandwidth, 78
  beamwidth, 54, 132, 409
  diversity, 140, 169
  height, 54, 81-82, 88, 136, 139, 167, 328
  isolation, 94-95
  pattern, 76, 82-83, 144
  temperature, 92
Aperture coherence, 154, 166
  limit, 154, 166
Apparent noise factor, 15, 198-201, 231, 329
ARQ, 35, 39, 155
Attenuation roll-off, 13, 252
Automatic frequency locking (AFL), 270
Auxiliary infrastructure, 4
AWGN, 156, 282
Backhaul, 17, 303, 306, 324, 332
  antenna, 260
  communications, 4
  delay, 307, 352
  diversity, 321
  dynamic range, 281, 306
  remote unit, 249
Band-pass filter (BPF), 236, 242, 255, 263, 307
Band repeater, 11, 251
Beam
  forming network, 76
  spreading, 318
  steering, 84, 154
  tilt, 83, 94, 130, 144, 351
  wander, 318
Bidirectional amplifier (BDA), 7
Blocking, 124-125, 189
Boresight, 78
Break point, 53, 62, 115, 116, 381
Brewster angle, 52-53
BSC, 2, 23
BTS, 1-18, 23, 29, 33, 102-107, 111, 139, 172, 188-190, 232, 236, 239, 243, 326, 328-336, 361, 373, 410
BTS hotelling, 4, 7
Canceller
  interference, 348
  isolation, 10, 209, 240, 346
Candidate set, 32
Capacity, 26, 105, 112, 120, 124-126, 137, 200, 214, 221, 223, 327
  equation, 137, 211
  limited cell, 113, 211, 215
  pole, 122, 123
CAPEX, 330
Cascade repeater, 229
CDF, 72, 150-152, 159-165
CDMA
  IS95, 10, 70, 103, 232
CDMA air interface, 20
CDMA2000, 10, 27, 35-41, 103, 169, 199, 232, 296, 300, 326
  1xEV-DO, 25, 39-42, 118
  1xEV-DV, 40-42

Cell
boundary, 107-108, 113
breathing, 16, 107, 109
optimization, 144
size, 330, 362
Cellular, 1-11, 23-42, 299, 338
antennas, 76, 90, 132, 166, 260, 319, 346, 351, 401,409
capacity, *see* capacity
cell planning, 10, 17, 193, 211, 326
coverage, 4, 7-8, 12, 14, 16, 32, 54, 63, 81-85, 102, 108-111, 113, 124, 126, 134, 194-232, 325-339, 357
frequency reuse, 2, 5, 10, 24, 134
interference, 26, 31, 34, 69, 74, 87, 97, 104, 111, 114-115, 122-124, 127, 134, 181-185, 196, 200, 204, 252-258, 272, 345, 347-350, 359, 366, 370, 373
Cellular bands, 24, 254, 415
Cellular communications, 7
Cellular operators, 5
Channel filters, 11, 251, 288
Channelized repeater, 11, 242
Circular polarization, 74
Clever antenna, 144
Cloverleaf pattern, 133
Coax, 304
Coding-interleaving, 27, 155
Coherent bandwidth, 70-71, 155, 179
Conductive coupling, 94
Conduit, 4, 6, 11
Control and monitoring (C&M), 248, 351
Correlation
coefficient, 87, 405
distance, 86, 88
receiver, 70
Cost, 4, 17, 144, 322-323, 326, 333
COST
WI model, 63-64
Coupling, 95
Coverage
balance, 3, 126, 266
extension, 14, 193
Coverage-limited cell, 211
Coverage shaping, 85, 131
Delay diversity, 155-156, 178-180, 231
Delay profile, 68-69
Delay spread, 69, 97, 155, 347
Diffraction coefficient, 57, 59, 63
Digital communications, 5, 6, 417
Digital filtering, 346
Digital gain, 16, 31, 124, 189
Directional couplers, 12, 237, 285
Distortion, 240, 244, 267
Distributed filtering, 253
Distributed repeater, 14, 250, 353
Diversity, 86-92, 117, 140, 149-191, 204, 210, 350, 373
branch, 117, 150, 173-178
channel, 150, 153, 170
gain, 117, 118, 151-156, 158-162, 164, 168, 171, 183, 187
order, 153, 157
reception *see* Receive diversity, 89, 106
Diversity gain, 151 *see* Diversity
Donor coverage, 14, 15, 194, 206, 210, 220, 223
Donor sector, 7, 303
Donor service antenna, 8, 176, 178
Donor unit, 8, 236
Doppler spread, 46, 155
Dropped calls, 124
Duplexer, 252, 313
Dynamic range, 238, 259, 308, 313, 400
Economy, 24, 325-339
Edge diffraction, 57, 58, 59
Effective noise factor, 198, 243, 263, 386
EGC, *see* Equal-gain combining
EIRP, 78, 84, 93, 329
Electrical tilt, 84, 351
Electromagnetic compatibility, 297
Emission mask, 239, 297, 299
Equal-gain combining, 90, 161, 162
Error-correction codes, 26
Error-vector magnitude (EVM), 240, 244
Facilities unit, 250
Fade margin, 320
Far-field coupling, 95
FDD, 9, 24, 38
FDMA, 10, 24
Finger, 26
Fins, 248
First Fresnel zone, 60, 61, 65
Flat fading, 46, 70, 86, 153, 155, 186
Forward link cell boundary, 113
Forward link gain, 194
Forward link power control, 31-32
Forward traffic channels, 29

Frame Error rate (FER), 30
Free-space optic (FSO) repeater, 13, 283-285, 305, 316-319, 323
Frequency allocation (FA), 9, 321
Frequency diversity, 154
Frequency offset, 270
Frequency shifted repeater (FSR), 12, 13, 17, 270, 285, 291, 292, 305
Frequency multiplexing, 306, 307
Fresnel zone, 66, 319, 320
Front to back (F/B) ratio, 78
Gain, 47, 241, 254, 276-293
Gain adjust, 296
Gain flatness, 242
Gain over temperature (G/T), 92
Grade of service (GoS), 23
Greenfield deployment, 326
Group delay, 267, 307
Group delay variation (GDV), 268, 269, 307
GSM, 2, 10, 24, 35, 99, 254, 296, 298, 309
Guard band, 13, 305
Handoff, 3
Har S-T model, 67
Headroom, 263
Heterodyne repeater, 11, 12, 270, 345
High data rate (HDR), *see* 1xEV-DO
High-power amplifier (HPA), 257
Highway coverage, 13, 140, 167, 260
Hole-filler, 14
Hot spot, 14, 134, 197, 215-216, 330
Hot spot microcell, 134
Hot spot repeater, 14
HSDPA, 40, 42, 187, 217
Ibrahim-Parsons model, 67
IF multiplexing, 13
Image rejection, 244, 245, 267
Impulse response, 67
In-band FSR, 13, 307
Indoor penetration, 17
Indoors microcell, 134
Indoors repeater, 14
Insertion loss, 238, 243, 267, 401, 402
Intercept point, 243, 393, 394, 397
Interference, 26, 87, 182, 253, 345, 347, 348, 359
Intermodulation (Intermod), 390
Inverse near-far effect, 120
IS 136, 10
IS 95, 10, 25, 27, 28
Isolation, 95, 209, 219, 240, 346
Isotropic antenna, 78
Large area scattering, 96-98
Lateral waves, 55
Lee's model, 63, 64
Linearity, 243, 262, 345
Link balance, 15-16, 126-127, 344
Link budget, 102
Link loss, 2, 16
LNA, 106, 141, 249, 255, 332
Load balance, 130, 352
Load control, 17, 352, 353
Load factor, 104, 121
Macrodiversity, 86
Maximal ratio combining (MRC), 162-165, 407
Microcell, 134, 137, 363, 366
Microwave repeater, 13, 292
MIMO diversity, 150
Multibeam Arrays, 84
Multicarrier, 13, 238, 304, 305
Multi-hop cascading, 175, 353
Multi-hop chain, 12, 229, 231
Multi-hop repeater, 8, 12, 14, 174-175, 196, 219, 222, 229, 231
Multi-lobe, 11, 14, 181, 219
Multimedia services, 25, 145
Multipath, 68, 114, 117, 131, 155, 187
  diversity gain, 119, 371
Multiple access, 1, 9
Nakagami-m distribution, 72
NBPF, 236, 240, 256
Neighbor cells, 3, 294, 354
Neighbor set, 33
Net gain, 15, 194, 198, 223, 329, 352
Net repeater gain, 198
Noise factor, 15, 199, 329, 384
Noise figure, 203, 223, 243, 254, 384
Noise floor, 238, 239, 264, 315
Noise rise, 15, 105, 111, 190, 201, 203, 220, 329, 352
Nominal load factor, 105
OFDMA, 354, 357
Okamura-Hata, 67
Omni cells, 138, 139
Omnidirectional, 169
On-frequency repeater (OFR), 11, 17, 275, 343, 346 *see also* Repeater -OFR
OPEX, 325, 330, 331

Optical fiber, 278, 311, 323
Optical fiber links, 6
Optical fiber repeater, 13, 278
Optical gain, 280
Optimization, 142, 144-146, 211, 213
Orthogonal transmit diversity, 170
Orthogonality factor, 26, 113, 115, 117, 183, 373
Orthogonality function, 116, 179
Oscillations, 277, 345
OTD, 36, 170
Out door unit (ODU), 250, 292, 316
Out-of-band, 244, 253, 255, 272, 277
Out-of-band FSR, 291, 305, 323
Over-the-air, 222, 236, 250, 267
Over-the-air backhaul, 175, 308
Packet-switched, 6, 35
Parabolic reflector antenna, 167, 290
Parasitic coupling, 272
Pass band, 240, 243, 253, 272, 306
Path-gain, 54, 56, 64, 362
PCDE, 245, 298
PCS, 415
PDC, 177
Phase noise, 240, 244, 271, 272
Phase sweeping, 156
Phase-sweeping transmit diversity (PSTD), 156, 170, 173, 187, 188, 354
Phased array, 84
Pilot pollution, 143
Pilot power, 16, 29, 113, 126-128, 130, 143, 190, 262
Pilot search window, 14
PN offset, 10, 29
Point-to-point (PTP), 13, 319, 321
Polarization diversity, 73, 92, 167-169, 176
Polarization matching, 74, 92, 140, 154, 168
Polarization shadow, 168
Polarization spread, 154, 155, 168
Pole capacity, 104-106, 123, 201
Power amplifier, 8, 123, 141, 172, 243, 258, 332, 346
Power control, 26-31, 38, 103, 120, 141, 179, 180, 359
  closed-loop, 30-31
  open-loop, 265
  subchannel, 29
Power Control Group, 29
Power margin, 238, 293, 296
Power offset-K, 30
Power per user, 125
Power ratio, 153
Power rise, 115, 123-125, 265
Power rise limit, 123
Power spectral density, 256, 271
Pseudodiversity combining, 177
QoS, 23, 35
  FER, 30
Radio access nodes (RAN), 7, 176, 177, 352
Radio nodes *see* Radio access nodes
Radio optimization, 19-21, 63, 84, 125, 211, 213, 330, 342, 351
Rake receiver, 26, 27, 32, 114, 155, 171, 182
RAN *see* Radio access nodes (RAN), 176, 177
Ray tracing model, 64
Rayleigh graph paper, 72, 164
Receive (Rx) diversity, 150, 158, 172, 237
Regenerative repeater, 6, 7, 357
Regulatory bodies, 296
Regulatory rules, 296
Reliability level, 150
Remaining set, 33
Remote coverage, 14
Remote electrical tilt (RET), 84, 145, 351
Remote sector, 7
Remote unit, 8, 236, 260, 270, 303, 342
Repeater, 6-22, 94, 149, 158, 170, 174, 178, 193-301, 306, 350, 355
  cascade, 8, 12, 178, 194, 196, 220-226, 330
  FSO, 11, 13, 283, 284, 305, 316, 323
  FSR, 11, 13, 17, 270, 285-294, 305, 323
  mesh, 358
  MW, 11, 13, 260, 292, 305-309, 319-324
  OFR, 11, 17, 236, 240, 250, 260, 273, 275, 343-346
  optical fiber, 278, 304, 305
  star, 8, 23, 220, 229, 304, 351
Repeater economics, 17, 322, 325-339
Repeater gain, 15, 47, 208, 210, 241, 254, 293, 344-346
Repeater network management system, 248, 249

Repeater power limit, 15
Repeater robustness, 341
Repeater selectivity, 267, 277
Repeater stability, 341
Repeater -embedded network, 20
Repeaters server, 249
Reverse access channel, 28
Reverse injection, 244, 298
Reverse interference, 298
RF access, 6, 144, 231
RF chain, 236, 239, 243, 253-257, 266-267
RF leakage, 242
RF transmission, 4, 237, 392
Rho, 240, 245, 246, 269
Ripple effect, 89, 98
RL repeater gain, 263
RNMS, 248, 275, 342, 343
Rural area, 3, 4, 96, 196, 333
SAW filter, 242, 243, 307
Scattering neighborhood, 68, 69, 89, 140, 166
Scheduler, 40, 41
Search window, 131, 232, 244, 309, 310
Sector average, 71
Sector beamwidth, 132, 133
Sector boundary, 126, 130, 189, 411
Sector coverage, 85, 132, 133, 303
Sectorization efficiency, 104
SEL, 160
Selection diversity, 159
Selective filtering, 250, 252, 267, 272, 285
Selectivity, 252, 297
Self-noise, 198, 199, 220, 256, 290, 291
Service antenna, 260
Set gain, 13, 194, 241, 263, 289, 296
Set level, 204, 259, 262, 352
Shadowed areas, 3, 14, 16, 143, 193, 196
Shelter, 4, 5, 7, 8, 333, 338
SHO, *see* Soft Handoff
SrHO, *see* Softer Handoff
Shut-down, 257
Sidelobe, 53, 78
Signal fidelity, 298
Slow fading, 71, 86, 149, 173, 180
Smart antennas, 5, 84, 101, 133, 355
Snell's law of refraction, 51
Soft Handoff, 3, 15, 20, 26, 29, 32, 33, 107, 111, 113, 126, 131-135
Softer Handoff, 32, 132, 353, 411
Space diversity, 98, 140, 154, 166
Space-Time Transmit Diversity (STTD), 36, 156, 170, 173
Splicing, 312, 313
Spurious coupling, 80, 209, 210
ST, *see* Subscriber terminal
Standard, 320
Star, 219, 220, 229
STAR network, 1, 220
Street canyon propagation, 64
Street microcells, 140
STTD, *see* Space-Time Transmit Diversity
Subscriber Terminal (ST), 15, 28-33, 107, 117, 126, 140, 167, 176, 190, 232, 342-352
Synchronization, 26, 29, 35, 38
System bandwidth, 27
TDD, 2, 9, 25
TDMA, 10, 24, 170, 357
TD-SCDMA, 25
TDTD - Time-delay transmit diversity, 156, 170-172, 176, 180-188, 192, 354
TE wave, 49, 50, 73
Terrestrial propagation, 18, 53
Tilt, 145, 351
Time diversity, 155
Time multiplexing, 24, 25, 40, 41
Time Switched Transmit Diversity (TSTD), 170
Time-multiplexed transmission, 118, 181
TM wave, 49, 52, 65, 74
TMA, 141
Tower, 106, 139, 141, 331-332
Tower-Top Electronics, 249, 332
Transmission equation, 47
Transmission gain, 15, 47, 62, 80, 83, 102, 136, 198, 319, 328, 329, 336
Transmit (Tx) diversity, 27, 36, 38, 169, 350
Transmit diversity
add-on, 27, 172, 174
TTLNA, 106
Two-tone signal, 247, 390
Type approval, 296-299
Ultimate rejection, 242, 252, 257, 267, 287
Undistorted power, 265
User diversity, 40, 187
Vendor financing, 5

Wavelength-division multiplexing (WDM), 13, 174, 304
WBPF, 236
WCDMA, 10, 25, 35, 38, 42, 170, 180, 238, 297-300, 306, 415
WiMAX, 357
Wireless modem, 248, 342-345, 350
XPD, 74, 75, 92, 140, 168, 175

Information Technology: Transmission, Processing, and Storage

(continued from page ii)

Principles of Digital Transmission
Sergio Benedetto, Ezio Biglieri